Cultural Heritage Science

Maria Perla Colombini
Ilaria Degano
Austin Nevin *Editors*

Analytical Chemistry for the Study of Paintings and the Detection of Forgeries

Springer

Cultural Heritage Science

The preservation and interpretation of our cultural heritage is one of the major challenges of today's society. Cultural Heritage Science is a highly interdisciplinary book series covering all aspects of conservation, analysis and interpretation of artworks, objects and materials from our collective cultural heritage. The series focuses on science and conservation in three main fields

- Art technology
- Active conservation and restoration
- Preventive conservation and risk management

The series addresses conservators and conservation scientists at museums, institutes, universities and heritage organizations. It also provides valuable information for curators and decision makers at museums and heritage organizations. Cultural Heritage Science comprises two subseries, one focusing on advanced methods and technology for conservation experts, the second presenting the latest developments in conservation science. All titles in the book series will be peer reviewed. Titles will be published as printed books and as eBooks, opening up the opportunity to include electronic supplementary material (videos, high-resolution figures, special data formats, and access to databases).

More information about this series at https://link.springer.com/bookseries/13104

Maria Perla Colombini • Ilaria Degano
Austin Nevin
Editors

Analytical Chemistry for the Study of Paintings and the Detection of Forgeries

Springer

Editors
Maria Perla Colombini
Department of Chemistry and
Industrial Chemistry
University of Pisa
Pisa, Italy

Ilaria Degano
Department of Chemistry and
Industrial Chemistry
University of Pisa
Pisa, Italy

Austin Nevin
Department of Conservation
Courtauld Institute of Art
London, United Kingdom

ISSN 2366-6226 ISSN 2366-6234 (electronic)
Cultural Heritage Science
ISBN 978-3-030-86864-2 ISBN 978-3-030-86865-9 (eBook)
https://doi.org/10.1007/978-3-030-86865-9

Cover illustration: Madonna and Child with two Angels (1495–1500) by Francesco Francia, stored at the North Carolina Art Museum (USA)

This Springer imprint is published by the registered company Springer Nature Switzerland AG
The registered company address is: Gewerbestrasse 11, 6330 Cham, Switzerland

Preface

Works of art have been copied and reproduced for millennia. The attribution of paintings to a specific artist often requires careful technical study, which can also assist in the detection of fakes. Indeed, forgeries are endemic in today's commercial art world, and the attribution of a painting, or the disproving of an attribution, or the identification of a deliberate fake is a curatorial and analytical challenge. Copying paintings and works of art has long been a tradition in art schools but did not have the purpose of creating false paintings. Instead, forging paintings, which requires ingenuity and invention, is an art in itself, and famous cases highlight the skill and deliberate intention of deceit by master forgers (e.g., Vermeer's paintings made by Han van Meegeren, Matisse's drawings by Elmyr de Hory, and Mantegna's or Van Dyck's or Brughel's paintings by Eric Hebborn). Forgeries gain illegal status when the act of falsification is linked to monetization. Established for old master paintings mainly during the nineteenth and twentieth centuries, the process of production of forgeries are known from the late Republican Age for the reproduction of Greek sculptures. It is noted that at the time, copies served a different purpose than modern forgeries, and the concept of authenticity had a quite different meaning than the one we will discuss in this book. Today, falsified paintings are plenty, including works by Monet, Renoir, Manet, Sisley, Modigliani, Picasso, Matisse, Gauguin, Cezanne, Tamara De Lempicka, and Klimt. Indeed, paintings existing in important museums and collections throughout the world or sold at auctions are still feared to be non-original, thus creating heated debates between art historians and experts. The unmasking of a forgery may require technical evidence to conclusively prove that a painting is a fake; indeed, the use of imaging techniques and instrumental analysis of materials has a fundamental role in the determination of the materials used by a painter, and this can be essential in the authentication of paintings, or the identification of a forgery. Indeed, the authenticity of a work carries significant value and contributes to reinforce the art market. It must, therefore, be highlighted that the protection of artistic heritage is strongly linked to our legal system, which prohibits illicit trade of works of art and their falsification. The aim of this book is to provide those with an interest in technical study and authentication with an overview of the analytical methods and imaging techniques that are used to study paintings, and that

are currently used to detect forgeries or provide scientific evidence that can corroborate or disprove authenticity. It is noted here and throughout the book that multiple evidence is used to inform attribution today.

The book guides the reader to understand first which approaches (Chaps. 1 and 2) are used in the authentication of works of art providing an overview on scientific studies and particularly analytical chemistry. An introductory chapter (Chap. 3) provides an overview of the different types of materials that may be encountered in paintings. An understanding of the chemical nature of materials aids in the interpretation of data obtained from imaging and analysis. With this information, curators and scientists can evaluate the likelihood that a particular material was available to artists in a particular period. In the chapters that follow, specific examples of how results of analytical methods are interpreted are given, together with examples of applications of specific techniques to address different questions that may relate to composition, condition, or technique.

Digital techniques are emerging as fundamental tools to assess paintings, permitting the comparison of similarities between paintings. These subjects are discussed in Chaps. 4 and 5.

Chapters 6, 7, 8, 9, 10, 11, and 12 deal with material characterization of paintings using instrumental methods, reporting the important updated techniques used in the field, complemented with several examples of application and exhaustive bibliography.

Isotope analysis for authentication is discussed in Chaps. 13 and 14, revealing the potential of radiocarbon dating and of the use of lead isotope ratios for identification of a pigment source or dating.

Finally, the book concludes with Chaps. 15 and 16 with the presentation of case studies and a discussion of art law. Recommendations for purchasing works and how art collectors and conservators may most safely approach the market are provided.

We hope that this book offers a useful source of information for those with an interest not only in authentication but, in a broader sense, in heritage science. Gathering knowledge on currently available techniques and case studies is an aid to those already working in this field, but this book aims to go further: it has the purpose to educate those entering the field by providing a comprehensible background of material characterization and analytical procedures for the study of paintings. We anticipate that new methods will be introduced in the future for examining paintings – a growing area of development includes the combination of spectroscopic data and the use of machine learning.

We also hope this work will continue to strengthen the collaboration between experts (art historians, connoisseurs, conservators, chemists, biologists, and physicists) in the decision-making required during authentication.

We acknowledge the many authors and reviewers who have contributed to this volume, who have embarked on this scientific challenge enduring the impatience of the editors. Finally, particular thanks go to the research group Scich (http://scich.dcci.unipi.it/) at the University of Pisa, who have worked for 30 years in the field of the development of analytical methods, particularly focusing on the complex

challenges of the identification of organic components in works of art; through their hard work and long-standing dedication, today we have developed multi-analytical approaches which provide key information both for the authentication and the conservation of our cultural heritage.

We hope that the present book will offer the opportunity to further consolidate links between art and science, and to bring young people to work in this fascinating field.

Pisa, Italy — Maria Perla Colombini

Pisa, Italy — Ilaria Degano

London, United Kingdom — Austin Nevin

Contents

Part I
Approaches to the Authentication of Works of Art

Chapter 1
The Eye Versus Chemistry? From Twentieth to Twenty-First Century Connoisseurship

Anna Tummers and Robert G. Erdmann

Abstract This essay traces the evolution of connoisseurship in the Netherlands from the early twentieth century to current and future challenges. In the twentieth century, the attitude of art historians towards chemistry varied from extreme distrust to extreme optimism about the possibilities of the discipline to provide conclusive evidence in authentication matters. While the chemical methods and technical means to research paintings have developed at an unprecedented pace in the twenty-first century, some of the key questions crucial to classifying works of art remain largely the same (e.g. how much consistency to expect in an artist's brushwork, painting technique and choice of materials?). However, other questions are new (e.g. how to interpret vast amounts of new data?) and call for a fundamentally different approach: for a cross-pollination of (technical) art history, chemistry and data science. While surveying recent developments, this essay discusses the merits and drawbacks of several modern analytical techniques (including as MA-XRF, HIS/RIS, isotope analysis and GC-MS) as well as the potential of digital aids (smart tools). The focal point of this essay is on the Netherlands since advances in the scientific investigation of works of art have repeatedly transformed the practice of connoisseurship here.

Keywords Connoisseurship · analytical methods · paintings · digital techniques

A. Tummers (✉)
Leiden University Centre for the Arts in Society, Leiden, the Netherlands
e-mail: j.c.tummers@hum.leidenuniv.nl

R. G. Erdmann
Rijksmuseum, Amsterdam, the Netherlands
e-mail: R.Erdmann@rijksmuseum.nl

M. P. Colombini et al. (eds.), *Analytical Chemistry for the Study of Paintings and the Detection of Forgeries*, Cultural Heritage Science,
https://doi.org/10.1007/978-3-030-86865-9_1

1.1 Connoisseurship, the Humanities and Some Recent Insights from Cognitive Psychology

Determining who painted what and when is one of the most difficult tasks of the art historian. Connoisseurship (i.e. the evaluation of the characteristic qualities, the dating and the attribution of works of art) involves estimating variabilities that can be tantalizingly difficult to determine. How much consistency can one expect in an artist's inventions, style and technique, choice of materials and workshop practice? Did the artist use one particular style that gradually developed over time or, instead, different manners at the same time? To what extent did he/she involve workshop assistants and was he/she consistent in doing so (or not doing so)? Even when secure evidence is scarce or missing, the art expert has to form a mental image –consciously or subconsciously– of what is characteristic of the artist in order to make a decision. Evidently, the validity of an attribution hinges on the correctness of the expert's assumptions.

Moreover, the determination of authorship also usually involves assessing the quality of the art work. Although key to the artist's goals and to the reception of the art work, the question how to define (high) quality is notoriously hard to tackle from an academic perspective.[1] For old master paintings, given the guild regulations and possible workshop assistance, the question is not just what level of quality can be expected of work by the master's hand but also –and perhaps more importantly– what level of quality the master demanded in the paintings he/she deemed worthy of carrying his/her name (Tummers 2011: 81–112). Here again, the issue of consistency is relevant: how much variation did the master allow in paintings produced in his/her workshop? And did the artist –as many old masters did– consciously produce works of different quality levels, that were priced accordingly?

In short, judging a picture is far from simple, no matter how swiftly the judgment is sometimes made. It involves myriad questions that touch on different academic disciplines, including art history and materials science. Moreover, the inherent complexity of the task entails a risk. As the psychologist and Nobel laureate Daniel Kahneman has shown, the human brain works with two different systems: a quick sub-conscious way of assessing (often referred to as 'intuitive') and a slower, conscious thought-process (Kahneman 2011). In daily life, the brain tends to simplify, thereby delegating the mental process to a sub-conscious part of our brain. When confronted with complex questions, the brain commonly substitutes a complex question with an easier one (Kahneman 2011). Though in many cases effective and efficient -and occasionally even better than conscious decisions- our intuitive tendency to simplify can also lead to dangerous biases and oversights in the decision-making process (Gladwell 2005: 48ff; 263–264 (example of a racial bias); see also Dijksterhuis 2007).

[1] One of the few scholars who attempted to answer this question is Jakob Rosenberg in his book *On Quality in Art* (Rosenberg 1967).

Given these insights into the workings of the brain (Kahneman 2011; Gladwell 2005), it is not surprising that there have long been discussions about the nature of connoisseurship among art experts. Throughout the twentieth century there have been two opposing views as to what should have the most weight in the attribution process: the connoisseur's intuition, that is, the sudden insight that the connoisseur experiences without fully grasping its origin (Kahneman's 'system 1'), or rational, communicable arguments (Kahneman's 'system 2'; Tummers 2011: 30–60). Although both aspects can be considered part of the same decision-making process, their different nature has long caused tension in both theory and practice.

The complexity of the decision-making process and the danger of oversimplifications may also explain the fierce criticism connoisseurs have often received. Already in the eighteenth century, the French scholar and theologist l'Abbé Du Bos dismissed 'the art of predicting the author of a painting by recognizing the master's hand' as 'the most faulty of all the arts, apart from medicine' (Du Bos 1719 [ed. 1993], 296). In the twentieth century, the attribution of paintings was reviled as subjective and intuitive, and as tainted by the market (Chapman and Weststeijn 2019: 10–15). Consequently, the term 'connoisseur' has acquired negative connotations, conjuring up the image of a presumptuous, outdated and inadequate judge of pictures –an attractive target for ridicule (Fig. 1.1).

As a result, academic art history repeatedly attempted to avoid connoisseurship at the start of the twentieth century, claiming it would not be quite 'theoretical' and

Fig. 1.1 Saul Steinberg, 'Gentlemen, it's a fake!', cartoon published in *The New Yorker*, 6 May 1950

'scholarly' enough to be worthy of serious academic attention (Muthesius 2013; Martin 1904). Avoiding connoisseurship did not solve the issue, however; it merely left academics vulnerable to the reproach that their discipline lacked a firm foundation (Pächt 1986 (ed. 1999): 66–67). For the history of art cannot be written without a basic classification of who created what and when. Therefore, other art experts chose the opposite strategy and attempted to mend the situation by creating a more 'objective' and 'scientific' connoisseurship. In the Netherlands the conservator Maurits van Dantzig in particular set out to develop a concrete (verifiable) method to attribute paintings based on rational arguments that could be checked (Van Dantzig 1936, 1978).[2] Despite his efforts, however, art historians remained divided. Even the prestigious Rembrandt Research Project (the largest and most advanced research project dedicated to sorting out the oeuvre of one single painter, pioneering several advanced scientific techniques) did not believe that the intuitive component could or should be taken out of the decision making process, as we will see (Bruyn et al., vol. 1, 1982: XVII; see below and note 22).

Meanwhile, another blow to the connoisseur's reputation came from the field of philosophy. In the 1950s and 1960s Arthur Koestler and Alfred Lessing argued that it made no aesthetic difference whether a painting is forged or not. Therefore, the person who pays a large sum of money for an original but would have no interest in a reproduction or imitation which he could not tell from the original, or worse, who prefers an aesthetically inferior original over an excellent forgery, is said to be at best confused and at worst a snob (Koestler 1955; Lessing 1965). It raised the question why connoisseurs should bother to tell originals and forgeries apart at all.

Although Koestler's and Lessing's claims were effectively refuted by the philosophers Nelson Goodman and Denis Dutton in the late 1960s and 1970s (see below), the fact that the validity of connoisseurship was questioned in this way, is telling. It is hard to imagine that a similar claim would be made for any other field of study (i.e. that it would make no difference if an expert's analysis and appreciation is based on an authentic or a forged piece of evidence). For example, should one value real and counterfeit money in the same manner if one cannot tell the difference? Should historians interpret and appreciate real and forged historical artefacts such as Hitler's diary or pieces of the dead sea scrolls in the same way if they cannot tell these apart? It is the emphasis on the *aesthetic* properties of course that makes the difference here. Yet the question was if the aesthetic properties could be separated entirely from any cultural or historical context.[3]

Goodman argued that since the exercise, training and development of our powers of discriminating among works of art are plainly aesthetic activities, the aesthetic

[2] The first one to devise concrete method to attribute paintings was the Italian art expert Giovanni Morelli. Although Van Dantzig did not refer back to him, his method seems indebted to his well-known Italian predecessor. See Tummers 2011: 30 ff.

[3] According to Goodman the idea that one should strip oneself of all the vestments of knowledge and experience when encountering a work of art derives from the Tingle-Immersion Theory which was developed around 1800 and has since then become part of the fabric of what Goodman calls our 'common nonsense' (Goodman 1983: 102).

properties of a picture include not only those found by looking at it but also those that determine how it is to be looked at (Goodman 1969: 111–112). In his view, the knowledge that a picture is an original and not a copy, imitation or forgery is a critical and valid factor in our response to it. [Indeed, the impact of such knowledge has recently been confirmed by neuroscientific research (see Huang et al. 2011; Wolz and Carbon 2014).]

Denis Dutton made a similar point but arrived at it differently. He stated that all visual art is necessarily performative, as it represents an achievement within a certain cultural and historical context. It is this achievement that determines its value as an art work (and makes it relevant to art history). Therefore, if our understanding of this achievement alters drastically when a work of art is exposed as a forgery, in his view it is no longer the same object, in so far as its position as a work of art is concerned (Dutton 1979: 314).

Although philosophers thus underscored the importance of connoisseurship, many academic art historians stayed clear of in-depth visual analysis and moved instead towards contextual and historical approaches in the 1970s and 1980s. Iconography, social history and socio-economic perspectives gained ground, causing art historians to rely heavily on verbal and contextual evidence rather than on their eyes. In an effort to change this, Harvard Professor and drawings expert Henri Zerner wrote an engaging essay on connoisseurship's bad reputation in 1987. "Ours is a logocentric culture", he stated: "We trust the written document much more than our visual understanding of an image. This must be changed and we must attend to visual clues if we want to get something out of our visual legacy" (Zerner 1987: 290).

While major research projects dedicated to individual artists such as Rembrandt, Rubens and Van Gogh greatly expanded our visual understanding of these masters at the end of the twentieth century, the advances in connoisseurship hardly impacted the academic curriculum. In 2009, Paul Craddock sharply observed: "the subject of authenticity does not seem to be seriously studied or taught to prospective art historians/curators, much less to materials scientists […] an honorable exception being the centre for study of forgery with its own museum at the University of Salerno" (Craddock 2009: 6). This lack of academic attention is disconcerting and yet somewhat understandable. Connoisseurship and authentication skills require arduous practice including extensive first-hand observation and in-depth study of important art works, copies and imitations, which not all universities can provide.

Nevertheless, the twenty-first century witnessed a renewed academic interest in connoisseurship as well as a theoretical refinement in thinking about issues of authenticity. Prominent academics who had not themselves dedicated their lives to sorting out the oeuvres of artists started to underscore the importance of this specific type of visual knowledge. David Freedberg eloquently argued that it was not just fundamental to art history but also potentially a 'core discipline in the humanities' as connoisseurship shared its 'evidential paradigm' with other types of scholarly detective work involving the interpretation of clues, symptoms and pictorial marks (Freedberg 2006; see also Ginzburg 1980). Stephanie Dickey stated that the continuing value of connoisseurship could be claimed both on theoretical and practical grounds: "Broad historical theories that build on works of art as evidence fall like a

house of cards if assumptions about the authenticity of those works prove incorrect" (Dickey 2015: 5). In 2019 the Dutch art historical yearbook was even dedicated entirely to connoisseurship, which is framed as the 'history of visual knowledge since the Renaissance'. According to Chapman and Weststeijn, connoisseurship is now widely understood as 'an essential and ever-evolving art-historical method'. Moreover, there is an 'enhanced rigor, [an] interdisciplinary reliance on materials science and neuroscience, and [a] new theoretical awareness' that represent a departure from the past (Chapman/Weststeijn 2019: 7).

This essay takes a closer look at the interaction between connoisseurs and chemists throughout the twentieth century, as well as at the current interdisciplinary character of authenticity research and its challenges. The main line of enquiry focuses on how advances in the scientific investigation of art works have repeatedly transformed the practice of connoisseurship in the Netherlands and on what is needed to effectively face future challenges.

1.2 The Eye Versus Chemistry: Early Interactions Between Connoisseurs and Chemists

No incident illustrates the deep distrust of an early twentieth century art expert towards chemical evidence better than a curious booklet of 89 pages with the title *Real or fake? Eye or Chemistry?,* dated 1925. It is written by Cornelis Hofstede de Groot, then one of the leading art historians and the author of a ten-volume survey book on Dutch seventeenth-century painting (Hofstede de Groot 1908–1927). He published the booklet in response to the lawsuit *Fred Muller & Co. vs H.A. de Haas*, the first court case in the Netherlands in which chemical evidence was brought to bear in an attribution matter. The bone of contention was the attribution of a small painting: the *Laughing Cavalier* (Fig. 1.2). Cornelis Hofstede de Groot had recognized it as an authentic Frans Hals (1582/83–1566) in 1923 and provided a certificate of authenticity. Both the certificate and painting had subsequently come into the possession of a certain H.A. de Haas, who had sold it via the auction house Fred Muller & Co. to a private collector for fl. 50.000,- (at the time the equivalent of fourteen years' salary for the average man[4]). A few months afterwards, however, the buyer demanded to be reimbursed claiming that the painting was in fact a forgery. The auction house looked into the matter, agreed with the buyer, reimbursed him, and subsequently asked Hofstede de Groot to cover a third of the damages suffered (circa fl.16.666,-). Hofstede de Groot refused to do so. He indicated that in his view he could not be held accountable for the prices fetched by paintings he had authenticated, and he offered to research the painting anew. After a second inspection, however, he concluded once again that in his view the painting was by Frans Hals.

[4] The equivalent is taken from Lopez 2008: 46

Fig. 1.2 Anonymous, *Laughing Cavalier*, ca. 1923, pastiche in the style of Frans Hals, current location unknown

The auction house then subpoenaed the seller, Mr. de Haas on the 9th of December 1923. Muller and Co. demanded that the purchase contract be annulled and that the purchase amount be reimbursed including interest as well as their litigation expenses. The burden of proof that the auction house presented was substantial. The painting had been researched by a team of experts who had jointly written a report: Sir Charles Holmes, director of the National Gallery in London, Prof. dr. Wilhelm Martin, director of the Royal Cabinet of Paintings, The Mauritshuis, in the Hague and Prof. dr. F.E.C. Scheller, chair of Inorganic Chemistry at Delft University of Technology.[5] Especially the materials science part of the investigation was disconcerting. Only the first test had yielded a positive result: the paint layer did not dissolve when treated with the usual 96% alcohol solution, which agrees with what one would expect of a seventeenth-century painting. However, when touched lightly with a cotton ball soaked in water, the paint became soft; with a soft brush and water the paint layer could even be entirely removed. Moreover, the researchers found artificial ultramarine in several locations throughout the painting, a pigment that had only been discovered in 1826. Furthermore, the researchers observed cobalt blue (through the microscope) in several locations in the background, a pigment that was not manufactured commercially until the early nineteenth century.[6] A chemical

[5] The report was published in its entirety as an appendix in Hofstede de Groot 1925: 74ff.

[6] According to the experts consulted during the trial, cobalt blue was first produced commercially around 1820/1830 (Hofstede de Groot 1925: 84); nowadays we believe it was somewhat earlier in 1807.

analysis of the white used in the painting identified it as zinc white, a pigment that has only been available since 1781. Also, a radiography of the picture revealed two nails that had been hammered into the picture from the front; these were machine-made and could therefore not have been produced before the nineteenth century. The conclusion was obvious: the painting could not be by Frans Hals or a contemporary; it was made by a modern forger or imitator.

The lawsuit received much press coverage and constituted a serious blow to the reputation of Cornelis Hofstede de Groot. After an impressive career as deputy director of the Royal Picture Gallery the Mauritshuis (1891–1896) and director of the Print Room at the Rijksmuseum (1896–1898) and dozens of prestigious publications, he lived as an independent art historian mostly from the certificates of authenticity that he provided (Ekkart 1979). When the court case had dragged on for one and a half years, he suddenly brought it to a halt, presumably in an attempt to prevent further damage to his reputation. Before the judge could reach a verdict, Hofstede de Groot purchased the contested painting for the full amount of fl. 50.000,-, which made the law suit redundant. He then defended his point of view in his publication *Real or Fake?* In a nutshell, he argued that his expert eye should outweigh the chemical evidence presented in court. It is a position one can hardly imagine taking nowadays, and therefore an interesting benchmark in our study of the development of connoisseurship. For what criteria did Cornelis Hofstede de Groot use to substantiate his attribution? And how did he come to dismiss 'chemistry' so radically?

Although Hofstede de Groot hardly defines criteria for assessing paintings, the way in which he attacks his opponents is revealing. Hofstede de Groot points his arrows mostly at Professor Wilhelm Martin, who is said to base himself too often on his 'feeling for style' (*stijlgevoel*).[7] Interestingly, Hofstede de Groot does not dismiss such a 'feeling for style' as a valid criterium; he just did not think Professor Martin possessed it. To Hofstede de Groot it seems to have been self-evident that an expert had a certain 'feeling' for the characteristic style of a painter, which enabled him to judge attributions better than a layman, an intuitive kind of insight that would normally not require much explanation. Given the circumstances, however, he felt obligated to refute the claims of his adversaries. Therefore, he wrote his argument in the form of a *negatio* (a denial of the contrary), a rebuttal of the expertise that had been used against him in court.

In doing so, he did not shy away from technical evidence. In particular, the discovery of modern nails in the picture and the solubility of the paint layer seem to have worried him. Therefore, he had confronted the painter and restorer who had asked him to assess the painting in 1923: Theo van Wijngaarden (1874–1952), nowadays better known as the mentor and business associate of master forger Han van Meegeren (1889–1947). Van Wijngaarden immediately admitted that he had hammered modern nails into the painting. These would not be situated underneath the paint layer, however; he claimed that he himself had covered their heads with tiny

[7] Hofstede de Groot 1925: 28–29.

retouches. He also provided an explanation for the solubility of the paint layer: he was in the possession of a product –invented by himself but kept a secret– that could render any old master painting in oil soluble in water, which he demonstrated on the spot on another seemingly old painting. Ignorant of the massive swindling for which van Wijngaarden would later become known, Hofstede de Groot did not raise further questions. He mentioned Van Wijngaarden in good faith in his publication and indicated that the restorer was willing to demonstrate his product on any old master painting (Hofstede de Groot 1925: 13).

Having thus 'refuted' the chemical evidence, Hofstede de Groot then proceeded to counter Martin's style analysis. In the expert report, Martin had indicated that he recognized a certain similarity to Hals' oeuvre (notably elements that seemed to have been copied from Hals's famous *Jolly Toper*), but that he did not encounter the distinctive characteristics of Hals' own hand, which he had described in rather broad terms as a 'playfulness of spirit' (*dartelheid van geest*), a 'secure hand' (*zekerheid van voordracht*), a '*virtuoso* manner of painting' (*gave schilderwijze*) and 'a lighthearted mobility in head and body' (*luchtige bewegelijkheid in hoofd en lichaam*) (Hofstede de Groote 1925: 82–83). Several elements in particular deviated from what Martin would have expected of Hals: the stockiness of the shoulder area in relation to the head, the rough indication of the left cheek and neck which did not show the underlying structure, the course definition of the hair roots, the way in which the mouth and teeth were depicted and the light reflection on the lower lip.

According to Hofstede de Groot, however, a 'secure hand' was a rather 'subjective feeling'. Although this remark seems to imply that he believed that Martin's criteria were perhaps not objective or clear enough, he merely objects to Martin's application of the criteria. Hofstede de Groot argues that the disputed picture does in fact show 'a secure hand'. He also believes that 'playfulness of spirit' is a valid criterium, but he claims that it does not apply to all Hals's works. Hals's late regent group portraits, for example, are far from playful in his view, thereby touching indirectly on the ambivalence of the term. For did it allude to a certain playfulness in the subject depicted or rather in handling of the brush? Moreover, in Hofstede de Groot's view, the coarse brushwork was not unusual for Hals, and neither was the stockiness of the shoulder area; he provides no fewer than 20 comparative examples to substantiate his claim(s). Ironically, one of the reference works he uses has the same provenance as the contested *Laughing Cavalier*: it is picture of a boy smoking that Theo van Wijngaarden had also asked him to assess in 1923 and that Hofstede de Groot had like so much that he had purchased it for himself. The similarities were not coincidental: the picture appears to be a forgery by the same hand, presumably by someone from Theo van Wijngaarden's workshop, possibly Han van Meegeren (Kraaijpoel and Van Wijnen 1996: 49; Lopez 2008: 24).

Many of Hofstede de Groot's reference works have been de-attributed since then. He thus did not just lack clear criteria to distinguish between an authentic Hals and an imitation, but also a clear frame of reference. Wilhelm Valentiner's oeuvre catalogue of the artists from 1923 lists 322 paintings as by the master without (much) further explanation (which is about 25% more than today's most positive estimate, see Slive 2014). It brings to mind how broadly Hals's oeuvre was defined at the

beginning of the twentieth century and how much the paintings ascribed to Hals's hand varied in quality.

While this unclear frame of reference gave Hofstede de Groot some leeway for new attributions, the chemical analyses did not leave room for doubt. If the painting had indeed been made with modern materials, it could not possibly be by Hals. Like an alley cat, and perhaps against his better judgment, Hofstede de Groot opted for the frontal attack: the samples taken would not be from the original paint layer but exclusively from later retouches. The Professor in chemistry had not understood what exactly he had been researching. In the introduction he explained that his defense was directed mostly at Professor Martin, not at Prof. F.E.C. Scheffer "for one cannot argue with a chemist about art. In painting the eye has to hold the highest authority, just like the ear does in matters of music. Here not the tuning fork; there not the test tube." (Hofstede de Groot 1925: 5)

The fact that Hofstede de Groot did not bother to have the paint layer that he believed to be original tested by a chemist, gives the impression that he must have at least suspected something was wrong. For the outside world, his booklet did not put an end to speculations about the status of the *Laughing Cavalier*. Shortly after its publication, a rumor spread that the picture was a forgery by Leo Nardus (1868–1955) or Han van Meegeren, a claim that Hofstede de Groot -once again- denied firmly and publicly. In an interview with the newspaper *Het Vaderland* of 10th of June 1926, he exclaimed: "they would wish they could paint like that!" Over the following decades, however, scientific evidence was no longer dismissed so radically by art historians; it became something to be reckoned with.

Two more forgery trials contributed to create a turning point in the history of connoisseurship. Just a few years after the trial about the *Laughing Cavalier* ended abruptly, a larger trial in Berlin in 1932 underscored importance of chemical evidence. The court case concerned 33 paintings in the style of Vincent van Gogh (Fig. 1.3). The dealer Otto Wacker stood on trial for fraud, falsification of documents and breach of contract (Charney 2015: 26–27; Koldehoff 2002). The paintings had been confiscated when the organizers of a commercial exhibition at Paul Cassirer in 1928, Grete de Ring and Walter Feilchenfeldt, had recognized four works as forgeries and grew suspicious of the other works supplied by Wacker. Before the lawsuit several prominent Van Gogh experts had provided certificates of authenticity for Wacker's Van Gogh pictures, including Jacob Baart de la Faille, Julius Meier-Graefe, H.P. Bremmer and Hans Rosenhagen. In anticipation of the court case, however, their opinions started to change. De la Faille published a book in which he dismissed all 33 paintings as forgeries: *Les Faux Van Gogh* (*The Van Gogh Forgeries*, De la Faille 1930).

During the trial, the experts continued to revise their opinions and were ultimately unable to reach a consensus. On the witness stand Baart de la Faille declared that he believed five of the 33 paintings to be genuine after all. Meier-Graefe, on the other hand, believed all works to be forgeries; Rosenhagen thought that fourteen works which he had previously authenticated were inferior works but nevertheless genuine; and H.P. Bremmer believed eight of the pictures were genuine and eight forgeries (Feilchenfeldt 1989: 294–295). Possibly, the fact that these same experts

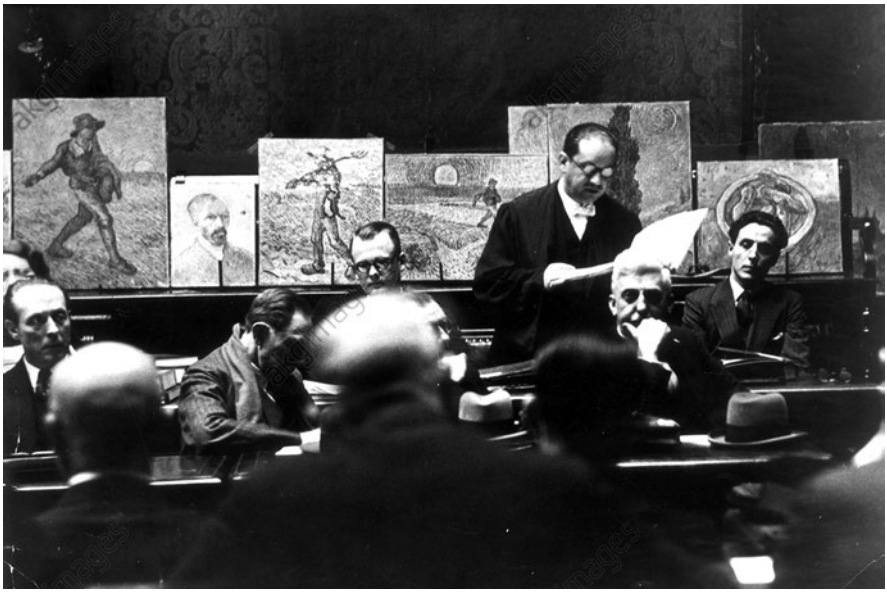

Fig. 1.3 Otto Wacker on trial with the suspected Van Gogh forgeries in the background, 1932

had previously provided certificates of authenticity for (some of) these works may have influenced their judgment. Their behavior resembles a curious phenomenon described by Daniel Kahneman and Amos Tversky as the *sunk cost fallacy*: investors who have already lost money on a project several times are nevertheless likely to re-invest in the project (Kahneman and Tversky 1979).[8] In any case, the court also invited a more independent expert to weigh in on the matter: Professor Ludwig Justi, director of the Nationalgalerie in Berlin, who had just exhibited Van Gogh paintings from the Kröller-Müller collection in the Kronprinzenpalais in December 1928 and used the occasion to compare these with ten of the Wacker Van Gogh pictures, which were hung nearby in his study. His conclusions were straightforward: all the Wacker pictures were "forgeries beyond any doubt"; each lacked the signs of the artist's struggle with his subject and they were, moreover, of varying quality in his view (Feilchenfeldt 1989: 295).

Furthermore, the court also consulted other specialists, including the Dutch chemist and restorer Martin de Wild, who had recently completed a PhD dissertation on the scientific analyses of paintings (De Wild 1928), and the German restorer Kurt Wehlte. De Wild tested the oil paint in the contested pictures and found some unusual components: resin and lead had been mixed in with the oil, presumably to

[8] The *sunk cost fallacy* may also explain Hofstede de Groot's perseverance in the Hals controversy described above. He had invested both his reputation and actual money in his attribution of the *Laughing Cavalier* and the *Boy Smoking*.

make it dry faster.[9] He had never encountered these chemicals in his analyses of securely attributed Van Gogh paintings and the chemical evidence was therefore persuasive. Wehlte made a close comparison of the painting technique based on x-radiographs of a Wacker painting and a reference work, demonstrating how the build-up of the paint layers differed noticeably. Ironically, the reference work he used has been de-attributed in 1970 and even labeled a forgery (De la Faille 1970: 594).[10]

In hindsight, Wehlte's analysis therefore underscores –once again– the necessity of a clear frame of reference. Chemical evidence such as a x-radiographs proved very useful to study the build-up of paintings; however, without sufficient and secure reference data, no valid conclusion could be drawn. Likewise, De Wild's scientific analysis was –to a large extent– a matter of interpretation. He could prove –without a doubt– the presence of resin and lead, but these were not anachronistic materials, as in the case of the Hals forgery.[11] The validity of his conclusion thus hinged on his expert knowledge of reference works (which he had researched in depth for his dissertation). In this respect, his analysis was rather similar to the approach of Ludwig Justi, who compared a large number of genuine Van Gogh paintings with a very secure provenance to ten contested works (see above). Such a side by side comparison of securely attributed works and contested pictures was quite rare at the time (and it still is – due to the limited accessibility of the high value original works); art experts usually had to rely heavily on their visual memory (Wallert and Van de Laar 2011: 70–71). Having secure reference material in sufficient quantity available greatly facilitated the interpretation. Only in this manner could one begin to answer crucial questions such as: How much consistency can one expect in an artist's inventions, style and technique, choice of materials and workshop practice?

Yet there was a sharp contrast between De Wild's observations and Justi's. While De Wild's data was clear and could be checked, Justi's observations remained more implicit. Like Hofstede de Groot and (Wilhem) Martin before him, Justi seems to have relied rather strongly on his intuitive insights, which he did not explain extensively. According to Justi one could recognize a genuine Van Gogh by studying the brushwork; each stroke 'has a very clear significance, because of its size and direction, its surface structure and colour, and also because of its relation to the surrounding brushstrokes'. He did not specify how exactly the brushwork deviated in the

[9] These elements had already been encountered in 1929 during a chemical analysis at the Nationalgalerie (*Die Kunstauktion*, 10 February 1929; *De Telegraaf*; Tromp 2006: 58 note 40). Presumably, the analysis was done by E. Täubner, chemist at the German National Museums, who declared in 1932 that he had researched 5 or 6 paintings at the Nationalgalerie, half of which were genuine and the others forgeries. Tromp 2006: 58.

[10] The work has gone missing during the Second World War, preventing further technical research. It can only be researched on the basis of photographs.

[11] Although de Wild is usually credited with the discovery of resin and lead (Charney 2015: 27), the presence of these elements was published already in 1929, see note 11.

Wacker paintings, stressing merely how 'obvious' it was to the eye. One 'had to be blind *not* to see it'! (Justi 1929; Feilchenfeldt 1989)

It was precisely this absence of rational, communicable arguments that was a thorn in the side of the Dutch restorer Maurits van Dantzig. In 1937 he published a book entitled *Frans Hals: Echt of vals? (Frans Hals: Genuine or Fake?)* in response to the first ever overview exhibition of paintings by Frans Hals in Haarlem (Van Dantzig 1937). In the introduction he sharply criticizes art experts 'who have the habit of answering every question relating to the value of an artwork with the Yes! Or No! of their aesthetic feeling' and their refusal to make the experiences that underpin their aesthetic judgement explicit.[12] In his view clear and verifiable criteria were needed to determine if a painting was an original, copy, imitation, forgery or other type of work. He developed a new method, which he would later call 'pictology' (Van Dantzig 1947; Van Dantzig 1973). On the basis of his own observations of the well-documented and securely attributed core oeuvre of Frans Hals, he made a list of 44 traits that he deemed characteristic of the artist. He subsequently applied the criteria to the 116 works on display and reached a devastating conclusion: only 33 were authentic works by Frans Hals in his view, 5 doubtful, 42 were wrongly attributed and 36 paintings were even forgeries in his opinion.[13]

Van Dantzig's harsh conclusions initially met with a lot of resistance in Dutch art community. Trained as a restorer, Van Dantzig had no formal art historical training and was mocked by academic art historians. Tellingly, the first Professor in Art History in the Netherlands, Wilhem Vogelzang (1875–1954), donated a copy of Van Dantzig's book to the Utrecht University library with the inscription: 'Handed over as an example of shoddy literature'.[14] Indeed, Van Dantzig's conclusions were far reaching and some of the works he dismissed are nowadays seen as undisputed originals, such as *Jasper Schade* (National Gallery, Prague) and *Laughing Boy* (Mauritshuis, The Hague). Nevertheless, his insistence that clear rational arguments were needed, constituted an important step forward in history of connoisseurship. Moreover, his careful observations of the works of Frans Hals, Rembrandt and Van Gogh (for each of which he eventually compiled a list of over 100 visual characteristics) are still of great value to art historians (Van Dantzig 1978; Hendriks and Hughes 2009).

In his lists Van Dantzig made no reference to his intuitive expertise or 'feeling for style' (contrary to predecessors such as Martin and Hofstede de Groot). Instead, he wrote down in great detail what he had observed. He noted, for example, how Frans Hals had a habit of depicting his figures in relaxed, natural poses, with limbs in angular constellations with each other and with the picture plane. "That is not coincidental. […] An angular position breaks through the picture plane and creates a connection with the viewer" (Van Dantzig 1937: 7). He also had a sharp eye for the

[12] Van Dantzig 1937: 2.

[13] Van Dantzig 1937: 3. Van Dantzig indicates in the introduction that he had seen more exhibitions that comprised doubtful works but this particular one exceeded all the others in his view: Van Dantzig 1937: 1.

[14] Storm van Leeuwen 1977: 89, note 3.

peculiarities of the brushwork: how Hals blended his final touches wet-in-wet with both foreground and background; and how he both painted and drew at the same time, indicating colours and shapes simultaneously, for example by depicting the highlight on the nose in the shape of the curvature of the nose. His systematic analysis of the oeuvre of Frans Hals constituted the first step in developing his new method. The central idea is that attributions should be quantified: buttressed by a large number of clearly and explicitly described characteristics, which could be checked and corrected by later scholars (Tummers 2011: 33 ff).[15] Given his emphasis on objective criteria that could be checked, it is interesting that Van Dantzig does not mention the potential of chemical analyses when discussing forgeries. Although chemical evidence had started to play a significant role in court cases, it was far from usual in the regular authentication practice. When one of Van Dantzig's most talented pupils, Storm van Leeuwen, evaluated his master's legacy in 1977 he mentioned this oversight as an important lacuna (Storm van Leeuwen 1977). It explained some of the resistance Van Dantzig had encountered in his view; he had dismissed paintings too quickly as forgeries, ignoring the potential of chemical analyses to confirm his suspicions.

While art experts were thus slow to incorporate chemical analyses in the authentication process, forgers were quick to use the chemical evidence presented in the different court cases to improve their skills (Wallert and Van de Laar 2011). They developed new techniques to make sure their paint layer would not dissolve when tested and they were more careful to select materials that were not anachronistic. Master forger Han van Meegeren, for example, started working with a new binding medium: he mixed fugitive oils with phenol-formaldehyde, also known as 'bakelite'. Using an oven to speed up the drying process, he created a paint layer that was just as hard as a naturally aged oil paint. Moreover, it allowed him to create a convincing pattern of cracks – which constituted another notoriously difficult challenge for forgers. Furthermore, he started to paint forgeries on top of actual seventeenth century canvases and made great efforts to obtain pigments that were consistent with the period (Fig. 1.4). Ironically, one of the most expensive pigments he purchased, natural lapis lazuli or ultramarine blue, later turned out to have been diluted with a cheaper modern blue (cobalt).[16] It was an oversight that amused the later master art forger Eric Hebborn, who had the advantage of knowing the outcome of the Van Meegeren trial in 1945–47 (Hebborn 1991: 121–122).

[15] His method is reminiscent of the method pioneered by his famous Italian predecessor, Giovanni Morelli (1816-1891), who also insisted on closely describing visual clues (although Van Dantzig never mentioned Morelli in his writings, see Storm van Leeuwen 1979). See also above, note 2.

[16] According to his own saying Van Meegeren paid 5000 guilders (current value circa 35.500 euros) for 100 grams of natural lapis lazuli, see Wallert and Van de Laar 2011: 79; see also Wallert and Van de Laar 2018.

Fig. 1.4 Tubes with pigments confiscated in Van Meegeren's workshop in Nice and entered as evidence in the Van Meegeren trial, Rijksmuseum Amsterdam

1.3 The Van Meegeren Scandal: A Turning Point

The Van Meegeren trial constitutes a definitive turning point in the history of connoisseurship. After having created forgeries of old master paintings with tremendous success for over a decade, Van Meegeren was arrested at the end of the Second World War. The charge did not concern the forgeries, however, but a far more serious crime: treason through collaboration with the Germans. He was accused of having sold a crucial part of the Dutch cultural heritage, a painting by Johannes Vermeer, *The Adulteress*, to the German marshall Herman Göring without the necessary export permission. Caught between a rock and a hard place, Van Meegeren decided to reveal his deceit: he defended himself by stating that he had not sold an authentic Vermeer painting but, instead, a forgery by his own hand. Moreover, he claimed authorship of six other paintings in the styles of Pieter de Hooch and Vermeer, including the well-known *Christ and his Disciples at Emmaus* at the Boijmans Museum in Rotterdam. It resulted in a highly unusual court case, in which the forger was keen to prove his guilt, as it would free him of more serious accusations (Fig. 1.5).

Despite an overwhelming amount of evidence, it was hard to accept the deceit for some of the art experts who had authenticated, bought or praised the paintings before. They had invested in the paintings in a material or immaterial way, and

Fig. 1.5 Court case against Han van Meegeren (lower left, on the accused bench) 29 October 1947 (featuring his forgery *Christ and his Disciples at Emmaus* in the background at the right)

therefore seem to have been prone to the so-called *sunk cost fallacy* (see above and Kahneman and Tversky 1979). For example, when the trial had already started Federica Bremmer still included the painting *Christ and his Disciples at Emmaus* in a revised edition of her survey of art history, stating: 'As my personal opinion I would like to state that it is completely unacceptable that this work, which has no equal in the expression of a deep religious emotion, could have been painted by a cowardly cheater […] If this work is indeed old, Vermeer would be the only painter who could have created it. After serious consideration, we have therefore decided to keep the painting in its place for the time being' (Bremer 1945: foreword).

After the trial reached a conclusion, it had become virtually impossible to deny Van Meegeren's claim.[17] Not only had the police found evidence of the forgeries he had created in his workshop in France, Van Meegeren had demonstrated how he

[17] Nevertheless, Dirk Hannema, the director of the Boijmans Museum who had purchased the painting, would continue to believe in its authenticity until his death in 1984, and so did D.G. van Beuningen, owner of one of the Vermeer forgeries (*The Last Supper*). Moreover, the Flemish art dealer Jean Decoen tried to disprove the chemical evidence presented in the court case by Professor Coremans in several publications and Van Beuningen repeatedly threatened to sue Coremans over the matter (Decoen 1951; Van de Brandhof 1979: 9–10). In 1968 Bernard Keisch published new

created his forgeries by making a new one in prison. Moreover, an elaborate expert report confirmed that the pictures could not possibly date from the seventeenth century. It was written by seven prominent paintings experts: Prof. dr. Paul Coremans, head of the Central Laboratory of Belgian Museums, Dr. Wiebo Froentjes, a chemist working for the Dutch Ministry of Justice, Dr. Harold J. Plenderleith, Keeper of the Research Laboratory of the British Museum in London, F. Ian G. Rawlins, Assistant Keeper of the National Gallery in London, Prof. dr. I.Q. van Regteren-Altena, Professor in art history at the University of Amsterdam, Dr. H. Schneider, former director of the National Institute for Art Historical Documentation (RKD) and Dr. Martin de Wild, the chemist and restorer who had also been consulted by the Berlin court during the Wacker trial.

The strongest evidence concerned the new binding medium Han van Meegeren had used. As we have seen, Van Meegeren painted his forgeries on top of authentic seventeenth century canvases and made great efforts to obtain pigments that were consistent with the period. In departure from seventeenth-century practice, however, he employed a modern binding medium, phenol-formaldehyde, which allowed him to imitate the cracked and hardened surface of centuries-old oil paintings. With two different tests involving a sulphuric acid solution and an ammonia solution, which caused yellow and blue discolourations, the chemists were able to demonstrate its presence throughout in the contested works (Huussen 2009: 99; Tummers et al. 2019b: 999). Phenol-formaldehyde had only been invented in 1907; thus, these paintings could not have been created before the twentieth century. [Furthermore, the presence of cobalt blue also pointed to a later date, see above.]

The stylistic analysis of the paintings written for the court emphasized many shortcomings which -according to the experts- did not agree with an attribution to Vermeer, such as the unclear definition of the space and the unhealthy flesh colour of the faces (Schneider 1947). For the purpose of legal proof it was not necessary to delve deeply into the stylistic interpretations. But it was certainly curious that the paintings had been described in radically different ways before and after Van Meegeren's confession, especially *Christ and his Disciples at Emmaus*. Both before and immediately after the trial, art historians described the picture in quite generic terms strongly infused with value judgments (Weerdenburg 1988). Before the trial the painting was said to be 'Vermeer's best work' (Bredius 1937); the composition was said to be well-balanced, the colors exquisite, the still life better than any other from the period, Christ's face was 'filled with secrecy' (Knuttel 1938) and the maid 'perhaps the most beautiful one Vermeer ever painted' (Van Thienen 1939). After the trial, the composition was seen as unbalanced and rather forced, the colors too gray, Christ's face decidedly effeminate (Kilbracken 1967), the maid cross-eye and bald, and her lips too thick (Van Dantzig 1947).[18]

scientific proof confirming the status of both these Van Meegeren paintings as forgeries based on the radioactivity of the lead (Keisch 1968).

[18] In attribution matters it is often striking how differently the quality of paintings is judged when their attribution changes, even when the same expert re- or de-attributes the work. Though this could be done maliciously to massage the evidence in order to convince the reader of one's judg-

The mistaken attribution was perhaps somewhat understandable. Van Meegeren had created such a convincing pattern of cracks that even the restorer who cleaned the painting for the Boijmans Museum failed to notice that the work did not date from the seventeenth century (Van Dantzig 1947: 63). In art-historical terms, the situation was not clear-cut. *Christ and his Disciples at Emmaus* had been recognized as an early work by the art historian who discovered the painting, Abraham Bredius, and in his early period, Vermeer varied his style and technique considerably.[19] Moreover, the reference material Bredius and others were using had been 'polluted' as similar forgeries had already been accepted as authentic (Wallert and Van der Laar 2011).

Nevertheless, the Van Meegeren trial exposed a serious shortcoming in connoisseurship. A large number of experts had clearly been unable to distinguish between an authentic old painting and a forgery. Moreover, they had even celebrated a forgery as one of Vermeer's best works. This painful conclusion not only affected the reputation of connoisseurs in the field of Dutch painting more than any previous error had done, it also heightened the awareness of the difficulties involved in attributing and dating paintings. In the aftermath of the court case, scholars became more cautious when authenticating and dating pictures. Attributions based on the intuition of an expert without much explanation were no longer acceptable. From now on arguments were needed. As Arie Bob de Vries, then director of both the Mauritshuis and the National Institute for Art Historical Documentation (RKD), put it: 'every attribution must be supported by evidence, insofar as one can provide proof in the thorny field of such conclusions' (De Vries 1939 [ed. 1948]: 71). De Vries, who had published a Vermeer oeuvre catalogue just before the start of the Second World War in 1939, revised his book considerably in 1948, bringing down the number of paintings he categorized as authentic Vermeers from 43 to 35 – a selection that has hardly been debated or altered since then (Tummers 2011: 27–29).

1.4 Excessive Optimism: The Potential and Limitations of Scientific Techniques

After the Van Meegeren scandal, art historians did not only specify in much greater detail what visual observations, archival and documentary evidence led to their attributions, but also gradually started to expand their visual analysis by systematically integrating scientific techniques. In Belgium, a National Centre for Research of the Flemish Primitives was established in 1949, which resulted in the publication

ment or save one's reputation, it could also be the effect of (altered) subconscious associations and expectations, which can truly make us look differently. It would be a fascinating subject for further research.

[19] Compare Johannes Vermeer, *Christ in the House of Martha and Mary*, c. 1655, National Gallery of Scotland, Edinburgh; Johannes Vermeer, *Diana and her Companions*, c. 1655-56, Royal Picture Gallery Mauritshuis, The Hague.

of numerous technical studies, including Prof. Coremans' technical analysis of Jan and Hubert van Eyck's famous *Ghent Altarpiece* in 1953 (Coremans 1953). Although early technical studies concentrated mostly on x-radiography and pigment analyses of paint samples, these were soon expanded with new techniques (Ainsworth 2005). Van Asperen de Boer, a physicist in the art history department at the University of Groningen in the Netherlands, was the first to develop infrared reflectography (IRR) for the study of paintings, a technique which proved particularly useful for examining early Netherlandish pictures as it exposed detailed underdrawings in these works (Van Asperen de Boer 1969).

In the field of seventeenth century paintings, the Rembrandt Research Project, founded in 1968, constituted a major step forward. At the initiative of Bob Haak, curator of old masters at the Amsterdam Historical Museum, a team of five leading Rembrandt experts set out to redefine Rembrandt's entire painted oeuvre: Josua Bruijn, Professor of art history at the University of Amsterdam, Haak himself, Simon Levie, the director of the Amsterdam Historical Museum, Pieter van Thiel, curator of old master paintings at the Rijksmuseum and Ernst van de Wetering, staff member of the Central Research Laboratory of Objects of Art and Science. At the start of the project, many connoisseurs were doubtful about the validity of existing attributions to Rembrandt. For example, Horst Gerson, professor of art history at Groningen University, noted in the introduction to his 1968 monograph on Rembrandt that he largely agreed with what British collectors tended to say about Dutch old masters, namely that 'nearly half of the old masters are wrongly attributed and the others are not old at all' (Gerson 1968: 160). He also pointed out that no Rembrandt scholar had ever even seen all possibly authentic Rembrandt paintings in real life (Tummers 2011: 40).

The members of the Rembrandt Research Project were the first to do so. In pairs of two they traveled the world, observed over 600 potential Rembrandt paintings in real life, described these in painstaking detail, and decided on the attributions as a group. Moreover, they tested a variety of scientific techniques systematically as to their merit in sorting out Rembrandt's oeuvre. Whereas previous generations of art historians had been hesitant and sometimes even skeptical about incorporating chemical research, the members of the Rembrandt Research Project signaled rather an excessive optimism: a relatively widespread belief that science held the answers and could potentially replace the eye in matters of attribution (Bruyn et al. 1982–, vol. I: XIIIff). However, their systematic application of technical research methods proved otherwise.

Dendrochronology proved useful in dating the oak panels Rembrandt used for his early paintings. By determining the approximate year in which the tree used to make the panel was felled, the technique provides a 'terminus post quem' that is, dates after which the painting had to have been made. Tests executed by Peter Klein and his team at the Ordinariat für Holzbiologie at the University of Hamburg provided surprising results when applied to paintings that the Rembrandt Research Project had originally considered later imitations (Bruyn et al. 1982–, vol. I: XII). Most of these turned out to be done on authentic seventeenth-century panels, which

in combination with other observations eventually led to the conclusion that the works *did* date from Rembrandt's time.

X-radiographs proved to be valuable in reconstructing Rembrandt's working process in terms of how he laid out his compositions and the order in which he executed various parts of a painting. X-ray images show especially lead-containing pigments very clearly, and since canvases were usually primed with a lead-containing coating, X-radiographs also allowed the group to study the structure and density of the original canvases on which the paintings were created (Van de Wetering 1986). This was important information that could not be acquired with the naked eye, since the canvas of most seventeenth-century paintings has since been covered by a second, more recent canvas. The Rembrandt Research Project's study of these canvases led to several striking conclusions, especially when the works had been cut down, or when the same flaw was found in the weaving of more than one painting, showing that they had been painted on canvas from the same bolt. Findings of that kind made it seem likely that the canvases had been bought in one batch and had all been used in Rembrandt's studio.

Ultraviolet radiation and photographs and infrared reflectographs proved less informative. The former can be helpful in identifying later retouches, though its use depends largely on the condition of the varnish, making it a rather inconsistent source of information. Infrared reflectography, which is mostly used to study carbon-containing underdrawings, did not yield a large amount of information, as no underlying drawing in an absorbent material was discovered in Rembrandt paintings. For this reason, the Rembrandt Research Project decided against investing in this technique.[20]

Neutron activation autoradiography yielded insights about the master's working method, but was too costly to be used on a large scale. Most significant in this respect was the investigation by the Metropolitan Museum of Art in New York in the early 1980s, the results of which were also studied by the Rembrandt project (Ainsworth et al. 1982). By making several paintings temporarily radioactive and subsequently recording the radiation of the various pigments in a number of photographic plates, a clear picture emerged of the areas in which the different pigments had been used. This gave scholars information on paint layers below the surface that could barely, if at all, be detected with other techniques.

Lastly, samples of the paint and ground layers gave mixed results. Rembrandt's pigments were found not to differ much from those of pupils and contemporaries, or even from those used by his followers. Analyses of paint samples were therefore hardly of any use when trying to identify the master's hand. Only in the rare instances when a pigment was found to have gone in or out of use at a certain moment did a paint sample give an indication as to when a painting was made. For example, the presence of lead-tin yellow made it likely that a painting was made

[20] Further research might still yield some interesting insights, as some information about the various paint layers can also be seen in infrared reflectographs and increasingly refined cameras make it possible to recognize thin underdrawings which earlier models cannot distinguish.

before 1750, as the pigment fell out of use at that point.[21] As to the ground layer, only one component was found to be significant for authentication purposes: after decades of study, the chemist Karin Groen discovered that the grounds in paintings by Rembrandt and his studio contain quartz from 1642 onwards, an element she had not encountered in other grounds from the period (Groen 2005). Presumably, Rembrandt trained his studio to prepare his own grounds when he was working on the *Nightwatch* and his studio continued to do so afterwards.

Gradually it became evident that technical examination seldom provided absolute certainty concerning attributions. While a technical or chemical analysis *can prove* that a work is *not authentic* by demonstrating, for example, that the materials used are anachronistic, a positive attribution cannot be done without a visual analysis. For if the materials are consistent with the period, one still needs to analyze the particular 'handwriting' of the artist in order to determine if the attribution is correct, to differentiate between different types of workshop products, contemporary copies and imitations. In practice, the researchers identified only one potential forgery among the more than 600 paintings they studied (Bruyn et al. 1982: XX, C12); the evidence was rarely conclusive.

Furthermore, regarding their methodology, the Rembrandt Research Project concluded: 'It is a mistake to think that even the most meticulous argument for or against the authenticity of a painting covers the whole of the visual experience that led to that opinion' (Bruyn et al. 1982–, vol. 1: XV).[22] Although the team members had made great efforts to make their arguments explicit, they did not think it covered all of their implicit knowledge (in other words, they had used both Kahneman's systems 1 and 2, see above). Nevertheless, their elaborate, systematic approach contributed significantly to refining the attribution process. Their lengthy and very detailed descriptions made it possible to analyze and check attributions, their underlying assumptions and possible biases to a much greater extent than had been possible before.

In the late twentieth century, technical art research came into its own as a significant new area of study that came to be known as 'technical art history'. The term was coined in the 1990s by David Bomford, senior paintings conservator at The National Gallery in London, who also called technical art history 'new school connoisseurship'. Bomford himself contributed significantly to the field, especially through the *Art in the Making* series, which he wrote together with conservation scientist Ashok Roy and curator Christopher Brown. This type of research was done mostly in a museum context as a collaboration between conservators, conservation scientists and curators, and commonly focused on a few related works of art rather than on sorting out an entire oeuvre. An excellent early example is the technical study of Rembrandt paintings at the Mauritshuis in The Hague which appeared a few years before the first *Corpus* volume was published (De Vries et al. 1978).

[21] When Van Meegeren created his forgeries, lead-tin yellow had not been discovered yet, so this finding was also useful for the identification of forgeries, see Wallert and Van der Laar 2011: 90 ff.

[22] On the changes in the project and its methodology throughout the years, see Tummers 2011: 39–50. See also Van de Wetering et al. 2005: XIII.

Bomford described the goal of this 'new school connoisseurship' as the study of all the processes for making art and the technical and documentary means which throw light on those processes. It is principally concerned with the physical material and structures of works of art but also charts the stages of invention, development, elaboration and revision (Bomford 2008). Like the members of the Rembrandt Research Project, Bomford was well aware of the limitations of the technical research for authentication purposes, and stated that 'new school connoisseurship is old school connoisseurship with technology'.[23]

The usefulness of the various techniques varied somewhat from one master to the next. For example, Vermeer seemed more distinct in his use of specific pigments, particularly in the use of the expensive lapis lazuli mixed in with other pigments to create background colours (Sheldon and Costaras 2006); and infrared reflectograms of works by one Rembrandt's most talented pupils, Carel Fabritius, gave some spectacular results in that these revealed the artist's signature in several darkened backgrounds (Duparc 2006). Nevertheless, many of the key questions for authenticating works of art remained the same, notably the question how much consistency one could expect in the masters technique, choice of materials and workshop practice. Only in the case of anachronistic materials, chemistry and other scientific analyses could provide conclusive evidence and expose forgeries or misattributions. In all other cases, the authentication or attribution process remained a matter of interpretation; it rather resembled detective work, combining circumstantial evidence and probabilities.

1.5 Paradigm Change and Myriad New Techniques

In the late twentieth and early twenty-first century an important paradigm change took place in the humanities that has far reaching consequences for the art authentication, especially in the field of old master paintings. Since the 1980s, there had been a growing concern that the twentieth-century practice of classifying old master paintings may be at odds with early modern categories of thought. Ernst van de Wetering, the leader of the Rembrandt Research Project (RRP), raised the issue most poignantly in 1992, when he gave a lecture entitled 'The Search for the Master's hand: An Anachronism?' at the 28th International Art History Congress in Berlin (Van de Wetering 1992). He wondered if the core mission of the RRP, namely to distinguish between the master's own hand and those of pupils, assistants and imitators, agreed with seventeenth-century workshop practice. Would early modern viewers have expected a 'Rembrandt' to be purely autograph? It was indeed a crucial issue, with serious implications for attribution issues. For how could one recognize the master's hand by studying the brushwork in a variety of details, if that

[23] Lecture 2013 at Bard Graduate Center in New York, 10 September 2013; cited in Chapman and Weststeijn 2019: 17.

brushwork was not necessarily executed by the master himself but possibly by a pupil or assistant?

According to Van de Wetering, not enough research was done to draw any conclusions with certainty. Nevertheless, several authors believed that early modern painters, such as Rembrandt, consciously produced paintings that give the effect of individuality without necessarily painting the pictures entirely by themselves (Alpers 1990; Kirby-Talley 1989; Grimm 1993). The debate highlighted the need for contextual knowledge.

In the early twenty-first century several larger studies yielded insights into early modern views on quality and authenticity, while raising awareness of various types of workshop collaborations (Tummers 2011; Guichard 2014). Gradually it became clear that old masters often had more than one style and working method (Gifford and Glinsman 2017). Their style and technique could vary considerably depending on the price of the painting, its subject, function and location. Furthermore, ingenious masters sometimes deliberately varied their styles to showcase their virtuosity, including notably Goltzius and Rembrandt (Van Mander 1604, fol. 284v; Melion 1990; Leeflang and Luijten (eds.) 2003: 210–215; Van de Wetering et al. 2005: 166). Moreover, there were many different types of workshop products and quality levels. What exactly a master painter deemed of high enough quality to carry his/her name, varied from one painter to the next, and could also vary over the course of an artist's career. Rubens, for example, distinguished between five different types of paintings produced in his workshop and prices these according to their quality, witness a letter by him dated 28 April 1618 (Rosenberg (ed.) 1888: 42 ff). Occasionally, master painters even sold pictures that were entirely by workshop assistants as their own. If the quality level was sufficient, the master painter had the right to do so according to guild regulations. Interestingly, some masters even used different signatures to indicate different quality levels – a practice that was long forgotten but must have been quite common in early modern times (Tummers 2011: 79–111, esp. 94–97).

In short, the very notion of what constituted 'authenticity' was redefined. As result, authentication decisions became more complex. In order to judge the authenticity and quality of a painting, one had to know what these terms meant at the time in which the painting was made and familiarize oneself with the then current categories of thought as well as with the specific master's workshop practice. An authentic Rembrandt could not be simply judged with the same criteria as an authentic Van Gogh (which one can reasonably expect to be autograph). A detailed understanding of the context in which a picture was created, provides insight as to what to look for and what not to look for. For example, seventeenth century experts had a rather hierarchical way of looking; they made a clear distinction between key elements and so-called 'bywork' and had developed nuanced terms for identifying mastery – which are useful when assessing paintings from this period. When judging pictures from this period, a simple binary perspective (either by the master or not) did no longer suffice.

While the framework for thinking about issue of authenticity within the humanities thus became increasingly nuanced, the technical means and chemical methods to research paintings developed at an unprecedented pace. As we have seen, early

twentieth century connoisseurs relied heavily on their visual memory when authenticating paintings (see Sect. 1.2). Since then, photographic material has become much more readily available, and its quality and resolution have improved dramatically, especially in the last decades. Moreover, numerous new analytical techniques were developed for the study of paintings. Especially macro x-ray-fluorescence scanning (MA-XRF) and hyperspectral imaging (HSI, also called reflectance image spectroscopy or RIS) are currently revolutionizing the field.

Macro x-ray-fluorescence scanning (MA-XRF) is a relatively new technique that allows for the visualisation of the distribution of elements in a flat sample, such as an easel painting, in a non-destructive manner. This is achieved by scanning the surface of the sample with a focused X-ray beam, and analysing the emitted fluorescence radiation. As the X-ray beam scans the whole painting, it produces thousands, sometimes millions, of data points. These can be plotted on elemental distribution maps, which may be interpreted as pigment distribution images (Alfeld et al. 2011, 2013). The technique is much more precise than x-radiography as it is able to distinguish between different chemical elements and therefore allows for a much more precise understanding of a painter's working process and the build-up of his pictures.

Hyperspectral imaging (HSI/RIS) is a technique that combines two-dimensional visualisation of the painting by optical imaging (such as photography) with optical spectroscopy. It is done in such a way that each pixel of the image is made to represent a complete spectrum of that pixel. Whereas a regular camera records three different wavelengths of the electromagnetic spectrum (corresponding to the colours red, blue and green), modern hyperspectral cameras can easily differentiate between hundreds of wavelengths, resulting in very precise digital images or 'data cubes' (see the article by John Delaney in this book). It is particularly useful for identifying the distribution of specific paint mixtures throughout a painting, although it can also be used to identify specific chemical elements.

Both MA-XRF and HSI proved useful to enhance our understanding of Frans Hals' hallmark techniques and materials, to give just one example (Tummers et al. 2019a). Furthermore, the insight MA-XRF provided in Hals' painting technique was also helpful for the identification of a potential forgery in style of Hals, rumored to be by Han van Meegeren (Tummers et al. 2019b). In the latter case, the son of the master forger had claimed that the painting was forgery by his father, but could be proven wrong with modern analytical techniques. Initially, GC-MS (a method of separating and identifying complex mixtures of organic molecules) seemed to prove that the binding medium did not contain phenol-formaldehyde, but when the same test also gave a negative result for a well-documented (and phenol-formaldehyde containing) Van Meegeren forgery in the style of Frans Hals, the test could not be seen as conclusive. A lead isotope analysis by Gareth Davies and Paolo d'Imporzano of the Geochemical Laboratory for Ultra-Low Isotopic Analyses in Amsterdam *did* provide solid evidence in combination with secure reference data gathered in the context of the NWO project *Frans Hals/not Frans Hals project* (2016–2018). The analyses indicated that the lead ores in the lead white used by Van Meegeren came from a completely different location than Hals's lead white (on this technique, see also the essay by Davies and d'Imporzano's in this book). The lead isotopes ratios

in the contested painting were consistent with those found in Hals paintings, not at all with those found in a Van Meegeren forgery: the painting could not possibly be by Van Meegeren. Subsequently, an in-depth analysis of the style, build-up and painting materials (using observations done with the naked eye, a dino-lite microscope, MA-XRF scans and an occasional paint sample) strengthened the attribution to Hals and his workshop, including Hals's distinctive use of indigo blue (identified with Raman spectroscopy).

In short, in this particular case, documentary evidence turned out to be unreliable and a modern analytical technique provided a false negative. Nevertheless, the range of possibilities in the attribution issue was greatly reduced with the aid of modern analytical techniques. Especially when combined with a visual analysis, in-depth technical research has great potential for art authentication.

Although technical art history has expanded enormously, especially in pioneering museum studies, in practice surprisingly little technical research is used for most attributions. In prominent oeuvre catalogues and scholarly attributions, it is often not used at all (Dumas et al. 2020). On the market, well-known auction houses use technical research only rarely to strengthen attributions (eg. Ginzburgh et al. 2019) – although its use is increasing since auction house Sotheby's founded a scientific department in 2016.[24] By far most well-known masters' oeuvres have not been researched yet with (all) the newest techniques and therefore the chances of discovering significant discrepancies between original paintings and forgeries and misattributions are currently high. Obviously, forgers and imitators from a different period cannot have mimicked specific materials and techniques, if these materials and techniques were not known to them.

In some instances, research into a specific artist's oeuvre with the newest techniques makes the creation of new forgeries virtually impossible. A good example is the project *REVIGO: Reassessing Vincent van Gogh* (2013–2017), a collaboration between researchers from the Van Gogh Museum, Tilburg University, Delft University of Technology, the Cultural Heritage Agency of the Netherlands and the Rochester Institute for Technology in New York, funded by the Dutch Science Foundation (NWO).[25] Because of the natural ageing and discoloration of Van Gogh drawings, recent forgeries are bound to fall short: either the ink contains the right pigment(s) and has the wrong colour or the ink has the right colour but not the right pigments. In most other cases, however, the situation is not so clear-cut, and additional research, reference data and analytical tools are urgently needed.

[24] Ironically, while serious in-depth technical studies for attributions are relatively rare, highly dubious paintings are often accompanied by questionable 'scientific' reports, as every active curator in the field knows. These reports are commonly presented as 'proof' for a concrete attribution on the basis of a logical fallacy: no anachronistic elements were discovered in the painting therefore it must be by the artist.

[25] https://www.vangoghmuseum.nl/en/about/knowledge-and-research/completed-research-projects/revigo

1.6 The Digitally Enhanced Eye: Connoisseurship and Smart Tools

While only a small fraction of the paintings of well-known masters have been subject to in-depth technical research, the data gathered is nevertheless substantial and increasingly rapidly. Especially the data collected with advanced photography and scanning methods such as MA-XRF and HSI/RIS is considerable. We have entered a digital age that comes with entirely new challenges and potential. How to manage and properly interpret vast amounts of data? In what way and to what extent can digital techniques facilitate art authentication?

In the early twenty-first century, various computer scientists have been developing computer programs with the intention of facilitating the attribution process, focusing in particular on brushstroke analysis. For example, at the end of 2004, a team from Dartmouth College in Hannover, New Hampshire, developed a method to analyze pen lines and brushstrokes, based on an algorithm that proved useful in court for the identification of manipulated photographs (Lyu et al. 2005/06). With the aid of so-called 'wavelets', Siwei Lyu, Daniel Rockmore and Hany Farid were able to isolate pen- and brushstrokes and analyze their direction, scale and relation to surrounding strokes. They assumed that every artist had a unique way of applying ink and paint to the surface, which results in a kind of virtual signature that can be analyzed by a computer without analyzing the subject matter. Since subject matter is however likely to affect the variability of the strokes, they only compared works with similar subjects.

The program they developed successfully confirmed existing attributions in a training set, and so did several other programs (Johnson et al. 2008; Hendriks and Hughes 2009; Li et al. 2012; Van Noord et al. 2015). However, thus far such programs have not been used to make new attributions or to confirm or exclude attributions in court – which is related to the complexity of such decisions. Complicating factors include, among other things, the condition of the painting studied (for example, old master paintings virtually always include restorations and later retouches which 'muddy' the data). Also, as we have seen, artists sometimes deliberately varied their styles and techniques, and/or used assistants in the execution of their works, which further complicates the analysis. In short, computer programs that can make decisions in the connoisseur's place remain -thus far- elusive. As of yet, it is unclear if these can be realized in the near future; the need for contextual knowledge may prove too formidable a hurdle.

However, digital techniques have shown great potential in facilitating in-depth comparisons. Based on Erdmann's work in this area over the past ten years and the ongoing NICAS project *21st Century Connoisseurship* we will discuss some of our main conclusions regarding the merits, challenges and potential of a number of digital techniques aimed to facilitate comparison below. These pioneering tools are currently mostly in use at the Rijksmuseum; the aim, however, is to open these up for wider use in the future.

Given the situation in which we now find ourselves, with an overabundance of data coming from a variety of sources, with an emphasis on imaging data, there is a strong need to process the data in a way that promotes honest comparisons. These comparisons rely heavily on accuracy and consistency since fundamentally, we must ensure that when the viewer sees differences between images artworks it is because they are in fact different, and not due to differences arising in the capture or subsequent processing of the imaging data. Furthermore, given the importance of materiality for judging both the condition and the attribution of paintings, imaging should strive to capture as much of the materiality of the artworks as practically possible. The following principles, while not comprehensive, serve as prescriptive guidelines for enhancing the utility of digital tools for authentication purposes:

- *Consistent high-resolution imaging*: Modern digital cameras and lens systems are capable of capturing images with extremely high spatial sampling resolutions, so that even small artworks can be captured with many overlapping tiles of high-resolution photographs. The value of such photographs is immense since they reveal microstructural details that are hidden at normal resolutions: paint pigment particles, cracks, retouches, areas of abrasion, nuances of brushstrokes or pen lines, subtle or small-scale pentimenti (corrections) and other details of artistic technique, details of the support, and many other aspects of the materiality of the artwork. In the absence of an ability to physically inspect all relevant artworks side-by-side, consistent sharp, and well-lighted digital photos are the best available option.
- *Consistent color management and processing*: Images collected by different photographers, with different light sources, or at different institutions will invariably display differences due to imaging technique. To the degree possible, these differences in equipment and technique should be minimized. Even so, differences will remain, but these variations can be minimized by performing careful color management during the processing of the raw photos. The variations in lighting and wavelength-dependent pixel sensitivity are minimized by always photographing a colorimetric standard (e.g., an XRite ColorChecker SG color card) as part of a standard workflow, so that a color profile can be made which will adjust the as-captured colors to their correct values. Imaging guidelines such as the Metamorphoze Guidelines[26] or the FADGI Guidelines[27] have proven useful in defining best practices and criteria for acceptable image quality.
- *Careful state-of-the art processing:* The use of high-resolution imaging generally leads to a collection of images spanning the artwork, and the use of additional technical imaging techniques such as radiography, infrared reflectography, or reflectance imaging spectroscopy further leads to multiple images describing any given point on the object. Among the desirable features of such a system are

[26] https://www.metamorfoze.nl/sites/default/files/publicatie_documenten/Metamorfoze_Preservation_Imaging_Guidelines_1.0.pdf, accessed 2021-03-04

[27] http://www.digitizationguidelines.gov/guidelines/FADGI%20Federal%20%20Agencies%20Digital%20Guidelines%20Initiative-2016%20Final_rev1.pdf, accessed 2021-03-04.

the following: (a) it should respect the details of human color perception since naive averaging of RGB pixel values does not result in perceptually averaged colors; (b) it should avoid any tears or duplications when assembling the component tiles in a single whole-artwork image; (c) it should use high-order interpolation kernels to avoid introducing blurring or ringing artifacts when performing the inevitable resampling of the images during the stitching; and (d) it should ensure subpixel precision when performing registration among the different imaging modalities, so that data from one imaging modality is fused with the data from another modality at the same physical location on the artwork. Erdmann (2016a, b) developed such a system as part of a comprehensive campaign of imaging and study of the oeuvre of Hieronymus Bosch, and this system is now in permanent use at the Rijksmuseum.

1.6.1 The Curtain Viewer

Meaningful comparisons between artworks or between different areas of an artwork are essential to the connoisseur's judgement. Even with a collection of consistent color-managed high-resolution images, traditional image-editing tools such as Photoshop are ill-suited to making frictionless comparisons among many works or among different imaging modalities of a single work. The problem is exacerbated when the images themselves are very large; 20 μm/pixel resolution (1270 ppi) 16-bit color imaging consumes 15 GB/m^2, so large-format paintings such as Hals' militia company portraits or Rembrandt's Nightwatch consume hundreds of gigabytes each. Side-by-side comparisons of such artworks may then be practically impossible using standard image-editing software due to memory limitations. Furthermore, such an approach makes it very difficult to save a comparison for later review, and collaborative inspections are impractical.

In response to these difficulties, in 2012 Erdmann developed an internet-based viewer for very high-resolution images with an explicit design goal of enabling frictionless comparisons between images. As with other web-based image viewers, the viewer, which he named the Curtain Viewer, utilizes image pyramids so that a cascade of image resolutions is pre-computed and stored on the server as small tiles to enable immediate on-demand zooming and panning without the need to pre-load large images.

The Curtain Viewer enables comparisons using a variety of modes, several of which are shown in Fig. 1.6: A "gallery mode" allows the user to juxtapose an unlimited number of viewing panes, each of which is unconstrained. Constraints can be placed among the panes in a "sync mode", so that they zoom or pan the same way simultaneously. The way an artist depicts a detail is strongly dependent on the scale of the depiction, so this feature enables a user to zoom in to a pair of details in different artworks while ensuring that each is presented at the correct scale, and by synchronizing their scales they can zoom out to compare their contexts or zoom in to compare their details without fear of being deceived by scale differences.

Fig. 1.6 The Curtain Viewer utilized in several of its viewing modes. (**a**) Hals' *Malle Babbe* (Gemäldegalerie) and Van Meegeren's forged version (Rijksmuseum); (**b**) a study of several similar figures appearing in the oeuvre of Bosch; (**c**) precisely co-registered high-resolution visible photograph, transmitted-light photograph, and raking light photographs from the left and above of Rembrandt's drawing *Young Woman Sitting by a Window (Saskia?)* (Rijksmuseum); (**d**) fading-mode fusion of 8 raking light images of Van Gogh's *Sunflowers* (F453, Van Gogh Museum) showing the texture of the artist's brush strokes around his signature; (**e**) curtain mode view of Bosch's John the Baptist in the Wilderness, using visible-light photography, infrared reflectography, radiography, and infrared photography, revealing a hidden figure behind the fruit and the underdrawing for John the Baptist

Fig. 1.6 (continued)

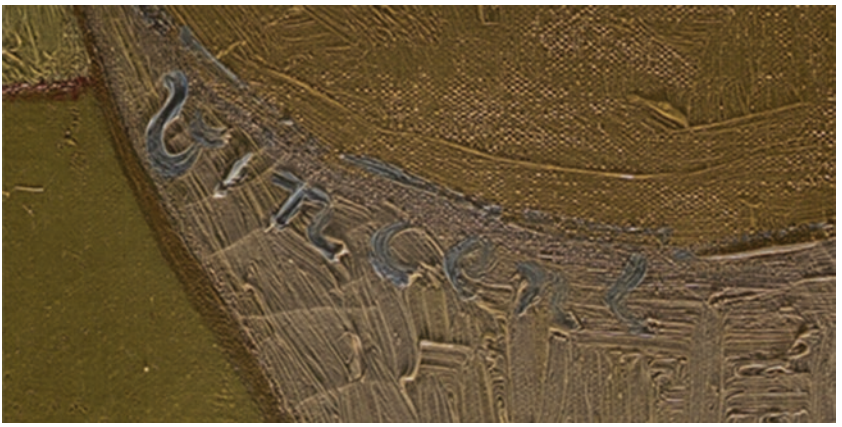

Fig. 1.6 (continued)

Fig. 1.6 (continued)

The sync mode is also useful in comparing different image modalities, since it is often difficult, for example, to associate a feature in a radiograph with the same feature in a visible-light photograph.

A "fade mode" enables an overlay of two or more panes, with relative opacities computed based on the position of the mouse. The fade mode has been used to create hybrid images such as those mixing visible-light and infrared photos, and has also been used to simulate a moving light source attached to the mouse by fading among a collection of raking-light images collected with the light source at different positions.

The Curtain Viewer is named after the "curtain mode", in which a single pane is split into multiple regions at the location of the mouse cursor, with a different imaging modality or artwork shown in each region. The movement of the mouse pointer thus gives an impression of "pulling back the curtain" or of "lifting the curtains" as it reveals additional imaging modalities. The system is designed to enable the user to focus carefully on an area of interest on the artwork and to repeatedly brush over it to show the exact relation among the features revealed by different imaging modalities. A traditional side-by-side view has been used to make these kinds of comparisons, but it induces a kind of "visual context switching" in which the user is forced to change focus from one location to another, diminishing the effectiveness of the comparison due to our limited visual memory. In contrast, the "curtain mode" enables the user to remain fixed on the same location in an artwork while comparing the different modalities.

The avoidance of visual context switching is another one of the major design goals of the Curtain Viewer system. Unlike other image viewers, its interface is not cluttered with visually distracting overlays such as logos, viewer control buttons, magnification sliders, and the like. The user is thus able to focus exclusively on studying the art without the visual noise of user interface elements. Furthermore, switching between modes is always done in a smooth way, with image panes animating their positions and opacities gradually to promote object constancy; the user is never forced to break their focus to reestablish their bearings in a new viewing configuration.

The Curtain Viewer also features a system where every aspect of the view is encoded in the URL, enabling easy bookmarking of an exact configuration for later study or for sharing and collaboration. As a demonstration of the technology, every figure from the Bosch Catalogue Raisonné (Ilsink et al. 2016), is also presented online (Erdmann et al. 2016) using the Curtain Viewer, enabling readers to understand the exact context and details of every featured detail.

As the book figures show, the Curtain Viewer's URL scheme allows for the design of displays that rely heavily on what Tufte (1990) calls "small multiples":

> At the heart of quantitative reasoning is a single question: Compared to what? Small multiple designs, multivariate and data bountiful, answer directly by visually enforcing comparisons of changes, of the differences among objects, of the scope of alternatives. For a wide range of problems in data presentation, small multiples are the best design solution.

These small multiple visualizations are crucial for connoisseurship since they ease and promote the fundamental act of comparison across scales, imaging modalities, and artworks.

1.6.2 Morelli's Vision

Facilitating fast and meaningful comparisons among small details from one or more artworks is the design goal of Erdmann's "Morelli's Vision" technique. It was named in honor of Giovanni Morelli, an art historian who advocated for the careful study of small habitually-painted details to discern the characteristic "handwriting" of an artist (see also note 2 and 15). It is driven by a system of user- or computer-generated rectangular selections on artworks which are given a semantic tag such as "ear" or "hand". The display is web-based and interactive: when a user clicks on a particular tag, the individual thumbnail images are dynamically sorted according to the pairwise similarity between the clicked image and all other images, placing the clicked tag first in the list with all the others sorted in decreasing order of their similarity to the clicked one. The pairwise similarity is computed as a cosine similarity between image features that are computed by a convolutional neural network. The system can be tuned to give different weights to semantic content, palette, texture, and other elements of style by giving different emphasis to the intermediate layers of the network.

The consequence for the connoisseur is that they can see as many comparisons in a single field of view as possible. Every detail can be easily compared with every other detail. The system also allows the selection of a subset of interesting details (shown in the figure outlined in blue) and to instantly launch a Curtain Viewer in "sync mode" to show the selected details side by side, zoomable and in high resolution. As an example of its use, consider its application to investigating attribution for paintings putatively by Bosch by studying the rendering of hands (Fig. 1.7). The user has selected a set of distinctive hands for further study, which they then use to launch a custom Curtain Viewer that enables studying the details in context. Zooming out completely from each detail reveals that they are actually all from the same painting, lending additional evidence to an argument that the picture was not painted by Bosch.

1.6.3 Draper

The Curtain Viewer affords great freedom to configure complex views involving multiple artworks, multiple imaging modalities, and a variety of viewer modes in terms of synchronization and display, all of which is captured in a human-readable URL. However, this flexibility comes at the price of complexity. The solution is an additional tool to help precisely configure a desired Curtain Viewer display, dubbed

Fig. 1.7 (**a**) The "Morelli's Vision" technique applied to a collection of painted hands from Bosch and followers of Bosch. The user has selected thumbnails of interest after using the system's dynamic sorting ability to group similar thumbnails. (**b**) a custom synchronized Curtain Viewer created automatically from the thumbnails. (**c**) zooming out of the details reveals that they all come from the same painting last images not sharp!

Fig. 1.7 (continued)

as the "Draper" (one who makes curtains) by the author (RE). The tool consults a database of technical images for a specified artwork and finds those which are co-registered with each other, presenting the user with a menu of different technical images. The resulting images can be arranged into a desired configuration via a drag-and-drop interface, and additional Curtain Viewer options can be specified. A live viewer preview at the bottom allows immediate exploration and tweaking of the viewer parameters (Fig. 1.8).

The consequence for the connoisseur is that it becomes basically frictionless to quickly answer complex questions about image collections that can easily occupy several terabytes on disk. For example, did Hals consistently use the rather costly red pigment vermillion for all the faces and hands of the 88 militia men he portrayed in his five prestigious large-scale militia group portraits? It also dramatically eases the process of documenting a judgement with supporting evidence.

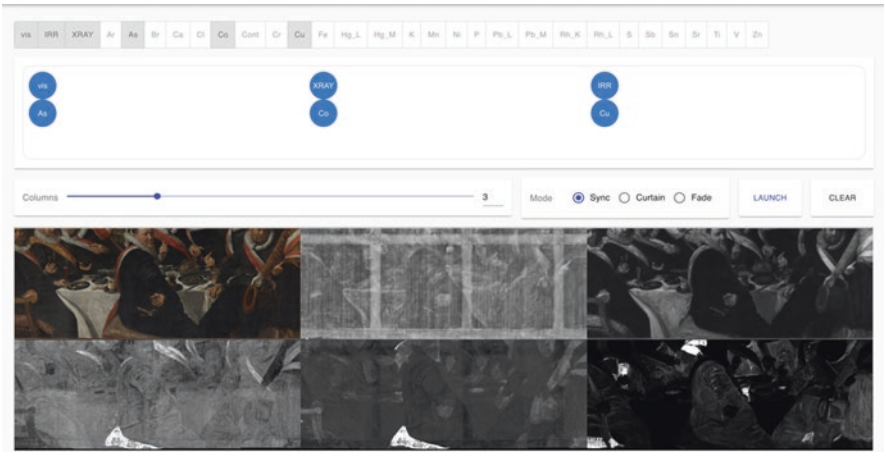

Fig. 1.8 The Draper applied to a Frans Hals militia company portrait as part of the NWO-funded *21st Century Connoisseurship* project. Precisely co-registered images from a visible-light photograph, a radiograph, an infrared reflectogram, and the arsenic, cobalt, and copper lines from MA-XRF scans are arranged into a desired configuration and Curtain Viewer viewing modality and previewed live in the bottom pane

1.6.4 PixelSwarm

The PixelSwarm tool is an online interactive tool to allow the user to draw insights from high-dimensional data arising from multimodal imaging of artworks. A visible-light photograph associates five numbers with each pixel: the three components of the color (RGB, e.g.), and two coordinates of its location in the painting. In this framing, every pixel can be conceived of as occupying a five-dimensional space. A pair of pixels close to each other on the painting and with similar colors will be near each other in this five-dimensional space, and large collections of similar pixels form clusters and complex topological structures there. When additional coregistered images are added, such as the many element maps arising from MA-XRF scanning, the dimensionality of the space grows because then every pixel has many elemental compositions, each of which corresponds to a separate axis in the high-dimensional space. Clusters and other structures in these high-dimensional elemental composition spaces form from areas of similar layer buildup, so visualizing them can help to make sense of the deluge of data.

Our solution to this problem of overwhelming amounts of data is allow the user to explore any combination of projections and colorings of the space interactively. In this approach, each pixel is drawn individually, and changes to the positions of the pixels are animated. Elemental compositions or colors can be used to position the pixels directly, or dimension-reduction techniques such as PCA, t-SNE (Van der Maaten and Hinton 2008), or UMAP (McInnes and Healy 2018) can be used to

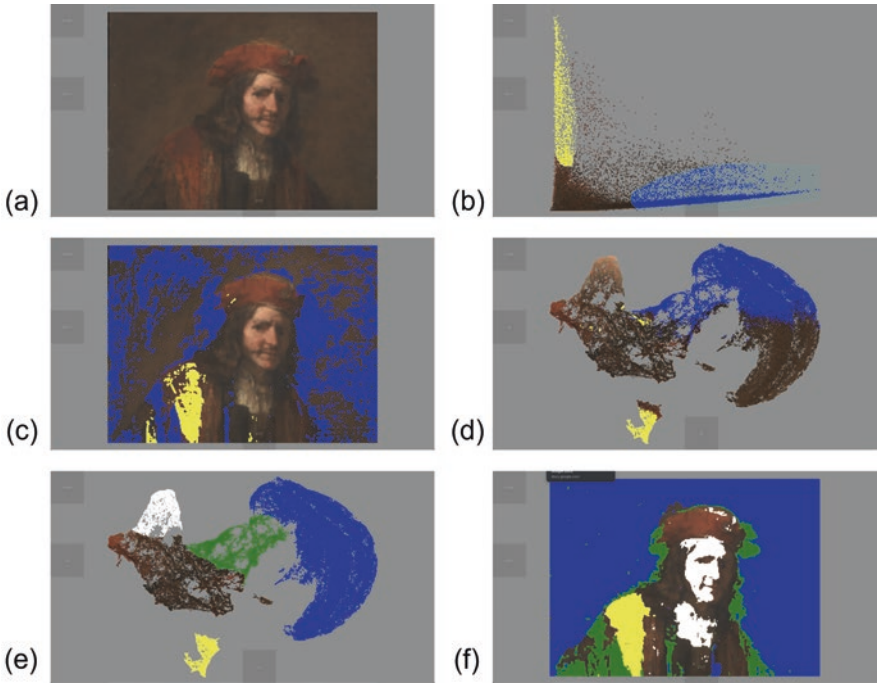

Fig. 1.9 (**a**)–(**f**): Screen captures of a sequence from a typical session with the PixelSwarm tool applied to the upper half of Rembrandt's (?) *Man with a Red Cap* (Boijmans Museum). Explanations of the sequence appear in the text.

cluster the pixels according to their composition or other criteria. In any configuration, the user is able to "lasso" points and temporarily color them so that they can be easily tracked from one view to another. The iterative projection-lasso-coloring-reprojection sequence thus allows the user to build up an understanding of the layer buildup and painterly technique that cannot easily be obtained by inspecting the individual technical images of the painting.

Figure 1.9 shows a sequence of states from a typical use in an investigation of the attribution of the Man with a Red Cap in the Boijmans Museum. In (a), the initial display shows the pixels of the upper half of the painting in their normal positions with normal colors. In (b) the display is animated to position the pixels according to their cobalt and arsenic concentrations on the x- and y-axes, after which the user temporarily lassoes pixels in the cobalt-rich branch (likely containing smalt particles) in blue and the arsenic-rich branch (likely containing orpiment or realgar) in yellow. In (c), the swarm of pixels is animated back to their initial positions, maintaining their colored tags from step (b), thereby revealing a background rich in smalt and portions of the jacket apparently rich in orpiment or realgar. Also, the outlines of a smaller hat are easily visible here. In (d), further insight is gained by positioning the pixels according to the first two components of a UMAP dimension reduction on the elemental compositions, where it is seen that the pixels are broadly grouped into two main lobes with a connecting isthmus. The compositional distinctiveness of the

arsenic-rich pixels is seen from their appearance as a separate island in the cluster plot. In (e), upon seeing that a large fraction of the right lobe is tagged with blue from step (b), the user hypothesizes that the right lobe corresponds to background pixels, the left lobe corresponds to foreground pixels, and the isthmus corresponds to pixels that have components typical of both, possibly due to overpainting of a painted background that was not originally held out. They then reset the tagging and freshly lasso the right lobe in blue, the isthmus in green, and the island in yellow. Additionally, the left lobe appears to have a distinctive clustered structure around the light-colored pixels, so the user tags those pixels in white. Finally, in step (f) the user again positions the pixels according to their original positions. There, it is seen that the light-colored foreground of the man's face is compositionally similar to the man's shirt, and that a large triangle in his jacket is compositionally distinct and contains orpiment or realgar. The visualization reveals that the widening of the hat corresponds to areas that are compositionally both foreground- and background-like, suggesting that they may be late-stage changes to the composition, made at the same time as changes to the pose of the man. Thus, the PixelSwarm tools allows the connoisseur to understand the materiality of the painting as it relates to painterly technique and to subsequently use this understanding in making judgements on attribution.[28]

1.7 Concluding Remarks: Challenges and Opportunities

Throughout the twentieth century, connoisseurship of old master and modern paintings evolved greatly in the Netherlands. From the implicit knowledge (or intuitive insight) of one specialist it became a predominantly evidence-based practice building on specialist insights of many different experts. Although implicit knowledge still plays a significant role in the authentication process, it is no longer accepted at face value; instead, the rational arguments underpinning authentication decisions have taken centre stage.

Chemical evidence was first introduced in court in 1925 to help settle a forgery dispute. Since then, chemical analyses have become increasingly integrated in the decision-making process. Having triggered both distrust and excessive optimism, chemical analyses and their potential in authentication issues were systematically assessed in several large-scale research projects aimed at sorting out the oeuvre of a specific artist, notably Rembrandt and Van Gogh.

In the late twentieth century, it gradually became clear that chemical evidence seldom yielded conclusive evidence concerning attributions. Only in the case of anachronistic materials, analytical chemistry could provide conclusive evidence and expose forgeries or misattributions. In all other cases, the authentication or

[28] The attribution of this particular painting is complicated by the fact that a previous owner of the work, the painter Joshua Reynolds (1723–1792) may have partially overpainted the work (which highlights the need for an in-depth assessment of the condition of the work and possible early overpaintings). With thanks to Katja Kleinert and Claudia Laurenze-Landsberg for this observation.

attribution process remained a matter of interpretation. Like detectives, art experts combine circumstantial evidence and probabilities. Significantly, no positive attribution (i.e. an attribution *to* a certain painter) can be done without a visual analysis. For even if the materials are consistent with the period and the specific painter's workshop practice, one still needs to analyze the particular 'handwriting' of the artist in order to determine if the attribution is correct, to differentiate between different types of workshop products, contemporary copies and imitations.

This latter task, the visual analysis, has become both more challenging and easier in the early twenty-first century, due to a paradigm shift in the humanities, myriad new technical possibilities and advanced digital tools. Within the humanities, the very notion of what constituted 'authenticity' was redefined, especially in the field of old master painting. As result, art experts moved away from a simple binary perspective (either by the master or not), became more aware of the complex range of possibilities, and started introducing more nuanced categories of thought.

With the aid of new analytical techniques, in particular MA-XRF scanning and HSI/RIS, pioneering teams of experts (often including conservators, conservations scientists and curators) have gained a deeper understanding of the art works they studied. Although their projects commonly focus on just a few works of art, the (digital) data thus generated is nevertheless substantial, and (increasingly) require digital tools to aid with the interpretation. The knowledge thus gained often helps to significantly reduces the number of possible attributions and occasionally yields unique insights that make the creation of new forgeries virtually impossible (as in the case of Van Gogh drawings). Moreover, there is currently a relatively high chance of discovering discrepancies when closely comparing originals with forgeries or imitations from a different time period. Most painters' oeuvres have not been researched yet with (all) the newest techniques, and it is unlikely that forgers and imitators mimicked specific materials and techniques, if these materials and techniques were not known to them.

Given the quantity of data already generated and the new data that will be generated in the near future, one of the main challenges of twenty-first century connoisseurship is to manage and process all the information and to effectively select the most relevant parts. While early twentieth-century connoisseurs heavily relied on their visual memory when judging attributions, their twenty-first-century equivalents face a different reality. Digital tools are increasingly facilitating one of their core tasks: making effective comparisons. Although various computer programs have been developed with more ambitious goals, namely to substitute the connoisseur's analysis of brushstrokes or overall visual assessment, these have not proven to be effective (yet) in practice (which must be due to the complexity of such decisions). By contrast, algorithms with more modest goals (namely simply facilitating comparisons) have a powerful impact on the field. For the first time, these tools make it possible to make precise in-depth comparison not just of the visible surface of paintings but also of the chemical properties of deeper layers in a heartbeat, zooming in and out from an overall view of a large-size painting to microscopic observation in less than a second, changing seamlessly from visible light to different

wavelengths, x-radiography, IRR and various elemental maps, while juxtaposing comparable elements in shape and size and material composition.

Although there is a relatively wide gap between pioneering authentication studies (using the newest techniques and tools) and the everyday attribution practice in the field, it is to be expected that connoisseurship will be become increasingly sophisticated as the techniques, tools and gathered data will become more widely available, and new techniques and tools will be developed. As in the past, the correct interpretation of both visual clues and chemical evidence will continue to require sufficient and secure reference data. For a positive attribution to a painter, an in-depth understanding of both the period in which a painting was made, and the specific master's characteristic habits and workshop practice, will undoubtedly remain indispensable (to best estimate of the amount of consistency one can expect in a master painter's style, technique and use of materials). For the detection of forgeries, a more widespread use of technical analyses is likely to make a significant difference, while the development of increasingly advanced methods is likely to facilitate the identification of anachronistic materials and other relevant discrepancies. As materiality tends to be harder to forge than it is to analyze nowadays, this might well tip the balance in favour of connoisseurs in the continuous arms race between forgers and art experts.

Acknowledgements The authors wish to thank Robert van Langh for his encouragement to write this chapter and his thoughtful comments on an earlier version of this text, Carlijn Vos for her copy editing and the Leiden University Centre for the Arts in Society for their generous support for writing this article. A substantial part of the research used in this article was done in the context of the NICAS Seed Money Project *21st Century Connoisseurship* (2018-2022) led by the authors and funded by the Dutch Science Foundation (NWO). The authors wish to thank the Frans Hals Museum, Haarlem and the Rijksmuseum, Amsterdam for supporting this project.

References

Ainsworth, M.W.: From connoisseurship to technical art history: the evolution of the interdisciplinary study of art. Conserv. Getty Conserv. Inst. Newsl. **20**(1), 4–10 (2005)

Ainsworth, M.W., Haverkamp-Begemann, E., Brealev, J., Meyers, P., et al.: Art and Autoradiography: Insights into the Genesis of Paintings by Rembrandt, Van Dyck, and Vermeer. Metropolitan Museum of Art, New York (1982)

Alfeld, M., Janssens, K., Dik, J., de Nolf, W., van der Snickt, G.: Optimization of mobile scanning macro-XRF systems for the in-situ investigation of historical paintings. J. Anal. At. Spectrom. **26**, 899–909 (2011)

Alfeld, M., Pedroso, J.V., van Eikema Hommes, M., Van der Snickt, G., Tauber, G., Blaas, J., et al.: A mobile instrument for in situ scanning macro-XRF investigation of historical paintings. J. Anal. At. Spectrom. **28**, 760–767 (2013)

Alpers, S.: Rembrandt's Enterprise: The Studio and the Market. University of Chicago Press, Chicago (1990)

Asperen de Boer, van J.R.J.: Reflectography of Paintings using an infrared vidicon television system. Stud. Conserv. **14**, 96–118 (1969)

Bomford, D.: Forbes Prize Lecture. International Institute for Conservation of Historic and Artistic Works annual congress, London (2008)
Brandhof, M.: van de. Een vroege Vermeer uit 1937: achtergronden van leven en werken van de schilder:vervalser Han van Meegeren. Het Spectrum, Utrecht/Antwerp (1979)
Bredius, A.: A New Vermeer. Burlingt. Mag. **71**, 210–211 (1937)
Bremer, F.: Inleiding tot de kunstgeschiedenis, 5th edn. Elsevier, Amsterdam/Brussels (1945)
Bruyn, J., et al.: A Corpus of Rembrandt Paintings (vols. I–III). Springer, The Hague/Boston (1982, 1986, 1989)
Chapman, H.P., Weststeijn, T.: Connoisseurship as knowledge: an introduction. In: Chapman, H.P., Weststeijn, T., Meijers, D. (eds.) Connoisseurship and the Knowledge of Art, pp. 6–41. Brill Academic Publishers (2019)
Charney, N.: The Art of Forgery: The Minds, Motives and Methods of Master Forgers. Phaidon Press, New York/London (2015)
Coremans, P.: L'Agneau Mystique au laboratoire: Examen et traitement. De Sikkel, Antwerp (1953)
Craddock, P.: Scientific Investigation of Copies, Fakes and Forgeries. Elsevier Ltd, Oxford (2009)
Dantzig, van M.: Frans Hals: echt of onecht. Amsterdam/Paris (1937)
Dantzig, van M.: Johannes Vermeer, de Emmausgangers en de Critici. Sijthof, Leiden (1947)
Dantzig, van M.: Pictology: An Analytical Method for Attribution and Evaluation of Pictures. E.J. Brill, Leiden (1973)
Decoen, J.: Terug naar de waarheid, twee authentieke schilderijen van Vermeer. Donker, Rotterdam (1951)
Dickey, S.: The art of connoisseurship. In: Podedworny, C., et al. (ed.) The Unvarnished Truth. Exploring the Material History of Paintings. McMaster University Museum of Art (2015). https://theunvarnishedtruth/mcmaster.ca. Accessed 1 Mar 2021
Dijksterhuis, A.P.: Het slimme onbewuste. Prometheus, Leiden (2007)
Du Bos, A.: Réflexions critiques sur la poésie et la painture. Jean Mariette, Paris (1719). cited ed. Paris: énsb-a (1993)
Dumas, C., Ekkart, R., van de Puttelaar, C. (eds.): Connoisseurship: Essays in Honour of Fred F. Meijer. Primavera Press, Leiden (2020)
Duparc, F.: Results of the recent art-historical and technical research on Carel Fabritius's early works. Oud Holland. **119**(2-3), 76–89 (2006)
Dutton, D.: Artistic Crimes: The Problem of Forgery in the Arts. Br. J. Aesthet. **19**(4), 302–314 (1979)
Ekkart, R.: Hofstede de Groot, Cornelis (1863–1930). In: Biografische Woordenboek van Nederland, pp. 248–249. Martinus Nijhoff, The Hague (1979)
Erdmann, R.G.: Image processing for the Bosch research and conservation project. In: Hoogstede, L., Spronk, R., Erdmann, R.G., Klein Gotink, R., Ilsink, M., Koldeweij, J., Nap, H., Veldhuizen, D. (eds.) Hieronymus Bosch, Painter and Draughtsman, Technical Studies, pp. 31–51. Yale University Press, Brussels (2016a)
Erdmann, R.G.: Bosch project (2016b). http://boschproject.org/#/book/. Accessed 4 Mar 2021
Faille, de la J.B.: Les faux Van Gogh. Impr. Arrault et Cie, Paris/Brussels (1930)
Faille, de la J.B.: The Works of Vincent van Gogh: His Paintings and Drawings. Reynal and Company, Amsterdam (1970)
Feilchenfeldt, W.V.: Gogh fakes: the Wacker affair, with an illustrated catalogue of the forgeries. Simiolus. **19**(4), 289–316 (1989)
Freedberg, D.: Why Connoisseurship matters. In: van der Stigghelen, K. (ed.) Minuscula Amicorum: Contributions on Rubens and his colleagues in honour of Hans Vlieghe, pp. 29–43. Brepols, Turnhout (2006)
Gerson, H.: Rembrandt Paintings. Translated from the German by Heinz Norden and edited by Gary Schwartz. Harrison House, New York (1968)
Gifford, M., Glinsman, L.D.: Collective style and personal manner: materials and techniques of high life genre painting. In: Waiboer, A., et al. (eds.) Vermeer and the Masters of Genre Paintings, pp. 65–83. Yale University Press, Paris/Dublin/Washington, DC (2017)

Ginsburgh, V., Radermecker, A., Tommasi, D.: The effect of experts' opinion on prices of art works: the case of Peter Brueghel the Younger. J. Econ. Behav. Organ. **159**(C), 36–50 (2019). https://doi.org/10.1016/j.jebo.2018.09.002

Ginzburg, C.: Morelli, Freud and Sherlock Holmes: Clues and scientific method. Hist. Work. **9**, 5–36 (1980)

Gladwell, M.: Blink: The Power of Thinking without Thinking. Little, Brown and Company, New York (2005)

Goodman, N.: Languages of Art. Oxford University Press, Oxford (1969)

Goodman, N.: Art and authenticity. In: Dutton, D. (ed.) The Forger's Art: Forgery and the Philosophy of Art, pp. 93–115. University of California Press, Berkerley/Los Angeles/London (1983)

Grimm, C.D.: Frage nach der Eigenhändigkeit und die Praxis der Zuschreibung. In: Thomas, W. (ed.) Künstlerische Austausch/Artistic Exchange: Akten des XXVIII. Internationalen Kongresses für Kunstgeschichte, Berlin, 15–20 juli 1992. Berlin, pp. 631–648 (1993). https://doi.org/10.11588/artdok.00004294

Groen, K.: Grounds in Rembrandt's workshop and in paintings by his contemporaries. In: van de Wetering, E. (ed.) A Corpus of Rembrandt Paintings (IV). Springer., pp. 318–334, 660–667, Dordrecht (2005)

Guichard, C. (ed.): De l'authenticité: Une histoire des valeurs de l'art (XVIe-XXe siècle). Publications de la Sorbonne, Paris (2014)

Hebborn, E.: Drawn to Trouble: The Forging of an Artist. Mainstream Publishing Projects, Edinburgh (1991)

Hofstede de Groot, C.: Beschreibendes und kritisches Verzeichnis der Werke der hervorragendsten holländischen Maler des XVII. Jahrhunderts (vols 1–10). Paul Neff Verlag/F. Kleinberger/MacMillan & Co, Esslingen/Paris/London (1908–1927)

Hofstede de Groot, C.: Echt of Onecht? Oog of Chemie? van Stockum, The Hague (1925)

Huang, M., Bridge, H., Martin, J., Kemp, M.J., Parker, A.J.: Human cortical activity evoked by the assignment of authenticity when viewing works of art. In: Frontiers in Human Neuroscience (2011). https://doi.org/10.3389/fnhum.2011.00134

Hughes, H., Hughes, E., Hughes, S.: Van Gogh's Brushstrokes: Marks of Authenticity? In: Proceedings of "Art, Conservation, and Authenticities: Material, Concept, Context", pp. 143–151. Archetype Publications, Scotland (2009)

Huussen, A.H. (ed.): Cahiers uit het Noorden XX: Henricus (Han) Antonius van Meegeren (1889–[1945]): documenten betreffende zijn leven en strafproces. Huussen, Zoetermeer (2009)

Ilsink, M., Koldeweij, J., Spronk, R., Hoogstede, L., Erdmann, R.G., Klein Gotink, R., Nap, H., Veldhuizen, D.: Hieronymus Bosch, Painter and Draughtsman, Catalogue Raisonné. Mercatorfonds, Brussels (2016) ISBN 978-94-6230-113-9

Jia, L., Yao, L., Hendriks, E., Wang, J.Z.: Rhythmic Brushstrokes distinguish van Gogh from his contemporaries: findings via automated Brushstroke extraction. IEEE Trans. Pattern Anal. Mach. Intell. **34**(6), 1159–1176 (2012). https://doi.org/10.1109/TPAMI.2011.203

Johnson, C.R., Hendriks, E., Berezhnoy, I., et al.: Image processing for artist identification. IEEE Signal Proces. Mag. **25**(4), 37–48 (2008)

Justi, L.: Van Gogh, die Kenner und Schriftsteller. Vossische Zeitung (1929)

Kahneman, D.: Thinking Fast and Slow. Farrar, Straus and Giroux, New York (2011)

Kahneman, D., Tversky, A.: Prospect theory: an analysis of decision under risk. Econometrica. **47**, 263–291 (1979)

Keisch, B.: Dating works of art through their natural radio-activity: improvements and applications. Science. **160**, 413–415 (1968)

Kirby-Talley, M.: Connoisseurship and the rembrandt research project. Int. J. Mus. Manag. Curatorship. **8**, 175–214 (1989)

Knuttel, D.G.: Nederlandsche Schilderkunst van Van Eyck tot Van Gogh. Becht, Amsterdam (1938)

Koestler, A.: The Anatomy of Snobbery. Anchor Rev. **1**, 1–25 (1955)

Koldehoff, S.: The Wacker forgeries: a catalogue. Van Gogh Mus. J. **20**, 138–149 (2002)

Kraaijpoel, D., van Wijnen, H.: Han van Meegeren. Waanders Uitgevers, Zwolle (1996)

Leeflang, H., Luijten, G. (eds.): Hendrick Goltzius (158–1617): Drawings, Prints and Paintings. Exh.cat. Waanders, Amsterdam/London (2003)
Lessing, A.: What is wrong with a forgery? J. Aesthet. Art Critic. **23**(4), 461–471 (1965). https://doi.org/10.2307/427668
Lopez, J.: The Man Who Made Vermeers: Unvarnishing the Legend of Master Forger Han van Meegeren. Harcourt, Inc., Orlando/Austin/New York/San Diego/London (2008)
Lord Kilbracken, J.G.: Van Meegeren: Master Forger. Scribner, London/Bristol (1967)
Lyu, S., Rockmore, D., Farid, H.: A digital technique for art authentication. Proc. Natl. Acad. Sci. **101**(49), 17006–17010 (2004)
Maaten, van der L.J.P., Hinton, G.E.: Visualizing high-dimensional data using t-SNE. J. Mach. Learn. Res. **9**, 2579–2605 (2008)
Mander, van K.: Het Schilder-boeck. Paschier van Wesbusch, Haarlem (1604)
Martin, W.: Kunstwetenschap in theorie en practijk. Martinus Nijhoff, The Hague (1904)
McInnes, L., Healy, J.: UMAP: uniform manifold approximation and projection for dimension reduction. ArXiv. **1**, 1–63 (2018)
Melion, W.S.: Hendrick Goltzius's project of reproductive engraving. Art Hist. **13**(4), 458–487 (1990)
Muthesius, S.: Towards an 'exakte Kunstwissenschaft'(?), Part II: the new German Art history in the nineteenth century: a summary of some problems. J. Art Hist. **9**, 1–16 (2013)
Noord, van N., Hendriks, E., Postma, E.: Toward discovery of the artist's style: learning to recognize artists by their artworks. IEEE Trans. Pattern Anal. Mach. Intell. **32**(4), 46–54 (2015)
Pächt, O.T.: Practice of Art History: Reflections on Method (1986). Translated by Britt D. Harvey Miller Publishers, London (1999)
Rosenberg, J.: On Quality in Art: Criteria of Excellence in Past and Present (The A.W. Mellon Lectures in the Fine Arts 1964). Princeton University Press, Princeton (1967)
Schneider, H., Regteren-Altena, J.Q.: Rapport van het stilistisch/aesthetisch onderzoek van zeven schilderijen welke een Vermeer-signatuur dragen of aan Jan Vermeer van Delft zijn toegeschreven en twee schilderijen die op den naam van Pieter de Hoogh staan en het merk PDH 1658 vertonen. Amsterdamse Rechtbank, Amsterdam (1947)
Seymour, S.: Frans Hals. Phaidon Press, London (2014)
Sheldon, L., Costaras, N.: Johannes Vermeer's 'Young Woman Seated at a Virginal'. Burlingt. Mag. **148**, 89–97 (2006)
Storm van Leeuwen, J.: The Concept of Pictology and its Application to Works by Frans Hals. In: Authentication in the Visual Arts: A Multi-Disciplinary Symposium, Amsterdam, 12th of March 1977, pp. 57–92. B.M. Israël, Amsterdam (1977)
Thienen, van F.: Vermeer. Palet-serie, Amsterdam (1939)
Tromp, H.: De Strijd om de Echte Vincent van Gogh: De kunstexpert als brenger van een onwelkome boodschap 1900–1970. Dissertation, Mets & Schilt, Amsterdam (2006)
Tufte, E.: Envisioning Information. Graphics Press, Cheshire (1990) ISBN 978-0961392116
Tummers, A.: The Eye of the Connoisseur, Authenticating Paintings by Rembrandt and His Contemporaries. Amsterdam University Press/Getty Publications, Amsterdam/Los Angeles (2011)
Tummers, A.: Connoisseurship in the Western World, developments since 1980. In: Grove Dictionary of Art, Oxford Art Online (2018). https://www.oxfordartonline.com/groveart/view/10.1093/gao/9781884446054.001.0001/oao-9781884446054-e-7000019062.
Tummers, A., Jonckheere, K. (eds.): Art Market and Connoisseurship: A Closer Look at Paintings by Rembrandt, Rubens and Their Contemporaries. Amsterdam University Press, Amsterdam (2008)
Tummers, A., Wallert, A., Kleinert, K., Hartwieg, B., Laurenze-Landsberg, C., Dik, J., Groves, R., Anisimov, A., Papadakis, V., Erdmann, R.: Supplementing the eye: the technical analysis of Frans Hals's Paintings – I. Burlingt. Mag. **161**, 934–941 (2019a)
Tummers, A., Wallert, A., de Keyser, N.: Supplementing the eye: the technical analysis of Frans Hals's Paintings – II. Burlingt. Mag. **161**, 996–1003 (2019b)

Vries, de A.B., Frountjes, W., Tóth-Ubbens, M.: Rembrandt in the Mauritshuis: An Interdisciplinary Study. Sijthoff & Noordhoff, The Hague (1978)
Wallert, A., van de Laar, M.: Werkwijzen, trucs, materialen en technieken: vervalsingen op het hoogste niveau. In: Lammertse, F., Garthoff, N., van de Laar, M., Wallert, A., van Es, J. (eds.) De Vermeers van Van Meegeren, Kennerschap en de techniek van het vervalsen, pp. 66–99. Boijmans studies, Rotterdam (2011)
Wallert, A., van de Laar, M.: Expertise in the Van Meegeren case: the contributions by Coremans, Froentjes and De Wild. In Proceedings of the Coremans Symposium. Brussels, pp. 202–214 (2018)
Weerdenbrug, S.: De Emmausgangers: een omslag in Waardering. MA thesis. University of Utrecht (1988)
Wetering, van de E.: The canvas support. In: Bruijn, J., et al. (eds.) A Corpus of Rembrandt Paintings, vol. 2, pp. 15–43. Springer, The Hague/Boston (1986)
Wetering, van de E.: The search for the master's hand: an anachronism? (A summary). In: Thomas, W. (ed.) Künstlerische Austausch / Artistic Exchange: Akten des XXVIII. Internationalen Kongresses für Kunstgeschichte, Berlin, 15–20 juli 1992. Berlin, pp. 627–630 (1993)
Wetering, van de E., et al.: A Corpus of Rembrandt Paintings (vols IV–VI). Dordrecht: Springer (2005, 2010, 2014)
Wild, de M.: Het natuurwetenschappelijk onderzoek naar schilderijen. Dissertation. TH Delft (1928)
Wolz, S.H., Carbon, C.: What's wrong with an art fake? Cognitive and emotional variables influenced by authenticity status of artworks. Leonardo. **47**(5), 467–473 (2014)
Zerner, H.: What gave connoisseurship its bad name? In: Strauss, W., Felker, T. (eds.) Drawings Defined, pp. 289–290. Abaris Books, New York (1987)

Chapter 2
Scientific Study, Condition Challenges, and Attribution Questions in Yves Tanguy's Oeuvre

Jennifer L. Mass, Rebecca Pollak, Aaron Shugar, Adam C. Finnefrock, Silvia A. Centeno, and Isabelle Duvernois

Abstract There can be no single scientific "road to attribution" for works by all artists. The primary factors of an attribution are widely considered to be provenance, connoisseurship, and technical analysis, but they are necessarily given different weights for different artists. The processes and challenges surrounding the attribution of a painting by Yves Tanguy are examined in this chapter. These include his use of a limited palette, a World War II forgery ring targeting his work, provenance gaps resulting from World War II, the lack of a complete catalogue raisonné for his works, and his documented reluctance to discuss his artistic process. Some of the difficulties encountered here are useful for review because they are common for other interwar painters, and others are common to the surrealists. The condition issues associated with surrealist paintings and their resulting conservation histories are discussed here, to our knowledge, for the first time. They provide a major challenge not only to attribution questions but also for the overall preservation of the

J. L. Mass (✉)
Scientific Analysis of Fine Art, LLC, Andrew W. Mellon Professor of Cultural Heritage Science, Bard Graduate Center, New York, NY, USA
e-mail: jen@scienceforfineart.com

R. Pollak
Scientific Analysis of Fine Art, LLC, New York, NY, USA

A. Shugar
Andrew W. Mellon Professor of Conservation Science, SUNY College at Buffalo, Buffalo, NY, USA

A. C. Finnefrock
Scientific Analysis of Fine Art, LLC, New York, NY, USA

S. A. Centeno
Department of Scientific Research, The Metropolitan Museum of Art, New York, NY, USA

I. Duvernois
Department of Paintings Conservation, The Metropolitan Museum of Art, New York, NY, USA

M. P. Colombini et al. (eds.), *Analytical Chemistry for the Study of Paintings and the Detection of Forgeries*, Cultural Heritage Science,
https://doi.org/10.1007/978-3-030-86865-9_2

surrealist oeuvre. The extant information about Tanguy's palette and working methods is provided, along with technical discoveries for the six paintings included in this study. This chapter also includes excerpts from interviews with two art historians, Charles Stuckey and Stephen Mack, who have worked intensively on a catalogue raisonné for Tanguy.

Keywords Attribution · Provenance · Connoisseurship · Technical analysis · Tanguy painting

2.1 Introduction

2.1.1 Attribution Challenges for Yves Tanguy and His Contemporaries

Questions of painting attribution are multifaceted, founded on a mixture of objective and subjective criteria that are commonly reevaluated as new information, interpretations, and investigative tools present themselves (Ragai 2013, 2015; Tromp 2010; Rhodes 2011; Saverwyns 2010). A comprehensive discussion of the challenges of painting attribution in general and even those facing the works of the surrealists is beyond the scope of this volume. However, general resources on the role of science in identifying forgeries and the interplay of connoisseurship and science are widely available (see, for example, Scott 2016; Wesley 2012; Teja Bach 1990; Spier 1990; Brewer 2009; Craddock 2009; Jones 1990; Sloggett 2014; Finn 2014). We have increasingly observed the need for distinct scientific protocols for different artists in our experiences using scientific examination of paintings to contribute to the attribution process (particularly with regard to prioritizing among the range of spectroscopic and imaging tools available). The weighting of these different types of data are unique to each artist, e.g., paint binding media identifications play a critical role in Jackson Pollock attributions (Khandekar et al. 2010). Even with such tailored approaches, the attributions that result are not always permanent in the absence of documentation conclusively demonstrating authorship (such as a verified period photograph of the work in the artist's studio) (van de Wetering 2014; Bijl and Kloek 2014). Reassessments, de-attributions, and re-attributions resulting from technical imaging and analysis data (such as, for example, infrared imaging and provenance dendrochronology) are particularly common in the world of Old Masters in which workshop practice plays a substantial role (Rønberg and Wadum 2006; Haneca et al. 2005). These reevaluations also occur in the surrealists' oeuvre (Robinson 2015). Three of the most important evaluation criteria are widely acknowledged to be a work's provenance, connoisseurship or stylistic merits, and the materials and working methods of the painter (Bellingham 2012; Rhodes 2011). However, the role of scientific data in the attribution process has been a subject of

contention and misunderstanding for over 100 years (Brewer 2005, 2009).[1] These considerations are examined here for a single artist, Yves Tanguy (1900–1955, active ca. 1925–1955). Tanguy's oeuvre reveals challenges that are illustrative of both artists working during the interwar period and the attribution of works by surrealist painters in general. We explore these issues from the perspective of our experiences as cultural heritage scientists and art conservators who form the scientific vetting committee for TEFAF New York, and who engage in attribution questions on a daily basis through our academic roles and our research at Scientific Analysis of Fine Art ("SAFA", New York). One consideration that we have observed repeatedly in our work with surrealist paintings is that their conservation histories can obfuscate attribution questions. The role of condition in attribution questions is not of course unique to the surrealists, and it has recently been considered by Scott and Mancini (Scott 2015, 2016; Mancini 2013).

The scientific identification of a favored set of materials or techniques such as J.M.W. Turner's striking and diverse yellow palette or Vincent van Gogh's geranium lake (eosin red) can provide evidence in support of an attribution for a specific artist, but this has yet to be widely applied to the attribution of surrealist works, even in the presence of substantial research having been carried out on their contemporaries the expressionists and the Russian avant-garde (Buckley 2018; Townsend 1993; Pozzi et al. 2021; Artesani et al. 2019). Instead, in the absence of materials databases on these artists, materials identification is predominantly carried out to identify anachronistic pigments or media that would rule out a particular attribution, or in special situations such as the use of hyperspectral and macro-area XRF imaging of a buried painting (as has been recently carried out in the case of René Magritte's 1935 *Le portrait* and his 1958 *La toile de Pénélope* (Van der Snickt et al. 2016; Defeyt et al. 2019a). Magritte's works have also been studied to address specific pigment degradation issues (Defeyt et al. 2019b). One of the objectives of this chapter is to begin the process of building a database for the material choices and methods of Yves Tanguy, which are of particular interest given his lack of any formal artistic training and the exacting and meticulous nature of his work (Maur 2001; Schalhorn 2001).

[1] The role of X-radiographic data versus the connoisseurship expertise of Joseph Duveen for a painting attributed to Leonardo da Vinci (*La Belle Ferronnière*) is one prominent early example of this debate (from a 1920 court case in which the painting's owners sued Duveen for slander). This case is discussed in detail by John Brewer in several publications. See, for example, "Art and Science: A Da Vinci Detective Story", *Engineering & Science* No. ½, 2005, 32–41. In scientific research we rely on the fact that the results we find are subject to re-evaluation and potential alteration as new evidence or better instrumentation is found. We have found that in fields outside of science, there is an expectation that a scientific result is immutable. Just as an attribution can change as a result of updated documentation or provenance data, it can also change as a result of new scientific data. This is analogous to the cumulative developments of the medical profession.

2.1.2 Science, Attribution, and the Art Market

The process involved in a positive attribution of a work by Rembrandt van Rijn provides one example of how this research can unfold within the art market (versus the research conducted at an art museum or in an academic context) (von Sonnenburg 1995a). In the museum context, Hubert von Sonnenburg at The Metropolitan Museum of Art provides an elaborate range of classifications for works in their collection that includes six categories: Rembrandt, Rembrandt(?), circle of Rembrandt, follower of Rembrandt, studio copy after Rembrandt, and Rembrandt forgery (von Sonnenburg 1995b). The art market, on the other hand (including the major auction houses), commonly accepts the evaluation of one or two renowned art historical experts for a positive Rembrandt van Rijn attribution such as those of Professor Ernst van de Wetering (University of Amsterdam) and the Dutch Old Masters dealer Jan Six (Van de Wetering 2008; Shorto 2019; Bandle 2015). Van de Wetering and Six's arguments about a work are supported by a large body of existing technical data on the artist's materials and techniques that has been published in peer-reviewed literature by paintings conservators and scientists in the Netherlands, England, and the United States[2] (Noble et al. 2018; Gonzalez et al. 2019). A similar situation exists for Leonardo da Vinci, with Martin Kemp (University of Oxford), Carmen Bambach (Metropolitan Museum of Art), and Frank Zöllner (Leipzig University) being examples of widely acknowledged stylistic experts for Leonardo's oeuvre even in the face of the often-spirited debate surrounding Leonardo attributions (Kemp 1992; Kemp 2018; Bambach 2019). Likewise, extensive technical studies of this artist's technique can be found in the art conservation and technical art history literature[3] (Walter 2013). In each of these situations art historians, provenance researchers, art conservators, and conservation scientists commonly work closely together to provide a global view of the work of art and its 'object biography'. These two structures for art attribution (the art market model and the museum model) have been discussed within the context of "singular or multiple authority delegation structures" by Loiselle for Modigliani and Renoir attributions (Loiselle 2017).

The attribution process described above is slow and laborious, but it benefits from the large amount of research and data available for these painters. While provenance gaps due to both world wars are problematic for both Old Masters and twentieth century artists, the attribution challenges for twentieth century artists are compounded by the presence of lacunae in other data sectors too (Yeide et al. 2001; Nicholas 1994; Tomkins and Humphries 2021). There may or may not be a

[2] Recent prominent examples include Noble et al.'s study of the Marten and Oopjen portraits, Gonzalez et al.'s identification of unusual lead compounds in Rembrandt's white impasto and the comprehensive scientific examination underway for the Rijksmuseum's 1642 *Night Watch*.

[3] See, for example, Phillippe Walter, "Chemical analysis and painted colours: the mystery of Leonardo's sfumato", *European Review*, 21(2), May 2013, 175–189.

catalogue raisonné available for the artist, or there may be multiple incomplete and competing ones as in, for example, the case of Amedeo Modigliani (Parisot et al. 1991; Lanthemann 1920; Ceroni et al. 1958; Cain 2016). For many preeminent twentieth century artists such as Joan Mitchell or Franz Kline, *catalogue raisonné* work is still ongoing, and there has been limited publication of their materials and techniques (with Kline's technique only having been studied thus far to address condition issues, see Rogge et al. 2019). In addition, foundations for many prominent twentieth century artists such as Jackson Pollock (the Pollock-Krasner Foundation) and Andy Warhol (the Andy Warhol Foundation for the Visual Arts) no longer accept works for attribution purposes (Pollock-Krasner Foundation 2021; Thomas 2005; Itzkoff and Vogel 2011). Other twentieth-century artists such as Pablo Picasso have extensive documentation of their oeuvre even in the face of an incomplete *catalogue raisonné* (Zervos 1951; Stolz 2013), as well as living close friends or family members to whom the French courts have granted *droit moral* for the attribution of their works (such as Claude Ruiz-Picasso, Stolz 2013). The uncomfortable (pro-Communist) politics of the surrealist painters were out of favor for much of the 1950s and early 1960s and during this time the monetary value of the paintings was also not high (Rasmussen 2004; Drost et al. 2019).[4] This may have had a role in a particular set of condition issues for these paintings – primarily issues such as mold damage that are associated with neglect and poor storage conditions. This circumstance, and a forgery scandal in Occupied Paris (discussed below) has led to confusion surrounding the condition and attribution of their paintings.

2.1.3 Background Information on Yves Tanguy's Influences and Life

Tanguy's artistic development and success was the result of his innate vision and talent, and he had the opportunity to benefit from a number of fortuitous connections. As noted above, Tanguy was born in Brittany and attended school in Paris with classmate and future dealer and executor Pierre Matisse. While in the French Army in 1920 Tanguy had met fellow Breton and future poet Jacques Prévert, and after finishing military service in Tunis in 1922 Tanguy was reunited with his friend

[4] While Joan Miró was popular in the United States and his influence on, for example, Mark Rothko and Arshile Gorky well-recognized, Breton struggled and failed to build a successful intellectual movement in the United States. Rasmussen has noted "Capitalism had no problem accepting the irrational and unusual objects of Surrealism. If only the objects of Surrealism could be separated from their historical and social context…" and Drost et al. "It is important to emphasize that a clear distinction should be made between the reception of surrealism in the United States, on one hand, and the artistic and intellectual interests of the exiles..."

in Paris. By 1924, the two were sharing a house with peer Marcel Duhamel at 54 Rue du Château. Working odd jobs, Tanguy had begun to make sketches on scraps of paper at Montparnasse cafes, which through mutual connections drew the attention of art critic Florent Fels (Schalhorn 2001, p. 213). This early interest may have encouraged Tanguy to pursue being an artist. The desire to paint, however, is linked to a revelatory moment in the Spring of 1922 when Tanguy and Prévert reportedly jumped off a bus platform to examine two works by Giorgio de Chirico in the window of a Paris gallery that had caught their eye (Sweeney 1946, p. 22; Maur 2001, p. 10). A reproduction of one of these, *A Child's Brain*, had just been included in the inaugural issue of *Littérature* (Breton and Soupalt 1922, pp. 12–13), in which editor André Breton proclaimed a break with the Dada movement before publishing his *Surrealist Manifesto* in 1924.

In 1925, Fels included three of Tanguy's drawings in an exhibition at the Salon de l'Araignee and introduced him to key surrealist figures in Paris (Mundy 1983, p. 200). Tanguy met Breton that December, and Tanguy's shared apartment soon became an important gathering place for the surrealists. By 1926, Tanguy's paintings would be reproduced in surrealist publications and he would be regarded as a surrealist painter (Schalhorn 2001, p. 216). Breton wrote the forward to the catalog of Tanguy's first solo exhibition in 1927, and Tanguy remained loyal to Breton though various internal divisions within the surrealist group (Maur 2001).[5] This exhibition, held at the Galerie Surréaliste, demonstrated the arrival of Tanguy's mature style that the artist continued to refine in the subsequent decades of his career.

Tanguy was among the first surrealists to arrive in America when he emigrated in 1939. His new life in the northeast would influence his artistic practice, although he insisted "geography has no bearing on it, nor have the interests of the community in which I work" (Tanguy 1954). Tanguy lived in the United States as a foreigner with a network of expats, a throng that dwindled as many eventually returned to Europe. As Tanguy and Sage settled permanently in Woodbury, Connecticut, Tanguy became somewhat isolated, expressing in 1954 that "there is little to gain by exchanging opinions with other artists concerning the ideology of art or technical methods" (Tanguy 1954).[6] The friendships Tanguy did forge with American artists, which included Alexander Calder and Arshile Gorky, among others, were facilitated by their geographic proximity and their knowledge of French (Davidson 2001, p. 189).

The current status of the different knowledge repositories, individual experts, and data sets available for Yves Tanguy are examined below. The provenance challenges, forgery issues, and dearth of materials research resources that we have encountered for Yves Tanguy exist for many other artists in the interwar period, making Tanguy a good case study for identifying both rewarding and challenging

[5] Although their relationship would cool in later years, in part due to Breton's dislike of Kay Sage and his perception of Tanguy's relative bourgeois.

[6] For a background on this period and the influence of Kay Sage on Tanguy see for example Miller et al. 2011.

avenues for pursuing an attribution. Similar to many other surrealist painters, Yves Tanguy's work has not been subject to careful evaluation and publication either by conservators or conservation scientists. In the absence of a body of scholarship about Tanguy's media, supports, techniques, and their evolution throughout his career, conservation scientists lack a database of comparative material with which to assist in forming judgements about works that may potentially be attributed to Tanguy.[7] Below we present new palette and working methods data from multiple periods of Tanguy's career. These data will provide context for subsequent materials analyses of Tanguy's oeuvre, and provide information beyond the identification of anachronistic materials that might eliminate a particular work being attributed to Tanguy.

2.1.4 Current Resources for Yves Tanguy Attribution Research

Kay Sage (1898–1963), surrealist artist and Yves Tanguy's second wife, authored a *catalogue raisonné* on Yves Tanguy's paintings and gouaches that was published in 1963 (Karpel et al. 1963). While still a very good resource, this work is now acknowledged to be incomplete.[8] A comprehensive *catalogue raisonné* on Tanguy's oeuvre will be an essential research tool for understanding the totality of his artistic output and for contextualizing unattributed works and new discoveries. Charles Stuckey, Head of Research on the Yves Tanguy *catalogue raisonné* project, participated in the research presented here on the materials and techniques of the artist. The *catalogue raisonné* project has, until spring of 2020, been carried out under the auspices of the Pierre and Tana Matisse Foundation. Also part of this project for 9 years was art historian Stephen Mack. Part of our research into the status of Tanguy's oeuvre involved interviewing Stuckey and Mack about their experiences working on the Yves Tanguy *catalogue raisonné* project and working with technical art history data. It is our hope that projects such as this will foster ongoing collaborative research that enables more complete documentation and preservation of surrealist collections.

2.1.5 Condition and the Surrealists

A complication that has emerged with the study of works by Tanguy and his surrealist contemporaries is the condition of the paintings. Surrealist works from this period are often expected to conform to a pristine aesthetic that does not lend itself

[7] Beyond the knowledge of which painting materials are anachronistic for his time.

[8] This was acknowledged by Sage at the time.

to the reality of a painting's appearance at approximately 100 years of age. This has resulted in aggressive and undocumented restoration treatments, likely carried out in the third quarter of the twentieth century, that have involved substantial overpainting. Similar to the color field abstract expressionist paintings of the 1940s and 1950s, surrealist works often have large planes of uninterrupted color which, when marred by a mark or abrasion, immediately draw the viewer's eye. Furthermore, the alteration and degradation of pigments that were common components of the artists' palette between the wars (such as the anatase form of titanium white) has led to some of these works having color fields that are now interrupted by age-related and photoinduced discoloration and staining.[9] We have also observed mold and water damage on a large percentage of the surrealist works we have examined. As a result, many surrealist works have large areas of overpaint, up to and including entirely overpainted backgrounds that can alter the overall balance of the work and challenge the possibility of a positive attribution. Given that these works often have extensive treatment histories, current conservation approaches must acknowledge that the smooth, unbroken appearance of surrealist paintings might be more compromised by minor disruptions than other works. As a result, more compensation for lost, damaged, or abraded paint might be considered for these works than, for example, an expressionist work from the same period. By the 1960s–1970s, the majority of surrealist works in museum collections were lined (with wax-resin, Beva, or PVAc hot-melt) and so documentation of prior structural treatment is not immediately apparent. Lastly, the effects of metal soap agglomerates on the appearance of the works are discussed in more detail below.

2.2 Background

2.2.1 Prior Technical Art History Studies of Surrealist Works

The surrealists are well-known targets for art forgers, with Giorgio de Chirico often being compared with Jean-Baptiste-Camille-Corot as the artist with the greatest number of forged works on the art market (Esterow 2005). The materials and techniques of the surrealist painters have not been as extensively studied as those of the abstract expressionists and the impressionists (Callen 2000; Pozzi 2014; Roy 1985). Famous forgeries of surrealist works include the "Max Ernst" and "Fernand Léger" paintings created by Wolfgang Beltracchi as part of Beltracchi's larger criminal enterprise that also included forgeries of works by Heinrich Campendonk and Kees van Dongen (Bambic 2014; Art Critique 2020). Salvador Dalí's oeuvre has suffered

[9] This can be observed in Joan Miró's *Dos Bañistas (Deux Baigneuses)*, 1936 (Colección El Convent, Barcelona) where a green background in the work has altered to a pale brown color.

from numerous forgery scandals, caused in large part by his having signed somewhere between 60,000 and 350,000 blank pieces of paper in the 1960s and 1970s to facilitate the production of prints of his works and to make rapid payment on his debts (Walker 1986; McGirk 1985).

Giorgio de Chirico not only stands out as a surrealist who notoriously suffered at the hands of forgers (including at the hands of his surrealist contemporaries Oscar Domínguez and Remedios Varo), but later in his career he also forged his own pre-1918 *Metaphysical Interior* works in response to a request by surrealist poet Paul Éluard (Kaplan 2010; Robinson 2001). Giorgio de Chirico's habit of painting his pre-1918 sparse and unsettling semi-industrial landscapes over his later compositions resulted from, in part, the early works being more marketable than some of his 1930s compositions (Robinson 2015; Soby 1949). These self-forgeries were called *verifalsi* by the artist, and have been the subject of technical imaging studies to elucidate their histories (Kaplan 2010). Joan Miró has since the 1970s been an incessant target of forgers, with the two most recent incidents being works produced by two separate criminal enterprises in Valencia and in Zaragoza, Spain, both in 2015 (Muñoz-Alonso 2015a, b). At the time of this writing, Man Ray theft and unauthorized replicas controversies have broken out with Christie's auction house being accused of selling works stolen from the artist's studio by his former assistant Lucien Treillard (Holmes 2021; Noce 2021).

One additional reason for forgery problems in the surrealists' oeuvre is that shrewd art forgers such as Wolfgang Beltracchi often intentionally avoid making forgeries of artists at the very top of the art market, knowing that a newly discovered Vincent van Gogh portrait or blue period work by Pablo Picasso would be subject to rigorous scrutiny and due diligence, but that a Leonora Carrington or André Masson might be more apt to sell "below the radar" and in the absence of scientific study. While the magnitude and driving forces behind the forgery problems involving the works of the surrealists cannot be fully discussed here, this is a serious and ongoing problem for these artists, starting from at least World War II and continuing into the present day. For those surrealist works that are scrutinized, the fact that many of the materials used in the 1930s and 1940s may still be available and even commonly used today may make differentiation through technical study harder still.

Given the scope of the problems surrounding forgery and the surrealists, the absence of technical literature on their materials and techniques is notable. The extant published literature on this topic is summarized here. Max Ernst's collage *Jean Hatchet and Charles the Bold*, 1929, was subjected to infrared imaging at the Cleveland Museum of Art to identify the signature of the engraver upon whose work the engraving is based. In the infrared, the signature is legible below a collage element, in this case a beetle whose legs comprise the bottom strokes of the signature (Real 1985). A volume detailing Max Ernst's trip to Southeast Asia with Paul Éluard and Gala Dalí describes Ernst's visit to Angkor Wat and the *estompage* images of stone carvings that he made there as being a possible source for his development of

the *frottage* technique (McNab 2004). Jim Coddington and Suzanne Siano have also conducted infrared imaging of works by Max Ernst and Joan Miró (Coddington and Siano 2000). Salvador Dalí and Max Ernst's materials and techniques are both briefly treated in the 1983 volume *Techniques of Modern Artists* (Collins et al. 1983). Caroline Lanchner's volume on Joan Miró briefly examines technical aspects of his collage work and curator Anne Umland and paintings conservator Anny Aviram discuss his incorporation of the painting's stretcher bar imprint in *The Birth of the World*, 1925, by using his paintbrush with sufficient force to produce a *frottage* image of the wood (Lanchner 1993; Umland and Aviram accessed 2021). Miró's painting techniques and materials throughout his career are described in more detail in an article in *Pátina* (Martínez 1999).

The role of technical analysis of surrealist works for attribution purposes is made particularly challenging by their works having been forged and sold to support the cause of the French *Résistance* in World War II (Kaplan 2010; Robinson 2001; Mack 2019). The paintings that were forged in Occupied Paris may have included the surrealist works of Max Ernst, Yves Tanguy, Salvador Dalí, and Joan Miró. Other artists who may have been victims of the wartime forgeries were Georges Braque and Pablo Picasso (Mack 2019). In the case of Yves Tanguy, the close associates who created these forgeries would have had intimate knowledge of his materials and direct access to them, although it is not known how intimately familiar they were with his working methods. It is probable that these forgeries have infiltrated both the art market and private collections. Given the disruptions of manufacturing and commerce caused by the war, it is also likely that some of these forgeries were made with materials that predate 1939–1940 (Rogge and Epley 2017). Ideally the most comprehensive method for studying a work of art would involve the expertise of the art conservator, the cultural heritage scientist (conservation scientist), and the art historian. The role of the scientist is hindered in the case of these wartime forgeries – these paintings are likely to have been created with materials contemporary to the artists, if not from the artists' own studios. This likely rules out the identification of anachronistic materials as a means of identifying copied or forged works. It also likely rules out bomb carbon dating unless the forgeries postdate 1945. In addition, many of these wartime forgeries were created by exceptionally skilled painters including prominent Spanish surrealists such as Oscar Domínguez and Remedios Varo (Kaplan 2010; Mack 2019). The forgeries continued to be produced and circulated after the war (Mack 2019).

2.3 The Extant Problems of Yves Tanguy and His Oeuvre

Yves Tanguy was married to surrealist painter Kay Sage at the time of his death in 1955. Following Tanguy's death, Sage, in collaboration with Pierre Matisse, started the work on what was to become the first comprehensive catalogue of Tanguy's oil

paintings and gouaches. The Pierre Matisse gallery published the volume, entitled *Yves Tanguy: un recueil de ses oeuvres* (*A Summary of His Works*) in 1963. Pierre Matisse was a childhood friend of Tanguy's, and his dealer from 1940 to 1955. After Sage's passing in 1963 and the publication of this first catalogue, Pierre Matisse began to be contacted by the owners of paintings that had been omitted from the Kay Sage volume. Matisse subsequently began evaluating these paintings with the intent to publish a new *catalogue raisonné*. When the endeavor remained incomplete at the time of his passing, Pierre's widow Tana Matisse convened a committee of four specialists in 1999 to complete the project. Charles Stuckey joined this committee as head of research in 2006. The undertaking of this revised *catalogue raisonné*, commissioned and funded by the Pierre and Tana Matisse Foundation, was aided by access to Pierre Matisse's gallery archives which included Kay Sage's papers. The production of this *catalogue raisonné* was discontinued in January of 2020 prior to its completion, however, due to a reevaluation of the Foundation's priorities. The Foundation currently retains all of the research and scholarship of the committee at this time, and is considering candidates from academic institutions for the catalogue's completion. However, the existing committee's research and decisions on particular works are not accessible to scholars. It is important to note that Tanguy did not have any children, and that no other family members have been part of any sustained endeavor to attribute his works.

The most comprehensive resources available to art conservators and scientists, then, include major monographs on Tanguy (Soby 1955; Karpel et al. 1963; Waldberg 1977; Cariou 2007; Le Bihan et al. 2001; Schmidt 1982; Maur and Davidson 2001) with the most complete biography of Tanguy's life documented in two books published to accompany the artist's retrospectives in 1982–83 and 2000 (Schmidt 1982; Maur and Davidson 2001). Other literature written by Tanguy and his peers such as André Breton, Marcel Jean, and Gordon Onslow Ford (Breton et al. 1946; Jean and Mezei 1960; Richter 1956; Onslow Ford 1978, 1983, 2001) provide insights into Tanguy's artistic process that are invaluable for technical research. These accounts were mostly written long after Tanguy's death and each reflect a single memory and perspective.

2.3.1 Condition Issues in Surrealist Paintings That Challenge Authenticity as a Dichotomy

The condition issues that we have observed in surrealist paintings further contribute to challenges in making definitive decisions regarding attributions. We have examined works by Fernand Léger, Max Ernst, Joan Miró, and Yves Tanguy that have had nearly their entire backgrounds overpainted, with the figures and the signatures left in reserve. The reasons for this treatment are sometimes obvious, as in the case of several works by Salvador Dalí and Yves Tanguy that were slashed in a political

attack (by the reactionary nationalist *Ligue des Patriotes*) in December of 1930 when they hung in the lobby at an early showing of *L'Age d'Or*, a movie by Dalí and Luis Buñuel (Durozoi and Anderson 2002; Crisp 2015; Breton et al. 1930). Tanguy exhibited three works in the lobby of Studio 28, where *L'Age d'Or* was shown. These works were titled *L'Orage*, *Les Mottes de Terre* (also known as *L'Homme* and *Homme et Femme*), and *Fraud dans le Jardin,* but it is not known which title belongs to which work. One of the Yves Tanguy paintings from this incident has recently been examined and appeared in seemingly excellent condition, resulting in questions about whether this could be a later copy of the destroyed painting.

Infrared and long-wave ultraviolet imaging did not reveal evidence of the painting's violent history, although the ultraviolet images did suggest that the tower, biomorphic figures, and signature have thin "halos" around them, suggesting that these components are now in reserve. X-radiography and x-ray fluorescence of the work together revealed evidence of both the *L'Age d'Or* damage, and that the painting had been subsequently cut down and relined. The original tacking margins are thus no longer extant, and there appear to be at least two restoration campaigns to the work. In the earlier campaign, a restorer inpainted the losses to the tower where the right-wing protestors had slashed through this element. The vanilla-hued background of the work was then largely overpainted to integrate the losses (with the signature left in reserve, Fig. 2.13). The materials used in this overpaint suggest that this occurred in a later campaign. A work in this condition, despite having overpaint covering approximately 60–70% of the work, is of tremendous historical and art historical value. The unique history of this work has written itself into the painting's condition, and is revealed by technical imaging that also contributes to a positive attribution for the work. The reasons for the overpainting of the white grounds of works by Fernand Léger, Max Ernst, and Joan Miró were less clear. However, in the case of the Fernand Léger painting the small amount of original white ground visible surrounding the signature left in reserve revealed brown staining of a zinc white ground, suggesting the reason for the overzealous restoration. Several of the overpainted works had zinc white grounds, but none of them showed evidence of the flaking associated with zinc soap formation and crystallization. The Max Ernst and Joan Miró works were treated similarly to the Fernand Léger and the Yves Tanguy, with the figural elements left in reserve and the overpaint tightly surrounding these figures. There was no visible evidence of discoloration of the original backgrounds for either the Max Ernst painting or the Joan Miró painting that would explain their having been given this treatment.

The observed discoloration appears to be organic in nature and may be due to the formation of chromophores in the oil binding medium (Levison 1985; de la Rie et al. 2017). Given the higher opacity and refractive index of the (invariably) titanium white overpaint, the overpainted backgrounds may simply have been carried out as an expedient solution for paintings that were starting to lose their freshness or brightness. This is a process that may have been accelerated by a general trend of

artists leaving their paintings unvarnished by the mid-twentieth century (Callen 1994; Richardson 1983).

Condition issues that we have observed on works by Tanguy include overcleaning, fading (of what appear visually to be synthetic organic pigments, particularly in the skies of his post-War works), darkened and discolored varnishes, and metal soap aggregation or agglomeration. The metal soap agglomerations are particularly problematic in his landscape compositions that have dark or black skies. The aggregation of lead soaps has led to the skies becoming paler and more translucent. This changes the balance of Tanguy's compositions leading to a lower contrast between the dark bands and the lighter bands, reducing some of the dramatic juxtapositions that the artist intended. The agglomerations formed originate within a preparation layer, resulting in the appearance of raised and off-white translucent spheres in the black skies. These not only subvert Tanguy's intended color dynamic, they also alter the planar surfaces that contribute to the unsettling power of many of his landscapes. Many Tanguy works in private collections have darkened overall with age (suggesting the degradation of a natural resin varnish) and there are works in public collections that appear to have been over-cleaned at some point in their histories.

2.3.2 Current Status of Yves Tanguy's Oeuvre

Our understanding of the current status of Yves Tanguy's oeuvre was acquired through interviews and discussions with Charles Stuckey and Stephen Mack that took place between 2018 and 2021; what follows below is a summary of these discussions. Because of the interruption of the most recent *catalogue raisonné* project, the number of extant works that can be confidently attributed to Tanguy is not known beyond the catalogue committee. In addition, Tanguy's friend Marcel Duhamel states in his biography that Tanguy himself destroyed an unknown number of his pre-surrealist works (Duhamel 1972; Soby 1955; Stuckey and Mack 2020). With respect to the physical integrity of his paintings, three of his works, including *Fantômas* (1925–1926), are known to have another work beneath them (discussed below). Figure 2.8 illustrates a nocturne that Tanguy painted over a nude figure, the Philadelphia Museum of Art's *The Storm (*or *Black Landscape)*, 1926. Tanguy did cut one of his larger works in half to create two independent paintings, one of which can be seen in the Mattatuck Museum (Connecticut).

Even the most rigorous attempt to document an artist's entire oeuvre in a *catalogue raisonné* cannot provide total protection against forged works contaminating the artist's legacy. In the process of compiling a *catalogue raisonné* it is almost never possible to inspect all of the artist's works in person, which can lead to omissions as in the case of Ambrogio Ceroni's Amedeo Modigliani *catalogue raisonné* (Ceroni et al. 1958). When a work is examined by photograph it can preclude the

possibility of identifying the finer details of the artist's technique in every painting (such as *grattage* lines, for example). In the case of the Yves Tanguy *catalogue raisonné* research, photodocumentation of each label on the verso of each work was obtained whenever possible, and any potentially spurious labels were subject to side-by-side comparison with extant examples from the institution in question[10] (Stuckey 2021). In addition, unless a work has gone directly from the artist into a museum collection and remained in that collection, provenance gaps in the twentieth century are likely. All of the provenance documentation was rigorously examined for each painting and the first mention and/or photographic documentation of each work was collected by Stephen Mack and Charles Stuckey as part of the *catalogue raisonné* project. Many of the paintings examined for the Yves Tanguy *catalogue raisonné* were first documented only after both Tanguy and Sage's deaths. While there has been no conservator working on the project to date, this is something that could be addressed in the next incarnation of the project. The technical data published here can begin to address the absence of a corpus of data on Tanguy's materials and techniques for identifying atypical works and should provide a starting point for scholars examining works by Tanguy in the future.

2.4 Extant Information on Tanguy's Working Methods

As mentioned above, Tanguy's painting materials and methods have not been widely studied or reported. The extant writings from the time reveal little about Tanguy's artistic motivations and practice. Thus, the summary of Tanguy's methods presented here is limited to physical and documentary evidence. Quotes from Tanguy and his peers relevant to the artist's process are considered invaluable but must also be qualified in the context of Tanguy's personal mythology and hearsay. Although Tanguy worked across various media, the focus of this text is on Tanguy's oil paintings on canvas, as these are the primary materials for the attribution concerns addressed in this chapter (Fig. 2.1).

No artworks survive from Tanguy's childhood, but by the mid-1920s Tanguy was painting in oil (Fig. 2.2). While he never sought formal training, he had by this time been exposed to the working methods of painters in Brittany and Paris.[11] It was Tanguy's close circle of friends who bought him his first oil painting materials, including a canvas, palette, brushes and oil paints, prompting Tanguy to build himself an easel (Duhamel 1972). Few of these early oils and gouaches survive.

[10] As is invariably the case in this type of research, not all of the labels found could be associated with a specific collection, sale, or exhibition.

[11] As a boy in Locronon Tanguy watched the Breton painter Charles Toche (1851–1916), who worked in dark glasses to record objects in chiaroscuro (Maur 2001, p. 13). As a teenager in Paris, Tanguy is known to have visited the studio of Pierre's father, the painter Henri Matisse (1869–1954) (Schalhorn 2001, p. 211).

Fig. 2.1 (*Left*) Yves Tanguy at work on *The Ears of a Deaf* in Paris, 1938. Photo: Denise Bellon © Estate of Yves Tanguy / DACS. Gordon Onslow Ford described Tanguy's 1938 one-room studio apartment in 1938 as "...spotlessly clean. The tubes of paint, palette and brushes were arranged in perfect order. He used his colors sparingly, and he still had not finished a tube of red paint from his original purchase at Etablissement Lefèbvre-Foinet"(Onslow Ford 1983, p. 15). (*Right*) *The Ears of a Deaf*, 1938, oil on canvas, 46 × 55 cm (18−1/8 × 21−5/8 in). The National Museum of Modern Art, Tokyo. Photo: MOMAT/DNPartcom

Fig. 2.2 Yves Tanguy, *Rue de la Santé*, 1925. Oil on canvas, 50.2 × 61.1 cm (19−3/4 × 24−1/8 in). The Museum of Modern Art, NY, Kay Sage Bequest, 338.1963 © Estate of Yves Tanguy / Artists Rights Society (ARS), NY. Photo: The Museum of Modern Art/ Licensed by SCALA / Art Resource, NY. Tanguy's first documented work in oil paint on canvas

After viewing his first surrealist exhibition in November 1925 Tanguy reportedly destroyed a large number of his works, Duhamel recalled Tanguy feeding many of these into a burning fireplace in "an hour of despair" (Soby 1955, p. 12).

Accounts of Tanguy's studios in Paris and Woodbury describe an ordered, spartan environment and an exacting painting method despite his use of less traditional techniques such as collage elements and sewn threads (*coudrage*) in several early works (Soby 1955, pp. 18–19) (examples of both techniques are seen in Fig. 2.3). From early in his career, Tanguy almost always dated his paintings (Soby 1955, p. 12). In the 1930s, Tanguy primarily lived and worked in one-room apartments. The effect of this austerity was described by fellow artist Gordon Onslow Ford, who

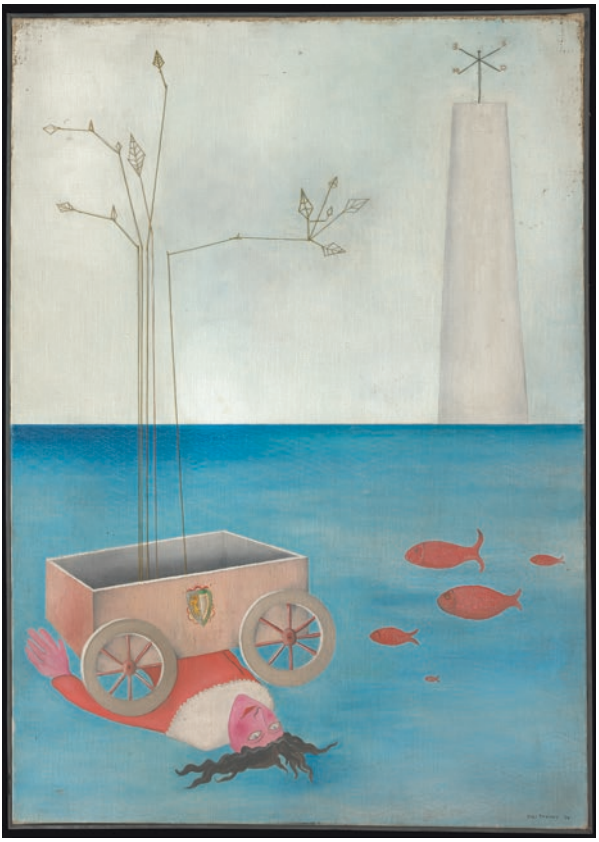

Fig. 2.3 Yves Tanguy, *Title Unknown*, 1926. Oil on canvas with string and collage, 92 × 64.8 cm (36 1/4 × 25 1/2 in). The Metropolitan Museum of Art, The Pierre and Maria-Gaetana Matisse Collection, 2002, 2002.456.6. © Artists Rights Society (ARS), NY. Photo credit: Art Resource, NY. Tanguy incorporated sewn threads (co*udrage*) to construct the linear plant forms and the weathervane in the ominous tower, which has been interpreted as a homage to de Chirico. The seal on the wagon is a paper collage element. Materials identified in this work are summarized in Table 2.1

Table 2.1 Comparison of palette found in Tanguy paintings executed between 1926 and 1942. All pigments and fillers were characterized noninvasively by X-ray fluorescence except where noted by an asterisk

Title, date, collection	*Title Unknown*, 1926, The Metropolitan Museum of Art, 2002.456.6	*He Did What He Wanted*, 1927, The Museum of Modern Art, 206.2008	*Mama, Papa is Wounded*, 1927, The Museum of Modern Art, 78.1936	*Title Unknown*, 1927, Private Collection, 5634	*Fraude dans le Jardin*, 1930, Private Collection	*Indefinite Divisibility, 1942,* Albright Knox Art Gallery
Red/ orange	Iron oxides Organic red lake[a] Vermilion[b]	Lead chromate Organic red lake Vermilion[b]	Iron oxides[c] Vermilion	Iron oxides Vermilion	Vermilion	Iron oxides Cadmium sulfoselenide Mixed cadmium yellow and iron oxide orange
Yellow	N.A.[d]	Cadmium yellow Chrome yellow Iron oxide yellow	Iron oxide yellow	N.A.	N.A.	Synthetic organic pigment Cadmium yellow
Blue	Prussian blue*	Cobalt blue Prussian blue	Cobalt cerulean blue	Cobalt blue Prussian blue	N.A.	Manganese blue Prussian blue*
Green	N.A.	Chrome green: lead chromate +Prussian blue[c] Viridian[e]	Chrome green: lead chromate +Prussian blue[c] Emerald green Viridian	Emerald green with lead chromate yellow	Chrome green: lead chromate + Prussian blue	Chrome green: lead chromate +Prussian blue Viridian +cadmium yellow
Brown/ black	Iron oxides Bone black Carbon-based black	Bone black	Umber Bone black	Iron oxides Umber indeterminate – carbon or bone black	bone black	Bone black*

(continued)

Table 2.1 (continued)

Title, date, collection	*Title Unknown*, 1926, The Metropolitan Museum of Art, 2002.456.6	*He Did What He Wanted*, 1927, The Museum of Modern Art, 206.2008	*Mama, Papa is Wounded*, 1927, The Museum of Modern Art, 78.1936	*Title Unknown*, 1927, Private Collection, 5634	*Fraude dans le Jardin*, 1930, Private Collection	*Indefinite Divisibility, 1942,* Albright Knox Art Gallery
White/ fillers	Lead white Zinc white Calcium-based white such as chalk or gypsum Barium-based, most likely barium sulfate	Lead white Zinc white Calcium-based white such as chalk or gypsum, traces of titanium	Lead white Zinc white Calcium-based white such as chalk or gypsum, with strontium and barium (likely barium sulfate filler)	Lead white Calcium-based filler such as chalk or gypsum Barium-based, most likely barium sulfate	Lead white Zinc white Calcium-based filler such as chalk or gypsum	Lead white Zinc white Titanium white Anatase and anhydrite coprecipitate* first ground, zinc white

*confirmed with molecular analysis by Raman spectroscopy
[a] Colorant (identified visually) precipitated on an alum-containing substrate, with Ba and Zn (identified by XRF)
[b]With Ba-based filler, most likely $BaSO_4$
[c]With Ba-based filler, most likely $BaSO_4$ and a calcium-based filler
[d]Not applicable
[e]With Ba-based filler, most likely $BaSO_4$ and a calcium-based filler
[f]Inferred from absence of elements indicative of inorganic components in XRF spectra

met Tanguy in 1938. According to Onslow Ford "There was only enough room in his studio, and in his mind, to make one painting at a time... A painting, once started, preoccupied him until it was finished" (Onslow Ford 2001, p. 200).

Although comparatively spacious, Tanguy's Connecticut studio was likewise "antiseptic...with no trace of the clutter of canvases, brushes, paint tubes, frames, or palettes ordinarily found in art studios. Tanguy kept all his tools on a table he had made himself that strongly resembled an operating table on wheels" (Soby 1949, p. 6; Richter 1956). "...Near his easel his colors were laid out in a compartmentalized wooden box he had made with as much skill and care as he lavished on a chess set he carved for his own and his wife's delectation" (Soby 1955, p. 18).

In 1940, shortly after Tanguy's arrival in New York, he entered into a contract with his old friend, Pierre Matisse which provided the artist with a monthly stipend in return for an agreed upon number of works. The contract was exceptional in that

it also allowed Tanguy to sell artworks privately at gallery prices with no commission to Matisse, with prices based on the European system of canvas sizes. However, according to Davidson and Rewald et al., Matisse and Tanguy quickly came to the realization that they would need to double the prices since Tanguy was such a meticulous and slow painter that neither could afford to keep them so low (Davidson 2001, p. 180; Rewald and Dabrowski 2009, p. 17).[12]

In 1954, Tanguy himself explained, "I work very irregularly and by 'crises' – sometimes for weeks at a stretch, but never on more than one painting at a time, not in more than one medium. Certain of my paintings are finished very quickly; others take two months or more. This does not depend on the size of the canvas" (Tanguy 1954).

2.5 Tanguy's Methods

Tanguy employed artistic techniques associated with other surrealist painters, who experimented in a collective effort to free the creative process from conscious restraint. Several of these methods, including collage and *grattage*, are especially evident in the artist's early work. De Chirico's profound influence is manifested in Tanguy's detached representation of objects and symbolic subject matter. The artist's use of hyperrealist techniques rooted in the conventions of pre-modern painting made tangible the unconscious world central to the surrealist ethos.

In 1926, Tanguy's compositions changed from figurative landscapes to symbolic images, where a select few motifs were arranged in a vast, divided space, sometimes with collage elements. In a transitional 1926 work at the Metropolitan Museum of Art (*Title Unknown*, Fig. 2.3), Tanguy incorporated sewn threads (*coudrage*) to construct the linear plant forms and the weathervane in the ominous tower, possibly with instruction from Tanguy's first wife Jeannette Ducrocq, who was an expert at applique work (Maur 2001, p. 24). Tanguy's earliest paintings have been described as "naïve in execution," and whether or not this was a conscious choice his technique developed quickly and his mature style emerged by 1927 (Soby 1955, p. 12).

Onslow Ford wrote that "Once Tanguy had found his technique, it stayed much the same, and became a personal calligraphy"(Onslow Ford 1983, p. 15). However, a clear evolution is evident in the artist's style and subject matter.[13] Tanguy's paintings typically depict thinly painted biomorphic forms and vegetation, dispersed over striated backgrounds, many of which are described as water, land, or sky elements of eerie and dreamlike landscapes. His forms become more refined and

[12] Original source cited in Davidson: Pierre Matisse to Gordon Washburn, 26 March 1940, The Pierre Matisse gallery Archives (note 7), box 80, file 14.

[13] The influence of artists such as de Chirico and other Surrealist painters on Tanguy's selection of specific materials must be assumed, but the lack of comparative data on the materials and techniques of many of these artists precludes confirmation of any conclusive similarities between artists or individual works.

overtly geological over time, ultimately crowding in the foreground of his late compositions of the 1950s.

Tanguy's use of *grattage*, in which he scratched into layers of darker wet paint to enable the lighter grounds to show through, has been attributed to his familiarity with Max Ernst's black ground panels of 1922–1923. These works incorporated processes used in printmaking, as well as the influence of photographic negatives and photograms utilized by contemporary artists such as Man Ray (Maur 2001, p. 31). In 1927s *He Did What He Wanted* (Fig. 2.4), the technique is visible in the biomorphic figure etched in the blue sky and black horizon. Vertical 'drips' through

Fig. 2.4 Yves Tanguy, *He Did What He Wanted*, 1927. Oil on canvas, 79.4 × 64.8 cm (31−1/4 × 25−1/2 in). The Museum of Modern Art, NY. Bequest of Richard S. Zeisler, 206.2008. © Estate of Yves Tanguy / Artists Rights Society (ARS), NY. Photo: The Museum of Modern Art/ Licensed by SCALA / Art Resource, NY. In several early works Tanguy populated his compositions with letters and numbers, in conversation with his graphic work of this period. *Grattage* lines are visible here in the biomorphic figure etched in the sky. Elemental analysis of the palette is summarized in Table 2.1

the black tentacled form in the foreground of the image are likely a form of *éclaboussure*, a technique used by surrealists where turpentine would be spattered or dripped through applied oil paint and soaked up to remove solubilized paint in these random areas.

This technique, which Tanguy also used in 1928 to create the sky of *Unspoken Depths*,[14] again evokes methods surrealists incorporated from printmaking to create abstract backgrounds and environments using solvents or monotyping. Gordon Onslow Ford described the artist's process[15] (Onslow Ford 1978, p. 18):

> This painting was made by allowing turpentine to run through a coat of blue-gray paint; then, paint was brushed across the canvas in undulating strokes. When the paint had dried for a day, personage-objects and etched lines were added...All that appeared was accepted just as it was.

Tanguy developed his technique in these transitional paintings (1926–1928) where vestiges of recognizable forms are retained. He used broad scraping, "manipulations of the semi-dry paint with a razor blade," and controlled the pressure of his brush to create long strokes with thin ribbons of impasto and exposed underlying paint (Onslow Ford 1983, p. 15) as exemplified in *Old Horizon*, Fig. 2.5. A photograph of Tanguy in his studio shows the artist with a mahl stick, a traditional painting tool used to steady the artist's hand (Fig. 2.6).[16] This tool consists of a stick or thin pole with a ball shaped pad on the end that can rest against the canvas edge or easel, allowing Tanguy to make very long, even paint strokes. This unique brushwork, as well as dry, wispy fumés are prevalent in works from the late 1920s and 1930s but are less frequent in the 1940s.

Although Tanguy's graphic output was prolific – he produced numerous significant drawings, prints, and gouaches throughout his career – he reportedly never made preparatory sketches for his paintings (see, for example, Soby 1955; Onslow Ford 2001, p. 200). Tanguy wanted it to be believed that not only were underdrawings not present in his mature work but that they would be antithetical to his surrealist artistic practice (Stuhlman 2013, p. 114), proclaiming "I found that if I planned a picture beforehand, it never surprised me, and surprises are my pleasure in painting" (Tanguy 1954, p. 15; Soby 1955, p. 17). Existing observations of Tanguy's works, while limited, conclude that the reality of the artist's process is more complicated (Stuhlman 2013, pp. 97–171).

Five paintings that Tanguy created after a visit to Tunis, North Africa, in 1930, were singled out by Tanguy as isolated exceptions where he planned out his compositions with graphite sketches on canvas (Soby 1955, p. 16; Solomon 1983, p. 8; Maur 2001, pp. 65–70). One of these paintings, *Promontory Palace* (Fig. 2.7)

[14] Yves Tanguy, Les Profondeurs tacites (Unspoken Depths), 1928. Oil on canvas, 100.3 × 73 cm (39−1/2 × 28−3/4 in). Private Collection. For an image of the painting see, http://kaitentou.blogspot.com/2013/09/yves-tanguy-and-multiplication-ofarcs.html (accessed October 7, 2021).

[15] It must be noted that Onslow Ford published this description decades after the work was created by Tanguy, and he is describing a painting made ten years prior to meeting the artist in 1938.

[16] This photograph depicts Yves Tanguy at work on the painting *Wine, Honey, and Oil*, 1942 (Schalhorn 2011, p. 230). The original source of this photograph could not be confirmed.

Fig. 2.5 Yves Tanguy, *Vieil horizon* (*Old horizon*), 1928. Oil on canvas, 100.0 × 73.0 cm. National Gallery of Australia, Canberra Purchased 1983, 83.3139. © Estate of Yves Tanguy/ARS/Copyright Agency. In this work, recognizable forms are still present in the two breasts that terminate the floating amoebic ribbon in the foreground. *Gratte* lines were used to form the sparse vegetation, as well as broad scraping to create the rhythmic waves receding into the horizon (Lloyd and Desmond 1992, p. 182). The effect is similar to a 'comb-stroke ' technique, which Tanguy also used to scratch parallel lines in thin layers of dark paint that exposed the lighter grounds

belongs to a series of works called *les coulées* (flowing forms) inspired by the African landscape. These paintings are unique in Tanguy's oeuvre, with their corrugated architecture and molten earth, as well as their desaturated palette and use of graphite to delineate forms.[17] Compared to Tanguy's more typical fluid, striated

[17] The use of graphite is inferred from the institutional media description and photographs and would need to be confirmed with physical examination.

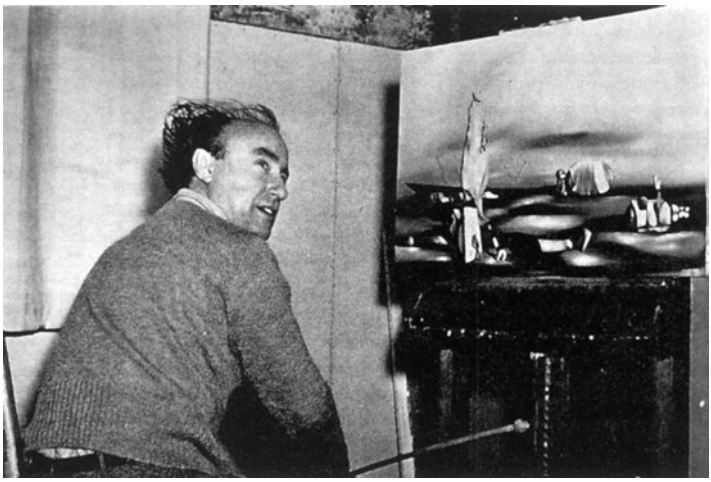

Fig. 2.6 Yves Tanguy at work on the painting *Wine, Honey, and Oil*, 1942. Photo: David Hare. Courtesy of the Estate David Hare (Maur 2001). Notable here is Tanguy's use of a mahl stick (here visible resting on the artist's knee), a traditional painting tool that would help Tanguy steady his hand to create his fine, steady lines and long, even brushstrokes

paint application, the surface of *Promontory Palace* appears chalky, with scattered fine black lines that look like scratches on a copper intaglio plate or projected film.[18] At least some of these lines, such as the rays emanating from the tower in the top left, were made by scratching into the paint surface with a sharp implement, and the resulting lines are much finer and etched into drier paint than the gratte lines visible in other Tanguy works (Rudenstine and Solomon 1985, p. 714).

A close examination of this painting reportedly reveals no traces of a preparatory drawing, so it is uncertain whether this preparation was only partial or erased by Tanguy as the composition developed (Rudenstine and Solomon 1985, p. 714). Additionally, no known technical imaging of these works has been carried out to confirm or refute this mythology. Only a small number of Tanguy's works have been subject to infrared photography or reflectography to document the presence or absence of underdrawing or pentimenti.[19] These imaging techniques, as well as radiography and XRF mapping, could also elucidate the extent to which Tanguy reused canvases. Evidence of this reuse exists for several works, including the work known as *The Storm (L'Orage)*,[20] 1926, currently in the collection of the Philadelphia Museum of Art, and *The New Nomads*, 1935, currently in the collection of the

[18] Tanguy began producing etchings in Stanley W. Hayter's Paris studio in 1932. Except for a brief hiatus during his move to the United States (1939–42), where Hayter also transferred his Atelier 17 in 1942, he continued to make etchings for the rest of his career.

[19] Personal communication with Charles Stuckey December 2020 e-mail interview.

[20] This work has been known as The Storm since 1936 only, and may have originally been known by another name.

Fig. 2.7 (*Left*) Yves Tanguy, *Palais promontoire* (*Promontory Palace*), 1931. Oil and graphite on canvas, 73 × 60 cm (28−3/4 × 23−3/8 in). Peggy Guggenheim Collection, Venice (The Solomon R. Guggenheim Foundation, New York) 76.2553 PG 094. © Estate of Yves Tanguy/Artists Rights Society (ARS), NY

Ringling Museum of Art.[21] In both works, the underlying image seems inconsistent with Tanguy's style, suggesting these were painted on canvases used by other artists. A radiograph of *The Storm* (Fig. 2.8) reveals an underlying standing nude figure in the center, with expressionist daubs of paint. An underlying standing figure in *The New Nomads* is faintly visible in normal illumination, executed in a formal linear style that does not evoke Tanguy.[22]

[21] The title of this painting may change in the forthcoming *catalogue raisonné*.

[22] Yves Tanguy, *Les Nouveaux Nomades (The New Nomads)*, 1935, oil on canvas, 31 3/4 × 27 7/16 in. (80.6 × 69.7 cm). Ringling Museum of Art, Gift of the Estate of Kay Sage Tanguy, 1964, SN782. An infrared image (900–1700 nm) of the painting captured in 2019 elucidates this underly-

Fig. 2.8 (Left) Yves Tanguy, *The Storm (Black Landscape)*, 1926. Oil on canvas. 81.6 × 65.4 cm (32−1/8 × 25−3/4 in). Philadelphia Museum of Art, The Louise and Walter Arensberg Collection, 1950, 1950-134-187 © Estate of Yves Tanguy / Artists Rights Society (ARS), NY. (Right) Composed X-radiograph of *The Storm*, revealing an underlying standing nude figure in the center, with expressionist daubs of paint. The x-radiograph was captured in 1979, prior to lining of the canvas. Photo: Philadelphia Museum of Art

In the early 1930s Tanguy appears to have produced relatively few paintings (based on his extant works), and experienced crushing poverty most acutely during 1931–1932.[23] While he took on book illustration projects to support himself during this period, he ultimately had to give up his studio and live a peripatetic life until his emigration to America (Le Bihan et al. 2001, p. 244). In 1933, there was a perceptible change in Tanguy's compositions, with chromatic, fluid shapes localized in the bottom of the image (*The Nest of the Amphioxus*, Fig. 2.9). Tanguy's use of color became more complex and varied, with extremes of lights and dark replacing the relatively even tonality of his previous pictures after his African voyage (Soby 1955, p. 18). In paintings after 1930, Tanguy tended to use a somewhat thicker application of paint and stronger colors compared to the glazed, translucent paintings of the 1920s with their subdued palette (Maur 2001, p. 75).

To create Tanguy's heavily thinned, blended backgrounds, visual inspection suggests that the artist diluted his oil paints with turpentine to almost liquid consistency. This allowed Tanguy to create subtle and controlled gradation of tones. However,

ing figure as well as additional landscape features. https://emuseum.ringling.org/emuseum/objects/26090/les-nouveaux-nomades (accessed 3/25/2021)

[23] A dozen or so known paintings by Tanguy were created between 1931 and 1933. Future research may revise this number.

Fig. 2.9 Yves Tanguy, *Nid d'Amphioxus (The Nest of the Amphioxus)*, 1936. Oil on canvas, 65 × 81 cm (25−9/16 x 31−7/8 in). Musée de Grenoble, gift of Peggy Guggenheim, 1954

there are works where drying cracks are evident that are attributed to the artist's process, suggesting that despite his sensitivity to his materials Tanguy did not always work within the limitations of the oil medium. The conditions in which this work survived World War II are likely also a contributing factor to the craquelure observed (Mack 2021). The smooth, often pristine surfaces of many of Tanguy's paintings make these condition issues much more visually disruptive, and so it is not surprising that these works have been subject to extensive retouching in conservation campaigns. The effects of 'inherent vice' in Tanguy's paintings was described (Onslow Ford 1983, p. 15): "The technique of oil paint was not in all respects suited to Tanguy's needs. Oil paint worked well when applied wet into wet, and when lines were etched into the paint, but in places where semi-dry paint was painted over, thin over fat, the surface cracked, as can be seen in many of the dark shadows and in *The Nest of Amphioxus*, 1936 (Fig. 2.9).[24] Tanguy occasionally used gouache, which dries fast, and so areas that could be blended while wet were limited in size; in this medium only small paintings were possible. Tanguy subordinated the requirements of technique to being true to the reality of Planet Yves."

In the 1930s, the miniature forms and structures in Tanguy's painting became increasingly solid, casting elongated shadows that evoke waxing or waning light that become fixtures in the artist's late works. Between 1936 and 1938, he created a

[24] Again it must be noted that Onslow Ford is making this observation about a work painted by Tanguy before the two artists met.

series of small landscape-oriented compositions. Tanguy's introduction to Kay Sage in the fall of 1938 facilitated the artist's emigration to the United States in late 1939. This move is thought to have had a significant impact on his work. In addition to a reorganization of his compositions, Tanguy acknowledged the expansion of his palette, and reflected "what the cause of this intensification of color is I can't say. But I do recognize a considerable change. Perhaps it is due to the light. I also have a feeling of greater space here – more 'room'. But that was why I came." (Sweeney 1946, p. 23). This expansion may have been spurred in part by the new pigments incorporated into artists' paints in this period, and is discussed in more detail in the Materials section below. A change is particularly noticeable in the brightly colored paints Tanguy used in many of his skies in this period.[25]

In the 1940s, as Tanguy settled in America, the complexity and texture of Tanguy's forms and their relationships to each other in his compositions began to develop in step with his prolific graphic output. For example, he had been creating drawings in which a single or occasionally a pair of forms dominated the composition since the late 1930s, but it was not until the early 1940s that his paintings began to move in this direction as well.[26] This is demonstrated in the 1942 work *Indefinite Divisibility* (Fig. 2.10), where figures occupy nearly half the picture's height and span its full width. Tanguy's painting technique, however, appears consistent, with figures and shadows meticulously applied over backgrounds of heavily thinned and blended paint.

In the 1950s, Tanguy's ossified forms propagated and became entangled, with monoliths and angular negative shapes punctuating his misty landscapes. These negative shapes are described as expanses of exposed off-white ground held in reserve (Maur 2001, p. 114). His cropping of the figures in the composition along the sides, as well as the bottom also becomes more common in this period. Among Tanguy's last paintings are his most monumental, with both a 1949 work, *Fear II*, and Tanguy's penultimate masterpiece *Multiplication of the Arcs*, 1954 (Fig. 2.11) respectively measuring 40 × 60 inches and 60 × 40 inches respectively.[27]

The artist's refinement and slow expansion of detail and scale in his late works demonstrates true evolution. Familiarity with the techniques he used at different points of his career provides context that is crucial to evaluating both attributed and autograph Tanguy works.

[25] This bright palette is especially evident in works such as Tanguy's 1940 work La Lumiere (The Solitude): https://arthistoryproject.com/artists/yves-tanguy/light-loneliness/ (accessed 8 October 2021).

[26] For a more complete discussion of the relationship between Tanguy's graphic output and his painting see (Stuhlman 2013, p. 91; Wolf 2001).

[27] *La Peur II* (*Fear II*), 1949, oil on linen, 60 × 40 in. (152.4 × 101.6 cm). Whitney Museum of American Art, New York; purchase, 49.21; *Multiplication of the Arcs*, 1954. Oil on canvas, 40 × 60″ (101.6 × 152.4 cm). Museum of Modern Art, Mrs. Simon Guggenheim Fund, 559.1954.

Fig. 2.10 Yves Tanguy, *Divisibilité indéfinie* (*Indefinite Divisibility*), 1942. Oil on canvas, 101.6 × 89 cm (40 × 35 in). Albright-Knox Art Gallery, Buffalo, NY, Room of Contemporary Art Fund, 1945, RCA1945:2. © Estate of Yves Tanguy / Artists Rights Society (ARS), NY. Photo: T. Loonan, Albright-Knox Art Gallery / Art Resource, NY. Materials identified in this work are summarized in Table 2.1

2.6 Tanguy's Materials

Although the initial source of the first canvas and oil paints given to Tanguy by his friends is unknown, Onslow Ford and Schalhorn suggest that by 1926 Tanguy was supplied with painting materials from the Lefèbvre-Foinet company in Paris and the artist continued to use these paints during his career (Onslow Ford 1983, p. 15; Schalhorn 2011, p. 216). The identification of three Tanguy works painted on reused canvases [*Fantômas* (1925–1926), *The Storm (*or *Black Landscape)* 1926, and *Les Nouveaux Nomades* 1935], however, indicates additional sources for Tanguy's materials in his career. For each of these reused canvases the infrared imaging suggests that the underlying painting was painted by another artist (based on stylistic assessment). Nonetheless, the Lefèbvre-Foinet company, which was located less

Fig. 2.11 Yves Tanguy, *Multiplication of the Arcs*, 1954. Oil on canvas, 101.6 × 152.4 cm (40 × 60 in). Museum of Modern Art, Mrs. Simon Guggenheim Fund, 559.1954. © Estate of Yves Tanguy / Artists Rights Society (ARS), NY. Despite Tanguy's dismissal of geographic influences on his imagery (Schmidt 1982, p. 273), frequent comparisons have been made to his works from this period and the monolithic stone structures and rocky shores of the Breton coastline near Tanguy's childhood home, as well as the American landscapes Tanguy encountered late in life

than a mile from Tanguy's shared apartment in Montparnasse, was an important supplier for Tanguy. The company was famous for their high-quality art materials, including prepared canvases and hand-prepared tube oil paints, as well as art storage and shipping.[28] In 1927 or 1928, Tanguy came to an arrangement with Lucien Lefèbvre-Foinet where he would receive painting supplies from the firm on credit, partly in exchange for pictures (Maur 2001, p. 50).[29] The firm's name is documented

[28] Lefèbvre-Foinet was a partnership between Lucien Lefèbvre and Paul Foinet established ca. 1897–1904. Paul Foinet had been making oil paints since the 1880s following 'a secret recipe,' and prepared canvases and paint brushes that he sold directly to artists. Lucien Lefèbvre was Paul's son-in-law who set up a storefront in the Montparnasse neighborhood. When Lucien Lefèbvre's son Maurice took over in the 1950s, relationships with artists developed on a grand scale, and the company remained in the family until it closed in 1994.

See, for example, British Artists' Suppliers 1650–1950. London: National Portrait Gallery; 2016. Paul Foinet; https://www.npg.org.uk/research/programmes/directory-of-suppliers/f.php (accessed March 11, 2021)

[29] Lefèbvre-Foinet regularly made such credit arrangements with artists and amassed a large art collection (Melikian 2009).

on the back of several Tanguy works, including *Noyer Indifférent,* 1929 (Maur 2001, p. 58, 233) and *Title Unknown*, 1936 (Schalhorn 2001, p. 229).[30]

There is evidence that Maurice Lefèbvre-Foinet (Lucien's son) safely stored canvases left in Paris by Tanguy during World War II (Davidson 2001, p. 187). Tanguy may have continued using the firm as a supplier and shipper of his works, as the firm was used extensively by American artists and was known internationally for covering the customs costs for transporting works abroad (Katlan and Falk 1987; Hélou-de La Grandière and Casadio 2019, p. 408). Documentation of materials prepared by Lefèbvre-Foinet are compiled here to inform technical study of Tanguy's works, including their condition, although the artist was likely also supplied by other as yet undocumented manufacturers, especially in the United States.

Supports A survey of the dimensions of Tanguy's published paintings on canvas suggests that the artist generally used standard French canvas sizes that would have been available pre-stretched with a commercially applied ground.[31] Each size would be identified by a number and available in three formats, *figure*, *paysage*, and *marine*.[32] Tanguy notably used a wide range of sizes throughout his career, with canvases correlating to 42 of the 78 or so standard French sizes typically available, and favored the portrait (vertical) orientation for his compositions. Suppliers such as Lefèbvre-Foinet would also prepare custom sizes to order, and canvases by Tanguy that do not conform to standard sizes may have been requested or prepared by Tanguy himself. From 1941, when Tanguy was working in the United States, he appears to have used standard American canvas sizes as well as the European sizes, suggesting he was not wedded to Lefèbvre-Foinet for his supports.

No meaningful size preferences in each decade of Tanguy's career are evident. The most common size is the No. 40 Portrait (100 × 81 cm), although this accounts for only 28 or so out of hundreds of canvases. Tanguy's poverty in the early 1930s is reflected in the small number of works he produced during this period, but is not obvious in the dimensions of his works. Tanguy's largest single-canvas works (measuring 40 × 60 inches) date later, to 1949 and 1954.[33] The six works examined in this

[30] *Noyer Indifferent*, 1929. Oil on canvas, 92 × 73 cm. Private collection. The work referred to here as Title Unknown has previously been published with a different title: Fragile, 1936. Oil on board with canvas structure, 9.1 × 21 cm, Private collection.

[31] Tanguy's paintings on canvas with published dimensions were derived from the 1963 *raisonné* and 1983 retrospective to give a *non-comprehensive* overview of Tanguy's preferences for supports, and included data from approximately 244 works. Additional works were on alternate supports, were multi-part works such as screens, or were listed with no dimensions. Different conclusions may be drawn from further documentation of more paintings by Tanguy. Sizes may differ slightly if a work has been restored, including relining and stretching, which may enlarge the original dimensions.

[32] For a history and explanation of standardized European canvas sizes, see for example Callen 1982.

[33] These include *Fear II*, 1949, 60 × 40 in. (153 × 102 cm) and *Multiplication of the arcs*, 1954, 40 × 60 in. (102 × 153 cm).

study were executed on plain-weave canvas. Tanguy painted on canvases with varying thread counts and textures that would impact the appearance of his thinly painted surfaces. His earlier works in particular highlight the texture of the support using dry brush effects, while some later works have relatively featureless surfaces. Canvas texture may become more apparent than the artist intended if a painting has suffered abrasion of the paint surface or overcleaning during an aggressive conservation campaign.

Preparatory Layer(s) The conclusion that Tanguy used commercially primed canvases is based on the few examined works in this study having priming layers that extended to the cut edge of the tacking margins of each canvas. Commercial priming was applied by the supplier on large pieces or rolls of canvas that would be later cut down and tacked onto their respective stretchers. Where canvases are primed by hand (i.e., by the artist) after stretching, only the face of the canvas is typically covered.

An examination of production methods for commercial priming and specifically those used by Lefèbvre-Foinet during Tanguy's career can help guide the assessment of potential condition issues when examining the artist's paintings. In the early twentieth century, the commercial priming would typically be composed of a glue sizing layer and one or more subsequent coats of opaque color bound with a drying oil. Canvases with different numbers of coats were offered to allow artists to control the absorbency of the ground and retain or reduce canvas texture to achieve different painterly effects. Insufficient drying time between coats or before an artist would apply paint to the surface was a risk for artists using these prepared supports, and cracking in the paint layer could result from a ground that continued to dry after it had been painted on. Canvases prepared by Lefèbvre-Foinet in the 1950s, for example, are known to be problematic, having an oil-rich lead-containing ground with a high concentration of lead palmitate (Barbarant and Hélou-de La Grandière 2012). Lifting and flaking of paint, most commonly at the ground/paint interface, have been observed in these works. During this period the supplier reportedly tried to reduce the manufacturing time for their grounds, but it is not known if driers were intentionally added to the lead white to accomplish this (Hélou-de La Grandière and Le Hô 2008). Additives such as metal soaps could be used to catalyse the drying of the priming, or sprinkling powder to prevent the priming from sticking when rolled were commonly used and could induce chemical or physical changes in the priming (Caldwell 2001).[34] Moisture would also play a significant role in the

[34] The composition of the powder used by Lefèbvre-Foinet is not specified. A number of nineteenth century sources describe the practice of sprinkling powder into the final layer of wet/tacky oil ground to absorb oil, improve the adhesive properties of the ground and subsequent paint layers, and protect a lead white ground layer from physical and chemical degradation (Stols-Witlox 2018, p. 121, 166). Excess powder on the ground surface would generally be removed before the priming was left to dry. Materials used include marble powder ((Kingston 1835, p. 35; Stols-Witlox 2018, p. 120), pumice powder (Hampel 1846, pp. 22–23; Stols-Witlox 2018, p. 120), flour (Hundertpfund

development of lead soaps in pre-primed canvases. A descendant of Lefèbvre-Foinet acknowledged that "...especially during the summer, when high temperatures caused exudation from the ground(!). Degreasing the surface with turpentine was then absolutely necessary" (Hélou-de La Grandière 2005; Hélou-de La Grandière and Casadio 2019, p. 396).[35] There are also accounts that the firm pre-oxidized their linseed oil by exposing it to the sun in order to 'bleach' it (Hélou-de La Grandière and Casadio 2019, p. 407). While the resulting oxidized fractions of the oil can improve the flexibility of the resulting paint layer, it can result in incomplete drying of the paint (Bronken and Boon 2014; Hélou-de La Grandière and Casadio 2019, p. 407).

The documented inconsistency of lead white pigment used by paint manufacturers in the early to mid-twentieth century has also played a role in condition issues in these works, in particular after World War II when new manufacturing processes for lead white were developed (Zucker 1999). Different forms of lead white pigment have been identified in Foinet's grounds of the 1950s, with varying chemical properties and morphologies that are thought to affect the drying of the oil in these ground layers (Helou-de La Grandière and Le Hô 2008).[36]

Elemental analysis of the white pigments and fillers used in the preparatory layers in the studied Tanguy works from the 1920s suggests that they were painted on a lead white-based ground with a zinc white-containing preparatory layer applied on top. A calcium-based extender such as chalk or gypsum was identified in the six works included in this study (executed between 1926 and 1942). Traces of titanium were also identified in the ground of *He Did What He Wanted* (1927), while the barium identified in *Mama, Papa is Wounded* (1927) and *Unknown Title* (1927) likely indicates the presence of a barium sulfate filler. *Indefinite Divisibility* (1942), in contrast, was executed on a titanium dioxide (anatase) based ground with a gypsum filler, likely with a zinc white preparatory layer. Additional stratigraphic and molecular analysis would be needed to confirm this interpretation and identify the presence or absence of metallic soaps and other chemical or physical changes in the preparatory layers.

Palette In addition to the issues in ground layers prepared by Lefèbvre-Foinet described above, high concentrations of lead soaps have also been observed in white tube paints supplied by the Parisian manufacturer, resulting in cleavage occurring between the white paint and overlying paint layers (rather than the ground and paint). This has been attributed to slower drying oils such as safflower and poppy-

1847, pp. 127–129; Stols-Witlox 2018, p. 166), and zinc white pigment (or 'filler') (Church 1890; p. 26, Stols-Witlox 2018, p. 166).

[35] Phone conversation with Lefebvre-Foinet's grandson, in reference to the supplier's three-layer oil grounds.

[36] A lead white ground made up of a plumbonacrite-hydrocerussite combination was used by Lefebvre-Foinet and has been found in paintings by other artists who bought their supplies there, such as Pierre Soulages and Paul-Emile Borduas.

seed that Lefèbvre-Foinet used to limit the yellowing of light-colored tube paints (in contrast to the linseed oil used in their white ground layers) as well as pigments with higher oil absorption such as cobalt blue and bone black (Corbeil et al. 2011, p. 40, 67).

Tanguy executed his paintings using a relatively limited palette of colors. His paints were often extensively thinned and blended on the canvas, but the colors themselves do not appear to be complex mixtures. Elemental analyses of Tanguy's paints in this study suggest that most of his hues are either single pigment colors (with fillers typical of commercial tube paints), simple mixtures that were likely prepared by the manufacturer (such as chrome green), or artist mixtures of a few pigments with white and/or black to modify the value.

The six paintings examined to date reveal that Tanguy's palette consisted of Prussian blue, cobalt blue, cerulean blue, manganese blue, emerald green, chromium-oxide based green, chrome green (a composite pigment where Prussian blue is precipitated with a chrome yellow pigment, here with barium sulfate and a calcium-containing filler), vermilion red (with barium sulfate), an organic red lake pigment on an alum substrate, cadmium yellow, chrome yellow, an organic yellow, zinc white, lead white (with calcium-based filler), bone or ivory black (note that any carbon blacks such as lamp cannot be identified with the techniques used), and iron oxide-based reds, yellows, and browns (see Table 2.1).

Additional pigments are likely to be present in the examined works, such as synthetic organic pigments, that will require future study using molecular analysis techniques or standoff molecular imaging methods such as FORS or hyperspectral imaging. Prior analyses of Lefèbvre-Foinet's artists' tube oil paints from the 1950s–1970s identified synthetic organic pigments such as Hansa Yellow 10G (PY 3), Toluidine Red (PR 3), chlorinated Para Red (PR 4), and Alizarin Red (PR 83), which would all have been commonly used by paint manufacturers during Tanguy's full career. Additional synthetic organic pigments identified in oil paints by Lefèbvre-Foinet include Copper Phthalocyanine Blue (PB 15) and Phthalocyanine Green (PG 7), which would have been available after the late 1930s (Corbeil et al. 2011, pp. 41–43). Visual examination and elemental analysis together support Tanguy's use of organic red pigments in his early works (see, for example, the dark red used in the conical figure in 1927s *He Did What He Wanted,* Fig. 2.4) as well as an organic yellow in the 1942 work in this study. The stability of these materials varies, and certain pigments such as para red (PR 4) or litho red (PR 49) are particularly vulnerable to degradation and fading from light exposure (Herbst and Hunger 1993). The fading of organic pigments in works by other artists such as Mark Rothko has dramatically altered their appearance (Standeven 2008), and it is important to consider this type of potential visual change in Tanguy's paintings. His thinly painted surfaces may also leave these materials more vulnerable to degradation.

Onslow Ford commented on Tanguy's sensitivity to the material qualities of his paints, noting that the artist "spoke of the year that the paints were made as if they

were wine (the 1934 paints were a bit too oily, et cetera)" (Onslow Ford 2001, p. 200). While this implies that the variable properties of artisanal artists' paints have a romantic charm, it should also be acknowledged that Tanguy created his paintings during a time of rapid change for artists' materials manufacturers. The dependency of art manufacturing on larger global events was especially impactful in the interwar period and after World War II. For example, the American paint company Bocour had problems obtaining cadmium- and cobalt-based pigments during and immediately after World War II, the latter shortage perhaps leading to the substitution of ultramarine for cobalt blue and Phthalocyanine Blue (PB 15) for a cobalt stannate cerulean blue in 'cobalt' oil paints analyzed from this period (Rogge and Epley 2017). These firms likely had several suppliers for raw materials, and the supplier or paint maker might be responsible for formulation changes unknown to the artist. Although these changes were most evident in pigments and synthetic resin paints (which are not known to be used by Tanguy), even Lefèbvre-Foinet purchased their linseed oil from various geographic regions (Hélou-de La Grandière 2005) and minor differences in each material and how they are processed might impact their characterization and interpretation.[37] The consequence of this complexity is that analytical results of paint samples can only capture snapshots in time and may or may not apply broadly to Tanguy's oeuvre (Golden 2016). This makes comprehensive studies of Tanguy's materials and methods imperative to drawing meaningful conclusions in the study of questioned artworks.

The historical information presented above is required to aid in the interpretation of the scientific study of Tanguy's works. His history as an artist, his influences and colleagues, and even his friendship and geographical proximity to Alexander Calder can all assist with understanding and interpreting the changes in materials and methods that we find during scientific investigations of his works. Knowing where he purchased his artist's supplies while in Paris, and when he moved to the United States provides us with insight into the potential changes in materials available to him and thus one reason why he may have deviated from his pre-war palette choices. As noted above, the war had a noticeable effect on artists' materials availability (particularly cobalt and cadmium-based pigments) which could easily change which pigments Tanguy had access to and used.[38] With the context provided above, scientific investigation can provide more germane data for both art conservators and art historians.

[37] The degree to which these potentially subtle physical and chemical differences are detected depends on the analytical technique(s) employed in each study.

[38] "Mark Golden said that his company had difficulty obtaining cobalt-based colorants during and immediately after World War II (Golden), which perhaps led to the substitution of ultramarine for cobalt blue and phthalocyanine blue (PB) for a cobalt stannate cerulean blue, the pigment found in the sample of Cerulean Blue Artist Oil Colors." (Rogge and Epley 2017)

2.7 Scientific Study of Yves Tanguy Works

2.7.1 Technical Imaging

The MA-XRF data presented above provides an overview of Tanguy's pigment mixtures for the foreground of the 1926 painting *Title Unknown* (Fig. 2.3), including the girl under the cart. The likely use of iron oxide brown pigment for painting the cart is shown in the Fe distribution map. The darker brown hues of the spokes of the wheels and the left wheel are also reflected in this map. The distribution of iron in the foreground (Fig. 2.12) is due to the use of Prussian blue ($Fe_4[Fe(CN)_6]_3$), whose presence was confirmed by Raman spectroscopy analysis, and adds to our understanding of its distribution. The Fe distribution map also allows for the identification of iron oxide pigments in the locks of her hair, as well as what appears to be additional Prussian blue surrounding her hair, creating a visual contrast between the brown hair and blue background. The lead and zinc distribution maps reveal what is likely to be a lead white commercial ground followed by a zinc white additional preparation layer. This layer structure is also suggested by the *gratte* lines that appear to have pushed aside the still-wet zinc white-based paint layer to expose the lead white-based paint layer. However, cross-section microanalysis would be required to confirm these observations. The girl's collar has both lead and zinc, with lead predominating in this element of the composition. Interestingly, the paint in the girl's face is composed of a purplish pink pigment mixed with lead white, while in her left hand, the mixture contains zinc white. The slightly yellow hue of the girl's collar may be due to the presence of an aging varnish, and likewise the yellowish hue of the girl's eyes.

The zinc distribution map also reveals that zinc white was used by Tanguy to add selected light brown highlights to the girl's hair. These highlights are near the girl's crown, and in the locks spreading to the left of the girl's head. Based on the calcium distribution, bone black is suggested as another component of the paint in the girl's hair. Tanguy used an iron oxide brown mixed with zinc white to make several locks of lighter brown hair that extend into the foreground of the image (see, for example, the leftmost upside-down v shape in the iron distribution map). Note that not all of the locks of hair that are rich in zinc white also have added iron oxide brown – this allows Tanguy to produce a variegated and naturalistic effect to this disquieting scene.

The mercury distribution map reveals that Tanguy used vermilion to paint the girl's lips, but the absence of this element in the rest of the girl's flushed face is consistent with its more purple tone which is often suggestive of a natural lake pigment or a synthetic organic pigment. While there is a strong lead signal in the girl's face this appears to be due to lead white rather than red lead because of its lack of correlation with the pinkish hues of her flesh, and, as noted above, to her flushed skin having a more purplish red (as opposed to an orangish red) hue. The elements of the composition that do have an orangish red hue include the fish and the girl's

Fig. 2.12 (*Top left*) Reference image of the analyzed Area 1 of *Title Unknown*, 1926 (The Metropolitan Museum of Art, 2002.456.6) together with the corresponding elemental distribution maps, clockwise from top right: iron (Fe Kα), mercury (Hg Lα), calcium (Ca Kα), zinc (Zn Kα), and lead (Pb Lα)

dress. Tanguy used vermilion to paint these elements, as can be observed in the mercury distribution map. Barium was detected by XRF in the paints that contain mercury, revealing that the vermilion Tanguy was using had been mixed with a barium-based filler, most likely barium white (barium sulfate).

The calcium distribution map obtained by MA-XRF is of particular interest because it indicates the use of both bone black, which contains Ca and P from hydroxyapatite, and a chalk or gypsum filler in the iron oxide brown of the wagon. The calcium signal at the end of the girl's left sleeve, which is rendered in black

paint, suggests that Tanguy used bone black here as well. Calcium based fillers were also revealed by this map in the white of the girl's collar and in the flesh of her face.

The six works selected for analysis represent three decades of Tanguy's output, with an emphasis on the late 1920s where some of the most important questions about his oeuvre and his technique lie. Tanguy's paint surfaces are invariably smooth with little craquelure and many of his canvases had their tacking margins cut down when the works were relined. As a result, our research has focused on noninvasive imaging and spectroscopic methods, with only rare opportunities to elucidate elemental findings with microanalysis on samples. The data in Table 2.1 are thus best understood by considering the artist's pre-war or French period as distinct from his postwar or American period. In both his pre-war and post-war periods Tanguy used a limited palette to create his uncanny landscapes and the biomorphs that populate them. He used a synthetic iron oxide red pigment in four of the six studied works, and vermilion red in the five pre-war paintings.[39] In the one post-war painting included in this study, Tanguy replaced the vermilion red in his palette with a cadmium sulfoselenide red. He used a lead chromate orange in two of his pre-war works. The vermilion paint Tanguy used (presumably from Lefèbvre-Foinet) is in all of the studied paintings, bulked with a barium-based filler, most likely barium sulfate. This was observed in the colocation of barium and mercury in the MA-XRF maps acquired in The Metropolitan Museum of Art , *Title Unknown* 1926 painting (2002.456.6). In the geometric figure of *He Did What He Wanted* (Fig. 2.4), Tanguy mixes a largely synthetic organic red paint with vermilion and lead chromate.

The presence of phosphorus and calcium or iron was used to categorize the black pigments noninvasively. In five of the six paintings studied, Tanguy used a bone black rather than another carbon-based black not containing Ca and P, such as charcoal or lamp black or Mars black. In the sixth painting, the signal was insufficient to distinguish between a bone black and another carbon-based black. These findings suggest that Tanguy had a distinct preference for the warmer undertones of bone black. The use of bone black for the hair of the little girl in the MMA's painting, together with the presence of a chalk or gypsum filler for the flesh tone of the figure, can be seen in Fig 2.12. Tanguy's use of chrome yellow, cadmium yellow, and Mars yellow in *He Did What He Wanted* (Fig. 2.4) reveals that his financial situation did not constrain him to the less expensive yellow pigments, and he used all three of these pigments together to create the number 17 in this painting. He used cadmium yellow to create the warm-hued yellow panel of the geometric object in the foreground.

One of the most prominent and recurring features of Tanguy's landscapes are large, variegated fields of predominantly blue paint that represent the sky or, less

[39] The determination of iron oxide red versus red ochre (which contains clay minerals in addition to iron oxides) was by visual inspection.

commonly, the sea. Five of the six works examined here contain blue painted backgrounds, and Prussian blue was identified or inferred from the data for four of these works. Tanguy mixes this pigment with a cobalt blue for the sky of *He Did What He Wanted*, while the blue sky of *Mama, Papa is Wounded* is entirely cobalt-based cerulean blue. After the War, the blues of Tanguy's skies become heightened and intensified. In the one post-war work studied here, this is a result of Tanguy mixing manganese blue, which has a brighter and more turquoise hue, into his Prussian blue. Manganese blue pigment is an unusual finding. The pigment is a barium manganate sulfate [$xBaSO_4.yBaMnO_4$] that was patented by I.G. Farbenindustrie in 1935 (although it may have been known as early as 1907) and was used until the 1990s (Clark 1995). Manganese blue was produced commercially in Europe starting in 1942 (Van den Berg 2019). Unlike the cobalt blue used in Tanguy's earlier works, manganese blue has a greenish-blue hue (Accorsi et al. 2014). Accorsi et al, in their recent study of the pigment were only able to find documented use of the pigment by a single artist – Diego Rivera (Accorsi et al. 2014). Visual inspection suggests that Tanguy selected synthetic organic pigments for the red and yellow components of his skies, and that in some instances these colors appear noticeably faded.

Five of the six works studied contain green biomorphic elements or foliage. In *He Did What He Wanted* Tanguy used both viridian and chrome green pigments, while in *Mama, Papa is Wounded* he used chrome green, viridian, and emerald green. The data for both of these seminal works suggest that he may also have used cobalt green, but molecular analysis would be required to confirm this. The 1927 work of unknown title (Fig 2.13) has one emerald green biomorphic figure that was toned with chrome yellow. The green portion of the tower in *Fraud in the garden*

Fig. 2.13 *Title Unknown*, oil on canvas, 1927**,** 60 × 45 cm (23−5/8 × 17−3/4 in). Tanguy's prewar palette and style are exemplified in this landscape, see Table 2.1 for the full palette description of this work

(unconfirmed title) (Fig 2.14) (1930) was colored with chrome green, and *Indefinite Divisibility* (1942) contains both chrome green and viridian green elements, the latter toned with cadmium yellow. The presence of a cobalt green pigment (CoO-ZnO) was inferred in two paintings, MoMA's *He Did What He Wanted* and *Mama, Papa is Wounded*. However, in the absence of molecular analysis to determine the origin of the zinc in the XRF spectra, these assignments have to remain inconclusive and so are not included in Table 2.1.

Elemental analysis of the white pigments and fillers used in the preparatory layers and tube paints in the four studied works executed between 1927 and 1930 suggests that they were painted on a lead-based ground with a zinc white preparatory layer. Areas of white paint used in the compositions of the three 1927 works were lead white with a calcium-based extender such as chalk or gypsum. Trace titanium was also identified in the ground of *He Did What He Wanted*, while barium

Fig. 2.14 An image of *Fraude dans le jardin (Fraud in the garden)*, 1930 following the vandalism of the L'Affaire de L'Age D'or (December 1930, Breton 1930) alongside a visible light image of the painting in 2020. A 2020 X-radiograph of the painting reveals the presence of mold damage in the top half of the work and the repair of the slashed canvas in the bottom half. A long-wave ultraviolet image shows no evidence of the L'Age D'or event or the repairs associated with it, but it reveals a vertical strip of restoration paint subsequently applied along the right edge

identified in *Mama, Papa is Wounded* and *Title Unknown* likely indicates the presence of a barium sulfate filler. *Indefinite Divisibility* (1942), in contrast, was executed on a titanium dioxide (anatase) based ground with a gypsum filler, likely with a zinc white preparatory layer. Additional stratigraphic and molecular analysis would be needed to confirm this interpretation.

Molecular analysis of the blue water in the Metropolitan's 1926 work using Raman microscopy confirmed the presence of Prussian blue pigment in this region. Molecular analysis on the Albright Knox Art Gallery 1942 *Indefinite Divisibility* work was carried out using FTIR and Raman spectroscopy. The grayish white foreground contains zinc stearate, a cobalt carboxylate drier, a drying oil binder, a proteinaceous component (possibly from an early glue lining), and an acrylic resin (the closest match is methyl methacrylate). The Raman data from this sample revealed the presence of the anatase form of titanium white pigment and bone black. The anatase white pigment has the characteristic Raman luminescence of titanium white pigments that are composed of co-precipitated anhydrite and anatase (Rogge and Arslanoglu 2019). This luminescence phenomenon, caused by the neodymium impurities in the titanium ore (ilmenite), has been previously observed in anatase paints dating from 1938–1967. This phenomenon corresponds with ilmenite ore derived from the McIntyre mine in Essex Co., New York, the primary mine for the Titanium Pigments Corporation and the TITANOX white pigments that they produced (Rogge and Arslanoglu 2019). This same phenomenon has been observed in paintings by Franz Kline, Hans Hoffmann, and Jackson Pollock, so this information may allow for the identification of Tanguy's source of paints once he moved to the United States (Rogge and Arslanoglu 2019). The 1942 date of this work precedes the introduction of acrylic-based artists paints resulting from Leonard Bocour and Sam Golden's experiments that took place between 1946 and 1949, and so this material is likely an impurity from a conservation treatment or mid-century varnish. A medium blue microsample from the sky removed from the tacking margin revealed the presence of Prussian blue, a drying oil such as linseed oil (or alkyd resin), a gypsum filler, cobalt stearate, and zinc stearate (data not shown).

The only work with collage and *coudrage* elements studied for this project is the Metropolitan Museum of Art's 1926 *Title Unknown* work. The collage element has applied color decorating a shield. This paint was studied by MA-XRF, but the data are not included in this article because one cannot determine if it was applied before or after the paper was incorporated into the composition, or if it was applied by Tanguy at all.

2.8 Conclusions

We have presented here for the first time information about the materials and working methods of the surrealist painter Yves Tanguy. Scientific examination of several of his works from the 1920s and through the 1940s revealed that his landscapes, populated by biomorphic forms and towers against hazy striated skies, were painted

simply using a limited palette of both inorganic and organic pigments with little pigment mixing. Among the materials we identified or inferred from the studied works are Prussian blue, cobalt blue, cerulean blue, manganese blue, emerald green, chromium-based green, chrome green (a co-precipitate of Prussian blue and chrome yellow), vermilion red, organic red pigments, cadmium yellow, chrome yellow, a synthetic organic yellow pigment, zinc white, lead white, bone black, and iron oxide reds, yellows, and browns. Contrary to his public statements Tanguy did use underdrawings (although limited) in his work, which is consistent with his prolific output of drawings and gouaches. In the works examined here, all of Tanguy's emerald green, cadmium yellow, and chrome yellow passages are in good condition. One condition issue that alters the intended balance of Tanguy's dark skies is the aggregation and agglomeration of metal carboxylates. These are causing regions of increased translucency and spherical protrusions that distract from an otherwise low impasto paint surface. The challenges to making an attribution of a work to Yves Tanguy in the absence of definitive provenance documentation have also been discussed. These complicating factors include an incomplete *catalogue raisonné*, forgeries of his works made by his contemporaries during World War II, the artist's own destruction of many of his early works, and the lack of extant research into Tanguy's materials and methods. In light of these challenges, the media identification presented here may assist with works misattributed to Tanguy that postdate the artist (for example paintings from the 1960s and 1970s when there was a marked uptick in the financial value of surrealist paintings). A larger body of technical imaging data may ultimately contribute to the discovery of one or more of World War II forgeries. As a result, it may be some time yet before Tanguy's cold and alien dreamscapes can be coaxed into revealing all of their mysteries.

2.9 Experimental Methods

2.9.1 Imaging methods

MMA

In *Title Unknown* (MMA 2002.456.6), infrared reflectography (IRR) was done using an OSIRIS InGaAs near-infrared camera with a 6-element, 150 mm focal length, f/5.6–f/45 lens; and 900–1700 nm spectral response.

MA-XRF analysis was performed in two areas of this painting with a Bruker M6 Jetstream system equipped with a Rh source operated at 50kV and 600uA. The focal spot size was 580 microns, the step size was 650 microns for Area 1 and 600 for Area 2, and the dwell time was 100 ms/pixel for both areas. The spatial distributions of the elements of interest were obtained using the Bruker software.

2.9.2 Spectroscopic methods

MMA
A microscopic paint sample was removed from the blue paint passage in the left edge of *Title Unknown* (MMA 2002.456.6). Raman spectroscopy measurements were done on this sample scraping using a Renishaw System 1000 coupled to a Leica DM LM microscope. The spectra were acquired using a 785 laser excitation focused on the sample using a 50x objective lens, with an integration time of 120 s. A 1200 lines/mm grating was used and power at the sample was set at 0.5 mW using a neutral density filter.

Albright Knox Art Gallery Buffalo
Infrared spectra of samples from *Indefinite Divisibility* were collected using a Nicolet 6700 FTIR spectrometer (Thermo Scientific). Samples were analyzed by compressing them against the Diamond ATR crystal. The spectra are the average of 64 scans at 4 cm^{-1} spectral resolution. Sample identification was aided by searching a spectral library of common conservation and artists' materials (Infrared and Raman Users Group, http://www.irug.org) using Omnic software (Thermo Scientific).

Dispersive Raman spectra of samples from *Indefinite Divisibility* were collected on a Bruker Senterra Raman microscope using a 785 nm excitation laser operating at a power of 10 or 25 mW at the source. A 10x or 50x ULWD objective was used to focus the excitation beam to an analysis spot of approximately 5–10 um directly onto a micro-sample placed on a microscope slide. The resulting Raman spectra are the average of 30 scans at 3 s integrations each. Spectral resolution was 9–15 cm^{-1} across the spectral range analyzed. Spectral spikes due to cosmic rays were removed. Sample identification was achieved by comparison of the unknown spectrum to spectra of reference materials.

2.9.3 Elemental Analysis – X-Ray Fluorescence (XRF)

MoMA, Private Collection 1930 Work
Qualitative energy-dispersive x-ray fluorescence spectroscopy (XRF) was carried out using a Bruker Tracer III-SD handheld XRF with a rhodium x-ray tube and a silicon drift detector. The analysis conditions were a tube voltage of 40 kV and 13 μA, no filter, and data collection time of 60 s live time.

Albright Knox Art Gallery Buffalo
A Bruker Tracer 5g handheld XRF equipped with a Rh source was used to collect XRF spectra of various locations on both Unknown Titled, 1927, and Indefinite Divisibility, 1942. The spectra were collected at 50 kV 35 uA using a 3 mm spot size

for 10 s on Untitled and 45 s on *Indefinite Divisibility*. Spectra were collected and interpreted using Bruker Artax software.

Acknowledgements We are grateful to a number of individuals and institutions for sharing their research and perspectives and providing access to paintings in their collections. We gratefully acknowledge the assistance of Christopher McGlinchey and Abed Haddad from the Museum of Modern Art (New York) for allowing us to collect data on *He Did What He Wanted*, 1927, and *Mama, Papa is Wounded*, 1927. We thank Laura Fleischmann and the Albright Knox Art Gallery for allowing us to collect data on *Indefinite Divisibility*, 1942. We also thank the Galerie Hervé Odermatt for access to *Fraude dans le jardin* (unconfirmed title), 1930 and Robert Landau of Landau Fine Art for providing us access to *Untitled*, 1927 for scientific study. Satoko Tanimoto of Scientific Analysis of Fine Art, LLC was essential to the X-ray fluorescence and X-radiography studies on *Fraude dans le jardin*.

The opportunities to examine paintings with Charles Stuckey and Stephen Mack were one of the most enjoyable aspects of this research, as were their many helpful discussions about their catalogue raisonné work. We are particularly grateful to them for their generosity with their time and expertise. We are also grateful to Alessandra Carnielli, Executive Director of the Pierre and Tana Matisse Foundation, for hosting us at the Foundation during several points of this project, and for her valuable insights into the Foundation's role in preserving Yves Tanguy's legacy.

References

Accorsi, G., Verri, G., Acocella, A., Zerbetto, F., Lerario, G., Gigli, G., Saunders, D., Billing, R.: Imaging, photophysical properties and DFT calculations of manganese blue [barium manganate(VI) sulphate] – a modern pigment. Chem. Commun. **50**(97), 15273–15466 (2014)

Art Critique.: The long game: how Wolfgang Beltracchi conned the art world, 24 January 2020. https://www.art-critique.com/en/2020/01/the-long-game-how-wolfgang-beltracchi-conned-the-art-world/. Accessed 28 Mar 2021

Artesani, A., Ghirardello, M., Mosca, S., Nevin, A., Valentini, G., Cornelli, D.: Combined photoluminescence and Raman microscopy for the identification of modern pigments: explanatory examples on cross-sections from Russian avant-garde paintings. Herit. Sci. **7**, 17 (2019)

Authentic de Chirico painting signalled as a fake by L'Archivio dell'Arte Metafisica: The construction of a fake "truth", Fondazione Giorgio e Isa de Chirico. https://fondazionedechirico.org/wp-content/uploads/2019/06/Authentic-de-Chirico-painting-signalled-as-a-Fake-by-L;Archivio-dell'Arte-Metafisica.pdf. Accessed 24 Mar 2021

Bambach, C.C.: Leonardo da Vinci Rediscovered. Yale University Press (2019)

Bambic, A.: Beltracchi. Widewalls (2014). https://www.widewalls.ch/magazine/case-wolfgang-beltracchi

Bandle, A.L.: Fake or Fortune? Art authentication rules in the art market and at court. Int. J. Cult. Prop. **22**, 379–399 (2015)

Barbarant, G., Helou-de La Grandière, P., Soulages, P.: l'art et le métier, la restauration de peinture, 130 x 165 cm, 18 avril 1959. In: Kairis, P.Y., et al. (eds.) Restauration des peintures et des sculpture, pp. 311–331. Armand Colin, Paris (2012)

Bellingham, D.: Attribution and the market: the case of Frans Hals. In: Aldrich, M.B., Hackforth-Jones, J., Humphries, L., Sotheby's (Firm) (eds.) Art and Authenticity. Institute of Art, Farnham/Lund Humphries/Sotheby's Institute of Art, Burlington/London/New York (2012)

Bijl, M., Kloek, W.: A painting re-attributed to Aelbert Cuyp: connoisseurship and technical research. Burlingt. Mag. **156**(1331), 91–98 (2014)

Breton, A.: Manifeste du surréalisme: poisson soluble. Éditions du Sagittaire, Paris (1924)

Breton, A., Soupalt, P.: Littérature. No. 1 (New Series) Paris (1922)

Breton, A., Alexandre, M., Aragon, Char, R., Crevel, R., Dalí, S., Eluard, P., Malkine, G., Peret, B., Ray, M., Sadoul, G., Tanguy, Y., Thirion, A., Tzara, T., Unik, P., Valentin, A., L'Affaire de "L'Age d'Or".: Four page leaflet and loose leaf with reproductions of the works destroyed in Studio 28. Paris (1930)

Breton, A., Tanguy, Y., Duchamp, M.: Yves Tanguy Par Andre Breton. Pierre Matisse Editions, New York (1946)

Brewer, J.: Art and science: a Da Vinci detective story. Eng. Sci ½, 32–41 (2005)

Brewer, J.: The American Leonardo. Oxford University Press, Oxford (2009)

Bronken, I., Boon, J.J.: Hard dry paint, softening tacky paint, and exuding drips on composition (1952) by Jean-Paul Riopelle. In: Van den Berg, K.J., Burnstock, A., de Tagle, A., de Keijzer, M., Heydenreich, G., Krueger, J., Learner, T. (eds.) Issues in Contemporary Oil Paint, pp. 247–262. Springer, Cham (2014). https://doi.org/10.1007/978-3-319-10100-2

Buckley, B.: The Modigliani technical research Study Modigliani's Paris portraits 1915-17. Burlingt. Mag. **160**(1381), 311 (2018)

Cain, A.: The controversy around Modigliani's many catalogues Raisonnes, explained. Artsy, July. **29** (2016)

Caldwell, M.: Some developments in british paint manufacture over the last two hundred years, and the occurrence of white surface deposits on paintings. In: Phenix, A. (ed.) Deterioration of Artists' Paints: Effects and Analysis, pp. 9–12. UKIC and British Museum, London (2001)

Callen, A.: Techniques of the Impressionists, pp. 58–61. Orbis, London (1982)

Callen, A.: The unvarnished truth: Mattness, 'Primitivism' and modernity in French painting, c. 1870-1907. Burlingt. Mag. **136**(100), 738–746 (1994)

Callen, A.: The Art of Impressionism: Painting Technique & The Making of Modernity. Yale University Press (2000)

Cariou, A.: Yves Tanguy – the surrealist universe. Exhibition Catalogue Musée des Beaux-Arts, Quimper (2007)

Ceroni, A., Czechowska, L..: Amedeo Modigliani : peintre. Edizioni Del Milione (1958)

Church, A.H.: The chemistry of paints and painting. Seeley, Service and Co., London (1890)

Clark, R.J.H.: Raman microscopy: application to the identification of pigments on medieval manuscripts. Chem. Soc. Rev., 187–196 (1995)

Coddington, J., Siano, S.: Infrared imaging of 20th century works of art, tradition and innovation: advances in conservation: contributions to the Melbourne Congress, 10–14 October 2000, pp. 39–44

Collins, J., Welchman, J., Chandler, D., Anfam, D.A.: Techniques of Modern Artists. Macdonald, London (1983)

Corbeil, M.C., Helwig, K., Poulin, J.: Jean Paul Riopelle: The Artist's Materials. Getty Publication, Los Angeles (2011)

Craddock, P.: Scientific Investigation of Copies, Fakes, and Forgeries. Butterworth-Heinemann, New York (2009)

Crisp, C. G. "L'Age d'or (2 October)" French cinema: a critical filmography, Volume 1. 1929–1939, Bloomington: Indiana University Press (2015)

Davidson, S.: A breton in connecticut. In: Maur, K.V. (ed.) Yves Tanguy and surrealism, pp. 175–197. Hatje Cantz, Ostfildern-Ruit (2001)

de la Rie, E.R., Michelin, A., Ngako, M., Del Federico, E., Del Grosso, C.: Photo-catalytic degradation of binding media of ultramarine blue containing paint layers: a new perspective on the phenomenon of "ultramarine disease" in paintings. Polym. Degrad. Stab. **144**, 43–52 (2017)

Defeyt, C., Vandepitte, F., Herens, E., Strivay, D.: Discovery and material study of the missing feet part from Magritte's L'évidence éternelle of 1954. Herit. Sci. **7**, 96 (2019a)

Defeyt, C., Vandepitte, F., Mazurek, J., Herens, E., Strivay, D.: Investigation on the Speckles Syndrome affecting late 1920s oil paintings by René Magritte. In: van den Berg, K.J., Bonaduce, I., Burnstock, A., Ormsby, B., Schar, M., Heydenreich, L.C.G., Keune, K. (eds.) Conservation of Modern Oil Paintings, pp. 255–263. Springer, New York (2019b)

Drost, J., Flahutez, F., Helmreich, A., Schieder, M.: Avida Dollars! Surrealism and the art market in the United States, 1930-1960. In: Networking Surrealism in the USA: Agents, Artists, and the Market, pp. 13–38. arthistoricum.net, Heidelberg (2019)
Duhamel, M.: Raconte pas ta vie. Mercure de France, Paris (1972)
Durozoi, G., Anderson, A.: History of the Surrealist Movement. University of Chicago Press, Chicago (2002)
Esterow, M.: The 10 most faked artists. Art News. **104**(6), 103 (2005)
Finn, C.: The Devil in the detail. Apollo, 50–54 (2014)
Golden, M.: Manufacturing Artist Paints: Keeping Pace with Change. Conservation Perspectives: Creation, Conservation, and Time: A Discussion About Modern Paints. Getty Conservation Institute, Los Angeles (2016)
Gonzalez, V., Cotte, M., Wallez, G., van Loon, A., de Nolf, W., Eveno, M., Keune, K., Noble, P., Dik, J.: Unraveling the composition of Rembrandt's Impasto through the identification of unusual Plumbonacrite by multimodal X-ray diffraction analysis. Angew. Chem. Int. Ed. **58**, 5619–5622 (2019)
Hampel, J.C.G.: Die restauration alter und schadhaft gewordener gemälde in ihrem ganzen umfange : nebst einer anleitung zur frescomalerei. Schäfer, Hannover (1846)
Haneca, K., Wazny, T., Van Acker, J., Beeckman, H.: Provenancing Baltic timber from art historical objects: success and limitations. J. Archaeol. Sci. **32**, 261–271 (2005)
Hélou-de La Grandière, P.: La restauration de Peinture 114 x 165 cm, 16 décembre 1959 de pierre soulages. Thesis for master restaurateur du patrimoine (2005)
Hélou-de La Grandière, P., Casadio, F.: A Montparnasse disease? Severe manifestations of metal soaps in paintings by pierre Soulages from around 1959 to 1960. In: Metal Soaps in Art: Conservation and Research, pp. 393–412. Springer, Cham (2019)
Hélou-de La Grandière, P., Le Hô, A.-S., Mirambet, F.: Delaminating paint films at the end of the 1950s: a case study on pierre soulages. In: Townsend, J.H., Doherty, T. (eds.) Preparation for painting, pp. 156–162 (2008)
Herbst, W., Hunger, K.: Industrial Organic Pigments: Production, Properties, Applications. Wiley Press, New Jersey (1993)
Holmes, H.: Man Ray Trust claims Christie's Auctioned Stolen Works. The Observer, 3 Mar 2021
Hundertpfund, L.: Die malerei auf ihre einfachsten und sichersten grundsätze zurückgeführt : eine anweisung, mit ganzen farben alle halbtöne und schatten ohne mischung zu malen. J. Walch, Augsburg (1847)
Itzkoff, D., Vogel, C.: Warhol foundation ends authentication board, arts, briefly. New York Times (2011)
Jean, M., Mezei, A.: The History of Surrealist Painting. Grove Press, London (1960)
Jones, M.: Fake? The Art of Deception. University of California Press, Berkeley/Los Angeles (1990)
Kaplan, L.A.: Traces of Influence: Giorgio de Chirico, Remedios Varo, and "Lo Real Maravilloso". Lat. Am., 25–51 (2010)
Karpel, B., Lippard, L.R., Sage Tanguy, K.: Yves Tanguy: Un Recueil De Ses Oeuvres. P. Matisse (1963)
Katlan, A.W., Falk, P.H.: American Artists' materials Suppliers Directory. The Conservation Series. Noyes Press, Park Ridge, pp. 328, 333, 347–349, 353, 357, 363 (1987)
Kemp, M.: Leonardo da Vinci The Mystery of the Madonna of the Yarnwinder, National Gallery of Scotland (1992)
Kemp, M.: Living with Leonardo: Fifty Years of Sanity and Insanity in the Art World and Beyond. Thames and Hudson, New York (2018)
Khandekar, N., Mancusi-Ungaro, C., Cooper, H., Rosenberger, C., Eremin, K., Smith, K., Stenger, J., Kirby, D.: A technical analysis of three paintings attributed to Jackson Pollock. Stud. Conserv. **55**(3), 204–215 (2010)
Lanchner, C.: Joán Miró. The Museum of Modern Art, New York (1993)
Lanthemann, J.: Modigliani, 1884–1920: catalogue raisonné: sa vie, son oeuvre complet, son art
Le Bihan, R., Mabin, R., Sawin, M.: Yves Tanguy. Éditions Palantines, Quimper (2001)

Levison, H.W.: Yellowing and bleaching of paint films. J. Am. Inst. Conserv. **24**(2), 69–76 (1985)
Lloyd, M., Desmond, M.: European and American Paintings and Sculptures 1870-1970 in the Australian National Gallery. Australian National Gallery, Canberra (1992)
Loiselle, M.: Multiple authority delegation in art authentication. Australas. Sci. **1**, 41–53 (2017)
Mack, S.: Forging Tanguy in Occupied Paris. College Art Association (2019)
Mack, S.: Personal Communication (2021)
Mancini, G.: History of a Fake: the Virgin and Child with an angel after Francesco Francia in the National Gallery, London, The Burlington Magazine, August 2013, Vol. 155, No. 1325, Art in Italy, 546–551 (2013)
Martínez, L.R.: Joán Miró en el MNCARS: tecnicas, materiales y problemas de conservación. Pátina. **9**, 56–63 (1999)
Maur, K.V.: The certainty of the never seen. In: Maur, K.V. (ed.) Yves tanguy and surrealism, pp. 11–133. Hatje Cantz, Ostfildern-Ruit (2001)
Maur, K.V., Davidson, S.: Staatsgalerie Stuttgart, Menil Collection (Houston, Tex.). Yves tanguy and surrealism. Hatje Cantz, Ostfildern-Ruit (2001)
Mcgirk, T.: Fake Dalis Flood the Art Market; Forged Surrealist Paintings. Sunday Times (London, England) (1985)
McNab, R.: Ghost Ships: A Surrealist Love Triangle. Yale University Press, London (2004)
Melikian, S.: Coining gold out of indifferent art. New York Times (2009)
Miller, S.R., Stuhlman, J., Wallach, N.: Katonah Museum of Art, Mint Museum (Charlotte, N.C.). Double solitaire : the surreal worlds of kay sage and yves tanguy. Katonah Museum of Art, Katonah (2011)
Mundy, J.V.: Tanguy, titles and mediums. Art Hist. **6**(2), 199–213 (1983). https://doi.org/10.1111/j.1467-8365.1983.tb00806.x
Muñoz-Alonso, L.: Picasso, Miró, and Matisse Forgery Ring Busted, Artnet News, Art and Law (2015a). https://news.artnet.com/art-world/picasso-miro-and-matisse-forgery-ring-busted-225600
Muñoz-Alonso, L.: *Artnet News*, Art and Law "271 Picasso, Warhol, and Miró Fakes seized in yet another Spanish Forgery Ring Bust :Has Spain become a fraudsters' paradise?" (2015b) https://news.artnet.com/art-world/271-picasso-warhol-and-miro-fakes-seized-in-yet-another-spanish-forgery-ring-bust-272394
Nicholas, L.H.: The Rape of Europa: The Fate of Europe's Treasures in the Third Reich and the Second World War. Random House, New York (1994)
Noble, P., Van Duijn, E., Hermens, E., Keune, K., Van Loon, A., Smelt, S., Tauber, G., Erdmann, R.: An Exceptional Commission: conservation history, treatment and painting technique of Rembrandt's Marten and Oopjen, 1635. Rijksmuseum Bull. **66**(4), 308–345 (2018)
Noce, V.: Surrealist collection of Man Ray's assistant sells out at Christie's despite 'serious concerns about ownership' of most of the works. The Art Newspaper (2021)
Onslow Ford, G.: Creation. Galerie Schreiner, Basel (1978)
Onslow Ford, G.: Yves tanguy and automatism. Bishop Pine Press, Inverness (1983)
Onslow Ford, G.: Yves tanguy and the new subject in painting. In: Maur, K.V. (ed.) Yves tanguy and surrealism, pp. 199–205. Hatje Cantz, Ostfildern-Ruit (2001)
Parisot, C., Guastella, G., Guastella, G.: Modigliani: catalogue raisonné (1991)
Pozzi, F., van den Berg, K.J., Fiedler, I., Casadio, F.: A systematic analysis of red lake pigments in French Impressionist and Post-Impressionist paintings by surface-enhanced Raman spectroscopy (SERS). J. Raman Spectrosc. **45**, 1119–1126 (2014)
Pozzi, F., Basso, E., Centeno, S.A., Smieska, L.M., Shibayama, N., Berns, R., Fontanella, M., Stringari, L.: Altered identity: fleeting colors and obscured surfaces in Van Gogh's landscapes in Paris, Arles, and Saint-Remy. Herit. Sci. **9**(15) (2021)
Ragai, J.: The scientific detection of forgery in paintings. Proc. Am. Philos. Soc. **157**(2), 164–175 (2013)
Ragai, J.: Scientist and the forger, the: insights into the scientific detection of forgery in paintings. World Sci. (2015)

Rasmussen, M.B.: The situationist international, surrealism, and the difficult fusion of art and politics. Oxford Art J. **3**(27), 367–387 (2004)
Rewald, S., Dabrowski, M.: The American Matisse : The Dealer, His Artists, His Collection : The Pierre and Maria-Gaetana Matisse Collection. Metropolitan Museum of Art, New York (2009)
Rhodes, A.-M.: Art law and transactions. Carolina Academic Press (2011), "Authenticity", 81
Richardson, J.: "Crimes against the Cubists", the New York Review of Books, June 16, (1983)
Richter, H.: In memory of two friends. yves tanguy, 1900-1956. College Art J. **15**(4), 343–346 (1956)
Robinson, W.H.: De Chirico forgeries: the treachery of the surrealists. IFAR J. **4**(1) (2001)
Robinson, A.S.: Giorgio de Chirico in the 1930s: the case of a hidden female nude. Burlingt. Mag. **157**(1347), 402–406 (2015)
Rogge, C.E., Arslanoglu, J.: Luminescence of coprecipitated titanium white pigments: implications for dating modern art. Sci. Adv. **5**, eaav0679 (2019)
Rogge, C.E., Epley, B.A.: Behind the bocour label: identification of pigments and binders in historic bocour oil and acrylic paints. J. Am. Inst. Conserv. **56**(1), 15–42 (2017). https://doi.org/10.1080/01971360.2016.1270634
Rogge, C.E., Bomford, Z.V., Leal, M.: Seldom Black and White: the works of Franz Kline. In: Casadio, F., Keune, K., Noble, P., Van Loon, A., Hendriks, E., Centeno, S.A., Osmond, G. (eds.) Metal Soaps in Art: Conservation and Research. Cultural Heritage Science, pp. 413–424. Springer, New York (2019)
Rønberg, L.B., Wadum, J.: Two paintings in Copenhagen re-attributed to Rembrandt. Burlington Magaz. Dutch Flemish German Art. **148**(1235), 82–88 (2006)
Roy, A.: The palettes of three impressionist paintings. Nat. Gallery Tech. Bull. **9**, 12–20 (1985)
Rudenstine, A.Z., Solomon, R.: Guggenheim Foundation. Peggy Guggenheim collection, Venice. H.N. Abrams, New York (1985)
Saverwyns, S.: Russian avant-garde. . . or not? A micro-Raman spectroscopy study of six paintings attributed to Liubov Popova. J. Raman Spectrosc. **41**, 1525–1532 (2010)
Schalhorn, A.: Yves tanguy 1900-55. In: Maur, K.V. (ed.) Yves Tanguy and Surrealism, pp. 211–230. Hatje Cantz, Ostfildern-Ruit (2001)
Schmidt, K.: Staatliche Kunsthalle Baden-Baden. Yves Tanguy. Prestel, München (1982)
Scott, D.A.: Conservation and authenticity: interactions and enquiries. Stud. Conserv. **60**(5), 291–305 (2015)
Scott, D.A.: Art: Authenticity, Restoration, Forgery. Cotsen Institute of Archaeology Press at UCLA, Los Angeles (2016)
Shorto, R.: Rembrandt in the blood: an obsessive aristocrat, rediscovered paintings and an art-world feud. New York Times Magaz. **27** (2019)
Sloggett, R.: Art crime: fraud and forensics. Aust. J. Forensic Sci. **47**(3), 253–259 (2014)
Soby, J.T.: Inland in the subconscious. Magaz. Art. **42**, 2–7 (1949)
Soby, J.T.: Yves tanguy. Museum of Modern Art, New York (1955)
Soby, J.T.: New York, Museum of Modern Art Archives, James Thrall Soby Papers, letter dated 17th December 1949
Solomon, R., Guggenheim Museum. Yves Tanguy: a Retrospective. New York: Solomon R. Guggenheim Foundation; (1983)
Spier, J.: Blinded with science: the abuse of science in the detection of false antiquities. Burlingt. Mag. **132**(1050), 623–631 (1990)
Standeven, H.A.L.: The history and manufacture of lithol red, a pigment used by Mark Rothko in is seagram and Harvard murals of the 1950s and 1960s. Tate Papers. **10**, 1–8 (2008)
Stols-witlox, M.: A perfect ground: preparatory layers for oil paintings 1550-1900. Archetype, London (2018)
Stolz, G.: Authenticating Picasso. ART News. **2** (2013)
Stuckey, C., Mack, S.:, e-mail interview, December 2020
Stuckey, Personal communication from Charles Stuckey, 2021
Stuhlman, J.: Navigating a constantly shifting terrain: yves tanguy and surrealism. Dissertation (2013) https://doi.org/10.18130/V3VR5J

Sweeney, J.J.: Eleven Europeans in America. Bull. Mus. Modern Art. **13**(4–5), 2–39 (1946)
Tanguy, Y.: Symposium: the creative process. Art Digest. **28**(8), 14–16 (1954)
Teja Bach, F.: Forgery: the art of deception. In: Becker, D., Fischer, A., Schmitz, Y. (eds.) Faking, Forging, Counterfeiting: Discredited Practices at the Margins of Mimesis, pp. 41–57. Transcript Verlag (1990)
The Pollock-Krasner Foundation (2021). https://pkf.org/general-faq/
Thomas, K.D.: The Newfound Pollocks: real or fake? (Pollock-krasner Foundation). ARTnews (0004-3273). **104**(7), 66 (2005)
Tomkins, A., Humphries, L.: Provenance Research Today: Principles, Practice, Problems (2021)
Townsend, J.H.: The materials of J.M.W. Turner: pigments. Stud. Conserv. **38**(4), 231–254 (1993)
Tromp, H.: Among art experts. In: A Real Van Gogh: How the Art World Struggles with the Truth, pp. 231–253, Amsterdam University Press (2010)
Umland, A., Aviram, A.: Materials and Processes. https://www.moma.org/audio/playlist/293/3853. Accessed 28 Mar 2021
van de Wetering, E.: Connoisseurship and Rembrandt's Paintings: new directions in the Rembrandt Research Project, Part II. Burlington Magaz. Northern European Art. **150**(1259), 83–90 (2008)
van de Wetering, E.: 'Old man in an armchair' re-attributed to Rembrandt. Burlingt. Mag. **156**(1335), 382–384 (2014)
van den Berg, K.J., Bonaduce, I., Burnstock, A., Ormsby, B., Scharff, M., Carlyle, L., Heydenreich, G., Keune, K. (eds.): Conservation of Modern Oil Paintings. Springer, New York (2019)
Van der Snickt, G., Martins, A., Delaney, J., Janssens, K., Zeibel, J., Duffy, M., McGlinchey, C., Van Driel, B., Dik, J.: Exploring a hidden painting below the surface of Rene Magritte's Le Portrait. *Appl. Spectrosc.* **70**(1), 57–67 (2016)
von Sonnenburg, H.: Paintings: Problems and issues. In: Rembrandt/Not Rembrandt in the Metropolitan Museum of Art: Aspects of Connoisseurship, vol. 1. Metropolitan Museum of Art and Harry N. Abrams, Inc., New York (1995a)
von Sonnenburg, H.: Rembrandt/Not Rembrandt in the Metropolitan Museum of Art: Aspects of Connoisseurship. Metropolitan Museum of Art and Harry N. Abrams, Inc., New York (1995b)
Waldberg, P.: Yves tanguy. Andre de Rache, Brussels (1977)
Walker, R.W.: New York cracks down on Dali forgeries. (Salvador Dali). ARTnews (0004-3273). **85**, 28 (1986)
Walter, P.: Chemical analysis and painted colours: the mystery of Leonardo's sfumato. Eur. Rev. **21**(2), 175–189 (2013)
Wesley, M.: A Dialogue of connoisseurship and science in constructing authenticity. In: Aldrich, M., Hackforth-Jones, J., Humphries, L. (eds.) Art and Authenticity. Sotheby's Institute of Art, New York (2012)
Wolf, B.: Genesis of a new world: the graphic art of yves tanguy. In: Maur, K.V. (ed.) Yves Tanguy and surrealism, pp. 135–174. Hatje Cantz, Ostfildern-Ruit (2001)
Yeide, N.H., Akinsha, K., Walsh, A.L.: The AAM Guide to Provenance Research. The American Association of Museums (2001)
Zervos, C.: Pablo Picasso 1881–1973 (1951)
Zucker, J.: From the ground up: the ground in 19th-century American pictures. J. Am. Inst. Conserv. **38**(1), 3–20 (1999)

Chapter 3
Analytical Approaches to the Analysis of Paintings: An Overview of Methods and Materials

Maria Perla Colombini, Ilaria Degano, and Austin Nevin

Abstract The analysis of paintings is based on a combination of non-invasive and sampling approaches – which provide different types of information about different areas of paintings. In this chapter the principal methods for analysis applied to the study of paintings are presented to provide information about the evidence that each can yield. This is followed by a review of the materials found in different layers of paintings, from the support to paint layers and coatings. While intended as an introduction, the chapter highlights the large variety of techniques employed, and the significant complexity of paintings which is an analytical challenge and requires very careful interpretation. Within the context of authentication, the interpretation of analysis requires understanding of the limitations and accuracy of analytical methods, and reference to historical trends and to the chronological use of materials for painting is necessary.

Keywords Analytical methods · Technical analysis · Chemistry · Dating · Chronology

3.1 Introduction

Scientists are often asked to evaluate unattributed works of art. Identifying the author of an artwork may be a crucial step in establishing its value from a cultural, historical, and economic perspective but it is our view that making decisions of attribution is not the responsibility of the scientist or conservator. Instead, scientists and conservators can provide key information that may refute the attribution of a

M. P. Colombini (✉) · I. Degano
Department of Chemistry and Industrial Chemistry, Università di Pisa, Pisa, Italy
e-mail: maria.perla.colombini@unipi.it

A. Nevin
Department of Conservation, Courtauld Institute of Art, Somerset House, Strand, London WC2R 0RN, UK

M. P. Colombini et al. (eds.), *Analytical Chemistry for the Study of Paintings and the Detection of Forgeries*, Cultural Heritage Science,
https://doi.org/10.1007/978-3-030-86865-9_3

work to a specific historical period, or identify paint materials or additions that may be consistent with a particular period or workshop practice.

Forgeries are endemic in the art world: old Masters and modern Masters paintings are commonly faked and forged. Therefore, great caution is necessary when providing assessments of attribution with a significant burden of proof resting on scientific and historical analysis. Sound knowledge of the history of a particular painting and its provenance, of the artistic technique of the painter, and on the identification of the constituent materials are often essential in the interpretation of the significance of results from the chemical analysis of works of art. Within this context, the accuracy and the limitations of scientific analysis are particularly important; while some techniques are ideal for the identification of bulk composition, others may provide evidence of trace materials or identify specific binders or pigments. In this book we have aimed to provide a balanced description of advantages and limitations of analytical methods and the extent to which each method provides qualitative and quantitative information.

Paintings are complex objects, and contain different materials (that may include wood, canvas, pigments, binders, varnishes, added materials from conservation, as well as degradation that may originate from the environment). Each component of a painting can be analysed or assessed using scientific methods and offer clues regarding the origin and physical history of paintings. A thorough visual examination by an art historian, curator, and conservator, all of whom may be familiar with the production of the supposed author, is a first step in assessing authorship of works of art. Scientific analysis and documentation rely on the choice and application of a large array of documentation techniques that range from consolidated methods including X-radiography and Infrared Reflectography and UV Fluorescence imaging (see Chaps. 4, 8, and 11), as well as hyperspectral imaging and complementary data analysis (see Chaps. 4 and 5). Imaging is often followed using analytical methods that rely on spot-analyses or sampling to identify artistic techniques and materials. Analysis may provide information that can be used to date a painting or to corroborate the compatibility of materials with a specific period. Synergistic interpretation of data between art historians, conservators, connoisseurs, and heritage scientists allows careful assessment of paintings, and can lead to the detection of forgeries.

Conservation and art history evidence will clarify the following issues:

– Documentary information and conservation history reveal the condition of a painting in terms of the presence of restoration and original material, damage and legibility. Past treatments of paintings may have introduced significant changes to the size and shape of a painting. For example, it is common that large canvases and panel paintings may be cut into smaller multiple paintings for sale, with well-known examples including Manet's 'Execution of Maximilian' (Execution of Maximilian n.d.). Past conservation treatments and in particular both lining of canvases where a new support is adhered to a canvas painting, or cradling where wooden panel paintings were thinned and a rigid structure (a cradle) was attached to the back may permanently change the appearance of a

painting and destroy evidence of the original materials. It is also worth noting that damage to paintings can be masked by restoration or reintegration – and it is critical for art historians and conservators to be able to assess the condition of a painting and distinguish original materials from past restorations. The use of UV Fluorescence imaging (see Chap. 8) is particularly important for highlighting varnishes and past retouching, and may be complemented by X-radiography, IRR and, more recently with data from elemental mapping with XRF. When a painting is significantly compromised due to damage, being able to assess restoration is particularly important since in this case the authenticity of the work may no longer be a prime concern. It is noted that decisions regarding acceptable damage and the extent to which reintegration can mask or restore a damaged painting are in the hands of curators and conservators of collections, and that in many cases paintings which have suffered damage may indeed be restored without compromising the legibility of the artist (e.g. the successful restoration of Raffaello's Madonna of the Goldfinch (Madonna of the Goldfinch n.d.)). Compensation for loss is commonplace in painting restoration but needs to be considered carefully and thoroughly documented. There are ethical guidelines for the use of easily identifiable restoration paint that can be removed with solvents for retouching (Schenck 1994). With the aim of making reintegration more easily identifiable to the public and to experts, conservators and indeed entire conservation schools have developed varying methods for retouching (see the documents produced by the Retouching of Cultural Heritage workgroup at (Rechgroup.pt. n.d.)).

– Provenance, or the history of ownership and documented sale history of a work is often essential in attributing a work. Insecure provenance or falsified provenance may compromise the authentication of paintings, while ownership and documented evidence of purchase can instead provide key and important art historical information regarding perception, taste and value. Excellent examples of the way documentary evidence can contribute to the study of provenance can be found in the Raphael Research Resource from the National Gallery London (https://www.nationalgallery.org.uk/paintings/research/provenance) (Cooper and Plazzotta 2004). While masterpieces in collections may have uninterrupted and documented provenance, this may not be the case for newly discovered paintings and this constitutes a significant dilemma: without provenance, authenticity is compromised.
– Another key aspect of studying a painting is the careful examination of the way a work is executed, or technical study. This may be as important as the identification of compatible materials in excluding or confirming authorship. For example, a close study of brushstrokes, drawings, signatures and other paint details are elements of the style of a painter (see Chap. 5). An intimate knowledge and visual memory of style and familiarity with the evolution of a painter's style is at the heart of close examination of paintings, and the work of the connosieur (Van De Wetering 2008). Advances in image-based automatic artist attribution is under development to improve visual examination by learning to recognize visual features from data rather than from prior knowledge (Noord et al. 2015).

Technical analysis entails the use of a large set of techniques to analyse the materials constituting a painting. Since it is fundamental to ensure that the paintings are not subjected to significant damage during sampling, analytical campaigns start with the application of non-invasive methods (Hyperspectral/multispectral imaging, point analysis and mapping by XRF, XRD, FTIR, FORS, Raman, X-ray radiography). Following non-invasive approaches, sampling is often required to obtain information about stratigraphy and specific components of paint layers and binding media. The principal methods applied during analysis are summarised in Table 3.1, and can be classified as:

– Non-destructive techniques (MO, SEM-EDX; microRaman, ATR, SIMS, XRD, XRF, Synchrotron based spectroscopies) applied on cross-sections or powdered samples;
– Sampling and microdestructive methods (analytical pyrolysis, GC-MS, HPLC-MS, ICP-MS, Raman SERS).

3.2 Materials

While different analytical methods provide data which can be used to identify materials, the interpretation of results requires significant knowledge of the composition of paintings and conservation materials. In order to provide context, a summary of the current understanding of the use of materials and their historical usage is given in the following sections.

3.2.1 Supports

The term "support", which is an integral part of the painting itself, refers to any material onto which paint is applied: it may be a flexible material like cotton or linen canvas (stretched over a wooden frame, the stretcher) and paper, or a rigid one as a wall, wooden panels, metal, glass or plastic. The types of materials used for supports are very much influenced by their availability in the historical periods: wooden panels and linen canvas were extensively used for tempera painting in medieval age; plywood and hardboard became prominent from the twentieth century onward; modern supports often consist of composite materials and include paper, illustration board, wood, tarpaulin, plywood and hardboard (Nevin and Sawicki 2019). Dendrochronology, X-radiography and Tomographic studies may be particularly important both for the dating and the identification of the type of wood employed as well as its condition, and are essential when considering complex constructions as commonly found in polychrome wood.

Canvases are widespread and often have a distinct texture that in most cases can be easily recognized in the painting: coarse canvas imparts a softness to the surface,

Table 3.1 Overview of the main analytical methods used for the analysis of the paint surface or on powder samples or on cross sections

Instrument	Information provided	Notes
Optical microscopy (OM)	Visual information in visible and ultraviolet light on the stratigraphy of cross sections	
Scanning electron microscopy with energy dispersive X-ray detection (SEM-EDX)	Cross section morphology and elemental identification in the paint layers	
Micro-Fourier transform infrared spectroscopy (μFTIR)	Molecular information on inorganic and organic composition in the painting and in cross sections	Inorganic signals are more intense. Being the paint layers very thin, the analysis of cross sections often refers to two layers
Micro-Raman spectroscopy (μRaman)	Molecular information on inorganic and organic composition. Particularly useful to identify inorganic and organic pigments	Important in the study of cross sections, but also used on paint fragments: spatial resolution is generally compatible with the paint layer thickness
X-ray fluorescence (XRF)	Elemental information on inorganic composition of the painting surface and of paint layers in the cross section	XRF of paint surface contains information from all the layers up to the preparation (Moens et al. 2000)
X-ray diffraction (XRD)	Identification of inorganic pigments	Particularly useful for differentiating pigments with the same chemical structure but with different crystalline phases
Fibre optics reflectance spectroscopy (FORS)	Identification of inorganic and organic pigments	The presence of sooth/particles, degraded varnishes can affect position and shape of reflectance bands
Direct mass spectrometry (DTMS, MALDI, ESI-MS, LDMS)	Ionization techniques enable the detection of organic compounds	Mostly used for varnish and organic pigments identification
Secondary ion mass spectrometry (SIMS)	Identification of organic and inorganic compounds also in cross sections	It shows a major sensitivity for glycerolipid compounds
Analytical pyrolysis (Py-GC-MS and EGA-MS)	Information on thermal behavior of organic compounds and detection of specific makers and profiles of synthetic and natural materials	To volatilize all compounds, it is necessary to use derivatization agents for acidic and alcoholic moieties. All the polymers are detected
Gas chromatography-mass spectrometry (GC-MS)	Information on specific profiles of proteins, glycerolipids, waxes, natural resins and pitches, gums	Wet treatments of samples to break chemical bonds in macromolecules
Liquid chromatography-mass spectrometry (LC-MS)	Information on specific profiles of proteins, lipid, waxes, resins and organic dyes	Wet treatment of samples to solubilize compounds of interest

whereas a painting on a wooden or metal panel looks hard and smooth. Interestingly, by X-radiography it is possible to understand the type of weave of the cloth, the orientation, thickness, and density of the threads (Hendriks and Van Tilborgh 2001). Thread counting, determination of the orientation of warp and weft, the width of canvas strips, and weave matches link certain canvases together, informing on their production and sometimes determine unexpected relationships between paintings. These features help to understand which canvases an artist used in a specific historical period and in a specific geographical location: this can help to confirm an attribution of a painting to a specific artist, or to date it in a specific period (Pozzi et al. 2021). Instead of manual thread counting, a software was designed to compute a trustworthy average thread count in a repeatable, readily documented procedure (Johnson et al. 2009; Johnson and Sethares 2017). This software can be applied to the X-rays digital images and can be freely downloaded from the GitHub repository [https://github.com/sethares/CountingVermeer]. Canvases by Vermeer and Van Gogh have been extensively analysed by this method (Van Tilborgh et al. 2012).

Generally, the support is sized by a diluted glue, most typically made from animal skins, to prevent absorption of the binder into the support. In the case of canvas, a ground covers the sized support to further protect it from the adverse effects of organic paint materials. The ground is a mixture made of materials compatible with the support and the paint to be used over it, acting as a reflective surface beneath the paint film. For centuries, a mixture composed of gypsum or chalk (calcium carbonate) and animal glue was used as a ground for both wooden panels and canvas. The most common ground preparation used today is gypsum dispersed in a binder of acrylic polymer, which replaces the animal skin glue used in “traditional gesso”.

3.2.2 Pigments

Both pigments and binders have been used since prehistory for paintings. Over the centuries, craftsmen and artists experimented with traditional and novel materials to impart colour to their paintings, improving the aesthetic appearance and durability of their works-of-art. In some lucky cases, we can estimate the first use of pigments, especially when dealing with synthetic ones. Nonetheless, scientific studies have led to new discoveries regarding the long-term use of historic pigments (e.g. Egyptian blue detected in Raffaello’s works of art (Anselmi et al. 2020), or natural carmine found in 19th C. Lefranc-Bourgeois archive materials (Degano et al. 2017; Gabrieli et al. 2016)). Thus, our ability to connect dating and provenance to the occurrence of specific pigments is dependent not only on geographic and historical research, but also on the study of specific artists and their workshops. Information on the most common pigments used in paintings are reported in Table 3.2.

Pigments can be classified by colour or origin, or broad chemical composition as inorganic and organic pigments. The latter can typically be obtained by complexation or adsorption on an inorganic, uncoloured salt, of an organic dye, extracted from natural sources, and are thus generally known as pigment lakes (see Chap. 9).

Table 3.2 Examples of the most commonly-used pigments found in paintings, adapted from (Colombini and Degano 2018)

	Name of the pigment	Formula/chemical class	Details	Notes
White	Lead white	$2PbCO_3 \cdot Pb(OH)_2$	Inorganic, artificial	Most used white until the nineteenth century
	Lime white (San Giovanni white)	$CaCO_3$	Inorganic	Mostly in wall paintings
	Titanium dioxide	TiO_2	Inorganic, synthetic	Synthetic (1920)
	Gypsum	$CaSO_4 \cdot 2H_2O$	Inorganic	Mostly used for ground layers
Blue	Azurite	$2CuCO_3 \cdot Cu(OH)_2$	Inorganic	
	Ultramarine blue (lazurite)	Lazurite is a tectosilicate mineral with sulfate, sulfur and chloride with formula $(Na,Ca)_8[(S,Cl,SO_4,OH)_2](Al_6Si_6O_{24})]$	Inorganic, natural (but a synthetic lazurite exists, first synthesized in 1828 (Plesters 1966))	Very precious
	Smalt (cobalt glass)	Obtained by including cobalt oxides in a glass melt and grinding the final product	Inorganic, artificial	Mostly used in the seventeenth–eighteenth centuries
	Indigo	Indigoid dye precipitated on an inert substrate (clay, gypsum), is composed mainly by indigotin, with possible secondary components (indirubin, isatin)	Organic, natural (but synthetic indigotin is available since 1882)	Extracted from several plants
	Maya blue	Indigo adsorbed on/ included in palygorskite clay	Lake pigment, artificial	Used in Mesoamerica
Green	Malachite	$CuCO_3 \cdot Cu(OH)_2$	Inorganic	
	Verdigris (copper acetate)	$Cu(CH_3COO)_2 \cdot 2Cu(OH)_2$	Inorganic, artificial	Synthesized by Greek and Roman painters
	Phthalo green	Copper phthalocyanine	Organic, synthetic pigment	Very stable, synthetic (1936)

(continued)

Table 3.2 (continued)

	Name of the pigment	Formula/chemical class	Details	Notes
Yellow	Lead chromate	$PbCrO_4$	Inorganic, synthetic	Commercially available since 1818
	Azo yellow pigments	Series of monoazo, diazo, BONA, etc.	Synthetic organic pigments (first, PY1, syntehsised in 1897 in Germany)	Commercially available since the end of nineteenth century
Yellow-red	Yellow and red ochre	Fe_2O_3 (from yellow to red depending on the hydration)	Inorganic, natural, artificial	
Red, violet and purple	Red lead (minium)	Pb_3O_4	Inorganic	
	Vermilion	HgS	Inorganic	From cinnabar mineral
	Madder lake	Anthraquinones precipitated as a complex with alum	Lake pigment, artificial	Since ancient times, from roots
	Carmine	Anthraquinones (carminic acid mainly) precipitated as a salt	Lake pigment, artificial	Very precious, seventeenth century
	Azo red pigments	Series of monoazo, diazo, etc.	Synthetic organic pigments (first, PR1, synthesized in 1880 in England)	Commercially available since the end of nineteenth century
	Eosin	Organic pigment (xanthene class)	Lake pigment, synthetic	Synthetic, very fugitive
	Crystal violet	Organic pigment, triarylmethine class	Much used in inks, until now	Synthetic, quite fugitive
Black	Ivory black	Amorphous carbon obtained from ivory and animal bones, also containing calcium phosphate and carbonate	Artificial	
	Carbon black/vine black	Amorphous carbon obtained from organic material	Artificial	

Amongst the synthetic organic pigments, some molecules are already insoluble in the paint binder, or can be precipitated as a salt, being strongly acid or alkaline.

Traditionally, pigments were obtained from coloured earth pigments (iron oxide containing clays) or by grinding precious stones. In few cases, specific products were obtained by chemically modifying natural substances, e.g. Egyptian blue, obtained in 3000 b.C. by heating silica, malachite, natron, calcium carbonate and

sodium carbonate; lead white, consisting of basic lead carbonate ($2Pb(CO_3)_2$ $Pb(OH)_2$) was made by stacking lead strips in porous jars with vinegar and burying the jars in animal manure, whose mild temperature promoted the reaction. Thanks to the modern understanding of chemical properties and processes, many synthetic inorganic pigments were produced during the eighteenth century: Prussian Blue (1704) replaced the more expensive ultramarine (Barnett et al. 2006). Cobalt containing pigments shortly followed: Cobalt blue, developed in 1802 by Thenard; Cobalt green developed by Rinmann, a Swedish chemist in 1780; Cobalt violet (either cobalt phosphate or cobalt arsenate) appeared in 1859 and Cobalt yellow (cobalt aluminium nitrite) discovered by Fischer in Breslau in 1830. Zinc was also very important: in 1834 Winsor & Newton of London, working with Michael Faraday, invented Chinese white (zinc oxide). Finally, Cadmium metal was discovered by Stromeyer in 1817, and Cadmium yellows were in use in Europe since 1829.

Lake pigments have been used since antiquity for colouring vases, for mural paintings, and later on wood panels and for easel paintings. Few water insoluble pigments were precipitated on inert supports as gypsum or clay, e.g. Maya blue (Grazia et al. 2020), or Tyrian purple used in Ancient Greek and Etruscan mural paintings (Sotiropoulou et al. 2021). Water soluble dyes were instead mostly precipitated as metal complexes on colourless salts, in particular with alum. Madder, kermes, lac and cochineal lakes are the most famous red ones, followed by brazilwood lake; few yellow lakes are known, such as weld lake. In the last decades of the nineteenth century, the deeper understanding of inorganic and organic chemistry influenced the availability of reactants, thus impacting on the preparation of a wider variety of new colours for paint materials. By modulating the extraction process and using different salts as precipitating agents, it became possible to obtain different modified madder and cochineal based products (e.g. carmine), with different colours.

The development of synthetic organic pigments (SOPs) was driven by the textile dying industry. In 1856, William Perkin synthetized the first organic dye, mauve. The success of the dye encouraged the production of other aniline/coal tar-based pigments used in paintings. At the beginning of twentieth century the number of colours available was still limited, while nowadays the paint industry has a wide variety of pigments to choose from. Due to their high performances, cheapness, and wide range of brilliant hues, SOPs were exploited for many industrial applications including printing inks, food and drink additives, plastics, and textiles. The first azo dye was Aniline Yellow, produced in 1861 by C. Mene. It was manufactured by reacting aniline with nitric acid and commercialized in 1864 as the first commercial azo dye. Several azo dyes were precipitated as lakes as new pigments for artists, but unfortunately many of the new products were not tested sufficiently for fastness properties before their introduction on the market. For instance, Eosin (Acid Red 87, C.I. 45,380), belonging to the family of xanthenes and commercialized as "Geranium lake", was one of the most attractive and interesting early synthetic colorants which unfortunately is highly fugitive. Vincent Van Gogh used this pigment lake in several paintings during the Arles period (1888–1890), which now show clear discoloration: the fading of the red lakes in still lives *Irises* and *Roses* has

resulted in pink paints that now look white and in purple paints that now look blue (Centeno et al. 2017).

Carbon based and organic pigments have been also used in the production of inks. The adoption of fluid inks has been attributed to China around 2700 b.C. (Edwards 2018). The first inks produced were made of carbon black suspended in water and gum Arabic solutions; sooth of different origin was later widely employed. In mediaeval times, iron gall ink replaced carbon black ink as the favored medium of writing, which was produced by reacting aqueous solution of iron(II) sulfate and extract of gallnuts with the addition of gum Arabic. Red inks were produced with brazilwood lakes, whose fugitive nature made it a better candidate for writing and manuscript illuminating than for painting purposes. Following upon Perkin's synthesis of mauveine in 1856, several developments in ink manufacture occurred, thanks to the availability of a new range of organic dye-based colored inks.

3.2.3 Traditional Paint Binders

Traditional binding materials are natural substances produced by plants or animals. Naturally occurring materials may contain proteins, lipids, carbohydrates, and waxes as reported in Table 3.3.

From a chemical point of view, these natural materials can be described as follows:

(a) **Proteins**. They are macromolecules made up of one or more unbranched chains of amino acids joined together by peptide bonds between the carboxyl and

Table 3.3 Classification of traditional natural binders

Class of organic compound	Natural material	Uses in painting
Proteins	Animal glue Egg white Egg yolk (proteins + lipids + sugars) Milk/Casein (+ lipids and sugars) Vegetable proteins (e.g. garlic)	Water-soluble binders for *tempera, tempera grassa* and *gilding* techniques
Carbohydrates	Honey, starch contain simple sugars Plant gums: Arabic gum, tragacanth, karaya, ghatti, guar, locust bean, fruit tree gum	Water-soluble polysaccharide binders mainly for *watercolor* and *gouache* techniques, ink components
Glycerolipids	Vegetable drying oils: linseed, walnut, poppy seed, Tung oil Animal fat	Not water-soluble binders for *oil* techniques
Waxes	Beeswax	*Encausto* and *ceroplastic* technique

amino groups of adjacent amino acid residues. Several (yet in limited number) amino acids are commonly found in animal and vegetable proteins: glycine (Gly), alanine (Ala), valine (Val), leucine (Leu), isoleucine (Ile), methionine (Met), proline (Pro), hydroxyproline, (Hyp), threonine (Thr), asparagine (Asn), glutamine (Gln), tyrosine (Tyr), cysteine (Cys), lysine (Lys), arginine (Arg), aspartic acid (Asp), phenylalanine (Phe), tryptophan (Trp), serine (Ser), glutamic acid (Glu), and hystidine (His).

(b) **Carbohydrates**. Plant gums are naturally occurring polysaccharide exudates from several species of plants or extracted from the endosperm of some seeds. The polymers consist of aldopentoses, aldohexoses and uronic acids joined together by glycosidic bonds. Natural gums present variable distributions in mean molecular mass of polymeric molecules, whereas the composition of the constituent sugar percentages remains reasonably constant and depends on the specie of the plant.

(c) **Glycerolipids**. Oils and fats are mixtures of triglycerides, namely esters of glycerol with fatty acids, containing smaller amounts of other compounds, as sterols and vitamins. Unsaturated and especially polyunsaturated fatty acids in the triacylglycerol molecule are commonly subject to oxidation via radical reactions with the inclusion of oxygen in the acyl chain, carbon-carbon bond formation, and the production of lower molecular weight species. This phenomenon causes polymerization and cross-linking processes during the curing of drying oils. It leads to the formation of a polymeric network, generating a solid paint film.

(d) **Waxes**. Beeswax, obtained from the hives of bees, is the most commonly used natural wax for manufacturing works of art, and used since prehistory. The qualitative average composition of beeswax is quite constant and is made up of hydrocarbons (14%), monoesters (35%), diesters (14%), triesters (3%), hydroxymonoesters (4%), hydroxypolyesters (8%), monoacid esters (1%), acid polyesters (2%), free acids (12%) and free alcohols (1%). The aliphatic chains of beeswax compounds are mainly saturated and consequently extremely resistant to ageing.

3.2.4 Modern Paint Binders

The chemical and compositional features of modern oil paints are different from those of classical oil paint used in antiquity. The main ingredients of the first commercial paint tubes, introduced at the beginning of the twentieth century, were traditional drying oils, as linseed or walnut oil, often used in mixtures with less expensive oils as castor, safflower or fish oil, added with new classes of additives such as surfactants, metal soaps and dispersing agents (La Nasa et al. 2015, 2021b). Pastel crayons were also widely used for sketching compositions with

precise details, and were ideal for different kinds of supports. The early commercial formulations of pastel crayons still remain undisclosed (La Nasa et al. 2021a).

In the twentieth century a wide range of new synthetic materials were also introduced. Modern art materials include a large number of formulations of synthetic polymers characterized by short drying times, excellent optical properties, flexibility and good resistance to light, humidity and heat. Synthetic polymers are extensively used not only as binders by the artists, but also as materials for conservation (i.e. as consolidants, adhesives or protective coatings). This means that almost any type of polymer structure can be found in historical and modern artworks, either added in some conservation treatment or as constituent materials. Anyway, the most representative classes of synthetic resins used by artists are acrylic, vinyl and alkyd ones, being the most used the acrylic resin. Table 3.4 reports some characteristics of the most used polymer paint binders.

Table 3.4 Characteristics of commonly used synthetic paint binders

Polymer	Production year	Chemical composition	Additives and plasticizers	Notes
Vinyl polymers	~1920	Poly(vinyl acetate): Polymerization of vinyl; poly(vinyl alcohol): acetate monomer hydrolysis of PVAc	Phthalate esters	Water-based paint binder
	~1960		VeoVa (vinyl versatates esters in vinyl acetate polymers)	VeoVa improves hydrolytic stability, adhesion, water and UV resistance
Alkyd resin	1927	Oil-modified polyesters synthesized from glycerol, phthalic anhydride and a drying oil	Unsaturated fatty acids, acrylic, styrene and silicone compounds, driers, dispersing agents	Semi-synthetic polymer
	1960	Glycerol was substituted by pentaerythritol		
Acrylic resins	~1940	*Homopolymers:* ethyl acrylate EA, butylmetacrilate, nBMA		Solvent soluble
	1956	*Copolymers* of MMA, EA, EMA, 2-EHA, nBA	Phthalates, surfactants	Aqueous emulsion, being p(EA/MMA) one of the most used
Polystyrene	~1940	Polymerization of the styrene monomer		Solvent soluble

3.2.5 Varnishes

Varnishes are mixtures of natural or synthetic resins that dry when spread thinly on a surface. Several recipes, reported in numerous historic sources, describe a variety of materials and techniques used to obtain natural varnishes. Basically, they can be classified into spirit varnishes and oil ones. Curing of spirit varnishes consists in the evaporation of the solvent and solidification of the resin; curing of oil varnishes is based on the polymerization capability of the (poly)unsaturated compounds present in both the oil and resin.

Natural varnishes were used by artists for easel painting, and by restorers to protect the paint layer from the environment (i.e. oxygen, moisture). Synthetic varnishes have been used for the same purposes, but also as binding media in modern and contemporary paintings.

Varnishes possess specific optical and physical properties, which confer them transparency and ability to form stable films on the surface of the paintings, without compromising the aesthetics of the work-of-art, and even improving its gloss and general color equilibrium. Plant terpenoid resins are the most used as varnish. They are a complex mixture of mono-, sesqui-, di- and triterpenes, which have, respectively, 10, 15, 20 and 30 carbon atoms per molecule.

In East Asia and Japan, natural polymers called lacquers were used both as varnishes and painting media since ancient times; lacquers consist of the sap extracted from trees and their composition is based on a specific mixtures of catechol derivatives (Heginbotham et al. 2011; Tamburini et al. 2020).

Amongst the natural and synthetic varnishes, the most common are reviewed in Table 3.5.

The detection of a specific varnish may provide the analyst with information on the painting technique, on the possible restoration occurred, on the presence of repaintings (especially whenever synthetic varnishes are applied) (Decq et al. 2019). Detecting synthetic or semi-synthetic varnishes may also yield information about the dating of the production of the painting or of a previous restoration (Bonaduce et al. 2013; La Nasa et al. 2017).

3.3 Conclusions

By providing a simplified overview of commonly applied techniques and many of the materials found in paintings it is clear that the identification of specific material in paintings is a complex analytical challenge, and requires experience and careful interpretation as well as caution. Commonly publications include as much data as necessary to support interpretation of results and should highlight accuracy and error as well as the potential analytical limitations, especially when the authorship

Table 3.5 Characteristics of the most used varnishes

Class	Common name	Main content	Provenance	Notes
Diterpenoid resin	Colophony/ turpentine	Abietadienic acids, pimaradienic acids	*Pinaceae* resins	
	Sandarac	Pimaradienic acids (sandaracopimaric acid), communic acid, totarol, agathic acid		Sandarac type I and II are available
Triterpenoid resin	Mastic resin	Euphanes (masticadienonic and isomasticadienonic acids), oleanananes (oleanonic and moronic acids), dammaranes	*Pistacia* tree resin	Plant resin from Chios island in the Aegean Sea; already used in ancient Egypt
	Dammar resin	Dammaranes (hydroxydammarenone, dammaradienol), ursanes (ursonic acid, ursonaldehyde)	*Hopea* genus tree	Plant resin, introduced into Europe in the nineteenth century
	Copal resin	Lupane (mainly), ursane and oleanane triterpenoids	*Bursera* spp., *Protium copal*, some *Pinus* spp. (e.g., *P. pseudostrobus*) and a few *Fabaceae* spp	
Sesquiterpenoid resin	Shellac	Mono- and polyesters of hydroxy-aliphatic and sesquiterpene acids, peaking at jalaric and laccijalaric acids, aleuritic and butolic acids	The glandular secretion of an Indian scaled insect (*Laccifer lacca* Kerr)	Animal resin, began to be used in Europe towards the end of the sixteenth century
East Asian Laquers	Japanese lacquer (*urushi*)	Catechol derivatives, peaking at 3-pentadecylcatechol	From the sap of *Rhus vernicifera* (*Anacardiaceae*), native to China, Japan and Corea	Plant resin, used as both varnishes and painting medium (see above) since ancient times
	Laccol	Catechol derivatives, peaking 3-heptadecylcatechol	From the sap of *Rhus succedanea* (*Anacardiaceae*), native to North Vietnam and Taiwan	
	Burmese lacquer (*thitsi*)	Catechol derivatives, including 3-pentadecylcatechol, 3-heptadecylcatechol, alkylphenylphenols and alkylphenyl-1,2-dihydroxybenzenes	From the sap of *Melanorrhoea usitate* (*Anacardiaceae*), native to Thailand and Burma	

Vinyl polymers	Polystyrene, PVC, polyethylene, polypropylene, polyacrylonitrile			Used in plastic objects, as water-based paint binder, adhesive and varnish
Acrylic resin	Perspex, PMMA, Paraloid			Synthetic polymers, available since c.a. 1930, used as varnishes, adhesives
Low-molecular-weight resins	Laropal K80	Urea-aldehyde polymer	Aldehyde resin synthesized from urea, isobutyraldehyde, and formaldehyde	Synthetic resins used as varnishes since c.a. 1930
	MS2A	Reduced ketone polymer	Condensation products of methylcyclohexanones and/or cyclohexanones	
	Regalrez	Hydrocarbon-based resin	Hydrocarbon resin synthesized from vinyltoluene and α-methylstyrene and subsequent hydrogenation of the unsaturated polymer	

or authenticity of works is under scrutiny. Indeed, the interpretation of results from analysis is often based on deduction and comparisons with results from the analysis of similar works, for which there may or may not be reliable studies.

References

Anselmi, C., Vagnini, M., Seccaroni, C., Azzarelli, M., Frizzi, T., Alberti, R., et al.: Imaging the antique: unexpected Egyptian blue in Raphael's Galatea by non-invasive mapping. Rend. Lincei. **31**, 913–917 (2020). https://doi.org/10.1007/s12210-020-00960-4

Barnett, J.R., Miller, S., Pearce, E.: Colour and art: a brief history of pigments. Opt. Laser Technol. **38**, 445–453 (2006). https://doi.org/10.1016/j.optlastec.2005.06.005

Bonaduce, I., Colombini, M.P., Degano, I., Di Girolamo, F., La Nasa, J., Modugno, F., et al.: Mass spectrometric techniques for characterizing low-molecular-weight resins used as paint varnishes. Anal. Bioanal. Chem. **405**, 1047–1065 (2013). https://doi.org/10.1007/s00216-012-6502-9

Centeno, S.A., Hale, C., Carò, F., Cesaratto, A., Shibayama, N., Delaney, J., et al.: Van Gogh's Irises and Roses: the contribution of chemical analyses and imaging to the assessment of color changes in the red lake pigments. Herit. Sci. **5**, 18 (2017). https://doi.org/10.1186/s40494-017-0131-8

Colombini, M.P., Degano, I.: Pigments and binders. Encycl. Archaeol. Sci., 1–5 (2018). https://doi.org/10.1002/9781119188230.saseas0458

Cooper, D., Plazzotta, C.: Raphael's Ansidei altarpiece in the National Gallery. Burlingt. Mag. (2004). https://doi.org/10.2307/20073744

Decq, L., Abatih, E., Van Keulen, H., Leyman, V., Cattersel, V., Steyaert, D., et al.: Nontargeted pattern recognition in the search for pyrolysis gas chromatography/mass spectrometry resin markers in historic lacquered objects. Anal. Chem. **91**, 7131–7138 (2019). https://doi.org/10.1021/acs.analchem.9b00240

Degano, I., Tognotti, P., Kunzelman, D., Modugno, F.: HPLC-DAD and HPLC-ESI-Q-ToF characterisation of early 20th century lake and organic pigments from Lefranc archives. Herit. Sci. **5**, 7 (2017). https://doi.org/10.1186/s40494-017-0120-y

Edwards, H.G.M.: Chapter 1. Analytical Raman Spectroscopy of Inks, vol. 2, pp. 1–15. The Royal Society of Chemistry (2018). https://doi.org/10.1039/9781788013475-00001

Execution of Maximilian. n.d. https://www.nationalgallery.org.uk/paintings/edouard-manet-the-execution-of-maximilian

Gabrieli, F., Doherty, B., Miliani, C., Degano, I., Modugno, F., Uldank, D., et al.: Micro-Raman and SER spectroscopy to unfold Lefranc's early organic pigment formulations. J. Raman Spectrosc. **47** (2016). https://doi.org/10.1002/jrs.5052

Grazia, C., Buti, D., Amat, A., Rosi, F., Romani, A., Domenici, D., et al.: Shades of blue: non-invasive spectroscopic investigations of Maya blue pigments. From laboratory mock-ups to Mesoamerican codices. Herit. Sci. **8**, 1 (2020). https://doi.org/10.1186/s40494-019-0345-z

Heginbotham, A., Schilling, M., Rivers, S., Faulkner, R., Pretzel, B. (eds.): East Asian Lacquer: Material Culture, Science and Conservation. Archetype Publications Ltd, London (2011)

Hendriks, E., Van Tilborgh, L.: Van Gogh's "garden of the asylum": genuine or fake? Burlingt. Mag. **143**, 145–156 (2001)

Johnson, R.J., Sethares, W.A. (eds.): Counting Vermeer: Using Weave Maps to Study Vermeer's Canvases. RKD Nederlands Instituut voor Kunstgeschiedenis, The Hague (2017)

Johnson, D.H., Johnson, C.R., Klein, A.G., Sethares, W.A., Lee, H., Hendriks, E.: A thread counting algorithm for art forensics. In: 2009 IEEE 13th Digital Signal Processing Workshop and 5th IEEE Signal Processing Education Workshop, pp. 679–684 (2009). https://doi.org/10.1109/DSP.2009.4786009

La Nasa, J., Zanaboni, M., Uldanck, D., Degano, I., Modugno, F., Kutzke, H., et al.: Novel application of liquid chromatography/mass spectrometry for the characterization of drying oils in art: elucidation on the composition of original paint materials used by Edvard Munch (1863–1944). Anal. Chim. Acta. **896**, 177–189 (2015). https://doi.org/10.1016/j.aca.2015.09.023

La Nasa, J., Di Marco, F., Bernazzani, L., Duce, C., Spepi, A., Ubaldi, V., et al.: Aquazol as a binder for retouching paints. An evaluation through analytical pyrolysis and thermal analysis. Polym. Degrad. Stab. **144**, 508–519 (2017). https://doi.org/10.1016/j.polymdegradstab.2017.09.007

La Nasa, J., Doherty, B., Rosi, F., Braccini, C., Broers, F.T.H., Degano, I., et al.: An integrated analytical study of crayons from the original art materials collection of the MUNCH museum in Oslo. Sci. Rep. **11**, 7152 (2021a). https://doi.org/10.1038/s41598-021-86031-6

La Nasa, J., Mazurek, J., Degano, I., Rogge, C.E.: The identification of fish oils in 20th century paints and paintings. J. Cult. Herit. **50**, 49–60 (2021b). https://doi.org/10.1016/j.culher.2021.06.003

Madonna of the Goldfinch. n.d. https://www.uffizi.it/en/artworks/mary-christ-and-the-young-john-the-baptist-known-as-the-madonna-of-the-goldfinch

Moens, L., von Bohlen, A., Vandenabeele: X-ray fluorescence. In: Ciliberto, E., Spoto, G. (eds.) Modern Analytical Methods in Art and Archaeology, pp. 55–79. Wiley, New York (2000)

Nevin, A., Sawicki, M.: Heritage Wood. Springer, Cham (2019). https://doi.org/10.1007/978-3-030-11054-3

Plesters, J.: Ultramarine blue, natural and artificial. Stud. Conserv. **11**, 62–91 (1966)

Pozzi, F., Basso, E., Centeno, S.A., Smieska, L.M., Shibayama, N., Berns, R., et al.: Altered identity: fleeting colors and obscured surfaces in Van Gogh's Landscapes in Paris, Arles, and Saint-Rémy. Herit. Sci. **9**, 15 (2021). https://doi.org/10.1186/s40494-021-00489-1

Rechgroup.pt. n.d. http://rechgroup.pt/postprints.htm

Schenck K. 30. Inpainting. B Pap Conserv Cat 1994

Sotiropoulou, S., Karapanagiotis, I., Andrikopoulos, K.S., Marketou, T., Birtacha, K., Marthari, M.: Review and new evidence on the molluscan purple pigment used in the early late Bronze Age Aegean Wall paintings. Heritage. **4**, 171–187 (2021). https://doi.org/10.3390/heritage4010010

Tamburini, D., Bonaduce, I., Ribechini, E., Gallego, C., Pérez-Arantegui, J.: Challenges in the data analysis of Asian lacquers from museum objects by pyrolysis gas chromatography/mass spectrometry. J. Anal. Appl. Pyrolysis. **151**, 104905 (2020). https://doi.org/10.1016/j.jaap.2020.104905

Van De Wetering, E.: Connoisseurship and Rembrandt's paintings: new directions in the Rembrandt Research Project, Part II. Burlingt. Mag. **150**, 83–90 (2008)

van Noord, N., Hendriks, E., Postma, E.: Toward discovery of the artist's style: learning to recognize artists by their artworks. IEEE Signal Process. Mag. **32**, 46–54 (2015). https://doi.org/10.1109/MSP.2015.2406955

Van Tilborgh, L., Meedendorp, T., Hendriks, E., Johnson, D.H., Johnson, C.R., Erdmann, R.G.: Weave matching and dating of Van Gogh's paintings: an interdisciplinary approach. Burlingt. Mag. **154**, 112–122 (2012)

Part II
Characterization of Paintings by Digital Techniques

Chapter 4
Visible and Infrared Reflectance Imaging Spectroscopy of Paintings and Works on Paper

John K. Delaney and Kathryn A. Dooley

Abstract In cultural heritage science, a variety of macroscale spectral imaging modalities have been developed to study the complete surface of paintings and works on paper. These spectral imaging modalities have been adapted from site-specific techniques such as reflectance spectroscopy and X-ray fluorescence that provide information about the molecular and elemental composition of materials. Such methods, especially when used in combination, provide a more comprehensive understanding of the artists' materials used and the artistic working process. This chapter focuses on the use of reflectance imaging spectroscopy. Specifically, topics on the collection of spectral image cubes include the definition of reflectance imaging spectroscopy, the spectral ranges most commonly used in cultural heritage science, and the types of hyperspectral cameras (i.e. single pixel and line-scanning imaging spectrometers that are sensitive in the visible-to-mid-IR), as well as the different ways mid-IR image cubes can be collected. In addition, a comprehensive discussion of data analysis starting from the most basic through to machine learning algorithms is given, with the focus on identifying and mapping artists' pigments and binders. Image processing strategies are presented to enhance the visualization of preparatory sketches or changes in the painted composition. Finally, two case studies show the use of reflectance imaging spectroscopy to map pigments and paint binders in illuminated manuscripts. Another case study uses reflectance and X-ray fluorescence imaging spectroscopies to help reveal sufficient detail of a hidden portrait such that a color simulation of the original painting could be made.

Keywords Reflectance imaging spectroscopy · Hyperspectral · Near-infrared · Mid-infrared · Pigment mapping

J. K. Delaney (✉) · K. A. Dooley
National Gallery of Art, Washington, DC, USA
e-mail: J-Delaney@NGA.GOV; k-dooley@NGA.GOV

M. P. Colombini et al. (eds.), *Analytical Chemistry for the Study of Paintings and the Detection of Forgeries*, Cultural Heritage Science,
https://doi.org/10.1007/978-3-030-86865-9_4

4.1 Introduction

Several spectral imaging modalities have been adopted for the analysis of fine works of art as well as polychrome archeological art objects on the macroscale. At present, the modalities that have been more widely explored fall into two classes: those that provide elemental information and those that provide molecular information about the artists' materials used. In all cases the information obtained is in the form of a three-dimensional image cube, consisting of two spatial dimensions representing the surface of the work of art and the third containing the spectral information. Thus, regardless of the spectral imaging modality or instrument used, the data can be considered as a large number of independent spectral measurements collected at regularly spaced spatial intervals over the surface of a work of art. These data sets are typically referred to as image cubes which are explored in order to find spatial pixels having similar spectral features that can be related to a material with a specific chemical composition. If X-ray fluorescence is measured, then the chemical elements can be identified, and if reflectance or luminescence is measured, then electronic transitions or vibrational transitions (reflectance only) can be used to identify artists' materials (pigments or binders). In this way all of these spectral imaging modalities can be considered forms of imaging spectroscopy.

This chapter focuses on diffuse reflectance imaging spectroscopy which has been used to provide a variety of information including identifying many of the artists' materials used and mapping their distribution across the surface of the work of art (e.g. paintings). The identification of artists' materials (pigments and paint binders) by reflectance imaging spectroscopy relies on the presence of absorption features in the spectra from electronic and vibrational transitions. Thus, in principle the optimal spectral range extends from the near-ultraviolet through the mid-infrared, where visible is defined as 400–750 nm, near-infrared (NIR) 750–3000 nm, and mid-infrared (mid-IR) as 3–25 μm.

4.2 Definition of Diffuse Reflectance Imaging Spectroscopy

Diffuse reflectance spectroscopy is used to provide information about absorption features associated with electronic and vibrational transitions of molecules and thus is analogous to absorption or transmission spectroscopy. However, unlike transmission spectroscopy, it involves the collection of light that is backscattered from the object. As such, the spectral signature encodes not only absorption features from electronic and vibrational transitions but also scattering characteristics of the sample as well. While this makes the interpretation of the spectra more complex, it does allow for the study of absorption features of opaque materials.

The formal definition of diffuse reflectance is the ratio of irradiance of light reflected back to the detector to that of the irradiance onto the surface of the art object as a function of wavelength. Thus, the measured reflectance spectrum is the

ratio of the spectral irradiances and will include contributions from the air/surface interface and vary with illumination and collection geometry. In practice for cultural heritage analysis, these specular contributions are not of interest and the diffuse reflectance spectrum is calculated by taking the ratio of irradiance of the illumination light off of the object of interest to that of a nearly Lambertian reflectance standard referred to as the white standard due to its ability to reflect approximately 99% of the illumination light. The implication of this practical simplification is that differences in the surface roughness between the white standard and the object can result in differences in the absolute reflectance values. Thus, reflectance spectra measured in this way are referred to as "Apparent Reflectance" to note this difference (Schaepman-Strub et al. 2006).

4.3 Use of Diffuse Reflectance Imaging Spectroscopy in Cultural Heritage Science

The central goal of reflectance imaging spectroscopy is the identification and mapping of artists' materials (pigments and paint binders) in situ (Cucci et al. 2016). The primary identification of the material is done using the spectral features (electronic and vibrational transitions) in the reflectance spectra and the mapping is done by identifying the spatial pixels that have similar spectral features to the material of interest. As discussed in the reflectance image cube processing section, this is done several ways. The most common way is to classify areas that have similar reflectance spectra and identify the reflectance spectra of the representative classes (i.e. characteristic or endmember spectra) as a specific artist material by mathematically comparing the endmember spectra with those from a spectral library or visually identifying the key spectral features.

A wide variety of paintings have been studied using reflectance imaging spectroscopy to map and identify artists' materials. These have included archaeological paintings from the ancient world (Delaney et al. 2017; Alfeld et al. 2018a, b), Byzantine paintings (Radpour 2019) and illuminated manuscripts from Italy (Ricciardi et al. 2013; Mounier and Daniel 2015; Cucci et al. 2018; Kleynhans et al. 2020a, b). Other Italian Renaissance paintings include those of Cosmé Tura (Dooley et al. 2014) and Bellini (Dooley et al. 2019) and Dutch painters such as Vermeer (Delaney et al. 2020). Late nineteenth and twentieth-century artists such as Van Gogh (Zhao et al. 2008; Dooley et al. 2020), Munch (Monico et al. 2020), Picasso (Delaney et al. 2010, 2016), and Pollock (Dooley et al. 2017) have been studied not only for pigments but in the latter case for paint binders as well.

Another use, especially when reflectance imaging spectroscopy is conducted in the NIR is to improve on the results obtained from traditional infrared reflectography (Delaney et al. 2016). Often NIR reflectance imaging spectroscopy provides more detailed information about preparatory sketches and changes in the painted composition than infrared reflectography. The optimal visualization of preparatory

sketches or compositional paint changes relies on imaging in a spectral region where the contrast is greatest between the background and the spatial features of interest. This optimal spectral window differs depending on the optical properties of the pigments in the paint layers and the underdrawing material as well as the reflectance properties of the ground layer they are on. Having a large number of spectral bands across this optimal spectral window allows for application of image processing tools that may increase the separation of overlapping features painted with different materials. For example, the use of principal component analysis, although more complicated than constructing false-color images (selection of three spectral bands placed in the RGB display channels), can often help a user better separate the drawing from partially penetrated paint. Or in the case of changes in the painted composition or the re-use of a canvas, the false-color images of transform images (i.e. the output images after performing PCA on an image cube) can provide clear images of earlier painted compositions. A variety of examples exist showing these added benefits from Picasso's famous re-used canvases of his Blue Period paintings to Italian Renaissance paintings such as *The Feast of the Gods* by Bellini whose landscape was subsequently altered twice, including by Titian (Bull 1993; Dooley et al. 2019).

Visible reflectance imaging spectroscopy has also been explored to improve on color accuracy of digital captures, as a tool to monitor color changes and produce simulations of paintings if an aged varnish was removed or if a faded pigment was restored. The large number of spectral bands allows a more accurate calculation of the color coordinates compared to a three-color channel camera since the functions of the standard observer can be used rather than the approximation provided by the three-color filters on the camera. The ability to monitor changes in color of an art object with time translates into looking for changes in the reflectance spectra but requires ensuring repeatable illumination conditions and image cube registration. The visible reflectance image cube allows for the possibility to estimate an average transmission cube for an aged varnish as well as scattering terms in order to simulate the visual effects of removing an aged varnish (Trumpy et al. 2015; Kirchner et al. 2018a). Such a data set allows the virtual replacement of areas of faded pigments with reflectance spectra obtained from Kubelka-Munk modeling of pigment concentrations determined by other means such as X-ray fluorescence (Kirchner et al. 2018b).

4.4 Spectral Range of Hyperspectral Reflectance Cameras Used in Cultural Heritage Science

Practically, the useful spectral range of reflectance spectra is set in part by the artists' pigments most often encountered and the types of hyperspectral reflectance imaging cameras or scanning single pixel spectrometers available. The electronic transitions associated with white pigments such as zinc white (384 nm) and both

forms of titanium white (anatase, 372 nm and rutile, 406 nm) set the lower wavelength limit to 350 nm or just into the near-UV (Bacci et al. 2007). The higher wavelength limit relates more to development of sensors used in remote sensing of the earth, where the thermal radiation of the earth dominates over the solar reflected radiation at wavelengths greater than about 3000 nm. Thus, in remote sensing of the earth (where the light source is the sun) hyperspectral cameras operating from 400 nm to 2500 or 3000 nm rely on reflected radiation and above 3000 nm they rely on thermal emitted radiation from the objects. In cultural heritage applications, most hyperspectral imaging experiments performed in the spectral region >3000 nm have relied on reflected radiation off of the art object from a thermal source (Rosi et al. 2013,;Legrand et al. 2014) and one study collected thermal emitted radiation from paintings (Gabrieli et al. 2019). In summary, the most used spectral ranges in cultural heritage hyperspectral imaging have been in the visible to 'optical near-infrared' (abbreviated VNIR) from 400 to 1000 nm, in the NIR region from ~1000 to 2500 nm, and in the mid-IR region at wavelengths longer than 3000 nm.

4.5 Instrumentation and Experimental Procedures for Reflectance Imaging Spectroscopic Studies (350–2500 nm)

A variety of spectral optical systems have been used to construct diffuse reflectance image cubes, such as single pixel and line scanners built around a dispersive spectrometer or Fourier transform imaging spectrometer that images areas. Camera systems that employ a large number of spectral filters or individual spectral lamps have also been used. The ultimate choice about which system is best for analysis of a collection of cultural heritage objects depends on several factors, including the range of artist materials expected, the spatial resolution desired, and object size. In cases where a small number of pigments are expected, a limited number of spectral bands may be all that is needed to spectrally separate and map them. The use of spectral filters or spectral lamps with an imaging array may suffice. For cases where a large number of pigments are expected to have similar spectral features, higher spectral resolution over a large spectral range is often required and an imaging spectrometer is needed. The simplest system is a single pixel 2-D scanner in which the collected light is directed to one or more spectrometers. Such systems often provide the widest spectral range, highest spectral resolution, and highest signal-to-noise, but have the lowest spatial sampling and scanning speed (spatial pixels per second). For example, single pixel scanners built around a commercial fiber optics spectroradiometer that spans the spectral range of 350–2500 nm have been found useful for laboratory measurements (Delaney et al. 2018a, b) and field work (Radpour 2019). The development of available line-scanning imaging spectrometers for the remote sensing community and more recently for industrial materials testing (pharmaceutical, manufacturing, food industry) has resulted in several commercial imaging

spectrometers which subsequently have been adapted for the study of cultural heritage objects. Compared to single pixel scanners, they have scan rates that are orders of magnitude faster with similar spectral resolution (Fig. 4.1). Such line-scanning systems can provide spatial sampling as fine as ~200 μm^2 and allow collecting image cubes of paintings as large as several square meters in less than one day. These hyperspectral cameras are typically built to operate in either the VNIR or the NIR spectral regions, although cameras that span the full range are becoming available.

The image collection geometry most commonly used for diffuse reflectance imaging spectroscopy has the hyperspectral reflectance camera oriented normal to the paintings surface with two illumination sources at 45 degrees to the normal.

Larger angles of the illumination sources are often used for paintings having a low average reflectance and glossy varnish in order to minimize glints from specular reflections from the lights. The illumination sources are often lamps with tungsten halogen bulbs whose vertical position coincides with the center of the slit of the spectrometer. Tungsten halogen bulbs powered with an external power supply can provide a stable light intensity. Alternatively, two fiber optic line-lights oriented parallel to the slit can be used to only illuminate a narrow vertical strip on the

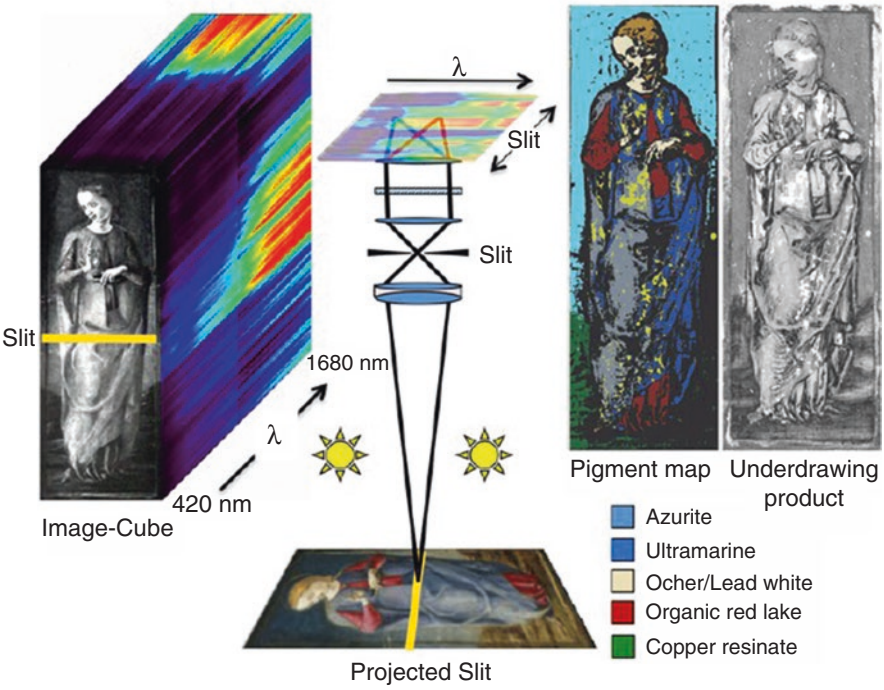

Fig. 4.1 Schematic operation of a line-scanning hyperspectral reflectance camera to acquire a 3-D reflectance image cube. A map of pigments and an image product showing the preparatory sketch can be obtained. (Cucci et al. 2016)

painting. Newer LED line lights designed for reflectance imaging spectroscopy are becoming available. In any illumination system used to study light-sensitive cultural heritage objects it is important to reduce the intensity of light (e.g. UV and thermal) outside the spectral region of interest and keep the illumination at acceptable levels as per conservation guidelines.

Data collection with single pixel or line scanners involves translating the scanner or the painting in order to collect the raw image cube, followed by collection of a 'dark' image cube (using a lens cap to prevent light from entering the hyperspectral camera) and finally the image cube of the white standard in order to calibrate the image cube of the artwork to apparent reflectance. This calibration set is typically incorporated into the collection software for commercial hyperspectral reflectance scanning cameras.

The key performance metrics of hyperspectral reflectance cameras includes both spatial and spectral parameters and it is important to include some of this information in publications. The spatial sampling is the projected size of a pixel at the painting and should be reported. Since the primary analysis of the reflectance image cube is performed in the spectral domain, the spectral sampling, the spectral resolution, and the signal-to-noise ratio are important metrics to measure. Spectral sampling is the number of nanometers a spectral pixel spans and should also be reported, but knowledge of the spectral resolution, which relates to the spectral response function (full width at half height in nanometers of an atomic emission line), is also useful. Note that the spectral sampling and resolution (at a given signal-to-noise ratio) that is deemed necessary to discriminate among materials depends upon the spectral position and width of their characteristic electronic and vibrational transitions. In materials that have similar spectral features that are shifted by only a few nanometers, sufficient spectral sampling and resolution is required to be able to confidently separate materials in the presence of noise.

Typically, specific electronic transitions in the visible and vibrational transitions in the NIR set the spectral sampling/resolution requirements for a hyperspectral camera. For example, the ability to distinguish among electronic transitions in the visible for cobalt pigments, iron earth pigments such as jarosite, and red lake pigments such as kermes and madder lake, are often important. This requires a spectral sampling of ~2–3 nm and a resolution of ~5–6 nm. To separate the NIR overtone due to hydroxyl stretching that occurs in azurite, gypsum and various clays, spectral sampling of about 3–6 nm and spectral resolution of 10–12 nm are generally required. Being able to measure the shift in NIR wavelength of the CH_2 combination band associated with different lipidic binders (egg yolk, drying oil, beeswax) requires spectral sampling of 4 nm or less. The signal-to-noise can be given in percent reflectance and a root mean square noise of $< 0.5\%$ reflectance (measured from a 2% 'black' reflectance standard) is preferred.

Low signal-to-noise, i.e. high random noise in the reflectance spectrum, is the most common problem with hyperspectral reflectance image cubes of paintings. Care needs to be taken to set the exposure time and light level such that the intensity of the light reflected off the white standard (99% diffuse reflectance reference) totals 80% of the dynamic range of the detector (i.e. utilizes 80% of the well

capacity of a pixel in the detector). Assuming the noise is random, the noise can be reduced by spatially averaging pixels in the image cube (but at a corresponding loss of the spatial sampling). Alternatively, noise can be reduced by spectral averaging although this decreases the spectral sampling. As a rule of thumb, the optimal spectral pixel aggregation should be set to match the width of the spectral slit. Most commercially produced VNIR hyperspectral cameras offer the user the ability to change the spectral sampling since they often contain focal plane arrays with pixel sizes that are smaller than the slit width of the spectrometer.

The intensity and duration of the illumination light used in collecting the reflectance image cube of cultural heritage objects, paintings, and works on paper needs to be addressed before any scanning is undertaken. Most commercial hyperspectral reflectance cameras were optimized for imaging outdoors where the natural light levels are 10 to 100x that of museum lighting conditions. Thus, care needs to be taken to ensure the light levels and their duration is adequate for the work of art being examined. A number of factors needs to be considered, including keeping the total accumulative exposure time as short as possible to minimize fading. This is often done by calculating the light exposure to be received using the experimental conditions in terms of the equivalent number of hours or days under normal gallery lighting conditions. Another factor of the illumination conditions to consider is ensuring the rise in temperature of the object, especially black paints, does not exceed acceptable conservation levels. The American Institute for Conservation provides practical guidelines for imaging works of art that can be used as a starting point.

4.6 Image Processing and Exploitation of Reflectance Image Cubes (350–2500 nm)

The analysis of reflectance image cubes is a multi-step process that depends just as much on the questions being asked as the skill level of the person analyzing the image cube. At one extreme, the analyst might only be interested in looking for a specific material whose unique spectral features they know. At the other extreme, the user wants to make labeled maps of all the artists' materials present such as pigments. Currently this can be done in two different ways. One way involves a two-step process that initially classifies the reflectance image cubes into a set of reflectance spectra, called endmembers, which have characteristic spectral features that represent specific regions of the image cube. Next, the pigments and binders represented by each endmember spectrum are assigned by using the spectral features of each endmember, along with information obtained by other site-specific methods (i.e. X-ray fluorescence, fiber optics reflectance spectroscopy, Raman spectroscopy). The other way is a one-step process that creates labeled maps of artists' materials directly without having to find spectral endmembers. This one-step

process is of great utility to the cultural heritage community, and development of such algorithms is still an active area of research.

In the case where the analyst is looking for a few specific materials whose unique spectral features are known, analysis can be performed by using a reference spectrum pulled from a spectral library, such as the one maintained by the United States Geological Survey (USGS). Next, an algorithm is used to identify the spatial pixels in the image cube that best match the library reference spectrum. Many matching algorithms exist for this purpose, such as Spectral Angle Mapper (Dooley et al. 2014). Since these libraries are typically of pure materials that are optically thick, they do not often work well for matching to reflectance image cubes of paintings, where the pigments are in paint layers that are not optically thick beyond the visible region and are applied on a preparatory ground layer having its own spectral properties. Because of the differences encountered between spectra from the collected image cube and a reference library, often the analyst tries to find a representative spectrum from the image cube that can serve as the reference spectrum. Successful results can usually be achieved by restricting the spectral range and removing the spectral continuum in order to isolate the spectral feature of interest.

When the user wants to make labeled maps of all the artists' materials present, either a two-step or a one-step process can be used. In the two-step process, the first step involves finding the spectral endmembers and separating the reflectance spectra in the image cube into classes. This can be achieved manually by visual inspection of the spectra in the image cube, but use of a statistical analysis algorithm is often a better approach. One of the more widely used algorithms to find endmembers in cultural heritage science is the ENVI spectral hourglass wizard (ENVI-SHW, Harris L3 Corp) which is rooted in convex geometry (Delaney et al. 2010). The ENVI-SHW algorithm uses principal component analysis (PCA) to reduce the number of spectral bands (dimensions) of the reflectance image cube, which can number in the 100's, down to between 10 and 30 principal component (PC) dimensions. Next, the Pixel Purity Index (PPI) algorithm is used. PPI uses a limited set of random projections (10's of thousands instead of millions) to find spectra that are the most spectrally diverse. The most diverse spectra are displayed as points in a cloud of n-dimensional space, where n is the number of PC dimensions, using the n-D visualizer tool. In principle, the spectral endmembers will be the spectra that reside at the vertices or corners of the point cloud. Although the ENVI-SHW can automatically identify endmembers, usually the best results are obtained when an experienced user refines the automatic selection or manually selects some endmembers that may have been previously missed. As a result, the method is only semi-automatic but through the interactive clustering process, the analyst can gain insight into the spectral data set.

In recent years, researchers have been testing existing remote sensing algorithms that automatically find spectral endmembers on reflectance image cubes of cultural heritage objects. Algorithms tested include ones based on k-means clustering (Rohani et al. 2016), and a combination of BH t-SNE (Barnes-Hutt t-Distributed

Stochastic Neighbour Embedding) and DBSCAN (Density-based spatial clustering of applications with noise) (Grabowski et al. 2018). Also, algorithms based on a convex hull, such as MaxD (Maximum Distance), are able to find the majority of spectral endmembers previously identified with ENVI-SHW (Kleynhans et al. 2020a). Once the endmembers are found, classification maps, defined by the endmember spectra, can be made. Commonly used classification algorithms include Spectral Angle Mapper (SAM) (Delaney et al. 2010), Maximum Likelihood (ML) (Balas et al. 2018) and Spectral Correlation Mapper (SCM) (Deborah et al. 2014). These algorithms compare each spectrum in the image cube with the endmembers to find matches. The classification map for a given endmember shows the spatial pixels whose spectra match those of the endmember. The second step of the two-step process involves the identification of the artists' materials represented by the endmember spectra. The artists' materials are determined by identifying the reflectance spectral features of each endmember, along with information obtained by other site-specific methods (i.e. X-ray fluorescence, fiber optics reflectance spectroscopy, Raman spectroscopy).

The second analysis approach creates the labeled material maps directly without having to find spectral endmembers in the image cube. This is the most challenging approach, but potentially of the most use to the cultural heritage community. The reason why it is so challenging is because, unlike most research questions encountered in remote sensing, the materials encountered in cultural heritage (like paint layers) are not optically thick over the full spectral range. The paint also consists of pigments that are intimately mixed, so their reflectance spectrum is not the weighted linear sum of their component spectra. One method that has been used to try and automatically identify materials includes attempts to linearize the intimate mixing problem by using an approximation to the radiative transfer equation for simple mixtures of optically thick paints (Zhao et al. 2008). The unknown spectrum from the image cube is linearly fit using a set of weighted absorption and scattering coefficients from a database, which limits its effectiveness because it requires a priori knowledge about what pigments and pigment mixtures will be encountered. It has been found to work well for mock paintings, but it has not been found yet to work in widespread applications and more than one mixture might produce acceptable results. An interesting approach to address these limitations has been the use of a neural network to preselect the pigments represented in the database (Rohani et al. 2018).

Another one-step approach for creating labeled material maps has restricted the number of pigments expected to be encountered to pigments found in particular schools of painting where the paint methods are similar in terms of the pigments and pigment mixtures used. A 1-D convolutional neural network was trained using four illuminations from the *Laudario of Sant'Agnese* c. 1340 attributed to two painters (Kleynhans et al. 2020a, b). The network was trained on large regions of these paintings whose pigment composition had been previously identified and mapped. These regions included areas with a range of pigment mixtures and areas with the same pigment having different optical thicknesses. The neural network was found successful in directly classifying and identifying the pigments in another painting from

the *Laudario*, as well as another painting from the same time period. These and other studies suggest a direct material mapping from reflectance image cubes is possible, and could be especially useful when information from other spectral imaging modalities is incorporated as well.

4.7 The Mid-IR Instrumentation, Experimental Procedures, and Image Processing (4000 cm^{-1} to 650 cm^{-1}, 2.5 to 15.4 μm)

In remote sensing, mid-IR hyperspectral cameras and analysis tools are well developed, but they are still an active area of research in the application to studying works of art. This spectral region is rich with absorption features from numerous functional groups which is what makes it attractive. However, the difficulty in obtaining affordable mid-IR hyperspectral cameras that can operate over the mid-IR spectral range, defined here as 4000–650 cm^{-1}, has limited most of the research to single pixel, FTIR spectrometer scanning systems, operating in reflectance mode, as first demonstrated by Legrand et al. 2014. Given their short air path length (<1 cm), these systems can collect spectra over the full mid-IR spectral range. However, they suffer from low spatial resolution/sampling (1–2 mm) and slow scan speeds (about 1 pixel per second versus 1000's of pixels per second for the VNIR and NIR hyperspectral reflectance cameras) even compared to XRF scanners. Still, results from these mid-IR scanners have shown the promise of mid-IR imaging spectroscopy by providing low resolution maps of many of the pigments (Legrand et al. 2014) as well as paint binders and paint fillers (Gabrieli et al. 2019) in unvarnished paintings such as illuminated manuscripts.

Efforts to increase the spatial pixel collection rates have focused on adapting mid-IR hyperspectral cameras that were optimized for remote sensing of the earth. Unlike the single pixel scanners discussed above, these cameras were designed to operate in one of two atmospheric spectral windows in the mid-IR, namely 3–5.5 μm (3333–1818 cm^{-1}) or 7.7 to ~14 μm (1298 to ~714 cm^{-1}). Using an imaging FTIR camera (1440–900 cm^{-1}), and operating in reflectance mode, Rosi et al. captured details from a Burri painting, *Sestante 10*, and identified and mapped organic (acrylic and alkyd binders) and inorganic (silicates and sulfates) compounds (Rosi et al. 2013). Gabrieli et al. used a line scanning imaging spectrometer (1240–760 cm^{-1}) in emissive mode and demonstrated the ability to map paint binders (oil, acrylic and alkyds), pigments, and fillers in a mock painting as well as in Edward Steichen's *Study for "Le Tournesol"* (Gabrieli et al. 2018).

With each mid-IR collection mode, reflectance or emissive, the origin of the spectral radiance collected to make the spectral image is different. In emissive mode, the spectral radiance collected is dominated by the thermal emission from the painting, whereas in reflectance mode, the collected radiance is dominated by the radiance that is reflected off the painting from an external thermal source. Reflectance

mode is common in laboratory measurements and requires some care to minimize the heating of the painting during the data cube collection. The conversion of the measured spectral data cube to apparent reflectance is done using a gold reflectance standard. Emissive mode in a laboratory environment emulates how mid-IR spectral imaging is done in remote sensing, namely the spectral radiance emitted by the object dominates over the downwelling spectral radiance from the sky that is reflected off of the object since the sky temperature is at a lower temperature than the object on the earth. To conduct emissive mode mid-IR imaging spectroscopy in a laboratory, a 'box' is placed between the painting and the camera to reduce the spectral radiance from the room which is at the same temperature as the painting under study. The 'box' is configured to be a source of radiance from a blackbody at a lower temperature than the room. Note that the measured spectra from each spatial pixel in the image cube is given by the product of the emissivity of the paint and the blackbody function, both of which vary with wavelength. Thus, in order to recover the emissivity spectrum at each spatial pixel, the collected image cube of the painting is first converted to units of spectral radiance, and then each spectrum is fit with a blackbody function. One of the advantages of emissive mode mid-IR imaging over reflectance mode mid-IR imaging is the signal strength, i.e. the spectral radiance from the signal of interest. This is because the emissivity of the paints is close to one and by Kirchhoff's law the reflectance is one minus the emissivity. Nevertheless, each mid-IR imaging mode has its strengths and weaknesses.

The data processing of the mid-IR reflectance or emission image cubes can be done using the same procedure used for the visible and NIR image cubes including the use of automatic and semi-automatic algorithms to find spectral endmembers. However, since most of the users are familiar with the spectra of many functional groups in the mid-IR, maps are most often made by limiting the spectral range used to that of the spectral feature of interest. Then an endmember spectrum is selected from the cube and a mapping algorithm such as spectral angle mapper is used to make the map. The identification of spectral features from functional groups for both the reflectance and the emissive spectra is often not as straightforward as absorptions seen in transmission FTIR spectra due to contributions from specular reflection by the pigment particles that leads to spectral distortion in the bands, a phenomenon that is well known (Miliani et al. 2012).

4.8 The Future of Reflectance Imaging Spectroscopy

The increased interest in macroscale spectral imaging modalities by conservation scientists, conservators, curators, and art historians can be expected to further invigorate the field. This is precisely because the image products are accessible to this wide audience. The desire for more spectral image cubes of paintings is not just for the new results they are giving but also because they help to confirm, and expand on,

earlier findings obtained from detailed chemical analysis of microsamples. The rapid adoption of reflectance imaging spectroscopy in the pharmaceutical, manufacturing, and food industry has resulted in the lowering of the cost of VNIR hyperspectral cameras for the cultural heritage science community. The increased availability and improved performance of NIR and mid-IR cameras is also decreasing the barrier to purchasing hyperspectral cameras in these spectral ranges as well. Finally, collection of reflectance image cubes from the near-UV through the mid-IR promises to offer a more robust ability to classify and identify artists' materials. New algorithms, including some used in machine learning, offer more automated processing of the reflectance image cubes. Finally, the fusion of reflectance imaging spectroscopy with the results from molecular and elemental fluorescence can be expected to provide a more complete understanding of artists' working methods and artists' materials.

4.9 Case Studies

A few case studies are provided that highlight the variety of results which can be obtained using reflectance imaging spectroscopy.

4.9.1 Identification and Mapping of Artists' Materials: Pigments

A central goal of reflectance imaging spectroscopy is the identification of classes of reflectance spectra that can be used to classify regions of the reflectance image cube into regions that have similar reflectance spectra. In this case study, the VNIR reflectance image cube of an illuminated manuscript cutting, *Christ and the Virgin Enthroned with Forty Saints*, from the *Laudario of Sant'Agnese,* attributed to Master of the Dominican Effigies c. 1340, was collected and analyzed. The reflectance image cube was analyzed using the ENVI Spectral Hourglass Wizard (ENVI, Harris L3 Corp). In the analysis, 16 spectral endmembers were obtained by manual clustering (Kleynhans et al. 2020a, b). These endmembers defined the classes used to construct the map. A combination of spectral features from the reflectance endmembers and results from site-specific X-ray fluorescence and fiber optics reflectance spectroscopy (350–2500 nm) were used to assign the pigments to each class (Fig. 4.2).

Fig. 4.2 (Left) *Christ and the Virgin Enthroned with Forty Saints*, Master of the Dominican Effigies c. 1340, National Gallery of Art, Washington. (Middle) Class map of the reflectance spectral endmembers (right) with their assigned pigments. (Kleynhans et al. 2020a)

4.9.2 Identification and Mapping of Artists' Materials: Paint Binders

Reflectance imaging spectroscopy in the NIR spectral region 2000–2400 nm offers the ability to separate and classify drying oils, egg yolk, wax and paint binders containing carbohydrates and proteins, depending on the substrate. However, mid-IR imaging spectroscopy (reflectance or emissive mode) offers more functional groups to better map and identify these binders, but currently at the expense of spatial resolution and time. In this example, the identification and mapping of paint binders is demonstrated in Lorenzo Monaco's *Praying Prophet*, a cutting from a fifteenth-century illuminated choir book commissioned by the Camaldolese monks of Santa Maria degli Angeli in Florence. NIR and mid-IR reflectance imaging spectroscopy were used to map spectral features associated with the binding media, including the NIR CH_2 lipidic feature at 2309 nm which has been associated with egg yolk tempera binder (Gabrieli et al. 2019). This assignment was confirmed by the map of the mid-IR carbonyl group and lipidic components of egg yolk tempera. The marginalia were found to possess mid-IR spectral absorptions associated with polysaccharides and not egg tempera (Fig. 4.3).

4.9.3 The Earlier Composition of Fragonard's Young Girl Reading

A previously collected X-ray radiograph of Jean-Honoré Fragonard's painting *Young Girl Reading*, c. 1769, showed another figure below the girl, although the features of this person were not clear. The painting also has a pentimento in the background above the girl's head that suggested the presence of a feather associated

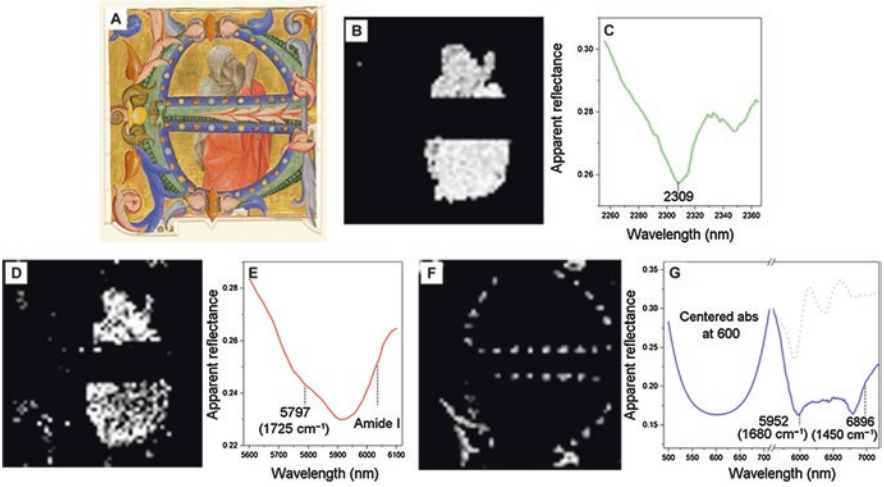

Fig. 4.3 (**a**) Color image of Lorenzo Monaco's *Praying Prophet,* 1410/1413, Rosenwald Collection, National Gallery of Art, Washington. (**b**) Map of the C─H lipidic spectral feature associated with egg yolk (**c**). (**d**) Map of carbonyl group (C═O) spectral features (**e**) associated with the proteic (amide I) and lipidic component (5797 nm or 1725 cm^{-1}) in egg yolk. (**f**) Map of ultramarine and polysaccharide spectral features (**g**) associated with the blue portions of the initial E and blue areas of the marginalia. (Gabrieli et al. 2019)

with the prior figure's head. This earlier figure has a face that is oriented towards the viewer, which was more in keeping with a series of portraits that Fragonard painted known as the Fantasy Figures. The underlying portrait was tenuously associated with the Fantasy Figures based on the similarity of the composition, but its association was confirmed when a Fragonard drawing of quickly executed thumbnail sketches of many paintings in this series was discovered in 2012 (Jackall et al. 2015). The first sketch on this drawing depicts a woman holding a book and looking towards the viewer. The combination of NIR (1000–2500 nm) reflectance imaging spectroscopy and XRF fluorescence imaging spectroscopy confirmed the prior figure was a woman and revealed new details, including the presence of a black ribbon tied around her neck and a feather in her hair with red beads. The appearance of the underlying woman not only matches the quick sketch in the Fragonard drawing, but also fits in with the style of the other Fantasy Figures (Jackall et al. 2015). The combination of the image products from the two imaging modalities allowed for a simulation to be made of the prior composition (Fig. 4.4).

Fig. 4.4 (Top left) Color detail of Jean-Honoré Fragonard's *Young Girl Reading*, c.1769, National Gallery of Art, Washington. Top right: False-color diffuse reflectance near-infrared image (1000, 1300, 2100 nm) (J. Delaney and K. Dooley). Bottom right: XRF image obtained from the mercury L-alpha line, likely associated with vermilion. Bottom left: Image simulation of figure underlying *Young Girl Reading* extrapolated from technical images (B. Goodman and D. Doorly). (Jackall et al. 2015)

References

Alfeld, M., et al.: MA-XRF and hyperspectral reflectance imaging for visualizing traces of antique polychromy on the Frieze of the Siphnian Treasury. Microchem. J. **141**, 395–403 (2018a)

Alfeld, M., et al.: Joint data treatment for Vis–NIR reflectance imaging spectroscopy and XRF imaging acquired in the Theban Necropolis in Egypt by data fusion and t-SNE. Comptes Rendus Physique. **19**(7), 625–635 (2018b)

Bacci, M., Picollo, M., Trumpy, G., Tsukada, M., Kunzelman, D.: Non-invasive identification of white pigments on 20th-century oil paintings by using fiber optic reflectance spectroscopy. J. Am. Inst. Conserv. **46**(1), 27–37 (2007). https://doi.org/10.1179/019713607806112413

Balas, C., Epitropou, G., Tsapras, A., Hadjinicolaou, N.: Hyperspectral imaging and spectral classification for pigment identification and mapping in paintings by El Greco and his workshop. Multimed. Tools Appl., 9737–9751 (2018)

Bull, D.: The feast of the Gods: conservation and investigation. Stud. Hist. Art. **45**, 366–373 (1993)

Cucci, C., Delaney, J.K., Picollo, M.: Reflectance hyperspectral imaging for investigation of works of art: old master paintings and illuminated manuscripts. Acc. Chem. Res. **49**(10), 2070–2079 (2016)

Cucci, C., Bracci, S., Casini, A., Innocenti, S., Picollo, M., Stefani, L., Rao, I.G., Scudieri, M.: The illuminated manuscript Corale 43 and its attribution to Beato Angelico: non-invasive analysis by FORS, XRF and hyperspectral imaging techniques. Microchem. J. **138**, 45–57 (2018). https://doi.org/10.1016/j.microc.2017.12.021

Deborah, H., George, S., Hardeberg, J.: Pigment mapping of the scream (1893) Based on Hyperspectral Imaging. In: 6th International Conference. ICISP. **8509**, 247–256 (2014). https://doi.org/10.1007/978-3-319-07998-1_28

Delaney, J.K., Zeibel, J.G., Thoury, M., Littleton, R., Palmer, M., Morales, K.M., et al.: Visible and infrared imaging spectroscopy of Picasso's Harlequin musician: mapping and identification of artist materials in situ. Appl. Spectrosc. **64**(6), 584–594 (2010)

Delaney, J.K., Thoury, M., Zeibel, J.G., Ricciardi, P., Morales, K.M., Dooley, K.A.: Visible and infrared imaging spectroscopy of paintings and improved reflectography. Herit. Sci. **4**(1), 1–10 (2016)

Delaney, J.K., Dooley, K.A., Radpour, R., Kakoulli, I.: Macroscale multimodal imaging reveals ancient painting production technology and the vogue in Greco-Roman Egypt. Nature Special Rep. **14** (2017)

Delaney, J., Conover, D., Dooley, K., Glinsman, L., Janssens, K., Loew, M.: Integrated x-ray fluorescence and diffuse visible-to-near-infrared reflectance scanner for standoff elemental and molecular spectroscopic imaging of paints and works on paper. Herit. Sci. **6**, 2050–7445 (2018a). https://doi.org/10.1186/s40494-018-0197-y

Delaney, J.K., Conover, D.M., Dooley, K.A., et al.: Integrated X-ray fluorescence and diffuse visible-to-near-infrared reflectance scanner for standoff elemental and molecular spectroscopic imaging of paints and works on paper. Herit. Sci. **6**, 31 (2018b). https://doi.org/10.1186/s40494-018-0197-y

Delaney, J.K., Dooley, K.A., van Loon, A., Vandivere, A.: Mapping the pigment distribution of Vermeer's Girl with a Pearl Earring. Herit. Sci. **8**, 4 (2020). https://doi.org/10.1186/s40494-019-0348-9

Dooley, K., Conover, D., Glinsman, L., Delaney, J.: Complementary standoff chemical imaging to map and identify artist materials in an early Italian Renaissance panel painting. Angew. Chem. Int. Ed. **126** (2014)

Dooley, K.A., Coddington, J., Krueger, J., Conover, D.M., Loew, M., Delaney, J.K.: Standoff chemical imaging finds evidence for Jackson Pollock's selective use of alkyd and oil binding media in a famous 'drip' painting". Anal. Methods. **9**(1), 28–37 (2017)

Dooley, K.A., Berrie, B., Delaney, J.K.: Appendix II technical reexamination of the *Feast of the Gods*. In: Brown, D.A. (ed.) Giovanni Bellini: The Last Works. Skira Editore, Milan (2019)

Dooley, K.A., Chieli, A., Romani, A., Legrand, S., Miliani, C., Janssens, K., Delaney, J.K.: Molecular fluorescence imaging spectroscopy for mapping low concentrations of red lake pigments: Van Gogh's painting The Olive Orchard. Angew. Chem. Int. Ed. Eng. **59**(15), 6046–6053. Epub 2020 Feb 11. PMID: 31961988 (2020). https://doi.org/10.1002/anie.201915490

Gabrieli, F., Dooley, K.A., Zeibel, J.G., Howe, J.D., Delaney, J.K.: Novel collection method for standoff mid-infrared hyperspectral imaging to identify and map materials in polychrome objects. Angew. Chem. Int. Ed. Eng. **57**(25), 7341–7345 (2018). https://doi.org/10.1002/anie.201710192

Gabrieli, F., Dooley, K.A., Facini, M., Delaney, J.K.: Near UV to mid-IR reflectance imaging spectroscopy of paintings on the macroscale. Sci. Adv. **5**(8) (2019). https://doi.org/10.1126/sciadv.aaw7794

Grabowski, B., Masarczyk, W., Lomb, P.G., Mendys-Frodyma, A.: Automatic pigment identification from hyperspectral data. J. Cult. Herit. **31**, 1–12 (2018). https://doi.org/10.1016/j.culher.2018.01.003

Jackall, Y., Delaney, J.K., Swicklik, M.: 'Portrait of a Woman with a Book': a 'Newly Discovered Fantasy Figure' by Fragonard at the National Gallery of Art, Washington. Burlingt. Mag. **157**(1345), 248–254 (2015)

Kirchner, E., van der Lans, I., Ligterink, F., Hendriks, E., Delaney, J.: Digitally reconstructing Van Gogh's *Field with Irises near Arles*. Part 1: varnish. Color. Res. Appl. **43**, 152–157 (2018a). https://doi.org/10.1002/col.22162

Kirchner, E., van der Lans, I., Ligterink, F., et al.: Digitally reconstructing Van Gogh's *Field with Irises near Arles* part 3: determining the original colors. Color. Res. Appl. **43**, 311–327 (2018b). https://doi.org/10.1002/col.22197

Kleynhans, T., Delaney, J.K., Messinger, D.: Towards automatic classification of diffuse reflectance image cubes from paintings collected with hyperspectral cameras. Microchem. J. **157** (2020a). https://doi.org/10.1016/j.microc.2020.104934

Kleynhans, T., Schmidt Patterson, C.M., Dooley, K.A., Messinger, D.W., Delaney, J.K.: An alternative approach to mapping pigments in paintings with hyperspectral reflectance image cubes using artificial intelligence. Herit. Sci. **8**, 84 (2020b). https://doi.org/10.1186/s40494-020-00427-7

Legrand, S., Alfeld, M., Vanmeert, F., De Nolf, W., Janssens, K.: Macroscopic Fourier transform infrared scanning in reflection mode (MA-rFTIR), a new tool for chemical imaging of cultural heritage artefacts in the mid-infrared range. Analyst. **139**, 2489–2498 (2014)

Miliani, C., Rosi, F., Daveri, A., Brunetti, B.G.: Reflection infrared spectroscopy for the non-invasive in situ study of artists' pigments. Appl. Phys. A Mater. Sci. Process. **106**, 295–307 (2012)

Monico, L., Cartechini, L., Rosi, F., Chieli, A., Grazia, C., De Meyer, S., Nuyts, G., Vanmeert, F., Janssens, K., Cotte, M., De Nolf, W., Falkenberg, G., Sandu, I.C.A., Tveit, E.S., Mass, J., de Freitas, R.P., Romani, A., Miliani, C.: Probing the chemistry of CdS paints in The Scream by in situ noninvasive spectroscopies and synchrotron radiation x-ray techniques. Sci. Adv., eaay3514 (2020)

Mounier, A., Daniel, F.: Hyperspectral imaging for the study of two thirteenth-century Italian miniatures from the Marcad'e collection, Treasury of the Saint-Andre Cathedral in Bordeaux, France. Stud. Conserv. **60**(sup1), S200–S209. arXiv (2015). https://doi.org/10.1179/0039363015Z.000000000225

Radpour, R.: Advanced imaging spectroscopy and chemical sensing in archaeometry and archaeological forensics. Dissertation. UCLA (2019)

Ricciardi, P., Delaney, J.K., Facini, M., Glinsman, L.: Comprehensive analysis of the materials and techniques of a 15th-century illuminated gradual using in situ analytical methods. J. Am. Inst. Conserv. **52**(1), 12–29 (2013)

Rohani, N, Salvant, J., Bahaadini, S., Cossairt, O., Walton, M., Katsaggelos, A.K.: Automatic pigment identification on roman Egyptian paintings by using sparse modeling of hyperspectral images. In: 24th European Signal Processing Conference (EUSIPCO), pp. 2111–2115 (2016)

Rohani, N., Pouyet, E., Walton, M., Cossairt, O., Katsaggelos, A.K.: Nonlinear unmixing of hyperspectral datasets for the study of painted works of art. Angew. Chem. **130**, 11076–11080 (2018)

Rosi, F., Miliani, C., Braun, R., Harig, R., Sali, D., Brunetti, B.G., Sgamellotti, A.: Noninvasive analysis of paintings by mid-infrared hyperspectral imaging. Angew. Chem. Int. Ed. **52**, 5258–5261 (2013)

Schaepman-Strub, et al.: Remote Sensing of Environment **103**, 27–42 (2006). https://doi.org/10.1016/j.rse.2006.03.002

Trumpy, G., Conover, D., Simonot, L., Thoury, M., Picollo, M., Delaney, J.K.: Experimental study on merits of virtual cleaning of paintings with aged varnish. Opt. Express. **23**, 33836–33848 (2015). https://doi.org/10.1364/OE.23.033836

Zhao, Y., Berns, R., Taplin, L., Coddington, J.: An investigation of multispectral imaging for the mapping of pigments in paintings. Proc. SPIE. **6810** (2008)

Chapter 5
Automated Analysis of Drawings at the Stroke Level for Attribution and Authentication Using Artificial Intelligence

Ahmed Elgammal, Yan Kang, and Milko Den Leeuw

Abstract This chapter summarizes research towards building a computational approach for analysis of strokes in line drawings by artists. We aim at developing a methodology that facilitates attribution of drawings of unknown authors in a way that is not easy to be deceived by forged art. The methodology used is based on quantifying the characteristics of individual strokes in drawings. We propose a novel algorithm for segmenting individual strokes. We designed and compared different hand-crafted and learned features for the task of quantifying stroke shape and tonal variation characteristics. We also propose and compare different classification methods at the drawing level. We experimented with a dataset of 300 digitized drawings with over 80 thousand strokes. The collection mainly consisted of drawings of Pablo Picasso, Henry Matisse, and Egon Schiele, besides a small number of representative works of other artists. The experiments show that the proposed methodology can classify individual strokes with accuracy 70–90%, and aggregate over drawings with accuracy above 80%, while being robust to be deceived by fakes (with accuracy 100% for detecting fakes in most of the case).

Keywords Artificial intelligence · Attribution · Authentication · Computer vision · Pictology

A. Elgammal (✉) · Y. Kang · M. Den Leeuw
Art and Artificial Intelligence Lab, Department of Computer Science, Rutgers University, New Brunswick, NJ, USA
e-mail: elgammal@cs.rutgers.edu

M. P. Colombini et al. (eds.), *Analytical Chemistry for the Study of Paintings and the Detection of Forgeries*, Cultural Heritage Science,
https://doi.org/10.1007/978-3-030-86865-9_5

5.1 Introduction

Attribution of art works is a very essential task for art experts. Traditionally, stylistic analysis by expert human eye has been a main way to judge the authenticity of artworks. This has been pioneered and made a methodology by Giovanni Morelli (1816–1891) who was a physician and art collector, in what is known as Morellian analysis. This connoisseurship methodology relies on finding consistent detailed "invariant" stylistic characteristics in the artist's work that stay away from composition and subject matter. For example, Morelli paid great attention to how certain body parts, such as ears and hands are depicted in paintings by different artists, not surprisingly given his medical background. This methodology relies mainly on the human eye and expert knowledge.

In contrast, technical analysis focuses on analyzing the surface of the painting, the underpainting, and/or the canvas material. As detailed on various chapters of this book, there is a wide spectrum of imaging (e.g. infrared spectroscopy and X-ray), chemical analysis (e.g. chromatography), and radiometric (e.g. carbon dating) techniques that have been developed for this purpose. Mostly, this analysis aims to get insights on the composition of the materials and pigments used in making the different layers of the work and how that relates to what materials, were available at the time of the original artist or what the artist typically used. These techniques are complementary and each of them has limitations to the scope of their applicability.

With advances in artificial intelligence in the last few decades, in particular advances in the subarea of computer vision, there have been several academic research projects that explored the use of such technology in analysis of paintings. Analysis using computer vision and image processing techniques has been very sparsely and cautiously investigated in the domains of attribution and forgery detection (e.g. Guo et al. 2000; Johnson et al. 2008; Li et al. 2012; Polatkan et al. 2009).

What role can the computer vision technology plays in this domain given the spectrum of the other available technical analysis techniques, which might seem more conclusive. The promise of this technology is that it offers potential methods for analysis of art at the stylistic level using visual spectrum. This naturally extend the traditional connoisseurship methodology by human expert.

We argue that developing this technology would complement other technical analysis techniques for three reasons. First, computer vision can uniquely provide a quantifiable scientific way to approach the traditional connoisseurship methodology of stylistic analysis, at the visual spectrum level. This in contrast to all other technical analysis methods that focus on the physical properties of the work. Image processing is not limited to visual spectrum and also extend to non-visual spectrum imaging. Examples of that are analysis of x-ray imaging to determine canvas material and thread count (e.g. Johnson et al. 2008; Liedtke et al. 2012).

Second, it would provide alternative tools for the analysis of art works that lie out of the scope of applicability for the other techniques. For example, this can be very useful for detecting forgery of modern and contemporary art where the forger would have access to pigments and materials similar to what original artist had used).

Third, computer vision has the potential to provide a cost-effective solution compared to the cost of other technical analysis methods. For example, in particular, related to the topic of this chapter, there are large volumes of drawings, prints, and sketches for sale and are relatively cheap (in the order of a few thousand dollars, or even few hundreds) compared to paintings. Performing sophisticated technical analysis in a laboratory would be more expensive than the price of the work itself. This prohibitive cost makes it attractive for forgers to extensively target this market.

It is worthy to mention that several papers have addressed art style classification, where style is an art movement (e.g. Impressionism), or the style of a particular artist (e.g. the style of Van Gogh) (Arora and Elgammal 2012; Khan et al. 2012; Sablatnig et al. 1998; Saleh et al. 2016; Tappert et al. 2005). Such stylistic analysis does not target authentication and is not suitable to solve such problem. Typically, such works, scale down the image of an artwork to a fixed size small thumbnail-size image that is then fed to a machine learning pipeline for processing. In some cases, the image is divided into a grid for computational reasons. Therefore, such works use holistic features taken from entire image of the artwork or a large part of it, which mainly capture the composition of the painting as well as the color palette and coarse texture. These makes such algorithms easily to be fooled by forgery. In fact, such algorithm will classify a painting done on the style of Van Gogh, for example, as Van Gogh, since it is designed to do so. That makes these methods not suitable for expert-level attribution and authentication.

In contrast, we focus on developing a methodology and a computational framework for the analysis of artworks at the stroke level, ignoring as much as possible the compositional elements and the color palette, which are typically easy to forge. To this end, we focus on drawings in particular as they are the most challenging for attribution and authentication.

5.2 From Pictology to AI-Pictology

The methodology explained in this chapter is based on quantifying the characteristics of individual strokes in drawings and comparing these characteristics to a large number of strokes by different artists using statistical inference and machine learning techniques. This process is inspired by the Pictology methodology developed by Maurits Michel van Dantzig (van Dantzig 1973) (1903–1960), see Fig. 5.1.

Van Dantzig suggested several characteristics to distinguish the strokes of an artist. His methodology focused on characteristics that capture the spontaneity of how original art is being created, in contrast to the inhibitory nature of imitated art.

Among the characteristics suggested by van Dantzig to distinguish the strokes of an artist are the shape, tone, and relative length of the beginning, middle and end of each stroke. The characteristics include also the length of the stroke relative to the depiction, direction, pressure, and several others. The list of characteristics suggested by van Danzig is comprehensive and includes, in some cases, over one hundred aspects that are designed for inspection by the human eye. The main motivation

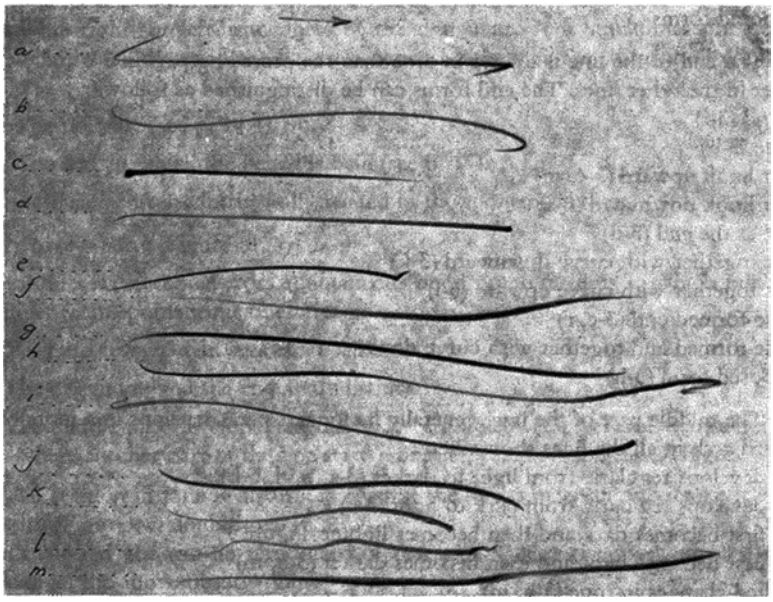

Fig. 5.1 Illustration of van Dantzig methodology on simple strokes. Spontaneous strokes differ in their shape and tone at their beginning, middle and end. (Figure from van Dantzig 1973)

is to characterize spontaneous strokes characterizing a certain artist from inhibited strokes, which are copied from original strokes to imitate the artist style.

In our work we do not plan to implement the exact list of characteristics suggested by van Dantzig; instead we developed methods for quantification of strokes that follow his methodology, trying to capture the same concepts in a way that is suitable to be quantified by the machine, is relevant to the digital domain, and facilitates statistical analysis of a large number of strokes by the machine rather than by human eye. The underlying assumption here is that the machine has much better ability to mass the statistical properties of the strokes across thousands of artworks in ways that are not possible for human experts.

We excluded using comparisons based on compositional and subject-matter-related patterns and elements. Most forged art works are based on copying certain compositional and subject-matter-related elements and patterns. Using such elements might obviously and mistakenly connect a test subject work to figures and composition in an artist known works. In contrast, to subject matter and compositional elements, the characteristics of individual strokes carry the artist's unintentional signature, which is hard to imitate or forge, even if the forger intends to do.

We propose a computational approach for analysis of strokes in line drawings that is inspired and follow the principles of Pictology, as suggested by van Dantzig. We propose and validate a novel algorithm for segmenting individual strokes. We designed and compared different hand-crafted and learned deep neural network features for the task of quantifying stroke characteristics. We also propose and compare

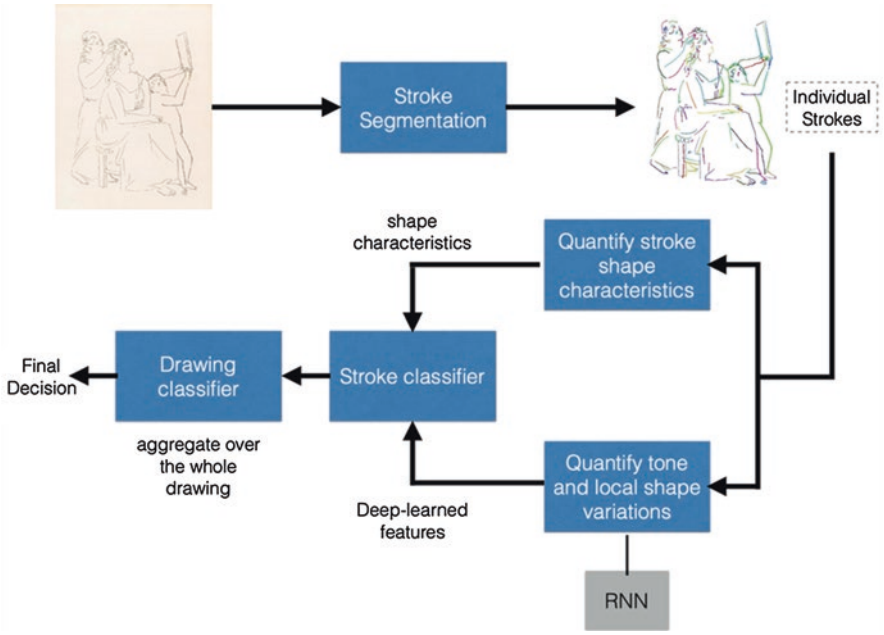

Fig. 5.2 Overview of the process of stroke analysis

different classification methods at the drawing level. Figure 5.2 illustrates the approach. We experimented with a dataset of 300 digitized drawings with over 70 thousand strokes. The collection mainly consisted of drawings of Pablo Picasso, Henry Matisse, and Egon Schiele, besides a small number of representative works of other artists. We extensively experimented on different settings of attributions to validate the proposed methodology. We also experimented with forged art works to validate the robustness of the proposed methodology and its potentials in authentication.

5.3 Challenges with Drawings

The variability in drawing technique, paper type, size, digitization technology, spatial resolution, impose various challenges in developing techniques to quantify the characteristic of strokes that are invariant to these variability. Here we highlight some these challenges and how we addressed them.

Drawings are made using different techniques, materials and tools, including, but not limited to drawings using pencil, pen and ink, brush and ink, crayon, charcoal, chalk, and graphite drawings. Different printing techniques also are used such as etching, lithograph, linocuts, wood cuts, and others. Each of these techniques results in different stroke characteristics. This suggests developing technique-specific

models of strokes. However, typically each artist prefers certain techniques over others, which introduce unbalance in the data collection, which need to be addressed. Therefore, we are tested two hypotheses: technique specific vs. across technique comparisons, to test if we can capture invariant stroke characteristic for each artist that persists across techniques.

Drawings are executed on different types of papers, which, along with differences in digitization, imply variations in the tone and color of the background. This introduces a bias in the data. We want to make sure that we identify artists based on their strokes and not based on the color tone of the paper used. Different types of papers along with the type of ink used result in different diffusion of ink at the boundaries of the strokes which, combined with digitization effects, alter the shape of the boundary of the stroke.

Drawings are made on different-sized papers, and digitized using different resolutions. The size of the original drawing as well as the digitization resolution are necessary to quantify characteristics related to the width or length of strokes. Therefore, in this paper we quantify the characteristics of the strokes in a metric basis after converting all the measurements to the metric system.

5.3.1 Case Study: Picasso, Matisse, and Schiele

A collection of 297 drawings were gathered from different sources to train, optimize, validate, and test the various classification methodologies used in this study. The drawings selected are restricted to line drawings, i.e, it excludes drawings that have heavy shading, hatching and water- colored strokes. The collection included drawings and prints by Picasso (130), Henry Matisse (77), Egon Schiele (36), Amedeo Modigliani (18), and a small representative works of other artists (36), ranging from 1910-1950AD. These artists were chosen since they were prolific in producing line drawings during the first half of the Twentieth century.

The collection included a variety of techniques including pen and ink, pencil, crayon, and graphite drawings as well as etching and lithograph prints. Table 5.1 shows the number of drawings for each artist and technique. In the domain of drawing analysis, it is very hard to obtain a dataset that is uniformly sampling artists and techniques. The collection is biased towards ink drawings, executed mostly with pen, or using brush in a few cases. There is a total of 145 ink drawings in the collection. The collection contains more works by Picasso than other artists. In all the validation and test experiments an equal number of strokes were sampled from each artist to eliminate data bias.

The collection included digitized works from books, downloaded digitized images from different sources, and screen captured images for cases where downloading was not permitted. The resolution of the collected images varies depending on the sources. The effective resolution varies from 10 to 173 pixel per cm depending on the actual drawing size and the digitized image resolution. Given this wide

Table 5.1 Case study: technique distribution

Technique	Pen/ brush (ink)	Etching	Pencil	Drypoint	Lithograph	Crayon	Charcoal	Unknown	Total
Picasso	80	38	8	2	2	0	0	0	130
Matisse	45	10	5	2	14	1	0	0	77
Schiele	0	0	10	0	0	5	4	17	36
Modigliani	0	0	9	0	0	8	1	0	18
Others	20	0	0	0	9	4	1	2	36
Total	145	48	32	4	25	18	6	19	297
Strokes	36,533	19,645	9300	914	6180	4648	666	2204	80,090

Others: Georges Braque, Antoine Bourdelle, Massimo Campigli, Marc Chagall, Marcel Gimond, Alexej Jawlensky, Henri Laurens, Andre Marchand, Albert Marquet, Andr Masson, Andre Dunoyer Dr. Segonzac, Louis Toughague

range of resolutions, the algorithms and features used were designed to be invariant to the digitization resolution.

Fake Drawing Dataset In order to validate the robustness of the proposed approaches against being deceived by forged art, we commissioned five artists to make drawings similar to those of Picasso (24), Matisse (39) and Schiele (20) using the same techniques. We collected a total of 83 drawings (24, 39, 20). None of these fake drawings was used in training the models. We only used them for testing.

Because we do not expect the reader to be experts in authentication in art, to be able to judge the quality of the fake drawings in isolation, we deliberately mixed up a collection of the fake drawings with real drawings in Figure 5.3. If the reader is interested to know which of these images are fake or real drawings, please refer to the end of the chapter.

5.4 Stroke Segmentation

A typical isolated stroke is a line or curve, with a starting point and endpoint. A stroke can have zero endpoints (closed curve) or 1 endpoint, which are special cases that do not need further segmentation. However, strokes typically intersect to form a network of tangled strokes that needs to be untangled. A network of strokes is characterized by having more than 2 endpoints. Since strokes are thin elongated structures; a skeleton representation would preserve their topological structure even in a network configuration (Lam et al. 1992). Therefore, the segmentation of strokes is done on such a skeleton representation.

There is a large classical literature in computer vision on detecting junctions on edge maps as a way to characterize object boundaries, infer about three-dimensional structure and form representations for recognition. Unlike classical literature which look at natural images, in our case detecting junctions and endpoints is fortunately

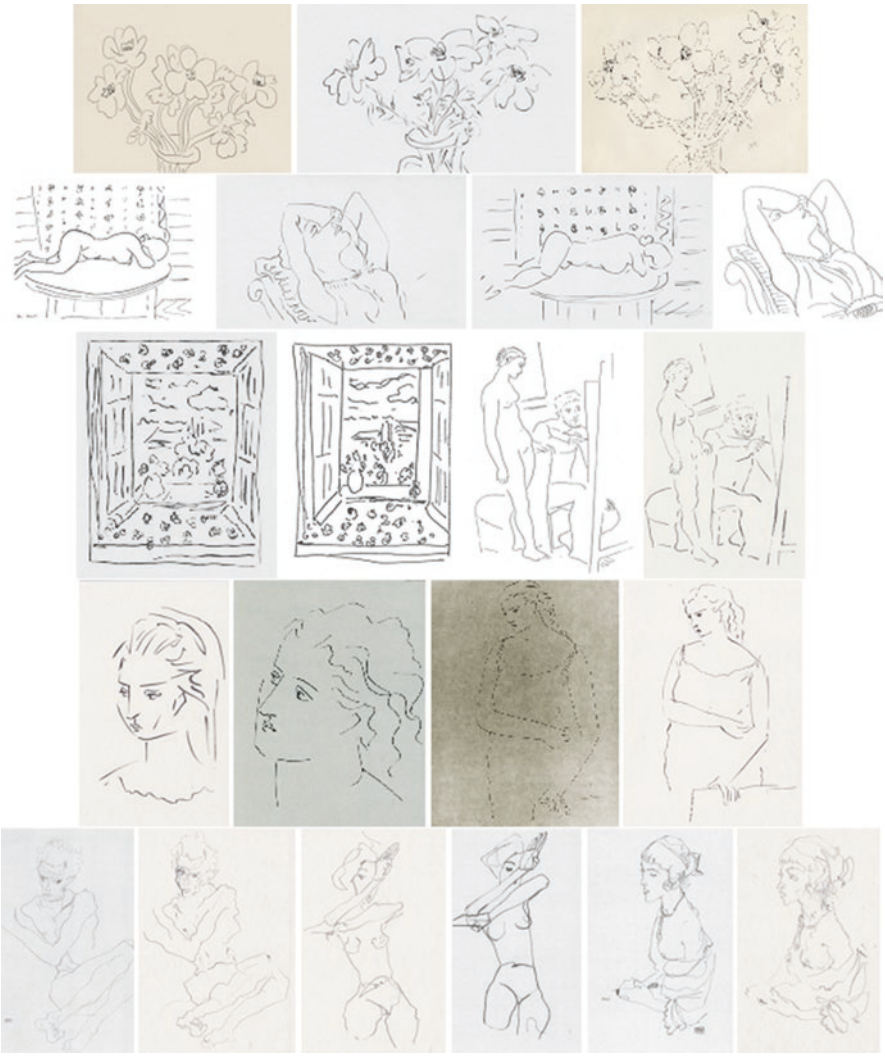

Fig. 5.3 Examples of images of the fake dataset mixed up with real images of drawings by Matisse, Picasso, and Schiele. See the key at the end of the document to tell which are real and which are fake!

relatively easy since they persist in a skeleton representation of the network of strokes. On the other hand, the challenge in our case is to use the information of such junctions and endpoints to segment individual strokes.

In our case, junctions play crucial role in identifying the intersections between strokes. There are two basic ways strokes intersect: an occluder-occluded configuration to form a T-junction or two strokes crossing each other to form an X-junction. A T-junction is a continuation point of the occluding stroke and an endpoint for the occluded stroke. We need to preserve the continuation of the occluding stroke at the T-junction.

The stroke segmentation algorithm takes a network of strokes and identifies one occluding stroke at a time and remove it from the network of strokes to form a residual network(s) that is recursively segmented. This is achieved by constructing a fully connected graph whose vertices are the endpoints in the network and edges are weighted by the cost of reaching between each two endpoints. The cost between two endpoints reflects the bending energy required at the junctions.

Let the endpoints in a network of strokes denoted by $e_1,\ldots, e_m$ and let the junction locations denoted by $j_1,\ldots, j_n$. The cost of the path between any two end points e_i to e_j is cumulative curvature along the skeleton path between them, where the curvature is only counted close to junctions. The rational is that it does not matter how much bending a stroke would take as long as it is not at junctions. Let $\gamma(t) : [0 : 1] \rightarrow R^2$ be the parametric representation of the skeleton curve connecting e_i and e_j. The cost is defined as

$$c\left(e_i, e_j\right) = \int_0^1 \kappa(t).\phi\left(\gamma\left(t\right)\right)dt,$$

where $\kappa(.)$ is the curvature and $\varphi(.)$ is a junction potential function, which is a function of the proximity to junction locations defined as

$$\phi\left(x\right) = \frac{1}{n}\sum_{i=1}^{n} e^{(x-j_i)^2/\sigma}.$$

After the graph construction, the minimum cost edge represents a path between two endpoints with minimum bending at the junctions, which corresponding to an occluding stroke. In case of a tie, the path with the longest length is chosen. The optimal stroke is removed from the skeleton representation and from the graph. This involves reconnecting the skeleton at X-junctions (to allow the detection of the crossing strokes) and new endpoints have to be added at T-junctions (to allow the detection of occluded strokes. Removing a stroke from the graph involves removing all edges corresponding to paths that go through the removed stroke. This results in breaking the graph to one or more residual subgraphs, which are processed recursively. Figures 5.4 and 5.5 illustrate examples of the stroke segmentation results.

5.5 Stroke Analysis and Recognition

5.5.1 Quantifying Stroke Characteristics

This section explains the process of quantifying the characteristics of individual strokes and the extracted features used to represent each stroke. The goal is to construct a joint feature space that captures the correlation between the shape of the stroke, its thickness variation, tone variation, local curvature variation. For this

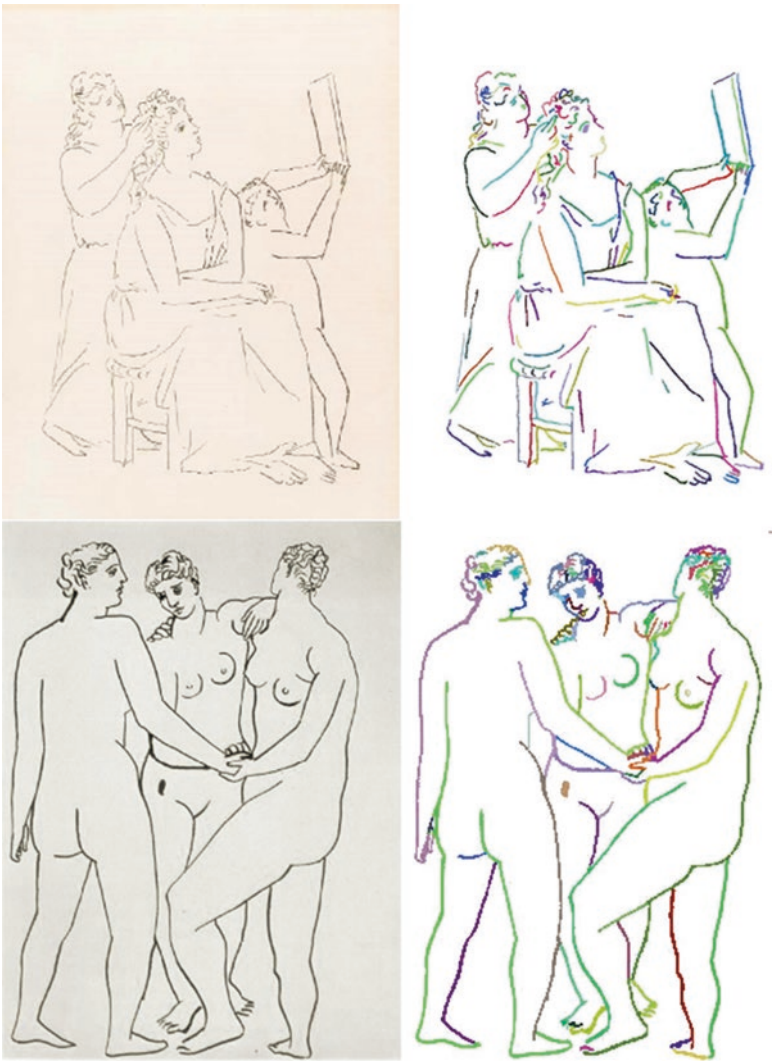

Fig. 5.4 Examples of segmentation results. Top: Picasso lithograph. Bottom: Picasso ink drawings. – best seen in color

purpose, we studied two different types of features and their combination: (1) Handcrafted features capturing the shape of each stroke and its boundary statistics, (2) Learned-representation features capturing the tonal variation as well as local shape characteristics. The next two subsection describe each of these features.

Fig. 5.5 Examples of segmentation results. Top: Matisse etching. Bottom: Schiele ink drawing

5.5.1.1 Stroke Shape Characteristics

In our study, each stroke is represented by its skeleton, its boundary, and the rib length around the skeleton. The following descriptors are extracted to quantify the characteristics of each stroke. All the descriptors are designed to be invariant to translation, rotation, scaling, and change in digitization resolution.

Shape of the Boundary The shape of the stroke boundary is quantified by Fourier descriptors (Burger and Burge 2016). Fourier descriptors are widely used shape

features for a variety of computer vision applications such as character recognition and shape matching. Fourier descriptors provide shape features that are proven to be invariant to translation, scaling, rotation, sampling, and contour starting points (Burger and Burge 2016). We used 40 amplitude coefficients (first 20 harmonics in each direction) to represent the shape of the boundary of the stroke.

Reconstruction Error Profile The mean reconstruction error, as a function of the number of harmonics used to approximate the shape of the strokes, is used as a descriptor of the smoothness of the contour and the negative space associated with the stroke. In particular, we compute the mean reconstruction error at each step while incrementally adding more harmonics to approximate the shape of the stroke. The reconstruction error profile is normalized by dividing by the stroke mean width in pixels to obtain a descriptor invariant to digitization resolution.

Contour Curvature Descriptor To quantify the curvature of the stroke contours, we use the first and second derivatives of the angular contour representation. The distributions of these derivatives are represented by their histograms.

Stroke Thickness Profile To quantify the thickness of the stroke, we compute the mean and standard deviation of the rib length around the skeleton of the stroke, as well as a histogram of the rib length. All rib length measurements are mapped to mm units to avoid variations in digitization resolution. *Stroke Length:* The length of the stroke is quantified as the ratio between the stroke skeleton length to the canvas diagonal length. This measure is invariant to digitization resolution.

5.5.1.2 Stroke Tonal Variations: Deep Learned Features Using RNNs

GRU Classification with Truncated Back Propagation Through Time Other than the traditional feed-forward neural networks specialized at fixed size input, e.g. images, recurrent neural network (RNN) could handle variable length sequence input $x = (\mathbf{x}_1, \ldots, \mathbf{x}_T)$ and either fixed length output or variable length output $y = (\mathbf{y}_1, \ldots, \mathbf{y}_T)$ by utilizing the hidden state within. RNN sequentially takes input $\mathbf{x}_t$ from the input sequence and update its hidden state. In each time step, a corresponding output could be generated through a nonlinear function.

Recently, it has been widely shown that the more complicated RNN model such as Long Short- Term Memory (LSTM; Hochreiter and Schmidhuber 1997) or Gated Recurrent Unit (GRU; Chung et al. 2014) would eliminate the problem of vanishing gradient (Bengio et al. 1994; Hochreiter et al. 2001). LSTM and GRU introduce some gating units that can automatically determine how much the information flow could be used in each time step, by which the vanishing gradient could be avoided.

Given a stroke, a sequence of patches of fixed size are collected along the skeleton of the stroke and fed to a GRU model as inputs. We tested both fixed size patches or adaptive size patches where the radius of the patch is a function of the

average stroke width in the drawing. In both cases the input patches are scaled to 11x11 input matrices. To achieve invariant to the direction of the stroke, each stroke is sampled in both directions as two separate data sequences (at classification, both a stroke and its reverse either appear in training or testing splits). We normalized the grey scale into range (−1, 1), and flattened the 11 11 image into a 121-dimension vector. The activation function we used in experiments is *tanh* function. Parameters are initialized from normal distribution with mean = 0, standard deviation = 1. After comparing several optimizer functions, we found that the RMSProp optimizer with learning rate 0.001 outperforms others.

The gradient is globally clipped to be less than 5 to prevent from gradient exploding,. And to avoid gradient vanishing, we calculated the gradient by the truncated Back Propagation Through Time. Each sequence is unrolled into a fixed size τ steps ($\tau = 30$ in the experiments) at each time to calculate the gradient and to update the network's parameters. The label of original sequence is assigned to each unrolling. Between each unrolling, the hidden state is passed on to carry former time steps information. And within each unrolling, only the last time step hidden state is used in the final linear transformation and Softmax function to get the predicted score of each class.

5.5.2 Stroke-Level Classification

For the case of hand-crafted features, strokes are classified using a support vector machine (SVM) classifier (Cortes and Vapnik 1995). We evaluated SVM using Radial basis kernels as well as polynomial kernels. The classifier produces posterior distribution over the classes. For the case of learned GRU features, the classification of strokes is directly given by the trained networks. SVM was used to combine hand-crafted features with the learned features in one classification framework. In such case, the activation of the hidden units were used as features, and combined to the hand-crafted features.

5.5.3 Drawing Classification

A given drawing is classified by aggregating the outcomes of the classification of its strokes. We used four different strategies for aggregating the stroke classification results, as described below.

- Majority Voting: In this strategy each stroke votes for one class. All strokes have equal votes regardless of the certainty of the output of the stroke classifier.
- Posterior aggregate: In this strategy each stroke votes with a weight equal to its posterior class probability. This results in reducing the effect of strokes that are not classified with high certainty by the stroke classifier.

- k-certain voting: In this strategy, only the strokes with class posterior greater than a threshold
- k are allowed to vote. This eliminates effect of uncertain strokes.
- certainty weighted voting: In this strategy each stroke vote is weighted using a gamma function based on the certainty of the stroke classifier in classifying it.

5.6 Example Results and Validations

We conducted extensive experiments conducted to test and validate the performance of the stroke segmentation, stroke classification, and the drawing classification approaches on the collected dataset. In particular, the experiments are designed to test the ability of the algorithms to determine the attribution of a given artwork and test its robustness to forged art. We highlight the major findings here. We refer the user to (Elgammal et al. 2018) for details.

5.6.1 Segmentation Validation

Validating the segmentation algorithm is quite challenging since there is no available ground truth segmentation and because of the difficulty of collecting such annotation. It is quite a tedious process for a human to trace individual strokes to provide segmentation of them, specially such task requires certain level of expertise. To validate the segmentation algorithm, we collected 14 drawings with medium difficulty (in terms of number of strokes) from the collection and showed the segmentation results to two artists and asked them independently to locate errors in the segmentations. Figure 5.6 shows an example of a drawing with its two annotations of the results. A closer look highlights that annotators make several mistakes (false positive, and false negatives). Table 5.2 the number of marked errors for each sample image by two evaluators. The overall error per annotator is computed as: Error rate = total marked errors at junctions / total number of strokes; where the total is aggregated over all evaluated images. The average error rate over the two annotators is 12.94%, counting all labelled errors by annotators. The annotation shows large deviations between the two annotators, with mean deviation 24.93 and standard deviation 12%. This highlight the challenge in validating the segmentation results by human annotation. However, most of the marked errors are at small detailed strokes that are hard to segment, even by the human eye, and does not contribute much to the classification of strokes since small strokes are filtered out anyway.

5.6.2 *Stroke Classification*

In all experiments the image datasets were split into five 80/20% folds to perform five-fold cross validation. Since strokes from the same drawings might share similar characteristics, we did these splits at the image level and not at the stroke level. For each fold, after splitting the images to train and test sets, equal number of strokes were sampled for each artist class for training and testing to avoid the bias in the data, which is significant in our case. We evaluated different classification settings including pair-wise classification, and one-vs-all classification, and multi-class classification. Extensive ablation studies are also performed to evaluate the different features and their effects, as well as to choose the optimal settings.

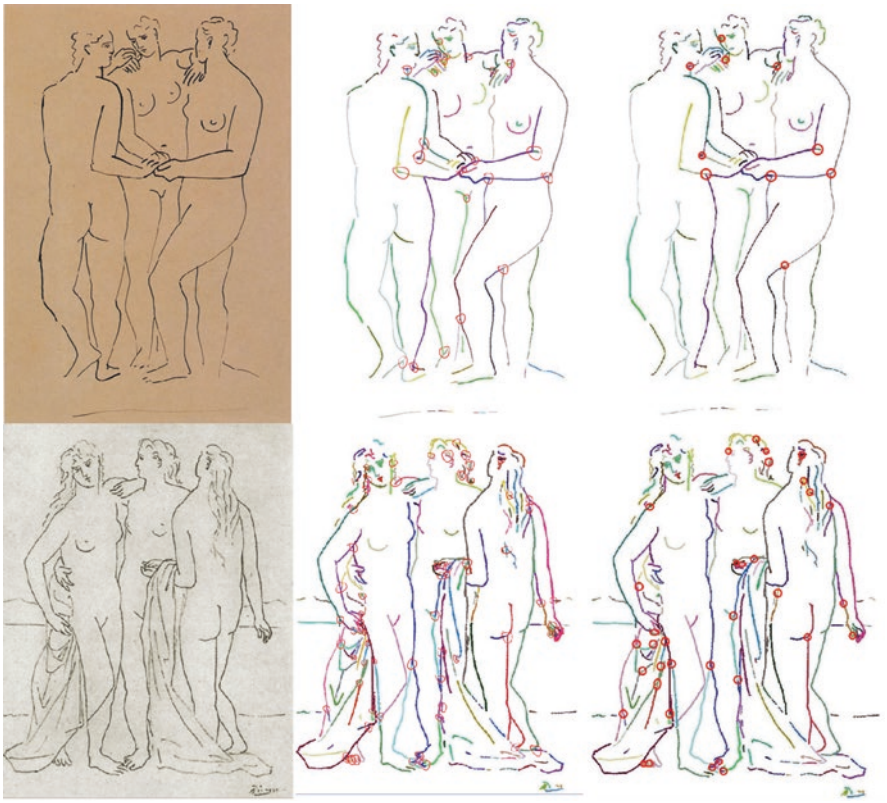

Fig. 5.6 Example of two drawings by Picasso, stroke segmentation results, and segmentation errors marked by two artists

Table 5.2 Validation of stroke segmentation

Sample	Number of strokes	Evaluator 1 marked errors	Evaluator 2 marked errors	Absolute deviation between evaluators
1	596	34	75	41
2	366	37	17	20
3	314	38	11	27
4	216	24	11	13
5	267	69	13	56
6	122	40	14	26
7	136	28	10	18
8	131	32	12	20
9	102	22	10	12
10	71	17	6	11
11	159	48	15	33
12	123	30	8	22
13	103	25	10	15
14	196	65	30	35
Total	2902	509	242	
Mean				24.93
Std				12.72

5.6.2.1 Stroke Classification Validation – Technique Specific – Pairwise

For testing technique-specific classifiers, we trained pairwise classifiers to discriminate between Picasso and Matisse drawings made using either pen/ink or etching. We chose these two techniques and these two artists since they have the largest representation in our collection. Table 5.3 shows the stroke classification results. The experiment is done using five-fold cross validation and the mean and standard deviations are reported. The table shows a comparison between the different types of proposed features.

5.6.2.2 Stroke Classification Validation – One-vs-All

In this experiment a one-vs-all classification settings is used to build classifiers for Picasso-vs- Non-Picasso, Matisse-vs-Non-Matisse, Schiele-vs-Non-Schiele. These three artists are chosen since they have enough data for training and testing the classifiers in a five-fold split setting. The classifiers are then evaluated on the fake dataset (see Sect. 5.6.3). We evaluated the performance of two settings:

1. Across-techniques: we evaluated the performance of the stroke classifiers on all techniques combined to evaluate whether the classifier can capture an invariant for the artist regardless of the technique used.
2. Technique-specific: in this setting each classifier is trained and tested using strokes from the same drawing technique. Given the data collection, we tested a)

Picasso-vs-Non-Picasso classifier using ink/pen, b) Matisse-vs-Non-Matisse classifier using ink/pen, c) Schiele-vs- Non-Schiele using pencil.

Table 5.4 shows the mean and standard deviations of the five folds for the hand-crafter features, the GRU features and the combination. Both types of features have very good stroke classification performance. GRU has better performance over the three artists tested. Combining the features further improved the results and reduced the cross-fold variances, which indicate that both types of features are complementary to each other as we hypothesized.

Comparing the performance of stroke classifiers on both the technique-specific and across- technique settings, we notice that in both cases the classifiers performed well. The GRU performed better in the across-technique settings than in the technique-specific setting, which can be justified by the lack of data in the latter case.

5.6.3 Drawing Classification and Detection of Fakes

Drawing Classification Validation Given the trained stroke classifiers, their performance is tested on drawing classification settings, also using one-vs-all settings. We used the four aforementioned strategies for aggregating the results from the stroke level to the drawing level. Given that the stroke classifiers are trained on a five-fold cross-validation setting, the drawing classification followed that strategy, i.e. in each fold, each drawing in the test split is classified using the classifier trained on the 80% of the images in the training split, hence there is no standard deviation to report. Table 5.5 shows the results for the across-technique setting and Table 5.6 shows the results for the technique- specific setting.

Evaluation on Fake Drawings The trained stroke classifiers were also tested on the collected fake drawings to evaluate whether the classifiers are really capturing artists' stroke characteristics and invariants or just statistics that can be easily deceived by forged versions. We used the Picasso- vs-all stroke classifiers to test the fake drawings that are made to imitate Picasso drawings (We denote them as Picasso

Table 5.3 Validation of stroke classifier – technique specific (Picasso vs Matisse)

Approach	Train	Test
Ink Drawing (Pen/Brush) (Picasso vs Matisse)		
Hand-crafted – SVM-RBF	87.99% (0.39%)	79.16% (0.26%)
Hand-crafted – SVM-POLY	79.88% (0.14%)	77.17% (0.58%)
GRU	84.92% (1.89%)	65.86 (13.58%)
Etching prints (Picasso vs Matisse)		
Hand-crafted – SVM-RBF	94.53% (0.22%)	84.18% (0.85%)
Hand-crafted – SVM-POLY	94.27% (0.21%)	93.09% (0.88%)
GRU	83.74% (4.60%)	75.08% (8.11%)

Table 5.4 Validation of stroke classifiers – one-vs-all

		Hand-crafted + SVM		GRU		Combined	
Classifier	Technique	Train	Test	Train	Test	Train	Test
Across-Techniques – Mean (std) of five folds							
Picasso vs. all	All	72.59% (1.19%)	67.26% (8.37%)	81.92% (2.59%)	75.09% (5.09%)	86.05% (1.08%)	78.54% (4.36%)
Matisse vs. all	All	65.83% (1.72%)	60.61% (8.71%)	81.01% (3.41%)	72.68% (5.58%)	87.92% (1.73%)	77.08% (4.33%)
Schiele vs. all	All	84.76% (0.91%)	81.49% (3.30%)	85.55% (1.74%)	78.54% (8.77%)	91.85% (0.87%)	86.20% (3.78%)
Technique-specific – Mean (std) of five folds							
Picasso vs. all	Pen/ink	73.20% (2.21%)	68.93% (7.04%)	84.08% (2.20%)	72.24% (1.87%)	88.40% (1.19%)	75.92% (4.22%)
Matisse vs. all	Pen/ink	73.35% (1.99%)	70.08% (7.94%)	86.88% (1.98%)	75.03% (6.47%)	91.56% (1.03%)	79.10% (6.65%)
Schiele vs. all	Pencil	82.58% (2.78%)	75.39% (20.64%)	94.33% (3.52%)	69.60% (20.62%)	91.30% (4.57%)	72.93% (19.67%)

fakes). A similar setting is used for Matisse fakes and Schiele fakes. Since the stroke classifiers are trained on a five-fold setting, we have five different classifiers trained per artist, one for each fold. Each test stroke is classified using the five classifiers and the majority vote is computed. The different aggregation methods are used to achieve a final classification for each drawing. Since one-vs-all setting is adapted, classifying a fake Picasso as others in a Picasso-vs-all setting is considered a correct classification, while classifying fake Picasso as Picasso is considered a wrong prediction. The bottom parts of Tables 5.5 and 5.6 shows the classification results for the fake dataset for the across-technique and technique-specific settings respectively.

The table shows that the trained one-vs-all stroke classifiers for all the three artists, are robustly rejecting fake drawing with accuracy reaching 100% in the across-technique case. A notable difference here is that the GRU failed to detect the fake drawings, in particular for the Picasso-vs-all, while the hand-crafted features detected all the fakes. Similar case happens for Schiele-vs-all as well. We hypothesize that this is because of the limited training data in the technique-specific case, which did not allow the GRU to learn an invariant model that generalizes well as in the across- technique case. In contrast the hand-crafted models did not suffer from this limitation. Overall, the hand-crafted features are outperforming in detecting the fakes.

5.7 Conclusions

In this chapter we presented research on an automated method for quantifying the characteristics of artist stokes in drawings. The approach is inspired by the Pictology methodology proposed by van Dantzig. The approach segments the drawing into

Table 5.5 Validation of drawing classifiers – one-vs-all -across techniques

	Picasso-vs-All			Matisse-vs-All			Schiele-vs-All		
Aggregation	Hand-crafted	GRU	Combined	Hand-crafted	GRU	Combined	Hand-crafted	GRU	Combined
Across-Techniques									
Majority	66.67%	76.77%	82.49%	54.88%	81.14%	80.47%	74.41%	82.49%	81.82%
Posterior	67.68%	77.44%	81.48%	56.90%	81.48%	79.12%	74.75%	83.50%	82.49%
85%-certain	73.06%	79.80%	82.83%	38.05%	80.47%	78.79%	75.42%	83.50%	83.84%
Certainty-weighted	67.34%	79.80%	82.83%	58.25%	80.81%	80.47%	75.42%	85.19%	83.16%
Detection of fake drawings									
Majority	100%	87.50%	100%	76.92%	100%	100%	100%	100%	100%
Posterior	100%	87.50%	100%	76.92%	100%	100%	100%	100%	100%
85%-certain	100%	87.50%	100%	76.92%	100%	100%	100%	100%	100%
Certainty-weighted	100%	87.50%	100%	76.92%	100%	100%	100%	100%	100%

Table 5.6 Validation of drawing classifiers – one-vs-all – technique-specific

	Picasso-vs-All			Matisse-vs-All			Schiele-vs-All		
Aggregation	Hand-crafted	GRU	Combined	Hand-crafted	GRU	Combined	Hand-crafted	GRU	Combined
Technique-Specific									
Majority	72.41%	82.76%	81.38%	65.52%	78.62%	82.76%	81.25%	78.12%	81.25%
Posterior	72.41%	82.76%	81.38%	66.21%	79.31%	80.69%	84.38%	78.12%	81.25%
85%-certain	72.41%	82.76%	82.76%	69.66%	76.55%	80.69%	84.38%	78.12%	81.25%
Certainty-weighted	71.72%	82.76%	82.07%	69.66%	77.93%	80.00%	87.50%	78.12%	81.25%
Detection of fake drawings									
Majority	100.00%	12.50%	16.67%	94.87%	100.00%	100.00%	100.00%	45.00%	55.00%
Posterior	100.00%	12.50%	16.67%	97.44%	100.00%	100.00%	100.00%	45.00%	55.00%
k-certain	100.00%	12.50%	20.83%	97.44%	100.00%	100.00%	100.00%	45.00%	60.00%
Certainty-weighted	100.00%	12.50%	20.83%	97.44%	100.00%	100.00%	100.00%	45.00%	60.00%

individual strokes using a novel segmentation algorithm. The characteristics of each stroke is captured using global and local shape features as well as a deep neural network that captures the local shape and tone variations of each stroke. We compared different types of features and showed results at the stroke classification and drawing classification levels.

The main conclusion is that we can distinguish between artists at the stroke-level with high accuracy, even using images of drawing of typical off-the-web or scanned books resolutions. We also tested the methodology using a collected data set of fake drawings and the results show that the proposed method is robust to such imitated drawings, which highlights that the method can indeed capture artists' invariant characteristics that is hard to imitate.

Answer Key of Fig. 5.3
Fake, Fake, Matisse
Matisse, Fake, Fake, Matisse
Fake, Matisse, Picasso, Fake
Fake, Picasso, Picasso, Fake
Schiele, Fake, Fake, Schiele, Schiele, Fake

Acknowledgments This research was done at Artrendex Inc.

References

Arora, R., Elgammal, A.: Towards automated classification of fine-art painting style: a comparative study. In: Proceeding of the 21st International Conference on Pattern Recognition, 2012, pp. 3541–3544. https://doi.org/10.7282/T3XP73QP

Bengio, Y., Simard, P., Frasconi, P.: Learning long-term dependencies with gradient descent is difficult. IEEE Trans. Neural Netw. **5**, 157–166 (1994). https://doi.org/10.1109/72.279181

Burger, W., Burge, M.J.: Fourier shape descriptors. In: Digital Image Processing Texts in Computer Science, pp. 665–711. Springer, London (2016). https://doi.org/10.1007/978-1-4471-6684-9_26

Chung, J., Gulcehre, C., Cho, K., Bengio, Y.: Empirical evaluation of gated recurrent neural networks on sequence modelling. In: NIPS'2014 Deep Learning Workshop (2014)

Cortes, C., Vapnik, V.: Support-vector networks. Mach. Learn. **20** (1995)

Elgammal, A., Kang, Y., Den, L.M.: Picasso, matisse, or a fake? Automated analysis of drawings at the stroke level for attribution and authentication. In: 32nd AAAI Conference on Artificial Intelligence, New Orleans, USA (2018)

Guo, J.K., Doermann, D., Rosenfield, A.: Off-line skilled forgery detection using stroke and substroke properties. In: Proceeding of the 15th International Conference on Pattern Recognition. ICPR-2000, vol. 2, IEEE Computer Society; 2000, pp. 355–358. https://doi.org/10.1109/ICPR.2000.906086

Hochreiter, S., Schmidhuber, J.: Long short-term memory. Neural Comput. **9**, 1735–1780 (1997). https://doi.org/10.1162/neco.1997.9.8.1735

Hochreiter, S., Bengio, Y., Frasconi, P., Schmidhuber, J.: Gradient flow in recurrent nets: the difficulty of learning long-term dependencies. In: Kremer, S.C., Kolen, J.F. (eds.) A Field Guide to Dynamical Recurrent Networks. IEEE Press, New York (2001)

Johnson, C., Hendriks, E., Berezhnoy, I., Brevdo, E., Hughes, S., Daubechies, I., et al.: Image processing for artist identification. IEEE Signal Process. Mag. **25**, 37–48 (2008). https://doi.org/10.1109/MSP.2008.923513

Khan, F.S., van de Weijer, J., Vanrell, M.: Who painted this painting? In: CREATE, 2012

Lam, L., Lee, S.-W., Suen, C.Y.: Thinning methodologies-a comprehensive survey. IEEE Trans. Pattern Anal. Mach. Intell. **14**, 869–885 (1992). https://doi.org/10.1109/34.161346

Li, J., Yao, L., Hendriks, E., Wang, J.Z.: Rhythmic brushstrokes distinguish van Gogh from his contemporaries: findings via automated brushstroke extraction. IEEE Trans. Pattern Anal. Mach. Intell. **34**, 1159–1176 (2012). https://doi.org/10.1109/TPAMI.2011.203

Liedtke, W., Johnson, C.R., Johnson, D.H.: Canvas matches in Vermeer: a case study in the computer analysis of fabric supports. Metrop. Mus. J. **47**, 101–108 (2012). https://doi.org/10.1086/670142

Polatkan, G., Jafarpour, S., Brasoveanu, A., Hughes, S., Daubechies, I.: Detection of forgery in paintings using supervised learning. In: Image Processing (ICIP), 2009 16th IEEE International Conference, 2009, pp. 2921–2924

Sablatnig, R., Kammerer, P., Zolda, E.: Hierarchical classification of paintings using face- and brush stroke models. In: Proceedings of the Fourteenth International Conference on Pattern Recognition (Cat. No.98EX170), vol. 1, IEEE Computer Society; 1998, pp. 172–174. https://doi.org/10.1109/ICPR.1998.711107

Saleh, B., Abe, K., Arora, R.S., Elgammal, A.: Toward automated discovery of artistic influence. Multimed. Tools Appl. **75**, 3565–3591 (2016). https://doi.org/10.1007/s11042-014-2193-x

Tappert, C., Cha, S., Lombardi, T.E.: The classification of style in fine-art painting. In: ETD Collection for Pace University, 2005, p. Paper AAI3189084

van Dantzig, M.M.: Pictology: an analytical method for attribution and evaluation of pictures. Leiden, E. J. Brill (1973)

Part III
Material Characterization of Paintings by Instrumental Techniques

Chapter 6
Analytical Pyrolysis of Organic Paint Materials for Authentication and Attribution

A. Andreotti, J. La Nasa, F. Modugno, and I. Bonaduce

Abstract The chemical analysis of organic paint material is still one of our most important tools for understanding an object, planning its conservation, and supporting speculations on the object's identity and history. Analytical pyrolysis is a micro-destructive analytical technique that chemically characterizes organic materials in a large range of molecular weights, directly in the solid state, without the need for any pretreatment. This makes the technique particularly useful when dealing with samples from a work of art and archaeological object, where typically the composition in terms of significant analytes and the matrix is not known before the analysis, and natural and synthetic materials may be expected simultaneously.

In this chapter the use of analytical pyrolysis for the molecular characterisation of organic materials in case studies from archaeological objects and works of art, spanning from the fourth century BC to the 1980s, is presented. The aim is to discuss how analytical pyrolysis can contribute to issues related to the identification of artistic techniques, to reconstruct the history of an object through the study of its chemical signature, and to differentiate between original and non-original materials in paintings.

Keywords Chemical analysis · Cultural heritage · Natural binders · Synthetic binders · Restoration materials

6.1 Introduction

Radiocarbon dating represents one of the greatest advances in the authentication of works of art. Accelerator mass spectrometry (AMS) (Hendriks et al. 2018) has enabled even just 20–30 micrograms of carbon to be analysed, opening the way to

A. Andreotti (✉) · J. La Nasa · F. Modugno · I. Bonaduce
Department of Chemistry and Industrial Chemistry, University of Pisa, Pisa, via Moruzzi, Italy
e-mail: alessia.andreotti@unipi.it

M. P. Colombini et al. (eds.), *Analytical Chemistry for the Study of Paintings and the Detection of Forgeries*, Cultural Heritage Science,
https://doi.org/10.1007/978-3-030-86865-9_6

the applications of radiocarbon dating to the study of paint forgeries (Hendriks et al. 2019b; Hodgins 2019). (^{14}C) AMS is capable to detect post-1955 imitations of pre-1955 works (Hodgins 2019), and it can also date materials in paintings more ancient than 500 years produced with natural binders (Fiorillo et al. 2021), as well as with lead white (Hendriks et al. 2019a). However, (^{14}C) AMS is not suitable for dating paintings produced in the past 500 years, because in these last centuries artists' materials have calibrated radiocarbon dates that span centuries (Hodgins 2019). Another issue is the frequent presence of restoration materials, that needs to be excluded to achieve accurate radiocarbon dating.

Analysing the materials that make up a work of art is thus still one of our most important tools for authentication purposes. In some cases, for example, a forgery can be identified based on the detection of anachronistic materials. For instance, some natural pigments have specific patterns of appearance and use, and in other cases, particle morphologies can help distinguish between hand versus machine-ground pigments. Finally, there are synthetic pigments with known dates of invention and adoption (Hodgins 2019).

In the case of organic materials used as paint media and varnishes, things are significantly more complex. Proteins have been detected in Neolithic paintings – possibly as paint binders (Roldán et al. 2018). Proteins and polysaccharides have been identified as paint binders in Bronze Age paintings (Brecoulaki et al. 2008, 2012, 2017; Linn et al. 2018). Oils were introduced as artistic media, possibly originally in a mixture with proteins, in the course of the fourteenth/fifteenth century, although the first documented artistic painting with a drying oil as a paint binder dates back to the seventh century (Cotte et al. 2008). Terpenoid resins are commonly found in paintings, mostly as ingredients of varnishes, and some of them have documented periods of appearance and use, such as dammar and shellac resin. Synthetic materials were introduced as paint materials or for conservation in the late nineteenth century.

Although there are a limited number of classes of organic materials in a painting, their identification in a work of art is a useful starting point in understanding an object, in planning its conservation, and, in supporting speculations on the object's identity and history.

The analytical techniques for identifying materials in an art object include analytical pyrolysis coupled to (gas chromatography-) mass spectrometry. This is an extremely versatile technique that allows a rapid molecular characterisation of an organic sample. The technique is used in heritage science and has evolved considerably for over 30 years (Bocchini and Traldi 1998; Degano et al. 2018).

Analytical pyrolysis is a fast micro-destructive analytical technique that chemically characterizes organic materials in a large range of molecular weights, directly in the solid state, without the need for any pretreatment. In pyrolysis, the sample is heated up for few seconds in anoxic conditions: volatile molecules evolve during the sample heating, thermally unstable compounds are degraded, and high molecular weight components are fragmented into reproducible molecular patterns. In a typical pyrolysis gas chromatography mass spectrometry (Py-GC-MS) experiment, the pool of molecules produced upon thermal degradation are transferred into the

gas chromatograph to be chromatographically separated and then analysed by a mass spectrometric detector. The molecular pattern that is obtained can be linked to the original chemical composition of the material. Molecular pattern recognition, semiquantitative analyses, or marker recognition are the main processes involved in data interpretation and in identifying a material (Degano et al. 2018).

Unlike all the other mass spectrometric based techniques, analytical pyrolysis characterizes the entire the organic fraction of a sample. While HPLC-MS and GC-MS based approaches can be used to characterise only the soluble/hydrolysable/volatile/thermally stable components of a sample, analytical pyrolysis also provides molecular insights into the highly insoluble, cross-linked and non-hydrolysable fractions of a material, including natural and synthetic macromolecules.

When HPLC-MS and GC-MS are used, several analytical protocols and experimental/instrumental conditions are required for different analytes. For example, for GC-MS analysis, lipids are best hydrolysed in alkaline conditions, proteins require acidic hydrolysis, and polysaccharides also require acidic hydrolysis, but with milder conditions (Bonaduce et al. 2016; Degano and La Nasa 2016). Derivatisation procedures are also often necessary in GC-MS, and again, different analytical conditions and reagents are used to maximise derivatisation yields for the different analytes (Andreotti et al. 2008b).

With analytical pyrolysis, all materials are the analysed at the same time. A paint sample can be introduced directly in its solid state, and no previous and customised wet-chemical pre-treatment is necessary. Thermally assisted reactions – e.g. hydrolysis and methylation as well as silylation – are commonly adopted as in-situ and on-line sample treatment in the analysis of hydrolysable and polar materials (Bonaduce and Andreotti 2009).

Analytical pyrolysis is thus ideal for the molecular characterisation of a micro sample from a work of art, where typically the composition in terms of significant analytes and the matrix is not known before the analysis. The constituent organic materials, both natural and synthetic, expected and unexpected, can be targeted simultaneously. This approach reduces the amount of sample required for the characterisation of different classes of organic materials, at the same time massively reducing the analytical workout.

The aim of this chapter is not to provide a comprehensive collection of all the work performed in the field, but rather to discuss mostly our experience in the use of analytical pyrolysis for the molecular characterisation of organic materials in case studies related to archaeological objects and works of art, which span from the fourth century BC to the 1980s.

We highlight how analytical pyrolysis can positively contribute to issues related to the identification of artistic techniques, to reconstruct the history of an artwork through the study of its chemical signature, and to differentiate between original and non-original materials in paintings. We aim to show the huge potential of the technique, and at the same time the challenges of reconstructing the chemical nature of the original artistic materials based on the recognition of its pyrolysis products.

6.2 The Analysis of Original and Restoration Materials in Ancient Polychromies and Paintings

6.2.1 An Etruscan Sarcophagus from the Fourth Century BC: "Sarcofago delle Amazzoni"

Our first case-study is an Etruscan masterpiece held in the Archaeological Museum of Florence. It is the fourth century BC architectural marble sarcophagus, known as the "Sarcofago delle Amazzoni" (Bottini and Setari 2007). For a detailed chemical characterization of the original and restoration materials, over twenty samples were taken from the *case* and *lid* of the sarcophagus (Andreotti et al. 2007). The analysis based on analytical pyrolysis with hexamethyldisilazane (Py(HMDS)-GC-MS) revealed the presence of alkyl pyrroles, pyrolysis products characteristic of animal glue proteins, and in lower amounts, hexadecanenitrile and octadecanenitrile, which are pyrolytic markers of egg yolk (Orsini et al. 2017). The uniform distribution of these materials in all the samples analysed suggests that these proteinaceous binders were used for the pictorial layers.

The presence of a lipid material was also evident in all the samples, as shown in the extract ion chromatogram relating to the fragment ion with *m/z* 117, (Fig. 6.1), common to all the trimethylsilyl esters of carboxylic acids, formed upon pyrolysis of lipids in the presence of HMDS.

However, the profile of the carboxylic acids was not the same in all the samples examined. In some of them, only monocarboxylic acids with 8–18 carbon atoms were present, while dicarboxylic acids such as azelaic acid were almost absent. For this set of samples, the profile showed that the lipids do not derive from a siccative oil: the observed molecular profile is indicative of a lipid with a low content of poly-unsaturated fatty acids, such as egg yolk lipids. In other samples, in addition to monocarboxylic acids, the dicarboxylic acids suberic, azelaic and sebacic were observed in significant amounts, suggesting the presence of lipids deriving from a drying oil.

Interestingly, all the samples containing drying oil also contained traces of butolic acid, a pyrolytic marker of shellac. Shellac is a resinous substance produced by the glandular secretion of some insects of the Cochineal family (Coccus lacca, Lakshadia indica Madhihassan, etc.) in the forests of India and Thailand, which was widely imported in Europe from 1500 and used as a varnish. The combined presence of drying oil and shellac present in several areas of the sarcophagus point to a varnish likely used in a past restoration.

In two of the samples collected from the lid, a triterpenoid material was detected, but not in any of the other samples examined. The terpenoid resin was identified as mastic resin (a resin exudated from the trees of *Pistacia genus*) based on the detection of, among others, 29-orlean-17en-3one (Fig. 6.2). Mastic was only identified on the lid, again possibly due to a past restoration.

Finally, the analyses revealed a synthetic polymer in all the samples examined. The trimethylsilyl ester of acetic acid, benzene and other aromatic compounds, such

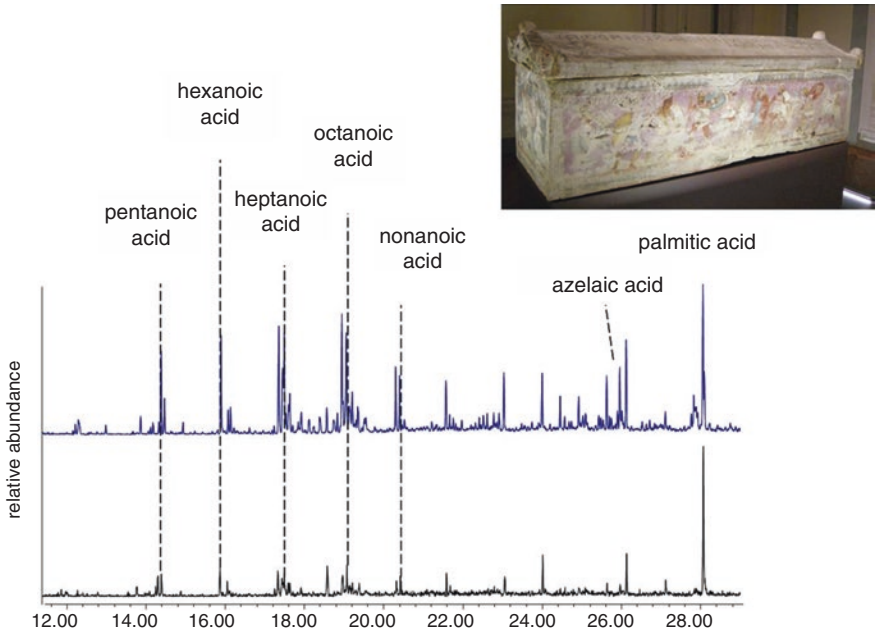

Fig. 6.1 Extract ion chromatogram of ion m/z 129, characteristic of the trimethylsilyl esters of carboxylic acids in two samples from Sarcofago delle Amazzoni. (Sarcofago delle Amazzoni picture from: I, Sailko, CC BY-SA 3.0 http://creativecommons.org/licenses/by-sa/3.0/, via Wikimedia Commons) Top: pyrolytic profile of a drying oil; bottom: pyrolytic profile of egg lipids

as styrene and alkylbenzenes are a characteristic signature of polyvinyl acetate (Bonaduce and Colombini 2003). This material was likely used since the early 1960s as to consolidate or protect pictorial surfaces. The protective based on polyvinyl acetate appeared to be evenly distributed over the polychromy.

6.2.2 Mural Painting in a Roman Villa Dated 10 BC–5 AD: The Casa del Bicentenario in Herculaneum

The *Casa del Bicentenario* was built during the Julio-Claudian period (from 27 BC to 68 AD), which was one of the most flourishing of the Imperial ages of Roman history. The *Casa del Bicentenario* in Herculaneum is one of the most magnificent houses in the forum area of Hercolaneum (Campania, Italy). The city was destroyed by the eruption of Vesuvius in 79 AD. After the eruption, all the buildings of the town were buried under approximately 20 meters of mud and ash. The *Casa del Bicentenario* has a large central *atrium*, two *alae*, the *tablinum*, and the *triclinium*, along the central axis. The walls are decorated with murals depicting architectural

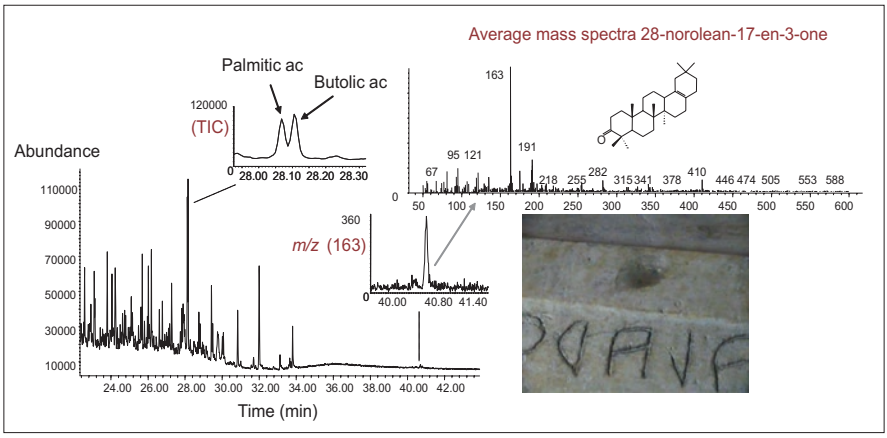

Fig. 6.2 Pyrogram of one of the Sarcophagus sample collected from the lid, with magnification of the peaks around 28 min (palmitic acid and butolic acid, shellac marker) and partial extract ion chromatogram of *m/z* 163, characteristic of the mass spectrum of 29-orlean-17en-3one (marker of mastic resin)

motives and animals, typical of the so-called artistic "Fourth Style" (50–62 AD) (Piqué et al. 2010, 2015).

A long national and international diagnostic campaign began in 2008 as part of a collaboration between the Getty Conservation Institute, the Herculaneum Conservation Project and the Parco Archeologico di Ercolano. The main aims were to identify the painting technique and compare the literature on Roman mural paintings (Andreotti et al. 2014; Casoli et al. 2006; Duran et al. 2010; Rainer et al. 2017; Berzioli and Casoli 2012; Chiantore et al. 2012), to study the plaster layering, identify the conservation issues, and develop environmental control strategies. In order to characterise the organic components of the pictorial layers, more than 20 microsamples from the mural paintings from the West and East Wall of the Tablinum were analysed by chromatographic – mass spectrometric techniques in our laboratory,

Two types of samples were analysed: raised flakes of pictorial film, and fragments that included the complete stratigraphy of the painting. An optical microscope revealed that all the samples had a translucent and brownish film on the surface – see Fig. 6.3 (layer E). The brownish film was mechanically separated from the paint fragments, and analysed by Py-GC-MS. Figure 6.3 (top) shows the extracted ion chromatogram of *m/z* 57 – characteristic mass fragment of aliphatic chains and is from the sample from the Medallion of the West Wall Tablinum. The chromatogram also highlights the presence of 15-hydroxy-hexadecanoic acid, tetracosanoic acid, long chain alcohols, and hydrocarbons. This molecular pattern is typical of beeswax (Riedo and Chiantore 2012). The wax is likely the superficial brownish layer in the cross sections, which is common to all the samples.

Since no other fixative or consolidating materials, either natural or synthetic, were detected, we hypothesized that beeswax was used as a protective layer, and that it penetrated the layers underneath through the paint layer and/or surface cracks.

The wax might have been applied to the wall paintings in undocumented restoration processes to consolidate the wall paintings and to make them shinier. In the pyrograms of all the samples collected from the decorated areas there were hexadecanenitrile and octadecanenitrile indicating the presence of egg (Orsini et al. 2017) probably used as a paint binder. Glycerol, levoglucosan, and other anhydro-sugars, which are typical pyrolysis products of a saccharide material, were also detected in all the samples (Fig. 6.3 bottom), with a chromatographic profile compatible with that of a fruit tree gum (Andreotti et al. 2009). The widespread presence of this gum might be due to its use as paint binder together with egg, or as a coating to protect the paintings. It is thus difficult to assert whether or not the saccharide material was part of the original paint layer.

The data interpretation is supported by investigations carried out on another villa in Hercolaneum, *Villa dei Papiri* (Amadori et al. 2015; Duran et al. 2010), which was discovered in 1750. What makes the wall paintings unique is that the villa was recently excavated (in 1991) and has not been restored, thus enabling the pictorial technique to be determined and the original paint materials to be investigated. The cross sections of the samples of the *Villa dei Papiri* wall painting showed a significantly less complex stratigraphy than the *Casa del Bicentenario samples*. Most interestingly, in the paintings of *Villa dei Papiri,* the brownish surface film was not

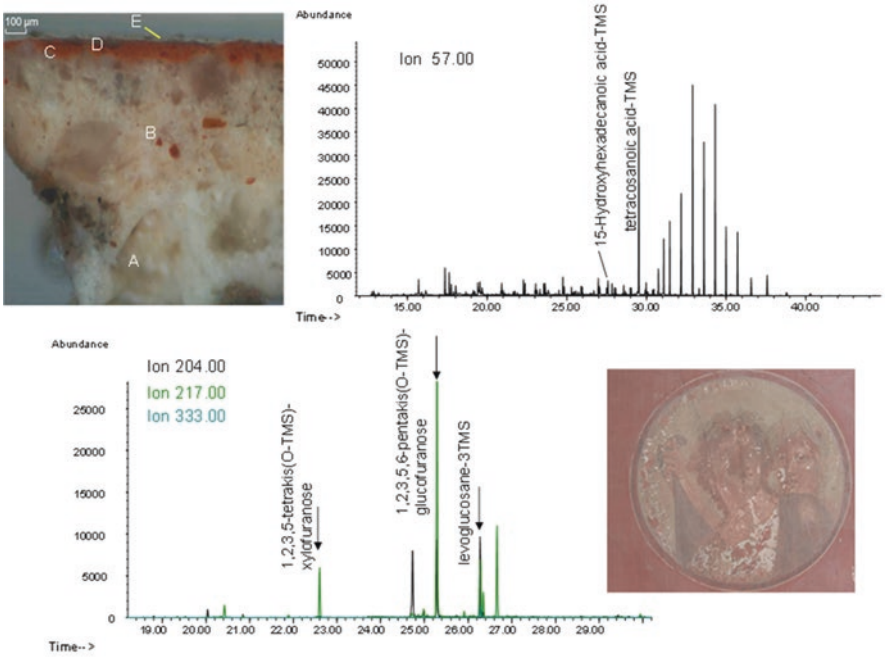

Fig. 6.3 Tablinum, West Wall – West Medallion 1 (South): cross section and extract ion chromatograms highlighting the typical beeswax (upper part, m/z 57) and saccharide (lower part, m/z 204, 217, 333) profiles

observed. Py-GC-MS evidenced the absence of beeswax. This strongly indicates that the wax layer found on the wall paintings of *Casa del Bicentenario* belongs to conservation work carried out after the excavations, which took place in the 1930s.

On the other hand, egg and a saccharide material were also detected in the paint samples from *Villa dei Papiri*, suggesting that the decorations in the two houses were painted with the same materials, and that the polysaccharides found in *Casa del Bicentenario* are original materials.

6.2.3 Hierapolis of Phrygia First-Third Century AD (Pamukkale, Denizli, Turkey)

During an archaeological campaign from 2014 to 2015 at the Hierapolis of Phrygia (Denizli, Turkey), evidence emerged of an ancient and extensive architectural restoration intervention of the Roman Imperial-era buildings. Determining the chronology of past restorations can be very difficult, and only rarely are epigraphic or stratigraphic data available. In the Hierapolis of Phrygia**,** the Corinthian portico was built in the Flavian age (68–96 AD) on the upper terrace of the Apollo Sanctuary, and the restoration work that followed the original construction consisted in a partial disassembly and reassembly of the columns and the repair and reinsertion of the capitals and decorative parts. The study of this restoration suggests that it was performed in the second or third century AD at the latest, likely following a seismic event, as suggested by the large number of interventions. The architectural blocks and the materials sampled were in an excellent state of conservation and have not been subject to any modern interventions. The type of architectural structures and the good state of these past conservation materials provided a unique opportunity to investigate the use of organic binders in ancient bonding mortars. Brocken blocks were reattached when possible, using metal cramps and dowels. In other cases, the damaged areas were mechanically removed, and replacements (in Greek *emblema*) were inserted. The composition of the adhesives used in these types of interventions was investigated, both for the large replacement parts and the small wedge-shaped *emblema.*

The mortars were investigated in the Sanctuary of Apollo, the Theatre, Temple B, the North Agora and the Ploutonion, dating back to the first to the third century AD. The analytical investigation together with the parallel archaeometric study of architectural blocks, revealed that different materials had been used simultaneously in the same monument, as in the case of the Corinthian Portico of the Apollo Sanctuary**.**

Py-GC-MS and/or EGA-MS analyses were performed on more than 20 samples (Cantisani et al. 2018). A large variety of materials was detected, above all plant oils, natural resins, beeswax, casein, egg and animal glue. In a few samples, the glues were made of a proteinaceous binder alone (egg-based or casein-based) where limited bonding was required, such as for a small section of a ‘gravity assisted

position' or for small decorations even held in place by a small dowel. The analytical results of the Hierapolis' samples, however, show that the use of one single organic material as a glue was not common at the time. Materials such as beeswax, resin or animal glue, which are reported as being used often alone in ancient texts, as in the *Historia animalium* III, 10, 5, Hesychius (sv. Κόλλεα), and Pliny (H.N., 33, 30, *resina plumbo et marmori* "resin is for lead and marble"), have been mainly detected in a mixture with one or more other materials.

In most cases, in fact, many organic ingredients were combined into mixtures containing up to four different components. As an exhample, the pyrogram for one sample collected from the Sanctuary of Apollo had pyrolysis products ascribable to a lipid, and proteinaceous materials, namely a mixture of casein and smaller amounts of egg and animal glue, as well as small amounts of beeswax. The complex pyrogram with numerous olefins and aromatic compounds, is reported in extracted ion mode (Fig. 6.4). It highlights the pyrolytic maker compounds of casein (benzeneacetonitrile and indole) (Bonaduce and Colombini 2003).

The absence of diketopiperazines, and the presence of aromatic compounds can be ascribed to the fact that the proteinaceous materials are very aged, and thus extremely cross-linked (Ho and Shahidi 2005).

In summary, the following combinations were found:

- plant oil and egg;
- plant oil, egg and animal glue;
- plant oil, plant resin and egg;
- plant oil, beeswax, egg, animal glue;
- beeswax, plant resin, egg and animal glue;
- plant oil, beeswax, plant resin, egg and animal glue;
- plant oil, beeswax, plant resin, proteinaceous material.

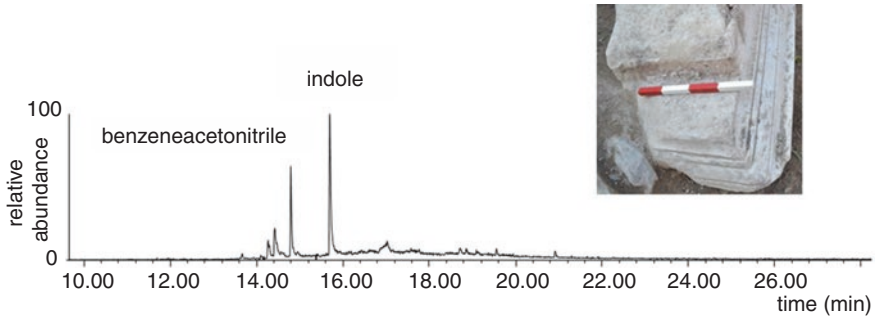

Fig. 6.4 Py-GC-MS extract ion chromatogram of m/z 90 to highlight the presence of benzeneacetonitrile and indole, markers of casein of a sample from the Sanctuary of Apollo

6.2.4 1385 AD ca – Annunciation and Saints by Giovanni del Biondo

The large polyptych *Annunciation and Saints* (406 cm × 377 cm) painted by Giovanni del Biondo (1356–1398 ca) around 1385 AD, was originally located in the sacristy of Santa Maria Novella (Florence, Italy) is now exhibited in the Galleria dell'Accademia in Florence. This masterpiece was painted in a period when egg yolk or *tempera grassa* (a mixture of oil and egg) were most commonly used as binders in panel paintings (Serefidou et al. 2016).

Although Giovanni del Biondo tended to follow the recipes provided by Cennino Cennini in his *Libro dell'Arte* (Brunello 1971) and other technical literature of his time (Brunello 1975), the surface of the panel looks unusually glossy, and is similar to the particular effects of medieval illumination and mural paintings, rather than traditional egg yolk tempera paints.

Analytical pyrolysis revealed the co-presence of different materials and identified the organic materials in the different paint layers.

The results showed that animal glue and a triterpene resin are the main constituents of those samples containing all the stratigraphy (preparation, paint layer and superficial brownish layer). Figure 6.5 shows the extracted ion pyrogram, highlighting the markers corresponding to animal glue and the plant resin. The peaks detected in the pyrogram are associated with characteristic dammar compounds: dammaredienol, ursonic acid, dammaradienone and oleanonic acid. In addition, smaller peaks, ascribable to egg yolk (Brunello 1975) and a saccharide material (Andreotti et al. 2009) were detected.

GC-MS analyses on the same samples showed that the saccharide material is honey. The pyrolysis of the material scraped from the surface containing mainly the brownish glossy layer, showed a low content of dicarboxylic acids, suggesting the absence of a lipid material, and detected the natural resin, animal glue and saccharide material. Analysis of the samples from an area that was cleaned before the sampling, showed only egg yolk and animal glue, based on the detection of hexadecanetrile and octadecanenitrile, pyrrole and alkylpyrroles (Brunello 1975). Analysis of the sample from the same cleaned area, after the preparation layer had been removed, revealed only egg.

It thus seems that del Biondo used an egg-tempera for the paint layers, applied on a ground made of using animal glue as binder. The stratigraphy is not complex, which highlights the high level of the egg-tempera technique at the turn of the fourteenth century. Lastly, the glossy surface was created using a coating made of a mixture of dammar resin, honey, and animal glue. Given that dammar resin was first introduced in Europe in around the seventeenth century, the darkened coating is likely due to past conservation work, known as a "beverone" which was commonly used to make the paint surface shinier. This interpretation is also corroborated by the absence of the coating over the areas protected by the twisted columns.

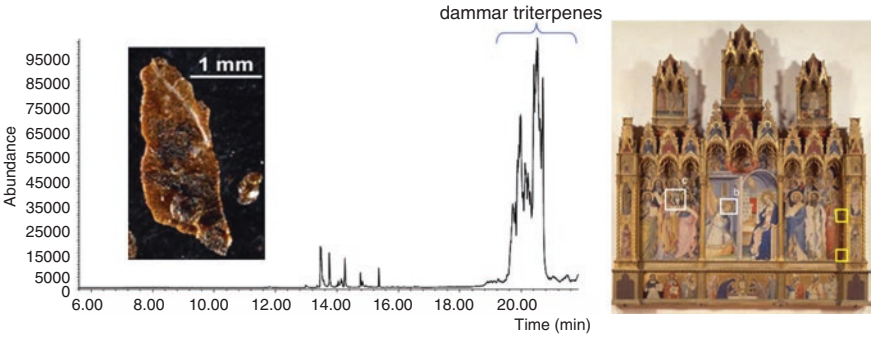

Fig. 6.5 Py-GC-MS extract ion chromatogram of m/z 189 of a sample taken from the central panel of the polyptych. The intense peaks are due to the presence of a triterpenoid resin, based on the identification of the mass spectra of oleanonic acid, ursonic acid, dammaradienol, and dammaradienone

6.2.5 Fourteenth–Seventeenth Century – Wall Paintings of the Monumental Cemetery of Pisa

The construction of the gothic cloister of the Monumental Cemetery in Pisa, also known as the *Campo Santo*, was begun in 1278 by the architect Giovanni di Simone. The walls were covered in over 2600 square meters of mural paintings (Fig. 6.6) created by an impressive number of famous artists including Francesco Traini, Buonamico di Martino da Firenze (Buonamico Buffalmacco), Spinello Aretino, Benozzo Gozzoli, Andrea Bonaiuti, Antonio Veneziano, Taddeo Gaddi, and Piero di Puccio. Due to their semi-outdoor position, the wall paintings have been subject to restorations since the fifteenth century, which became even more frequent during the eighteenth and nineteenth centuries. During the Second World War, an bomb exploded in the cemetery, burning the wood and melting the lead of the roof, thus damaging the paintings underneath. The recovery of these paintings began immediately and is still ongoing.

In 1945 the mural paintings were detached from the walls and relocated on asbestos cement supports, using a glue based on a mixture of casein and calcium hydroxide. A variety of materials were used in the post-war restorations, and already in the 1980s, the restored mural paintings had darkened, covered with efflorescence and flaking (Andreotti et al. 2008a, b). A new conservation campaign started, which is almost concluded (2021, the year of publication of the present volume). During these recent restorations, several paintings presented unexpected challenges that needed diagnostic campaigns to support conservation decisions.

An example of this complexity is the ‘Giudizio Universale’ by Bonamico Buffalmacco (Andreotti et al. 2008a; Bonaduce and Colombini 2003). The paint surface of a section of this mural was completely waterproof, preventing any restoration attempt using traditional approaches. Py-GC-MS analyses revealed the simultaneous presence of several materials. An example of the complexity of the

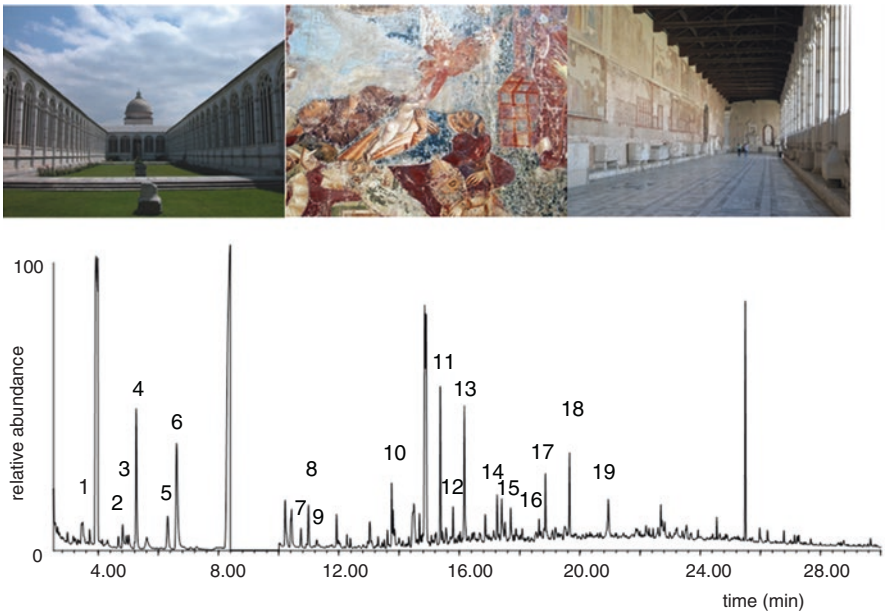

Fig. 6.6 Py-GC-MS chromatogram of one sample from the 'Giudizio Universale' by Bonamico Buffalmacco, Monumental Cemetery in Pisa. The TMS derivatives compounds identified are: 1: Benzene, 2: Ethyl acrylate, 3: Methyl methacrylate, 4: Acetic acid, 5: Pyrrole, 6: Toluene, 7: 2-Methylpyrrole, 8: 3-Methylpyrrole, 9: Benzaldehyde, 10: Phenol, 11: 2-Methylphenol, 12: 4-Methylphenol, 13: 2,4-Dimethylphenol, 14: benzene acetonitrile, 15: 3-Phenylpropionitrile, 16: Indole, 17: Phthalate, 18: Phthalate, 19: Benzyl benzoate

pyrograms obtained is shown in Fig. 6.6. Ethyl acrylate, methyl methacrylate, ethyl methacrylate, isobutyl methacrylate, and butyl methacrylate were detected, unevenly distributed on the surface of the 'Giudizio Universale', and ascribable to Primal and Elvacite, two acrylic resins used in an attempt to detach the painting from the support.

Pyrolysis products derived from egg yolk, casein, and animal glue were also detected in the chromatograms. Hexadecanenitrile, octadecanenitrile, cholesterol derivatives, and carboxylic acids are the characteristic pyrolysis products used for egg yolk, indole for casein, whereas pyrrole, alkyl pyrroles, benzyl nitrile and 3-phenylpropionitrile are used for animal glue (Andreotti et al. 2008a, b). Egg yolk had been used possibly as a paint binder, or in a past conservation treatment. Casein and animal glue belong to post-war conservation interventions. Polyvinylacetate was also detected, based on the detection of high relative amounts of acetic acid trimethylsilyl ester, benzene and other aromatic compounds. This synthetic material also belongs to the post-war restoration. The presence in the pyrogram of high amounts of phenols, pointed to the presence of a phenol-formaldehyde resin. This material is not documented and it is not a conservation material. The hypothesis is that copolymerisation occurred between the casein (the glue between the paint layer

and the canvas) and polyvinyl acetate (the glue placed between the canvas and the asbestos support), producing a phenol-formaldehyde-like material. Copolymerisation probably occurred due to the addition of formaldehyde to the casein glue, as an antimicrobial agent, which explains the high hydrophobicity of the paint surface.

6.2.6 Sixteenth Century Madonna con Bambino, Giovanni Pietro Rizzoli

The range of synthetic materials used by restorers over the last few decades has expanded significantly. A variety of modern materials have been tested based on different optical properties and durability, as well as solubility and performance, and their identification in an artwork contributes to reconstruct its history. In particular, modern varnishes include low molecular weight resins, and the two most common classes in conservation practice are hydrogenated hydrocarbon resins and urea-aldehyde resins.

Regalrez 1094 is a hydrocarbon resin synthesized from vinyl-toluene and α-methyl-styrene and subsequent hydrogenation of the unsaturated polymer. The Py-GC-MS profile of this resin is characterized by three different peak clusters, the first associated with the monomers of cyclohexane and cyclohexene, and another two at a higher retention time associated with cyclohexane dimers and trimers. Figure 6.7 reports the profile of a sample from a restored sixteenth century painting by Giovanni Pietro Rizzoli, part of the The Sander Collection, in which the three clusters of pyrolysis products of Regalrez 1094 are clearly visible.

6.3 Py-GC-MS Analysing Modern Paint Materials

In the twentieth century a wide range of synthetic materials were introduced as artists' media. The first commercial formulation of acrylic resin was marketed in the 1950s, and consisted of acrylic polymers dissolved in organic solvents, such as toluene and xylene. The evolution of the formulations and synthetic processes used to produce acrylic resins led to the introduction in the 1970s to copolymers based on different acrylic monomers, together with other monomeric species, such as styrene. This enabled producers to formulate acrylic resins for use as aqueous emulsions, which are still in use today.

Analysing the chemical structure of the acrylic resins, in order to clarify whether they were applied as emulsions or as solvent resins, and identifying specific additives, such as modern plasticizers or surfactants, is extremely useful in dating modern paints and detecting possible forgeries.

Py-GC-MS is the preferred method in the analysis of synthetic paints (Learner 2004).

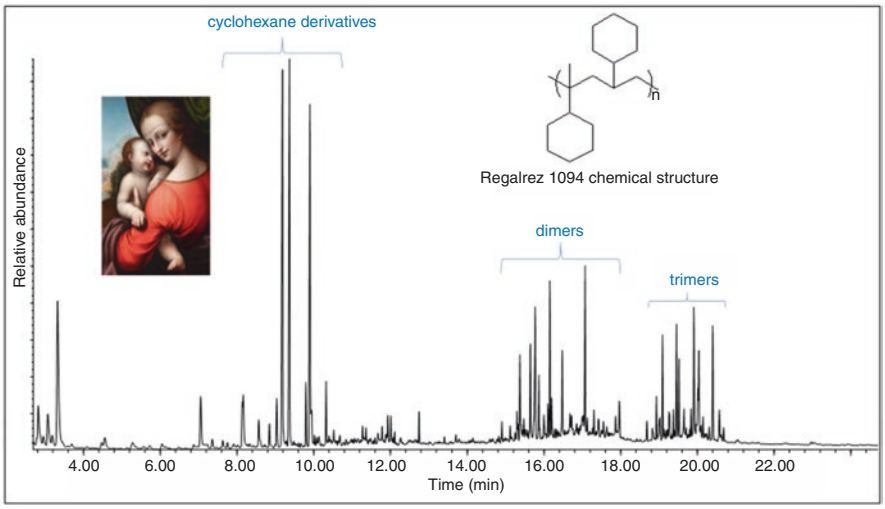

Fig. 6.7 Py-GC-MS profile of a sample from a sixteenth century painting by Giovanni Pietro Rizzoli (The Sander Collection) showing the presence of the modern varnish Regalrez 1094

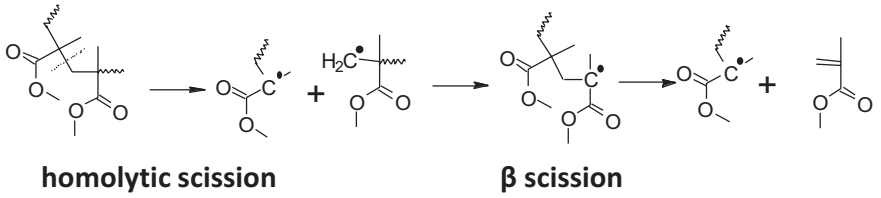

Fig. 6.8 Example of the unzipping pyrolysis mechanism of a generic acrylic resin

Acrylic resins undergo unzipping mechanism upon pyrolysis, which is a radical mechanism of thermal cleavage whereby the polymer is converted into the respective monomers. As an example, Fig. 6.8 reports the unzipping of a generic acrylic resin.

Acrylic resins with formulations compatible with the use of solvent paints have been detected in the works of several Italian artists. For example, Py-GC-MS analyses of *Superficie 207* (1957), a painting by Giuseppe Capogrossi (Galleria Nazionale di Arte Moderna, Rome), showed the presence of a resin based on ethyl acrylate (Fig. 6.9). Ethylacrylate was commonly used in the first formulations of acrylic resins dissolved in solvents (La Nasa et al. 2020).

Examples of acrylic formulations compatible as emulsions were detected in Anselm Kiefer's "Cette Obscure Clarté qui Tombe des Etoiles" dated 1996 (Fig. 6.10), which contained styrene-acrylic copolymers typically used in these formulations (Bartolozzi et al. 2016; Pellegrini et al. 2013). This type of resin was identified due to the presence in the pyrolysis profile of both the monomers, n-butyl acrylate and styrene, together with the corresponding dimers and trimers. This was

confirmed by the absence of the characteristic homo-oligomers, which are instead associated with polystyrene and n-butyl acrylate homopolymers. This formulation is one of the most common acrylic copolymers produced as an aqueous emulsion and used in several other applications as well as painting.

The same formulation based on *n*-butyl acrylate modified with styrene has also been detected as a paint binder in outdoor murals such as Tuttomondo (1989) in Pisa (La Nasa et al. 2016, 2021). Other common acrylic emulsions are produced by the copolymerization of different monomers, such as methyl acrylate, methyl methacrylate and ethyl acrylate, which have different commercial names, such as the families of Paraloid, Plextol and Primal (Osete-Cortina and Doménech-Carbó 2006). This type of resin is identified by both the pyrolysis markers characteristic of the monomers and their relative combined oligomers. Interestingly, acrylic emulsions are not only produced using copolymers. The analysis of the work of art "*The Italian Flag*" by Fernando Melani (1955–1960) revealed an ethylhexyl-acrylate homopolymer, identified by the monomer together with 2-hexanol, and 2-ethyl hexanol (Carlesi et al. 2016). This type of resin is generally applied as an aqueous emulsion. Polyvinylacetate, when subject to pyrolysis, undergoes a two-step elimination process. The cleavage starts with a concerted mechanism that involves two adjacent carbon atoms to produce a double bond. The second step in the reaction leads to chain scission and aromatization reactions. Figure 6.11 shows the elimination reaction characteristic of polyvinyl resins.

Pure PVAc is too hard to form a film from an emulsion, thus the paint formulations contain massive amounts of plasticizers. These plasticizers are usually the most abundant in the pyrolysis profile of PVAc and can be divided into: external plasticizers, such as phthalate esters, and internal plasticizers, such as VeoVa (vinyl-versatate esters), copolymerized with the PVAc monomer (Learner 2001; Silva et al. 2010).

Polyvinyl acetate used as a paint binder has been detected in several works of art. For example, PVAc was detected in the paint samples from the "*La Caverna*

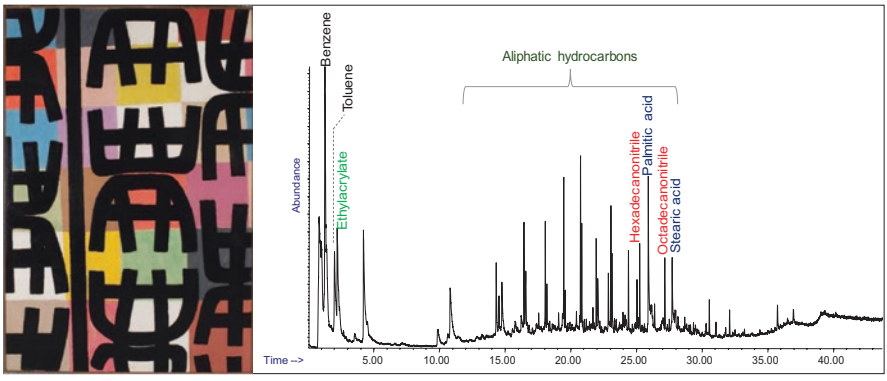

Fig. 6.9 Py-GC-MS chromatogram for a paint sample from "Superficie 207" (1957) by Giuseppe Capogrossi (La Nasa et al. 2020)

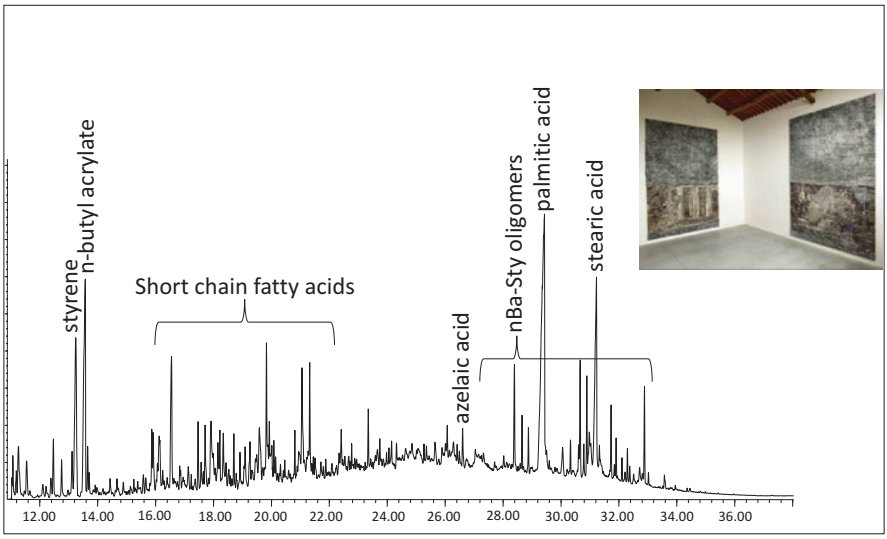

Fig. 6.10 Py-GC-MS profile of a paint sample from "Cette Obscure Clarté qui Tombe des Etoiles"(1996) by Anselm Kiefer (Pellegrini et al. 2013)

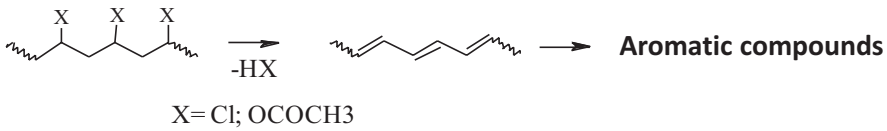

Fig. 6.11 The elimination reaction characteristic of the pyrolysis of polyvinyl resins

dell'Antimateria" (1958–1959) by Pinot Gallizzio (Bartolozzi et al. 2014). The pyrolytic profiles of the samples were characterized by the presence of acetic acid, benzene, and the aromatic species characteristic of the pyrolysis of this material (indene, naphthalene, fluorene and, anthracene), which were generally found with relatively high amounts of external plasticizers (phthalates) (Fig. 6.12). Several commercial materials containing PVAc were identified in the painting materials stored in two of the artist's former studios (Gottschaller et al. 2012).

Py-GC-MS can also be used to detect PVAc mixed with other synthetic polymers. Multi-shot analytical pyrolysis on the samples from the artworks Disgelo (Piero Gilardi, 1968) and Superficie Lunare (Giulio Turcato, 1969) showed how powerful this approach is in differentiating between different types of polymers: the polyurethane used in the 3D structure, from the paint binder on the surface, based on PVAc (Fig. 6.13) (Zuena et al. 2020).

PVAc is also often encountered as a paint binder in outdoor murals, such as those produced by Keith Haring in the Necker Hospital mural in Paris painted in 1987. Py-GC-MS analyses showed that Haring used a PVAc paint binder with VeoVa as an internal plasticizer (La Nasa et al. 2016, 2021).

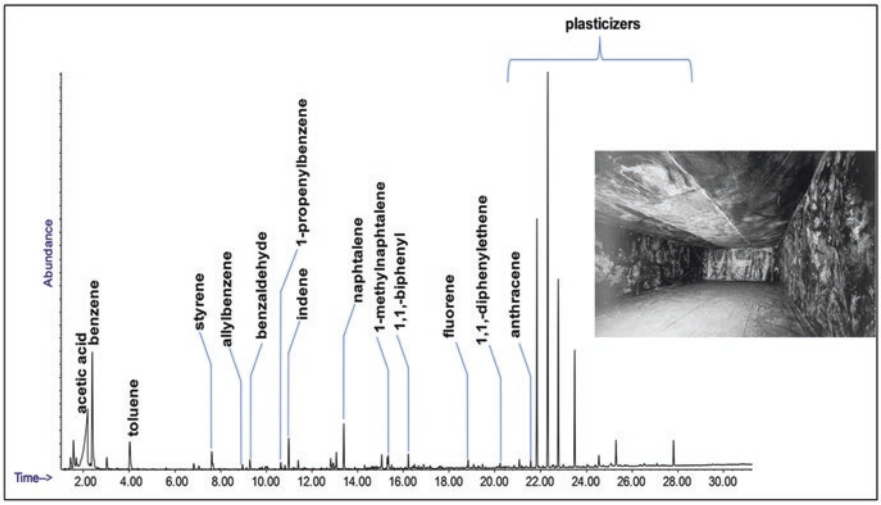

Fig. 6.12 Py-GC-MS profile of a paint sample from "La Caverna dell'Antimateria" (1958–1959) by Pinto Gallizio (Bartolozzi et al. 2014)

Another important class of resins is **alkyd resins**. These resins, often referred to as "smalts" when used in art, consist of oil-modified polyesters synthesized from polyols, aromatic polybasic acids, with different oil contents (or a source of fatty acids) (Fig. 6.14). They have been used as commercial binders for paints and coatings since the 1940s (Ploeger et al. 2008).

The pyrolysis profiles of alkyd paints are similar to drying oils, due to the acylglycerol/fatty acid portion in the polymer network. However, the presence of pyrolysis products related to the polyols and aromatic polybasic acid portion of the resin distinguishes them from drying oils.

Given that the formulation of alkyd resins has been modified over the years, their characterization by analytical pyrolysis is key to understanding painting techniques and to identifying forgeries (La Nasa et al. 2021). More recent alkyd formulations are characterized by specific components, such as styrene, which distinguish them from the first alkyds based mainly on lipids.

Pablo Picasso and Jackson Pollock are good examples of painters who used alkyd paints. The analysis of Pablo Picasso's *Nude Woman in a Red Armchair* (1932) showed the presence of fatty acids, dicarboxylic acids, glycerol, and phthalic anhydride, which are characteristic markers of alkyds (Cappitelli and Koussiaki 2006). The same pyrolysis markers associated with the use of alkyd resin were detected in a paint sample from Pollock's *Yellow Island* (1952).

Alkyd resins have also been detected in *Superficie 207* (1957) by Giuseppe Capogrossi (La Nasa et al. 2020), amongst other Italian artists, where an alkyd resin was used in a mixture with a styrene resin (Figs. 6.14 and 6.15), thus highlighting the use of analytical pyrolysis to detect more than one paint binder in the same

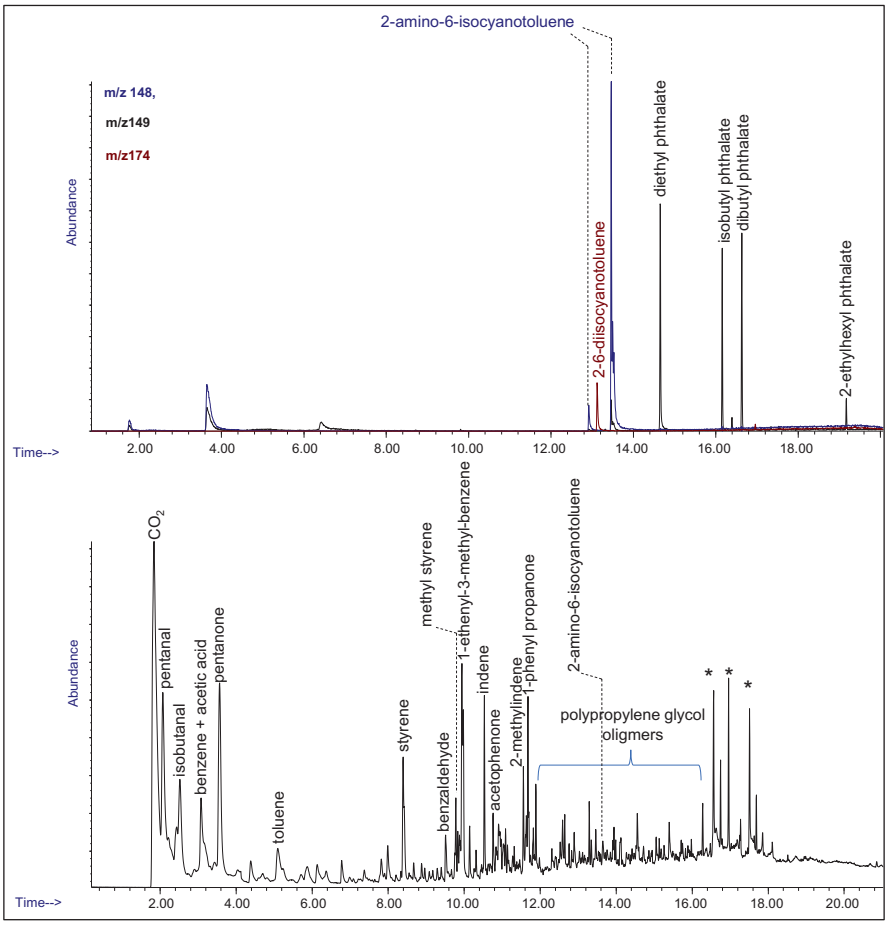

Fig. 6.13 Py-GC-MS chromatograms obtained at 350 °C and 600 °C by a double shot approach on a paint sample from "Superficie Lunare" (1969) by Giulio Turcato (Zuena et al. 2020)

sample. Finally, several alkyd resins have been identified in the commercial painting materials stored in Lucio Fontana's former studios (Cappitelli 2004).

As with the other classes of paint binders mentioned in this chapter, alkyds have also been used in outdoor murals. For example, an alkyd resin paint binder was detected in the samples from Keith Haring's mural in Collingwood (1984), Melbourne (La Nasa et al. 2016, 2021).

In the last few years, low molecular weight urea-aldehyde resins have been introduced as paint binders in retouch paints. Although the nature of the monomers used in synthesizing these classes of resins is generally known, the specific synthetic pathways and the final chemical composition of the materials are patented and thus such information is not publicly available. Tentative structure elucidations together with their relative mass spectra have been published in the literature for Laropal

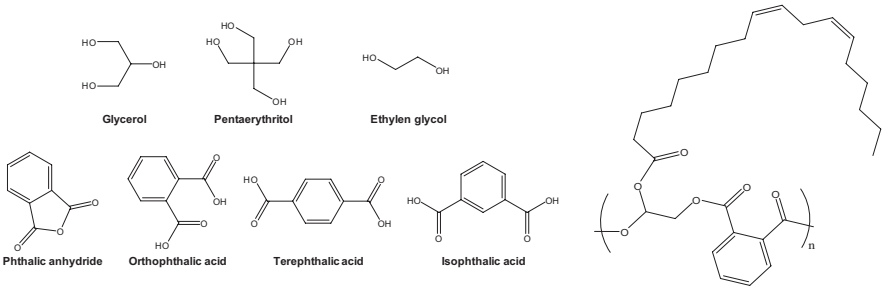

Fig. 6.14 Polyols and polybasic acids used in artistic alkyd paint formulations, and model structure of alkyd resin containing phthalic anhydride, glycerol, and linoleic acid

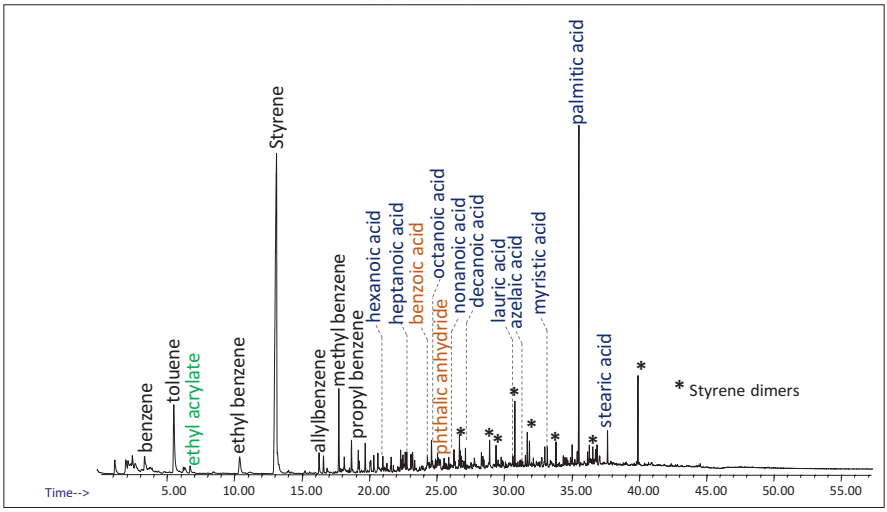

Fig. 6.15 Py-GC-MS chromatogram of a paint sample from "Superficie 207" (1957) by Giuseppe Capogrossi (La Nasa et al. 2020)

A81 (Bonaduce et al. 2013) (Fig. 6.16). This information can be used to detect these polymers in paint samples, highlighting retouches in the paintings.

6.4 Characterization of Organic Pigments

Besides the characterization of the paint binders, analytical pyrolysis can also be used to characterize organic pigments. Identifying pigments is crucial to improve the knowledge of an artwork, its historical context, and painting technique. In the nineteenth century organic pigments were continuously being developed, each characterized by a specific synthesis and commercialization year. Knowing the type of

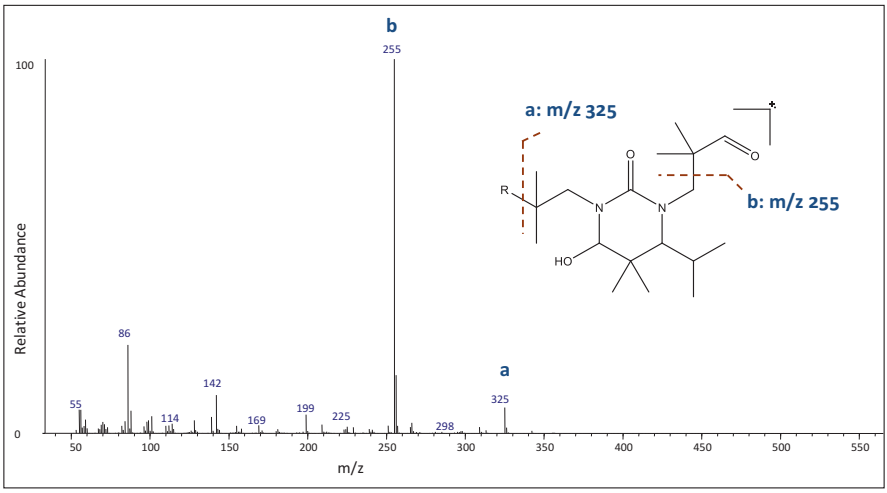

Fig. 6.16 Mass spectra (EI) of the most abundant pyrolysis products of the resin Laropal A81 (Bonaduce et al. 2013)

organic pigment may also help to solve authenticity, attribution, and conservation problems.

Py-GC-MS has been applied for the characterization and ageing of several classes of organic pigments: β-naphthol pigment lakes, BONA pigment lakes, disazopyrazolone, triarylcarbonium, dioxazine, anthraquinone, indanthrone, isoindoline, and thioindigo (Ghelardi et al. 2015; Russell et al. 2011). Each pigment has specific pyrolysis markers that can be used to identify these chemical species in paint samples.

Good examples of analytical pyrolysis are the results obtained for the identification of the organic pigments used by Francis Bacon, Clyfford Still, and Jackson Pollock in their paintings (Ghelardi et al. 2015; Russell et al. 2011).

A list of all the organic pigments that can currently be identified by Py-GC-MS is reported in Table 6.1 (Ghelardi et al. 2015; Russell et al. 2011).

6.5 Conclusions

The case studies illustrated in this chapter demonstrate how Py-GC-MS is extremely efficient at identifying both natural and synthetic artistic materials, in a wide range of molecular weights, including synthetic resins that are not suitable for investigation by conventional GC-MS.

The material analysis of an artwork constitutes a complementary and fundamental tool in the authentication of an artwork. This is because the chemical analysis and identification of paint materials provide important information on the artistic technique, which is essential in relation to attribution and dating issues.

Table 6.1 The organic pigments that can currently be identified by Py-GC-MS (Ghelardi et al. 2015; Russell et al. 2011)

Red	PR1, PR3, PR4, PR5, PR6, PR7, PR9, PR12, PR14, PR17, PR22, PR23, PR31, PR41, PR48:1, PR48:2, PR49:1, PR49:2, PR52:1, PR53:1, PR57:1, PR63:1, PR83, PR90, PR112, PR123, PR144, PR147, PR149, PR166, PR170, PR175, PR176, PR178, PR179, PR185, PR188, PR190, PR208, PR214, PR221, PR254, PR255, PR264
Orange	PO16, PO36, PO46, PO61, PO62, PO73
Violet	PV1, PV3, PV19, PV23, PV27, PV32, PV37, PV39, PV42, PV44, PV51, PV52, PV53
Green	PG7, PG8, PG10, PG13, PG36
Brown	PBr23, PBr25, PBr38, PBr41
Blue	PB1, PB15:0, PB15:1, PB15:2, PB15:3, PB15:4, PB15:6, PB17, PB60, PB62, PB76
Yellow	PY1, PY2, PY3, PY6, PY12, PY13, PY14, PY17, PY55, PY65, PY73, PY74, PY75, PY81, PY87, PY97, PY109, PY110, PY120, PY126, PY127, PY151, PY154, PY173, PY175

Cross-checking the information obtained from the chemical analysis of paint materials with knowledge on the history and evolution of artistic techniques – not only over centuries but also decades as in the twentieth century – helps to date a painting or identify a forgery if any anachronistic materials are detected. When the object of study concerns modern and contemporary art, the chemical analysis of the materials used in an artist's workshop also provides a valuable source of additional information for cross-reference in order to reinforce or confirm possible attributions.

Acknowledgements The authors are grateful to all the conservators, curators and conservation scientists that collaborated to the researches described in the chapter, and contributed to the publication of the results in the cited references. The Sander Collection, the restorer Stefano Ticci, and Adarte (Florence) are kindly acknowledged for providing the varnish sample from the Madonna con Bambino by Giovanni Pietro Rizzoli, and for allowing us to include the analytical results in this contribution.

References

Amadori, M.L., Barcelli, S., Poldi, G., Ferrucci, F., Andreotti, A., Baraldi, P., Colombini, M.: Invasive and non-invasive analyses for knowledge and conservation of Roman wall paintings of the Villa of the Papyri in Herculaneum. Microchem. J. **118**, 183–192 (2015)

Andreotti, A., Bonaduce, I., Colombini, M., Modugno, F.: in Sarcofago delle Amazzoni. In: Bottini, A., Setari, E. (eds.) Le componenti organiche della pittura, pp. 157–162. Mondatori Electa, Milano (2007)

Andreotti, A., Baracchini, C., Bonaduce, I., Caleca, A., Colombini, M., Paolucci, A.: *Saving the Medieval Paintings by the Master Painter of the Triumph of Death in Pisa*. Paper presented at the Proceedings of 2008 ICOM-CC Triennial Conference (2008a)

Andreotti, A., Bonaduce, I., Colombini, M.P., Modugno, F., Ribechini, E.: Characterisation of natural organic materials in paintings by GC/MS analytical procedures. In: New Trends in Analytical, Environmental and Cultural Heritage Chemistry, pp. 389–423 (2008b)

Andreotti, A., Bonaduce, I., Colombini, M.P., Modugno, F., Ribechini, E.: A diagnosis of the yellowing of the marble high reliefs and the black decorations in the chapel of the tomb of Saint Anthony (Padua, Italy). Int. J. Mass Spectrom. **284**(1–3), 123–130 (2009)

Andreotti, A., Bonaduce, I., Colombini, M.P., Degano, I., Lluveras, A., Modugno, F., Ribechini, E.: Characterisation of natural substances in ancient polychromies. In: Liverani, P., Santamaria, U. (eds.) Diversamente bianco-La policromia della scultura romana, pp. 191–206. Edizioni Quasar, Roma (2014)

Bartolozzi, G., Cucci, C., Marchiafava, V., Masi, S., Picollo, M., Grifoni, E., et al.: A multidisciplinary approach to the investigation of "La Caverna dell'Antimateria" (1958–1959) by Pinot Gallizio. Herit. Sci. **2**(1), 29 (2014). https://doi.org/10.1186/s40494-014-0029-7

Bartolozzi, G., Picollo, M., Marchiafava, V., Centeno, S.A., Duvernois, I., Di Girolamo, F., et al.: Anselm Kiefer: a study of his artistic materials. Archaeol. Anthropol. Sci. **8**(3), 563–574 (2016). https://doi.org/10.1007/s12520-015-0238-3

Berzioli, M., Casoli, A.: FTIR spectroscopy as a fingerprint for waxes. In: Omarini, S. (ed.) Encaustic. History, Technique and Research, pp. 154–155. Nardini Ed (2012)

Bocchini, P., Traldi, P.: Organic mass spectrometry in our cultural heritage. J. Mass Spectrom. **33**(11), 1053–1062 (1998)

Bonaduce, I., Andreotti, A.: Py-GC/MS of organic paint binders. In: Organic Mass Spectrometry in Art and Archaeology, pp. 304–326. Wiley (2009)

Bonaduce, I., Colombini, M.P.: Gas chromatography/mass spectrometry for the characterization of organic materials in frescoes of the Momumental Cemetery of Pisa (Italy). Rapid Commun. Mass Spectrom. **17**(22), 2523–2527 (2003)

Bonaduce, I., Colombini, M.P., Degano, I., Di Girolamo, F., La Nasa, J., Modugno, F., Orsini, S.: Mass spectrometric techniques for characterizing low-molecular-weight resins used as paint varnishes. Anal. Bioanal. Chem. **405**(2), 1047–1065 (2013). https://doi.org/10.1007/s00216-012-6502-9

Bonaduce, I., Ribechini, E., Modugno, F., Colombini, M.P.: Analytical approaches based on gas chromatography mass spectrometry (GC/MS) to study organic materials in artworks and archaeological objects. Top. Curr. Chem. **374**(1), 6 (2016)

Bottini, A., Setari, E.: Il sarcofago delle Amazzoni. Electa, Milano (2007)

Brecoulaki, H., Zaitoun, C., Stocker, S.R., Davis, J.L., Karydas, A.G., Colombini, M.P., Bartolucci, U.: An Archer from the Palace of Nestor: a new wall-painting fragment in the Chora Museum. Hesperia. **77**(3), 363–397 (2008)

Brecoulaki, H., Andreotti, A., Bonaduce, I., Colombini, M.P., Lluveras, A.: Characterization of organic media in the wall-paintings of the "Palace of Nestor" at Pylos, Greece: evidence for a Secco painting techniques in the Bronze Age. J. Archaeol. Sci. **39**(9), 2866–2876 (2012)

Brecoulaki, H., Sotiropoulou, S., Perdikatsis, V., Lluveras-Tenorio, A., Bonaduce, I., Colombini, M.P., Tournavitou, I.: Appendix A: a technological investigation of the painting materials. In: The Wall Paintings of the West House at Mycenae, vol. 54, pp. 147–158. INSTAP Academic Press (2017)

Brunello, F.: Il Libro dell'Arte di C. Cennini, p. 589. Neri Pozza Editore, Vicenza (1971)

Brunello, F.: De arte illuminandi e altri trattati sulla tecnica della miniatura medievale. N. Pozza, Vicenza (1975)

Cantisani, E., Vettori, S., Andreotti, A., Ismaelli, T.: Ancient restorations at Hierapolis: research on the artificial binders. In: Ismaelli, T., Scardozzi, G. (eds.) Ancient Quarries and Building Sites in Asia Minor: Research on Hierapolis in Phrygia and Other Cities in South-Western Anatolia: Archaeology, Archaeometry, Conservation. Bari Edipuglia (2018)

Cappitelli, F.: THM-GCMS and FTIR for the study of binding media in Yellow Islands by Jackson Pollock and Break Point by Fiona Banner. J. Anal. Appl. Pyrolysis. **71**(1), 405–415 (2004). https://doi.org/10.1016/S0165-2370(03)00128-1

Cappitelli, F., Koussiaki, F.: THM-GCMS and FTIR for the investigation of paints in Picasso's still life, weeping woman and nude woman in a Red Armchair from the Tate Collection, London. J. Anal. Appl. Pyrolysis. **75**(2), 200–204 (2006). https://doi.org/10.1016/j.jaap.2005.05.008

Carlesi, S., Bartolozzi, G., Cucci, C., Marchiafava, V., Picollo, M., La Nasa, J., et al.: Discovering "The Italian Flag" by Fernando Melani (1907–1985). Spectrochim. Acta A Mol. Biomol. Spectrosc. **168**, 52–59 (2016). https://doi.org/10.1016/j.saa.2016.05.027

Casoli, A., Violante, C., Mastrobattista, E., Santoro, S.: Le pitture dell'Insula del Centenario a Pompei: Le indagini sulle sostanze organiche. Paper presented at the IV Congresso nazionale di Archeometria, Pisa (2006)

Chiantore, O., Riedo, C., Andreotti, A., Colombini, M.P., Lluveras, A., Tenorio, et al.: Organic materials in the wall paintings of the Vesuvian area. In: Omarini, S. (ed.) Encaustic. History, Technique and Research, pp. 41–122. Nardini Ed (2012)

Cotte, M., Susini, J., Solé, V.A., Taniguchi, Y., Chillida, J., Checroun, E., Walter, P.: Applications of synchrotron-based micro-imaging techniques to the chemical analysis of ancient paintings. J. Anal. At. Spectrom. **23**(6), 820–828 (2008)

Degano, I., La Nasa, J.: Trends in high performance liquid chromatography for cultural heritage. Top. Curr. Chem. **374**(2), 20 (2016)

Degano, I., Modugno, F., Bonaduce, I., Ribechini, E., Colombini, M.P.: Recent advances in analytical pyrolysis to investigate organic materials in heritage science. Angew. Chem. Int. Ed. **57**(25), 7313–7323 (2018)

Duran, A., Jimenez De Haro, M., Perez-Rodriguez, J., Franquelo, M., Herrera, L., Justo, A.: Determination of pigments and binders in Pompeian wall paintings using synchrotron radiation–high-resolution X-ray powder diffraction and conventional spectroscopy–chromatography. Archaeometry. **52**(2), 286–307 (2010)

Fiorillo, F., Hendriks, L., Hajdas, I., Vandini, M., Huysecom, E.: The rediscovery of Jan Ruyscher and its consequence. J. Am. Inst. Conserv., 1–9 (2021). https://doi.org/10.1080/01971360.2020.1822702

Ghelardi, E., Degano, I., Colombini, M.P., Mazurek, J., Schilling, M., Learner, T.: Py-GC/MS applied to the analysis of synthetic organic pigments: characterization and identification in paint samples. Anal. Bioanal. Chem. **407**(5), 1415–1431 (2015)

Gottschaller, P., Khandekar, N., Lee, L.F., Kirby, D.P.: The evolution of Lucio Fontana's painting materials. Stud. Conserv. **57**(2), 76–91 (2012). https://doi.org/10.1179/2047058411Y.0000000002

Hendriks, L., Hajdas, I., Ferreira, E.S., Scherrer, N.C., Zumbühl, S., Küffner, M., et al.: Combined 14 C analysis of canvas and organic binder for dating a painting. Radiocarbon. **60**(1), 207–218 (2018)

Hendriks, L., Hajdas, I., Ferreira, E.S., Scherrer, N.C., Zumbühl, S., Küffner, M., et al.: Selective dating of paint components: radiocarbon dating of lead white pigment. Radiocarbon. **61**(2), 473–493 (2019a)

Hendriks, L., Hajdas, I., Ferreira, E.S., Scherrer, N.C., Zumbühl, S., Smith, G.D., et al.: Uncovering modern paint forgeries by radiocarbon dating. Proc. Natl. Acad. Sci. **116**(27), 13210–13214 (2019b)

Ho, C.-T., Shahidi, F.: Flavor components of fats and oils. In: Bailey's Industrial Oil and Fat Products (2005). https://doi.org/10.1002/047167849X.bio009

Hodgins, G.W.L.: Identifying art forgeries by radiocarbon dating microgram quantities of artists' paints. Proc. Natl. Acad. Sci. **116**(27), 13158–13160 (2019). https://doi.org/10.1073/pnas.1907933116

La Nasa, J., Orsini, S., Degano, I., Rava, A., Modugno, F., Colombini, M.P.: A chemical study of organic materials in three murals by Keith Haring: a comparison of painting techniques. Microchem. J. **124**, 940–948 (2016). https://doi.org/10.1016/j.microc.2015.06.003

La Nasa, J., Moretti, P., Maniccia, E., Pizzimenti, S., Colombini, M.P., Miliani, C., et al.: Discovering Giuseppe Capogrossi: study of the painting materials in three works of art stored at Galleria Nazionale (Rome). Heritage. **3**(3) (2020). https://doi.org/10.3390/heritage3030052

La Nasa, J., Campanella, B., Sabatini, F., Rava, A., Shank, W., Lucero-Gomez, P., et al.: 60 years of street art: a comparative study of the artists' materials through spectroscopic and

mass spectrometric approaches. J. Cult. Herit. **48**, 129–140 (2021). https://doi.org/10.1016/j.culher.2020.11.016
Learner, T.: The analysis of synthetic paints by pyrolysis-gas chromatography-mass spectrometry (PyGCMS). Stud. Conserv. **46**(4), 225–241 (2001). https://doi.org/10.1179/sic.2001.46.4.225
Learner, T.: Analysis of Modern Paints. Getty Publications (2004)
Linn, R., Bonaduce, I., Ntasi, G., Birolo, L., Yasur-Landau, A., Cline, E.H., et al.: Evolved gas analysis-mass spectrometry to identify the earliest organic binder in Aegean style wall paintings. Angew. Chem. **130**(40), 13441–13444 (2018)
Orsini, S., Parlanti, F., Bonaduce, I.: Analytical pyrolysis of proteins in samples from artistic and archaeological objects. J. Anal. Appl. Pyrolysis. **124**, 643–657 (2017). https://doi.org/10.1016/j.jaap.2016.12.017
Osete-Cortina, L., Doménech-Carbó, M.T.: Characterization of acrylic resins used for restoration of artworks by pyrolysis-silylation-gas chromatography/mass spectrometry with hexamethyldisilazane. J. Chromatogr. A. **1127**(1–2), 228–236 (2006)
Pellegrini, D., Modugno, J.L.N.F., di Girolamo, F., Colombini, M.P.: Indagini scientifiche su Cette obscure clartè qui tombe des étoiles di Anselm Kiefer. EDIFIR, Florence (2013)
Piqué, F., Chiari, G., Colombini, M.P., Torraca, G.: I dipinti murali della Casa del Bicentenario ad Ercolano: Degrado e prevenzione. In: Driussi, G.B.A.G. (ed.) Scienza e Beni Culturali, vol. 26, pp. 837–847. Arcadia Ricerche, Marghera (2010)
Piqué, F., Macdonald-Korth, E., Rainer, L.: Observations on materials and techniques used in Roman wall paintings of the tablinum, House of the Bicentenary at Herculaneum. In: Beyond Iconography: Materials, Methods, and Meaning in Ancient Surface Decoration. Selected Papers on Ancient Art and Architecture, pp. 57–76. Archaeological Institute of America, Boston (2015)
Ploeger, R., Scalarone, D., Chiantore, O.: The characterization of commercial artists' alkyd paints. J. Cult. Herit. **9**(4), 412–419 (2008)
Rainer, L., Graves, K., Maekawa, S., Gittins, M., Piqué, F.: Conservation of the Architectural Surfaces in the Tablinum of the House of the Bicentenary, Herculaneum Phase I: Examination, Investigations, and Condition Assessment. Getty Conservation Institute, Los Angeles (2017)
Riedo, B., Chiantore, O.: Py-GC/MS to evaluate waxy materials. In: Omarini, S. (ed.) Encaustic. History, Technique and Research, pp. 156–158. Nardini Ed (2012)
Roldán, C., Murcia-Mascarós, S., López-Montalvo, E., Vilanova, C., Porcar, M.: Proteomic and metagenomic insights into prehistoric Spanish Levantine Rock Art. Sci. Rep. **8**(1), 1–10 (2018)
Russell, J., Singer, B.W., Perry, J.J., Bacon, A.: The identification of synthetic organic pigments in modern paints and modern paintings using pyrolysis-gas chromatography–mass spectrometry. Anal. Bioanal. Chem. **400**(5), 1473 (2011). https://doi.org/10.1007/s00216-011-4822-9
Serefidou, M., Bracci, S., Tapete, D., Andreotti, A., Biondi, L., Colombini, M.P., et al.: Microchemical and microscopic characterization of the pictorial quality of egg-tempera polyptych, late 14th century, Florence, Italy. Microchem. J. **127**, 187–198 (2016)
Silva, M.F., Doménech-Carbó, M.T., Fuster-López, L., Mecklenburg, M.F., Martin-Rey, S.: Identification of additives in poly(vinylacetate) artist's paints using PY-GC-MS. Anal. Bioanal. Chem. **397**(1), 357–367 (2010). https://doi.org/10.1007/s00216-010-3505-2
Zuena, M., Legnaioli, S., Campanella, B., Palleschi, V., Tomasin, P., Tufano, M.K., et al.: Landing on the moon 50 years later: a multi-analytical investigation on Superficie Lunare (1969) by Giulio Turcato. Microchem. J. **157**, 105045 (2020). https://doi.org/10.1016/j.microc.2020.105045

Chapter 7
Direct and Hyphenated Mass Spectrometry to Detect Glycerolipids and Additives in Paint

Inez van der Werf and Klaas Jan van den Berg

Abstract This chapter gives a short overview of the way glycerolipids have been used in paints and varnishes. Their chemistry is discussed in relation to pretreatment, modifications and ageing processes.

Hyphenated and direct mass spectrometry techniques are presented. Their capacity for detecting lipids and additives in paintings and for studying their ageing and degradation processes is discussed. While the potential of these techniques for authentication or discovery of forgeries may be problematic in many cases, there are some exceptions. Molecular markers of ageing and the occurrence of certain additives may provide information on the age and making of the paintings.

Keywords Glycerolipids · Binding media · Direct mass spectrometry · GCMS · LCMS

7.1 Introduction

Glycerolipids form a large group of biological molecules containing three long-chain fatty acids in ester linkage to a glycerol backbone. The natural fats and oils composed of these glycerolipids have been extensively used, in paints and varnishes, to create works of painted art.

From the nineteenth century onwards, the distinction and division between commercial artists' paints and house paints has become increasingly significant. However, since especially avant-garde artists have used house paints extensively (Crook and Learner 2000; Standeven 2011), both types of paints will be treated.

This chapter discusses the application of direct and hyphenated mass spectrometric techniques to detect glycerolipids, their modifications, lipid and non-lipid

I. van der Werf · K. J. van den Berg (✉)
Cultural Heritage Agency of the Netherlands, Amsterdam, The Netherlands
e-mail: k.van.den.berg@cultureelerfgoed.nl

M. P. Colombini et al. (eds.), *Analytical Chemistry for the Study of Paintings and the Detection of Forgeries*, Cultural Heritage Science,
https://doi.org/10.1007/978-3-030-86865-9_7

additives. The potential of these techniques to authenticate paintings or discover forgeries is investigated in relation to the historical context of use of oil paints and -varnishes together with their ageing properties.

7.1.1 Overview of the Use of Oil Paint Binders

7.1.1.1 Oil Paint

The earliest reported use of drying oils is as protective coatings by gilders and encaustic painters in the fifth century CE. In the eighth century in the *Lucca* manuscript, an oil varnish was described that was made by dissolving resin into oil (Laurie 1988).

In paint, glycerolipid binders have been employed by artists since early medieval times, at least in northern Europe (White and Kirby 2006), and especially in the form of linseed oil. In southern Europe, and initially in the form of walnut oil, they were introduced later and gradually replaced the use of egg tempera during late medieval times (Higgitt and White 2007).

To this day, linseed oil has remained the most popular medium for artists' paint despite the introduction of synthetic media around WW2. This is in contrast with interior and exterior house painting, where synthetic media have almost completely replaced glycerolipids.

Drying oil was the first medium that allowed artists to create a perfect illusion of depth and space on a two-dimensional support. The variety of transparency and opacity in the paints enabled artists to make nuances of warm and saturated transparent colours over relatively cold opaque paints, such as folds in dresses, flesh tones in human figures, foliage in trees, gradations in the sky. Linseed oil is a perfect paint medium in terms of drying and working properties, but has also the tendency to yellow. Therefore, the less yellowing, but slower drying, walnut and poppy oils have been used as well. In the 1950s and 1960s, artists' paint makers gradually replaced these oils by cheaper and more readily available 'semidrying' safflower oil, dehydrated castor oil and, occasionally, sunflower oil (Burnstock and van den Berg 2014; Van den Berg et al. 2021). In China and other Asian countries, tung (wood) and perilla oils have been used for lacquerware (Heginbotham et al. 2016).

7.1.1.2 Oil Varnishes

Drying oils have been used in varnishes from the early middle ages (Phenix and Townsend 2021), to provide gloss, saturation and protection to painted surfaces. Traditional oil-varnish media, as described by Theophilus in the eleventh century, contain most often sandarac resin that was crushed and added to linseed, and perhaps, walnut or hempseed oils; alternatively, other natural resins such as mastic or the cheaper colophony have been employed (Phenix and Townsend 2021). However,

the potential for authentication of paintings based on the detection of these varnishes is extremely low, since the vast majority of pre-nineteenth or twentieth century varnishes has been removed in repeated varnish removal and re-varnishing campaigns. More interesting may be the notion that such natural resins may in turn have been used as, or added to, oil paint media (see Sect. 7.1.1.3).

7.1.1.3 Additives and Modifications

One of the attractive features of oil paint is that it dries relatively slowly, allowing for long working times, which may be modified with the addition of other lipid materials, driers and bulking agents or by pre-treatment of the oil (Carlyle 2001; Hermens and Townsend 2021).

Pre-treatment may involve washing with water or alkaline water, causing the removal of water soluble, non lipid materials and free fatty acids. Some degree of pre-polymerisation of the oil is achieved by e.g. blowing the oil with air or heat pre-treatment, sometimes in the presence of metal driers (Carlyle 2001; Van den Berg et al. 2004) (see Sect. 7.1.2.2).

Oil paint will appear transparent or opaque, depending on the refractive index of the pigments. Its optical properties can thus be modified by varying the pigment to medium ratio, but also by admixing other media, such as resin, wax, or proteins. These additives may render the paint surface more or less glossy and saturated. For example, the fifteenth century Strasburg Manuscript mentions that (resin) varnish should be added to oil paint (Borradaile and Borradaile 1966), probably to improve the gloss and the transparency (White and Kirby 2006; Van den Berg et al. 2015). Modifications especially popular in some sections of the nineteenth century are megilp (addition of gum mastic to leaded linseed oil), amber and copal oil varnishes used as paint media (Carlyle 2001; Hackney et al. 2001). In addition, some artists used paint with copaiba balsam, such as Vincent van Gogh in his early years (Van der Werf et al. 2000). A commercially available oleoresinous paint introduced in the 1890s was Ripolin. This enamel paint, consisting of drying oil and diterpenoid resins, was not meant as artist paint, but used by e.g. Picasso (Muir et al. 2011). Similar resin/oil paints have been detected in works by various artists including Pollock (Wijnberg and van den Berg 2019).

Around 1900, contemporary ‘tempera’ or emulsion paints that contain significant amounts of drying oil and soaps, became popular especially in and around central Europe (Beltinger and Nadolny 2016).

Non-drying lipid materials such as metal stearates and free fatty acids are added by (artists’) paint manufacturers to facilitate mixing of pigments into the oil medium. Hydrogenated castor oil, beeswax and metal stearates have been used by manufacturers to stabilise paints in the paint tubes (Mills et al. 2008; Izzo et al. 2014; Van den Berg et al. 2019). These and other added non-drying oils such as palm oil (La Nasa et al. 2015a) and rapeseed oil (Van Keulen 2014) extend the paint drying times, by reducing the relative amount of polyunsaturated fatty acids. On the other

hand, driers based on cobalt, manganese and lead have been common additives to accelerate the drying process.

Arguably the most important invention related to drying oil media in the twentieth century is the discovery of alkyd resin media, which allows for a large variability in the properties of paints (Standeven 2011). These oil-modified polyesters were introduced in the early 1930s and represented a revolution in paint technology. Although largely used in decorative house and industrial paints, their use in artists' paints is rather limited. One of the first alkyd paint products was the DuLux series marketed by DuPont introduced in 1931. Jackson Pollock (Cappitelli 2004) shifted from oleoresin to alkyd paints around 1947 (Wijnberg and van den Berg 2019); other artists using alkyd paints are, Pablo Picasso, Pierre Soulages, Frank Stella (Crook and Learner 2000) and Alexis Harding (La Nasa et al. 2020). Alkyds were introduced in artists grounds from the 1960s (Ormsby and Gottsegen 2021); Winsor & Newton Griffin was the first range of artists' alkyd paints which came on the market in 1980, after a short-lived attempt in the early 1970s (Garrett 2019). Therefore, in works of art from before 1980, alkyd resins are mainly resulting from artists using oil-based house paints.

7.1.2 Chemistry of Oil Paints

7.1.2.1 Oil Composition

Drying oil binders used in painting are natural glycerolipids with a high content of polyunsaturated acyl moieties (fatty acids esterified with glycerol). The most important reactive polyunsaturated fatty acids are linoleic (9,12-octadecadienoic, C18:2) and linolenic (9,12,15-octadecatrienoic, C18:3) acids. Not very reactive is oleic (9-octadecanoic, C18:1) acid, whereas palmitic (hexadecanoic, C16:0) and stearic (octadecanoic, C18:0) acids are non-reactive. These five fatty acids are the main acyl moieties in most oils and fats used for painting (Mills and White 1987a, b). Fresh drying oils usually consist of 65–80% of these C18:2 and C18:3 acids; in semi-drying oils, such as sunflower or soybean oils, this content is closer to 60%, with mostly the less reactive 18:2 acid; non-drying oils (e.g. rapeseed and castor oil) contain much less (Dubois et al. 2007; Hulshof 2019). Oils may also include minor quantities of other saturated and unsaturated acids. Linseed oil, for example, also shows C12:O, C14:O, C20:O, C22:O, C24:O, C16:1 and C20:1 fatty acids (Swern 1979). With few exceptions (see Sect. 7.5.2), these fatty acids are generally not diagnostic for the type of oil.

7.1.2.2 Pre-heating Process

Heat pre-treatment of the oil may lead to the formation of dimers (and oligomers) from the triglyceride molecules (Van den Berg 2002), as well as internally cyclised structures (Dobson et al. 1996; Van den Berg et al. 2004) as a result of Diels-Alders reactions. The heating process will also cause isomerisation of the double bonds in the (poly-)unsaturated molecules, not only conversion from the *cis* to the *trans* configuration, but also shifts of the double bonds to other positions (Van den Berg 2002). For example, unsaturated triglycerides contain acyl groups with double bonds typically at the Δ9 position; heat treatment will produce acyl groups with double bonds on Δ8, Δ10 and other positions. This isomerisation has implications for the oxidation process (see Sect. 7.1.2.3).

7.1.2.3 Drying Process

In the drying or curing process, the polyunsaturated triglycerides undergo radical-oxidative cross-linking reactions involving atmospheric oxygen. This process may be catalysed by drying agents or certain pigments. The bis-allylic carbon atoms present in linoleic and linolenic acid are very reactive and their hydrogen atoms can be extracted, accelerated by light and heat, leading to the formation of radicals which will react further with molecular oxygen to form alkoxyl and peroxyl radicals (Schaich 2005). Such radicals will recombine to form dimers (Van den Berg 2002; Bonaduce et al. 2019). Upon further reaction the formation of oligomers will take place (Muizebelt et al. 1994). These oligomers, with complex molecular structures and associated masses way above 2000 Da, are responsible for the formation of the paint film. Such high-molecular weight species are not very accessible analytically with mass spectrometry, although pyrolysis will provide fragments which are only of low diagnostic value.

Within the curing process, the formation of oligomers is in competition with the creation of smaller molecules, oxidative degradation products that do not participate in the polymerization process (Fig. 7.1) (Burnstock and van den Berg 2014; Bonaduce et al. 2019). The main products are dicarboxylic acid moieties which may be analysed with mass spectrometry as unpolymerised monoglycerides, or after hydrolysis from the glyceride backbone as free dicarboxylic acids (see Sects. 7.1.2.4 and 7.1.2.5). Other oxidation products are midchain oxidised fatty acids (hydroxy and epoxy stearates), formed as products during the oxidative curing and ageing of the oil (Fig. 7.1) (Van den Berg 2002).

Since the majority of the unsaturated fatty acid moieties contain double bonds at the Δ9 position, the diacid product will be mostly nonane dicarboxylic acid or azelaic acid. As already mentioned, when the oil is heat-treated, double bonds may shift to other positions, leading to less azeleic acid and higher quantities of other diacids, such as octane and decane dicarboxylic acids (suberic and sebacic acid, respectively) (Van den Berg 2002).

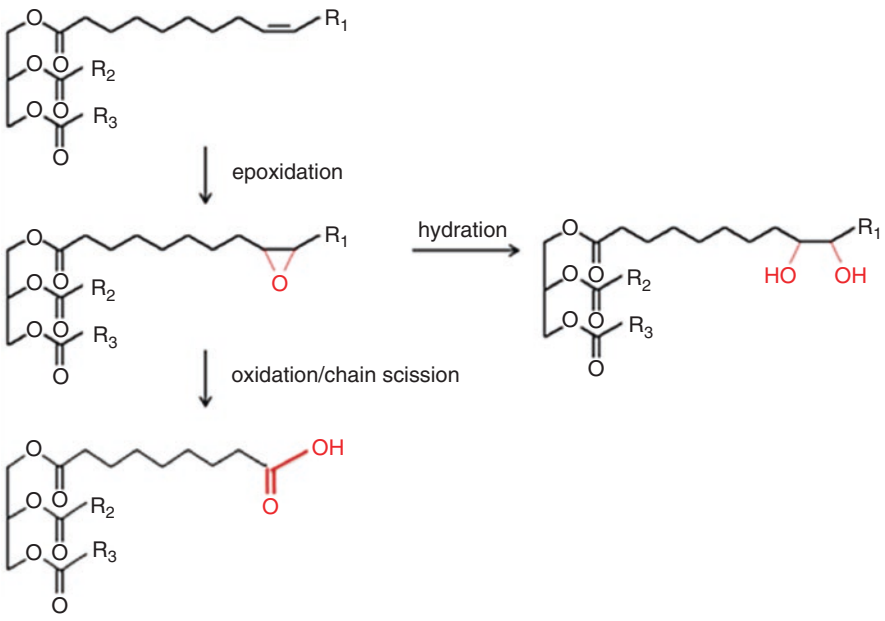

Fig. 7.1 Oxidative degradation reactions to form dihydroxy, epoxy and diacid glycerides. Diacid glycerides may also be formed through different oxidation pathways

7.1.2.4 Ageing Process

Already during the process of preparation and curing (drying), ageing reactions may take place that alter the chemical composition of the paints and strongly influence the chemical composition and thus the properties of the resulting paint film (Bonaduce et al. 2019).

In addition to the oxidative degradation processes (see Sect. 7.1.2.3), which are in competition with the polymerisation process, hydrolysis plays a crucial role. Hydrolysis involves the reaction with water, or with metal (hydr)oxide or carbonates catalysed by water, and leads to the formation of hydroxyl groups and, ultimately, of free glycerol molecules on one hand, and carboxylic acid or metal carboxylate groups on the other. In the presence of (polyvalent) metal ions, this may generate a relatively stable paint with an ionomeric character. In the absence of these ions, paints will form a chemical structure that is relatively soft and vulnerable to solvents (Fig. 7.2) (Van den Berg et al. 1999a; Burnstock and van den Berg 2014).

Modugno et al. (2019) showed that high moisture contents not only enhance hydrolysis, but also degradation, thus reducing the degree of oxidative polymerisation of the oil network by neutralising the radicals that are required for the polymerisation of the oil binder.

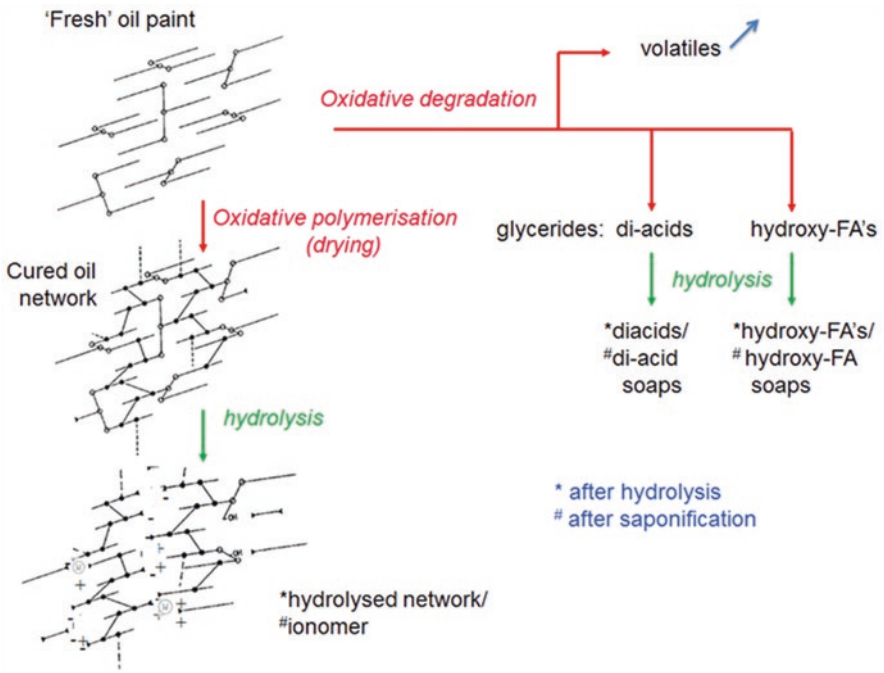

Fig. 7.2 Schematic overview of curing, oxidation, hydrolysis and/or saponification of drying oil media. (Adapted from Van den Berg et al. 1999a; Burnstock and van den Berg 2014)

7.1.2.5 Degradation Phenomena

Paintings may exhibit problems of ageing and deterioration, related to changes in optical, physical and chemical properties (Van Loon et al. 2021). Chemical alterations generally lie at the base of modifications in solubility and other optical and physical changes. Optical phenomena include variations in colour or formation of white hazes; physical changes may be structural deformations, resulting in embrittlement, loss of cohesion between layers, loss of adhesion and powderiness of the paint. The alterations may be related to the use of certain paint formulations and their application, environmental conditions, and past conservation interventions. Knowledge of these phenomena is important for authentication studies.

Well studied examples of deterioration are those of protrusions (Keune 2005; Keune and Boon 2007) and increased transparency (Noble et al. 2005; Shimadzu et al. 2008; Shimadzu 2015). These phenomena are related to the formation of metal soaps in oil paint, especially lead and zinc soaps. These are reaction products of alkaline pigments, metal carbonates and oxides such as lead white (Noble et al. 2005) and zinc white (Osmond 2014), with carboxylic acids originating from the paint medium.

Especially modern paintings show problems which are, at least partly, related to the binding medium (Van den Berg et al. 2021). Typical degradation phenomena are

medium exudation, dripping, flaking, crumbling, softening, water sensitivity and efflorescence. These are often related to the paint composition. Especially when paints with a high medium content, a lack of inorganic pigments capable of forming ionomers, and/or low amounts of drying oils, are used, these may be degraded and become sensitive to solvents and prone to deformation (Fig. 7.2) (Van den Berg et al. 2021).

For example, the addition of metal stearates have been shown to create problems in zinc oxide white paints, due to excessive formation of zinc soaps and reduction of the binding capacity of the medium (Osmond 2014). Fatty acid efflorescence, which is often observed on twentieth century oil paintings, is frequently caused by such metal soap additives (Tempest et al. 2013).

An increasing number of MS studies has been focused on degradation mechanisms of modern oil paint (Van den Berg et al. 2001, 2002; Colombini et al. 2002; Keune et al. 2008; Izzo 2011; Izzo et al. 2014; Boon and Hoogland 2019; Bronken and Boon 2014; Lee et al. 2018; Bonaduce et al. 2019; Modugno et al. 2019; La Nasa et al. 2019a) (see Sect. 7.5.4).

7.2 Mass Spectrometry

Mass spectrometry (MS) is one of the most powerful techniques used for the identification, structural characterisation and quantitation of small and big organic molecules. It is based on the production of ions, which are separated according to their mass-to-charge (*m/z*) ratios.

The first step in MS is the introduction of the sample into the mass spectrometer. Here the molecules must be ionised, i.e. transformed into ions, using one of a range of ionisation techniques (see below). Once produced, the ions are accelerated and driven from the source to the analyser in order to be separated according to their *m/z* ratios, and finally to be revealed by the detector, such as an electron multiplier. The analyser and detector – and sometimes also the ion source –are kept under high vacuum.

A wide variety of ionisation techniques is available and can be chosen on the basis of the chemical-physical properties of the analyte, such as molecular weight, polarity, etc. In electron ionisation (EI) an electron is extracted from gas phase molecules, yielding radical ions, which may in turn form fragment ions and neutral molecules or radicals. Otherwise, one – in the case of chemical ionisation (CI) or matrix assisted laser desorption ionisation (MALDI) – and more – as in electrospray ionisation (ESI) – protons can be added. Similarly, negative ions can be formed due to single (CI, MALDI) or multiple (ESI) proton abstraction. In static secondary ion MS (SIMS), several ions, (de-) protonated or fragmented, can be formed.

EI and CI are the most common ionisation techniques for the MS analysis of volatile, nonpolar, low molecular weight and thermally stable compounds. The so-called ‘soft’ ionisation techniques, such as MALDI, static SIMS and ESI, allow for the study of non-volatile and thermally unstable compounds.

With EI, CI and MALDI the ion sources are maintained under high vacuum, whereas spray ionisation techniques, such as ESI and atmospheric pressure chemical ionization (APCI), operate at ambient pressure. In this way non-volatile, polar and large compounds can be analysed.

With EI and CI, gas phase molecules need to be introduced, while with ESI and APCI, the analytes are dissolved in a liquid. With the other techniques mentioned in this chapter, ions are formed through desorption from a surface, using a laser (MALDI), an ion beam (SIMS) or an electrospray (desorption ESI (DESI)).

The MS analyzers are classified into two main groups, based on the separation of ions in space, or in time. In the first case, ions are separated while travelling over a certain distance (some metres in the case of sector instruments, centimetres in the quadrupole). In the second case, ions are confined in a small region of space and their separation is obtained by varying parameters such as electric field and radio frequency. Magnetic and electrostatic sector instruments, quadrupoles, and time of flight (ToF) analysers belong to the first group; ion trap, orbitrap and Fourier transform ion cyclotron resonance (FT-ICR) analysers to the second. The choice of the MS analyser depends on the application. Parameters such as *m/z* range, mass resolution, mass accuracy, scan speed, and number of mass separations are considered (Giorgi 2009).

In the last two decades a range of new types of mass spectrometers have entered the field of conservation science, and are increasingly used. While the sector mass spectrometer is almost obsolete, the most widely used is the inexpensive, rugged linear quadrupole system, which is most commonly used in combination with GC. This mass spectrometer provides mass spectra with unit mass resolution and the GC-MS combination is most useful for routine applications.

Increasingly, sensitive and high resolution mass spectrometers are used. Their high mass resolution provides information on elemental composition of molecular and fragment ions, which aides in further elucidation of unknown molecules. Such mass spectrometers – ToF, orbitrap and FT-ICR – may be used as stand-alone systems, or in combination with LC. These mass spectrometers are pulsed systems, which can be used in combination with lasers, such as in MALDI-MS (see Sect. 7.4.2).

From the mid-1970s onward, instruments were designed for tandem MS experiments with final configurations as triple quadrupole (TQ), multistage ion-trap, hybrid quadrupole–time-of-flight (Q–ToF), hybrid quadrupole-linear ion-trap (Q–LIT), ToF–ToF and hybrid LIT–orbitrap. These instruments allow for the study of the fragment ions of selected precursor ions and represent an essential tool in fundamental studies on ion generation, ion–molecule reactions, unimolecular fragmentation reactions, and identity of ions.

In a mass spectrum for each *m/z* value the abundance of ions is plotted. When using a chromatographic technique in combination with MS – GC-MS or LC-MS (see Sects. 7.3.1 and 7.3.2) – the mass spectra of individual compounds are obtained and can be compared with mass spectral databases or interpreted to elucidate the molecular structure. Tandem mass spectrometry, regardless of the way the primary ions are formed, produces fragment ions and can also be applied to provide

additional structural information of the parent ion and thus the parent molecule. In case of EI or another technique which produces radical ions, the quality of information derived from the tandem mass spectra is higher than for even electron ions produced from 'softer' ionisation techniques.

Scan mode is most frequently used and a total ion chromatogram (TIC) is usually presented. Otherwise, the abundance of ions of selected *m/z* values can be displayed as extracted ion chromatograms (EIC). In this way the visibility of particular compounds, or a class of compounds, can be enhanced. In order to increase the sensitivity and detect specific molecules, selected ion monitoring (SIM) may be applied. In this mode the MS is set to detect only a small group of ions that are characteristic of the analytes of interest.

7.3 Chromatography – Mass Spectrometry

7.3.1 GC-MS

Due to its high sensitivity and specificity, gas chromatography mass spectrometry (GC-MS) has been the tool most used for organic analysis in artworks for several decades (Sutherland 2019; Marinach et al. 2004; Doménech-Carbó 2008; Colombini et al. 2009; Bonaduce et al. 2016). GC-MS is often applied to characterise glycerolipid binders and additives, both for their identification and degradation processes.

This analytical technique combines the benefits of GC, gas-phase separation of organic molecules, with MS for identification and/or quantification. Since paint samples are in solid form, preparation is required in order to make the components volatile enough to be separated. This process typically involves hydrolysis and derivatization (see below). After this step, a solution of sufficiently volatile molecules is injected into a heated GC inlet and volatilised. Alternatively, pyrolysis – heating in an inert atmosphere – can be used to generate small molecules to be transferred directly to the inlet (see below).

In GC, a capillary column is used for separation of the molecules. It is coated on the inside with the stationary phase, a viscous liquid, typically polysiloxane or polyethylene glycol. The volatilized molecules are transported through the column by the mobile phase, a stream of inert carrier gas such as helium or nitrogen. The relative affinity of the analyte molecules for the stationary phase and their boiling point determines the retention time. An oven allows for temperature control in order to improve separation. The analyte molecules elute directly into the ion source of the mass spectrometer where they are ionised with EI or CI (see Sect. 7.2).

With regard to glycerolipids, GC identification usually requires sample pretreatment. Alkaline saponification can be used to obtain free fatty acids, followed by derivatisation. Various methods have been successfully used, often in combination with high temperatures also employed with pyrolysis (see below). These methods mostly involve methylation or trimethyl-silylation (Table 7.1).

Table 7.1 Online and off-line reagents used for (Py-)GC-MS analysis of lipids and other organic materials

Reagent	Et/ Me/ TMS	Trans-esterification	Off-line	Py	References
Diazomethane	Me	–	x	–	Sutherland (2000)
Trimethylsilyldiazomethane (TMSDM)	Me	x	x	x	Van den Berg (2002)
Ethyl or methyl chloroformate	Et/ Me	–	x	–	Nowik (1995) and Mateo-Castro (1997)
Tetramethylammonium hydroxide (TMAH)	Me[a]	x	x	x	Echard (2007), White and Roy (1998), Sutherland (2007), Manzano (2011), Piccirillo (2005) and Tammekivi (2019)
Phenyltrimethylammonium hydroxide (PhTMAH)	Me[a]	x	x	x	
m-trifluoromethylphenyl) trimethylammonium hydroxide (TMTFTH), called Meth-PrepII	Me[a]	x	x	x	
Hexamethyldisilazane (HMDS)	TMS	x	x	x	La Nasa (2015a) and Bonaduce (2016)
Bis(trimethylsilyl) trifluoroacetamide (BSTFA)	TMS	–	x	–	Van den Berg (2002) and Tammekivi (2019)

Et formation of ethyl esters, *Me* formation of methyl esters, *TMS* formation of trimethylsilyl esters/ethers

[a]May also form ethers from hydroxyl functionalities

Most paint samples contain complex mixtures of natural and/or synthetic (polymeric) materials and inorganic compounds such as pigments and fillers. Therefore, various analytical protocols have been developed that address a broad range of material types. These protocols are comprehensive, involving multiple stages of extraction, derivatization and analysis, but are also rather laborious and require relatively large samples (Lluveras et al. 2010; Bersani et al. 2014; Bonaduce et al. 2016; Amadori et al. 2016; Mazurek et al. 2019).

For the study of organic components in paint samples GC-MS is often combined with analytical pyrolysis (Degano et al. 2018; Bonaduce and Andreotti 2009; Learner 2004; La Nasa et al. 2019b). Py-GC-MS allows to analyse complex mixtures, including synthetic resins and pigments, and is widely employed for the analysis of traditional binding media, such as lipids (Chiavari et al. 1998; Van den Berg 2002). Pyrolysis requires a rather easy sample pre-treatment, reducing contamination and increasing sensitivity (Sutherland 2019; Calvano et al. 2016, and references therein). Different pyrolysis devices are available and can be classified into: (a) furnaces, both isothermal and programmable; (b) inductively heated (Curie-point) filaments; (c) resistively heated filaments. Furnace pyrolyzers are kept at a certain temperature and the sample molecules are rapidly pyrolysed in the hot volume. In the case of heated filaments, the sample is placed onto the cold heater to be quickly heated with resistance or inductive heating.

The use of the double shot technique – first thermal desorption (TD) of volatile molecules at temperatures of about 300 °C, then pyrolysis of less volatile polymers – is nowadays applied to the study of a wide range of paint materials (Van den Berg et al. 1999b; Prati et al. 2004; Pintus and Schreiner 2011; Pintus et al. 2012; Wei et al. 2013; Nakamura et al. 2001), including additives (Pintus and Schreiner 2011).

Py-GC-MS also requires suitable derivatisation to increase the detectability of fatty acids and dicarboxylic acids present in the aged paint film, whether they are present as free acids, metal soaps or esterified with glycerol. Methylation with TMAH and silylation with HMDS are mostly used for Py-GC-MS analysis of oils in paint samples (Table 7.1) (Colombini et al. 2009). Fatty acid profiles can be easily obtained. Next to the long chain fatty acids, both saturated and unsaturated short chain fatty acids are generated from the pyrolytic fragmentation of the cured network and the fatty acids themselves (La Nasa et al. 2019a; Colombini et al. 2009). This can provide useful information on the degree of network formation. It should, however, be taken into account that complex side reactions may occur in the pyrolysis process. Unspecific fragmentation of triglycerides and the polymeric network, isomerisation of double bonds, loss of functional groups such as hydroxyl functions, and α-methylation of acidic moieties (observed with TMAH) may occur and modify the fatty acid profile. Several studies highlighted that the concentration and the solvent of the reagent as well as the instrumental setup may influence the degree of transesterification, derivatisation (Van den Berg 2002) and the formation of side products (Van den Berg et al. 2001; Sutherland 2007).

For these reasons, Py-GC-MS may not be exhaustive for ageing studies of lipid materials. GC-MS (after off-line hydrolysis), and/or LC-MS/MS, are useful and valuable complements to analytical pyrolysis in the study of oxidation/degradation processes of glycerolipids, including alkyds (La Nasa et al. 2013a; Lee et al. 2018; Modugno et al. 2019).

Schilling et al. (2016) developed systematised Py-GC-MS data analysis by exploiting the features of AMDIS (Automated Mass spectral Deconvolution and Identification System), a freeware program of the National Institute of Standards and Technology (NIST). With this system chromatograms can be rapidly deconvoluted, individual peaks identified, and the results searched against a user library of marker compounds. A simple report is produced that lists the names, retention indices, and peak areas for all the compounds identified in the sample. The authors have created custom compound libraries, compiled from in-house studies of reference samples, and supplemented by published work from other researchers.

7.3.2 LC-MS

Electrospray ionization (ESI) can be used for direct MS analysis (see Sect. 7.4.1.1), but is most commonly applied in a tandem liquid chromatography MS (LC-ESI-MS) configuration. This is widely used for qualitative and quantitative analysis in many

application areas, and since a few decades also in the cultural heritage field. Firstly, for the analysis of protein binders (Dallongeville et al. 2016), but more recently also for the study of other biomacromolecules, natural and synthetic dyes and pigments (Zhang and Laursen 2009; Degano et al. 2017), terpenoids (Van der Doelen 1999), and lipids (vide infra).

ESI is a soft ionization technique that involves the introduction of a solution, which may be the LC mobile phase, into an atmospheric pressure source. There the solution droplets are nebulised by a strong electric field, eventually assisted by nitrogen as a nebulising and heating gas. In this way small (1–10 μm) and highly charged droplets are generated. Concurrently to droplet evaporation and field-induced droplet disintegration, gas-phase ions are produced (Cech and Enke 2001). The gas-vapour mixture of nitrogen and solvents with analyte ions is extracted into the vacuum interface where further desolvation and collisional cooling of the ions occur (Gabelica and De Pauw 2005). In most cases, protonated ions are generated, together with lithiated, sodiated and potassiated adduct cations. At the same time, negative ions are formed, deprotonated or, occasionally and dependent on the co-eluting salts, adduct anions.

ESI is impacted by the presence of high salt concentrations, non-volatile salts, and surface-active components which cause ionisation suppression. Therefore, ESI is often preceded by liquid chromatography, where optimisation of the sample composition and/or mobile-phase composition are important to achieve the best MS results in terms of response and selectivity (La Nasa et al. 2015a; Van Dam et al. 2017; Modugno et al. 2019).

In liquid chromatography separation of the analytes is accomplished with a liquid mobile phase and a stationary phase which fills a column, a capillary or a plane. For lipid analysis reversed phase high performance liquid chromatography (HPLC) is used. Here, the mobile phase, usually methanol, acetonitrile and water, is more polar than the stationary phase, which is generally composed of apolar groups, such as octadecyl groups (C18), bound to silica particles. The retention of the molecules is strongly influenced by their degree of hydrophobicity. This can be modified by adding acids, bases or buffers (Degano 2019). Good separations in short runs have been obtained employing core-shell stationary phases (La Nasa et al. 2013b). HPLC coupled with high resolution mass spectrometry (ESI-Q-ToF) can be efficiently used to characterize the lipid profile of a paint sample. Recently a new derivatization method was introduced based on the use of 2-hydrazinoquinoline, that increases the retention of free fatty acids on a C18 column. With this, extractable acyl glycerides (monoglyceride, diglycerides, and triglycerides), their oxidation products and free fatty acids can be characterised and semi-quantified in a single chromatographic run (Blanco-Zubiaguirre et al. 2018; La Nasa et al. 2013b, 2018b).

7.4 Direct MS

Direct MS methods may provide a good alternative for hyphenated MS approaches. Since a chromatograph with interface is present, the latter approaches are generally easier to interpret and less prone to instrument failure. Conversely, direct analyses will be, in general, faster and require somewhat smaller samples. The disadvantage of loss of separation of molecules in complex mixtures may be partly compensated by tandem MS possibilities and high resolution MS. Moreover, the relatively quick analysis also allows for faster gathering of data and ensuing statistical analysis such as PCA (Modugno et al. 2019).

Direct methods are very useful for fingerprinting, meaning that certain compounds are easily recognised in the spectra. This is the case for example with triglycerides in fresh oils (Van den Berg 2002), mono-, di- and triacylglyceride clusters (MAG, DAG, TAG) (Lee et al. 2018), resins (Van der Doelen et al. 1998), waxes, synthetic oligomers (La Nasa et al. 2013a), etc.

7.4.1 Spray Ionisation

7.4.1.1 ESI-MS

As explained above, ESI is a soft ionization technique, often used in combination with LC. When used as standalone technique, direct introduction of a solution with flow injection analysis (FIA) in the mass spectrometer is performed. Extraction may take place and most often ethanol, sometimes hexane, are employed (Boon and Hoogland 2019; La Nasa et al. 2013a; Lee et al. 2018; Modugno et al. 2019). Ammonium acetate added to the extract produces ammonium adducts ($[M+NH_4]^+$) from mono, di- and triglyceride molecules (MAGs, DAGs and TAGs, respectively). If no ammonium acetate is added, the molecules will transform into sodium adducts ($[M+Na]^+$). Sometimes $[M+Li]^+$ or $[M+K]^+$ are formed along (Van Dam et al. 2017). In the negative ion mode, [M-H]- ions are produced from fatty acids and glycerides containing diacid functionalities. This means, that in both polarities partly complementary information from the extracted lipids, i.e., fatty acids and glycerides, is obtained.

7.4.1.2 SAWN-MS

Recently, a novel method was introduced to generate gaseous ions which can then be analysed with direct MS. Surface acoustic wave nebulisation (SAWN) mass spectrometry employs acoustic waves that are propagated through a sampling chip on which a drop of liquid sample is applied. The waves that are conducted to the liquid generate fine mist-like droplets of nanometre to micrometre diameter. Similar

to electrospray, the droplets generate gaseous analyte ions through fission and evaporation. As with direct electrospray MS, extracts of minute samples at femtomole sensitivity can be analysed (Astefanei et al. 2020).

7.4.1.3 DESI-MS

A potentially very useful method for analysis of glycerolipids is Desorption electrospray ionization (DESI)-MS. This technique employs an electrospray set-up, but instead directs the plume to a surface, simultaneously desorbing and ionising the analyte molecules. In this way imaging of lipidic materials on paint surfaces is possible semi-non-destructively, without the need of taking samples. Watts and Lagalante showed the potential of the technique in distinguishing between lipid-containing and modern binding materials present in paint cross-sections. They identified lipid-binding media in a seventeenth century baroque painting (Watts and Lagalante 2018).

7.4.2 MALDI MS

Matrix-assisted laser desorption/ionization (MALDI) is a soft ionization technique applied in mass spectrometry for the analysis of large, non-volatile and labile biomolecules, such as DNA, proteins, peptides, and carbohydrates. It consists of three-steps. At first, the sample is mixed with a matrix material, applied to a metal plate and allowed to crystallize. Then, a pulsed laser irradiates the analyte-matrix mixture, causing its ablation and desorption. Lastly, the molecules are ionised in the hot plume of ablated gases and accelerated into the mass analyser. The advantages of MALDI MS are: rapid sample preparation and analysis, sensitivity (sample amounts of pico-atto-moles), high tolerance towards salts, suitability for analysis of heterogeneous and semi-complex samples. Indeed, samples are analysed as solids due to the crystallization process after solvent evaporation. All these features are important when taking into account the application in the field of cultural heritage where it has been used for analysis of proteins (Dallongeville et al. 2016), peptides (Fremout et al. 2011; Kuckova et al. 2009), dyes (Maier et al. 2004), resins (Scalarone et al. 2005) and lipids, both from oil and egg yolk binders (Calvano et al. 2011; Van den Brink 2001; Van den Brink et al. 2001; Herrera et al. 2016) (see Sect. 7.5.1.3).

7.4.3 ToF-SIMS

Time of flight secondary ion mass spectrometry (ToF-SIMS) can be employed for the simultaneous identification of inorganic and organic compounds on the surface of solids and thin films. With this technique the samples are sputtered with a focused

primary ion beam and the ejected secondary ions are detected with a mass spectrometer. In this way the elemental, isotopic, or molecular composition of the surface (max depth: 1–2 nm) can be determined with elemental detection limits ranging from parts per million to parts per billion. For organic ions, only static SIMS can be used.

Due to its very high lateral resolution (micrometres) and its minimal sample preparation, ToF-SIMS is frequently used for chemical imaging (Mazel and Richardin 2009; Spoto 2000, Spoto and Grasso 2011). In lipid analysis this technique has been applied in studying the distribution of fatty acids (Keune and Boon 2004; Keune 2005, Keune et al. 2009) (see Sect. 7.5.4.1).

7.4.4 Thermal Desorption and Pyrolysis Techniques

7.4.4.1 DTMS

Direct temperature resolved mass spectrometry (DTMS) is an effective technique for characterising mainly organic, but also some inorganic components, present in paint layers. It can be applied to a wide variety of materials, ranging from volatile low-molecular-mass compounds to polymers, and is a powerful tool for the analysis of complex mixtures.

DTMS requires no chemical pre-treatment, is fairly sensitive and provides reliable analysis in a short time, typically 2 min (Boon 1992; Van den Berg 2002). A direct exposure probe is used where a drop of sample solution/dispersion is deposited on a filament wire. After solvent evaporation the probe is directly inserted into the source of the mass spectrometer where it is rapidly heated to temperatures up to 1000 °C and different fractions evolve from the filament. Different types of ionization techniques can be applied, such as EI and CI. Mainly low voltage EI ionisation (16 eV) DTMS is performed in order to minimise fragmentation and obtain molecular information. Moreover, since heating is accomplished on-line under vacuum, thermal dissociation products, once formed, evaporate quickly, while the probability of molecular collisions is very low and the occurrence of secondary reactions is therefore reduced (Boon 1992). Although separation at the compound level as in GC-MS does not occur and the MS summation spectra of multi-component mixtures have to be interpreted, DTMS gives temperature-resolved information. Low molecular mass compounds such as free fatty acids are volatilized at low temperatures up to 250 °C, while metal soaps dissociate and form products at slightly higher temperatures (c. 350 °C); polymeric materials undergo pyrolytic degradation temperatures above c. 430 °C (Van den Berg et al. 2019). By gradually raising the temperature of the sample, a physical separation is achieved between low molecular weight compounds in the evaporation phase, and the cross-linked fraction of a sample in the pyrolysis-phase. The temperature-resolved information facilitates the interpretation of the results. Moreover, marker ions for different compounds have been established (Oudemans et al. 2007).

7.4.4.2 EGA-MS

In Evolved Gas Analysis (EGA) the paint sample is introduced in a microfurnace (as used for Py-GC-MS) installed on the GC injector. The latter is connected by a thermostated deactivated metal tube inside the GC oven with the MS analyser. By programmed heating of the sample, the released gases are detected by MS. The resulting chart is called an EGA thermogram. The analyses are performed under an inert gas such as helium.

This technique has been used to analyse proteins (Orsini et al. 2017) and lipids (La Nasa et al. 2019a) in paint samples. In the latter study EGA-MS has been applied to explore the polymeric fraction of paints and the thermal stability of the different molecular fractions. Mixtures of oil and added metal stearates were studied by Van den Berg (Van den Berg et al. 2019). It was found that the EGA profiles can be divided in three different thermal zones. At T < 250 °C fatty and dicarboxylic acids are desorbed, and monoglycerides are partially degraded, at T 250–400 °C thermal degradation of acylglycerides and metal carboxylates occurs, and above 400 °C the average mass spectrum is characterised by fragment ions at *m/z* 91 and 105, which can be ascribed to alkylated benzenes. The latter are due to decomposition of the cross-linked network.

7.5 Glycerolipid Markers, Modifications and Additives

Glycerolipids have been discussed as relatively problematic in terms of identification. This is especially the case after curing and ageing, where information on the biological origin may be lost due to oxidation and hydrolysis.

Most paint samples contain complex mixtures of natural and/or synthetic (polymeric) materials and inorganic compounds such as pigments and fillers. Especially for the study of ageing behaviour, but also for the detection of e.g. additives in complex samples, analyses are increasingly done using multistep preparations (generally employing only GC-MS, see Sect. 7.3.1) and/or ‘multianalytical approaches’ involving several (hyphenated) MS techniques and e.g. Fourier Transform Infrared (FTIR) spectroscopy. A versatile addition to this range of techniques for the study of complex paint samples is DTMS. This was first used by Boon et al. (Boon 1992). For instance, in a single sample from the background in Vermeer’s “Girl with a pearl earring” information was obtained from a mixture of materials, including organic pigments (indigo), proteins, (bees)wax, diterpenoid resins, and lead metal ions from lead white (Groen et al. 1998) (see also Sect. 7.5.1.2).

Table 7.2 Overview of the different MS methods presented in this study, and their propensity for the detection of individual lipid marker compounds

	Non polymerised fraction					Polymerised fraction		
MS method	Free fatty acids	Dicarboxylic acids	Free metal soaps of fatty acids and diacids	Non-crosslinked glycerides containing dicarboxylic acids	Full glyceride profile	Metal soaps of diacids connected to a covalently bound network, only via ester bonds	Fatty acids and non-saponified diacids connected to a covalently bound polymeric network, only via ester bonds	Cross-linked material (fatty acids and diacids) that would remain covalently bound (C-C and C-O-C bonds), even if hydrolysis of all ester bonds present in the binder occurred
GC-MS (BSTFA)	Yes	Yes	Yes	No[a]	No[a]	No	No	No
GC-MS (HMDS)	Yes	Yes	No	No[a]	No[a]	No	No	No
GC-MS (Meth Prep II)	Yes[b]	Yes	Yes[2]	Yes[a]	Yes[a]	Yes	Yes	No
Py-GC-MS	Yes	Yes/part.	Part.	Part.	Yes	Part.	Part.	Part.
(LC and direct) ESI-MS, SAWN-MS (positive mode)	No	No	No	Yes	Yes	No	No	No

(LC and direct) ESI-MS, SAWN-MS (negative model)	Yes	Yes	No	Yes	No	No	No	No
EGA-MS, DT-MS[c]	Yes	Part.	Yes	(Yes)	Yes	Part.	Part.	Part.
MALDI-MS	No	No	No	Yes	Yes	No	No	No
TOF-SIMS	Yes[b]	Part.	Yes[b]	Part.	No	No/part.	No/part.	No/part.

part. = generic fraction is detected, but not recognisable as individual molecules
This table is based on and inspired by Lee et al. (2018) and La Nasa et al. (2019a, b)
[a]Chromatographic separation may be challenging
[b]No distinction between free carboxylic acids and soaps
[c]DTMS better temperature resolution; more efficient pyrolysis

7.5.1 Lipid Markers and Relation to Ageing

As discussed in paragraphs Sects. 7.5.3 and 7.5.4, a range of direct and hyphenated MS applications have been developed for the analysis of lipid markers in oil paints and varnishes. Table 7.2 lists these techniques in relation to the detection of different fractions of oil binders and additives in various stages of curing and ageing.

7.5.1.1 Detection and Identification of Glycerolipid Binders

During the last decades a large number of publications have reported on the application of (Py)-GC-MS techniques to the identification of glycerolipid materials, both original constituents and superposed materials, in artworks. The identification of an oil binder – and its distinction from other binding media such as egg tempera – is generally based on the fatty acid profile, where palmitic (P) and stearic acid (S) are the most abundant, together with azelaic (A) acid. Every type of drying oil presents a characteristic range of P/S ratios, and since these saturated fatty acids are considered to be hardly involved in oxidative degradation processes, their ratio is thought to remain constant during ageing.[1] The P/S ratio is therefore often used as an indicator of the kind of oil present in a paint sample (Mills 1966; Mills and White 1987b).

However, the parameters used to identify drying oils are deeply influenced by the history of the paint. Bonaduce et al. (2012) showed that the P/S ratio is extremely dependent on the pigments present and the age of the paint, and that neither the P/S parameter nor the ratios between the relative amounts of the various dicarboxylic acids (A/Sub and A/Seb) can be used to provide definite information on the type of oil or on the pre-treatment undergone by the oil. Indeed, preferential migration of free fatty acids, or triglycerides if the paint is not fully cured, could influence the P/S ratio, at least of the surface layers. This was demonstrated by Keune et al. (Keune 2005) in a study on the P/S ratios in two layers of paint containing linseed and poppyseed oil. After ageing, the P/S ratios found from either layer was the same, whereas the P/S ratios of linseed and poppyseed oil are c. 1.5 and 5, respectively.

Especially in modern paint formulations, P/S ratios alone are not reliable to determine the kind of oil. This is due to the different contributions which may interfere. An example is given by the analysis of a relatively sticky, thick paint sample taken from 'Rosy-Fingered Dawn at Louse Point' (1963) by Willem de Kooning (1904–1997). The GC-MS data (Fig. 7.3) provide a P/S ratio, which is virtually meaningless, since at least three, and more probably four, sources of fatty acids are present. The cadmium yellow paint, presumably based on linseed oil and/or poppyseed oil binder, may have been mixed with a slow-drying oil such as safflower to allow for longer working, something De Kooning reportedly used to do (Lake 2010). This may also explain the stickiness of the paint, 45 years after its creation.

[1] Recent work has shown that also palmitic and stearic acid may be prone to oxidation on the α-position relative to the carbonyl (Bonaduce et al. 2019; Pizzimenti et al. 2021)

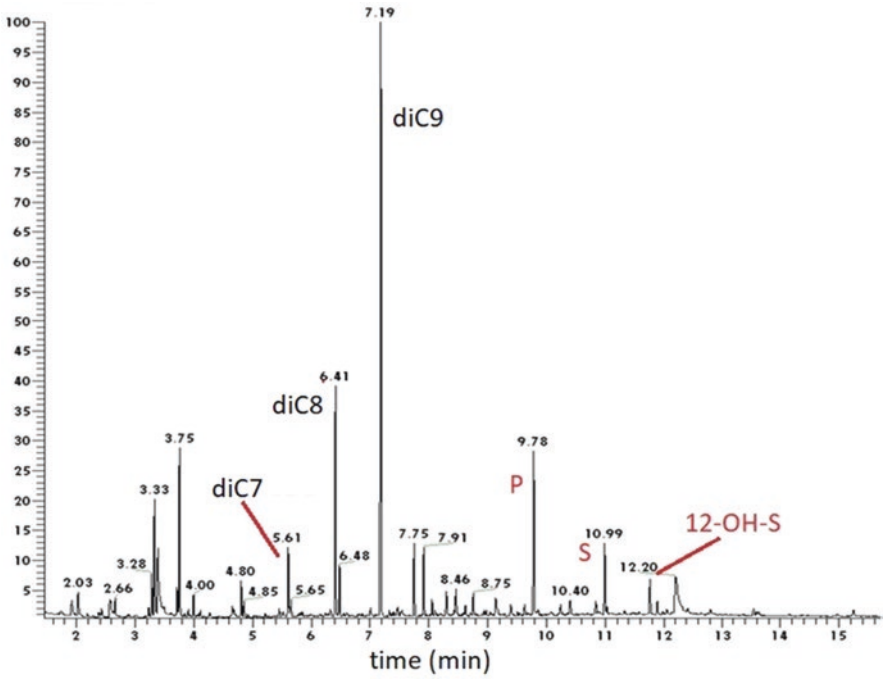

Fig. 7.3 GCMS TIC chromatogram of 'Rosy-Fingered Dawn at Louse Point' (1963), by Willem de Kooning (1904–1997); collection Stedelijk Museum Amsterdam; inv. Nr. A 22662. Methyl esters of fatty acids; diC9, diC8, diC7: diacids with number of carbon atoms. Analysis Henk van Keulen, RCE, 2008

In addition, FTIR spectroscopy had shown that the paint contains zinc stearate and possibly aluminium stearate additives.

Indeed, the addition of metal stearates, beeswax, castor wax, semi-drying and non-drying oils may alter the fatty acid profile, especially when all present lipids are hydrolysed and derivatised as usually happens in (Py)-GC-MS.

Specific markers can sometimes give a clue on the occurrence of certain oils, such as rapeseed or castor oil (Izzo 2011; Mills and White 1987b). For instance, erucic (13-docosenoic) and gondoic (11-eicosenoic) acids and their oxidation products (13,14-dihydroxydocosanoic acid and 11,12-dihydroxyeicosanoicacid) are considered to be biomarkers of oils obtained from the seeds of *Cruciferae*, such as rapeseed oil (Colombini and Modugno 2009). Otherwise, some fatty acids are not specific, but, if present in higher amounts, can be indicative for the use of a certain oil. This is for example the case of arachidic and behenic acid in sunflower oil (Izzo 2011; Colombini and Modugno 2009).

A powerful approach to gain information on glycerolipids composition was developed by scientists from the University of Pisa. TAGs were identified by using HPLC-ESI-MS, whereas GC-MS and Py-GC-MS were employed for the overall characterization of lipid materials in oil paint (La Nasa et al. 2015a). The protocol

was applied to study the sketch 'New Rays' painted by Edvard Munch owned by the Munch Museum (Oslo, Norway) as well as original paint materials from the painter's atelier. The collected data permitted to unambiguously identify the lipids of walnut and linseed oils used for the production of the paint tubes and linseed and palm oil in the paint sample.

7.5.1.2 Distinction of Glycerides, Free Fatty Acids and Metal Carboxylates

Recently, various new MS approaches have been introduced which allow for distinction between the different fractions of oil paints, i.e., glycerides, free fatty acids and metal stearates, both added and formed, based on P/S ratios.

Discrimination between added metal stearates and glycerolipid binders can be made on the basis of distinctly different P/S ratios of the materials. Oils are glycerides that contain palmitic and stearic acyl moieties with a P/S ratio that is always higher than 1. Metal stearate additives contain up to 20% free fatty acids and have a very low palmitate/stearate (P/S) ratio of typically 0.4–0.7, which can be used to distinguish the stearates from other fatty components in the oil paints, using mass spectrometry (Izzo et al. 2014; Van den Berg et al. 2019).

Figure 7.4 shows an example of a simple direct ESI-MS approach to illustrate this. An ethanol extract of the material taken from black paint, originally from Winsor&Newton, used in a 4 year-old painting by Mia Tarney, was analysed (Van den Berg et al. 2019). The spectrum of the positive ions provides an indication of the

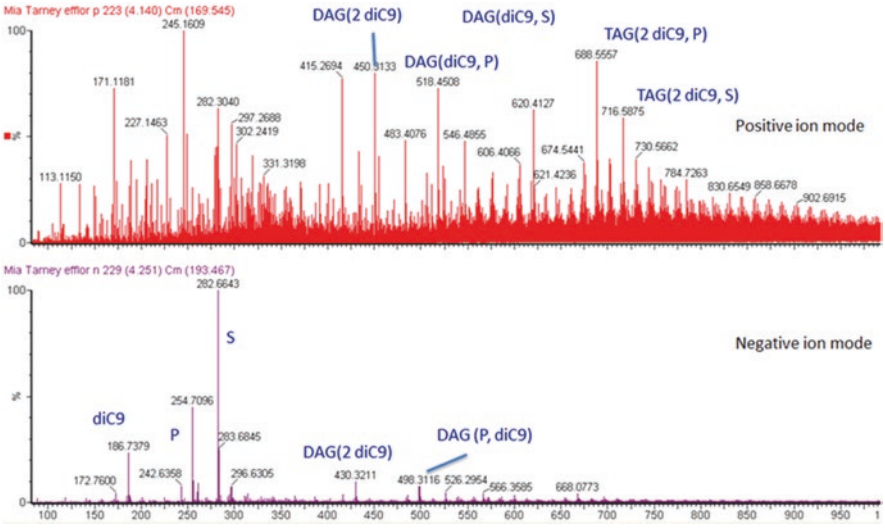

Fig. 7.4 Direct ESI-MS spectra of a scraping from the surface of a blanched painting by Mia Tarney (private collection). DAG = diacylglyceride; TAG = triacylglyceride; between brackets the acyl moieties present. (Adapted from Van den Berg et al. 2019)

glycerolipid fraction of the paint showing various ammonium adduct molecular ions. The diglycerides and triglycerides containing one saturated fatty acid at *m/z* 518/546 and *m/z* 688/716, assigned to DAG diC9, P and diC9, S and TAG 2 diC9, P and 2 diC9, S, respectively, both show a P/S ratio of 1.5. These ions are related to the partially oxidised glycerolipid molecules; their P/S ratios are consistent with that of linseed oil, which is commonly used in black paints. In the negative mode, the $M\text{-}H^-$ ions of the free fatty acids are detected. They show a P/S ratio of 0.5, suggesting that these fatty acids are related to added metal soaps additives.

GC-MS can also be used to yield information on the presence of metal stearates by separating the oil binder from the added metal soaps using a mix of chloroform/methanol (2:8 v/v) (Izzo 2011; Izzo et al. 2014). Both the extract and residue were treated with TMTFTH. The presence of metal stearates could be detected in the residues on the basis of the P/S ratios.

A GC-MS method to detect metal soaps and free fatty acids in paint layers has been proposed by La Nasa et al. (2018a). It is based on the sequential use of silylating reagents, BSTFA for the analysis of free acids plus metal carboxylates, and HMDS for the analysis of free acids, in order to detect these fractions separately.

As mentioned, DTMS has been successfully used to study painting materials in samples from many Old Master paintings (Groen et al. 1998). DTMS was applied to study the surface coatings and paint layers of post-Byzantine icons (Katsibiri 2010). The spectra showed molecular and fragment ions of palmitic and stearic acids, together with the mass peaks of alkylated benzenes, generated from the polymeric oil network. The P/S ratio indicated the presence of linseed oil. The *m/z* peaks of the lead isotopes in the pyrolysis/organic region together with the mass peak of carbonates at *m/z* 44, point to the thermal decomposition of the lead white pigment. Cholesterol and its degradation products in the region of *m/z* 368–400 suggested the presence of egg and other molecular ion peaks related to the occurrence of beeswax.

7.5.1.3 Influence of Heat Treatment on Degree of Oxidation

The A/P ratio is generally used to obtain an indication on the degree of oxidation of the drying oil, being azelaic acid the most abundant dicarboxylic acid formed (see Sect. 7.1.2.3). Moreover, the relative abundance of azelaic acid and suberic acid (A/Sub) is often determined in order to get an indication on the pre-treatment of an oil. If the ratio is >6, the oil is considered raw, not preheated, while a value ranging between 2 and 3 could refer to a "cooked" oil, with pre-polymerisation of the binder (Mills and White 1987a; Izzo 2011). An important indication of the heating of linseed oil is the detection of characteristic cyclic markers – alkylphenylcarboxylic acids – predominantly 9-(2-propylphenyl)nonanoate and 8-(2-butylphenyl)octanoate) – which are present as methyl or silyl esters in the GC chromatograms (Mills and White 1987b; Van den Berg 2002).

A study by Bonaduce et al. (2012) demonstrated, however, that the ratios between the relative amounts of the various dicarboxylic acids (A/Sub and A/Seb) cannot be used to provide information on the pre-treatment undergone by the oil (see also Sect. 7.5.1.2).

7.5.2 *Lipid Additives*

As mentioned, various additives are used in glycero-lipid paint binders as stabilisers, antioxidants, driers etc. Therefore, stearates, phthalates, waxes, metal octanoates and naphthanates, can be found. Alkyd resins, moreover, are often modified to improve certain properties as drying time, film hardness, water resistance. To that purpose the following materials are added: styrene, vinyl toluene, isocyanates, epoxy, and silicone compounds (Learner 2004).

Lipid additives may be waxes, semi-drying oils or fatty acids. For instance, in all LeFranc and Old Holland paints produced in the 2000s, the addition of castor wax could be detected, based on the identification of the specific marker 12-hydroxy-octadecanoic acid (Izzo et al. 2014). GC-MS also allowed to establish the occurrence of beeswax in Emerald Green paint from the Haagsche Kunstschilderverven Fabriek and in two Winsor & Newton paints dating 1969 (Izzo et al. 2014). Beeswax is a more traditional stabilizer and can be rather easily detected from the occurrence of 15-hydroxy-palmitic acid and long chain odd-numbered alkanes, being C_{27} generally the most abundant (Asperger et al. 1999; Bonaduce and Colombini 2004).

The detection of safflower oil in a De Kooning painting (see Sect. 7.4.1.2) and palm oil in Munch's 'New Rays' (La Nasa et al. 2015a) has already been mentioned (see Sect. 7.5.1.1).

7.5.3 *Oil Paint Modifications*

7.5.3.1 Oleoresinous Media

The addition of natural resins to oil paint media through the ages has been ascertained in several works and can give sometimes a clue on authenticity.

Copal-oil medium used by pre-Raphaelites artists (Hackney et al. 2001) was successfully analysed with a two-step Py-GCMS method by van den Berg et al. (1999b). Copals can, indeed, be efficiently analysed with Py-GC-MS (Scalarone et al. 2003a; Modugno and Ribechini 2009) or DTMS (Scalarone et al. 2003b).

Peculiarly, copaiva balsam – an oleoresin from Brasil – was added by Van Gogh with the intention to deepen the dark colours in some of his early paintings and in some Talens recipes of the 1920s and in the Roberson archives of the 1920–1930s the addition of this resin to oil colours has also been reported (Van der Werf et al. 2000). The occurrence of copaiba balsam has been ascertained as well in Talens tempera (Van den Berg et al. Forthcoming).

The composition of some modern enamel paints was determined with a combination of mass spectrometric techniques including THM–Py–GCMS, DTMS and ESI–MS (see also ESI-MS) (Kokkori et al. 2015). Specifically, DTMS allowed for distinction between unbound and cross-linked organic fractions. The low molecular weight (volatile) species are detected early in the analytical temperature program,

while cross-linked or macromolecular components are subject to pyrolysis and analyzed later at higher temperatures. The DTMS data of the Ripolin paints provided information on the chemical form of the resin component in the paint, which was present both unbound and linked to the oil.

7.5.3.2 Alkyd Paints

GC-MS and Py-GC-MS are very powerful techniques for the characterization of alkyd resins (Ploeger et al. 2014; La Nasa et al. 2013a, 2015b). The different constituents of alkyd resins can be relatively easily identified with Py-GC-MS and detailed information on their formulation obtained. The polyol, i.e. glycerol, penthaerytrytol, or sorbitol, and polybasic acids are transesterified forming methylated or silylated products. The detection of pentaerythritol indicates that the paint was produced after 1960. It should, however, be observed that pentaerythritol can also be associated with the surface treatment of titanium white (Laver 1997). Various polybasic acids can be used. For house paints phthalic anhydride is generally employed, whereas isophtalic, terephthalic, maleic, fumaric, adipic, and sebacic acids can be found in industrial alkyd resins. Adipic and sebacic acids yield less rigid molecules, forming plasticizing alkyds (Learner 2004). Schilling et al. (2007) used GC-MS to quantify the oil content in alkyd paints.

A combination of (Py-)GC-MS and HPLC-ESI-MS was also employed to characterise commercial alkyd paint materials used as binder (La Nasa et al. 2013a) and to evaluate the interactions between alkyd paints and acetic acid during the curing process of the paint layers (La Nasa et al. 2014). In the first work, the integrated platform was applied to three commercial artistic oil-based alkyd resin paints (Ferrario, Winsor & Newton Griffin and Kremer) and to a paint sample from the artwork "Salto di qualità" by Patrizia Zara (2008). The protocol allowed to characterize the fatty acid profile, the aromatic fraction and the triglyceride profiles.

The same alkyd paints were also analysed with direct ESI-MS. A "fingerprint" profile of the glyceride fraction and possible additives was obtained in just 2 min by analysing hexane extracts. As can be observed in Fig. 7.5, the mass spectrum of Ferrario alkyd resin is dominated by the presence of a cluster of peaks around *m/z* 555 characterized by $\Delta m/z$ of 44 units. These can be assigned to polyethylene glycol (PEG), which is known to be used as additive in alkyd formulations. In particular, since the PEGs ions of the main cluster are doubly charged ($[M]^{2+}$), the authors concluded that the profile is compatible with that of PEG2000. The TAG fraction can be observed in the range 800–910 *m/z* (Fig. 7.5b).

In a successive study by La Nasa et al. (2014), the previously characterized Winsor & Newton alkyd paints were exposed to acetic acid vapour for 6 months to evaluate their interactions, mimicking a curing process of the paint layers. The exposure to acetic acid vapour led to hydrolysis of the phthalic acids used for the synthesis of the resin thus deteriorating the polymeric film, a rapid degradation of the organic fraction producing several oxidized triglycerides and a loss of the aromatic fraction.

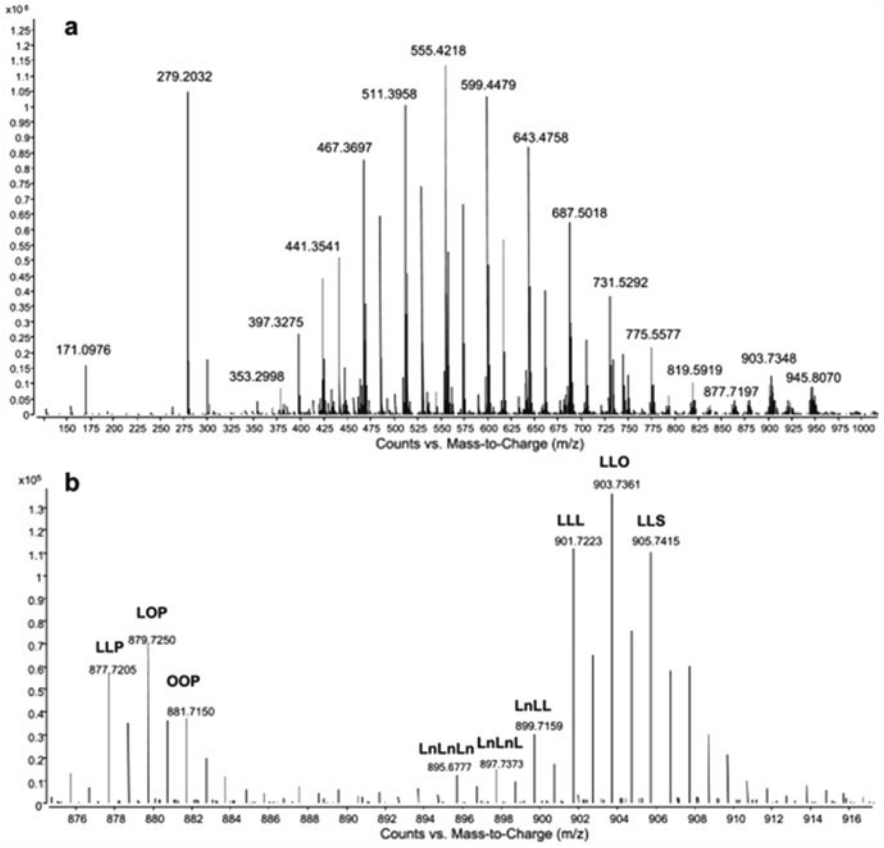

Fig. 7.5 Direct ESI-MS spectra of Ferrario Alkyd paint showing envelopes of PEGs (**a**) and TAGs (**b**). (From La Nasa et al. 2013a, b)

7.5.3.3 Oil/Protein Mixtures

MALDI-MS has been applied in the simultaneous study of proteins and lipids, including TAGs and phospholipids (Calvano et al. 2011; Van der Werf et al. 2012). Extraction with methanol/chloroform allowed to obtain a lipid and protein fraction, which could then be analysed separately with MALDI-MS (after the tryptic digestion of the protein extract). A similar analytical protocol was used in a recent study where the impact of urban air pollution on egg yolk tempera paint dosimeters was evaluated with MALDI-MS. The changes of the lipid profiles of TAGs and phospholipids and their oxidation products were monitored over time (Herrera et al. 2016).

The simultaneous identification of proteinaceous and lipid markers was also achieved directly on paint fragments, without extraction, fixed on the target plate with colloidal graphite (Calvano et al. 2015). Graphite-assisted laser desorption

ionisation (GALDI) had been used for the analysis in solvent extracts of paint samples of natural resins, oils, waxes, and ketone resins (Dietemann and Herm 2009).

MALDI-MS had already been shown efficient in detecting alteration products of TAGs and phosphatidylcholines in egg tempera dosimeters (Van den Brink 2001) or to study the effects on TAGs composition of traditional processing methods of drying oils (i.e., washing with water, heating to different temperatures, addition of lead-based siccatives) (Van den Berg and Boon 2001; Van den Berg et al. 2004). It was shown that in presence of lead more oxygen was incorporated and that high temperature treatment caused oligomerization of the starting TAGs. DTMS and DTMSMS were also applied to the study of molecular changes in egg tempera paint dosimeters (Van den Brink 2001). DTMS and derivatisation with BSTFA were specifically used to identify cholesterol and its degradation products.

As to the detection of additives, MALDI has been used for the characterisation of poly(ethylene glycol) (PEG) in aqueous extracts of acrylic emulsions and emulsion paints as well in paintings. In this way detailed information such as the weight average molar mass, number average molar mass and the polydispersity, could be obtained (Hoogland and Boon 2009).

A combination of GC-MS and LC/MS was applied to identify the lipids and natural resins of Leonardo's 'Donna Nuda' (Hermitage Museum, St. Petersburg, Russia). In this case sampling was carried out by the application of an ethylene vinyl acetate (EVA) polymer embedded with strong cation and anion exchangers and with C8 and/or C18 resins. "Tempera grassa" (consisting of linseed oil admixed with egg yolk) seems to have been used in the entire painting. Essential oils and conifer resin were also found (Barberis et al. 2019).

The composition of ETA paint, introduced by Royal Talens in 1933 and discontinued in the 1980s, was determined with Py-GC/MS (Van den Heuvel et al. 2019). This emulsion paint consists of stand oil, casein and various additives including ketone resin.

7.5.4 Degradation Studies

7.5.4.1 Saponification

As described in Sect. 7.1.2.5, the formation of metal soaps may cause degradation phenomena inside the paint layer (increased transparency, crumbling) and on its surface (disruption, protrusions). The detection of these metal carboxylates in paint cross sections can be performed with FTIR spectroscopy (metal carboxylate absorptions) and SEM-EDX (distribution of the metal ions involved) (Keune 2005).

In addition, ToF-SIMS imaging has also been used to obtain more information about the molecular structure of the soaps. This technique was, for instance, applied on a sample from a painting by Rogier van der Weyden (1399/1400–1464) (Keune and Boon 2004). In this study an indium liquid metal ion gun allowed to obtain a map of the cross section with elemental and molecular information of the pigments

and oil binder. The paint layer showed deprotonated palmitic and stearic acids as well as short chain fatty acids (C8, C9 and C10) and correlations with the distribution of lead could be determined. In a later study Keune et al. (2005)presented the results of oil identification and fatty acid speciation, based on positive ion ToF-SIMS. In this way it was possible to establish if the fatty acids exist as free fatty acids, ester bound fatty acids or metal soaps. A few years later, the potential of SIMS as compared with GC-MS and DT-MS was evaluated (Keune et al. 2009). Although ToF-SIMS presents the advantages of simultaneous detection of both organic and inorganic components in combination with spatial distribution, limitations in sensitivity and bias towards certain constituents were evidenced. Dicarboxylic fatty acids and their glyceryl derivatives could be hardly detected. Conversely, detailed information on metal soap formation can be obtained, as has also been illustrated by a study of Rembrandt van Rijn's painting materials (Sanyova et al. 2011). More recently, oil-based wall paintings in Santa Maria della Pace in Rome were examined with ToF-SIMS and high-resolution spatial maps of cross-sectional paint samples were obtained. Drying oils could be identified based on the detection of stearic acid ($C_{18}H_{35}O_2^-$) and palmitic acid ($C_{16}H_{31}O_2^-$) ions, lacking that of dicarboxylic acids (De Ghetaldi et al. 2017).

7.5.4.2 Influence of Moisture

GC-MS is a powerful tool to investigate in detail the modification of the organic components of the paint formulation with time and the influence of external factors like heat, moisture, light and noxious gases (Modugno et al. 2019; Colombini et al. 2002). Midchain oxidized fatty acids (hydroxy and epoxy stearates), as well as 2-hydroxy diacids that are formed as intermediate products during the oxidative curing and ageing of the oil, can be identified with (Py-)GC-MS (Van den Berg 2002). More highly oxidised hydroxylated fatty acids (with up to four oxygen atoms on the fatty acid chains, possibly hydroxyperoxides) could only be detected with ESI-MS (Van den Berg et al. unpublished); these fatty acids do not survive the derivatisation procedure required for GC-MS analysis of the lipids.

7.5.4.3 Water Sensitivity

Recently, ESI-MS was successfully applied in studies concerning water sensitivity of oil paints (Lee et al. 2018). These, often unvarnished (uncoated), twentieth and twenty-first century paintings limit or preclude the use of water or protic solvents for cleaning treatments and removal of polar coatings, because this may result in loss of pigment and/or binder and gloss changes due to surface disruption (Cooper et al. 2014). Lee et al. (2018) examined water sensitive Winsor & Newton oil paint swatches and twentieth century oil paintings with GC-MS, HPLC-ESI-Q-ToF and direct injection ESI-MS. The latter analyses were carried out on the ethanol extract of paint samples mixed with ammonium acetate in ethanol prior to analysis.

Negative mode ESI-mass spectra provided interesting information about the extractable polar glycerides and fatty acids. A set of most abundant ions was assigned and selected for principal component analysis (PCA). The study highlighted a relationship between the molecular composition of the binding medium and the type of pigment, which relates to water sensitivity.

The double derivatisation procedure based on the sequential use of BSTFA and HMDS (La Nasa et al. 2018a) was applied to study the water sensitivity of two naturally aged oil colour paint swatches, dating 1993 and 2003. Very similar compositions in terms of unbound and esterified medium fractions were found with HPLC-MS and GC-MS. Differences were, however, noticed in the polymeric network. This was investigated using analytical pyrolysis (Py-GC-MS) as well as EGA-MS. It was found that the polymeric material was relatively more abundant in the non-water-sensitive paint, showing a correlation between water sensitivity and the degree of polymerisation of the oil medium (La Nasa et al. 2019a). Another study had already demonstrated that additives may also influence the water sensitivity (Banti et al. 2018). In particular, the addition of Zn or Al stearates was shown to cause a small decrease of water sensitivity, while added free fatty acids did not show a consistent trend. It was therefore concluded that not only pigments, but also additives can modify the curing process of the paint, determining, together with external factors, the degree of oxidation/crosslinking, and finally the nature of the mature polymeric/ionomeric network, which indeed determines the formation of water sensitive or water resistant paint.

7.5.5 Studies on Forgeries

The number of studies involving hyphenated or direct MS techniques for authentication studies or detection of forgeries are relatively limited. Some of the studies reported in the previous paragraphs explain the type of information that MS techniques may provide in support of these, such as the detection of certain additives. That is partly the reason that, as yet, very few dedicated studies have been carried out.

As an example, the degree of oxidation of the painting material from Pablo Picasso's cubist period was examined in order to verify its authenticity (Stella et al. 2019). An integrated protocol based on in situ non-invasive and micro-invasive techniques demonstrated the compatibility of the constituent materials of the painting with its period of creation, 1912, confirming the results of expert opinions based on stylistic data and study of documentary sources. Py-GC-MS and HPLC-ESI-Q-ToF were carried out. Comparison of the lipid profile with the literature allowed to establish the presence of highly oxidised material characterised by an original high amount of triglycerides containing linolenic acid. It could be concluded that the profile was consistent with an oxidised linseed oil, which might be consistent with the alleged year of creation.

ESI-MS has been applied in the study of oil paints that were subject to accelerated drying with high temperatures (Blumenroth et al. 2019). The purpose of this study was to investigate if it is possible to detect differences between 'baked' and naturally cured oil paints. Art forgers may apply various methods to speed up the drying and hardening of oil paints (Blumenroth et al. 2019and references therein). It is known that Van Meegeren added phenol formaldehyde resin to the paint medium to obtain a hard and cracked surface. Then he used to bake the painting for 2 h at ca. 100 °C. The forger Beltracchi also baked his paintings. In the study by Blumenroth et al. commercially prepared zinc and lead white containing paints were used. ESI-MS analyses were carried out on chloroform/methanol extracts in positive mode and a 100-year old lead white paint sample was compared with a lead white sample aged for 1 week at 60 °C. It came out that the concentration of free fatty acids and fragments was significantly higher in the 'baked' sample.

7.6 Conclusion

This chapter has presented an overview of the use and chemistry of oil paints as well as of various direct and hyphenated mass spectrometric techniques. These techniques may provide valuable information on the use of lipid materials and the degree of oxidation, polymerisation, hydrolysis and saponification, allowing for a better understanding of the optical and physical state of a painting. However, since these indicators are not only related to age, but also to the particular composition as well as the environmental circumstances under which the artworks were aged, their value for authentication studies is limited.

As to the detection of forgeries, an analysis can only prove that a painting is forged when it is clear that the 'original' paint contains components that could not have been used at the alleged time of making of the work of art. Indeed, as shown in this chapter, the identification of certain additives in a paint may give a clue on the manufacturer and sometimes suggest a *terminus post quem*. For this reason, the building of databases with chemical data and archival information of the formulations of different paint manufacturers is highly important (Clarke and Carlyle 2005; Carlyle et al. 2011; Van den Berg et al. 2016; Phenix et al. 2017). As an increasing body of information is currently collected on the specific use of materials by artists, specific formulations of artists paints, and artists' working methods, it is not entirely illusory that it will be possible to obtain increasingly specific indications of both authenticity and forgery through the detection of certain paint components.

References

Amadori, M.L., Poldi, G., Barcelli, S., Baraldi, P., Berzioli, M., Casoli, A., Marras, S., Pojana, G., Villa, G.C.F.: Lorenzo Lotto's painting materials: an integrated diagnostic approach. Spectrochim. Acta A. **164**, 110–122 (2016)

Asperger, A., Engewald, W., Fabian, G.: Advances in the analysis of natural waxes provided by thermally assisted hydrolysis and methylation (THM) in combination with GC/MS. J. Anal. Appl. Pyrolysis. **52**, 51–63 (1999)

Astefanei, A., van den Berg, K.J., Burnstock, A., Corthals, G.: Surface acoustic wave nebulization−mass spectrometry as a new tool to investigate the water sensitivity behavior of 20th century oil paints. J. Am. Soc. Mass Spectrom. (2020). https://doi.org/10.1021/jasms.0c00272

Banti, D., La Nasa, J., Lluveras Tenorio, A., Modugno, F., van den Berg, K.J., Lee, J., Ormsby, B., Burnstock, A., Bonaduce, I.: A molecular study of modern oil paintings: investigating the role of dicarboxylic acids in the water sensitivity of modern oil paints. RSC Adv. **8**, 6001 (2018)

Barberis, E., Manfredi, M., Marengo, E., Zilberstein, G., Zilberstein, S., Kossolapov, A., Righetti, P.G.: Leonardo's Donna Nuda unveiled. J. Proteome. **207** (2019). https://doi.org/10.1016/j.jprot.2019.103450

Beltinger, K., Nadolny, J. (eds.): Painting in Tempera, c. 1900. Archetype, London (2016)

Bersani, D., Berzioli, M., Caglio, S., Casoli, A., Lottici, P.P., Medeghini, L., Poldi, G., Zannini, P.: An integrated multi-analytical approach to the study of the dome wall paintings by Correggio in Parma cathedral. Microchem. J. **114**, 80–88 (2014)

Blanco-Zubiaguirre, L., Ribechini, E., Degano, I., La Nasa, J., Carrero, J.A., Iñañez, J., Olivares, M., Castro, K.: GC–MS and HPLC-ESI-QToF characterization of organic lipid residues from ceramic vessels used by Basque whalers from16th to 17th centuries. Microchem. J. **137**, 190–203 (2018)

Blumenroth, D., Dietz, S., Müller, W., Zumbühl, S., Caseri, W., Heydenreich, G.: Inside the Forger's oven: identification of drying products in oil paints during and after accelerated drying with increased temperatures. In: van den Berg, K.J., et al. (eds.) Conservation of Modern Oil Paintings, pp. 437–450. Springer (2019)

Bonaduce, I., Andreotti, A.: Py-GC/MS of organic paint binders. In: Colombini, M.P., Modugno, F. (eds.) Organic Mass Spectrometry in Art and Archaeology, pp. 303–326. Springer, Cham (2009)

Bonaduce, I., Colombini, M.P.: Characterisation of beeswax in works of art by gas chromatography–mass spectrometry and pyrolysis–gas chromatography–mass spectrometry procedures. J. Chrom. A. **1028**, 297–306 (2004)

Bonaduce, I., Carlyle, L., Colombini, M.P., Duce, C., Ferrari, C., Ribechini, E., Selleri, P., Tiné, M.R.: New insights into the ageing of linseed oil paint binder: a qualitative and quantitative analytical study. PLoS One. **7** (2012). https://doi.org/10.1371/journal.pone.0049333

Bonaduce, I., Ribechini, E., Modugno, F., Colombini, M.P.: Analytical approaches based on gas chromatography mass spectrometry (GC/MS) to study organic materials in artworks and archaeological objects. Top. Curr. Chem. **374**, Article number: 6 (2016)

Bonaduce, I., Duce, C., Lluveras-Tenorio, A., Lee, J., Ormsby, B., Burnstock, A., van den Berg, K.J.: Conservation issues of modern oil paintings: a molecular model on paint curing. Acc. Chem. Res. **52**(12), 3397–3406 (2019)

Boon, J.J.: Analytical pyrolysis mass spectrometry: new vistas opened by temperature resolved in-source PYMS. Int. J. Mass Spectrom. Ion Process. **118/119**, 755–787 (1992)

Boon, J., Hoogland, F.: Investigating fluidizing dripping pink commercial paint on Van Hemert's seven-series works from 1990–1995. In: van den Berg, K.J., et al. (eds.) Conservation of Modern Oil Paintings, pp. 227–246. Springer (2019)

Borradaile, V., Borradaile, R.: The Strasburg Manuscript, A Medieval Painters' Handbook, pp. 36–65, New York (1966)

Bronken, I., Boon, J.: Hard dry paint, softening tacky paint, and exuding drips on composition 1952. In: van den Berg, K.J., et al. (eds.) Issues in Contemporary Oil Paints, pp. 247–262. Springer, Cham (2014)

Burnstock, A., van den Berg, K.J.: Twentieth century oil paint. The interface between science and conservation and the challenges for modern oil paint research. In: van den Berg, K.J., et al. (eds.) Issues in Contemporary Oil Paints, pp. 1–19. Springer, Cham (2014)

Calvano, C.D., van der Werf, I.D., Palmisano, F., Sabbatini, L.: Fingerprinting of egg and oil binders in painted artworks by matrix-assisted laser desorption ionization time-of-flight mass spectrometry analysis of lipid oxidation by-products. Anal. Bioanal. Chem. **400**, 2229–2240 (2011)

Calvano, C.D., van der Werf, I.D., Palmisano, F., Sabbatini, L.: Identification of lipid- and protein-based binders in paintings by direct on-plate wet chemistry and matrix-assisted laser desorption ionization mass spectrometry. Anal. Bioanal. Chem. **407**, 1–8 (2015)

Calvano, C.D., van der Werf, I.D., Palmisano, F., Sabbatini, L.: Revealing the composition of organic materials in polychrome works of art: the role of mass spectrometry-based techniques. Anal. Bioanal. Chem. **408**(25), 6957–6981 (2016)

Cappitelli, F.: THM-GCMS and FTIR for the study of binding media in Yellow Islands by Jackson Pollock and Break Point by Fiona Banner. J. Anal. Appl. Pyrolysis. **71**, 405–415 (2004)

Carlyle, L.: The Artist's Assistant: Oil Painting Instruction Manuals and Handbooks in Britain 1800–1900 with Reference to Selected Eighteenth-Century Sources. Archetype, London (2001)

Carlyle, L., Alves, P.C., Otero, V., Melo, M.J., Vilarigues, M.: A question of scale and terminology, extrapolating from past practices in commercial manufacture to current laboratory experience: the Winsor & Newton 19th century artists' materials archive database. In: Bridgland, J. (ed.) ICOM-CC 16th Triennial Meeting Preprints, Lisbon, 9–23 September 2011 (2011)

Cech, N.B., Enke, C.G.: Practical implications of some recent studies in electrospray ionization fundamentals. Mass Spectrom. Rev. **20**, 362–387 (2001)

Chiavari, G., Gandini, N., Russo, P., Fabbri, D.: Characterisation of standard tempera painting layers containing proteinaceous binders by pyrolysis (/methylation)-gas chromatography-mass spectrometry. Chromatographia. **47**, 420–426 (1998)

Clarke, M., Carlyle, L.: Page-image recipe databases, a new approach for accessing art technological manuscripts and rare printed sources: the Winsor & Newton archive prototype. In: Bridgland, J. (ed.) ICOM-CC 14th Triennial Meeting Preprints, The Hague, 12–16 September 2005, vol. I, pp. 24–29 (2005)

Colombini, M.P., Modugno, F.: Organic materials in art and archaeology. In: Colombini, M.P., Modugno, F. (eds.) Organic Mass Spectrometry in Art and Archaeology, pp. 3–36. Springer, Cham (2009)

Colombini, M.P., Modugno, F., Fuoco, R., Tognazzi, A.: A GC-MS study on the deterioration of lipidic paint binders. Microchem. J. **73**(1), 175–185 (2002)

Colombini, M.P., Modugno, F., Ribechini, E.: GC/MS in the characterisation of lipids. In: Colombini, M.P., Modugno, F. (eds.) Organic Mass Spectrometry in Art and Archaeology, pp. 191–213. Springer, Cham (2009)

Cooper, A., Burnstock, A., van den Berg, K.J., Ormsby, B.: Water sensitive oil paints in the 20th century: a study of the distribution of water-soluble degradation products in modern oil paint films. In: van den Berg, K.J., et al. (eds.) Issues in Contemporary Oil Paints, pp. 295–310. Springer, Cham (2014)

Crook, J., Learner, T.: The Impact of Modern Paints. Tate Gallery publishing, London (2000)

Dallongeville, S., Garnier, N., Rolando, C., Tokarski, C.: Proteins in art, archaeology, and palaeontology: from detection to identification. Chem. Rev. **116**, 2–79 (2016)

De Ghetaldi, K., Wiggins, M.B., Bertorello, C., Voras, Z., Norbutus, A., Beebe Jr., T.P., Baadea, B.: In-depth examination and analysis of Domenico Cresti's oil on wall paintings in Santa Maria della Pace in Rome. J. Cult. Herit. **28**, 48–55 (2017)

Degano, I.: Liquid chromatography: current applications in Heritage Science and recent developments. In: Sabbatini, L., Van der Werf, I.D. (eds.) Chemical Analysis in Cultural Heritage, pp. 205–226. De Gruyter, Berlin/Boston (2019)

Degano, I., Tognotti, P., Kunzelman, D., Modugno, F.: HPLC-DAD and HPLC-ESI-Q-ToF characterisation of early 20th century lake and organic pigments from Lefranc archives. Herit. Sci. **5**, 7 (2017)

Degano, I., Modugno, F., Bonaduce, I., Ribechini, E., Colombini, M.P.: Recent advances in analytical pyrolysis to investigate organic materials in heritage science. Angew. Chem. Int. Ed. **57**, 7313–7323 (2018)

Dietemann, P., Herm, C.: GALDI-MS applied to characterise natural varnishes and binders. In: Colombini, M.P., Modugno, F. (eds.) Organic Mass Spectrometry in Art and Archaeology, pp. 131–163. Springer, Cham (2009)

Dobson, G., Christie, W.W., Sebedio, J.L.: Gas chromatographic properties of cylic dienoic fatty acids formed in heated linseed oil. J. Chromatogr. **723**, 349–354 (1996)

Doménech-Carbó, M.T.: Novel analytical methods for characterizing binding media and protective coatings in artworks. Anal. Chim. Acta. **621**, 109–139 (2008)

Dubois, V., Breton, S., Linder, M., Fanni, J., Parmentier, M.: Fatty acid profiles of 80 vegetable oils with regard to their nutritional potential. Eur. J. Lipid Sci. Technol. **109**, 710–732 (2007)

Echard, J.P., Benoit, C., Peris-Vicente, J., Malecki, V., Gimeno-Adelantado, J.V., Vaiedelich, S.: Gas chromatography/mass spectrometry characterization of historical varnishes of ancient Italian lutes and violin. Anal. Chim. Acta. **584**, 172–180 (2007)

Fremout, W., Kuckova, S., Crhova, M., Sanyova, J., Saverwyns, S., Hynek, R., Kodicek, M., Vandenabeele, P., Moens, L.: Classification of protein binders in artist's paints by matrix-assisted laser desorption/ionisation time-of-flight mass spectrometry: an evaluation of principal component analysis (PCA) and soft independent modelling of class analogy (SIMCA). Rapid Commun. Mass Spectrom. **25**, 1631–1640 (2011)

Gabelica, V., De Pauw, E.: Internal energy and fragmentation of ions produced in electrospray sources. Mass Spectrom. Rev. **24**(4), 566–587 (2005). https://doi.org/10.1002/mas.20027

Garrett, I.: Winsor&Newton, retired Technical Director, with KJvdB, private conversation (January 2019)

Giorgi, G.: Overview of mass spectrometric based techniques applied in the cultural heritage field. In: Colombini, M.P., Modugno, F. (eds.) Organic Mass Spectrometry in Art and Archaeology, pp. 37–74. Springer, Cham (2009)

Groen, C.M., van der Werf, I.D., van den Berg, K.J., Boon, J.J.: The scientific examination of Vermeer's 'The girl with the pearl earring'. In: Gaskell, I., Jonker, M. (eds.) Vermeer Studies, pp. 168–183. National Gallery of Art, Washington (1998)

Hackney, S., Ridge, J., Townsend, J.H., Carlyle, L., van den Berg, K.J.: Visual deterioration in Pre-Raphaelite paintings, in Deterioration of Artists' Paints: effects and analysis. Extended abstracts of the presentations. In: Phenix, A. (ed.) ICOM-CC Working Groups Paintings 1 & 2 and the Paintings Section, UKIC. British Museum, London. 10th and 11th September 2001, pp. 54–56. ICOM and UKIC (2001)

Heginbotham, A., Chang, J., Khanjian, H., Schilling, M.R.: Some observations on the composition of Chinese lacquer. Stud. Conserv. **61**(sup3), 28–37 (2016)

Hermens, E., Townsend, J.: Binding media. In: Hill Stoner, J., Rushfield, R. (eds.) Conservation of Easel Paintings Conservation of Easel Paintings: Principles and Practice, pp. 262–273. Routledge (2021)

Herrera, A., Navas, N., Cardell, C.: An evaluation of the impact of urban air pollution on paint dosimeters by tracking changes in the lipid MALDI-TOF mass spectra profile. Talanta. **155**, 53–61 (2016)

Higgitt, C., White, R.: Analyses of paint media: new studies of Italian paintings of the fifteenth and sixteenth centuries. National Gallery Tech. Bull. **26**, 88–97 (2007)

Hoogland, F.G., Boon, J.J.: Analytical mass spectrometry of poly(ethylene glycol) additives in artists acrylic emulsion media, artists paints, and microsamples from acrylic paintings using MALDI-MS and nanospray-ESI-MS. Int. J. Mass Spectrom. **284**, 66–71 (2009)

Hulshof, P.J.M.: Fatty acid composition of selected edible fats and oils. Online report Division of Human Nutrition & Health, Wageningen University (2019). https://www.mvo.nl/media/report_fatty_acid_composition_of_selected_fats_and_oils_2019.pdf

Izzo, F.C.: 20th Century artists' oil paints: a chemical-physical survey, PhD Dissertation, Ca' Foscari University (2011)

Izzo, F.C., van den Berg, K.J., van Keulen, H., Ferriani, B., Zendri, E.: Modern oil paints – formulations, organic additives and degradation: some case studies. In: van den Berg, K.J., et al. (eds.) Issues in Contemporary Oil Paints, pp. 75–104. Springer, Cham (2014)

Katsibiri, O., Howe, R.F.: Characterisation of the transparent surface coatings on post-Byzantine icons usingmicroscopic, mass spectrometric and spectroscopic techniques. Microchem. J. **94**, 14–23 (2010)

Keune, K.: Binding medium, pigments and metal soaps characterised and localised in paint cross-sections. PhD thesis, University of Amsterdam, Amsterdam (2005)

Keune, K., Boon, J.J.: Imaging secondary ion mass spectrometry of a paint cross section taken from an Early Netherlandish painting by Rogier Van Der Weyden. Anal. Chem. **76**, 1374–1385 (2004)

Keune, K., Boon, J.J.: Analytical imaging studies of cross-sections of paintings affected by lead soap aggregate formation. Stud. Conserv. **52**(3), 161–176 (2007)

Keune, K., Ferreira, E.S.B., Boon, J.J.: Characterization and localization of the oil binding medium in paint cross sections using imaging secondary ion mass spectrometry. In: Preprints of the 14th Triennial Meeting of ICOM CC Committee for Conservation, The Hague, vol. 2, pp. 796–802 (2005)

Keune, K., Hoogland, F.G., Peggie, D., Higgitt, C., Boon, J.J.: Comparative study of the effect of traditional pigments on artificially aged oil paint systems using complementary analytical techniques. In: Bridgland, J. (ed.) Preprints 15th Triennial Conference, New Delhi, 22–26 September 2008, pp. 833–842. Allied Publishers Pvt. Ltd (2008)

Keune, K., Hoogland, F., Boon, J.J., Peggie, D., Higgitt, C.: Evaluation of the "added value" of SIMS: a mass spectrometric and spectroscopic study of an unusual Naples yellow oil paint reconstruction. Int. J. Mass Spectrom. **284**, 22–34 (2009)

Kokkori, M., Sutherland, K., Boon, J.J., Casadio, F., Vermeulen, M.: Synergistic use of Py–THM–GCMS, DTMS, and ESI–MS for the characterization of the organic fraction of modern enamel paints. Herit. Sci. **3**(Article number: 30), 1–14 (2015)

Kuckova, S., Hynek, R., Kodicek, M.: MALDI-MS applied to the analysis of protein paint binders. In: Colombini, M.P., Modugno, F. (eds.) Organic Mass Spectrometry in Art and Archaeology, pp. 165–187. Springer, Cham (2009)

La Nasa, J., Degano, I., Modugno, F., Colombini, M.P.: Alkyd paints in art: characterization using integrated mass spectrometry. Anal. Chim. Acta. **797**, 64–80 (2013a)

La Nasa, J., Ghelardi, E., Degano, I., Modugno, F., Colombini, M.P.: Core shell stationary phases for a novel separation of triglycerides in plant oils by high performance liquid chromatography with electrospray-quadrupole-time of flight mass spectrometer. J. Chrom. A. **1308**, 114–124 (2013b)

La Nasa, J., Degano, I., Modugno, F., Colombini, M.P.: Effects of acetic acid vapour on the ageing of alkyd paint layers: multi-analytical approach for the evaluation of the degradation processes. Polym. Degrad. Stab. **105**, 257–264 (2014)

La Nasa, J., Zanaboni, M., Uldanck, D., Degano, I., Modugno, F., Kutzke, H., Storevik Tveit, E., Topalova-Casadiego, B., Colombini, M.P.: Novel application of liquid chromatography/mass spectrometry for the characterization of drying oils in art: elucidation on the composition of original paint materials used by Edvard Munch (1863-1944). Anal. Chim. Acta. **896**, 177–189 (2015a)

La Nasa, J., Degano, I., Modugno, F., Colombini, M.P.: Industrial alkyd resins: characterization of pentaerythritol and phthalic acid esters using integrated mass spectrometry. Rapid Commun. Mass Spectrom. **29**, 225–237 (2015b)

La Nasa, J., Modugno, F., Aloisi, M., Lluveras-Tenorio, A., Bonaduce, I.: Development of a GC/MS method for the qualitative and quantitative analysis of mixtures of free fatty acids and metal soaps in paint samples. Anal. Chim. Acta. **1001**, 51–58 (2018a)

La Nasa, J., Degano, I., Brandolini, L., Modugno, F., Bonaduce, I.: A novel HPLC-ESI-Q-ToF approach for the determination of fatty acids and acylglycerols in food samples. Anal. Chim. Acta. **1013**, 98–109 (2018b)

La Nasa, J., Lee, J., Degano, I., Burnstock, A., van den Berg, K.J., Ormsby, B., Bonaduce, I.: The role of the polymeric network in the water sensitivity of modern oil paints. Sci. Rep. **9**, 3467 (2019a)

La Nasa, J., Biale, G., Sabatini, F., Degano, I., Colombini, M.P., Modugno, F.: Synthetic materials in art: a new comprehensive approach for the characterization of multi-material artworks by analytical pyrolysis. Herit. Sci. **7**, 8 (2019b)

La Nasa, J., Nodari, L., Nardella, F., Sabatini, F., Degano, I., Modugno, F., Legnaioli, S., Campanella, B., Tufano, M.K., Zuena, M., Tomasin, P.: Chemistry of modern paint media: the strained and collapsed painting by Alexis Harding. Microchem. J. **155**, 104659 (2020)

Lake, S.: Willem de Kooning: the Artist's Materials. Getty Publications, Los Angeles (2010)

Laurie, A.P.: The Painter's Methods. Dover Publications, Inc, Mineola (1988)

Laver, M.: Titanium white. In: West Fitzhugh, E. (ed.) Artists' Pigments: A Handbook of Their History and Characteristics, vol. 3, pp. 295–355. National gallery of Art, Archetype Publications, London (1997)

Learner, T.: Analysis of Modern Paints. The Getty Conservation Institute, Los Angeles (2004)

Lee, J., Bonaduce, I., Modugno, F., La Nasa, J., Ormsby, B., van den Berg, K.J.: Scientific investigation into the water sensitivity of twentieth century oil paints. Microchem. J. **138**, 282–295 (2018)

Lluveras, A., Bonaduce, I., Andreotti, A., Colombini, M.P.: GC/MS analytical procedure for the characterization of glycerolipids, natural waxes, terpenoid resins, proteinaceous and polysaccharide materials in the same paint microsample avoiding interferences from inorganic media. Anal. Chem. **81**, 376–386 (2010)

Maier, M.S., Parera, S.D., Seldes, A.M.: Matrix-assisted laser desorption and electrospray ionization mass spectrometry of carminic acid isolated from cochineal. Int. J. Mass Spectrom. **232**, 225–229 (2004)

Manzano, E., Rodriguez-Simón, L.R., Navas, N., Checa-Moreno, R., Romero-Gámez, M., Capitan-Vallvey, L.F.: Study of the GC-MS determination of the palmitic-stearic acid ratio for the characterisation of drying oil in painting: La Encarnación by Alonso Cano as a case study. Talanta. **84**, 1148–1154 (2011)

Marinach, C., Papillon, M.C., Pepe, C.: Identification of binding media in works of art by gas chromatography–mass spectrometry. J. Cult. Herit. **5**, 231–240 (2004)

Mateo-Castro, R., Doménech-Carbó, M.T., Peris-Martínez, V., Gimeno-Adelantado, J.V., Bosch-Reig, F.: Study of binding media in works of art by gas chromatographic analysis of amino acids and fatty acids derivatized with ethyl chloroformate. J. Chromatogr. A. **778**, 373–381 (1997)

Mazel, V., Richardin, P.: ToF-SIMS study of organic materials in cultural heritage: identification and chemical imaging. In: Colombini, M.P., Modugno, F. (eds.) Organic Mass Spectrometry in Art and Archaeology, pp. 433–457. Springer, Cham (2009)

Mazurek, J., Svoboda, M., Schilling, M.: GC/MS characterization of beeswax, protein, gum, resin, and oil in Romano-Egyptian paintings. Heritage. **2**(3), 1960–1985 (2019). https://doi.org/10.3390/heritage2030119

Mills, J.S.: The gas chromatographic examination of paint media. Part I, fatty acid composition and identification of dried oil films. Stud. Conserv. **11**, 92–108 (1966)

Mills, J., White, R.: Analyses of paint media. National Gallery Tech. Bull. **11**, 92–95 (1987a)

Mills, J.S., White, R.: The Organic Chemistry of Museum Objects. Butterworths, London (1987b)

Mills, L., Burnstock, A., Duarte, F., de Groot, S., Megens, L., Bisschoff, M., van Keulen, H., van den Berg, K.J.: Water sensitivity of modern artists' oil paints. In: Bridgland, J. (ed.) ICOM

Committee for Conservation, 15th Triennial Conference, New Delhi, 22–26 September 2008: Preprints, pp. 651–659. ICOM Committee for Conservation, Paris (2008)
Modugno, F., Ribechini, E.: GC/MS in the characterisation of resinous materials. In: Colombini, M.P., Modugno, F. (eds.) Organic Mass Spectrometry in Art and Archaeology, pp. 215–235. Springer, Cham (2009)
Modugno, F., Di Gianvincenzo, F., Degano, I., van der Werf, I.D., Bonaduce, I., van den Berg, K.J.: On the influence of relative humidity on the oxidation and hydrolysis of fresh and aged oil paints. Sci. Rep. **9**, 5533 (2019)
Muir, K., Gautier, G., Casadio, F., Vila, A.: Interdisciplinary investigation of early house paints: Picasso, Picabia and their "Ripolin" Paintings – Revision 1. In: ICOM Committee for Conservation, 16th Triennial Meeting, Lisbon 19–23 September 2011. International Council of Museums (2011)
Muizebelt, W.J., Hubert, J.C., Venderbosch, R.A.M.: Mechanistic study of drying of alkyd resins using ethyl linoleate as a model substance. Prog. Org. Coat. **24**, 263–279 (1994)
Nakamura, S., Takino, M., Daishima, S.: Analysis of waterborne paints by gas chromatography–mass spectrometry with a temperature-programmable pyrolyzer. J. Chromatogr. A. **912**, 329–334 (2001)
Noble, P., Van Loon, A., Boon, J.J.: Chemical changes in old master paintings II: darkening due to increased transparency as a result of metal soap formation. In: Preprints of the ICOM Committee for Conservation 14th Triennial Meeting, 12–16 Sept 2005, The Hague, pp. 496–503 (2005)
Nowik, W.: Acides amines et acides gras sur un même chromatogramme—un autre regard sur l'analyse des liants en peinture. Stud. Conserv. **40**, 120–126 (1995)
Ormsby, B., Gottsegen, M.: Grounds in the twentieth century and beyond. In: Hill Stoner, J., Rushfield, R. (eds.) Conservation of Easel Paintings Conservation of Easel Paintings: Principles and Practice, pp. 187–191. Routledge (2021)
Orsini, S., Parlanti, F., Bonaduce, I.: Analytical pyrolysis of proteins in samples from artistic and archaeological objects. J. Anal. Appl. Pyrolysis. **124**, 643–657 (2017)
Osmond, G.Z.: White and the influence of paint composition for stability in oil based media. In: van den Berg, K.J., Burnstock, A., Keijzer, M., Tagle, A., Heydenreich, G. (eds.) Issues in Contemporary Oil Paint, pp. 263–282. Springer (2014)
Oudemans, T.F.M., Eijkel, G.B., Boon, J.J.: Identifying biomolecular origins of solid residues preserved in iron Age pottery using DTMS and MVA. J. Archaeol. Sci. **34**, 173–193 (2007)
Phenix, A., Townsend, J.: A brief survey on historical varnishes. In: Hill Stoner, J., Rushfield, R. (eds.) Conservation of Easel Paintings Conservation of Easel Paintings: Principles and Practice, pp. 262–273. Routledge (2021)
Phenix, A., Soldano, A., Van Driel, B., van den Berg, K.J.: 'The Might of White': formulations of titanium dioxide-based oil paints as evidenced in archives of two artists' colourmen, mid-twentieth century. In: Bridgland, J. (ed.) ICOM-CC 18th Triennial Conference Preprints, Copenhagen, 4–8 September 2017, p. art. 0104. International Council of Museums, Paris (2017)
Piccirillo, A., Scalarone, D., Chiantore, O.: Comparison between off line and on line deriva tisation methods in the characterisation of siccative oils in paint media. J. Anal. Appl. Pyrolysis. **74**, 33–38 (2005)
Pintus, V., Schreiner, M.: Characterization and identification of acrylic binding media: influence of UV light on the ageing process. Anal. Bioanal. Chem. **399**, 2961–2976 (2011)
Pintus, V., Wei, S., Schreiner, M.: UV ageing studies: evaluation of lightfastness declarations of commercial acrylic paints. Anal. Bioanal. Chem. **402**, 1567–1584 (2012)
Pizzimenti, S., Bernazzani, L., Tinè, M.R., Treil, V., Duce, C., Bonaduce, I.: Oxidation and Cross-Linking in the Curing of Air-Drying Artists' Oil Paints. ACS Polymer Material Science (2021)
Ploeger, R., Scalarone, D., Chiantore, O.: The characterization of commercial artists' alkyd paints. J. Cult. Herit. **9**, 412–419 (2014)
Prati, S., Smith, S., Chiavari, G.: Characterisation of siccative oils, resins and pigments in art works by thermochemolysis coupled to thermal desorption and pyrolysis GC and GC-MS. Chromatographia. **59**, 227–231 (2004)

Sanyova, J., Cersoy, S., Richardin, P., Laprévote, O., Walter, P., Brunelle, A.: Unexpected materials in a Rembrandt painting characterized by high spatial resolution cluster-TOF-SIMS imaging. Anal. Chem. **83**, 753–760 (2011)

Scalarone, D., Lazzari, M., Chiantore, O.: Ageing behaviour and analytical pyrolysis characterisation of diterpenic resins used as art materials: Manila copal and sandarac. J. Anal. Appl. Pyrolysis. **68**, 115–136 (2003a)

Scalarone, D., van der Horst, J., Boon, J.J., Chiantore, O.: Direct-temperature mass spectrometric detection of volatile terpenoids and natural terpenoid polymers in fresh and artificially aged resins. J. Mass Spectrom. **38**, 607–617 (2003b)

Scalarone, D., Duursma, M.C., Boon, J.J., Chiantore, O.J.: MALDI-TOF mass spectrometry on cellulosic surfaces of fresh and photo-aged di- and triterpenoid varnish resins. J. Mass Spectrom. **40**, 1527–1535 (2005)

Schaich, K.: Lipid Oxidation: Theoretical Aspects. Wiley (2005)

Schilling, M.R., Mazurek, J., Learner, T.J.S.: Studies of modern oil-based artists' paint media by gas chromatography/mass spectrometry. In: Modern Paints Uncovered, Proceedings from the Modern Paints Uncovered Symposium, Tate Modern, pp. 129–139 (2007)

Schilling, M.R., Heginbotham, A., van Keulen, H., Szelewski, M.: Beyond the basics: a systematic approach for comprehensive analysis of organic materials in Asian lacquers. Stud. Conserv. **61**(sup3), 3–27 (2016)

Shimadzu, Y.: Chemical and Optical Aspects of Appearance Changes in Oil Paintings from the 19th and Early 20th Century. University of Amsterdam (2015)

Shimadzu, Y., Keune, K., van den Berg, K.J., Boon, J.J., Townsend, J.H.: The effects of lead and zinc white saponification on surface appearance of paint. In: Bridgland, J. (ed.) Preprints of the ICOM Committee for Conservation: Preprints of the 15th Triennial Meeting, New Delhi, 22–26 Sept 2008, pp. 626–632. Allied Publishers Pvt Ltd (2008)

Spoto, G.: Secondary ion mass spectrometry in art and archaeology. Thermochim. Acta. **365**, 157–166 (2000)

Spoto, G., Grasso, G.: Spatially resolved mass spectrometry in the study of art and archaeological objects. Trends Anal. Chem. **30**, 856–863 (2011)

Standeven, H.A.L.: House Paints, 1900–1960: History and Use. Getty Publications, Los Angeles (2011)

Stella, E.M., Bracci, S., Iannaccone, R., La Nasa, J., Colombini, M.P.: Violon. Céret by Pablo Picasso: the case of a lost painting. A methodological approach. J. Cult. Herit. **35**, 199–208 (2019)

Sutherland, K.: The extraction of soluble components from an oil paint film by a varnish solution. Stud. Conserv. **45**, 54–62 (2000)

Sutherland, K.: Derivatisation using m-(trifluoromethyl)phenyltrimethylammonium hydroxide of organic materials in artworks for analysis by gas chromatography-mass spectrometry: unusual reaction products with alcohols. J. Chrom. A. **1149**(1), 30–37 (2007)

Sutherland, K.: Gas chromatography/mass spectrometry techniques for the characterization of organic materials in works of art. In: Sabbatini, L., van der Werf, I.D. (eds.) Chemical Analysis in Cultural Heritage, pp. 181–203. De Gruyter (2019)

Swern, D.: In: Swern, D. (ed.) Bailey's Industrial Oil and Fat Products, vol. 1. Wiley, New York (1979)

Tammekivi, E., Vahur, S., Kekisev, O., van der Werf, I.D., Toom, L., Herodesa, K., Leito, I.: Comparison of derivatization methods for the quantitative gas chromatographic analysis of oils. Anal. Methods. **11**, 3514 (2019)

Tempest, H., Burnstock, A., Saltmarsh, P., van den Berg, K.J.: Progress in the water sensitive oil project. In: Mecklenburgh, M.F., Charola, A.E., Koestler, R.J. (eds.) Proceedings of the Cleaning 2010 Conference, Valencia, 26–28 May 2010, pp. 107–117. Smithsonian Institute (2013)

Van Dam, E., van den Berg, K.J., Ness Proaño Gaibor, A., van Bommel, M.: Analysis of triglyceride degradation products in drying oils and oil paints using LC-ESI-MS. Int. J. Mass Spectrom. **413**, 33–42 (2017)

Van den Berg, J.D.J.: Analytical Chemical Studies on Traditional Linseed Oil Paints. University of Amsterdam (2002)

Van den Berg, J.D.J., Boon, J.J.: Unwanted alkylation during direct methylation of fatty acids using tetramethyl ammonium hydroxide reagent in a Curie-point pyrolysis unit. J. Anal. Appl. Pyrolysis. **61**, 45–63 (2001)

Van den Berg, J.D.J., van den Berg, K.J., Boon, J.J.: Chemical changes in curing and ageing oil paints. In: Bridgland, J. (ed.) ICOM Committee for Conservation 12th Triennial Meeting, Lyon, France, 29 August-3 September 1999, vol. 1, pp. 248–253. James & James, London (1999a)

Van den Berg, K.J., van der Horst, J., Boon, J.J.: Recognition of copals in aged resin/oil paints and varnishes. In: Bridgland, J. (ed.) ICOM Committee for Conservation 12th Triennial Meeting, Lyon, France, 29 August-3 September 1999, pp. 855–861. James & James, London (1999b)

Van den Berg, J.D.J., van den Berg, K.J., Boon, J.J.: Determination of the degree of hydrolysis of oil paint samples using a two-step derivatisation method and on-column GC/MS. J. Progr. Org. Coatings. **1074**, 1–13 (2001)

Van den Berg, J.D.J., Vermist, N.D., Carlyle, L., Holcapek, M., Boon, J.J.: The effects of traditional processing methods of linseed oil on the composition of its triacylglycerols. J. Sep. Sci. **27**, 181–199 (2004)

Van den Berg, K.J., Keune, K., de Groot, S., van Keulen, H.: Binding media in Tudor and Jacobean paintings. In: Cooper, T., Howard, M., Burnstock, A. (eds.) Painting in Britain 1500–1630: Production, Influences, and Patronage, pp. 146–157. OUP, Oxford (2015)

Van den Berg, K.J., Bayliss, S., Burnstock, A., van Gurp, F., Klein, O.B.: Making paint in the 20th century: the Talens Archive. In: Eyb Green, S., Townsend, J.H., Pilz, K., Kroustallis, S., Van Leeuwen, I. (eds.) Sources on Art Technology; Back to Basics. Proceedings of the 6th Symposium of ATSR, 16 and 17 June 2014, pp. 43–50. Archetype (2016)

Van den Berg, K.J., Burnstock, A., Schilling, M.: Notes on metal soap extenders in modern oil paints – history, use, degradation and analysis. In: Casadio, F., et al. (eds.) Metal Soaps in Art – Conservation & Research, pp. 329–342. Springer (2019)

Van den Berg, K.J., Lee, J., Ormsby, B.: Modern oil paints. In: Hill Stoner, J., Rushfield, R. (eds.) Conservation of Easel Paintings Conservation of Easel Paintings: Principles and Practice, pp. 262–273. Routledge (2021)

Van den Berg, K.J., van den Heuvel, L., Pause, R., van der Werf, I.: Talens' emulsion paints 1900–1950. (Forthcoming)

Van den Brink, O.F.: Molecular changes in egg tempera paint dosimeters as tools to monitor the museum environment. Molart Report 4. PhD thesis, University of Amsterdam (2001)

Van den Brink OF, Boon, J.J., O'Connor, P.B., Duursma, M.C., Heeren, R.M.A.: Matrix-assisted laser desorption/ionization Fourier transform mass spectrometric analysis of oxygenated triglycerides and phosphatidylcholines in egg tempera paint dosimeters used for environmental monitoring of museum display conditions. J. Mass Spectrom. **36**, 479–492 (2001)

Van den Heuvel, L., van der Werf, I., van Waas, C., van den Berg, K.J.: Approaches to the identification of Royal Talens ETA (emulsion) paint in objects of art. In: van den Berg, K.J., et al. (eds.) Conservation of Modern Oil Paintings, pp. 97–107. Springer, Cham (2019)

Van der Doelen, G.A.: Molecular studies of fresh and aged triterpenoid varnishes. Molart Report 1. PhD thesis, University of Amsterdam (1999)

Van der Doelen, G.A., van den Berg, K.J., Boon, J.J.: Comparative chromatographic and mass spectrometric studies of triterpenoid varnishes: fresh material and aged samples from paintings. Stud. Conserv. **43**(4), 249–264 (1998)

Van der Werf, I.D., van den Berg, K.J., Schmitt, S., Boon, J.J.: Molecular characterisation of copaiba balsam as used in painting techniques and restoration procedures. Stud. Conserv. **45**, 1–18 (2000)

Van der Werf, I.D., Calvano, C.D., Palmisano, F., Sabbatini, L.: A simple protocol for Matrix Assisted Laser Desorption Ionization- time of flight-mass spectrometry (MALDI-TOF-MS) analysis of lipids and proteins in single microsamples of paintings. Anal. Chim. Acta. **718**, 1–10 (2012)

Van Keulen, H.: Slow-drying oil additives in modern oil paints and their application in conservation treatments. An analytical study in technical historical perspective. In: Bridgland, J. (ed.) ICOM-CC 17th Triennial Conference Preprints. Melbourne, 15–19 September 2014, p. Paper 349 (2014)

Van Loon, A., Noble, P., Burnstock, A.: Ageing and deterioration of traditional oil and tempera paints. In: Hill Stoner, J., Rushfield, R. (eds.) Conservation of Easel Paintings Conservation of Easel Paintings: Principles and Practice, pp. 216–243. Routledge (2021)

Watts, K., Lagalante, A.: Method development for binding media analysis in painting cross-sections by desorption electrospray ionization-mass spectrometry (DESI-MS). Rapid Commun. Mass Spectrom. **32** (2018). https://doi.org/10.1002/rcm.8184

Wei, S., Pintus, V., Schreiner, M.: A comparison study of alkyd resin used in art works by Py-GC/MS andGC/MS: the influence of aging. J. Anal. Appl. Pyrolysis. **104**, 441–447 (2013)

White, R., Kirby, J.: Some observations on the binder and dyestuff composition of glaze paints in early European panel paintings. In: Nadolny, J. (ed.) Medieval Techniques in Northern Europe: Techniques, Analysis, Art History, pp. 215–222, London (2006)

White, R., Roy, A.: GC-MS and SEM studies on the effects of solvent cleaning on old master paintings from the National Gallery, London. Stud. Conserv. **43**, 159–176 (1998)

Wijnberg, L., van den Berg, K.J.: Reflection of the Big Dipper (1947). In: Pensabuene Buemi L et al., editors. Alchimia di Jackson Pollock. Viaggio all'interno della materia, pp. 157–169. Edifir Edizione, Firenze (2019)

Zhang, X., Laursen, R.: Application of LC–MS to the analysis of dyes in objects of historical interest. Int. J. Mass Spectrom. **284**, 108–114 (2009)

Chapter 8
Fluorescence for the Analysis of Paintings

Austin Nevin

Abstract This chapter aims to provide an overview of fluorescence as it is employed for the examination of works of art, with specific examples of the technique applied to the assessment of condition of paintings. The physical phenomena that underlie fluorescence are reviewed briefly, together with an overview of the methods used for the inspection of easel paintings. Fluorescence spectroscopy and advanced imaging methods based on time-resolved luminescence are useful for the discrimination of materials, and the characterisation of modern pigments, as well as to monitor the ageing of materials, but require careful calibration and the use of suitable reference materials. This chapter has the specific aim of illustrating how fluorescence can be used to inspect the condition of the surface of paintings, for the identification of reintegration, and for the detection of emissions from inorganic and organic pigments; in some cases how luminescence may allow the identification of the presence of non-original materials, aged varnishes or surface treatments.

Keywords Fluorescence · Ultraviolet · Varnish · Imaging · Non-invasive documentation

8.1 Introduction

The use of ultraviolet light sources for the visual examination or photography (and imaging) of fluorescence is common as part of routine examination of works of art. The advantage of using UV sources is that they provide excitation of fluorescence from the materials on surfaces, allowing the documentation of condition as is well known and reviewed widely. Indeed UV fluorescence images of paintings are

A. Nevin (✉)
Department of Conservation, Courtauld Institute of Art, London, United Kingdom
e-mail: austin.nevin@courtauld.ac.uk

M. P. Colombini et al. (eds.), *Analytical Chemistry for the Study of Paintings and the Detection of Forgeries*, Cultural Heritage Science,
https://doi.org/10.1007/978-3-030-86865-9_8

commonly published alongside images in visible incident and raking light in technical publications, or as part of condition reports.

The application of UV fluorescence for the examination of paintings is not new. In 1931, in his book "Ultra-violet Rays and Their Use in the Examination of Works of Art" published by the Metropolitan Museum of Art, Rorimer reviews the principles of fluorescence photography. Noteworthy today are the long exposure times reported for photographing fluorescence signals using conventional lamps (5–30 min) (Rorimer 1931). As noted by Rorimer (p. 47): "Restorations, though perhaps not to be distinguished in ordinary light, are readily apparent in ultra-violet light, owing to the difference in fluorescence between the old and the new paints." Rorimer notes that "in addition, it is probable that by comparing and analyzing under ultra-violet rays paintings of a particular period or by particular individuals it will be possible to arrive at conclusions about authenticity and attribution (p. 48)." Examples in his book reflect the "reactions of various pigments to the rays, as well as the manner of working" of artists, and the presence of "repairs and surface condition." Indeed, conservators routinely employ UV fluorescence for examining repairs and to rapidly assess the extent of past restorations; conveniently UV Fluorescence is a rapid, economical, and non-invasive method for documentation and can assist in the characterisation of pigments (Carden 1991).

IUPAC defines fluorescence as luminescence which occurs during the irradiation of a substance by electromagnetic radiation. Only particular materials are fluorescent and include some pigments used in paintings, many binding media, and varnishes. Several authors report systematic studies documenting the appearance of pigments and binders under UV (Carden 1991; Feller 1986; Grant 2000; Pelagotti et al. 2005). While there are different origins of fluorescence in materials, luminescence always relates to chemical composition. Materials may be intrinsically fluorescent. Alternatively fluorescence may be generated with the formation of new molecules as a consequence of age-related degradation. Another cause of fluorescence is the presence of additives and impurities in pigments and media.

Key texts regarding fluorescence and applications in chemistry include Principles of Fluorescence Spectroscopy by Lakowitz (Lakowicz 2006). Within conservation literature, luminescence is often part of routine documentation (Hickey-Friedman 2002), and advances and an overview of applications of UV fluorescence in conservation have been well described in publications and in recent texts (Picollo et al. 2019).

Simply, fluorescence is a phenomenon that occurs when a portion of the electromagnetic spectrum (within conservation, this is commonly UV light from a Wood's lamp, LED source, or a laser beam) is absorbed by a material causing excitation of its electrons. Following excitation, many of the excited electrons relax to the ground state and in so doing emit radiation at a longer wavelength (which may be visible to the eye and perceived as colour, or measured with a spectrometer). The proportion of excited electrons resulting in the emission of fluorescence is known as the quantum yield, which is generally not reported for materials in conservation science literature and complex to calculate for solids; quantum yield nonetheless gives an

indication of the efficiency of molecules in converting excited electrons into luminescence signal.

The detection limits of fluorescence spectroscopy are generally very low, and the concentration of solutions used in fluorescence spectroscopy is often below 10^{-6} M (Lakowicz 2006). Fluorescence is not a weak effect (in comparison, for example, with scattering) and signal from fluorescence can be detected easily and photographed using suitable settings. Indeed in truly dark conditions when a light that emits only UV is used, it is only fluorescence and not reflected light that is generated. In forensic applications, fluorescent markers added to documents and currency yield bright signals that can be easily checked under inspection lamps. Fluorescent dyes and reagents have also been used for identification of materials in cross-sections, and include rhodamine as well as more specific immunological stains for binding media (Plesters 1956; Magrini et al. 2013).

The timescale of the absorption of UV photons or light is instantaneous while emissions occur on the picosecond and nanosecond scale for fluorescence, and at a slower rate for phosphorescent materials. Generally fluorescence is encountered in the materials found in works of art. Recent research has demonstrated phosphorescence of artists pigments, with appreciable signal from ZnS-based pigments, for example, that can be photographed in exceptional circumstances, or detected using time-resolved imaging devices (Capua 2014; Bellei et al. 2015).

Absorption spectra (that plot the proportion of light absorbed vs. wavelength), excitation spectra (that plot the intensity of an emission at a specific wavelength vs. excitation wavelength), emission spectra (that plot the intensity of signal vs. wavelength of emitted light) and luminescence lifetimes (a calculation of the exponential decay, in seconds) are all characteristic of fluorescent materials. This does not mean that any of these phenomena are unique or diagnostic, but each can give insights into the excitation and emission processes that occur when radiation interacts with the molecules in works of art. Data regarding photostability (quantum yield), as well as defects or impurities that may relate to synthesis or degradation can also be obtained (Comelli et al. 2019).

While the measurement of absorption is not possible for paintings, fibre optic reflectance of surfaces can allow the estimation of the absorption of materials (Bacci and Picollo 1996). Electrons can be excited easily with commonly available light sources (including UV-flash lamps, LED lights (Verri 2019), or with spectrometer set-ups (fibre optic probes, or laser induced fluorescence (LIF)) for fluorescence spectrum and lifetime measurements (Comelli et al. 2005), hence emission spectra and fluorescent lifetimes can be measured from works of art. The use of fluorescence spectroscopy as an analytical technique, while common in chemistry and biological applications, requires purification of samples, and calibration. Instead, in applications within conservation science, fluorescence is most commonly encountered as part of documentation and routine examination, or as part of analytical imaging using multispectral or hyperspectral imaging devices (Comelli et al. 2008).

In this text applications of fluorescence are shown and relate chiefly to the examination and assessment of easel paintings (Saunders 2012). Within the context of authentication and the condition of surfaces, the main reason we are interested in

fluorescence is that it provides key information regarding damage and restoration, as well as insights into materials present in paint. Indeed, while the analysis and identification of specific materials will usually require sampling and more specific analytical approaches, photography of fluorescence may still yield important insights into the pigments and materials present on a surface. With more advanced multispectral and hyperspectral instrumentation it is possible to capture spectral data from images, which is particularly useful for the discrimination of luminescence from different materials (Ghirardello et al. 2020).

8.2 Documentation of Paintings

The documentation of paintings using UV light is standard practice, as is the examination of paintings with UV to assess their condition (Saunders 2012). Health and safety considerations are important when using UV light sources and suitable protective eyewear needs to be worn during examination. Moreover, radiation from UV light can cause irreversible degradation and rapid photooxidation of fugitive pigments and should be employed cautiously. Fluorescence microscopy is another area that is particularly important for the examination of paint samples, and may allow scientists and conservators to distinguish between multiple layers of organic materials, or identify properties that may be associated with particular pigments, using standard UV lamps (Easthugh et al. 2001) or advanced time-resolved multispectral imaging systems (Comelli et al. 2005). For an excellent review on the application of UV inspection to the analysis of cross-sections see Berrie and Thoury (Berrie and Thoury 2020). Important reference collections and charts and the response of materials to UV and IR have been produced, with research by Aldrovandi et al. on False Colour IR particularly useful for distinguishing blue pigments (Aldovrandi et al. 2004).

It is common to refer to UV Fluorescence as a method of examination, but this terminology does not reveal how the effect is measured. Technology with sensitive digital cameras, lasers and portable light sources based either on modified flashes or LEDs have significantly changed the parameters used for recording fluorescence today (Aldovrandi et al. 2004; Verri 2019). Photography of the results of UV fluorescence is tricky and the colour recorded from digital photographs of fluorescence may vary considerably with different setups; only recently have there been convincing attempts to introduce suitable fluorescence calibration standards within images that will greatly improve the comparison of images in the future (Cosentino 2014; Keller et al. 2020).

A secondary purpose of the application of fluorescence spectroscopy and analytical imaging to paintings is the identification of materials. This aim is frustrated by the general lack of specificity of luminescence emissions from the multiple materials often found in works of art. Spectrofluorimetry may yield more specific signals (spectra) and data which aids the identification of pigments and binders. Due

to the complexity of fluorescence from multi-layered surfaces, the majority of literature has focused on the identification of pure materials or reference samples.

UV fluorescence has been the subject of extensive discussion in conservation and recent research, with some authors providing workflows for identifying materials based on the behaviour of sets of reference pigments and paints as they reflect and emit UV light (Aldovrandi et al. 2004). Despite encouraging results on model samples, claims that UV photography or measurements of UV fluorescence using colorimetry can distinguish varnishes should be treated with caution. It is recognised that fundamental studies are essential for the understanding of the optical properties of artistic materials. Indeed, while much has been written about emissions from different materials, readers should be cautions of the difficulties in interpretation of data and the attribution of fluorescence to specific materials (Rogge and Lough 2016). Varnished tin type prints were examined by Rogge and Lough who convincingly demonstrate the risks in adopting techniques based on UV-induced fluorescence based on UV fluorescence and reflectance: in the study on tin-types, dammar and shellac could not be distinguished based on fluorescence properties (Rogge and Lough 2016). For these reasons great caution should be exercised when describing fluorescence, in attempting to identify specific materials based on fluorescence emissions and when interpreting results from UV photographs.

Fluorescence Spectroscopy (that includes application of Laser Induced Fluorescence (LIF)) has been employed to study the emissions from paintings and materials including pigments and binding media. Spectrofluorimetric analysis of protein-based binding media, oils and varnishes has highlighted the potential of fluorescence spectroscopy for the study of binders, but also the sometimes very small differences in the broad emissions found in media (Larson et al. 1991). While spectrally-resolved applications require more expensive equipment (based on multiple filters, or spectrometers, hyperspectral lidar systems (Colao et al. 2008), timegated fluorescence cameras (Miyoshi 1987), or multispectral imaging (Fischer and Kakoulli 2006), photographic techniques based on commonly available excitation sources and adapted digital cameras are more common (Dyer and Sotiropoulou 2017).

8.3 Capturing Fluorescence Images

UV lamps are ubiquitous in conservation studios and hand-held inspection lights with LED illumination in the UV can be used to illuminate paintings for the excitation of luminescence during routine inspection. Different sources can be used for exciting fluorescence, and recent publications have suggested significant improvements using interference filters and photographic cameras which allow more low-cost photography of paintings and works of art (2006). UV lamps are based on either Xenon gas or Mercury arc lamps or fluorescent black lamps – and provide either broad (Xenon) or narrow (365 nm) excitation respectively. It is common to use either for microscopy, where intense light is needed for examination. Adapted photographic flashes without UV-filters can be used to excite surfaces of paintings

(Dyer et al. 2013). Another option for excitation is found with LED sources but these are generally more focused and less intense than the light found in traditional lamps; LED sources can also be found in hand-held lights.

UV photography is carried out in the dark, by blocking visible light sources. Uniform illumination during UV photography is challenging and often not possible. To improve illumination, multiple lamps may be used. Another further complication during photography is that many UV lamps emit visible as well as UV light – and visible light needs to be filtered prior to excitation in order to observe only fluorescence and not reflected light. Filters can be placed in front of the lamps to block all visible light or in front of the flash for the same reason. Many published images of fluorescence of paintings may seem either blue or even purple in tone as the images are a combination of fluorescence and reflected light.

After excitation, photography requires careful use of filters to block reflected UV light from entering the camera so that only visible (or IR) luminescence is recorded. Gelatine filters placed in front of objectives provide good screening of UV. It is common to use relatively long exposure times for UV photography that may be limited by the signal-to-noise ratio of the CCD sensors in digital cameras, unless intense flash sources are used. Flash sources are particularly powerful for capturing fluorescence in low-light conditions. A striking example of the application of flash photography to photograph the bright yellowish emission from Indian Yellow (Martin de Fonjaudran et al. 2017), due to aromatic xanthonoid structure, is shown in Fig. 8.1.

Another important factor to consider when capturing fluorescence is that different materials present on the same painting will emit at different intensities and with different spectra. As a consequence, it is often the most intense fluorescence signal that is captured in photography, and this signal can dominate or mask signal from other much weaker fluorescence. This is seen in examples of paintings later in this chapter but needs to be kept in mind during examination and photography; it can be useful to mask areas of strong fluorescence to assess varnish (which tends to fluoresce with weak intensity) compared to, for example, semiconductor pigments such as ZnO or some red lake pigments.

8.4 On the Fluorescence of Varnishes

The most common application of fluorescence in the assessment of paintings is for the examination of the condition of varnishes and for the identification of the presence of restorations and retouching or inpainting, which may appear darker than the original varnishes. Many traditional varnishes are intrinsically fluorescent, and become increasingly fluorescent with ageing and the formation of double bonds and chromophores or coloured molecules that change the absorption of varnishes (yellowing). New fluorophores are also generated during aging and account for the greater fluorescence of aged oils and varnishes, and also for changes in the fluorescence of proteins (Nevin et al. 2008, 2009a). Thus, inspection of paint surfaces with

Fig. 8.1 Ceiling of the Badal Mahal, Garh Palace, Bundi (Rajasthan, India) depicting Krishna dancing with the gopis; (top) visible image and (bottom) UV-induced luminescence image, showing the yellow-orange emission of Indian yellow. Due to the distance between the camera and the ceiling, the use of a white board and Spectralon® reflectance standards was impossible, thus precluding correction for inhomogeneous light distribution and ambient stray light. (Reproduced with permission from Martin de Fonjaudran et al. 2017)

UV light is powerful to distinguish the presence of aged varnishes, areas of reintegration or restoration that have been executed in different media that may have aged differently, and hence may appear less or more fluorescent.

In Fig. 8.2 the fluorescence excitation emission properties of dammar varnish are shown. The graph reflects the multiple indistinguishable fluorophores present in the varnish that all contribute to the emission. In excitation emission spectra, both excitation and emission are measured from a film of varnish by varying the wavelength

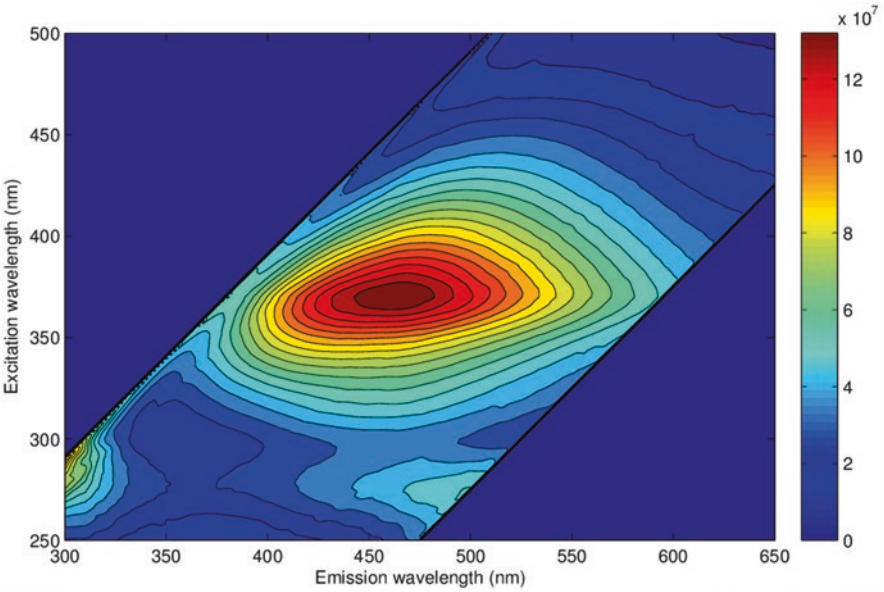

Fig. 8.2 False colour Excitation emission spectrum of Dammar varnish which highlights the broad band emission from the varnish with a maximum at 360/435; the scale refers to the intensity/counts of the emission. (Reproduced with permission from reference Nevin et al. 2009a)

of excitation using a monochromator and a spectrometer equipped with a Xe-lamp source. Depending on the excitation used, a different emission spectrum will be produced. This is relevant for conservation because different lamps/sources with different emissions may produce slightly different coloured fluorescence results. The broad signal and asymmetric shape of the maxima reflect the presence of multiple fluorescent materials that absorb and emit at different wavelengths. Moreover, by studying the excitation emission spectrum of dammar it is possible to measure how fluorescence changes as a consequence of aging and to compare dammar with other similar varnishes.

The fluorescence of varnishes and organic materials continues to fascinate conservators and has received much attention recently – perhaps encouraged by a desire to find simple non-invasive methods for identifying materials that require sampling analysis for their differentiation (Pelagotti et al. 2005). Emission spectra from oil-based films (de la Rie 1982a) and varnishes have broad and often visible signals (de la Rie 1982a; Thoury et al. 2007). Research has confirmed seminal work by De la Rie in 1982 that describes the luminescence of varnishes and the modifications of fluorescence spectra of oil films, dammar and mastic as a consequence of ageing (de la Rie 1982a, 1982b). Indeed the molecular changes that occur in paint media and varnishes as a consequence of photooxidation are detected by fluorescence spectroscopy but cannot be resolved Borgia et al. (1998); for the characterisation of changes on the molecular and atomic level, molecular spectroscopy and mass spectrometry are required (Dietemann et al. 2009).

Table 8.1 Laser Induced Fluorescence of Varnishes, adapted with permission from Nevin, Spoto and Anglos. (Nevin et al. 2012)

Varnish	Laser wavelength/nm	Emission maximum/nm	Lifetime/ns
Amber	337	475	
Colophony	337	420–530	2–8
		480	
	355	435	
Copal	337	405–430	2–9
		450	
	355	456	
Dammar	337	430	
	355	437	7
Elemi	337	410–480	2–9
Mastic	337	430–40	2–8
		450	
	363.8	450	
Sandarac	337	410–460	2–8
		480	
Shellac	337	430–580	2–9
		600–640	2–9
		580/630	3–5
	457.9	606, 632, 680	
Turpentine Resin	337	410–480	2–9
	355	450	16

Table 8.1 summarises the emissions from varnishes excited with a UV laser, and demonstrates how many varnishes give similar emission maxima, with some materials presenting more than one emission band. Variations in emission maxima reflect the complex composition of varnishes and the many molecules present within natural media. Fluorescence is a generated by many molecules within varnishes, hence broad and variable emissions reported in the literature are reasonable (Miyoshi 1990; Nevin et al. 2012). It should be noted that small variations in spectra may give rise to differences in perceived colour. While most varnishes present broad and essentially similar spectra, a notable exception is shellac, a varnish commonly used on furniture, that is known for its orange-red fluorescence emission from laccaic acids. These anthraquinones, also used as pigments, are still present in trace concentrations even in bleached shellac, which has been chemically treated to specifically remove laccaic acids. The emission maxima of other varnishes occur between 410 and 490 nm (Miyoshi 1990) and may depend on their composition, but the identity of the many fluorophores present in aged varnishes is still unknown. It is finally noted that while the shape (colour) of the emission spectrum may be similar, the intensity (brightness) of the fluorescence signal may depend on the type of varnish and ageing (Nevin et al. 2009b). Indeed multiple layers of a linseed oil and colophony based varnish containing madder lake particles in cross-sections may be

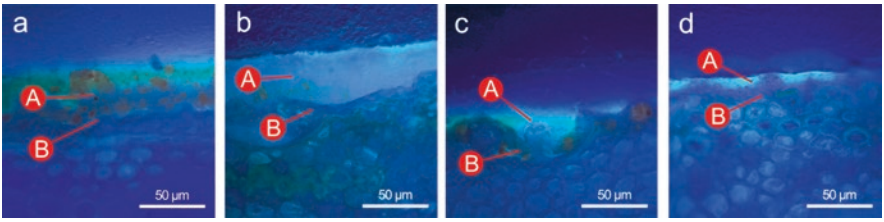

Fig. 8.3 Cross sections observed through the optical microscope under UV illumination: P3 (with madder lake in the varnish) at (a) t = 0 h (before ageing) and (b) at t = 520 h (after ageing); P8 (with madder lake in the priming layer) at (c) t = 0 h (before ageing) and (d) at t = 520 h (after ageing). The letter A indicates the outer linseed oil-colophony varnish layer and B indicates the ammonium caseinate primer layer under the outer varnish coat reproduced from (Fiocco et al. 2018), creative common licence. (http://creativecommons.org/licenses/by/4.0/)

indistinguishable in reflected light, but under UV illumination layers may be clearly identified (Fiocco et al. 2018). Different varnish layers on model samples of wood simulating the coloured varnishes, and the changes in the colour of emissions following exposure to UV light that includes the fading of madder are seen in cross-sections shown in Fig. 8.3.

8.4.1 Examples of Inspection of Varnish and Restorations on Paintings

In the panel painting in Fig. 8.4 there is widespread evidence of reintegration or overpainting – and large brushstrokes of different coloured paint appear dark in UV. Some of the reintegration is apparent in the visible image, especially that on the flesh tones and drapery; in contrast the dark background is not legible in reflected light and instead UV fluorescence gives immediate information about the extent of reintegration, in large brushstrokes used in much of the background and the flesh tones of the male figures, including the area under the turban. In addition to the dark paint, there is another layer of varnish covering other reintegration, which is uniformly bluish. The second type of reintegration painting appears to be finer and is widespread on the drapery of the left figure in hatching, and on Christ's body and face, and appears slightly darker than the brightly fluorescent original paint. This example shows how signal from multiple layers of paint and varnish can contribute to a complex series of treatments that are immediately apparent under UV illumination. The UV image of the panel painting of Saint Lawrence in Fig. 8.5 highlights areas of damage and reintegration, that include paint losses, including an area of paint over a nail hole that served to attach the panel to the altarpiece. Widespread loss of paint around the figure is due to poor adhesion between around areas of gilding; these losses have been restored. The gold background appears light yellow due

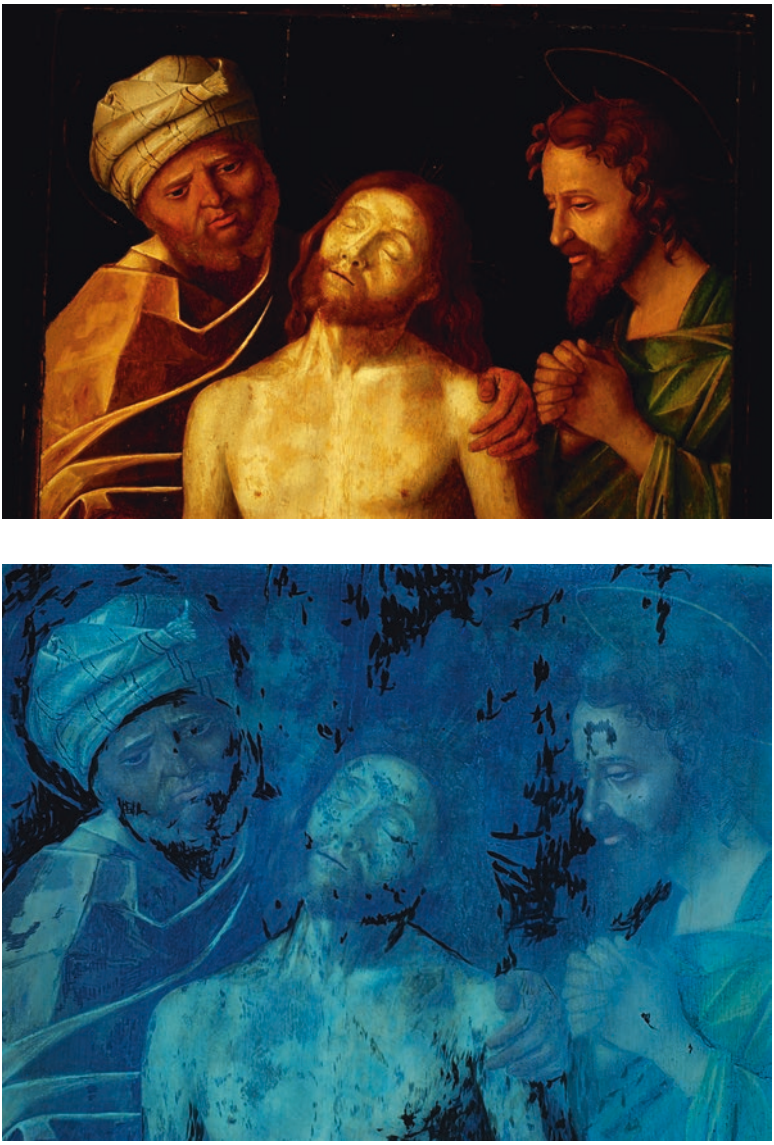

Fig. 8.4 A panel painting by an unknown artist depicting the Lamentation over the dead Christ, private collection, shown in visible (top) and UV light (bottom). A faint bluish hue is seen in a varnish, and the paint in the flesh tones is strongly fluorescent. Slightly pink lips of the figures suggest a red lake pigment. Significant reintegration of paint losses, and likely overpaint is visible in UV-induced fluorescence

Fig. 8.5 Saint Lawrence, Master of the Fogg Pietá, Courtauld Gallery of Art, London, in visible (top) and UV (bottom). Strong luminescence of the flesh tones is apparent, as are areas of reintegration at the top of the head, in fine craquelure pattern and in a rectangular region on the blue drapery

to an ageing varnish. In this painting the red colour of the book under UV is likely an optical effect that is the consequence of the partial absorption of the fluorescence of the superficial varnish by the red paint rather than the emission from the red paint itself. This effect is important and has been described optically by Elias et al. (2009); here the luminescence signal from the varnish is isotropic, or will be generated in forward and backward directions. As a consequence, the luminescent radiation will be reflected/absorbed by underlying pigments, hence the final appearance of the luminescence is not only due to the varnish emission but also from the differential reflection of the underlying layers.

Another example of UV fluorescence applied to study the extent and distribution of restoration is found in Fig. 8.6. The dark background of the painting has areas of reintegration, but these are not visible under normal light. Instead UV fluorescence highlights areas of reintegration over an aged varnish and around the perimeter of the painting and partial reintegration of an area of the face. The authors note that "The actual damage to the paint is more limited than what the UV picture suggests; retouching was carried out on a wider area than the damage" (Saverwyns et al. 2018).

The example of UV fluorescence in Fig. 8.7 shows strongly emitting paint and the use of calibration standards for UV as well as visible photography. Examination of the painting under magnification confirmed the presence of a yellowing varnish. FTIR spectroscopy and mass spectrometric analysis suggest the presence of Laropal K 80 and Dammar on the paint surface but it is not only these varnishes that account for the luminescence of the paint, which includes lead white and cadmium yellows (Ford et al. 2019).

Fig. 8.6 Portrait of Jan Brant, formerly attributed to workshop or school of Pieter Paul Rubens (1577–1640), oil on canvas (65.5 × 56.5 cm), private collection, under a) normal light and b) UV-light illumination. (Reproduced with permission from Saverwyns et al. 2018)

8.4.2 A Note on UV Stabilised Varnishes and Assessing Condition

Significant research has been dedicated to stabilising varnishes with additives to stop them from yellowing, in an effort to minimise retreatment (de la Rie and de la Rie 1988). Different classes of UV light stabilisers include Ultraviolet Light Absorbers (UVA) and Hindered-Amine Light Stabilizers (HALS); Tinuvin ® (which comes in a variety of different formulations identified by numbers) is one commonly used additive that is also available within conservation. Within the context of fluorescence examination, the presence of additives to varnish is of particular relevance as these varnishes may absorb UV and not fluoresce, or, if fluorescent brighteners are added, may produce a broad emission that masks the fluorescence of underlying layers (Ara et al. 2003). In cases where UV absorbers are present, a total barrier to the transmission of UV in the varnish layer is produced, and thus the excitation of underlying materials and retouching is also blocked. As a consequence alterations and modifications to paintings during restorations may no longer be visible under UV light. There are ethical implications in the use of such varnishes for painting conservation: by blocking UV, or by creating a broad fluorescent layer, it is also possible to mask the extent of damage and restoration of paintings (Ara et al. 2003). While this may be less important for museum collections, these considerations are essential for the art market, where the condition of a painting (and the extent of restoration) will have obvious economic consequences.

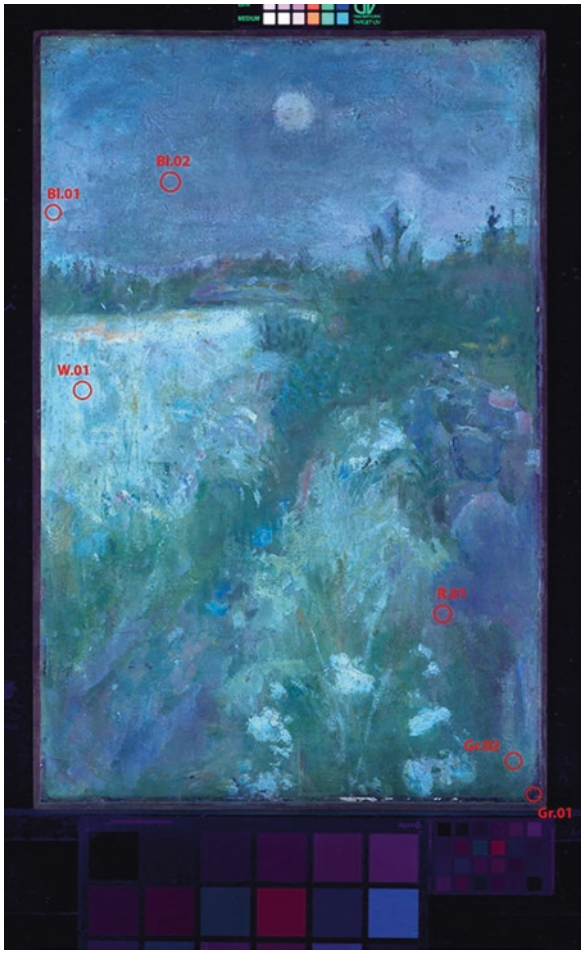

Fig. 8.7 Flower Meadow Field (Woll 148), Edvard Munch, UVA-induced fluorescence photography, showing fluorescence of the upper varnish coating, reproduced with permission from Ford et al. (2019). (http://creativecommons.org/licenses/by/4.0/)

8.5 UV Fluorescence for the Analysis of Binding media

Analysis of binding media – proteins and oils – used as paint has been performed with LIF spectroscopy on a variety of model samples, films and mock-ups of oil- and protein-based binding media, as summarised in Tables 8.2 and 8.3. The reported results of various applications of LIF for binding media analysis are summarised in (Nevin et al. 2012). Although there is potential for discriminating between classes of proteins using fluorescence, as in oils and varnishes, there are multiple molecules including amino acids which give rise to fluorescence in binding media, and thus emission spectra are broad and not specific to particular materials. Therefore, despite excellent results on model samples (Nevin et al. 2006), the identification of binding media is not generally possible based on fluorescence spectroscopy.

Table 8.2 Fluorescence and binding media, after (Nevin et al. 2012)

Substrate	Excitation/ nm	Emission/ nm	Attribution
Oil-Linseed films	363.8	685	Mainly assessment for diagnostic purposes; generally LIF signal too broad, fluorescence ascribed to 'large organic molecules'
Oil-Linseed and Lead white films		588	
Protein-casein films		456	
Protein-egg white films		588	
Resin-Mastic films/lumps		450	
Varnish-Shellac films/lumps	457.9	606, 632, 680	
Oil-Linseed films	365	460–530	Autooxidation/Polymerisation

Table 8.3 Laser Induced fluorescence spectroscopy of binding media, attributions are given only when reported, after (Nevin et al. 2012)

Binding medium	Excitation wavelength/nm	Emission wavelength/nm	Attribution
Animal glue	355	440, 415, ~480	Pyridinoline, di-tyrosine, dihydroxyphenylalanine and related products
Casein	355	435	Oxidation products
	363.8	456	
Egg White	355	435	Oxidation products
Egg Yolk	337	425	
Egg yolk -linseed oil- tempera	248	450	
Oil-Linseed - aged 1 year	363.8	492	
Oil-Linseed - aged 50 years	363.8	685	
Wax	337	500–550	

The fluorescence of selected tryptophan-containing binding media (egg white, egg yolk and casein) in solution has been proposed (Tseitlina and Kozhukn 1990), following the analysis of gluten-based binders. Laser Induced Fluorescence of selected films of proteinaceous materials (casein and egg white) has been published that suggest that if excited in below 300 nm, it is possible to discriminate signals that originate from amino acids tryptophan and tyrosine (Nevin et al. 2007). If longer wavelengths closer to those from standard UV lamps are employed, UV will not excite fluorophores from amino acids, and hence results from fluorescence analysis

may not allow the discrimination between proteins. Indeed spectroscopic discrimination between protein-based binding media (egg white and casein, egg yolk and animal glues) requires the use of excitation below 300 nm (thus far below the commonly found UV excitation sources). While egg yolk films emit at 425 nm, addition of a drying oil causes a shift to 450 nm (Castillejo et al. 2002). Fluorescence from films of linseed oil shifts from 490 to 685 nm with natural ageing. In some cases, the addition of pigment to protein-based and oil-based films does not necessarily obscure the fluorescence from the binder, but may cause spectral distortions of fluorescence (Pelagotti et al. 2005), that can be mathematically corrected. Generally, the strength of the emission from binding media is weak in comparison with that from varnishes and many inorganic and organic pigments.

8.6 UV Fluorescence for the Analysis of Pigments

For the purposes of this work, it is important to note that fluorescence may help in the detection of modern anachronistic pigments on historical paintings (for example to detect repainting). Broadly, fluorescent pigments can be classified as natural organic pigments (for example cochineal lakes, sappanwood), synthetic organic pigments (for example di-azo pigments) or synthetic inorganic pigments (including doped glasses and semiconductor pigments) (Pozza et al. 2000). A summary of the fluorescence properties of different pigments which have been analysed with LIF is given in (Nevin et al. 2012) and in Table 8.4.

Applications of fluorescence spectroscopy for the analysis of inorganic pigments (Pelagotti et al. 2005) and organic pigments have distinguished materials based on differences in fluorescence emissions and time-resolved measurements of fluorescence emissions (Clementi et al. 2008). Indeed a major application of fluorescence spectroscopy is in the analysis of pigments, many of which fluoresce, and painting conservators often have training in the identification of pigments using optical microscopy and UV fluorescence excitation (Easthugh et al. 2001).

Table 8.4 Laser Induced Fluorescence Spectroscopy of selected pigments, adapted from (Nevin et al. 2012)

Pigment	Excitation wavelength/nm	Emission maxima/nm
Egyptian Blue	various	950
Sappanwood	337	600
Lake (cochineal)	337,	630–640
Curcumin	248, 337	540–560
TiO_2	248, 355	473
ZnO	248, 337, 355	385, 530
Cd Yellows	337, 355	485–528
Cd Reds	355, 337	585–640

While it may not be straightforward to distinguish specific anthraquinone-based pigments based on fluorescence, some organic and inorganic pigments give specific and recognisable luminescence that may allow their identification (Clementi et al. 2012; Melo and Claro 2010). For example, semi-conductor pigments including cadmium yellow and reds present characteristic luminescence in the visible and IR (Anglos et al. 1996).

Semi-conductor pigments including ZnO, and cadmium-based yellows and reds exhibit emissions that may produce striking emissions in the UV (see Fig. 8.7 for examples of the orangish emission from Cd yellows). For cadmium pigments, both the colour of the pigment and the fluorescence emissions increase in wavelength with increasing concentration of Se. It is also noted that degradation of Cd yellows may generate a change in the fluorescence emission of pigments (Comelli et al. 2019). Another remarkable case of well-known and unique luminescence comes from the trapped Cu^{+2} ions in cuprorivaite, and the B2g-B1g transition in Cu^{2+} (Pozza et al. 2000). As a consequence Egyptian Blue, which exhibits a strong IR emission centred at 950 nm can be detected rapidly using IR photography for the study of ancient painted artifacts (Verri 2009). Surprising examples of traces of the blue pigment on ancient polychromy highlight the very high quantum yield of the pigment, allowing the efficient detection of the pigment in trace concentrations.

8.6.1 Inorganic Pigments

Zinc White has a sharp emission at 380 nm, a consequence of the band gap between the excited and ground state of the molecule, and a greenish emission due to trapped electrons in defects (Artesani et al. 2017; Thoury et al. 2011). The spectrum of the visible emission, which is due to trapped states in the molecule, will depend on the intensity of the excitation, a feature also observed for Cd pigments where band gap and trap states both produce luminescence (Cesaratto et al. 2014). As mentioned above, the fluorescence of zinc white is related to the band gap in the pigment as well as defects that may be introduced during its synthesis. In a survey of paintings by Alessandro Milesi, Laser induced fluorescence, Fluorescence lifetime imaging and other X-ray fluorescence spectroscopy highlighted significant differences in the emission spectra of areas containing zinc white as seen in the graph in Fig. 8.8 (Giorgi et al. 2019). The main emission of ZnO is at approximately 380 nm, which falls beneath the detection by the human eye, while other signals are from the emission from trapped states or defects in the ZnO pigments – these appear greenish in colour but the hue of emissions differs among the paintings studied.

Another striking example of semiconductor luminescence is found in the study of Van Gogh's painting "Les bretonnes et le pardon de pont Aven" in Fig. 8.9 (Omelli 2012). In this example the luminescence was recorded with a multispectral imaging device which allowed the capture of the spectrum of the UV luminescence. Additional analysis using Fluorescence Lifetime Imaging confirmed a long lived

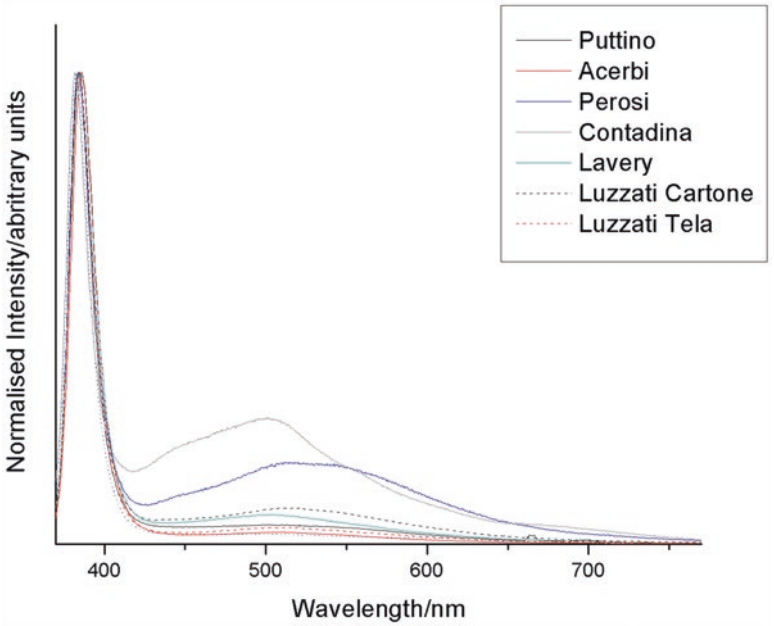

Fig. 8.8 Laser Induced Fluorescence spectra demonstrate significant differences in the green emission from white areas recorded from different paintings by Alessandro Milesi from the Collection of Ca' Pesaro, Venice. Spectra are shown normalised to the emission between 380 and 390 nm for clarity. (Reprinted with permission from Giorgi et al. (Clementi et al. 2008; Giorgi et al. 2019))

phosphorescence signal from the white pigment with lifetime of 1500 ms, similar to emissions found from ZnO in other nineteenth C. paintings (Giorgi et al. 2019).

It is worth noting finally that, on the macro scale, luminescence may appear to be relatively uniform, while on the micro scale, there are large variations in the luminescence of powdered pigments. For example, in studies of historical lithopone pigment ($ZnS+BaSO_4$), Bellei et al. demonstrated how different coloured emissions relate to the impurities from trace elements that include ions from Cu, Mn and Ag, giving rise to heterogenous emissions which are best appreciated under the microscope (Bellei et al. 2015).

8.6.2 Organic Pigments

While the emissions from inorganic pigments may be from a variety of physical phenomena, for organic pigments (both synthetic and natural) fluorescence occurs due to the presence of delocalised electrons in molecules containing multiple aromatic rings (for example anthraquinones), long-chains of conjugated double bonds and aromatic rings (curcumin), di-azo pigments (for example Hansa yellow)

Fig. 8.9 Luminescence from Vincent Van Gogh's painting on paper «Les bretonnes et le pardon de pont Aven», Galleria dell'Arte Moderna, Milano (bottom). Here the bright green emissions from Zinc White (top) are apparent where the white pigment is mixed with blue in the multiple headdresses of the figures in the painting. Other emissions are seen in the yellow paint, and are likely from a Cd-yellow. (Reproduced with permission from Comelli et al. (2012))

(Romani et al. 2008). Nonetheless, generally emission bands from organic molecules are broad which may compromise the differentiation between similar pigments with fluorescence spectroscopy. Measurements of fluorescence lifetime have been proposed as a viable method for discriminating between laccaic acids and carminic acids (Clementi et al. 2012), the main anthraquinone components of two organic dyes and related pigments (Indian lac and cochineal, respectively) that have similar fluorescence emissions but different bi-exponential fluorescence lifetimes.

Calculations of the quantum yield of Lac suggest that the dye was applied in manuscripts rather than a pigment based on a precipitated aluminium complex Melo and Claro (2010).

An example of the bright pink emission found in red lake pigments is found in the painting of a Bishop Saint in Fig. 8.10. Based on the fourteenth C. dating of the painting the red paint is likely to be madder, but this has not been confirmed. In the UV image paint losses (again related to the presence of a nail in the wooden panel) and reintegration are both immediately apparent and appear dark, as is the relatively dark signal from the varnish covering the gilding. Luminescence is also observed in the flesh tones and the white gloves and other areas of white paint.

In another example in Fig. 8.11, UV fluorescence is used during preliminary investigations to map the presence of a red pigment which is ascribed to madder lake in a ceiling painting by Bignami (Conejo-Barboza et al. 2020). Comparisons with a colour checker containing a set of reference paintouts support the attribution to madder, based on the orange-red fluorescence, but the positive identification of madder requires sampling and complementary analysis – including but not limited to spectrofluorescence. The blueish hue seen in the image is attributed to a varnish on the painting.

8.7 Conclusions

UV fluorescence examination plays a fundamental role in the documentation of paintings and the routine use of the UV lights in conservation studies. Careful interpretation of fluorescence images and fluorescence spectra requires experience and complementary information – that may be from X-radiography, Infrared reflectography or other elemental and molecular analyses. In some cases, fluorescence spectroscopy can yield unique information regarding the electronic transitions and surface reactions that occur in semi-conductor pigments and may allow the identification of specific classes of pigments – especially when pigments are observed under the microscope so that data about their colour and morphology can be used to inform interpretation. Within the context of authentication and assessment of condition fluorescence may be used to better guide analysis of pigments, and establish the extent of restoration in a painting. However, barrier varnishes need to be carefully assessed in case these may mask past treatments.

Fig. 8.10 Bishop Saint, Master of the Fogg Pietà, Courtauld Gallery, Visible (top) and UV fluorescence (bottom) images of the panel highlight the condition of the painting, areas of reintegration, and the bright fluorescence signal from lake pigments (pink) and white paint. Note also the dark background, and lack of fluorescence from the greens.

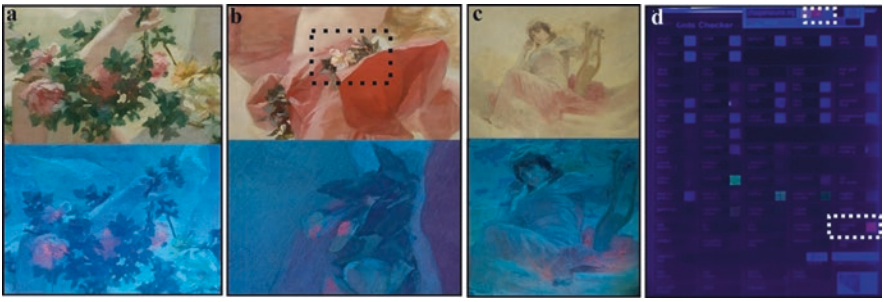

Fig. 8.11 Comparison between Vis and Fluorescent response under UV radiation in areas of (**a**) The Poetry, (**b**) The Dance, (**c**) The Music, and (**d**) Pigment Checker from CHSOS, white rectangles show the Madder lake from Conejo-Barboza et al. (Conejo-Barboza et al. 2020)

References

Aldovrandi, A., Buzzegoli, E., Keller, A., Kunzelman, D.: Indagini su superfici dipinte mediante immagini UV riflesse in falso colore. OPD Restauro. **16**, 83–199 (2004)

Anglos, D., Solomidou, M., Zergioti, I., Zafiropulos, V., Papazoglou, T.G., Fotakis, C.: Laser-induced fluorescence in artwork diagnostics: an application in pigment analysis. Appl. Spectrosc. **50**, 1331–1334 (1996). https://doi.org/10.1366/0003702963904863

Ara, K., Folkes, S., Green, T., Howell, S., Tasker, N., Walker, A.: Some ethical implications of using ultra-violet barrier varnishes. Pict. Restor. **24** (2003)

Artesani, A., Gherardi, F., Nevin, A., Valentini, G., Comelli, D.: A photoluminescence study of the changes induced in the zinc white pigment by formation of zinc complexes. Materials (Basel). **10**, 340 (2017). https://doi.org/10.3390/ma10040340

Bacci, M., Picollo, M.: Non-destructive spectroscopic detection of cobalt(II) in paintings and glass. Stud. Conserv. **41**, 136–144 (1996). https://doi.org/10.1179/sic.1996.41.3.136

Bellei, S., Nevin, A., Cesaratto, A., Capogrosso, V., Vezin, H., Tokarski, C., et al.: Multianalytical study of historical luminescent lithopone for the detection of impurities and trace metal ions. Anal. Chem. **87**, 6049–6056 (2015). https://doi.org/10.1021/acs.analchem.5b00560

Berrie, B., Thoury, M.: Examination of luminescence of cross sections. UV-Vis Lumin. imaging Tech. Técnicas imagen luminiscencia UV-Vis, (2020)

Borgia, R., Fantoni, C., Flamini, T.M.D., Palma, A.G., Guidoni, A.: Mele, luminescence from pigments and resins for oil paintings induced by laser excitation. Appl. Surf. Sci. **127**, 95–100 (1998). https://doi.org/10.1016/S0169-4332(97)00616-8

Capua, R.: The obscure history of a ubiquitous pigment: phosphorescent lithopone and its appearance on drawings by John La Farge. J. Am. Inst. Conserv. **53**(2), 75–88 (2014). https://doi.org/10.1179/1945233014Y.0000000022

Carden, M.L.: Use of ultraviolet light as an aid to pigment identification. APT Bull. **23**, 26 (1991). https://doi.org/10.2307/1504337

Castillejo, M., Martín, M., Oujja, M., Silva, D., Torres, R., Manousaki, A., et al.: Analytical study of the chemical and physical changes induced by KrF laser cleaning of tempera paints. Anal. Chem. **74**, 4662–4671 (2002). https://doi.org/10.1021/ac025778c

Cesaratto, A., D'Andrea, C., Nevin, A., Valentini, G., Tassone, F., Alberti, R., et al.: Analysis of cadmium-based pigments with time-resolved photoluminescence. Anal. Methods. **6**(1), 130–138 (2014). https://doi.org/10.1039/C3AY41585F

Clementi, C., Doherty, B., Gentili, P.L., Miliani, C., Romani, A., Brunetti, B.G., et al.: Vibrational and electronic properties of painting lakes. Appl. Phys. A Mater. Sci. Process. **92**, 25–33 (2008). https://doi.org/10.1007/s00339-008-4474-6

Clementi, C., Rosi, F., Romani, A., Vivani, R., Brunetti, B.G., Miliani, C.: Photoluminescence properties of zinc oxide in paints: a study of the effect of self-absorption and passivation. Appl. Spectrosc. **66**, 1233–1241 (2012). https://doi.org/10.1366/12-06643

Colao, F., Caneve, L., Palucci, A., Fantoni, R., Fiorani, L.: Scanning hyperspectral lidar fluorosensor for fresco diagnostics in laboratory and field campaigns. In: Proc. Int. Conf. LACONA, Vol. 7, pp. 149–155 (2008)

Comelli, D., MacLennan, D., Ghirardello, M., Phenix, A., Schmidt Patterson, C., Khanjian, H., et al.: Degradation of cadmium yellow paint: new evidence from photoluminescence studies of trap states in Picasso's Femme (Époque des "Demoiselles d'Avignon"). Anal. Chem. **91**, 3421–3428 (2019). https://doi.org/10.1021/acs.analchem.8b04914

Comelli, D., Nevin, A., Brambilla, A., Osticioli, I., Valentini, G., Toniolo, L., et al.: On the discovery of an unusual luminescent pigment in Van Gogh's painting "Les bretonnes et le pardon de pont Aven". Appl. Phys. A Mater. Sci. Process. **106**, 25–34 (2012). https://doi.org/10.1007/s00339-011-6665-9

Comelli, D., Valentini, G., Cubeddu, R., Toniolo, L.: Fluorescence lifetime imaging and fourier transform infrared spectroscopy of Michelangelo's David. Appl. Spectrosc. **59**, 1174–1181 (2005). https://doi.org/10.1366/0003702055012663

Comelli, D., Valentini, G., Nevin, A., Farina, A., Toniolo, L., Cubeddu, R.: A portable UV-fluorescence multispectral imaging system for the analysis of painted surfaces. Rev. Sci. Instrum. **79**, 086112 (2008). https://doi.org/10.1063/1.2969257

Conejo-Barboza, G., Libby, E., Marín, C., Herrera-Sancho, O.A.: Discovery of Vespasiano Bignami paintings at the National Theatre of Costa Rica through technical photography and UV–Vis spectroscopy. Herit. Sci. **8**, 125 (2020). https://doi.org/10.1186/s40494-020-00470-4

Cosentino, A.: Identification of pigments by multispectral imaging; a flowchart method. Herit. Sci. **2**, 8 (2014). https://doi.org/10.1186/2050-7445-2-8

de la Rie, E.R.: Fluorescence of paint and varnish layers (Part 1). Stud. Conserv. **27**, 1–7 (1982a). https://doi.org/10.1179/sic.1982.27.1.1

de la Rie, E.R.: Fluorescence of paint and varnish layers (Part II). Stud. Conserv. **27**, 65–69 (1982b). https://doi.org/10.1179/sic.1982.27.2.65

de la Rie, E.R.: Polymer stabilizers. a survey with reference to possible applications in the conservation field. Stud. Conserv. **33**, 9–22 (1988). https://doi.org/10.2307/1506236

Dietemann, P., Higgitt, C., Kälin, M., Edelmann, M.J., Knochenmuss, R., Zenobi, R.: Aging and yellowing of triterpenoid resin varnishes – Influence of aging conditions and resin composition. J. Cult. Herit. **10**, 30–40 (2009). https://doi.org/10.1016/j.culher.2008.04.007

Dyer, J., Sotiropoulou, S.: A technical step forward in the integration of visible-induced luminescence imaging methods for the study of ancient polychromy. Herit. Sci. **5**, 24 (2017). https://doi.org/10.1186/s40494-017-0137-2

Dyer, J., Verri, G., Cupitt, J.: Multispectral Imaging in Reflectance and Photo-induced Luminscence Modes: A User Manual. The British Museum, London (2013)

Easthugh, N., Walsh, V., Chapman, T., Siddall, R.: Pigment Compendium: A Dictionary and Optical Microscopy of Historic Pigments. Elsevier Butterworth Heinemann, Oxford (2001)

Elias, M., Magnain, C., Barthou, C., Nevin, A., Comelli, D., Valentini, G.: UV-fluorescence spectroscopy for identification of varnishes in works of art: influence of the underlayer on the emission spectrum. In: Pezzati, L., Salimbeni, R. (eds.) O3A Opt. Arts, Archit. Archaeol. II, Vol. 7391, p. 739104. International Society for Optics and Photonics (2009). https://doi.org/10.1117/12.825093

Feller, R.L. (ed.): Artists' Pigments A Handbook of Their History and Characteristics, vol 1. National Gallery of Art, Washington, D.C. (1986)

Fiocco, G., Rovetta, T., Gulmini, M., Piccirillo, A., Canevari, C., Licchelli, M., et al.: Approaches for detecting madder lake in multi-layered coating systems of historical bowed string instruments. Coatings. **8**, 171 (2018). https://doi.org/10.3390/coatings8050171

Fischer, C., Kakoulli, I.: Multispectral and hyperspectral imaging technologies in conservation: current research and potential applications. Stud. Conserv. **51**, 3–16 (2006). https://doi.org/10.1179/sic.2006.51.Supplement-1.3

Ford, T., Rizzo, A., Hendriks, E., Frøysaker, T., Caruso, F.: A non-invasive screening study of varnishes applied to three paintings by Edvard Munch using portable diffuse reflectance infrared Fourier transform spectroscopy (DRIFTS). Herit. Sci. **7**, 84 (2019). https://doi.org/10.1186/s40494-019-0327-1

Ghirardello, M., Valentini, G., Toniolo, L., Alberti, R., Gironda, M., Comelli, D.: Photoluminescence imaging of modern paintings: there is plenty of information at the microsecond timescale. Microchem. J. **154**, 104618 (2020). https://doi.org/10.1016/j.microc.2020.104618

Giorgi, L., Nevin, A., Comelli, C., Frizzi, T., Alberti, R., Zendri, E., Piccolo, M., Izzo, F.C.: In-situ technical study of modern paintings - part 2: imaging and spectroscopic analysis of zinc white in paintings from 1889 to 1940 by Alessandro Milesi (1856–1945). Spectrochim. Acta A Mol. Biomol. Spectrosc. **219**, 504–508 (2019). https://doi.org/10.1016/j.saa.2019.04.084

Grant, M.S.: The use of ultraviolet induced visible-fluorescence in the examination of museum objects, part II. Museum. **10**(1), 4 (2000)

Hickey-Friedman, L.: A review of ultra-violet light and examination techniques. Objects Spec. Gr. Postprints, Vol. 9, pp. 161–168. The American Institute for Conservation of Historic & Artistic Works, Washington, DC (2002)

Keller, A., Lenz, R., Artesani, A., Mosca, S., Comelli, D., Nevin, A.: Exploring the ultraviolet induced infrared luminescence of titanium white pigments. In: Fuster López, L., Stols-Witlox, M., Picollo, M. (eds.) UV-vis Luminescence Imaging Techniques/Técnicas de Imagen de Luminiscencia UV-vis. Editorial Univ. Politècnica de València (2020)

Lakowicz, J.R.: Principles of Fluorescence Spectroscopy. Springer, Boston (2006). https://doi.org/10.1007/978-0-387-46312-4

Larson, L.J., Shin, K.-S.K., Zink, J.I.: Photoluminescence spectroscopy of natural resins and organic binding media of paintings. J. Am. Inst. Conserv. **30**, 89–104 (1991). https://doi.org/10.1179/019713691806373231

Magrini, D., Bracci, S., Sandu, I.C.A.: Fluorescence of organic binders in painting cross-sections. Procedia Chem. **8**, 194–201 (2013). https://doi.org/10.1016/j.proche.2013.03.025

Martin de Fonjaudran, C., Acocella, A., Accorsi, G., Tamburini, D., Verri, G., Rava, A., et al.: Optical and theoretical investigation of Indian yellow (euxanthic acid and euxanthone). Dyes Pigments. **144**, 234–241 (2017). https://doi.org/10.1016/j.dyepig.2017.05.034

Melo, M.J., Claro, A.: Bright light: microspectrofluorimetry for the characterization of lake pigments and dyes in works of art. Acc. Chem. Res. **43**(6), 857–866 (2010). https://doi.org/10.1021/ar9001894

Miyoshi, T.: Fluorescence from varnishes for oil paintings under n2 laser excitation. Jpn. J. Appl. Phys. **26**, 780–781 (1987). https://doi.org/10.1143/JJAP.26.780

Miyoshi, T.: Fluorescence from resins for oil painting under N2 laser excitation. Jpn. J. Appl. Phys. **29**, 1727–1728 (1990). https://doi.org/10.1143/JJAP.29.1727

Nevin, A., Cather, S., Anglos, D., Fotakis, C.: Analysis of protein-based binding media found in paintings using laser induced fluorescence spectroscopy. Anal. Chim. Acta. **573–574**, 341–346 (2006). https://doi.org/10.1016/j.aca.2006.01.027

Nevin, A., Comelli, D., Valentini, G., Anglos, D., Burnstock, A., Cather, S., et al.: Time-resolved fluorescence spectroscopy and imaging of proteinaceous binders used in paintings. Anal. Bioanal. Chem. **388**, 1897–1905 (2007). https://doi.org/10.1007/s00216-007-1402-0

Nevin, A., Anglos, D., Cather, S., Burnstock, A.: The influence of visible light and inorganic pigments on fluorescence excitation emission spectra of egg-, casein- and collagen-based painting media. Appl. Phys. A Mater. Sci. Process. **92**, 69–76 (2008). https://doi.org/10.1007/s00339-008-4460-z

Nevin, A., Comelli, D., Osticioli, I., Toniolo, L., Valentini, G., Cubeddu, R.: Assessment of the ageing of triterpenoid paint varnishes using fluorescence, Raman and FTIR spectroscopy. Anal. Bioanal. Chem. **395**, 2139–2149 (2009a). https://doi.org/10.1007/s00216-009-3005-4

Nevin, A., Echard, J.-P., Thoury, M., Comelli, D., Valentini, G., Cubeddu, R.: Excitation emission and time-resolved fluorescence spectroscopy of selected varnishes used in historical musical instruments. Talanta. **80**, 286–293 (2009b). https://doi.org/10.1016/j.talanta.2009.06.063

Nevin, A., Spoto, G., Anglos, D.: Laser spectroscopies for elemental and molecular analysis in art and archaeology. Appl. Phys. A Mater. Sci. Process. **106**, 339–361 (2012). https://doi.org/10.1007/s00339-011-6699-z

Pelagotti, A., Bevilacqua, N., Vascotto, V., Daffara, C.: A study of UV fluorescence emission of painting materials. Art '05–8th Int. Conf. Non-Destructive Investig. Microanal. Diagnostics Conserv. Cult. Environ. Herit., Lecce (Italy), pp. 1–14 (2005)

Picollo, M., Stols-Witlox, M., Fuster-López, L.: UV-Vis Luminescence imaging techniques/Técnicas de imagen de luminiscencia UV-Vis. Editorial Universitat Politècnica de València. (2019). https://doi.org/10.4995/360.2019.110002

Plesters, J.: Cross-sections and chemical analysis of paint samples. Stud. Conserv. **2**(3), 110–157 (1956). https://doi.org/10.1179/sic.1956.015

Pozza, G., Ajò, D., Chiari, G., De Zuane, F., Favaro, M.: Photoluminescence of the inorganic pigments Egyptian blue, Han blue and Han purple. J. Cult. Herit. **1**, 393–398 (2000). https://doi.org/10.1016/S1296-2074(00)01095-5

Rogge, C.E., Lough, K.: Fluorescence fails: analysis of UVA-induced visible fluorescence and false-color reflected UVA images of tintype varnishes do not discriminate between varnish materials. J. Am. Inst. Conserv. **55**, 138–147 (2016). https://doi.org/10.1080/01971360.2016.1155813

Romani, A., Clementi, C., Miliani, C., Brunetti, B.G., Sgamellotti, A., Favaro, G.: Portable equipment for luminescence lifetime measurements on surfaces. Appl. Spectrosc. **62**, 1395–1399 (2008). https://doi.org/10.1366/000370208786822250

Rorimer, J.: Ultra-violet rays and their use in the examination of works of art. The Metropolitan Museum of Art, New York (1931)

Saverwyns, S., Currie, C., Lamas-Delgado, E.: Macro X-ray fluorescence scanning (MA-XRF) as tool in the authentication of paintings. Microchem. J. **137**, 139–147 (2018). https://www.sciencedirect.com/science/article/abs/pii/S0026265X17307051. https://doi.org/10.1016/j.microc.2017.10.008

Saunders, D.: Image documentation for paintings conservation. In: Stoner, J.H., Rushfield, R. (eds.) Conservation Easel Paint, pp. 277–280. Routledge, Abingdon (2012)

Thoury, M., Elias, M., Frigerio, J.M., Barthou, C.: Nondestructive varnish identification by ultraviolet fluorescence spectroscopy. Appl. Spectrosc. **61**, 1275–1282 (2007). https://doi.org/10.1366/000370207783292064

Thoury, M., Echard, J.-P., Réfrégiers, M., Berrie, B., Nevin, A., Jamme, F., et al.: Synchrotron UV−visible multispectral luminescence microimaging of historical samples. Anal. Chem. **83**, 1737–1745 (2011). https://doi.org/10.1021/ac102986h

Tseitlina, M., Kozhukn, N.: Luminescence study of protein binders used in painting. ICOM Comm. Conserv. 9th Trienn. Meet. Prepr., Dresden, German Democratic Republic (1990)

Verri, G.: The spatially resolved characterisation of Egyptian blue, Han blue and Han purple by photo-induced luminescence digital imaging. Anal. Bioanal. Chem. **394**, 1011–1021 (2009). https://doi.org/10.1007/s00216-009-2693-0

Verri, G.: Broad-band, photo-induced, steady-state luminescence imaging in practice. In: Fuster López, L., Nicoline Witlox, M.-J., Picollo, M. (eds.) UV-Vis Lumin. Imaging Tech. Técnicas imagen luminiscencia UV-Vis, Editorial Universitat Politècnica de València (2019). https://doi.org/10.4995/360.2019.110002

Chapter 9
Analysis of Natural and Synthetic Organic Lakes and Pigments by Chromatographic and Mass Spectrometric Techniques

Francesca Sabatini and Ilaria Degano

Abstract This chapter aims to provide an overview of natural and synthetic organic lakes and pigments and of how their analysis by chromatography and mass spectrometry can provide useful information in the examination of works of art. The characteristics of natural organic colourants are reviewed, including information on their provenance and uses in the production of lakes; information on the date of production, availability as paint products and application in artworks of the most important synthetic organic pigments is also provided. This chapter specifically illustrates the state-of-the-art of organic pigments analysis by high performance liquid chromatography with different detectors, and by gas chromatography – mass spectrometry also coupled to analytical pyrolysis. Different mass spectrometry based techniques used both as detector and directly applied on a sample or its extract are also presented. Particular attention is paid to sample preparation; further issues related to difficulties in finding relevant standards or reference materials and understanding photo-degradation processes occurring in degraded organic pigments are also discussed. Several case studies are presented, showing the potentialities of liquid chromatography interfaced with mass spectrometry in determining properties of the samples which can be of assistance for assessing the provenance, dating or even the authenticity of a painting.

Keywords High performance liquid chromatography · Mass spectrometry · Organic lakes · Synthetic organic pigments · Paint materials

F. Sabatini · I. Degano (✉)
Dipartimento di Chimica e Chimica Industriale, Pisa, Italy
e-mail: ilaria.degano@unipi.it

M. P. Colombini et al. (eds.), *Analytical Chemistry for the Study of Paintings and the Detection of Forgeries*, Cultural Heritage Science,
https://doi.org/10.1007/978-3-030-86865-9_9

9.1 Introduction

Organic lakes and pigments have been used in paintings and in ink formulations since pre-history. Their composition is, in some cases, specific to a time period or a geographical area, thus their identification may provide data for dating purposes or even for establishing authorship. Unfortunately, the analysis of organic lakes and pigments in artworks and in painting matrices is particularly arduous for the chemist. In addition to the analytical issues that must be overcome when we deal with the analysis of any microsample from a work of art, such as the small amount and representativeness of the sample available and the low concentration in which analytes are present, several other factors have to be considered, such as the lack of reliable recipes for lake preparation, or the uninformative product names provided by modern manufacturers due to patent wars. Finally, organic colourants are amongst the most fugitive species in works-of-art, and thus their composition as determined today strongly depends on the condition of the painting, which may have undergone irreversible degradation.

Consequently, the study of the composition in terms of colouring molecules of organic dyes and pigments can provide important information on the origin and dating of an object, given that a thorough comparison with reference materials, possibly also subjected to natural and artificial ageing, is correctly performed.

This chapter presents the main natural and synthetic organic lakes along with their most important characteristics for establishing provenance and dating. State-of-the-art methods of detection and identification of organic pigments and lakes based on chromatography and mass spectrometry will be reviewed, and specific issues related to sample treatment and photo-ageing processes will be presented. The level of information achievable by the analysis of organic pigments will be illustrated through selected case studies.

9.1.1 Natural Organic Lakes

In antiquity, organic coloured paint materials were obtained from natural sources derived from plant extracts or from the metabolism of insects or molluscs. Ancient Egyptians were the first to develop dye extraction procedures and to document them accurately in hieroglyphics (Zollinger 2003). The introduction of indigo, Tyrian purple, and the reds madder and cochineal were main milestones in the artistic and economical history of natural dyes (Zollinger 2003). Notably, different cultures around the globe developed methods to extract such colours, even if from different autochthonous plants or animal species. These dyes were used for colouring textiles, and for the preparation of organic pigments. Organic dyes and pigments differ in their solubility in water and in other binding media: dyes are soluble in binding media while pigments are insoluble (Colombini and Modugno 2009), and lakes are generally obtained by precipitation as salts, absorption on inert and colourless

substrates and/or complexed as metal salts (Herbst et al. 2004; Kirby et al. 2005a, 2014). By this procedure, coloured insoluble particles are formed (through complexation or absorption phenomena), and can be separated by precipitation and filtration, washed and dried to obtain a solid lake pigment. The most commonly salt used in lake production was alum, and in particular hydrated potassium aluminium sulphate ($KAl(SO_4)_2 \cdot 12H_2O$), which was also employed as a mordant for textile dyeing. Other salts used in lake production were chalk (calcium sulphate, $CaSO_4$) and gypsum (calcium sulphate dihydrate, $CaSO_4 \cdot 2H_2O$). The metallic cation chosen may change and influence the colour shades that are produced.

Over the centuries, artists have applied lakes with different painting techniques and on several supports. Lakes have performed a less important role in classic painting compared to inorganic pigments because most of them exhibit lower lightfastness and great sensitivity to atmospheric agents and to pH variations. As a consequence, lakes were applied in a great extent for miniatures in illuminated manuscripts, and in a less extent in mural paintings and in easel or canvas painting. Notwithstanding this, evidence of the use for millennia of madder lake, purple and indigo pigments in wall painting and paint decorations on ceramics, and in codices, has been found by scientific examinations. Madder was identified on funerary vessels and in Pompei's pigments (Andreotti et al. 2017; Colombini et al. 2017) while purple was used in Thera wall paintings (Karapanagiotis et al. 2017), in Macedonia and Magna Grecia funerary paintings (Andreotti et al. 2017), and indigo is the main ingredient of Maya blue (Grazia et al. 2020). Finally, yellow organic dyestuffs such as saffron (*Crocus sativus*), Buckthorn/Persian berries (*Rhamnus* spp.), and weld (*Reseda luteola* L.) have been used to produce lake pigments in works of art since antiquity (Ciatti and Marini 2009; Mayhew et al. 2013; Saunders and Kirby 1994).

If a survey is made of the recipes used in Europe between the fifteenth and the nineteenth centuries, the dyestuffs most frequently mentioned are those extracted from redwoods (brazilwood), madder, and the scale insects kermes, cochineal and Indian lac (Kirby and White 1996). Most of these natural sources were available in Europe since antiquity, while some others have been imported since early times from India and South and Central America (Kirby et al. 2014). In Fig. 9.1, the geographical locations of some natural sources of red dyes used to produce lake pigments are depicted. Lakes produced with these materials are characterized by a low colouring power given by the dye and translucency provided by substrate (Kirby and White 1996). From the study of recipes from the European and Mediterranean area and the material analysis of paintings, a timeline can be identified in the use of these materials: up to the early seventeenth century, brazilwood, lac and shearings of cloth dyed with kermes ("cimatura de grana") were the most common sources for lake production. It is worth noting that some confusion can be generated by the inconsistent nomenclature of raw materials and final products reported in ancient treatises and recipes, and the paucity of details provided, which sometimes refer to undefined "common practices". Fake pigments (e.g. "fake purple") are attested since medieval times, and guild regulations were often disregarded by dyers and manufacturers (Saez et al. 2019). From the late sixteenth century onwards, cochineal became more common, because of the increased availability of scale insects

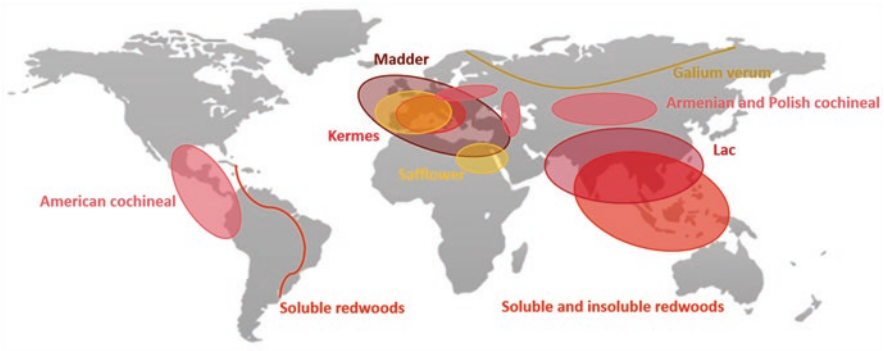

Fig. 9.1 Map showing the geographical location of natural sources of red dyes. (Adapted from Kirby et al. 2014)

from South America, and by the nineteenth century the most important sources have been cochineal and madder, while lac and kermes are barely mentioned. For their low covering propriety, these lakes have been widely employed in glazing on canvas, or to modify the hues of other inorganic red pigments. This technique, exhibited by several European painters of fifteenth and sixteenth century, consisted in the overlapping of coloured paint layers on already dried paint layers in order to achieve different nuances (Kirby et al. 2005a, 2014). Moreover, anthraquinoid lakes were used in illuminating manuscripts, where colours were protected from degradation processes induced by light and external agents. Different species were used to produce organic lakes in the East, such as safflower (Wouters et al. 2010).

Starting from the end of the eighteenth century, thanks to the advances in knowledge of the chemistry of organic substance and the availability of strong acid and bases, progress led to the production of higher quality organic dyes, pigments, and lake pigments. The distinction between natural and synthetic materials becomes blurred due to manufacturers experimentation of new approaches such as the exploitation of natural dyes as pigments, by precipitating the natural extracts as salts in alkaline conditions (Degano et al. 2017). In particular, several methods to extract the colouring materials from madder were already tested at the end of the eighteenth century, yielding products with slightly different names, such as Brown Madder. Later, the availability of sulphuric and sulphurous acids led to the isolation of alizarin and purpurin in 1826. Different modified madder-based products, e.g. garancine (1828), enriched in alizarin and purpurin, Kopp's purpurin (also known in France as "purpurine commerciale"), enriched in both purpurin and pseudopurpurin, or "carmine de garance", supposedly pure madder dyestuff without the addition of an inorganic salt, were then commercialized (Kirby et al. 2007). Several "carmines" based on cochineal are also reported in nineteenth – twentieth century catalogues, in a wide range of hues and prices, prepared using different recipes and inorganic salts (Kirby et al. 2007). New lakes based on brazilwood were also introduced, produced by varying the pH of the reagents used or employing tin in the precipitating agent (Doherty et al. 2021).

Natural organic lakes can be classified based on their colour. The main organic lakes and pigments prepared with natural dyes are listed in Table 9.1.

9.1.2 Synthetic Organic Pigments (SOPs)

The successful synthesis of molecules responsible for the coloration of natural extracts was performed in 1868 during the synthesis of alizarin by the German chemists Carl Gräbe and Carl Lieberman (Kirby et al. 2005b), leading to the gradual decrease of the production of natural dyes and organic pigments. In an early stage, synthetic and natural pigments were often admixed, but after the 1930s, synthetic pigments totally dominated the market. The following step in the history of organic pigments was the synthesis of completely new formulations from the late nineteenth century, which could be tuned for the desired hue and chemical properties. The first synthetic organic pigments produced was Picric acid. In 1742, the German alchemist Johann Glauber prepared this dye by treating wool or animal horn and resins with nitric acid (Read 2014). Picric acid was rarely used due to its high intense yellow hue and thus the history of synthetic organic dyes officially started in 1856, when William Henry Perkin first synthesized mauveine. He was experimenting under the direction of August von Hofmann at the Royal College of Chemistry in London, and he was trying to produce a synthetic alternative to quinine from coal tar, when he accidentally obtained a purple compound, characterize by a high wash- and lightfastness, that he called mauveine (Lomax et al. 2006). Notably, the advances in synthetic chemistry and the discovery of mauveine occurred during the industrial revolution, a period of great change and expansion for Europe, particularly in the textile trade. The availability of cheaper synthetic dyes made coloured textiles more accessible to the wider population. Mauveine rapidly became the most fashionable colour for Victorian ladies, and Perkin became a rich entrepreneur (Garfield 2011). The commercial success of mauveine, the potential wide variety of hues achievable by slightly modifying the synthetic route, the cheapness, and the availability of the reagents, pushed chemists to experiment with new colorant formulations.

In 1863, the first azo dye, a bright yellow colour named “Field’s yellow”, was synthesized by Fredrick Field (Skelton 1999). Several aniline based dyes, obtained by diazotization reaction and differing by the kind of substituents (Ball 2001), were produced: they are the so called *coal-tar colors* (Lomax et al. 2006). Many of these products were precipitated as lakes (“laked”) to offer new pigments for artists: the availability of synthetic organic pigments in different hues, the possibility to admix them with binding media and additives in paint tubes and the relatively low costs of production, all made these new materials more appealing for manufactures not only of natural organic lakes, but also of traditional inorganic pigments. Unfortunately, many of these products were commercialized without testing for fastness properties and fugitivity in oils and severely faded few years after their application. The experimental trial-and-error strategy showed severe limits and a more reliable approach based on understanding the chemistry of the colorants and extraction processes was

Table 9.1 Classification of the main natural organic lakes

Colour	Chemical class	Raw material	Common lake names	Main components
Blue and purple	Indigoids	Indigo plants (*Isatis*, *Indigofera*)	Indigo pigment, Maya blue (in America)	Indigotin, indirubin
		Shellfish purple (*Hexaplex trunculus*, *Bolinus brandaris* and *Stramonita haemastoma*)	Purple pigment, *purpurissum* (Latin name)	6,6′-dibromoindigotin, 6-bromoindigotin, indigotin (6,6′-dibromoindirubin, 6-bromoindirubin, indirubin)
Red and pink	Homoisoflavonoids	Sappanwood (*Caesalpinia sappan*), brazilwood (*Caesalpinia* spp. from South America)	*Verzino* (Latin, medieval Italy), brazilwood lake	Brazilin, brazilein, urolithin C
	Chalcones	Safflower (*Carthamus tinctorium*)	Safflower lake	Carthamin
	Anthraquinones	Madder (*Rubia spp.*)	Madder lake, *garanza* (medieval Italy), garancine, Kopp's purpurine, *carmine de garance*	Alizarin, purpurin
		Scale insect *Kerria lacca*	Indian Lac	Laccaic acid A, Laccaic acid B
		Scale insect *Kermes vermilio*	Kermes	Kermesic acid, flavokermesic acid (carminic acid)
		Scale insects *Porpyrophora hemelii*, *Porphyrophora polonica*, *Dactylopius coccus*	Cochineal lake, carmine	Carminic acid (dcII, kermesic acid, flavokermesic acid)
Yellow	Carotenoids	Saffron (*Crocus sativus*)	Saffron lake	Crocin, crocetin
	Flavonoids	Buckthorn/Persian berries (*Rhamnus* spp.)	Stil de Grain/ Buckthorn lake	Quercetin, rhamnetin
		Weld (*Reseda luteola L.*)	Reseda lake, *arzica* (medieval Italy)	Luteolin, apigenin

developed for producing high performing formulations and adequately meeting market demands. In this regard, the discovery of the benzene structure by Kekulé (Herndon 1974) and the following elucidation of alizarin structure by Adolf Bayer, Carl Grabe and Carl Lieberman in 1868 (Graebe and Liebermann 1879) were fundamental in laying the foundation for the comprehension of colour chemistry.

In 1910, the production of Pigment Yellow 1, alternatively named "Hansa Yellow G", by Meister Lucius & Brüning, introduced the important class of Monoazo or Hansa pigments on the market (Meister Lucius and Brüning 1909). This very bright yellow pigment was the first of many to be produced with great commercial success (Schulte et al. 2008).

In 1936, phthalocyanines were the first class of organic colorants introduced directly into the market as 'true' pigments without prior use as dyes or lakes (De Keijzer 2002). This new class of pigments quickly conquered the blue and green pigment markets in all ranges of applications due to their incredibly high performance in terms of tinting strength, fastness and chemical resistance (Skelton 1999). Phthalocyanines replaced synthetic indigo lake pigments as a popular artists' pigments. Quinacridones (1950's) and diketopyrrolopyrroles (1983) were later introduced and used in high-quality artists' materials due their excellent fastness and resistance properties (Lomax et al. 2006). By the 1990s more pigment classes of synthetic organic origin, such as perylenes and pyrrols, were synthesized and are now sold as artist's materials.

Synthetic organic pigments now dominate the colorant market and have almost completely replaced traditional natural organic colorants.

Keeping track of the huge variety of currently available SOPs and those used in the pastis nearly impossible and an attempt to define the most important classes, based on literature (Herbst et al. 2004; Lutzenberger and Stege 2009), is summarized in the diagram below (Fig. 9.2).

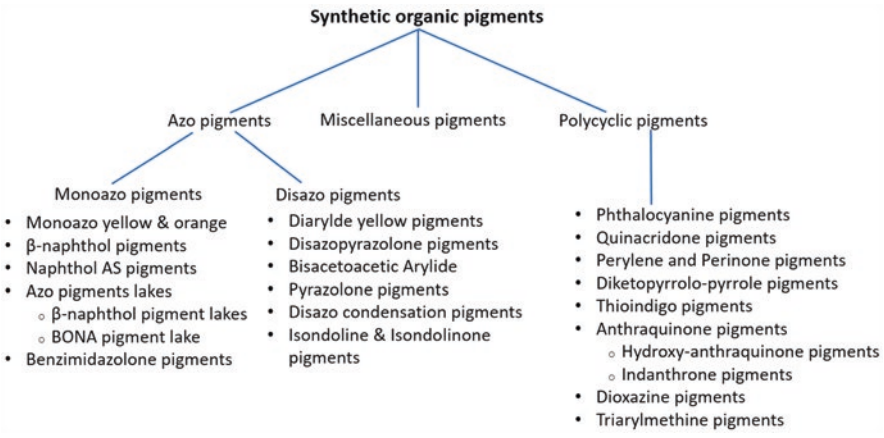

Fig. 9.2 Classification of SOPs. (Adapted from Herbst et al. 2004; Lutzenberger and Stege 2009)

Synthetic pigments can be divided in two main groups: the azo pigments and the polycyclic ones. Amongst each group, pigments are further classified on the basis of their chemical structure. The azo pigments are characterized by the azo functional group (-N=N-): monoazo pigments contain one azo group, while disazo two. The synthetic strategy to produce azo pigments is easy and economical, and based on the reaction of a diazonium compound with a coupling component. The kind of coupling agent selected allows the grouping of monoazo and disazo pigments in subclasses. Conversely, polycyclic pigments can be distinguished by the number or type of rings constituting the aromatic structure (Lutzenberger and Stege 2009). The pigments which cannot be included in one of these two big groups are generally classified as miscellaneous.

Throughout the last 150 years, creative and not informative names have been ascribed to formulations of synthetic organic dyes and pigments by manufacturers and resellers. The total absence of scientific rigour in the naming has led to a general confusion which still does not easily allow the understanding of the composition of the commercialized formulations. Patent wars between manufacturers have compounded such confusion. Indeed, in 1924, the Society of Dyers and Colourists (SDC) and the American Association of Textile Chemists and Colorists (AATCC) recorded the most extensive compendium of dyes and pigments: Colour Index™ (C.I.) (Colour index n.d.). A "Colour Index generic name" (e.g. PY1 for Pigment yellow 1) and a "Colour Index constitution number" (e.g. C.I. 11680 for Pigment yellow 1) was assigned to every coloured compound. The first is referred to the application field/coloration method, the latter to the chemical structure (Evans 1990).

A summary of the most important synthetic pigments, along with the year of synthesis and introduction on the market, their use as paint materials and some case studies (paintings and paint fabrics only) in which they were detected are reported in Table 9.2. However, in consulting patents and manufacturers' logbooks, it should be kept in mind that the commercial nomenclature of synthetic dyes and pigments is often uninformative or undeclared due to patent restrictions, and the recipes of paint tubes often contain mixtures of more than one pigment belonging to the same or different classes. Moreover, the several by-products present in different ratios, as a consequence of the various synthetic strategies adopted to produce the same pigment, have contributed to generate confusion regarding the composition of the starting materials (Lech et al. 2013). Additionally, artists themselves further complicate the composition of the final paint by mixing colours, as well as through the addition of media, thinners, driers, waxes, diluents and extra oils to obtain the desired effects in their artworks (Townsend 1994). Furthermore, artists have experimented with new and old materials, blending highly heterogeneous components, including those that were low cost and not specifically suitable for artistic purposes (Learner et al. 2006).

Table 9.2 Compendium of the most common synthetic organic pigments with the year of synthesis and introduction on the market. Their use as paint materials and some case studies (paintings only) in which they have been detected are reported. Adapted from (de Keijzer 2014)

	Pigment code	First discoveries	Industrial introduction	Paint materials and paint artworks	Features
Red and orange pigments	**β-naphthol pigments**				
	PR1, 12070	1880: England	1899: Farbwerke vorm Meister Lucius und Brüning manifacturer (Germany)	1955: M. Rothko, *Red band* (Lomax et al. 2014) 1955–1960: F. Melani, *Bandiera* (Carlesi et al. 2016) 1968: P. Gilardi, *Disgelo* (La Nasa et al. 2019)	Low light and heat fastness, high migration fastness, low tinting strength
	PR3, 12120	1905: Germany		Since 1905*: Rouge Japonais Foncé*, Lefranc archive paint tube (France) (Degano et al. 2017) 1905: F. Melani's atelier material (Italy) (Carlesi et al. 2013) 1923–1924: V. Huszar, *Miss Blanche advertisement* (Netherlands) 1927: Royal Talens N.V., list of artists' paints, Rembrandt series (Netherlands) 1964: J. Dubuffet, *Chain de mémoire III* 1964: J. Dubuffet, *Le train de pendules* 1970: M. Rothko, Untitled (Lomax et al. 2014) Mid. 1980s: *Bright Red and Vermillion Hue*, Windsor & Newton, Artists' oil colour and Winton oil colour (England) 1988: *Karmin, Krapplack hell, Kadmiumrot dunkel, Zinnober dunkel*, Lukas, A and B quality artists' oil colours (Germany)	
	PR4, 12085	1906: Germany, France		1918: E.L. Kirchner, *Plastik: Mann and Frau* 1929: Missiemuseum Steyl-Tegelen, pigment archive (Netherlands) 1949: M. Rothko, Untitled (Lomax et al. 2014) 1988: *Helio-Echtrot, Helio-Echtorange, Kadmiumorange, Zinnoberrot hell*, Lukas, A and B quality artists' oil colours (Germany)	
	PR6, 12090	1906: Germany, England		1955–1960: F. Melani, *Bandiera* (Carlesi et al. 2016)	

(continued)

Table 9.2 (continued)

	Pigment code	First discoveries	Industrial introduction	Paint materials and paint artworks	Features
	PO5, 12075	1907: Germany	1908: AGFA (Germany)	1931: Royal Talens N.V., list of artists' paints, Rembrandt series (Netherlands) 1933–1934: W. Kandinsky's Paris palette 1936: M. Beckmann, *Stillleben mit Ausblick auf dem Wannsee* 1968: P. Gilardi, *Disgelo* (La Nasa et al. 2019) 2003: A. Harding, *Quartet* (La Nasa et al. 2020)	
	Naphthol AS pigments				
	PR2, 12310	1911: Germany		1967: G. Baselitz, *Drei Feldarbeiter*	Good lightfastness
	PR8, 12335	1911: France, Germany, England		1988: *Indischgelb, Geraniumlack, Gruner Lack hell*, Lukas, A quality artists' oil colours (Germany) 1988: *Geraniumlack, Kobaltviolett dunkel*, Lukas, B quality artists' pigments (Germany)	
	PR5, 12490	1931: Germany, England		1982: G. Baselit, *Orangenesser IV*	
	PR7, 12420	1921: Germany		1955–1960: F. Melani, *Bandiera* (Carlesi et al. 2016)	
	PR12, 12385	1922: Germany, French			
	PR9, 12460	1922: Germany		1970: B. Rancillac, *La Suite Américaine* 1970–71: D. Hockney, *Mr and Mrs Persey* 1993: G. Baselitz, *Bildsechzehn*	
	PR112, 12370	1939: Germany		1960s: D.A. Siqueiros, murals of the Polyforum Cultural Siqueiros building (Mexico) (La Nasa et al. 2021) 1975: A.R. Penck, *Young Generation* (Lutzenberger and Stege 2009) 1987: K. Haring, *Necker* (Magrini et al. 2017) 1991: *Vermiljoen chin., Talensrood donker and Permanentrood*, Royal Talens B.V., list of artists' paints, Rembrandt oil colours (Netherlands) 2013–14: BLU, mural painting on the wall of an old military warehouse (La Nasa et al. 2021)	

	PR146, 12485	1953: Germany			
	PR170, 12475	1963: Germany		1983: J. Dubuffet, *Mire G 137 Kowloon* 1985–86: P. Caulfield, *Interior with a picture*	
	β-naphthol pigment lakes				
	PR49, 15630	1899: Germany		1961: M. Rothko, *Untitled*, Harvard Murals (Stenger et al. 2010)	Poor lightfastness, good solvent fastness
	PR53, 15585	1902: Germany		1993: M. Lupertz, *Männer ohne Frauen. Parsifal*	
	PO46, 15602	1949: USA			
	BONA pigment lakes				
	PR57, 15850	1903: Germany, England		1958: F. Winter, *Teile* 1958: F. Winter, *Später Garten* 1958: F. Winter, *Winterliches Geäst* 1991: *Geraniumlack, Talensrood purper*, Royal Talens B.V., list of artists' paints, Rembrandt oil colours (Netherlands) 1991: *Cadmiumrood azo, Vermiljoen, Karmin*, Royal Talens B.V., list of artists' paints, Van Gogh oil colours (Netherlands) 1991: *Donkerrose*, Royal Talens B.V., list of artists' paints, Amsterdam oil colours (Netherlands)	Similar proprieties to β-naphthol pigment lakes but more lightfast
	PR48, 15865	1904: Germany		Late 1920s: *Watchung Red*, A. Siegel, E.I. du Pont de Nemours & Company (USA) 1991: *Cadmiumrood donker azo*, Royal Talens B.V., list of artists' paints, Van Gogh oil colours (Netherlands) 2011: A. Pasquini, Untitled (Bosi et al. 2020) 2014: A. Luchko, *Straniera* (Bosi et al. 2020)	
	PR52, 15860	1910: Germany			
	PR63, 15880	1906: Germany			

(continued)

Table 9.2 (continued)

	Pigment code	First discoveries	Industrial introduction	Paint materials and paint artworks	Features
	Benzimidazolone pigments				
	PR171, 12512	1960: Germany	1964: Farbwerke Hoechst AG (Germany)		Good lightfastness and solvent fastness
	PR175, 12519	1960: Germany	1964: Farbwerke Hoechst AG (Germany)		
	PR176, 12515	1960: Germany	1965: Farbwerke Hoechst AG (Germany)	1988: *Karmin, Krapplack hell dunkel and dunkelst, Casslerbraun, Septa, Vandyckbraun and Indigo*, Lukas, A quality artists' pigments (Germany) 1988: *Karminrot, Krapplack hell and dunkel*, *Casslerbraun and Vandyckbraun,* Lukas, B quality artists' pigments (Germany)	
	PBr25, 12510	1960: Germany	1966: Farbwerke Hoechst AG (Germany)		
	PR185, 12516	1962: Germany	1967: Farbwerke Hoechst AG (Germany)		
	PV32, 12517	1963: Germany	1965: Farbwerke Hoechst AG(Germany)		
	PR208, 12514	Belgium	1970: Farbwerke Hoechst AG (Germany)		
	PO36, 11780	1961: Germany	1964: Farbwerke Hoechst AG (Germany)		
	PY120, 11783	Germany	1969: Farbwerke Hoechst AG (Germany)		

	Pyrazolone pigments				
	PO13, 21110	1910: Germany			Versatile fastness proprieties
	PR38, 21120	1934: Germany	1934: I.G. Farbenindustrie, (Germany)		
	PO34, 21115	1934: USA	1934: I.G. Farbenindustrie (Germany)		
	PR41, 21200	1935: USA			
	Perylene pigments				
	PR123, 71145	1948: USA			Excellent lightfastness and solvent fastness
	PR149,71137	1956: Germany	1961: Farbwerke Hoechst AG (Germany)	1961: Lefranc (France) 1996: *Scarlet*, Royal Talens B.V., list of artists' paints (Netherlands)	
	PR179, 71130	1913: Germany, England			
	Perinone pigments				
	PO43, 71105	1924: Germany	1953: Farbwerke Hoechst AG (Germany)	1978: Royal Talens B.V., list of artists' paints, Rembrandt oil colours (Netherlands) 1978: S. Francis; *Untitled* 1991: *Geraniumlack, Talensrood purper, Cadmiumrood donker,* Royal Talens B.V., list of artists' paints, Rembrandt oil colours (Netherlands) 1991: *Cadmiumrood donker azo, Vermiljon, Karmin,* Royal Talens B.V., list of artists' paints, Van Gogh oil colours (Netherlands)	Excellent lightfastness and solvent fastness

(continued)

Table 9.2 (continued)

	Pigment code	First discoveries	Industrial introduction	Paint materials and paint artworks	Features
	Quinacridone pigments				
	PR122, 73915	1958: USA		1974: Royal Talens B.V., list of artists' paints, Rembrandt oil colours (Netherlands) 1978: S. Francis, Untitled 1991: *Rembrandtrose, Permanentviolet, Permanent troodviolet*, Royal Talens B.V., list of artists' paints, Rembrandt oil colours (Netherlands) 1991: *Permanenrose, Permanent roodviole, Permanent blauwviolet*, Royal Talens B.V., list of artists' paints, Van Gogh oil colours (Netherlands) 1991: Violet, Royal Talens B.V., list of artists' paints, Amsterdam oil colours (Netherlands) 2013–14: BLU, mural painting on the wall of an old military warehouse (La Nasa et al. 2021)	Excellent lightfastness and solvent fastness
	PR192, 739155	1958: USA			
	PR202, 73907	1958: USA		1982: G. Baselitz, *Orangenesser IV*	
	PR206, 73900+73920	1958: USA			
	PR207, 73900+73906	1958: USA			
	PR209, 73905	1958: USA			
	Diketopyrrolo-Pyrrole pigments				
	PR254, 56110	1982: Switzerland		1996: Royal Talens B.V., list of artists' paints, Rembrandt oil colours (Netherlands) 2000: Schmincke, MUSSINI (Germany) 2003: Schmincke, PRIMAcryl (Germany) 2004: Lukas (Germany)	Excellent lightfastness and solvent fastness

	PR255, 561050	1982: Switzerland		1996: Royal Talens B.V., list of artists' paints, Rembrandt oil colours (Netherlands) 2000: Schmincke, MUSSINI (Germany) 2003: Schmincke, PRIMAcryl (Germany) 2004: Lukas(Germany)	
	PR264, 561300	1982: Switzerland		1996: Royal Talens B.V., list of artists' paints, Rembrandt oil colours (Netherlands) 2000: Schmincke, MUSSINI (Germany) 2004: Lukas (Germany)	
	PO71, 561200	1982: Switzerland		2000: Schmincke, MUSSINI (Germany) 2003: Schmincke, PRIMAcryl (Germany)	
	PO73, 561170	1982: Switzerland		1996: Royal Talens B.V., list of artists' paints, Rembrandt oil colours (Netherlands) 2000: Schmincke, MUSSINI (Germany)	
	Anthraquinone pigments				
	PR83, 58210	1868: Germany		Since 1804: Lefranc archive paint tube (France) (Degano et al. 2017) Since 1900: *Laque de garance rose*, Felice Alman (Italy) (Christiansen et al. 2017) Since 1900: P. Picasso's atelier material, Ripolin (Netherlands) (Gautier et al. 2009) 1947: M. Rothko, Untitled (Lomax et al. 2014) 1950: M. Beckmann, *Frau mit Mandoline in Gelb und rot* (Lutzenberger and Stege 2009)	Poor lightfastness and solvent fastness

(continued)

Table 9.2 (continued)

	Pigment code	First discoveries	Industrial introduction	Paint materials and paint artworks	Features
Yellow pigments	**Monoazo yellow pigments**				
	PY1, 11680	1897: Germany		Since 1909: *Vert Anglais n. 3*, Lefranc archive paint tube (France) (Degano et al. 2017) Since 1909: F. Melani's atelier material (Italy) (Carlesi et al. 2013) 1912: Schmincke (Germany) 1919: A. Rodchenk, *Konstruktivistische Komposition* 1919: L. Meidner, *Der Krieg* 1924: Daler-Rowney (England) 1925: M. Ullmann, *Komposition mit zwei Akten* 1926: *Pigment Fast Yellow HGL*, J.W. Leitch and Co. (England) 1931: Royal Talens B.V., list of artists' paints, Rembrandt series (Netherlands) 1935: *Sunproof Yellow 1*, Gouache paint-outs, Schmincke (Germany) 1948: V. Pasmore, *Abstract Design for a Poster* 1958: A. Pellan, *Jardin Vert* 1958: H. Frankenthaler, *Basque Beach* 1960s: D.A. Siqueiros, murals of the Polyforum Cultural Siqueiros building (Mexico) (La Nasa et al. 2021) 1968: P. Gilardi, *Disgelo* (La Nasa et al. 2019) 1982: F. Bacon, *Figure with cricket pads* (Russell et al. 2011) 1982: S. Polke, *Stairwell (Treppenhaus)* 2003: A. Harding, *Quartet* (La Nasa et al. 2020) 2013–14: BLU, mural painting on the wall of an old military warehouse (La Nasa et al. 2021)	Good lightfastness and poor solvent fastness

	PY3, 11710	1909: Germany		Since 1909: F. Melani's atelier material (Italy) (Carlesi et al. 2013) Since 1909: *Vert Anglais n. 3*, Lefranc archive paint tube (France) (Degano et al. 2017) 1927: *Talens Groen Licht*, Royal Talens B.V., list of artists' paints, Rembrandt tempera paints (Netherlands) 1935: *Sunproof Yellow II*, Gouache paint-outs, Schmincke (Germany) 1935: V. Vytlacil, *Construction No. 3* 1936: A. Calder, *From against yellow* 1936: M. Beckmann, *Stillleben mit Ausblick auf den Wannsee* 1938: *P. Picasso, Portrait of Dora Marr* 1939: *V.* Vytlacil, *Construction* 1945: J. Pollock, *There were seven in eight* 1945: J. Pollock, *Summertime number 9A* 1949: B. Newman, *Dionysius* 1953: E. Briggs, *Untitled* 1957: Y. Klein, *Monochrome Vert* 1958: A. Pellam, *S'abstenir* 1965: T. Wesselmann, *Study for First illuminated Nude* 1968: Lucebert, *Baby elephant* 1968: P. Gilardi, *Disgelo* (La Nasa et al. 2019) 1970: P. King, *Dunstable Reel* 1973: B. Riley, *Cantus Firmus* 1982: T. Setch, *Once upon a time there was oil III* 1985: P. Caulfield, *Interior with picture* 1989: K. Fritsch, *Display stand with Madonnas* 2003: A. Harding, *Quartet* (La Nasa et al. 2020)	
	PY65, 11740	1936: Germany, England	Before world war II: IG. Farbenindustrie (Germany)		

(continued)

Table 9.2 (continued)

	Pigment code	First discoveries	Industrial introduction	Paint materials and paint artworks	Features
	PY73, 11738	1961: USA, Germany, England			
	PY74, 11741	1959: USA	1958: E.I. du Pont de Nemours & Company (USA) 1961: Sherwin Williams Comp. (USA) 1961: Farbwerke Hoechst AG (Germany)	1973: A. Jensen, *The sun rises twice (Per I, Per II, Per III, Per IV)* 1994: G. Ayres, *Sundark blues* 2011: A. Pasquini, Untitled (Bosi et al. 2020)	
	PY97, 11767	1950: Germany	1960: Farbwerke Hoechst AG (Germany)		
	PY98, 11727	1960: Germany	1960: Farbwerke Hoechst AG (Germany)		
	PO1, 11725	1925: USA			
	Benzimidazolone pigments				
	PY151, 13980	1960s	1971: Farbwerke Hoechst AG (Germany)		Good lightfastness and solvent fastness
	PY154, 11781	1960s	1975: Farbwerke Hoechst AG (Germany)	1996: *Permanent Yellow, light, medium and dark, Permanent Green light, medium and dark, Permanent Yellowish Green, Cinnabar Green light and medium*, Royal Talens B.V., list of artists' paints, Rembrandt oil colours (Netherlands)	
	PY175, 11784	1960s	1980: Farbwerke Hoechst AG (Germany)		

	Diarylide yellow pigments				
	PY12, 21090	1911: Germany		1988: *Indischgelb, Geraniumlack*, *Gruner Lack hell*, Lukas, A quality artists' oil colours (Germany) 1988: *Geraniumlack*, Lukas, B quality Artists' oil colours (Germany)	Moderate lightfastness and good solvent fastness
	PY13, 21100	1911: Germany			
	PY14, 21095	1911: Germany			
	PY17, 21105	1911: Germany			
	PY81, 21127	1958: Germany			
	PY83, 21108	1949: Germany	1958: Farbwerke Hoechst AG (Germany)	1993: M. Lüpertz, *Parsifal or men without women* (Lutzenberger and Stege 2009) 2006: Peeta, *Writings* (La Nasa et al. 2021) 2006: Deban and M. Ment, *Writings* (La Nasa et al. 2021)	
	PY127, 21102	1964: Germany			
	Isoindoline and isoindolinone pigments				
	PY109, 56284	1956: Germany		1980: Royal Talens B.V., list of artists' paints, Rembrandt oil colours (Netherlands)	Excellent lightfastness and solvent fastness
	PY110, 56280	1977: Germany		1978: *Indian Yellow,* Royal Talens B.V., list of artists' paints, Rembrandt oil colours (Netherlands)	
	PY139, 56298	1980: Germany			
Blue pigments	**Phthalocyanine pigments**				
	PB15, 74160	1928: England	1935–1936: I.G. Farbenindustrie (Germany) 1937: E.I. du Pont de Nemours & Company (USA)	1937: Winsor & Newton, artists'paint (England) 1940: Royal Talens B.V., list of artists' paints (Netherlands) 1953: G. Capogrossi, *Cinema Airone* (La Nasa et al. 2021) 1967: B. Newman, *Who is afraid of red, yellow and blue III* 1975: A.R. Penck, *Young generation* 1989: K. Haring, *Tutto mondo* (Cucci et al. 2016) 2011: A. Pasquini, Untitled (Bosi et al. 2020)	Excellent lightfastness and solvent fastness

(continued)

Table 9.2 (continued)

	Pigment code	First discoveries	Industrial introduction	Paint materials and paint artworks	Features
	PB16, 74100	1931: England	1939: I.G. Farbenindustrie (Germany) 1939: Imperial Chemical Industries Ltd. (England)	1962: G. Baselitz, *Der Zwerg* 1964: E. Kelly, *Blue green red I*	
	Triarylmethine pigments				
	PV39, 42535	1884: Germany		1886: V. van Gogh, *Glass with yellow roses* (Van Bommel et al. 2005) 1888: V. van Gogh, *Montmajour drawing* (Confortin et al. 2010) 1956–1959: *Ultramarine*, Yang Tse permanent inks, L. Fontana's atelier material, J.M. Paillard (France) (Zaffino et al. 2017) Since 1960: felt-tip pen, L. Bo Bardi's atelier material, Johann Faber (Germany) (Moretti et al. 2019) 1965: G. Turcato, *Composizione-Superficie Lunare* (Sabatini et al. 2020c)	Poor lightfastness
Green pigments	**Phtalocyanine pigments**				
	PG7, 74260	1935: Germany, England	1936: Imperial Chemical Industries Ltd. (England) 1938: I.G. Farbenindustrie (Germany) 1940: E.I. du Pont de Nemours & Company (USA)	1940: Royal Talens B.V., list of artists' paints (Netherlands) 1950: M. Beckmann, *Frau mit Mandoline in Gelb und Rot* (Lutzenberger and Stege 2009) 1956–1957: F. Bacon, *Study for a portrait IV* (Russell et al. 2011) 1961: M. Louis, *Alpha Phi*	Excellent lightfastness and solvent fastness
	PG36, 74265	1935: England	1957: Harmon Colors (USA) 1959: E.I. du Pont de Nemours & Company (USA) 1960: BASF (Germany)	1962: G. Baselitz, *Der Zwerg* 1964: E. Kelly, *Blue green red I*	

	Triarylmethine pigments				
	PG1, 42040	1887: Germany		1960s: D.A. Siqueiros, murals of the Polyforum Cultural Siqueiros building (Mexico) (La Nasa et al. 2021) Since 1960: felt-tip pens, L. Bo Bardi's atelier material, Johann Faber (Germany) (Moretti et al. 2019)	Poor lightfastness
Violet pigments	**Quinacridone pigments**				
	PV19, 46500	1955: USA	1955: E.I. du Pont de Nemours & Company (USA)	1965–1970: Royal Talens B.V., list of artists' paints, Rembrandt oil colours (Netherlands) 1980: Schmincke (Germany) 1983: G. Richter, *Bild 525, Prag*	Excellent lightfastness and solvent fastness
	Dioxazine pigments				
	PV23, 51319	1928: Germany	1953: Farbwerke Hoechst AG (Germany)	1938: G. Baselitz, *Roadwarker* 1973: G. Baselitz, *Straßenbauarbeiter* 1974: Royal Talens B.V., list of artists' paints, Rembrandt oil colours (Netherlands) 1988: J. Schnabel, *Ri de pomme* (E. Ghelardi et al. 2015)	Excellent lightfastness and moderate solvent fastness

(continued)

Table 9.2 (continued)

	Pigment code	First discoveries	Industrial introduction	Paint materials and paint artworks	Features
	Triarylmethine pigment				
	BV14, 42510	1859: France			Poor lightfastness
	PR90, 45380	1873: Germany		1888–1890: V. van Gogh paintings (Geldof et al. 2013) 1889: V. van Gogh, *Two white butterflies* (Claro et al. 2010) 1890: V. van Gogh, *Wheat field under clouded sky* (Claro et al. 2010) 1890: V. van Gogh, *La maison blanche, la nuit* (Sabatini et al. 2020a) 1888: V. van Gogh, *Landscape with Snow* (Pozzi et al. 2021)	
	BV10, 45170	1887: Germany		Since 1905*: Rouge Japonais Foncé*, Lefranc archive paint tube (France) (Degano et al. 2017) 1955–1960: F. Melani, *bandiera* (Carlesi et al. 2016)	
	PR81, 45160	1887: Germany		1956–1959: *Natural Sienna earth*, Yang Tse permanent inks, L. Fontana's atelier material J.M. Paillard (France) (Zaffino et al. 2017) 1955–1960: F. Melani, *bandiera* (Carlesi et al. 2016)	

9.2 Analysis: Methods, Instrumentation, and Specific Issues

9.2.1 High Performance Liquid Chromatography (HPLC) and Ultra Performance Liquid Chromatography (UPLC)

Liquid Chromatography has been widely employed in the analysis of organic materials in Heritage Science objects. In particular, it can be considered the method of choice because of its reliability and performance for the analysis of organic colorants whenever sampling is allowed. The first applications were based on Thin Layer Chromatography (TLC) that was gradually supplanted by High Performance Liquid Chromatography (HPLC) due to higher selectivity and sensitivity, great chromatographic efficiency, and the possibility of performing quantitative analysis (if analytical standards are available), or semiquantitative evaluations (Degano 2019). Reversed-phase chromatography (RP-HPLC) has been applied for the last 30 years for the characterization of organic dyes and pigments, which are most often complex mixtures of organic molecules that are mostly aromatic and polar, generally water soluble and characterized by a strong absorption in the UV-Vis range (Degano and La Nasa 2016). While natural colorants are inherently composed by mixture of different compounds, synthetic dyes were often admixed to obtain specific hues, or contained synthesis by-products whose identification can provide interesting information on the manufacturer. Thus, the identification of materials is usually achieved by comparing the chromatographic profiles of extracts of unknown samples to those obtained for known reference materials.

The analytical column is the core of the chromatographic separation. Amongst the several columns available, the most commonly used in the analysis of organic pigments and lakes are constituted by C8 or C18 stationary phase, with sizes of 150 × 4.6 or 150 × 2 mm, with 3 or 5 μm particle size. UHPLC (Ultra High-Pressure Liquid Chromatography) allows the use of sub-2-μm particle size, bearing relatively higher back-pressures. While HPLC can operate continuously at high pressure, up to 6000 psi, UHPLC can operate up to 10,000 psi. The recent success of UHPLC is given by its higher chromatographic efficiency and sensitivity, shorter runtimes and thus faster analysis, saving solvent cost and waste (Serrano et al. 2013; Taujenis and Olšauskaite 2012; Troalen et al. 2014). The solvent flow generally ranges between 0.2 and 10 mL/min, while for nano-LC setups a flow 0.002 mL/min is required. For an efficient separation of mixtures of differently polar compounds, the fine-tuning of a suitable elution program in gradient mode is fundamental. Binary systems of water and methanol or acetonitrile acidified with formic acid or trifluoroacetic or acetic acids are generally selected (Halpine 1996). For the analysis of some classes of synthetic pigments, counter ion chromatography making use of ion pair reagents such as tetrabutylammonium hydroxide may be more efficient in achieving a better separation and improved peak symmetry (van Bommel et al. 2007). When dealing with strongly polar dyes or uncoloured degradation compounds, the use of a RP-amide i.e. a polar embedded reversed-phase column, may be effective (Restivo et al. 2014). Finally, 2D-HPLC, entailing the use of two columns exploiting

different retention mechanisms, can be employed as a universal system to separate both extremely polar and relatively less polar organic dyes (Pirok Bob et al. 2016, 2019a, b).

For the detection of separated compounds, the most commonly employed detectors are spectrophotometric (UV-Vis, Diode Array and Fluorescence Detectors) and mass spectrometric (ESI-MS, APCI-MS) detectors. Whenever possible, the use of both spectrophotometric and mass spectrometric detectors in series is advisable, to exploit the ability of the first to assess the colour of the eluted components through the acquisition of the UV/Visible spectrum, and the sensitivity and selectivity of the latter. Fluorimetric detection is extremely sensitive and selective (van Bommel 2005; Colombini et al. 2004; Surowiec et al. 2003) due to the high sensitivity of fluorescence in low concentrations. On the other hand, the fact that only a few chromophores exhibit fluorescence can be a drawback in the application of this method of detection. Thus, in most cases, pre- or post-column derivatisation is applied; particularly using aluminium and gallium salts in post-column derivatisation (van Bommel 2005; Szostek et al. 2003). In recent years, the application of high resolution mass spectrometry has aided the resolution of complex mixtures containing unknown species (including degradation products and synthetic by-products) in replicas, in atelier materials and in paint samples (Chieli et al. 2019; La Nasa et al. 2020; Sabatini et al. 2018, 2020b, c).

9.2.2 Gas Chromatography – Mass Spectrometry (GC/MS) and Analytical Pyrolysis (Py-GC/MS)

In the study of natural dyes, gas chromatographic techniques have not been exploited extensively, due to the relatively high-molecular mass and polarity of target compounds. Derivatisation of coloured compounds is thus mandatory. Although uncommon, GC/MS based methods have been proposed mainly for dyed textiles and objects, based on the extraction of colouring molecules followed by their derivatization with a silylating agent, both by Colombini (Colombini et al. 2007) and Degani (Degani et al. 2014). Poulin instead developed a procedure for the simultaneous extraction and derivatization of molecules by TMTFTH (Poulin 2018). To bypass any sample pre-treatment, pyrolysis coupled with gas chromatography has been used. While for natural colours research is limited (Andreotti et al. 2004; Casas-Catalán and Doménech-Carbó 2005; Fabbri et al. 2000), several studies tackled the analysis by Py-GC/MS of synthetic organic pigments (SOPs), which are often insoluble or bound in synthetic binders that prove difficult to solubilize. Synthetic pigments are usually analysed without any derivatising reagent; recently, several libraries, listing the characteristic pyrolysis products of several classes of SOPs, have been created (Germinario et al. 2017; Ghelardi et al. 2015b; Learner 2005; Rehorek and Plum 2007; Russell et al. 2011; Sonoda 1999).

In spite of its ability to detect pigments which are not soluble in any extraction solvent, pyrolysis does not provide information on the chemically and thermally stable pigments. Moreover, many families of pigments have a common skeletal structure, differing only in the nature or position of the substituents on the aromatic rings, and thus they often yield common pyrolysis fragments. Notwithstanding this, differences between pyrograms of unaged and artificially aged paint model systems have been detected and have allowed the hypothesis of degradation pathways (Ghelardi et al. 2015a).

9.2.3 Mass Spectrometry Based Techniques

Mass spectrometry based techniques can be applied as detectors for liquid or gas chromatography, or as self-standing analytical tools. For liquid chromatography, the most widely used systems are based on electrospray ionization (ESI) tandem mass spectrometry. ESI allows the interfacing of a high pressure system such as HPLC with a mass spectrometer, which requires high vacuum, and performs the ionization of the analytes. Being a soft ionization technique, for small molecules as dyes ESI mostly produces monocharged molecular ions, whose mass to charge ratio corresponds to $[M+H]^+$ or $[M-H]^-$ ions, for positive and negative analysis modes, respectively. A second stage of analysis after a further fragmentation of the molecular ion in a collision chamber is thus required to perform qualitative analysis and ultimately to improve sensitivity. Consequently, tandem mass spectrometry is employed in most applications, including ion traps, triple quadrupoles and quadrupole-time of flight analysers.

Other mass spectrometry based techniques used to detect organic dyes and pigments without any prior separation of the sample components are: direct temperature mass spectrometry (DTMS); laser-desorption/ionization (LDI) and matrix assisted laser desorption/ionization (MALDI) mass spectrometry; direct analysis in real time (DART) and surface acoustic wave nebulization (SAWN). Through the rapid acquisition and observation of positive and negative ion spectra, acidic, basic and neutral natural and synthetic colorants can be distinguished and characterized by their m/z values. The absence of preliminary separation means that the detection of minor components is quite difficult, but the features of these techniques make them suitable for the analysis of poorly soluble organic pigments and for the screening of large collections of samples.

DTMS was pioneered by Boon and Learner, but has essentially been abandoned in the last 10 years (Boon and Learner 2002; Lomax et al. 2007; Menke et al. 2009) in favour of more robust and more widely available techniques. LDI and MALDI-MS have been widely used for the analysis of synthetic organic pigments (Boon and Learner 2002; Kirby et al. 2009), but also applied to the detection of natural organic lakes (Boon et al. 2007; Sabatini et al. 2016; Soltzberg et al. 2007).

DART has been tested on organic dyes, even directly on textiles (Armitage et al. 2015, 2019), while it has only been applied to the detection of organic lakes on paint

mock-ups in the recent publication by Alvarez-Martin on eosin lake (Alvarez-Martin et al. 2019).

SAWN has been employed by Astefanei for the identification of synthetic dyes in reference powder materials and historical textiles (Astefanei et al. 2017).

9.2.4 Sample Preparation

The application of liquid chromatography, gas chromatography and some of the direct MS techniques requires the preliminary extraction of the chromophore containing molecules from the matrix. The selection of the most suitable extraction method is crucial, considering the uniqueness of samples and the tiny amount of colorant they often contain (Bacci et al. 2006). The effectiveness of the pretreatment is strongly dependent on the solubility and stability of the colorants in solvents and the nature and the ageing of the matrix (Padfield n.d.). Thus, there is as yet no universal method of extraction applicable to all the many dye classes in every kind of heterogenous matrix. The most commonly used extraction methods for the analysis of organic pigments are listed below:

- Boiling mixture of organic solvent and strong acid: this is the strongest and more aggressive extraction method, the organic solvent usually used is methanol (MeOH) and the acid is hydrochloric (HCl) or sulfuric acid (H_2SO_4) (Abrahart 1977; Halpine 1996). HCl 0.5 M and MeOH (1:1) (Halpine 1996) solution or 2 HCl: 1 MeOH: 1 H2O (v/v/v) (Wouters 1985) are the most effective and used methods. Nevertheless, some undesired effects such as the cleavage of labile bonds, esterification of carboxylic compounds and oxidation of moieties limit its utilization (Ferreira et al. 2002). Moreover, HCl is corrosive and difficult to evaporate;
- Transmethylation with boron trifluoride and methanol (BF_3/MeOH): a suitable method for disrupting highly polymerized painting films and extracting dyes from lake pigments. If BF_3 is highly concentrated, interactions among compounds in the matrix and esterification may occur (Kirby and White 1996);
- Hydrofluoric acid (HF): a weak acid and, in its dissociated form, also a strong aluminium-complexing agent as efficient as a strong acid (Sanyova 2008). This is a mild extraction preferrable for unstable colorants and applicable to a wide range of colorant classes and mixtures precipitated with different metal cations, applied on different supports and in various matrices (Padfield n.d.; Sanyova and Reisse 2006). It allows working at much milder pH (c.a. 1.5) than with HCl (Sanyova 2008) obtaining high yields for many colorants. The drawbacks of this method consist in the precautions for manipulation and treatment of HF. Its toxicity both for contact and for inhalation requires protections and its corrosive power, especially toward glass, requires the use of Teflon laboratory ware;

- Formic acid (HCOOH): a weak acid which is used in an extracting solution of 5 HCOOH: 95 MeOH (v/v) which enable a mild extraction of the chromophore containing molecules (Zhang and Laursen 2005);
- Complexation agents: ethylenediaminetetracetic acid (EDTA) is used for its capability as a strong chelator of aluminium and of other ions, enabling the release of dyes molecule without decomposing them. An efficient extracting solution used is 2 H_2EDTA: 10 ACN: 88 MeOH (v/v/v) (Zhang and Laursen 2005). Finally, in order to improve the extraction yields of complexation agents, it is also possible to use an organic solvent such as dimethylformamide (DMF) (Surowiec 2008). Another method exploiting a complexing agent entails the use of oxalic acid in a mixture of oxalic acid/MeOH/acetone/H_2O (1:30:30:40, v/v/v/v) (Guinot and Andary 2006; Manhita et al. 2011);
- Organic solvent: pyridine, dimethylsulfoxide, or dimethylformamide (Kirby and White 1996; Wouters 1991) are commonly used, heating at maximum 100 °C for short times (Manhita et al. 2011).

9.2.5 Data Interpretation

The interpretation of chromatographic and mass spectrometric data relies on the identification of specific molecules, typical of organic dyes, based on their retention time, mass spectra and possibly spectroscopic properties (e.g. UV-Vis or fluorescence spectra). The unambiguous identification of the source of colour is a much more complex task, since minor components and in some cases even the ratio between different molecules can enable the distinction between different species, or synthetic routes. Thus, data can only be interpreted by comparing both the qualitative and semi-quantitative profile of the extract of an unknown sample with that of reference materials, possibly subjected to artificial ageing. Comparison with published data should be performed by keeping in mind that different extraction protocols may lead to slightly different results, thus extra caution is needed whenever using novel sample treatments. Finally, multivariate statistical data analysis can be successfully employed to discriminate between closely related materials, such as the dyes and organic pigments extracted from scale insects, as demonstrated by Serrano et al. in extensive research on cochineal (Serrano et al. 2011).

9.3 A Further Analytical Issue: Photo-Degradation of Coloured Compounds

Organic lakes and pigments are among the most labile materials used in works-of-art. They are coloured, which means that they absorb light in the UV-Visible range and are susceptible to photochemical reactions i.e. photo-oxidation processes that

lead to a change in colour or even to bleaching. The photo-oxidation of synthetic organic pigments already heavily affects the appearance of modern and contemporary paintings; therefore, specific storage and display conditions need to be designed to minimize reactions leading to the degradation of chromophore-containing molecules. Thus, improving our comprehension of photooxidation chemical pathways and fading mechanism is the only way to develop suitable preventive conservation strategies.

The stability of materials to photo-oxidation and damages induced by light is defined as photostability (Anghelone et al. 2018). The absorption of photons of suitable energy by an organic molecule provides an electronically excited state, which is the starting point for the subsequent reactions (Weyermann et al. 2009). The presence of oxygen frequently accelerates the degradation via radical-initiated oxidation and only in a few cases it can retard dye-fading by re-oxidizing reduced molecules.

Artificial accelerated ageing of reference materials is commonly used to mimic and study the degradation process undergone by colorants and of other materials present in artworks. In most cases, accelerated ageing procedures are performed in order to assess rates of fading and identify the factors that lead to lightfastness. Accelerated ageing is based on the reciprocity principle: degradation is assumed to be proportional to net exposure calculated as the product of intensity of illuminance and exposition time (Feller 1994). There are many examples of deviations from the reciprocity principle in natural materials. Furthermore artificial accelerated ageing is not able to accurately reproduce natural ageing due to the impossibility to recreate the variety of different conditions an artwork might be exposed during its life (Weyermann and Spengler 2008). Nonetheless, artificial ageing is the only tool available to simulate photo-oxidation. The cross-checking between results collected from the analysis of artificially aged reference materials with historical samples is mandatory to validate the reliability of accelerated ageing procedures.

With regard to natural lake pigments, the most studied chromophores in terms of photo-stability are flavonoids (Colombini et al. 2007; Ferreira et al. 1999, 2002; Saunders and Kirby 1994); degradation products have been identified in aged specimens that were prepared in the laboratory and sampled from works of art. Hydroxybenzoic acids were detected in the extracts from aged specimens, the presence of which may be due to the photo-oxidation of the double bond C2-C3 of the flavonoids, leading to the formation of a depside. This latter is formed by condensation of two or more hydroxybenzoic acids whereby the carboxyl group of one molecule is esterified with a phenolic hydroxyl group of a second molecule. Cleavage also yields low-molecular mass products, such as dihydroxybenzoic acids and trihydroxybenzoic acids (Fig. 9.3). Some of these degradation products were identified in historical and archaeological samples as well (Ferreira et al. 2003; Zhang et al. 2007).

Madder degradation has been extensively investigated, due to its wide occurrence in works of art (Ahn and Obendorf 2004; Clementi et al. 2007; Saunders and Kirby 1994). Ahn and co-workers worked on alizarin in water solution and identified possible degradation products such as phthalic acid and phtalic anhydride, and benzoic acid. However, Clementi and co-workers did not identify any degradation products after accelerated ageing of wool yarns dyed with madder.

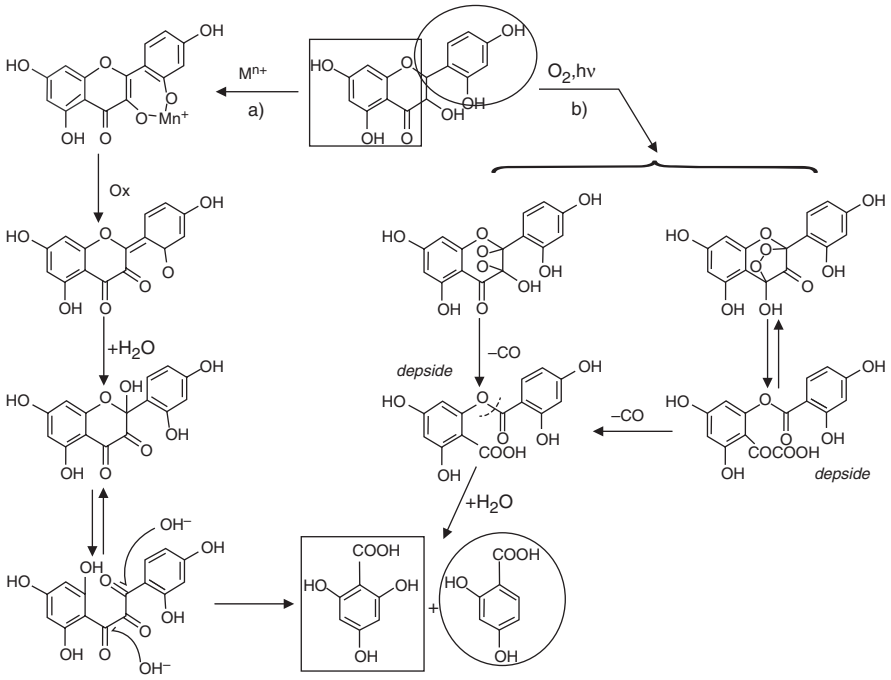

Fig. 9.3 Suggested degradation pathway for morin: (**a**) oxidation catalysed by a metallic ion (Mn^+) and (**b**) oxidation by atmospheric oxygen activated by light (O_2, hν). The square and the circle evidence the fates of the two aromatic rings (Colombini et al. 2007)

Many studies have been carried out on the synthetic dyes and pigments characterization while few have been performed on their artificial ageing and in particular on the identification of the relative degradation compounds in paintings, drawings or historical textiles (Alvarez-Martin and Janssens 2018; Anghelone et al. 2018; Burnstock et al. 2005; Confortin et al. 2010, n.d.; Crews 1987; Dunn et al. 2003; Favaro et al. 2012; Ghelardi et al. 2015a; Weyermann et al. 2006, 2009). Extensive publications describe the detection of synthetic dyes in wastewaters along with remediation strategies, whereas only few discuss in detail the photodegradation pathways in solution (Pirok Bob et al. 2019a, b; Sabatini et al. 2021). Thus, the database of reference systems and case studies analysed needs to be enlarged in order to reveal degradation processes of SOPs.

9.4 Case Studies

In the previous section, the potential of chromatography-mass spectrometry and several of the anlytical issues involving the analysis of synthetic organic pigments were discussed. In this section, some case studies will be described to hightlight

how chromatography-mass spectrometry allows the analyst to overcome analytical challenges and to produce data that can be used for authentication purposes.

9.4.1 Commercial Paint Materials: Database of Manufacturers

One of the main causes of confusion on the effective composition of commercial paint materials is the use of creative and non-informative names by the manufacturers, who even used the same name for defining formualtions with different compositions. An explicative example of this latter case is constituted by three red historical colorants from LeFranc Archive in Le Mans (France) and one paint tube, dated to the early twentieth century. The three powders were all labelled as *Laque de Garance*, while the paint tube was named *Lac Fine*. The containers of the powders and the paint tube are shown in Fig. 9.4, along with the chromatograms acquired on the extracts of microsamples (Degano et al. 2017).

In all the chromatograms a peak ascribable to alizarin was detected but, while in the paint tube alizarin was the main colorant, in the three powders it was present in

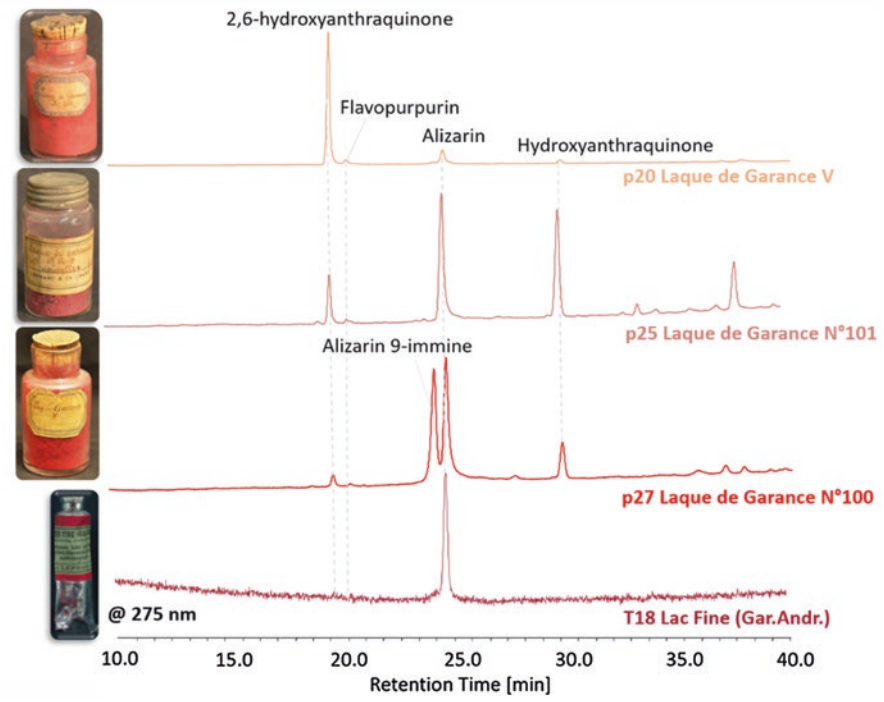

Fig. 9.4 HPLC-DAD chromatograms (extracted at 480 nm) of the extracts of one Lefranc paint tube and three powders (from the bottom to the top): *Lac Fine (Gar. Andr.)*; *Laque de Garance N°100*; *Laque de Garance N°101*; *Laque de Garance V* (Degano et al. 2017)

variable amounts and together with other abundant coloured compounds. These species were identified by chromatography with high resolution tandem mass spectrometry (HPLC-ESI-Q-ToF) as 2,6-dihydroxyanthraquinone, flavopurpurin and a hydroxyanthraquinone (possibly 2-hydroxyanthraquinone), which are synthetic species and plausible by-products in the synthesis alizarin, as suggested on the basis of the process reported in (Degano et al. 2017; Fieser 1930). "Laque de Garance Number 100" also contains alizarin-9-imine, possibly formed by treating synthetic alizarin with ammonia. The qualitative and quantitative differences in composition of the three powders from the same period, manufacture and labelled with the same name highlight how important it is to characterise reference materials in order to build rich databases. At the same time, this example clarifies how extensive knowledge of commercial paint formulations may allow the scientist to trace specific manufacture on the basis of the profile collected for a sample from a disputed work of art. Therefore, this information can be correlated with the dating of the artwork and the information related to paint suppliers.

9.4.2 Commercial Paint Materials: Comparison of Yellow Formulations

Four case studies have reported the detection of Hansa Yellow pigments by chromatography with spectrophotometric and mass spectrometric detection (HPLC-DAD and HPLC-ESI-Q-ToF), in materials and works-of-art dating from the beginning of the twentieth century to 2003. The chromatographic profiles obtained for the extracts of a LeFranc green paint tube labelled as *Vert Anglais N°3* (Degano et al. 2017), a yellow powder from Fernando Melani's archive (1907–1985, *yellow 3_Melani*) (Carlesi et al. 2013), a red sample taken from the pop-art sculpture *Disgelo* by Piero Gilardi (1942) (La Nasa et al. 2019) and a yellow sample taken from the painting *Quartet* by Alex Harding (2003) (La Nasa et al. 2020) are provided in Fig. 9.5.

The combined information provided by the two detectors disclosed the composition of these four formulations. Even if the four samples are coloured in different hues, the yellow base for all of them is a Hansa Yellows (PY1, PY1 isomer and PY3) suggesting a common trend to use these pigments together. Nevertheless, the relative amount of PY1 and PY3 differs in the samples suggesting different recipes that were possibly adapted on the basis of the other organic and/or inorganic pigments present in the formulations. In particular, the LeFranc tube, *Quartet* and *Disgelo* chromatograms are richer in PY3 while the *yellow 3_Melani* in PY1. Considering the good lightfastness of Hansa Yellow pigments and their stability in time, the ratio between these two pigments may be used to discriminate formulations of different paint manufactures detected in artworks. If the painter's atelier materials are available, the evaluation of the authenticity of artworks may be performed by comparing not only the qualitative but also the semi-quantitative composition of the pigments identified.

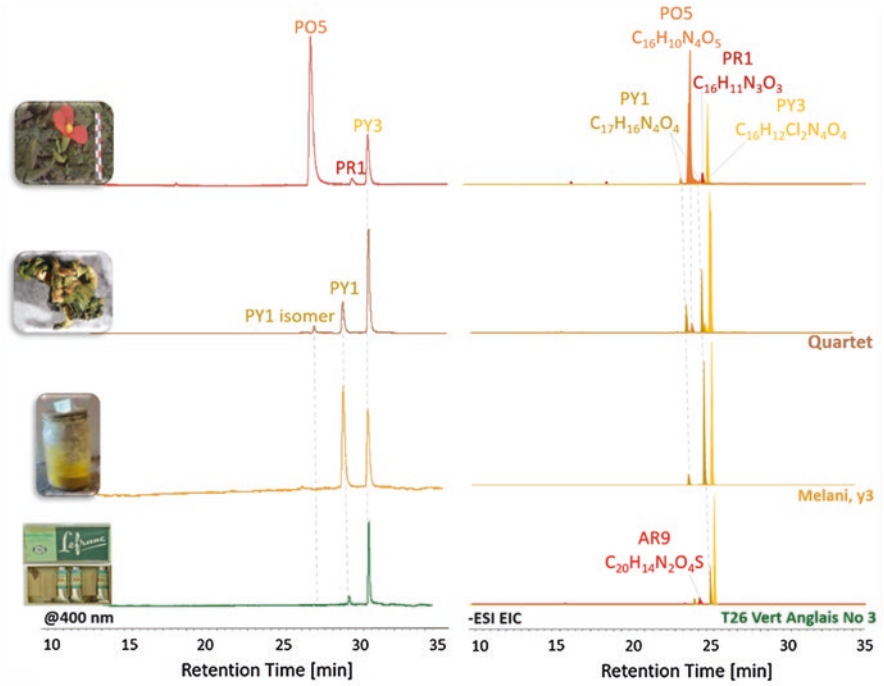

Fig. 9.5 HPLC-DAD chromatograms (extracted at 400 nm) on the left, HPLC-ESI-Q-ToF Extract Ion Chromatograms (EIC) (acquired in negative ionization mode) of $C_{17}H_{16}N_4O_4$, $C_{16}H_{10}N_4O_5$, $C_{16}H_{11}N_3O_3$ and $C_{16}H_{12}Cl_2N_4O_4$ of the extracts of atelier materials and artworks (from the bottom to the top): *Vert Anglais N°3* (Degano et al. 2017), *yellow 3_Melani* (Carlesi et al. 2013), the painting *Quartet* (Alex Harding 2003) (La Nasa et al. 2020); the pop-art sculpture *Disgelo* (Piero Gilardi, 1942) (La Nasa et al. 2019)

9.4.3 Ageing and a Cautionary Tale

Unfortunately, the evaluation of the relative pigment ratio cannot be used as a reliable criterion for all classes of pigments. Many of them, such as triarylmethines and xanthenes, exhibit poor lightfastness, resulting in degradation and consequent modification of the chromatographic profiles. Methyl violet, a triarylmethine pigment, was one of the colours employed by Giulio Turcato to create the effect of a lunar surface in his painting *Composizione-Superficie Lunare* (1965) (Sabatini et al. 2020c). The artwork was overheated and damaged by fire. The HPLC-ESI-Q-ToF analysis of two samples collected from two areas of the painting suggested the use of methyl violet, even though different profiles were obtained: sample 1 shows lower amount of hexa-N-methyl pararosaniline (hexa MP) and an increase in intensity of the respective demethylated compounds (Fig. 9.6).

Methyl violet is a complex mixture generally constituted by tetra, penta and hexa-N-methyl pararosaniline (tetra MP, penta MP, hexa MP, respectively) but many formulations were available that vary based on the synthetic strategy adopted.

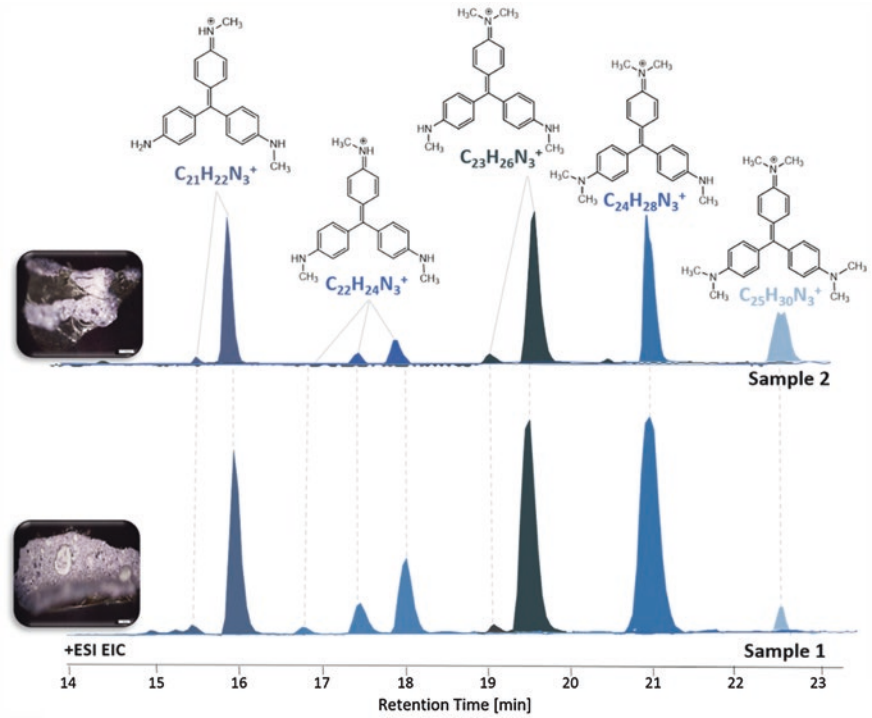

Fig. 9.6 HPLC-ESI-Q-ToF Extract Ion Chromatograms (EIC) (acquired in positive ionization mode) of $C_{19}H_{18}N_3^+$, $C_{20}H_{20}N_3^+$, $C_{21}H_{22}N_3^+$, $C_{22}H_{24}N_3^+$, $C_{23}H_{26}N_3^+$, $C_{24}H_{28}N_3^+$ and $C_{25}H_{30}N_3^+$ of the extracts of two samples (1 and 2) taken from the painting *Composizione-Superficie Lunare* (Giulio Turcato, 1965) (Sabatini et al. 2020c)

Moreover, the composition of methyl violet formulations might be altered by degradation, proceeding via demetylation (Confortin et al. 2010). Thus, the relative ratio of the different N-methyl pararosaniline products is not distinctive for a specific formulation. Finally, the only conclusion to be drawn for the present case study is that sample 1 is more degraded than sample 2.

9.4.4 Ageing and a Tale of Success

Artificial ageing of reference materials may be a reliable simulation of the natural ageing possibly occurring in an artwork, as demonstrated in the following case study. The drawing *Montmajour* by Vincent Van Gogh (1888) appears brownish but purple shades are present on the edges where the ink has been protected from light by the frame (Confortin et al. 2010). The purple ink resembled that used for drawings and letters produced in the same period by the artist, in which methyl violet had been already found. The positive matching between the chromatographic

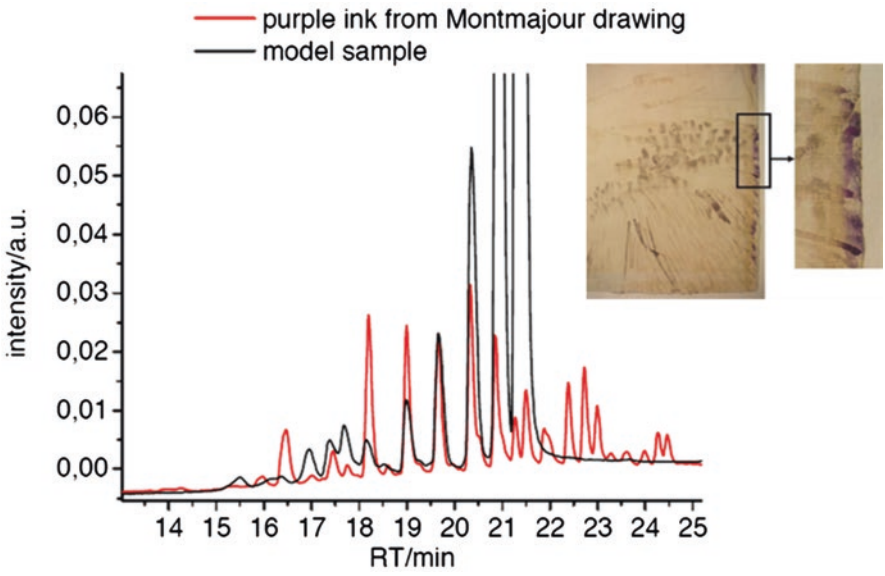

Fig. 9.7 HPLC-PDA chromatograms (extracted at 590 nm) of model sample of crystal violet faded on paper and of purple ink from the drawing *Montmajour* (Vincent Van Gogh 1888). Adapted from (Confortin et al. 2010)

(HPLC-PDA) profile collected for aged model samples of historical crystal violet (mainly constituted by hexa-N-methyl pararosaniline) faded on paper (irradiated by UV light for 340 h) and a sample from a purple ink area of *Montmajour* (Fig. 9.7) gave evidence of the reliability of the model samples prepared, at the same time, validating the authenticity of the drawing.

9.5 Conclusions

The review of scientific publications and the case studies presented demonstrate the ability of chromatographic and mass spectrometric techniques to provide qualitative and even semi-quantitative information on the complex mixtures constituting organic lakes and pigments. Such detailed information, if corroborated by a comparison with a suitable set of reference materials, can be used to supplement other scientific data to refute a specific historical period, or identify paint materials or additions that may be consistent with a particular period or artist's practice.

References

Abrahart EN. Dyes and Their Intermediates 1977

Ahn, C., Obendorf, S.K.: Dyes on archaeological textiles: analyzing alizarin and its degradation products. Text. Res. J. **74**, 949–954 (2004). https://doi.org/10.1177/004051750407401102

Alvarez-Martin, A., Janssens, K.: Protecting and stimulating effect on the degradation of eosin lakes. Part 1: Lead white and cobalt blue. Microchem. J. **141**, 51–63 (2018). https://doi.org/10.1016/j.microc.2018.05.005

Alvarez-Martin, A., Cleland, T.P., Kavich, G.M., Janssens, K., Newsome, G.A.: Rapid evaluation of the debromination mechanism of eosin in oil paint by direct analysis in real time and direct infusion-electrospray ionization mass spectrometry. Anal. Chem. **91**, 10856–10863 (2019). https://doi.org/10.1021/acs.analchem.9b02568

Andreotti, A., Bonaduce, I., Colombini, M.P., Ribechini, E.: Characterisation of natural indigo and shellfish purple by mass spectrometric techniques. Rapid Commun. Mass Spectrom. (2004). https://doi.org/10.1002/rcm.1464

Andreotti, A., Colombini, M.P., Ribechini, E., D'Alessio, A., Frezzato, F.: The characterisation of red-violet organic colours in ancient samples. In: The Diversity of Dyes in History & Archaeology, pp. 97–106 (2017)

Anghelone, M., Stoytschew, V., Jembrih-Simbürger, D., Schreiner, M.: Spectroscopic methods for the identification and photostability study of red synthetic organic pigments in alkyd and acrylic paints. Microchem. J. **139**, 155–163 (2018). https://doi.org/10.1016/j.microc.2018.02.029

Armitage, R.A., Jakes, K., Day, C.: Direct analysis in real time-mass spectroscopy for identification of red dye colourants in Paracas Necropolis Textiles. Sci. Technol. Archaeol. Res. **1**, 60–69 (2015). https://doi.org/10.1179/2054892315Y.0000000009

Armitage, R.A., Fraser, D., Degano, I., Colombini, M.P.: The analysis of the Saltzman Collection of Peruvian dyes by high performance liquid chromatography and ambient ionisation mass spectrometry. Herit. Sci. **7**, 81 (2019). https://doi.org/10.1186/s40494-019-0319-1

Astefanei, A., van Bommel, M., Corthals, G.L.: Surface acoustic wave nebulisation mass spectrometry for the fast and highly sensitive characterisation of synthetic dyes in textile samples. J. Am. Soc. Mass Spectrom. **28**, 2108–2116 (2017). https://doi.org/10.1007/s13361-017-1716-x

Bacci, M., Casini, A., Picollo, M., Radicati, B., Stefani, L.: Integrated non-invasive technologies for the diagnosis and conservation of the cultural heritage. J. Neutron. Res. **14**, 11–16 (2006). https://doi.org/10.1080/10238160600672930

Ball, P.: Bright Earth: Art and the Invention of Color. Straus, New York (2001)

Boon, J.J., Learner, T.: Analytical mass spectrometry of artists' acrylic emulsion paints by direct temperature resolved mass spectrometry and laser desorption ionisation mass spectrometry. J. Anal. Appl. Pyrolysis. **64**, 327–344 (2002). https://doi.org/10.1016/S0165-2370(02)00045-1

Boon, J.J., Hoogland, F.G., van der Horst, J.: Mass spectrometry of modern paints. In: Modern Paints Uncovered: Proceedings from the Modern Paints Uncovered Symposium (2007)

Bosi, A., Ciccola, A., Serafini, I., Guiso, M., Ripanti, F., Postorino, P., et al.: Street art graffiti: discovering their composition and alteration by FTIR and micro-Raman spectroscopy. Spectrochim Acta Part A Mol. Biomol. Spectrosc. **225**, 117474 (2020). https://doi.org/10.1016/j.saa.2019.117474

Burnstock, A., Lanfear, I., van den Berg, K.J., Carlyle, L., Clarke, M., Hendriks, E., et al.: Comparison of the fading and surface deterioration of red lake pigments in six paintings by Vincent van Gogh with artificially aged paint reconstructions. In: ICOM Committee for Conservation 14th Triennial Meeting. Den Haag, p. 4569. James and James, London (2005)

Carlesi, S., Bartolozzi, G., Cucci, C., Marchiafava, V., Picollo, M.: The artists' materials of Fernando Melani: a precursor of the Poor Art artistic movement in Italy. Spectrochim Acta Part A Mol. Biomol. Spectrosc. **104**, 527–537 (2013). https://doi.org/10.1016/j.saa.2012.11.094

Carlesi, S., Bartolozzi, G., Cucci, C., Marchiafava, V., Picollo, M., La Nasa, J., et al.: Discovering "the Italian Flag" by Fernando Melani (1907-1985). Spectrochim Acta – Part A Mol. Biomol. Spectrosc. **168**, 52–59 (2016). https://doi.org/10.1016/j.saa.2016.05.027

Casas-Catalán, M.J., Doménech-Carbó, M.T.: Identification of natural dyes used in works of art by pyrolysis-gas chromatography/mass spectrometry combined with in situ trimethylsilylation. In: Analytical and Bioanalytical Chemistry, vol. 382, pp. 259–268. Springer (2005). https://doi.org/10.1007/s00216-005-3064-0

Chieli, A., Romani, A., Degano, I., Sabatini, F., Tognotti, P., Miliani, C.: New insights into the fading mechanism of Geranium lake in painting matrix. New J. Chem. Della RCS. (2019) submitted

Christiansen, M.B., Baadsgaard, E., Sanyova, J., Simonsen, K.P.: The artists' materials of P. S. Krøyer: an analytical study of the artist's paintings and tube colours by Raman, SEM--EDS and HPLC. Herit. Sci. **5**, 39 (2017). https://doi.org/10.1186/s40494-017-0153-2

Ciatti, M., Marini, P. (eds.): Andrea Mantegna. La Pala di San Zeno: studio e conservazione. Edifir, Firenze (2009)

Claro, A., Melo, M.J., de Melo, J.S.S., van den Berg, K.J., Burnstock, A., Montague, M., et al.: Identification of red colorants in van Gogh paintings and ancient Andean textiles by microspectrofluorimetry. J. Cult. Herit. **11**, 27–34 (2010). https://doi.org/10.1016/j.culher.2009.03.006

Clementi, C., Nowik, W., Romani, A., Cibin, F., Favaro, G.: A spectrometric and chromatographic approach to the study of ageing of madder (Rubia tinctorum L.) dyestuff on wool. Anal. Chim. Acta. **596**, 46–54 (2007). https://doi.org/10.1016/j.aca.2007.05.036

Colombini, M.P., Modugno, F.: Organic materials in art and archaeology. In: Colombini, M.P., Modugno, F. (eds.) Organic Mass Spectrometry in Art and Archaeology, pp. 1–36. Wiley (2009). https://doi.org/10.1002/9780470741917.ch1

Colombini, M.P., Carmignani, A., Modugno, F., Frezzato, F., Olchini, A., Brecoulaki, H., et al.: Integrated analytical techniques for the study of ancient Greek polychromy. Talanta. **63**, 839–848 (2004). https://doi.org/10.1016/j.talanta.2003.12.043

Colombini, M.P.M.P., Andreotti, A., Baraldi, C., Degano, I., Łucejko, J.J.: Colour fading in textiles: a model study on the decomposition of natural dyes. Microchem. J. **85**, 174–182 (2007). https://doi.org/10.1016/j.microc.2006.04.002

Colombini, M.P., Degano, I., Ribechini, E.: A multi analytical approach to determine Madder lake in a funerary clay vessel found in a chamber tomb in Taranto. In: Kirby (ed.) The Diversity of Dyes in History & Archaeology. Archetype, London (2017)

Colour index. https://colour-index.com/

Confortin, D., Neevel, H., Brustolon, M., Franco, L., Kettelarij, A.J., Williams, R.M., et al.: Crystal violet: study of the photo-fading of an early synthetic dye in aqueous solution and on paper with HPLC-PDA, LCMS and FORS. J. Phys. Conf. Ser. **231**, 1–9 (2010)

Confortin, D., Neevel, H., Van Bommel, M., Reissland, B.: Study of the degradation of an early synthetic dye. Crystal Violet, 197–201 (n.d.)

Crews, P.C.: The fading rates of some natural dyes. Stud. Conserv. **32**, 65–72 (1987). https://doi.org/10.1179/sic.1987.32.2.65

Cucci, C., Bartolozzi, G., De Vita, M., Marchiafava, V., Picollo, M., Casadio, F.: The colors of Keith Haring: a spectroscopic study on the materials of the mural painting Tuttomondo and on reference contemporary outdoor paints. Appl. Spectrosc. **70**, 186–196 (2016). https://doi.org/10.1177/0003702815615346

De Keijzer, M.: The history of modern synthetic inorganic and organic artists' pigments. In: Contributions to Conservation: Research in Conservation at the Netherlands Institute for Cultural Heritage (ICN Instituut Collectie Nederland), pp. 42–54. James & James, London (2002)

de Keijzer, M.: The delight of modern organic pigment creations. In: van den Berg, K.J., Burnstock, A., de Keijzer, M., Krueger, J., Learner, T., Tagle, A., et al. (eds.) Issues in Contemporary Oil Paint, pp. 45–73. Springer, Cham (2014). https://doi.org/10.1007/978-3-319-10100-2_4

Degani, L., Riedo, C., Gulmini, M., Chiantore, O.: From plant extracts to historical textiles: characterization of dyestuffs by GC–MS. Chromatographia. **77**, 1683–1696 (2014). https://doi.org/10.1007/s10337-014-2772-z

Degano, I.: Liquid chromatography: current applications in heritage science and recent developments. Phys. Sci. Rev. **4**, 20180009 (2019)

Degano, I., La Nasa, J.: Trends in high performance liquid chromatography for cultural heritage. Top. Curr. Chem. **374**, 20 (2016). https://doi.org/10.1007/s41061-016-0020-8

Degano, I., Tognotti, P., Kunzelman, D., Modugno, F.: HPLC-DAD and HPLC-ESI-Q-ToF characterisation of early 20th century lake and organic pigments from Lefranc archives. Herit. Sci. **5**, 7 (2017). https://doi.org/10.1186/s40494-017-0120-y

Doherty, B., Degano, I., Romani, A., Higgitt, C., Peggie, D., Colombini, M.P., et al.: Identifying Brazilwood's marker component, Urolithin C, in historical textiles by surface-enhanced Raman spectroscopy. Heritage. **4**, 1415–1428 (2021). https://doi.org/10.3390/heritage4030078

Dunn, J., Siegel, J., Allison, J.: Photodegradation and laser desorption mass spectrometry for the characterization of dyes used in red pen inks. Sci. J. Foren. **48**, 652 (2003)

Evans, D.G.: The Color Index international papers for 1992. J. Soc. Dye. Colour. **106**, 192–193 (1990)

Fabbri, D., Chiavari, G., Ling, H.: Analysis of anthraquinoid and indigoid dyes used in ancient artistic works by thermally assisted hydrolysis and methylation in the presence of tetramethylammonium hydroxide. J. Anal. Appl. Pyrolysis. **56**, 167–178 (2000). https://doi.org/10.1016/S0165-2370(00)00092-9

Favaro, G., Confortin, D., Pastore, P., Brustolon, M.: Application of LC-MS and LC-MS-MS to the analysis of photo-decomposed crystal violet in the investigation of cultural heritage materials aging. J. Mass Spectrom. **47**, 1660–1670 (2012). https://doi.org/10.1002/jms.3110

Feller, R.L.: Accelerated Aging-Photochemical and Thermal Aspects. The Getty Conservation Institute (1994)

Ferreira, E., Quye, A., McNab, H., Hulme, A., Wouters, J., Boon, J.J.: The analytical characterisation of flavonoid photodegradation products: a novel approach to identifying natural yellow dyes in ancient textiles. ICOM-CC 12th Trienn. Meet. Lyon. **1**, 221–227 (1999)

Ferreira, E.S., Quye, A., McNab, H., Hulme, A.N.: Photo-oxidation products of quercetin and morin as markers for the characterisation of natural flavonoid yellow dyes in ancient textiles. Dye Hist. Archaeol. **18**, 63–72 (2002)

Ferreira, E., Quye, A., Hulme, A., McNab, H.: LC-Ion trap MS and PDA HPLC complementary techniques in the analysis of flavonoid dyes in historical textiles: the case study of an 18th century herald's tabard. Dye. **19**, 13–18 (2003)

Fieser, L.: The dicovery of synthetic alizarin. J. Chem. Educ. **7**, 2609–2633 (1930)

Garfield, S.: Purple Patch. Faber, London (2011)

Gautier, G., Bezur, A., Muir, K., Casadio, F., Fiedler, I.: Chemical fingerprinting of ready-mixed house paints of relevance to artistic production in the first half of the twentieth century. Part I: inorganic and organic pigments. Appl. Spectrosc. **63**, 597–603 (2009). https://doi.org/10.1366/000370209788559584

Geldof, M., de Keijzer, M., van Bommel, M.R., Pilz, K., Salvant, J., van Keulen, H., et al.: Van Gogh's geranium lake. In: Vellekoop, M., Muriel, G., Hendriks, E., Jansen, L., de Tagle, A. (eds.) Van Gogh's Studio Practice, pp. 268–289. Yale University/Mercatorfonds, Amsterdam/Brussels (2013)

Germinario, G., Rigante, E.C.L.L., van der Werf, I.D., Sabbatini, L.: Pyrolysis gas chromatography–mass spectrometry of triarylmethane dyes. J. Anal. Appl. Pyrolysis. **127**, 229–239 (2017). https://doi.org/10.1016/j.jaap.2017.08.001

Ghelardi, E., Degano, I., Modugno, F., Colombini, M.P.: An integrated approach to the study of Ri de pomme, a painting by Julian Schnabel. Int. J. Conserv. Sci. **6**, 51–62 (2015)

Ghelardi, E., Degano, I., Colombini, M.P., Mazurek, J., Schilling, M., Khanjian, H., et al.: A multi-analytical study on the photochemical degradation of synthetic organic pigments. Dyes Pigments. **123**, 396–403 (2015a). https://doi.org/10.1016/j.dyepig.2015.07.029

Ghelardi, E., Degano, I., Colombini, M.P., Mazurek, J., Schilling, M., Learner, T.: Py-GC/MS applied to the analysis of synthetic organic pigments: characterization and identification in paint samples. Anal. Bioanal. Chem. **407**, 1415–1431 (2015b). https://doi.org/10.1007/s00216-014-8370-y

Graebe, G., Liebermann, C.: L'alizarine artificielle. Montieur. Sci. **21**, 394 (1879)

Grazia, C., Buti, D., Amat, A., Rosi, F., Romani, A., Domenici, D., et al.: Shades of blue: non-invasive spectroscopic investigations of Maya blue pigments. From laboratory mock-ups to Mesoamerican codices. Herit. Sci. **8**, 1 (2020). https://doi.org/10.1186/s40494-019-0345-z

Guinot, P., Andary, C.: Molecules involved in the dyeing process with flavonoids. Dye Hist. Archaeol. **25**, 21–22 (2006)

Halpine, S.M.: An improved dye and lake pigment analysis method for high-performance liquid chromatography and diode-array detector. Stud. Conserv. **41**, 76–94 (1996). https://doi.org/10.2307/1506519

Herbst, W., Hunger, K., Wilker, G., Ohleier, H., Winter, R.: Industrial Organic Pigments, 3rd edn. Wiley (2004). https://doi.org/10.1002/3527602429

Herndon, W.C.: Resonance theory and the enumeration of Kekule structures. J. Chem. Educ. **51**, 10 (1974). https://doi.org/10.1021/ed051p10

Karapanagiotis, I., Sotiropoulou, S., Chryssikopoulou, E., Magiatis, P., Andrikopoulos, K.S., Chryssoulakis, Y.: Investigation of Tyrian purple occurring in prehistoric wall paintings of Thera. In: The Diversity of Dyes in History & Archaeology, pp. 82–89 (2017)

Kirby, J., White, R.: The identification of red lake pigment dyestuffs and a discussion of their use. Natl. Gall. Tech. Bull. **17**, 56–80 (1996)

Kirby, J., Spring, M., Higgitt, C.: The technology of red lake pigment manufacture: study of the dyestuff substrate. Natl. Gall. Tech. Bull. **26**, 71–87 (2005a)

Kirby, J., Townsend, K.H., Stijnman, A.: The reconstruction of late 19th-century French red lake pigments. In: Archetype Publications (ed.) Art of the Past – Sources and Reconstructions, p. 69. Archetype Publications, London (2005b)

Kirby, J., Spring, M., Higgitt, C.: The technology of eighteenth- and nineteenth-century red lake pigments. Natl. Gall. Tech. Bull. **28**, 69–87 (2007)

Kirby, D.P., Khandekar, N., Sutherland, K., Price, B.A.: Applications of laser desorption mass spectrometry for the study of synthetic organic pigments in works of art. Int. J. Mass Spectrom. **284**, 115–122 (2009). https://doi.org/10.1016/j.ijms.2008.08.011

Kirby, J., van Bommel, M.R., Verhecken, A.: Natural Colorants for Dyeing and Lake Pigments: Practical Recipes and Their Historical Sources. Archetype Publication, London (2014)

La Nasa, J., Biale, G., Sabatini, F., Degano, I., Colombini, M.P., Modugno, F.: Synthetic materials in art: a new comprehensive approach for the characterization of multi-material artworks by analytical pyrolysis. Herit. Sci. **7**, 8 (2019). https://doi.org/10.1186/s40494-019-0251-4

La Nasa, J., Nodari, L., Nardella, F., Sabatini, F., Degano, I., Modugno, F., et al.: Chemistry of modern paint media: the strained and collapsed painting by Alexis Harding. Microchem. J. **155**, 104659 (2020). https://doi.org/10.1016/J.MICROC.2020.104659

La Nasa, J., Campanella, B., Sabatini, F., Rava, A., Shank, W., Lucero-Gomez, P., et al.: 60 years of street art: a comparative study of the artists' materials through spectroscopic and mass spectrometric approaches. J. Cult. Herit. **48**, 129–140 (2021). https://doi.org/10.1016/j.culher.2020.11.016

Learner, T.J.S.: Analysis of Modern Paints. The Getty (2005)

Learner, T.J.S., Smithen, P., Krueger, J.W., Schilling, M.R.: Modern Paints Uncovered Symposium. Tate Modern, London (2006)

Lech, K., Wilicka, E., Witowska-Jarosz, J., Jarosz, M.: Early synthetic dyes – a challenge for tandem mass spectrometry. J. Mass Spectrom. **48**, 141–147 (2013). https://doi.org/10.1002/jms.3090

Lomax, S.Q.L.T., Lomax, S.Q., Learner, T.: A review of the classes, structures, and methods of analysis of synthetic organic pigments. J. Am. Inst. Conserv. **45**, 107–125 (2006). https://doi.org/10.1179/019713606806112540

Lomax, S., Schilling, M., Learner, T.: The Identification of Synthetic Organic Pigments by FTIR and DTMS. Mod. Paint. Uncovered (2007)

Lomax, S.Q., Lomax, J.F., De Luca-Westrate, A.: The use of Raman microscopy and laser desorption ionization mass spectrometry in the examination of synthetic organic pigments in modern works of art. J. Raman Spectrosc. **45**, 448–455 (2014). https://doi.org/10.1002/jrs.4480

Lutzenberger, Stege, H.: From Beckmann to Baselitz-towards an improved micro-identification of organic pigments in paintings of 20th century art. Preserv. Sci. **6**, 89–100 (2009)

Magrini, D., Bracci, S., Cantisani, E., Conti, C., Rava, A., Sansonetti, A., et al.: A multi-analytical approach for the characterization of wall painting materials on contemporary buildings. Spectrochim Acta Part A Mol. Biomol. Spectrosc. **173**, 39–45 (2017). https://doi.org/10.1016/j.saa.2016.08.017

Manhita, A., Ferreira, T., Candeias, A., Barrocas, D.C.: Extracting natural dyes from wool-an evaluation of extraction methods. Anal. Bioanal. Chem. **400**, 1501–1514 (2011). https://doi.org/10.1007/s00216-011-4858-x

Mayhew, H.E., Fabian, D.M., Svoboda, S.A., Wustholz, K.L.: Surface-enhanced Raman spectroscopy studies of yellow organic dyestuffs and lake pigments in oil paint. Analyst. **138**, 4493–4499 (2013). https://doi.org/10.1039/c3an00611e

Meister Lucius & Brüning. DRP 257 488 1909

Menke, C.A., Rivenc, R., Learner, T.: The use of direct temperature-resolved mass spectrometry (DTMS) in the detection of organic pigments found in acrylic paints used by Sam Francis. Int. J. Mass Spectrom. **284**, 2–11 (2009). https://doi.org/10.1016/j.ijms.2008.12.006

Moretti, P., Germinario, G., Doherty, B., van der Werf, I.D., Sabbatini, L., Mirabile, A., et al.: Disclosing the composition of historical commercial felt-tip pens used in art by integrated vibrational spectroscopy and pyrolysis-gas chromatography/mass spectrometry. J. Cult. Herit. **35**, 242–253 (2019). https://doi.org/10.1016/j.culher.2018.03.018

Padfield, J.: Mild Extraction Methods for Organic Colorant Analysis, A Bibliographic Reference Database. Charisma Project Website, Natl Gall Sci Dep (http://research.ng-london.org.uk/scientific/colourant/)

Pirok Bob, W.J., Moro, G., Meekel, N., SVJ, B., Schoenmakers, P.J., van Bommel, M.R.: Mapping degradation pathways of natural and synthetic dyes with LC-MS: influence of solvent on degradation mechanisms. J. Cult. Herit. (2019a). https://doi.org/10.1016/j.culher.2019.01.003

Pirok Bob, W.J., den Uijl, M.J., Moro, G., Berbers, S.V.J., Croes, C.J.M., van Bommel, M.R., et al.: Characterization of dye extracts from historical cultural-heritage objects using state-of-the-art comprehensive two-dimensional liquid chromatography and mass spectrometry with active modulation and optimized shifting gradients. Anal. Chem. **91**, 3062–3069 (2019b). https://doi.org/10.1021/acs.analchem.8b05469

Pirok, B.W.J.J., Knip, J., van Bommel, M.R., Schoenmakers, P.J.: Characterization of synthetic dyes by comprehensive two-dimensional liquid chromatography combining ion-exchange chromatography and fast ion-pair reversed-phase chromatography. J. Chromatogr. A. **1436**, 141–146 (2016). https://doi.org/10.1016/j.chroma.2016.01.070

Poulin, J.: A new methodology for the characterisation of natural dyes on museum objects using gas chromatography–mass spectrometry. Stud. Conserv. **63**, 36–61 (2018). https://doi.org/10.1080/00393630.2016.1271097

Pozzi, F., Basso, E., Centeno, S.A., Smieska, L.M., Shibayama, N., Berns, R., et al.: Altered identity: fleeting colors and obscured surfaces in Van Gogh's Landscapes in Paris, Arles, and Saint-Rémy. Herit. Sci. **9**, 15 (2021). https://doi.org/10.1186/s40494-021-00489-1

Read, R.: Q and A: picric acid. Chem. Aust. (2014)

Rehorek, A., Plum, A.: Characterization of sulfonated azo dyes and aromatic amines by pyrolysis gas chromatography/mass spectrometry. Anal. Bioanal. Chem. **388**, 1653–1662 (2007). https://doi.org/10.1007/s00216-007-1390-0

Restivo, A., Degano, I., Ribechini, E., Colombini, M.P.: Development and optimisation of an HPLC-DAD-ESI-Q-ToF method for the determination of phenolic acids and derivatives. PLoS One. **9**, e88762 (2014). https://doi.org/10.1371/journal.pone.0088762

Russell, J., Singer, B.W., Perry, J.J., Bacon, A.: The identification of synthetic organic pigments in modern paints and modern paintings using pyrolysis-gas chromatography-mass spectrometry. Anal. Bioanal. Chem. **400**, 1473–1491 (2011). https://doi.org/10.1007/s00216-011-4822-9

Sabatini, F., Lluveras-Tenorio, A., Degano, I., Kuckova, S., Krizova, I., Colombini, M.P.: A matrix-assisted laser desorption/ionization time-of-flight mass spectrometry method for the identifica-

tion of anthraquinones: the case of historical lakes. J. Am. Soc. Mass Spectrom. **27** (2016). https://doi.org/10.1007/s13361-016-1471-4

Sabatini, F., Giugliano, R., Degano, I.: Photo-oxidation processes of Rhodamine B: a chromatographic and mass spectrometric approach. Microchem. J. **140**, 114–122 (2018). https://doi.org/10.1016/j.microc.2018.04.018

Sabatini, F., Degano, I., Colombini, M.P.: Development of a method based on high performance liquid chromatography coupled with diode array, fluorescence and mass spectrometric detectors for the analysis of eosin at trace levels. Sep. Sci. Plus. **3**, 207–215 (2020a). https://doi.org/10.1002/sscp.202000002

Sabatini, F., Eis, E., Degano, I., Thoury, M., Bonaduce, I., Lluveras-Tenorio, A.: The issue of eosin fading: a combined spectroscopic and mass spectrometric approach applied to historical lakes. Dyes Pigments. **180**, 108436 (2020b). https://doi.org/10.1016/j.dyepig.2020.108436

Sabatini, F., Manariti, A., Di Girolamo, F., Bonaduce, I., Tozzi, L., Rava, A., et al.: Painting on polyurethane foam: "Composizione-Superficie Lunare" by Giulio Turcato. Microchem. J. **156**, 104872 (2020c). https://doi.org/10.1016/j.microc.2020.104872

Sabatini, F., Degano, I., Bommel, M.: Investigating the in-solution photodegradation pathway of Diamond Green G by chromatography and mass spectrometry. Color. Technol., cote.12538 (2021). https://doi.org/10.1111/cote.12538

Saez, N.O., Vanden, B.I., Schalm, O., De Munck, B., Caen, J.: Material analysis versus historical dye recipes: ingredients found in black dyed wool from five Belgian archives (1650-1850). Conserv. Patrim. **31**, 115–132 (2019). https://doi.org/10.14568/cp2018025

Sanyova, J.: Mild extraction of dyes by hydrofluoric acid in routine analysis of historical paint microsamples. Microchim. Acta. **162**, 361–370 (2008). https://doi.org/10.1007/s00604-007-0867-z

Sanyova, J., Reisse, J.: Development of a mild method for the extraction of anthraquinones from their aluminum complexes in madder lakes prior to HPLC analysis. J. Cult. Herit. **7**, 229–235 (2006)

Saunders, D., Kirby, J.: Light-induced colour changes in red and yellow lake pigments. Natl. Gall. Tech. Bull. **15**, 79–97 (1994). https://doi.org/10.1017/CBO9781107415324.004

Schulte, F., Brzezinka, K.W., Lutzenberger, K., Stege, H., Panne, U.: Raman spectroscopy of synthetic organic pigments used in 20th century works of art. J. Raman Spectrosc. **39**, 1455–1463 (2008). https://doi.org/10.1002/jrs.2021

Serrano, A., Sousa, M.M., Hallett, J., Lopes, J.A., Oliveira, M.C.: Analysis of natural red dyes (cochineal) in textiles of historical importance using HPLC and multivariate data analysis. Anal. Bioanal. Chem. **401**, 735–743 (2011). https://doi.org/10.1007/s00216-011-5094-0

Serrano, A., Van Bommel, M., Hallett, J.: Evaluation between ultrahigh pressure liquid chromatography and high-performance liquid chromatography analytical methods for characterizing natural dyestuffs. J. Chromatogr. A. **1318**, 102–111 (2013). https://doi.org/10.1016/j.chroma.2013.09.062

Skelton, H.: A colour chemist's history of Western art. Rev. Prog. Color. Relat. Top. **29**, 43–64 (1999). https://doi.org/10.1111/j.1478-4408.1999.tb00127.x

Soltzberg, L.J., Hagar, A., Kridaratikorn, S., Mattson, A., Newman, R.: MALDI-TOF mass spectrometric identification of dyes and pigments. J. Am. Soc. Mass Spectrom. **18**, 2001–2006 (2007). https://doi.org/10.1016/j.jasms.2007.08.008

Sonoda, N.: Characterization of organic azo-pigments by pyrolysis–gas chromatography. Stud. Conserv. **44**, 195–208 (1999). https://doi.org/10.1179/sic.1999.44.3.195

Stenger, J., Kwan, E.E., Eremin, K., Speakman, S., Kirby, D., Stewart, H., et al.: Lithol red salts: characterization and deterioration. E-PreservationScience. **7**, 147–157 (2010)

Surowiec, I.: Application of high-performance separation techniques in archaeometry. Microchim. Acta. **162**, 289–302 (2008). https://doi.org/10.1007/s00604-007-0911-z

Surowiec, I., Orska-Gawryś, J., Biesaga, M., Trojanowicz, M., Hutta, M., Halko, R., et al.: Identification of natural dyestuff in archeological Coptic textiles by HPLC with fluorescence detection. Anal. Lett. **36**, 1211–1229 (2003). https://doi.org/10.1081/AL-120020154

Szostek, B., Orska-Gawrys, J., Surowiec, I., Trojanowicz, M.: Investigation of natural dyes occurring in historical Coptic textiles by high-performance liquid chromatography with UV-Vis and mass spectrometric detection. J. Chromatogr. A. **1012**, 179–192 (2003). https://doi.org/10.1016/S0021-9673(03)01170-1

Taujenis, L., Olšauskaite, V.: Identification of main constituents of historical textile dyes by ultra performance liquid chromatography with photodiode array detection. Chemija. **23**, 210–215 (2012)

Townsend, J.H.: Whistler's oil painting materials. Burlingt. Mag. **136**, 690–695 (1994)

Troalen, L.G., Phillips, A.S., Peggie, D.A., Barran, P.E., Hulme, A.N.: Historical textile dyeing with *Genista tinctoria* L.: a comprehensive study by UPLC-MS/MS analysis. Anal. Methods. **6**, 8915–8923 (2014). https://doi.org/10.1039/C4AY01509F

van Bommel, M.R.: The analysis of dyes with HPLC coupled to photodiode array and fluorescence detection. Dye. Hist. Archaeol. **20**, 30–38 (2005)

Van Bommel, M.R., Gedolf, M., Hendriks, E.: An investigation of organic red pigments used in paintings by Vincent Van Gogh. ArtMatters. **3**, 111–137 (2005)

van Bommel, M.R., Vanden Berghe, I., Wallert, A.M., Boitelle, R., Wouters, J.: High-performance liquid chromatography and non-destructive three-dimensional fluorescence analysis of early synthetic dyes. J. Chromatogr. A. **1157**, 260–272 (2007). https://doi.org/10.1016/j.chroma.2007.05.017

Weyermann, C., Spengler, B.: The potential of artificial aging for modelling of natural aging processes of ballpoint ink. Forensic Sci. Int. **180**, 23–31 (2008). https://doi.org/10.1016/j.forsciint.2008.06.012

Weyermann, C., Kirsch, D., Costa-Vera, C., Spengler, B.: Photofading of ballpoint dyes studied on paper by LDI and MALDI MS. J. Am. Soc. Mass Spectrom. **17**, 297–306 (2006). https://doi.org/10.1016/j.jasms.2005.11.010

Weyermann, C., Kirsch, D., Vera, C.C., Spengler, B.: Evaluation of the photodegradation of crystal violet upon light exposure by mass spectrometric and spectroscopic methods. J. Forensic Sci. **54**, 339–345 (2009). https://doi.org/10.1111/j.1556-4029.2008.00975.x

Wouters, J.: High performance liquid chromatography of anthraquinones: analysis of plant and insect extracts and dyed textiles. Stud. Conserv. **30**, 119–128 (1985). https://doi.org/10.1179/sic.1985.30.3.119

Wouters, J.: A new method for the analysis of blue and purple dyes in textiles. Dye Hist. Archaeol. **10**, 17–21 (1991)

Wouters, J., Grzywacz, C.M., Claro, A.: Markers for identification of faded safflower (Carthamus tinctorius L.) colorants by HPLC-PDA-MS – ancient fibres, pigments, paints and cosmetics derived from antique recipes. Stud. Conserv. **55**, 186–203 (2010). https://doi.org/10.1179/sic.2010.55.3.186

Zaffino, C., Passaretti, A., Poldi, G., Fratelli, M., Tibiletti, A., Bestetti, R., et al.: A multi-technique approach to the chemical characterization of colored inks in contemporary art: the materials of Lucio Fontana. J. Cult. Herit. **23**, 87–97 (2017). https://doi.org/10.1016/j.culher.2016.09.006

Zhang, X., Laursen, R.A.: Development of mild extraction methods for the analysis of natural dyes in textiles of historical interest using LC-diode array detector-MS. Anal. Chem. **77**, 2022–2025 (2005). https://doi.org/10.1021/ac048380k

Zhang, X., Boytner, R., Cabrera, J.L., Laursen, R.: Identification of yellow dye types in Pre-Columbian Andean Textiles. Anal. Chem. **79**, 1575–1582 (2007). https://doi.org/10.1021/ac061618f

Zollinger, H.: Color Chemistry: Syntheses, Properties, and Applications of Organic Dyes and Pigments. Wiley (2003)

Chapter 10
Raman Analysis of Inorganic and Organic Pigments

Anastasia Rousaki and Peter Vandenabeele

Abstract Raman spectroscopy is one of the most favorable techniques applied in the art analysis field. Its unique characteristics, namely the organic and inorganic components identification, spatial resolution down to micrometers scale, control of the laser power and measuring conditions and fast identification are just some of the remarkable features of the technique. Moreover, Raman spectroscopy can be applied directly on the artefact and on the field, with mobile systems, without jeopardizing the integrity of the work of art. Other Raman approaches can be considered namely, microspatially offset Raman spectroscopy (micro-SORS) and surface-enhanced Raman spectroscopy (SERS) when it comes to the direct non-destructive stratigraphic analysis of art works and the characterization of organic compounds such as dyes.

Keywords Benchtop Raman spectroscopy · Mobile Raman spectroscopy · Microspatially offset Raman spectroscopy · Surface enhanced Raman spectroscopy · Resonance Raman spectroscopy

A. Rousaki
Department of Chemistry, Raman Spectroscopy Research Group, Ghent University, Ghent, Belgium
e-mail: Anastasia.Rousaki@UGent.be

P. Vandenabeele (✉)
Department of Chemistry, Raman Spectroscopy Research Group, Ghent University, Ghent, Belgium

Department of Archaeology, Archaeometry Research Group, Ghent University, Ghent, Belgium
e-mail: Peter.Vandenabeele@UGent.be

M. P. Colombini et al. (eds.), *Analytical Chemistry for the Study of Paintings and the Detection of Forgeries*, Cultural Heritage Science,
https://doi.org/10.1007/978-3-030-86865-9_10

10.1 Introduction

Over the years, Raman spectroscopy has grown to become a frequently applied technique that is available to conservation scientists. The approach has many advantages, such as allowing a relatively quick identification of the artists' pigments while being non-destructive. By focussing a low power laser beam on a sample or even directly on the artwork, it is possible to record a molecular spectrum of the pigments, accounting for their identification.

Almost a century ago, in 1923, based on theoretical considerations, the German scientist Adolf Smekal predicted the inelastic scattering of light interacting with molecules. It lasted until 1928, till the Raman effect was for the first time observed by the Indian physicist Chandrasekhara Venkata Raman and his student Kariamanikkam Srinivasa Krishnan. In 1930, Sir Raman was awarded the Nobel prize of physics for this discovery that was named after him. In the initial days of Raman spectroscopy, Raman spectra were recorded using filtered sunlight and required a large (room-size) spectrometer to record spectra of large volumes (ca. 600 ml) of pure liquids (Gardiner and Graves 1989; Vandenabeele 2013). Soon, the introduction of mercury arch lamps accounted for a more stable light source and allowed to record spectra of smaller volumes of liquids. Often, mercury lamps were spiral-shaped and the sample was positioned in the center of the lamp, allowing to record spectra in a 90°-geometry. Photographic plates were used as detectors. However, setting-up and aligning the spectrometer was a complex and time-consuming task, which hampered the broad application of Raman spectroscopy outside specialised laboratories. Often, scientists preferred the use of infrared spectroscopy as a way to identify molecules, in a more routine way.

As Raman spectroscopy requires the use of a monochromatic light source, the introduction of lasers – which are intense and monochromatic – to excite the molecules, the time required to record a Raman spectrum was drastically reduced. Moreover, steadily the introduction of optical components improved the sensitivity of the instrumentation. This included, amongst others the introduction of charge-coupled-device (CCD) detectors, that are sensitive in the visual region of the electromagnetic spectrum. Until recently, as no sensitive detectors were available in this spectral region, spectrometers using infrared excitation (1064 nm) relied on the Fourier-transform technology to record high-quality spectra. Also, the introduction of high-quality notch filters allowed that for many applications the large double-monochromator spectrometers could be replaced by more compact instruments. Another milestone in the development of Raman spectroscopy was the coupling of Raman spectrometers with microscope optics, allowing to record Raman spectra of small solid particles, while the introduction of fibre-optics probes accounted for a flexible set-up. Since the first decade of current century, smaller and mobile spectrometers were introduced, allowing the technique to move away from a strictly controlled laboratory environment, introducing the possibilities to perform *in situ* measurements.

Along with these technological evolutions, new possibilities of implementing Raman spectroscopy for the investigation of art objects, became increasingly more available. It was soon after the introduction of confocal Raman microscopy by

M. Delhaye and P. Dhamelincourt (1975) that they realised that this approach could be of great advantage for the analysis of micrometer-sized particles, like minute pigment grains. Moreover, the technique was also applied for the direct Raman analysis of small-sized mediaeval manuscripts (Best et al. 1992; Clark 1995a, b). Laboratories created their reference databases with Raman spectra of artists' materials (Table 10.1).

As the field of applications broadened, different methods of data processing were developed, including chemometrical approaches. As an example, when studying

Table 10.1 Overview of some published collections of reference spectra of artists' materials

Collection	Description	References
UCL- Raman Spectroscopic Library of Natural and Synthetic Pigments	Collection with downloadable Raman spectra of mostly inorganic pigments. Many spectra were recorded with an Ar^+ laser, others with a HeNe laser. In a second paper, the database was extended with other laser wavelengths (http://www.chem.ucl.ac.uk/resources/raman/)	Bell et al. 1997; Burgio and Clark 2001
e-VISART database	Password protected database	Castro et al. 2005
ColoRaman	Raman and fluorescence spectroscopy of oil, tempera and fresco paint pigments	Burrafato et al. 2004
Medieval pigments	Collection of spectra of mediaeval pigments	Marucci et al. 2018
Natural organic binding media and varnishes	Collection and discussion of Raman spectra of artists' oils, polysaccharides, proteins and resins, recorded with 785 nm	Vandenabeele et al. 2000b; Daher et al. 2010
Archaeological resins	Collection of spectra of archaeological resins recorded with FT-Raman spectroscopy (1064 nm).	Edwards and Ali 2011
Mexican Copal resins	Local Mexican copal resins	Vandenabeele et al. 2003
RRUFF database	Extensive collection of spectra of minerals	Lafuente et al. 2016
Biological molecules	Raman spectral database of biomolecules	De Gelder et al. 2007
Natural silicate glasses	Collection of spectra of natural silicates	Giordano et al. 2019
Green minerals	Raman spectra of green mineral pigments	Coccato et al. 2016; Gilbert et al. 2003
Black pigments	Raman spectra and discussion of black pigments	Coccato et al. 2015
Synthetic Organic pigments	Collection of downloadable Raman spectra of synthetic organic pigments. https://soprano.kikirpa.be	Fremout et al. 2012
Azo-pigments	Spectra and discussion on azo-pigments	Vandenabeele et al. 2000a
Synthetic Organic pigments	Collection of synthetic organic pigments	Scherrer et al. 2009; Schulte et al. 2008
Cupper-phthalocyanine	Spectra and discussion on the discrimination between different forms of copper phthalocyanine pigment.	Defeyt et al. 2012

Raman spectra of glassy materials, it is possible to do a Raman band deconvolution and based on the polymerisation index, information on the glass composition and the production temperature can be obtained (Colomban 2003a; Colomban et al. 2006). On the other hand, the evolution towards the introduction of smaller instruments and the use of flexible probeheads counted for the development of the first mobile Raman instrument (Vandenabeele et al. 2004), dedicated to the analysis of artefacts. This allowed for the first on-site investigations, where direct analysis of the artworks could be performed, including the analysis of wall-paintings (Maguregui et al. 2012; Vandenabeele et al. 2005a, b; Vandenabeele et al. 2009) and the direct analysis of objects in a museum environment (Vandenabeele et al. 2007a, b; Vandenabeele et al. 2008).

In this chapter, we will first shortly discuss some theoretical aspects of the Raman effect, including some information on cases where the technique can be successfully applied, as well as some possible interferences. To obtain interesting results with Raman spectroscopy, it is of the utmost importance to select an appropriate approach. On the one hand, one can use benchtop instrumentation to perform molecular analysis with a spatial resolution down to ca. 1 μm, while on the other hand, when using mobile Raman instrumentation, the spot size is typically larger. Furthermore, microspatially offset Raman spectroscopy (micro-SORS) is described as an innovative technique towards the direct stratigraphic analysis, without sample requirements. Finally, when the focus is on the analysis of organic dyes, surface-enhanced Raman Spectroscopy (SERS) approaches can be implemented.

10.2 Theory of the Raman Effect

To understand the working principles of Raman spectroscopy, one should think about scattering; one of the most basic interactions of electromagnetic radiation with molecules. In other words, the Raman effect elegantly describes the inelastic scattering of the incident radiation from molecules (Lombardi 2007; Vandenabeele 2013). On the other hand, the elastic scattering of light is referred to as Rayleigh scattering (Vandenabeele 2013). The difference between the elastic and inelastic scattering is whether or not the vibrational energy of the system is changed or not. In the following paragraphs, only the basic scientific terminology will be given accompanied with the description of the phenomena relevant to Raman spectroscopy. Detailed information regarding the physical and chemical background of Raman spectroscopy can be found in dedicated literature (Cialla-May et al. n.d.; Ferraro and Nakamoto 2003; Lombardi 2007; Long 2002; McCreery 2000; Smith and Dent 2004; Tobias 1967; Vandenabeele 2013).

In order to understand the difference between elastic and inelastic scattering we need to imagine the interactions of photons with molecules. If the incident and the scattered photon have the same energy, Rayleigh scattering (*i.e.* elastic scattering) occurs (energy difference between incident and emitted photon equals 0) (Ferraro and Nakamoto 2003; McCreery 2000; Smith and Dent 2004; Tobias 1967;

Vandenabeele 2013). However, in some cases the incident photon collides with a molecule and the scattered one increases or decreases its energy, as the molecule transfers some of its vibrational energy from or to the photons. If the scattered photon increases its energy, anti-Stokes Raman scattering occurs and if the energy decreases the Stokes Raman scattering takes place. The intensity of the Raman scattering, plotted against the difference in energy, defined in wavenumbers (cm^{-1}), gives the Raman spectrum of the molecule (Vandenabeele 2013). Raman scattering is a weak phenomenon compared to Rayleigh scattering and thus the latter is supressed by appropriate filtering, not to overwhelm the entire spectrum (Vandenabeele 2013). A Raman spectrum is symmetrical: on the one hand some photons gain energy, while on the other hand some loose energy. As the loosing of energy is more abundant, the latter form, which is called Stokes Raman spectroscopy, is most frequently used in cultural heritage research. In Fig. 10.1, the most fundamental radiation-molecule interactions relevant to this chapter are described.

Raman scattering is occurring between vibrational/rotational states and so-called virtual states. The virtual state is not a solution of the time independent Schrödinger's equation and thus it is an 'imaginary' state The Raman Effect: A Unified Treatment of the Theory (Long 2002). As a consequence, the Raman shift is independent of the wavelength of the incident radiation. However, what is changing, is fluorescence emission (Fig. 10.1). With sufficient energy, a molecule can transit from the ground to the excited energy state, relax and return to the ground state.

With the appropriate laser and thus the appropriate energy, the molecule can be forced to be excited to an electronic state, instead of to a virtual one (Vandenabeele 2013). This transition enhances considerably the Raman signal, a process that is called resonance enhancement. If the energy of the laser is sufficiently low (i.e. at longer wavelengths), the molecules cannot be excited to the electronic state, hence

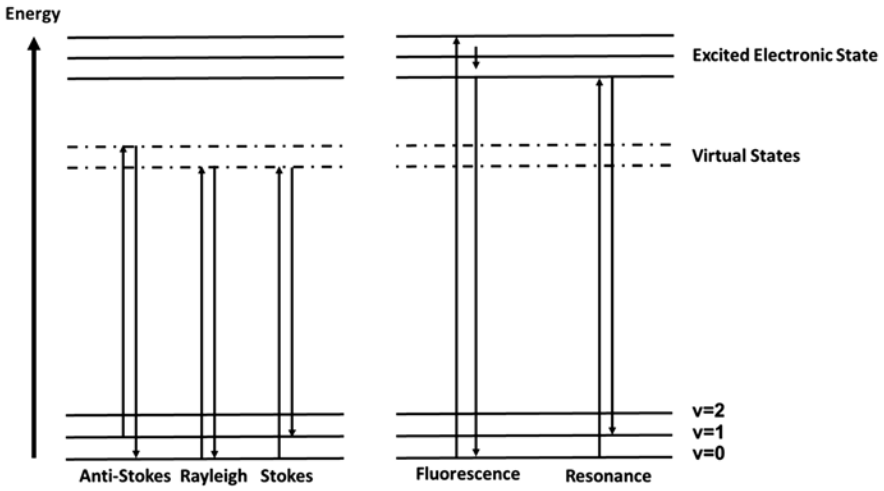

Fig. 10.1 Ideal energy diagram visualizing some of the fundamental radiation-molecule interactions

no fluorescence is observed. On the other hand, with lasers with a higher energy, it is more likely to achieve resonance Raman spectra of pigments used in cultural heritage objects (Clark and Franks 1975; Colomban 2003b). This technique is widely known as Resonance Raman spectrsocopy (RRS).

10.3 Laboratory Raman Spectroscopy

Benchtop Raman systems are stable spectrometers used for laboratory applications. These instruments are used extensively in archaeometrical research as they can provide fast analysis and reliable data. Nowadays, multi-laser systems are commercially available: these spectrometers are coupled with multiple laser sources covering the ultraviolet (UV) to the near-infrared (near-IR) region of the electromagnetic spectrum. In the Raman analysis of art objects, the most useful excitation wavelengths are situated from the visible to the near-IR region.

Laboratory Raman systems are securing wavenumber stability, a feature that is essential for the correct identification of the unknown (attributing the accurate wavenumber vibration to the correct substance). In many benchtop instruments, focusing of the laser beam is performed via a coupled Raman microscope, that allows to analyse directly the surface of the sample and/or artefact. Different objective lenses are attached on the microscope turret, changing the working distance (the larger the magnification the smaller the working distance) and the spatial resolution (depended on the objective lens and the laser wavelength). Indeed, micro-Raman spectroscopy instruments can achieve really small spatial resolutions comparable to the size of the pigments' granules (micrometre scale). Moreover, high-quality laboratory instruments are typically able to achieve high spectral resolutions, which can make it possible to discriminate between molecular vibrations that result in Raman signals that are just few wavenumbers (or less) apart.

A true confocal Raman microscope can achieve high lateral (XY) and depth (Z) resolutions by incorporating a confocal pinhole at the laser illumination path to detect only the signal from the focal plane. Any other Raman signal that originates from material that is above or below the focal plane, is removed.

The aforementioned advantageous features of benchtop Raman spectrometers are ideally coupled to the fact that the selection of excitation wavelength, laser power on the sample, measuring conditions (usually referring to the number of accumulations and measuring time) and the size of the confocal pinhole is controlled and selected upon the needs of the analysis. Thus, the user can select all possible settings and take full advantage to measure the scattering properties of the material under study, investigate resonance effects, avoid thermally induced degradation due to elevated laser power and/or measuring time etc.

A variation of solids, liquids and gasses can be characterized with micro-Raman spectroscopy. For art analysis research, both inorganic and organic materials found in works of art are successfully identified. The minimal amount of sample can be placed under the Raman microscope and can be measured without any sample preparation, while small artefacts can be positioned directly on the microscope stage. Due to the

high spatial resolution of the Raman technique, q-tip sampling (Vandenabeele et al. 1999) can be an alternative approach to the scrapping or razor sampling. For this, q-tips (cotton tipped swabs) are gently swabbed on the coloured surface. Removing just few pigment grains (theoretically a single grain is sufficient) allow to perform a micro-Raman analysis. When stratigraphic analysis is requested, cross sections are required. In order to direct the sections, these are embedded in resins and after curing and appropriate polishing the components of each layer can be differentiated. Raman micro-spectroscopy is an non-destructive technique when the size of the object allows its placement under the Raman microscope for direct analysis.

Since the first successful examples of Raman spectroscopy studies on pigment identification of colourful mediaeval manuscripts (Best et al. 1992; Clark 1995b; Guineau 1984; Guineau et al. 1986; Vandenabeele et al. 1999; Wehling et al. 1999), the technique has been applied to various pigments found on works of art including materials on: oil paintings (Benquerença et al. 2009), wall paintings (Vandenabeele et al. 2005a, b), rock art paintings (Hernanz et al. 2008, 2016; Morillas et al. 2018; Rousaki et al. 2015), ceramics (Lucas et al. 2018; Tomasini et al. 2020), porcelains (Jiang et al. 2018) etc.. Micro-Raman spectroscopy produces tremendous results on the synthetic organic pigments analysis (Scherrer et al. 2009; Schulte et al. 2008; Vandenabeele et al. 2000a) including plastics (Angelin et al. 2021) and graffiti/street art colours (Bosi et al. 2020; Cucci et al. 2016; La Nasa et al. 2021) with not only characterizing the main colorants but also allowing to discriminate between polymorphs (Defeyt et al. 2012, 2013).

Regarding the analysis of polymorphs found in modern artists' palette, indeed Raman spectroscopy is a very powerful tool for their non-destructive analysis and solid characterization. As an example the copper phthalocyanine (CuPc) blue compounds, a modern synthetic group of pigments, are among the most interesting pigments in art and art analysis. Not only can be found in different polymorphs characterized by different crystal arrangements, stability properties, shade among others (α form: PB15:0, PB15:1, PB15:2; β form: PB15:3, PB15:4 γ form: PB15:5 and ε form: PB15:6) but also can be used as dating and/or authenticity markers of the artefact (Defeyt et al. 2012, 2013; Defeyt and Strivay 2014; Kehe 1963). It was only in 1935 that the α form reached the market followed by the β form at the early 1950s and the ε form being commercially available in 1962 (Defeyt et al. 2012, 2013; Defeyt and Strivay 2014; Kehe 1963). Defeyt et al., in 2012 (Defeyt et al. 2012) and 2013 (Defeyt et al. 2013) used micro-Raman spectroscopy in combination with other techniques or alone for the identification of the α- β- and ε- form of copper phthalocyanine (CuPc) blue pigments. Moreover, for the latter forms she employed linear discriminant analysis (LDA) by using twelve Raman intensity ratios for the discrimination (Defeyt et al. 2013).

As most of the works of art are exposed to environmental conditions that introduce degradation of the pigments, Raman spectroscopy has proven a valuable tool on the study of alteration mechanisms. Many examples can be given, such as the study of the degradation of lead and copper (Costantini et al. 2020; Smith and Clark 2002), and iron based pigments (Costantini et al. 2020), experiments on the darkening of haematite and formation of coquimbite ($Fe_2(SO_4)3{\cdot}9H_2O$) on paintings from Pompei – a multi stepped procedure (Maguregui et al. 2014), degradation of the

blue colour found on Pompeian wall paintings (Prieto-Taboada et al. 2021), formation of copper oxalates on Cypriot wall painting (Nevin et al. 2008) etc.

Except from identifying the artist's palette and discovering the degradation processes, both having a great impact on conservation treatments, Raman spectroscopy is ideal for tracking possible forgeries and can contribute against the illegal trafficking of works of art. Titanium dioxide is a widely known white pigment used on art objects. Its most debated polymorphs are anatase and rutile whilst brookite seems less relevant to cultural heritage studies. Anatase and rutile seem to have a well-defined occurrence in the art world which coincides with its commercial availability (Edwards et al. 2006; Laver 1997) especially its use on easel paintings (Saverwyns 2010), on modern graffiti colours (or on modern and contemporary art) etc. Anatase, being a rare mineral, is expected not to be a major pigment in ancient art objects but rather an impurity, indicating when found as a pigment, a possible forgery (Edwards et al. 2006). However, this is debated as anatase has been found to be a pigment in antiquity artefacts (Edwards et al. 2006).

Tracking the manufacture and commercial availability dates of pigments throughout the centuries (Brown and Clark 2013; Eastaugh et al. 2008; Laver 1997) is of utmost importance when conducting research in order to identify copied work. Micro-Raman spectroscopy is a very useful technique for authentication studies as it proved very successful in the case of Russian avant-garde paintings characterization (Saverwyns 2010).

For Raman spectroscopy retrieving spectra with good signal-to-noise ratios is partially depending on the laser power and measuring time applied. But the retrieval of a Raman signal in general can be based also on resonance phenomena or fluorescence emission. Fluorescence emission can be avoided by selecting a laser in the near-IR region, typically with a 1064 nm wavelength. Fourier transformations (FT-) were incorporated to Raman spectroscopy and FT-Raman spectroscopy was used for the identification of various organic and inorganic pigments (Baran et al. 2010; Edwards et al. 2004). Recording spectra with near-infrared excitation requires typically liquid-nitrogen-cooled solid state semiconductors as detector, and as a consequence it has to rely on the FT-principle. When using excitation with visible lasers, dispersive Raman spectrometers can be used, with thermoelectrically cooled (TEC) charge-coupled device (CCD) detectors. Moving towards lower excitation energies helps to avoid fluorescence, but as the energy decreases the Raman scattering is decreasing. Indeed, the Raman signal is proportional to the 4th power of the excitation frequency. Thus for achieving a good quality signal elevated laser power should be introduced. (Bersani et al. 2016; Bersani and Lottici 2016; Conti et al. 2016a; Rousaki et al. 2018a). Besides the 1064 nm excitation usually coupled to semiconductor detectors, recently multi-channel detector chips became available, that are able to deal with this long-wavelength excitation, allowing to introduce the near-infrared dispersive Raman instrumentation.

Associating the chemical information with the spatial distribution of the unknown is an approach called mapping. Micro-Raman spectrometers, because of their stability, confocality and high spatial resolution, can retrieve quality mappings producing high quality molecular images. Most of the micro-Raman systems are using calibrated stages for positioning and focusing in the x,y and z axis, respectively. By

arranging a number of point measurements in the x,y space, these can be stored, combined and manipulated (with the appropriate chemometrical methods) to produce chemical images. Flat objects are always preferable when conducting Raman mappings, as otherwise correction for focusing needs to be incorporated.

Raman mappings can be performed on embedded samples, by using a (confocal) Raman microscope. Among others, a cross section from the cork model of the Pantheon in Rome made by Antonio Chichi was collected from the dome of the maquette and stratigraphically characterized to reveal the consequent layers and prior conservation treatments (Rousaki et al. 2019). Also, cross sections from the sixteenth century 'Portrait of a Youth' painting were characterized to map the materials used by the painter (Lau et al. 2008). High quality molecular mappings of areas of few cm^2 were performed in the case of a nineteenth century porcelain card in order for the spatial distribution of the pigments to be revealed (Deneckere et al. 2012). In Fig. 10.2 the optical microscope image with the measuring area is indicated against its molecular images.

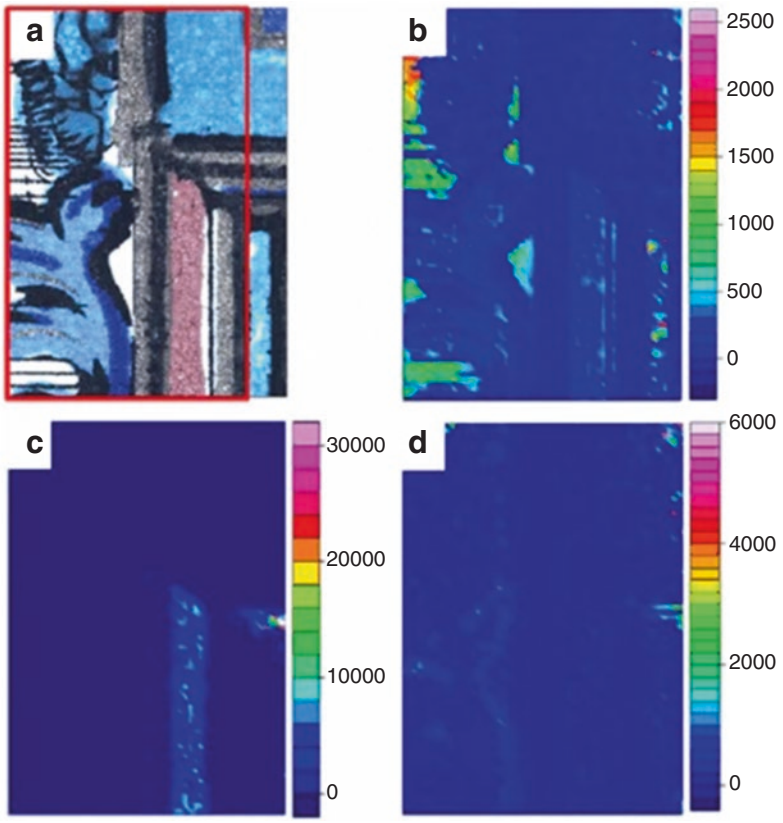

Fig. 10.2 (**a**) Optical microscope image of the area under study together with its molecular images constructed by intergrading the most prominent Raman band of (**b**) lead white ($2PbCO_3{\cdot}Pb(OH)_2$); (**c**) vermillion (HgS) and (**d**) ultramarine ($Na_{8-10}Al_6Si_6O_24S_{2-4}$). (Reproduced from ref. (Deneckere et al. 2012) with permission from Springer Nature, Copyright 2011)

10.4 Direct and Mobile Raman Spectroscopy

It is undeniable that one of the most advantageous characteristics of Raman spectroscopy, is its mobility. Over the years, the spectrometers scaled down in size and became compact and/or autonomous in order to enhance the experience of non-destructive analysis. This was a milestone of the technique that was quickly embraced by the archaeometrical community. Indeed, nowadays one can say that there is a clear turn on the direct, non-invasive and/or on field analysis as extensive sampling on artefacts is faced with scepticism.

Review papers, dedicated partially or entirely on Raman spectroscopy mobile applications (Bersani et al. 2016; Colomban 2012; Vandenabeele et al. 2014; Vandenabeele and Donais 2016) underline not only the importance and the instrumental improvements of the technique itself but also reveal the huge amount of applications on works of art from prehistory until today. Thus, it is safe to say that a hundred years' technique or even almost two decades of Raman mobility successfully reflects on masterpieces of thousands of years old.

The nomenclature concerning the Raman spectrometers, for non-invasive analysis or direct analysis, is separating the systems in transportable, mobile, portable, handheld and palm sized (Lauwers et al. 2014b; Rousaki et al. 2018a; Vandenabeele et al. 2014; Vandenabeele and Donais 2016). Mobile spectrometers, compared to their benchtop counterparts, are suffering more from wavenumber instability and are more prompt to wavenumber fluctuations due to unstable environmental conditions etc., especially when they are brought on field. The correct and frequent calibration of the systems can compensate for the wavenumber instability. Calibration can be achieved by measuring a single product and verify the wavenumber position of the most prominent band against the theoretical value. This is not an exact calibration but rather a fast calibration check of the validity of the output of the spectrometer. Accurate calibration can be performed by measuring products with Raman signals covering a wide spectral region (Hutsebaut et al. 2005). Corrections, recalculations and final calibration of the x-axis can be performed by comparison with the theoretical positions (reference band positions) of the products used (Hutsebaut et al. 2005). Moreover, absolute calibration (to obtain the calibration in nm) can also be performed by using a light source, e.g. neon light calibration.

Mobile Raman spectrometers are usually single laser systems, although dual laser mobile systems exist on the market. They are dispersive instruments coupled to TEC CCD or TEC solid state (semiconductor) detectors, depending on the laser excitation used. Generally, they have lower spatial and spectral resolution than benchtop systems. The most common mobile instruments used in cultural heritage research are the ones attached to long fibre optics cables, thus enabling the characterization of surfaces that are situated away from the main unit. These systems are usually relatively compact and allow the full control of the measuring conditions by the operator. Without cameras or objective lenses and when the probehead is mounted on positioning accessories (e.g. tripods), the focusing of the beam is achieved by evaluating the signal-to-noise ratio in distinct positions. When focusing

by hand and positioning the probehead in close contact with the object, special caps can be slided over the probe's lens (Lauwers et al. 2014b; Rousaki et al. 2017b). Using these caps serves a twofold reason: they are introducing a known focal distance, thus enabling stable focusing and are simultaneously blocking the sunlight. For extra protection of the artefact, a thin layer of semi hard foam can be placed on top of the cap. The thickness of the foam must not interfere with the focal length of the lenses cap. If the caps are not used, blocking the ambient light can be achieved by using black non transparent thick cloths or measuring during the night. One should note, in Raman spectroscopy, blocking the environmental signal is very important as this can interfere seriously with the actual Raman signal, hampering the identification of the unknown.

Mobile Raman instruments can perform the analysis on field or in the laboratory directly on the artefact or even on samples and cross sections. Although their spot size is in the mm scale, when the fibre optics probehead is combined with magnification objectives, high magnifications can be reached. Handheld Raman spectrometers are less frequently mentioned in cultural heritage studies. These have fixed optical heads and the users have less freedom to change some measuring parameters (according to the model or the software mode).

In art analysis, the beginning of the 2000s signified the need of conducting direct analysis straight on the artefact. One solution explored the possibility of connecting fibre optics to an FT-Raman spectrometer (Vandenabeele et al. 2001). Among the paintings examined with this method were the Baby Elephant by Lucebert, La Toilette by Degas, La Mort d'un Esprit by Giorgio de Chirico, and La Promenade du Monstre by Rene Magritte. Three years later, in 2004, an in-house developed mobile Raman spectrometer dedicated to cultural heritage studies was realized (Vandenabeele et al. 2004).

Among others (Deneckere et al. 2010, 2011), this mobile art analyser (MArtA) was used for the identification of the pigments in Mad Meg ("Dulle Griet") by Pieter Bruegel the Elder (1561) (Van de Voorde et al. 2014) (Fig. 10.3). The Raman analysis which was conducted in the Museum Mayer van den Bergh in Antwerp, Belgium was accompanied by a handheld X-Ray fluorescence (XRF) spectrometer and a portable X-ray fluorescence/X-ray diffraction (XRF/XRD) instrument in order for the outcome of the direct and on field analysis to be complemented.

Since the first attempts for direct analysis with in-house or adapted solutions, mobile Raman spectrometers are now widely commercially available and researchers can opt for using a combination of systems according to the art project or investigation (Rousaki et al. 2020; Vandenabeele et al. 2007a, b). Mobile Raman spectroscopy is responsible for high-quality data retrieved from a numerous of masterpieces including pigments and degradation products of Pompeian wall paintings (Conti et al. 2015; Maguregui et al. 2012) and preserved Pompeian pigments (Marcaida et al. 2018), illuminated mediaeval manuscripts (Lauwers et al. 2014a), materials and weathering products of decorated plasterwork in the Alhambra (Dominguez-Vidal et al. 2012, 2014). Concerning three-dimensional (3D) objects, direct Raman analysis was able to identify materials used as original pigments and overpainting components of the interior and exterior of the cork maquette of the

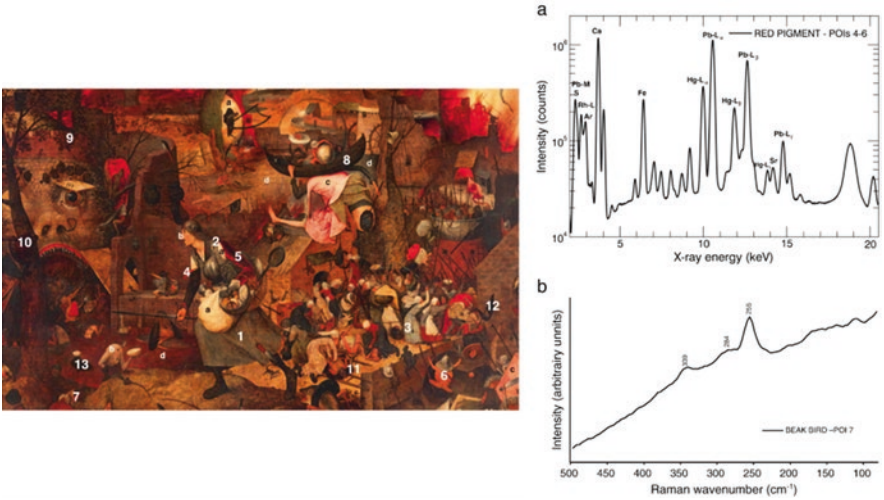

Fig. 10.3 (Left) Mad Meg ("Dulle Griet") by Pieter Bruegel the Elder with points of interest indicted on the painting (Right) (**a**) XRF sum-spectrum of the 4 and 5 points of interest (sleeves) and of the point of interest 6 (creature on the bridge) and (**b**) Raman spectrum confirming vermillion confirming as a red pigment on the surface of the painting (point of interest 7, (beak of the bird). (Adapted from ref. (Van de Voorde et al. 2014) with permission from Elsevier, Copyright 2014)

Pantheon in Rome made by Antonio Chichi (Rousaki et al. 2019). The long fibre optics probehead of the portable Raman instrument used was mounted on a articulating arm for positioning and focusing. The direct Raman study was accompanied with handheld X-ray fluorescence (hXRF), ultraviolet-induced visible fluorescence photography (UIVFP), digital microscopy (Hirox), micro-XRF and benchtop Raman spectroscopy. The results of this project, that also included computer tomography (CT)-scanning and 3D-scanning, assisted towards the restoration campaign of the cork model now exposed to the Ghent University Museum (GUM).

Remarkable results were produced from the direct Raman analysis of rock art paintings (Rousaki etal. 2017b; Tournié et al. 2011; Lahlil et al. 2012; Pitarch et al. 2014; Rousaki et al. 2018b). In particular, the pigments of the ancient population inhabited rock shelters in Patagonia (Argentina) were thoroughly investigated together with the conservation sate of the magnificent works of rock art (Rousaki et al. 2017b, 2018b). Portable Raman spectroscopy was able to identify the existence of a green earth pigment, a challenging task due to its poor Raman scattering capabilities (Fig. 10.4) (Rousaki et al. 2018b).

Concerning the Raman mapping of works of art performed with mobile Raman spectrometers, this still remains a challenging task. In 2016, the proof-of-concept of an *in situ* Raman mapping of a nineteenth century porcelain card, was published (Lauwers et al. 2016), suggesting possible hardware connections and processing tools.

Fluorescence emission is a valid problem in mobile Raman spectroscopy and new approaches have been suggested for overcoming such a disadvantage. 1064 nm

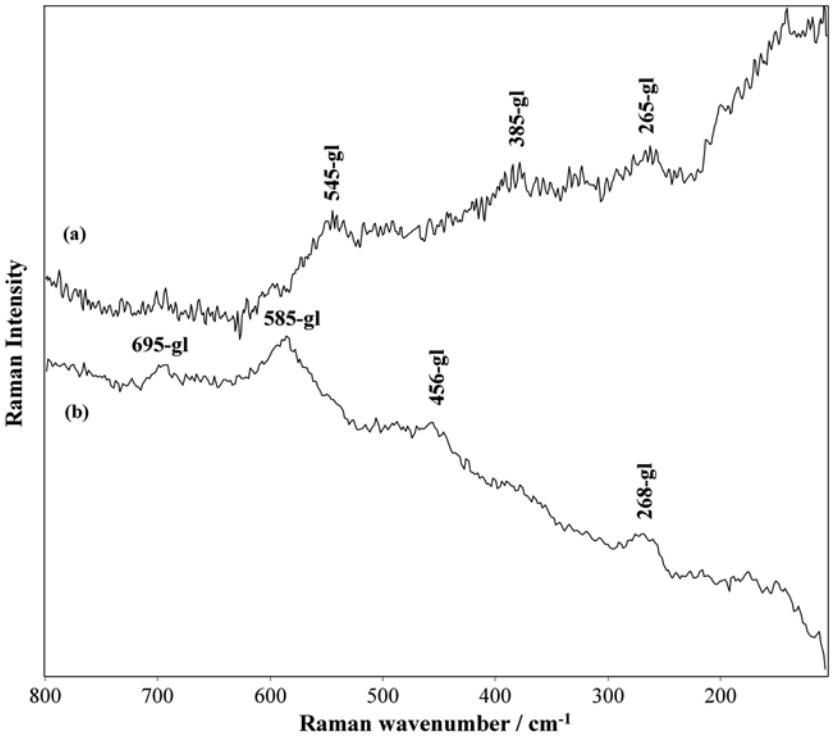

Fig. 10.4 Raman spectra collected with (**a**) with the 785 nm and (**b**) with the 532 nm laser of the Nr. 10 green rock art painting from the shelter Angostura Blanca, Chubut province. Portable Raman spectroscopy point out the likely presence of glauconite (gl), (K,Na)$(Fe^{3+},Al,Mg)_2(Si,Al)_4O_{10}(OH)_2$. (Reproduced from ref. [Rousaki et al. 2018b] with permission from Elsevier, Copyright 2018)

dispersive mobile Raman spectrometers can be used by the scientists profiting from the long wavelength excitation characteristics. As the 1064 nm excitation was associated with FT-spectrometers (required optics and interferometers), the entire unit was able to be scaled down by swapping from FT- to dispersive systems and from cooling with liquid nitrogen to TEC-solid state detectors. The loss of scattering capabilities is compensated with increased laser powers and measuring times (Conti et al. 2016a; Rousaki et al. 2020).

For advancing the analysis and processing experience, it was introduced on the market a handheld Raman spectrometer using the sequentially shifted excitation technology (SSE™) (patent number: US8570507B1) (Rousaki et al. 2020) [Bravo by Bruker]. This is a compact spectrometer with a fixed optical head and a fixed operational power at 100 mW, in-built calibration and a software that autonomously collects the Raman spectra (except when it is positioned on its docking stage where the user can decide for the measuring time of the data). It is a dual laser system, projecting its results in a wide spectral region. The shifted excitation procedure

corrects for fluorescence emission allowing the actual Raman signal, from the measured object, to be revealed (Cooper et al. 2013; Rousaki et al. 2020). The system is tested on cultural heritage objects and materials such as mosaics (Rousaki et al. 2020), a series of laboratory samples and colourful sculptures (Conti et al. 2016a), works of art from some of the New York City museums (Pozzi et al. 2019), organic components found in modern art (Vagnini et al. 2017), etc.

10.5 Non-invasive Stratigraphic Analysis: SORS

Art and Raman spectroscopy is a combination of fields and disciplines that is proven to give fruitful results. Until recently, the concept of stratigraphic analysis of complex layered structures found on works of art was exclusively accomplished by the use of benchtop Raman instruments. For carrying out the analysis, the painting, sculpture or object should be sampled in a specific manner (cross sections) in order for the stratigraphy to be revealed. The sample should then be embedded and polished. As direct research is gaining steam in the art analysis world, new techniques are immerging. Raman spectroscopy is one of the first techniques to embrace the 'new trends' in archaeometry and propose new concepts of non-invasive and non-destructive, direct stratigraphic analysis.

P. Matousek et al. (Eliasson et al. 2014; Matousek et al. 2005) in 2005, proposed the concept of spatially offset Raman spectroscopy (SORS) as a method for deeper-than-the-surface analysis. In SORS the laser beam and the collection zone are spatially separated. The larger the separation and/or the spatial offset the greater the subsurface information. And although, the technique can be applied when the thickness for the layers are at the millimetres or centimetres range (Eliasson and Matousek 2007; Rousaki et al. 2018a; Stone et al. 2007), its application on cultural heritage object was questionable.

The typical thicknesses of the layers of work of art objects are at the micrometre scale. One simple drawback; when applying SORS without any modification on micrometre thick layers, could have been the altered retrieval of signal; a rough sum of subsequent layers. Moreover, as many pigments are sensitive under the laser, restrictions should be made in both the laser frequency, laser power and measuring time. To overcome possible obstacles, microspatially offset Raman spectroscopy (micro-SORS) was proposed as an alternative for work of art analysis, when the sublayers are situated under turbid/opaque one (Bersani et al. 2016; Botteon et al. 2020a, b; Conti et al. 2015; Conti et al. 2015c; Conti et al. 2020; Matousek et al. 2016; Rousaki et al. 2018a). Micro-SORS is using the same basic idea of SORS, the spatial separation of the illumination and signal retrieval zone adapted to the needs of archaeometric research (micrometres spatial offsets, lower laser powers etc.) (Rousaki et al. 2018a). Furthermore, focusing through objectives reduces the volume size of the collection zones significantly. The most straightforward approach/variant of micro-SORS is when this is applied via conventional unmodified micro-Raman spectrometers. *Defocusing* micro-SORS can be achieved by distancing in

steps, the objective lens from the focusing position of the microscope (Bersani et al. 2016; Conti et al. 2015b; Conti et al. 2020; Matousek et al. 2016). On the other hand, *full* micro-SORS demands the modification of the apparatus, to separate the beam delivery from the signal collection areas by using different lenses (Bersani et al. 2016; C. Conti et al. 2015; Conti et al. 2020). In the miniaturized variant of micro-SORS, namely fibre-optics micro-SORS (Vandenabeele et al. 2017), two glass fibres are spatially separated; one to deliver and one to collect the Raman signal. The delivery fibre is unmovable while the collection glass fibre is mounted on a translation stage. The spot size is roughly equal with the diameter of the fibres used. As micro-SORS is still under investigation and research other approaches have been proposed in the literature (Buckley et al. 2016; Khan et al. 2016; Liao et al. 2016; Matthiae and Kristensen 2019).

Micro-SORS methods, with applications on cultural heritage research, have been tested on artificial samples (Conti et al. 2014, 2016c, 2017) and art works including sculptures (Conti et al. 2015a) and street murals (Botteon et al. 2018). Extensive research has been done for studying the possibilities and abilities of micro-SORS for subsurface analysis of painted structures (Conti et al. 2016b, d, e; Matousek et al. 2015), for combining confocal XRF with micro-SORS (Conti et al. 2018), for exploring the diffusion profile, of products used in conservation, into a matrix (Botteon et al. 2020a, b) etc.

In respect to subsurface mapping this has been tested on artificial samples using the *full* micro-SORS variant (Botteon et al. 2017) or on real samples using the *defocusing* variant (Rousaki et al. 2017a). For the latter a nineteenth century porcelain card was used as an ideal object for such research. The experiments were separated in two stages: one to retrieve and evaluate the *defocusing* Raman signal from subsequent layers from differently coloured zones and two to perform the *defocusing* Raman mapping and construct the sublayers images. In Fig. 10.5 the distribution of vermillion (normalized to lead white) is given is the focused position and in two different *defocusing* ones.

In the imaged position (Fig. 10.5a), vermillion is situated on the correct zone, while by increasing defocusing its signal is losing intensity (Fig. 10.5b, c). Indeed, lead white is situated below all the couloured zones of the porcelain card (Rousaki et al. 2017a). In terms of portability towards the *in situ* investigations the defocusing

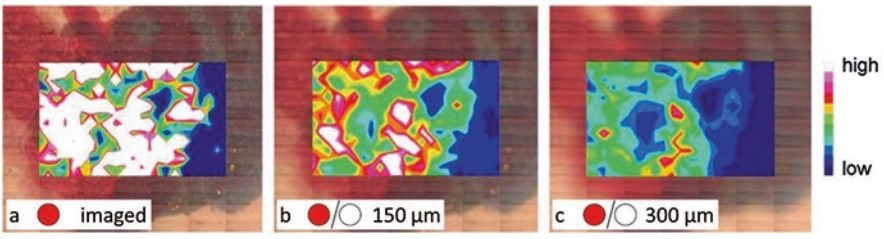

Fig. 10.5 Spatial distribution of vermillion normalized to lead white on an area of a nineteenth century porcelain at (**a**) zero offset or focusing position; (**b**) 150 µm and (**c**) 300 µm. (Adapted from ref. (Rousaki et al. 2017a) with permission from the Royal Society of Chemistry, Copyright 2017)

and the full micro-SORS variants have successfully demonstrated (Botteon et al. 2020a, b; Realini et al. 2016, 2017).

In order to achieve subsurface contrast between layers, frequency offset Raman spectroscopy (FORS) has been proposed (Sekar et al. 2017). This approach is based on the idea that the optical properties of the medium are changing upon shifting the laser frequency thus achieving sublayer information (Sekar et al. 2017). Moreover, it was reported that a FORS-SORS method is producing increased enhancement (Sekar et al. 2017).

10.6 Surface-Enhanced Raman Spectroscopy (SERS)

Raman spectroscopy is an ideal first choice technique for the identification of inorganic and organic materials in cultural heritage objects. However, especially for the analysis of organic components often fluorescence occurs. Therefore, for this analysis, one can simply benefit from changing the laser wavelength to supress fluorescence phenomena and retrieve the actual Raman signal. Although this is valid for some classes of organics or synthetic organic molecules, 'traditional' Raman spectroscopy seems to lack sensitivity to identify several organic colorants such as the natural dyes. Complications especially arise when the concentration of the colorant is low or if this colorant is largely dispersed inside the artwork's layers. Moreover, often these colorants don't have very good Raman scattering capabilities. The development of surface–enhanced Raman spectroscopy (SERS) produced successful results on materials like dyes, by enhancing considerably their Raman signal.

Fleischmann et al. (Fleischmann et al. 1974), in 1974, observed the enhancement of the Raman signal of pyridine on silver, creating the base of SERS experiments. A bit over a decade later, B. Guineau and V. Guichard (1987) reported its application on cultural heritage objects, characterizing madder. Nowadays, SERS is widely applied and extensively researched for the characterization of organic colorants. Even though, separation techniques seems to produce better discrimination between dyestuffs, SERS is considered more cost efficient, less invasive or less destructive and faster (Casadio et al. 2016; Pozzi and Leona 2016).

In SERS, both chemical and field enhancement are effectively occurring, for describing the analyte-metal interaction and the increase of the power of the electromagnetic field (wavelength depended), respectively (Vandenabeele 2013). Parameters of outmost importance are the preparation and application of the metallic substrate on which the analyte is to be absorbed (Agarwal et al. 2014; Cañamares et al. 2009; Leona 2009; Leona et al. 2006; Pozzi and Leona 2016; Retko et al. 2014; Sessa et al. 2018; Zalaffi et al. 2020) and the meticulous, sometimes aggressive, sample treatment and sophisticated methodologies (Bruni et al. 2011; Chen et al. 2006; Jurasekova et al. 2010; Pozzi et al. 2012; Pozzi and Leona 2016). The technique has been demonstrated and applied widely on samples and real works of art identifying dyes and lakes (Campanella et al. 2020; Cañamares et al. 2006;

Casadio et al. 2010; Gui et al. 2013; Leona et al. 2011; Newman et al. 2007; Pozzi et al. 2013, 2014; Sessa et al. 2018; Zoleo et al. 2020).

Several methodological approaches and techniques for upgrading the SERS experience have been proposed in literature, including laser-ablation surface-enhanced Raman spectroscopy (Cesaratto et al. 2014; Londero et al. 2013) and the implementation of the appropriate laser excitation for surface-enhanced resonance Raman spectroscopy (SERRS) (Leona 2009).

Towards the direct analysis of art objects by using SERS, some approaches include mobile, removable film (Doherty et al. 2011), inkjet colloidal application (Benedetti et al. 2014) and application of tip-enhanced Raman spectroscopy (TERS) with even a combination of TERS and atomic force microscopy (AFM) (Kurouski et al. 2014).

10.7 Conclusions

Almost a century after the discovery of the Raman effect, Raman spectroscopy has grown to be one of the core stone techniques applied in cultural heritage studies. Its undeniable that advantages together with the variation of the Raman approaches developed, bring the technique in the front line of analytical studies. Moreover, the hardware advantages of the last two decades detach the method from its traditional immobile approach and brought it on the field, allowing measuring directly on the artefact and breaking out from the laboratory. Furthermore, the implementation of SERS for the identification of dyes, a very important class of organic colorants and the development of novel techniques such as micro-SORS proves the versatility of Raman spectroscopy.

Although, Raman spectroscopy shares some undeniably powerful characteristics, the users should be very cautious before starting a Raman analysis. In general, the laser power should be kept under control and sufficiently low in order not to invoke alterations on the measuring sample or object. Moreover, the Raman data should be meticulously treated not only against a spectral library of pure substances but considering also the literature. Lastly, one should be aware of spectral interferences, such as noise, fluorescence background and fluorescence bands, cosmic rays, ambient light etc when interpreting the Raman spectra.

Conclusively, Raman spectroscopy is able to answer contemporary conservation questions and create pathways for the identification of inorganic and organic pigments and colorants found on artistic masterpieces.

Acknowledgements Anastasia Rousaki thanks the Research Foundation–Flanders (FWO-Vlaanderen) for her postdoctoral fellowship, project number 12X1919N.

References

Agarwal, N.R., Tommasini, M., Fazio, E., Neri, F., Ponterio, R.C., Trusso, S., et al.: SERS activity of silver and gold nanostructured thin films deposited by pulsed laser ablation. Appl. Phys. A Mater. Sci. Process. **117**, 347–351 (2014). https://doi.org/10.1007/s00339-014-8401-8

Angelin, E.M., França de Sá, S., Picollo, M., Nevin, A., Callapez, M.E., Melo, M.J.: The identification of synthetic organic red pigments in historical plastics: developing an in situ analytical protocol based on Raman microscopy. J. Raman Spectrosc. **52**, 145–158 (2021). https://doi.org/10.1002/jrs.5985

Baran, A., Fiedler, A., Schulz, H., Baranska, M.: In situ Raman and IR spectroscopic analysis of indigo dye. Anal. Methods. **2**, 1372 (2010). https://doi.org/10.1039/c0ay00311e

Bell, I.M., Clark, R.J.H., Gibbs, P.J.: Raman spectroscopic library of natural and synthetic pigments (pre-≈ 1850 AD). Spectrochim. Acta A Mol. Biomol. Spectrosc. **53**(12), 2159–2179 (1997)

Benedetti, D.P., Zhang, J., Tague, T.J., Lombardi, J.R., Leona, M.: In situ microanalysis of organic colorants by inkjet colloid deposition surface-enhanced Raman scattering. J. Raman Spectrosc. **45**, 123–127 (2014). https://doi.org/10.1002/jrs.4424

Benquerença, M.-J., Mendes, N.F.C., Castellucci, E., Gaspar, V.M.F., Gil, F.P.S.C.: Micro-Raman spectroscopy analysis of 16th century Portuguese Ferreirim Masters oil paintings. J. Raman Spectrosc. **40**, 2135–2143 (2009). https://doi.org/10.1002/jrs.2383

Bersani, D., Lottici, P.P.: Raman spectroscopy of minerals and mineral pigments in archaeometry. J. Raman Spectrosc. **47**, 499–530 (2016). https://doi.org/10.1002/jrs.4914

Bersani, D., Conti, C., Matousek, P., Pozzi, F., Vandenabeele, P.: Methodological evolutions of Raman spectroscopy in art and archaeology. Anal. Methods. **8**, 8395–8409 (2016). https://doi.org/10.1039/C6AY02327D

Best, S.P., Clark, R.J., Withnall, R.: Non-destructive pigment analysis of artefacts by Raman microscopy. Endeavour. **16**, 66–73 (1992). https://doi.org/10.1016/0160-9327(92)90004-9

Bosi, A., Ciccola, A., Serafini, I., Guiso, M., Ripanti, F., Postorino, P., et al.: Street art graffiti: discovering their composition and alteration by FTIR and micro-Raman spectroscopy. Spectrochim. Acta. Part A Mol. Biomol. Spectrosc. **225**, 117474 (2020). https://doi.org/10.1016/j.saa.2019.117474

Botteon, A., Conti, C., Realini, M., Colombo, C., Matousek, P.: Discovering hidden painted images: subsurface imaging using microscale spatially offset Raman spectroscopy. Anal. Chem. **89**, 792–798 (2017). https://doi.org/10.1021/acs.analchem.6b03548

Botteon, A., Colombo, C., Realini, M., Bracci, S., Magrini, D., Matousek, P., et al.: Exploring street art paintings by microspatially offset Raman spectroscopy. J. Raman Spectrosc. **49**, 1652–1659 (2018). https://doi.org/10.1002/jrs.5445

Botteon, A., Colombo, C., Realini, M., Castiglioni, C., Piccirillo, A., Matousek, P., et al.: Non-invasive and in situ investigation of layers sequence in panel paintings by portable microspatially offset Raman spectroscopy. J. Raman Spectrosc. **51**, 2016–2021 (2020a). https://doi.org/10.1002/jrs.5939

Botteon, A., Yiming, J., Prati, S., Sciutto, G., Realini, M., Colombo, C., et al.: Non-invasive characterisation of molecular diffusion of agent into turbid matrix using micro-SORS. Talanta. **218**, 121078 (2020b). https://doi.org/10.1016/j.talanta.2020.121078

Brown, S., Clark, R.J.H.: Anatase: Important industrial white pigment and date-marker for artwork. Spectrochim. Acta. Part A Mol. Biomol. Spectrosc. **110**, 78–80 (2013). https://doi.org/10.1016/j.saa.2013.03.041

Bruni, S., Guglielmi, V., Pozzi, F., Mercuri, A.M.: Surface-enhanced Raman spectroscopy (SERS) on silver colloids for the identification of ancient textile dyes. Part II: pomegranate and sumac. J. Raman Spectrosc. **42**, 465–473 (2011). https://doi.org/10.1002/jrs.2736

Buckley, K., Atkins, C.G., Chen, D., Schulze, H.G., Devine, D.V., Blades, M.W., et al.: Non-invasive spectroscopy of transfusable red blood cells stored inside sealed plastic blood-bags. Analyst. **141**, 1678–1685 (2016). https://doi.org/10.1039/C5AN02461G

Burgio, L., Clark, R.J.H.: Library of FT-Raman spectra of pigments, minerals, pigment media and varnishes, and supplement to existing library of Raman spectra of pigments with visible excitation. Spectrochim. Acta A Mol. Biomol. Spectrosc. **57**(7), 1491–1521 (2001)

Burrafato, G., Calabrese, M., Cosentino, A., Gueli, A.M., Troja, S.O., Zuccarello, A.: ColoRaman project: Raman and fluorescence spectroscopy of oil, tempera and fresco paint pigments. J. Raman Spectrosc. **35**(10), 879–886 (2004)

Campanella, B., Botti, J., Cavaleri, T., Cicogna, F., Legnaioli, S., Pagnotta, S., et al.: The shining brightness of daylight fluorescent pigments: Raman and SERS study of a modern class of painting materials. Microchem. J. **152**, 104292 (2020). https://doi.org/10.1016/j.microc.2019.104292

Cañamares, M.V., Garcia-Ramos, J.V., Domingo, C., Sanchez-Cortes, S.: Surface-enhanced Raman scattering study of the anthraquinone red pigment carminic acid. Vib. Spectrosc. **40**, 161–167 (2006). https://doi.org/10.1016/j.vibspec.2005.08.002

Cañamares, M.V., Leona, M., Bouchard, M., Grzywacz, C.M., Wouters, J., Trentelman, K.: Evaluation of Raman and SERS analytical protocols in the analysis of Cape Jasmine dye (Gardenia augusta L.). J. Raman Spectrosc. **41** (2009). https://doi.org/10.1002/jrs.2462

Casadio, F., Leona, M., Lombardi, J.R., Van Duyne, R.: Identification of organic colorants in fibers, paints, and glazes by surface enhanced Raman spectroscopy. Acc. Chem. Res. **43**, 782–791 (2010). https://doi.org/10.1021/ar100019q

Casadio, F., Daher, C., Bellot-Gurlet, L.: Raman spectroscopy of cultural heritage materials: overview of applications and new frontiers in instrumentation, sampling modalities, and data processing. Top. Curr. Chem. **374**, 62 (2016). https://doi.org/10.1007/s41061-016-0061-z

Cesaratto, A., Leona, M., Lombardi, J.R., Comelli, D., Nevin, A., Londero, P.: Detection of organic colorants in historical painting layers using UV laser ablation surface-enhanced Raman microspectroscopy. Angew. Chem. Int. Ed. **53**, 14373–14377 (2014). https://doi.org/10.1002/anie.201408016

Castro, K., Pérez-Alonso, M., Rodríguez-Laso, M.D., Fernández, L.A., Madariaga, J.M.: On-line FT-Raman and dispersive Raman spectra database of artists' materials (e-VISART database). Anal. Bioanal. Chem. **382**(2), 248–258 (2005)

Chen, K., Leona, M., Vo-Dinh, K.-C., Yan, F., Wabuyele, M.B., Vo-Dinh, T.: Application of surface-enhanced Raman scattering (SERS) for the identification of anthraquinone dyes used in works of art. J. Raman Spectrosc. **37**, 520–527 (2006). https://doi.org/10.1002/jrs.1426

Cialla-May, D., Schmitt, M., Popp, J.: Theoretical principles of Raman spectroscopy. Phys Sci Rev. **4**, 20170040 (n.d.). https://doi.org/10.1515/psr-2017-0040

Clark, R.J.: Pigment identification on medieval manuscripts by Raman microscopy. J. Mol. Struct. **347**, 417–427 (1995a). https://doi.org/10.1016/0022-2860(95)08564-C

Clark, R.J.H.: Raman microscopy: application to the identification of pigments on medieval manuscripts. Chem. Soc. Rev. **24**, 187 (1995b). https://doi.org/10.1039/cs9952400187

Clark, R.J.H., Franks, M.L.: The resonance Raman spectrum of ultramarine blue. Chem. Phys. Lett. **34**, 69–72 (1975). https://doi.org/10.1016/0009-2614(75)80202-8

Coccato, A., Jehlicka, J., Moens, L., Vandenabeele, P.: Raman spectroscopy for the investigation of carbon–based black pigments. J. Raman Spectrosc. **46**(10), 1003–1015 (2015)

Coccato, A., Bersani, D., Coudray, A., Sanyova, J., Moens, L., Vandenabeele, P.: Raman spectroscopy of green minerals and reaction products with an application in cultural heritage research. J. Raman Spectrosc. **47**(12), 1429–1443 (2016)

Colomban, P.: Polymerization degree and Raman identification of ancient glasses used for jewelry, ceramic enamels and mosaics. J. Non-Cryst. Solids. **323**, 180–187 (2003a). https://doi.org/10.1016/S0022-3093(03)00303-X

Colomban, P.: Lapis lazuli as unexpected blue pigment in Iranian Lâjvardina ceramics. J. Raman Spectrosc. **34**, 420–423 (2003b). https://doi.org/10.1002/jrs.1014

Colomban, P.: The on-site/remote Raman analysis with mobile instruments: a review of drawbacks and success in cultural heritage studies and other associated fields. J. Raman Spectrosc. **43**, 1529–1535 (2012). https://doi.org/10.1002/jrs.4042

Colomban, P., Tournie, A., Bellot-Gurlet, L.: Raman identification of glassy silicates used in ceramics, glass and jewellery: a tentative differentiation guide. J. Raman Spectrosc. **37**, 841–852 (2006). https://doi.org/10.1002/jrs.1515

Conti, C., Colombo, C., Realini, M., Zerbi, G., Matousek, P.: Subsurface Raman analysis of thin painted layers. Appl. Spectrosc. **68**, 686–691 (2014). https://doi.org/10.1366/13-07376

Conti, C., Colombo, C., Realini, M., Matousek, P.: Subsurface analysis of painted sculptures and plasters using micrometre-scale spatially offset Raman spectroscopy (micro-SORS). J. Raman Spectrosc. **46**, 476–482 (2015a). https://doi.org/10.1002/jrs.4673

Conti, C., Realini, M., Colombo, C., Sowoidnich, K., Afseth, N.K., Bertasa, M., et al.: Noninvasive analysis of thin turbid layers using microscale spatially offset Raman spectroscopy. Anal. Chem. **87**, 5810–5815 (2015b). https://doi.org/10.1021/acs.analchem.5b01080

Conti, C., Realini, M., Colombo, C., Matousek, P.: Comparison of key modalities of microscale spatially offset Raman spectroscopy. Analyst. **140**, 8127–8133 (2015c). https://doi.org/10.1039/C5AN01900A

Conti, C., Botteon, A., Bertasa, M., Colombo, C., Realini, M., Sali, D.: Portable sequentially shifted excitation Raman spectroscopy as an innovative tool for in situ chemical interrogation of painted surfaces. Analyst. **141**, 4599–4607 (2016a). https://doi.org/10.1039/C6AN00753H

Conti, C., Botteon, A., Colombo, C., Realini, M., Matousek, P.: Fluorescence suppression using micro-scale spatially offset Raman spectroscopy. Analyst. **141**, 5374–5381 (2016b). https://doi.org/10.1039/C6AN00852F

Conti, C., Realini, M., Botteon, A., Colombo, C., Noll, S., Elliott, S.R., et al.: Analytical capability of defocused μ-SORS in the chemical interrogation of thin turbid painted layers. Appl. Spectrosc. **70**, 156–161 (2016c). https://doi.org/10.1177/0003702815615345

Conti, C., Realini, M., Colombo, C., Botteon, A., Bertasa, M., Striova, J., et al.: Determination of thickness of thin turbid painted over-layers using micro-scale spatially offset Raman spectroscopy. Philos. Trans. R. Soc. A Math. Phys. Eng. Sci. **374**, 20160049 (2016d). https://doi.org/10.1098/rsta.2016.0049

Conti, C., Realini, M., Colombo, C., Botteon, A., Matousek, P.: Contrasting confocal with defocusing microscale spatially offset Raman spectroscopy. J. Raman Spectrosc. **47**, 565–570 (2016e). https://doi.org/10.1002/jrs.4851

Conti, C., Botteon, A., Colombo, C., Realini, M., Matousek, P.: Investigation of heterogeneous painted systems by micro-spatially offset Raman spectroscopy. Anal. Chem. **89**, 11476–11483 (2017). https://doi.org/10.1021/acs.analchem.7b02700

Conti, C., Botteon, A., Colombo, C., Realini, M., Matousek, P., Vandenabeele, P., et al.: Contrasting confocal XRF with micro-SORS: a deep view within micrometric painted stratigraphy. Anal. Methods. **10**, 3837–3844 (2018). https://doi.org/10.1039/C8AY00957K

Conti, C., Botteon, A., Colombo, C., Pinna, D., Realini, M., Matousek, P.: Advances in Raman spectroscopy for the non-destructive subsurface analysis of artworks: micro-SORS. J. Cult. Herit. **43**, 319–328 (2020). https://doi.org/10.1016/j.culher.2019.12.003

Cooper, J.B., Abdelkader, M., Wise, K.L.: Sequentially shifted excitation Raman spectroscopy: Novel algorithm and instrumentation for fluorescence-free Raman spectroscopy in spectral space. Appl. Spectrosc. **67**, 973–984 (2013)

Costantini, I., Lottici, P.P., Bersani, D., Pontiroli, D., Casoli, A., Castro, K., et al.: Darkening of lead- and iron-based pigments on late Gothic Italian wall paintings: energy dispersive X-ray fluorescence, μ-Raman, and powder X-ray diffraction analyses for diagnosis: presence of β-PbO 2 (plattnerite) and α-PbO 2 (scrutinyite). J. Raman Spectrosc. **51**, 680–692 (2020). https://doi.org/10.1002/jrs.5817

Cucci, C., Bartolozzi, G., De Vita, M., Marchiafava, V., Picollo, M., Casadio, F.: The colors of Keith Haring: a spectroscopic study on the materials of the mural painting Tuttomondo and on reference contemporary outdoor paints. Appl. Spectrosc. **70**, 186–196 (2016). https://doi.org/10.1177/0003702815615346

Daher, C., Paris, C., Le Hô, A.S., Bellot-Gurlet, L., Échard, J.P.: A joint use of Raman and infrared spectroscopies for the identification of natural organic media used in ancient varnishes. J. Raman Spectrosc. **41**(11), 1494–1499 (2010)

De Gelder, J., De Gussem, K., Vandenabeele, P., Moens, L.: Reference database of Raman spectra of biological molecules. J. Raman Spectrosc. **38**(9), 1133–1147 (2007)

Defeyt, C., Strivay, D.: PB15 as 20th and 21st artists' pigments: conservation concerns. E-Preserv. Sci. **11**, 6–14 (2014)

Defeyt, C., Vandenabeele, P., Gilbert, B., Van Pevenage, J., Cloots, R., Strivay, D., et al.: Contribution to the identification of α-, β- and ε-copper phthalocyanine blue pigments in modern artists' paints by X-ray powder diffraction, attenuated total reflectance micro-fourier transform infrared spectroscopy and micro-Raman spectroscopy. J. Raman Spectrosc. **43**, 1772–1780 (2012). https://doi.org/10.1002/jrs.4125

Defeyt, C., Van Pevenage, J., Moens, L., Strivay, D., Vandenabeele, P.: Micro-Raman spectroscopy and chemometrical analysis for the distinction of copper phthalocyanine polymorphs in paint layers. Spectrochim. Acta. Part A Mol. Biomol. Spectrosc. **115**, 636–640 (2013). https://doi.org/10.1016/j.saa.2013.04.128

Delhaye, M., Dhamelincourt, P.: Raman microprobe and microscope with laser excitation. J. Raman Spectrosc. **3**, 33–43 (1975). https://doi.org/10.1002/jrs.1250030105

Deneckere, A., Schudel, W., Van Bos, M., Wouters, H., Bergmans, A., Vandenabeele, P., et al.: In situ investigations of vault paintings in the Antwerp cathedral. Spectrochim. Acta. Part A Mol. Biomol. Spectrosc. **75**, 511–519 (2010). https://doi.org/10.1016/j.saa.2009.10.032

Deneckere, A., Leeflang, M., Bloem, M., Chavannes-Mazel, C.A., Vekemans, B., Vincze, L., et al.: The use of mobile Raman spectroscopy to compare three full-page miniatures from the breviary of Arnold of Egmond. Spectrochim. Acta. Part A Mol. Biomol. Spectrosc. **83**, 194–199 (2011). https://doi.org/10.1016/j.saa.2011.08.016

Deneckere, A., Vekemans, B., Voorde, L., Paepe, P., Vincze, L., Moens, L., et al.: Feasibility study of the application of micro-Raman imaging as complement to micro-XRF imaging. Appl. Phys. A Mater. Sci. Process. **106**, 363–376 (2012). https://doi.org/10.1007/s00339-011-6693-5

Doherty, B., Brunetti, B.G., Sgamellotti, A., Miliani, C.: A detachable SERS active cellulose film: a minimally invasive approach to the study of painting lakes. J. Raman Spectrosc. **42**, 1932–1938 (2011). https://doi.org/10.1002/jrs.2942

Dominguez-Vidal, A., Jose de la Torre-Lopez, M., Rubio-Domene, R., Ayora-Cañada, M.J.: In situ noninvasive Raman microspectroscopic investigation of polychrome plasterworks in the Alhambra. Analyst. **137**, 5763 (2012). https://doi.org/10.1039/c2an36027f

Dominguez-Vidal, A., de la Torre-López, M.J., Campos-Suñol, M.J., Rubio-Domene, R., Ayora-Cañada, M.J.: Decorated plasterwork in the Alhambra investigated by Raman spectroscopy: comparative field and laboratory study. J. Raman Spectrosc. **45**, 1006–1012 (2014). https://doi.org/10.1002/jrs.4439

Eastaugh, N., Walsh, V., Chaplin, T.D., Siddall, R.: The Pigment Compendium – A Dictionary of Historical Pigments. Butterworth-Heinemann, Oxford (2008)

Edwards, H.G., Ali, E.M.: Raman spectroscopy of archaeological and ancient resins: problems with database construction for applications in conservation and historical provenancing. Spectrochim. Acta A Mol. Biomol. Spectrosc. **80**(1), 49–54 (2011)

Edwards, H.G.M., Jorge Villar, S.E., Eremin, K.A.: Raman spectroscopic analysis of pigments from dynastic Egyptian funerary artefacts. J. Raman Spectrosc. **35**, 786–795 (2004). https://doi.org/10.1002/jrs.1193

Edwards, H.G.M., Nik Hassan, N.F., Middleton, P.S.: Anatase – a pigment in ancient artwork or a modern usurper? Anal. Bioanal. Chem. **384**, 1356–1365 (2006). https://doi.org/10.1007/s00216-005-0284-2

Eliasson, C., Matousek, P.: Noninvasive authentication of pharmaceutical products through packaging using spatially offset Raman Spectroscopy. Anal. Chem. **79**, 1696–1701 (2007). https://doi.org/10.1021/ac062223z

Eliasson, C., Matousek, P., Leona, M., Stenger, J., Ferloni, E., Jurasekova, Z., et al.: Numerical Simulations of subsurface probing in diffusely scattering media using spatially offset Raman Spectroscopy. J. Raman Spectrosc. **43**, 1–29 (2014). https://doi.org/10.1515/psr-2017-0040

Ferraro, J.R., Nakamoto, K.: Introductory Raman Spectroscopy, 2nd edn. Elsevier, Amsterdam (2003). https://doi.org/10.1016/B978-0-12-254105-6.X5000-8

Fleischmann, M., Hendra, P.J., McQuillan, A.J.: Raman spectra of pyridine adsorbed at a silver electrode. Chem. Phys. Lett. **26**, 163–166 (1974). https://doi.org/10.1016/0009-2614(74)85388-1

Fremout, W., Saverwyns, S.: Identification of synthetic organic pigments: the role of a comprehensive digital Raman spectral library. J. Raman Spectrosc. **43**(11), 1536–1544 (2012)

Gardiner, D.J., Graves, P.R. (eds.): Practical Raman Spectroscopy. Springer, Berlin/Heidelberg (1989). https://doi.org/10.1007/978-3-642-74040-4

Gilbert, B., Denoël, S., Weber, G., Allart, D.: Analysis of green copper pigments in illuminated manuscripts by micro-Raman spectroscopy. Analyst. **128**(10), 1213–1217 (2003)

Giordano, D., González-García, D., Russell, J.K., Raneri, S., Bersani, D., Fornasini, L., Di Genova, D., Ferrando, S., Kaliwoda, M., Lottici, P.P., Smit, M., Dingwell, D.B.: A calibrated database of Raman spectra for natural silicate glasses: implications for modelling melt physical properties. J. Raman Spectrosc. **51**, 1822–1838 (2019)

Gui, O.M., Fălămaş, A., Barbu-Tudoran, L., Aluaş, M., Giambra, B., Cîntă Pînzaru, S.: Surface-enhanced Raman scattering (SERS) and complementary techniques applied for the investigation of an Italian cultural heritage canvas. J. Raman Spectrosc. **44**, 277–282 (2013). https://doi.org/10.1002/jrs.4186

Guineau, B.: Microanalysis of painted manuscripts and of colored archeological materials by Raman laser microprobe. J. Forensic Sci. **29**, 471–485 (1984)

Guineau, B., Guichard, V.: Identification des colorants organiques naturels par microspectrometrie Raman de resonance et par effet Raman exalte de surface (SERS); Exemple d'application à l'étude de tranchefiles de reliures anciennes teintes à la garance. ICOM Comm. Conserv. In 8th Triennal Meeting, vol. 2, Sydney, Australia, 1987, pp. 659–666.

Guineau, B., Coupry, C., Gousset, M.T., Forgerit, J.P., Vezin, J.: Identification de bleu de lapis-lazuli dans six manuscrits à peintures du XIIe siècle provenant de l'abbaye de Corbie. Scriptorium. **40**, 157–171 (1986)

Hernanz, A., Gavira-Vallejo, J.M., Ruiz-López, J.F., Edwards, H.G.M.: A comprehensive micro-Raman spectroscopic study of prehistoric rock paintings from the Sierra de las Cuerdas, Cuenca, Spain. J. Raman Spectrosc. **39**, 972–984 (2008). https://doi.org/10.1002/jrs.1940

Hernanz, A., Chang, J., Iriarte, M., Gavira-Vallejo, J.M., de Balbín-Behrmann, R., Bueno-Ramírez, P., et al.: Raman microscopy of hand stencils rock art from the Yabrai Mountain, Inner Mongolia Autonomous Region, China. Appl. Phys. A. **122**, 699 (2016). https://doi.org/10.1007/s00339-016-0228-z

Hutsebaut, D., Vandenabeele, P., Moens, L.: Evaluation of an accurate calibration and spectral standardization procedure for Raman spectroscopy. Analyst. **130**, 1204 (2005). https://doi.org/10.1039/b503624k

Jiang, X., Ma, Y., Chen, Y., Li, Y., Ma, Q., Zhang, Z., et al.: Raman analysis of cobalt blue pigment in blue and white porcelain: a reassessment. Spectrochim. Acta. Part A Mol. Biomol. Spectrosc. **190**, 61–67 (2018). https://doi.org/10.1016/j.saa.2017.08.076

Jurasekova, Z., del Puerto, E., Bruno, G., García-Ramos, J.V., Sanchez-Cortes, S., Domingo, C.: Extractionless non-hydrolysis surface-enhanced Raman spectroscopic detection of historical mordant dyes on textile fibers. J. Raman Spectrosc. **41**, 1455–1461 (2010). https://doi.org/10.1002/jrs.2651

Kehe, H.J.: Phthalocyanine compounds (Moser, Frank H.; Thomas, Arthur L.). J. Chem. Educ. **40**, A974 (1963). https://doi.org/10.1021/ed040pA974.2

Khan, K.M., Ghosh, N., Majumder, S.K.: Off-confocal Raman spectroscopy (OCRS) for subsurface measurements in layered turbid samples. J. Opt. **18**, 095301 (2016). https://doi.org/10.1088/2040-8978/18/9/095301

Kurouski, D., Zaleski, S., Casadio, F., Van Duyne, R.P., Shah, N.C.: Tip-Enhanced Raman Spectroscopy (TERS) for in situ identification of indigo and iron gall ink on paper. J. Am. Chem. Soc. **136**, 8677–8684 (2014). https://doi.org/10.1021/ja5027612

La Nasa, J., Campanella, B., Sabatini, F., Rava, A., Shank, W., Lucero-Gomez, P., et al.: 60 years of street art: a comparative study of the artists' materials through spectroscopic and mass spectrometric approaches. J. Cult. Herit. **48**, 129–140 (2021). https://doi.org/10.1016/j.culher.2020.11.016

Lafuente, B., Downs, R.T., Yang, H., Stone, N.: The power of databases: the RRUFF project. In: Armbruster, T., Danisi, R.M. (eds.) Highlights in Mineralogical Crystallography, pp. 1–29. Walter de Gruyter GmbH (2016)

Lahlil, S., Lebon, M., Beck, L., Rousselière, H., Vignaud, C., Reiche, I., Menu, M., Paillet, P., Plassard, F.: The first in situ micro-Raman spectroscopic analysis of prehistoric cave art of Rouffignac St–Cernin, France. J. Raman Spectrosc. **43**, 1637–1643 (2012)

Lau, D., Villis, C., Furman, S., Livett, M.: Multispectral and hyperspectral image analysis of elemental and micro-Raman maps of cross-sections from a 16th century painting. Anal. Chim. Acta. **610**, 15–24 (2008). https://doi.org/10.1016/j.aca.2007.12.043

Lauwers, D., Cattersel, V., Vandamme, L., Van Eester, A., De Langhe, K., Moens, L., et al.: Pigment identification of an illuminated mediaeval manuscript De Civitate Dei by means of a portable Raman equipment. J. Raman Spectrosc. **45**, 1266–1271 (2014a). https://doi.org/10.1002/jrs.4500

Lauwers, D., Hutado, A.G., Tanevska, V., Moens, L., Bersani, D., Vandenabeele, P.: Characterisation of a portable Raman spectrometer for in situ analysis of art objects. Spectrochim. Acta. Part A Mol. Biomol. Spectrosc. **118**, 294–301 (2014b). https://doi.org/10.1016/j.saa.2013.08.088

Lauwers, D., Brondeel, P., Moens, L., Vandenabeele, P.: In situ Raman mapping of art objects. Philos. Trans. R. Soc. A Math. Phys. Eng. Sci. **374**, 20160039 (2016). https://doi.org/10.1098/rsta.2016.0039

Laver, M.: Titanium dioxide whites. In: FitzHugh, E.W. (ed.) Artist's Pigment A Handbook of Their Historical Character, vol. 3, pp. 295–339. National Gallery of Art, Washington & Oxford University Press, Oxford (1997)

Leona, M.: Microanalysis of organic pigments and glazes in polychrome works of art by surface-enhanced resonance Raman scattering. Proc. Natl. Acad. Sci. **106**, 14757–14762 (2009). https://doi.org/10.1073/pnas.0906995106

Leona, M., Stenger, J., Ferloni, E.: Application of surface-enhanced Raman scattering techniques to the ultrasensitive identification of natural dyes in works of art. J. Raman Spectrosc. **37**, 981–992 (2006). https://doi.org/10.1002/jrs.1582

Leona, M., Decuzzi, P., Kubic, T.A., Gates, G., Lombardi, J.R.: Nondestructive identification of natural and synthetic organic colorants in works of art by surface enhanced Raman scattering. Anal. Chem. **83**, 3990–3993 (2011). https://doi.org/10.1021/ac2007015

Liao, Z., Sinjab, F., Gibson, G., Padgett, M., Notingher, I.: DMD-based software-configurable spatially-offset Raman spectroscopy for spectral depth-profiling of optically turbid samples. Opt. Express. **24**, 12701 (2016). https://doi.org/10.1364/OE.24.012701

Lombardi, J.R.: In: Brown, T.G., Creath, K., Kogelnik, H., Kriss, M.A., Schmit, J., Weber, M.J. (eds.) Radiation Interaction with Molecules Opt. Encyclopedia, pp. 2603–2635. Wiley-VCH Verlag GmbH & Co. KGaA, Weinheim (2007). https://doi.org/10.1002/9783527600441.oe082

Londero, P.S., Lombardi, J.R., Leona, M.: Laser ablation surface-enhanced Raman microspectroscopy. Anal. Chem. **85**, 5463–5467 (2013). https://doi.org/10.1021/ac400440c

Long, D.: The Raman Effect: A Unified Treatment of the Theory of Raman Scattering by Molecules. Wiley, Chichester (2002)

Lucas, H.B., Silva, H.J.A., Tasayco, C.M.S., Munayco, P., Faria, J.L.B.: Archaeological pottery from Nasca culture studied by Raman and Mössbauer spectroscopy combined with X-ray diffraction. Vib. Spectrosc. **97**, 140–145 (2018). https://doi.org/10.1016/j.vibspec.2018.06.010

Maguregui, M., Knuutinen, U., Martínez-Arkarazo, I., Giakoumaki, A., Castro, K., Madariaga, J.M.: Field Raman analysis to diagnose the conservation state of excavated walls and wall

paintings in the archaeological site of Pompeii (Italy). J. Raman Spectrosc. **43**, 1747–1753 (2012). https://doi.org/10.1002/jrs.4109

Maguregui, M., Castro, K., Morillas, H., Trebolazabala, J., Knuutinen, U., Wiesinger, R., et al.: Multianalytical approach to explain the darkening process of hematite pigment in paintings from ancient Pompeii after accelerated weathering experiments. Anal. Methods. **6**, 372–378 (2014). https://doi.org/10.1039/C3AY41741G

Marcaida, I., Maguregui, M., Morillas, H., Prieto-Taboada, N., de Vallejuelo, S.F.-O., Veneranda, M., et al.: In situ non-invasive characterization of the composition of Pompeian pigments preserved in their original bowls. Microchem. J. **139**, 458–466 (2018). https://doi.org/10.1016/j.microc.2018.03.028

Marucci, G., Beeby, A., Parker, A.W., Nicholson, C.E.: Raman spectroscopic library of medieval pigments collected with five different wavelengths for investigation of illuminated manuscripts. Anal. Methods. **10**(10), 1219–1236 (2018)

Matousek, P., Clark, I.P., Draper, E.R.C., Morris, M.D., Goodship, A.E., Everall, N., et al.: Subsurface probing in diffusely scattering media using spatially offset Raman spectroscopy. Appl. Spectrosc. **59**, 393–400 (2005). https://doi.org/10.1366/0003702053641450

Matousek, P., Conti, C., Colombo, C., Realini, M.: Monte Carlo simulations of subsurface analysis of painted layers in micro-scale spatially offset Raman spectroscopy. Appl. Spectrosc. **69**, 1091–1095 (2015). https://doi.org/10.1366/15-07894

Matousek, P., Conti, C., Realini, M., Colombo, C.: Micro-scale spatially offset Raman spectroscopy for non-invasive subsurface analysis of turbid materials. Analyst. **141**, 731–739 (2016). https://doi.org/10.1039/C5AN02129D

Matthiae, M., Kristensen, A.: Hyperspectral spatially offset Raman spectroscopy in a microfluidic channel. Opt. Express. **27**, 3782 (2019). https://doi.org/10.1364/OE.27.003782

McCreery, R.: Raman Spectroscopy for Chemical Analysis. Wiley, New York (2000)

Morillas, H., Maguregui, M., Bastante, J., Huallparimachi, G., Marcaida, I., García-Florentino, C., et al.: Characterization of the Inkaterra rock shelter paintings exposed to tropical climate (Machupicchu, Peru). Microchem. J. **137**, 422–428 (2018). https://doi.org/10.1016/j.microc.2017.12.003

Nevin, A., Melia, J.L., Osticioli, I., Gautier, G., Colombini, M.P.: The identification of copper oxalates in a 16th century Cypriot exterior wall painting using micro FTIR, micro Raman spectroscopy and Gas Chromatography-Mass Spectrometry. J. Cult. Herit. **9**, 154–161 (2008). https://doi.org/10.1016/j.culher.2007.10.002

Newman, J., Chen, K., Leona, M., Vo-Dinh, T.: Surface-enhanced Raman scattering for identification of organic pigments and dyes in works of art and cultural heritage material. Sens. Rev. **27**, 109–120 (2007)

Pitarch, A., Ruiz, J.F., Fdez-Ortiz De Vallejuelo, S., Hernanz, A., Maguregui, M., Madariaga, J.M.: In situ characterization by Raman and X-ray fluorescence spectroscopy of post-Paleolithic blackish pictographs exposed to the open air in Los Chaparros shelter (Albalate del Arzobispo, Teruel, Spain). Anal. Methods. **6**, 6641–6650 (2014)

Pozzi, F., Leona, M.: Surface-enhanced Raman spectroscopy in art and archaeology. J. Raman Spectrosc. **47**, 67–77 (2016). https://doi.org/10.1002/jrs.4827

Pozzi, F., Lombardi, J.R., Bruni, S., Leona, M.: Sample treatment considerations in the analysis of organic colorants by surface-enhanced Raman scattering. Anal. Chem. **84**, 3751–3757 (2012). https://doi.org/10.1021/ac300380c

Pozzi, F., Lombardi, J.R., Leona, M.: Winsor & Newton original handbooks: a surface-enhanced Raman scattering (SERS) and Raman spectral database of dyes from modern watercolor pigments. Herit. Sci. **1**, 23 (2013). https://doi.org/10.1186/2050-7445-1-23

Pozzi, F., van den Berg, K.J., Fiedler, I., Casadio, F.: A systematic analysis of red lake pigments in French Impressionist and Post-Impressionist paintings by surface-enhanced Raman spectroscopy (SERS). J. Raman Spectrosc. **45**, 1119–1126 (2014). https://doi.org/10.1002/jrs.4483

Pozzi, F., Basso, E., Rizzo, A., Cesaratto, A., Tague Jr., T.J.: Evaluation and optimization of the potential of a handheld Raman spectrometer: in situ, noninvasive materials characterization in artworks. J. Raman Spectrosc. **50**, jrs.5585 (2019). https://doi.org/10.1002/jrs.5585

Prieto-Taboada, N., Fdez-Ortiz de Vallejuelo, S., Santos, A., Veneranda, M., Castro, K., Maguregui, M., et al.: Understanding the degradation of the blue colour in the wall paintings of Ariadne's house (Pompeii, Italy) by non-destructive techniques. J. Raman Spectrosc. **52**, 85–94 (2021). https://doi.org/10.1002/jrs.5941

Realini, M., Botteon, A., Conti, C., Colombo, C., Matousek, P.: Development of portable defocusing micro-scale spatially offset Raman spectroscopy. Analyst. **141**, 3012–3019 (2016). https://doi.org/10.1039/C6AN00413J

Realini, M., Conti, C., Botteon, A., Colombo, C., Matousek, P.: Development of a full micro-scale spatially offset Raman spectroscopy prototype as a portable analytical tool. Analyst. **142**, 351–355 (2017). https://doi.org/10.1039/C6AN02470J

Retko, K., Ropret, P., Cerc Korošec, R.: Surface-enhanced Raman spectroscopy (SERS) analysis of organic colourants utilising a new UV-photoreduced substrate. J. Raman Spectrosc. **45**, 1140–1146 (2014). https://doi.org/10.1002/jrs.4533

Rousaki, A., Bellelli, C., Carballido Calatayud, M., Aldazabal, V., Custo, G., Moens, L., et al.: Micro-Raman analysis of pigments from hunter-gatherer archaeological sites of North Patagonia (Argentina). J. Raman Spectrosc. **46**, 1016–1024 (2015). https://doi.org/10.1002/jrs.4723

Rousaki, A., Botteon, A., Colombo, C., Conti, C., Matousek, P., Moens, L., et al.: Development of defocusing micro-SORS mapping: a study of a 19th century porcelain card. Anal. Methods. **9**, 6435–6442 (2017a). https://doi.org/10.1039/C7AY02336G

Rousaki, A., Vázquez, C., Aldazábal, V., Bellelli, C., Carballido Calatayud, M., Hajduk, A., et al.: The first use of portable Raman instrumentation for the in situ study of prehistoric rock paintings in Patagonian sites. J. Raman Spectrosc. **48**, 1459–1467 (2017b). https://doi.org/10.1002/jrs.5107

Rousaki, A., Moens, L., Vandenabeele, P.: Archaeological investigations (archaeometry). Phys. Sci. Rev. **3** (2018a). https://doi.org/10.1515/psr-2017-0048

Rousaki, A., Vargas, E., Vázquez, C., Aldazábal, V., Bellelli, C., Carballido Calatayud, M., et al.: On-field Raman spectroscopy of Patagonian prehistoric rock art: pigments, alteration products and substrata. TrAC Trends Anal. Chem. **105**, 338–351 (2018b). https://doi.org/10.1016/j.trac.2018.05.011

Rousaki, A., Pincé, P., Lycke, S., Harth, A., Martens, M., Moens, L., et al.: In situ and laboratory analysis on the polychromy of the Ghent Pantheon cork model by Antonio Chichi. Eur. Phys. J. Plus. **134**, 375 (2019). https://doi.org/10.1140/epjp/i2019-12754-3

Rousaki, A., Costa, M., Saelens, D., Lycke, S., Sánchez, A., Tuñón, J., et al.: A comparative mobile Raman study for the on field analysis of the Mosaico de los Amores of the Cástulo Archaeological Site (Linares, Spain). J. Raman Spectrosc. **51**, 1913–1923 (2020). https://doi.org/10.1002/jrs.5624

Saverwyns, S.: Russian avant-garde … or not? A micro-Raman spectroscopy study of six paintings attributed to Liubov Popova. J. Raman Spectrosc. **41**, 1525–1532 (2010). https://doi.org/10.1002/jrs.2654

Scherrer, N.C., Stefan, Z., Francoise, D., Annette, F., Renate, K.: Synthetic organic pigments of the 20th and 21st century relevant to artist's paints: Raman spectra reference collection. Spectrochim. Acta Part A Mol. Biomol. Spectrosc. **73**, 505–524 (2009). https://doi.org/10.1016/j.saa.2008.11.029

Schulte, F., Brzezinka, K.W., Lutzenberger, K., Stege, H., Panne, U.: Raman spectroscopy of synthetic organic pigments used in 20th century works of art. J. Raman Spectrosc. **39**, 1455–1463 (2008). https://doi.org/10.1002/jrs.2021

Sekar, S.K.V., Mosca, S., Farina, A., Martelli, F., Taroni, P., Valentini, G., et al.: Frequency offset Raman spectroscopy (FORS) for depth probing of diffusive media. Opt. Express. **25**, 4585 (2017). https://doi.org/10.1364/OE.25.004585

Sessa, C., Weiss, R., Niessner, R., Ivleva, N.P., Stege, H.: Towards a Surface Enhanced Raman Scattering (SERS) spectra database for synthetic organic colourants in cultural heritage. The effect of using different metal substrates on the spectra. Microchem. J. **138**, 209–225 (2018). https://doi.org/10.1016/j.microc.2018.01.009

Smith, G.D., Clark, R.J.H.: The role of H2S in pigment blackening. J. Cult. Herit. **3**, 101–105 (2002). https://doi.org/10.1016/S1296-2074(02)01173-1

Smith, E., Dent, G.: Modern Raman Spectroscopy – A Practical Approach. Wiley, Chichester (2004). https://doi.org/10.1002/0470011831

Stone, N., Baker, R., Rogers, K., Parker, A.W., Matousek, P.: Subsurface probing of calcifications with spatially offset Raman spectroscopy (SORS): future possibilities for the diagnosis of breast cancer. Analyst. **132**, 899 (2007). https://doi.org/10.1039/b705029a

Tobias, R.S.: Raman spectroscopy in inorganic chemistry. J. Chem. Educ. **44**, 70 (1967). https://doi.org/10.1021/ed044p70

Tomasini, E., Palamarczuk, V., Zalduendo, M.M., Halac, E.B., Porto López, J.M., Fuertes, M.C.: The colors of San José pottery from Yocavil valley, Argentine Northwest. Strategy for the characterization of archaeological pigments using non-destructive techniques. J. Archaeol. Sci. Rep. **29**, 102123 (2020). https://doi.org/10.1016/j.jasrep.2019.102123

Tournié, A., Prinsloo, L.C., Paris, C., Colomban, P., Smith, B.: The first in situ Raman spectroscopic study of san rock art in South Africa: procedures and preliminary results. J. Raman Spectrosc. **42**, 399–406 (2011)

Vagnini, M., Gabrieli, F., Daveri, A., Sali, D.: Handheld new technology Raman and portable FT-IR spectrometers as complementary tools for the in situ identification of organic materials in modern art. Spectrochim. Acta. Part A Mol. Biomol. Spectrosc. **176**, 174–182 (2017). https://doi.org/10.1016/j.saa.2017.01.006

Van de Voorde, L., Van Pevenage, J., De Langhe, K., De Wolf, R., Vekemans, B., Vincze, L., et al.: Non-destructive in situ study of "Mad Meg" by Pieter Bruegel the Elder using mobile X-ray fluorescence, X-ray diffraction and Raman spectrometers. Spectrochim. Acta Part B At. Spectrosc. **97**, 1–6 (2014). https://doi.org/10.1016/j.sab.2014.04.006

Vandenabeele, P.: Practical Raman Spectroscopy – An Introduction. Wiley, Chichester (2013). https://doi.org/10.1002/9781119961284

Vandenabeele, P., Donais, M.K.: Mobile spectroscopic instrumentation in archaeometry research. Appl. Spectrosc. **70**, 27–41 (2016). https://doi.org/10.1177/0003702815611063

Vandenabeele, P., Wehling, B., Moens, L., Dekeyzer, B., Cardon, B., von Bohlen, A., et al.: Pigment investigation of a late-medieval manuscript with total reflection X-ray fluorescence and micro-Raman spectroscopy. Analyst. **124**, 169–172 (1999). https://doi.org/10.1039/a807343k

Vandenabeele, P., Moens, L., Edwards, H.G.M., Dams, R.: Raman spectroscopic database of azo and application to modern art studies. J. Raman Spectrosc. **31**, 509–517 (2000a). https://doi.org/10.1002/1097-4555(200006)31:6<509::AID-JRS566>3.0.CO;2-0

Vandenabeele, P., Wehling, B., Moens, L., Edwards, H., De Reu, M., Van Hooydonk, G.: Analysis with micro-Raman spectroscopy of natural organic binding media and varnishes used in art. Anal. Chim. Acta. **407**(1–2), 261–274 (2000b)

Vandenabeele, P., Verpoort, F., Moens, L.: Non-destructive analysis of paintings using Fourier transform Raman spectroscopy with fibre optics. J. Raman Spectrosc. **32**, 263–269 (2001). https://doi.org/10.1002/jrs.691

Vandenabeele, P., Grimaldi, D.M., Edwards, H.G., Moens, L.: Raman spectroscopy of different types of Mexican copal resins. Spectrochim. Acta A Mol. Biomol. Spectrosc. **59**(10), 2221–2229 (2003)

Vandenabeele, P., Weis, T.L., Grant, E.R., Moens, L.J.: A new instrument adapted to in situ Raman analysis of objects of art. Anal. Bioanal. Chem. **379**, 137–142 (2004). https://doi.org/10.1007/s00216-004-2551-z

Vandenabeele, P., Bodé, S., Alonso, A., Moens, L.: Raman spectroscopic analysis of the Maya wall paintings in Ek'Balam, Mexico. Spectrochim. Acta. Part A Mol. Biomol. Spectrosc. **61**, 2349–2356 (2005a). https://doi.org/10.1016/j.saa.2005.02.034

Vandenabeele, P., Lambert, K., Matthys, S., Schudel, W., Bergmans, A., Moens, L.: In situ analysis of mediaeval wall paintings: a challenge for mobile Raman spectroscopy. Anal. Bioanal. Chem. **383**, 707–712 (2005b). https://doi.org/10.1007/s00216-005-0045-2

Vandenabeele, P., Castro, K., Hargreaves, M., Moens, L., Madariaga, J.M., Edwards, H.G.M.: Comparative study of mobile Raman instrumentation for art analysis. Anal. Chim. Acta. **588**, 108–116 (2007a). https://doi.org/10.1016/j.aca.2007.01.082

Vandenabeele, P., Tate, J., Moens, L.: Non-destructive analysis of museum objects by fibre-optic Raman spectroscopy. Anal. Bioanal. Chem. **387**, 813–819 (2007b). https://doi.org/10.1007/s00216-006-0758-x

Vandenabeele, P., Christensen, M.C., Moens, L.: Analysis of South-Asian Shaman paintings at the national museum of Denmark. J. Raman Spectrosc. **39**, 1030–1034 (2008). https://doi.org/10.1002/jrs.1905

Vandenabeele, P., Garcia-Moreno, R., Mathis, F., Leterme, K., Van Elslande, E., Hocquet, F.-P., et al.: Multi-disciplinary investigation of the tomb of Menna (TT69), Theban Necropolis, Egypt. Spectrochim. Acta. Part A Mol. Biomol. Spectrosc. **73**, 546–552 (2009). https://doi.org/10.1016/j.saa.2008.07.028

Vandenabeele, P., Edwards, H.G.M., Jehlička, J.: The role of mobile instrumentation in novel applications of Raman spectroscopy: archaeometry, geosciences, and forensics. Chem. Soc. Rev. **43**, 2628 (2014). https://doi.org/10.1039/c3cs60263j

Vandenabeele, P., Conti, C., Rousaki, A., Moens, L., Realini, M., Matousek, P.: Development of a fiber-optics microspatially offset Raman spectroscopy sensor for probing layered materials. Anal. Chem. **89**, 9218–9223 (2017). https://doi.org/10.1021/acs.analchem.7b01978

Wehling, B., Vandenabeele, P., Moens, L., Klockenkämper, R., von Bohlen, A., Van Hooydonk, G., et al.: Investigation of pigments in medieval manuscripts by micro raman spectroscopy and total reflection X-ray fluorescence spectrometry. Microchim. Acta. **130**, 253–260 (1999). https://doi.org/10.1007/BF01242913

Zalaffi, M.S., Agostinelli, I., Karimian, N., Ugo, P.: Ag-nanostars for the sensitive SERS detection of dyes in artistic cross-sections – Madonna della Misericordia of the National Gallery of Parma: a case study. Heritage. **3**, 1344–1359 (2020). https://doi.org/10.3390/heritage3040074

Zoleo, A., Rossi, C., Poggi, G., Rossi, M., Meneghetti, M., Baglioni, P.: Spotting aged dyes on paper with SERS. Phys. Chem. Chem. Phys. **22**, 24070–24076 (2020). https://doi.org/10.1039/D0CP04099A

Chapter 11
Non-invasive and Non-destructive Examination of Artists' Pigments, Paints and Paintings by Means of X-Ray Imaging Methods

Frederik Vanmeert, Steven De Meyer, Arthur Gestels, Ermanno Avranovich Clerici, Nina Deleu, Stijn Legrand, Piet Van Espen, Geert Van der Snickt, Matthias Alfeld, Joris Dik, Letizia Monico, Wout De Nolf, Marine Cotte, Victor Gonzalez, Steven Saverwyns, Livia Depuydt-Elbaum, and Koen Janssens

Abstract Recent studies in which X-ray beams of (sub)micrometre to millimetre dimensions have been used for non-destructive analysis and characterization of pigments, minute paint samples and/or entire paintings from fifteenth to twentieth century artists are discussed. The overview presented encompasses the use of laboratory and synchrotron radiation-based instrumentation and deals with the use of several variants of X-ray fluorescence (XRF) as a method of elemental analysis and imaging as well as with the combined use with X-ray diffraction (XRD). Microscopic XRF (μ-XRF) is a variant of the XRF method able to visualize the elemental distri-

F. Vanmeert
AXIS Research Group, NANOLab Centre of Excellence, University of Antwerp, Antwerp, Belgium

Laboratory Department, Royal Institute for Cultural Heritage, Brussels, Belgium
e-mail: frederik.vanmeert@uantwerpen.be

S. De Meyer · A. Gestels · P. Van Espen
AXIS Research Group, NANOLab Centre of Excellence, University of Antwerp, Antwerp, Belgium
e-mail: steven.demeyer@uantwerpen.be; arthur.gestels@uantwerpen.be; piet.vanespen@uantwerpen.be

E. A. Clerici
AXIS Research Group, NANOLab Centre of Excellence, University of Antwerp, Antwerp, Belgium

Department of Materials Science and Engineering, Delft University of Technology, Delft, The Netherlands
e-mail: ermanno.avranovichclerici@uantwerpen.be

M. P. Colombini et al. (eds.), *Analytical Chemistry for the Study of Paintings and the Detection of Forgeries*, Cultural Heritage Science,
https://doi.org/10.1007/978-3-030-86865-9_11

bution of key elements, mostly metals, on the scale from 1 μm to 100 μm present inside multi-layered micro samples taken from paintings. In the context of the characterization of artists' pigments subjected to natural degradation, in many cases the use of methods limited to elemental analysis or imaging does not suffice to elu-

N. Deleu · S. Legrand · G. Van der Snickt
AXIS Research Group, NANOLab Centre of Excellence, University of Antwerp, Antwerp, Belgium

ARCHES Research Group, Conservation/Restauration Department, University of Antwerp, Antwerp, Belgium
e-mail: nina.deleu@uantwerpen.be; stijn.legrand@uantwerpen.be; geert.vandersnickt@uantwerpen.be

M. Alfeld · J. Dik
Department of Materials Science and Engineering, Delft University of Technology, Delft, The Netherlands
e-mail: M.Alfeld@tudelft.nl; J.Dik@tudelft.nl

L. Monico
AXIS Research Group, NANOLab Centre of Excellence, University of Antwerp, Antwerp, Belgium

CNR-SCITEC and Centro SMAArt, Department of Chemistry, Biology and Biotechnology, University of Perugia, Perugia, Italy
e-mail: letizia.monico@cnr.it

W. De Nolf
European Synchrotron Radiation Facility, Experimental Division, Grenoble, France
e-mail: wout.de_nolf@esrf.fr

M. Cotte
European Synchrotron Radiation Facility (ESRF), Experimental Division, Grenoble, France

Laboratoire d'Archéologie Moléculaire et Structurale, Sorbonne Université, CNRS, Paris, France
e-mail: marine.cotte@esrf.fr

V. Gonzalez
Rijksmuseum, Amsterdam, The Netherlands
e-mail: v.gonzalez@rijksmuseum.nl

S. Saverwyns
Laboratory Department, Royal Institute for Cultural Heritage, Brussels, Belgium
e-mail: steven.saverwyns@kikirpa.be

L. Depuydt-Elbaum
Conservation-Restoration Department, Royal Institute for Cultural Heritage, Brussels, Belgium
e-mail: livia.depuydt@kikirpa.be

K. Janssens (✉)
AXIS Research Group, NANOLab Centre of Excellence, University of Antwerp, Antwerp, Belgium

ARCHES Research Group, Conservation/Restauration Department, University of Antwerp, Antwerp, Belgium

Rijksmuseum, Amsterdam, The Netherlands
e-mail: koen.janssens@uantwerpen.be

cidate the chemical transformations that have taken place. However, at synchrotron facilities, combinations of μ-XRF with related methods such as μ-XAS (microscopic X-ray absorption spectroscopy) and μ-XRD have proven themselves to be very suitable for such studies. Since microscopic investigation of a relatively limited number of minute paint samples may not yield representative information about the complete artefact they were taken from, several methods for macroscopic, non-invasive imaging have recently been developed. Combined macroscopic XRF/XRD scanning is able to provide a fairly complete overview of the inorganic pigments employed to create a work of art, to answer questions about ongoing degradation phenomena and about its authenticity. As such these newly developed non-invasive and highly specific imaging methods are of interest for many cultural heritage stakeholders.

Keywords X-ray imaging methods · Macro- and micro- XRF · XRD · Mapping · Degradation assessment

11.1 Introduction

In the last decades, the constructive interplay between analytical and conservation sciences has permitted numerous advances towards a better documentation of the conservation state of cultural heritage (CH) artefacts and a more objective assessment of their authenticity. Though very precious to mankind, there is an increasing awareness that cultural heritage objects are not eternal: they deteriorate inexorably at a certain rate, according to their material composition, the environmental conditions they are subjected to, and the chemical reactions that are taking place within their structure or at their surface. For centuries, the conservation of CH has been solely based on empirical knowledge, often resulting in an underestimation of the chemical phenomena at play, many of which are invisible to the naked eye as they unfold at the micro or even the nanoscale, but with potentially devastating effects for the physical integrity or macroscopic appearance of the artefacts involved.

Collecting reliable chemical information on the materials constituting CH artefacts is essential for developing new preservation and conservation strategies, as well as for distinguishing between genuine and counterfeit artefacts. However, to gather such data, some hurdles must be overcome: CH objects are hybrid (organic/inorganic) and hierarchically organized systems of high complexity. Their material components were often obtained either directly from nature or through elaborate synthesis procedures, resulting in chemical products of various degrees of purity. Those components were then mixed and used following the artists' skill and expertise, which might no longer be known today.

The palette of materials used by an artist can have temporal and geographical specificities and may contain information about possible technical practices and commercial exchanges. A continuous challenge for art historians and conservators is to precisely distinguish between the materials actually used by artists in the past

and potentially non-original compounds that were applied later or that formed *in-situ* over time. In particular, past conservation treatments, often undocumented, can result in the presence of "foreign" materials within the analyzed artwork. Unexpected materials may also result from the interactions between mineral and organic compounds that take place over time and can potentially induce the formation of degradation products. Monitoring of these non-original compounds can be crucial, as they may threaten the integrity of the object by causing delamination phenomena, color changes, etc.

From an analytical point of view, the use of imaging techniques for the study of painted cultural heritage artefacts has followed a clear positive trend in the last decade. Several imaging techniques are now regularly employed to identify and map artistic materials, from the nano and micro scale to the macro scale. 2D and 3D techniques are particularly rewarding considering the "heterogeneous hierarchy of cultural heritage materials". (Trentelman 2017) Among the imaging methods, UV imaging is the simplest and most commonly used, both at the macro and micro scales, to visualize areas containing organic media. (Trentelman 2017) With visible and infrared imaging spectroscopies, both organic (e.g. binders in paintings) and inorganic (e.g. pigments in paintings) compounds can be identified and mapped. (Delaney et al. 2010, 2017) The understanding of reflectance and luminescence spectra can be assisted by the determination of the elemental composition, obtained via 2D macroscopic X-ray fluorescence scanning (MA-XRF). (Delaney et al. 2017) For this particular technique, the penetrating power of X-rays also permits to detect materials present deeper within the object's stratigraphy, in some cases revealing paint layers invisible to the naked eye. In this way, even completely hidden compositions can be made visible again in a non-invasive manner. (Dik et al. 2008a, b; Thurrowgood et al. 2016) Two extensive reviews about the various applications of MA-XRF illustrate the wide use of this technique within cultural heritage science. (Alfeld and Broekaert 2013; Alfeld and de Viguerie 2017) Moreover, more in general, penetrative X-ray radiation offers the possibility of obtaining information on the inner morphology of artefacts, either by employing simple absorption contrast (X-ray radiography, XRR), which has been applied to paintings since the very early discovery of X-rays, (Bridgman 1964) or by exploiting state-of-the-art methods such as for example synchrotron based phase-contrast computed tomography. (Porcier et al. 2019) In summary, imaging techniques using short wavelengths (such as X-rays) and long wavelengths (such as UV, visible, or infrared) can be efficiently combined at all scales, from the macroscale imaging study of entire objects (e.g. Greco-Roman Fayum portraits) (Delaney et al. 2017) to the microscopic analysis of fragments (e.g. from Buddhist wall paintings in Bamyian). (Cotte et al. 2008)

An obvious advantage of any chemical imaging technique is that it yields information in the form of images, allowing to easily visualize the chemical (e.g. molecular, elemental) composition of the artefact in question. This image data, obtained using different contrasts or imaging modes, in turn, can be superimposed/combined with each other or with (higher resolution) optical images, greatly facilitating the readability of the result for the various stakeholders of cultural heritage research (scientists, art conservators, museum curators, art historians, …). Ultimately, the

identification and charting of the chemical compounds help to document the current and past condition of paintings and insures their safeguard for future generations.

Over the last few years, to complement MA-XRF and XRR, another type of X-ray based imaging technique has been developed exploiting a different contrast: X-ray diffraction, providing information on the crystal structure rather than the elemental composition of solid materials. Similar to MA-XRF, MA-XRD mapping generally consists in acquiring (often several tens of thousands) XRD patterns at each pixel in a two dimensional area (Fig. 11.1). This technique is capable of directly identifying crystalline phases in complex mixtures and also allows to quantitatively determine the relative abundance of these components.

All above-mentioned non-invasive imaging methods may be combined to (dis) prove subjective art-expert opinions on the authenticity of specific artworks, to detect fake paintings but also to allow art restorers to distinguish in a clearer manner between the original and the non-original parts of a large work of art. In what follows, after discussing the principles of XRF and XRD mapping at different length scales, a few examples of their combined use for authentication and 'fake-detection' purposes will be given next to its uses to ascertain the state of conservation of painted artworks. This chapter is largely based on two previously published reviews, focusing on respectively μ-XRF/MA-XRF (Janssens et al. 2016a, b) and μ-XRD/MA-XRD. (Gonzalez et al. 2020)

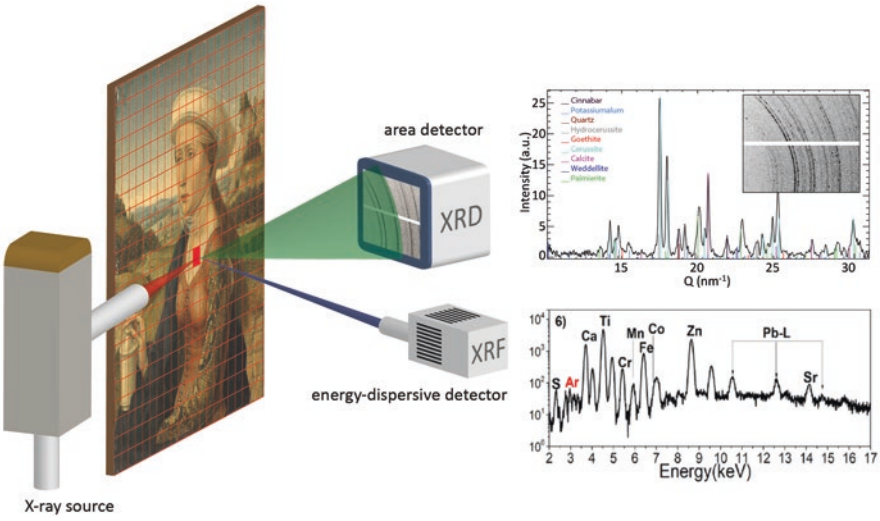

Fig. 11.1 Principle of Macroscopic XRF and XRD scanning. A primary X-ray beam (red) is sequentially scanned over a work of art while at each irradiated position, XRF (blue) and XRD (green) signals are recorded by means of suitable detectors. Either the work of art is moved in an XY fashion while the X-ray source and detectors remain stationary or the X-ray components are moved relative to a stationary artwork. Next to each detector, a typical example of the resulting spectral distributions per pixel are shown

11.2 Principles of XRF and XRD Mapping

11.2.1 Principles of XRF

X-ray fluorescence analysis (XRF) is a well-established method of (semi-)quantitative elemental analysis that is based on the ionization of the atoms of the material being irradiated by an energetic beam of primary X-rays. Quantitative XRF on heritage and archaeological samples is mainly used in reflection geometry to probe the stratigraphy of polished cross-sections of micro samples or the exposed surfaces of objects but can also be employed in a semi-quantitative to qualitative manner directly on cultural heritage artefacts, i.e. without any sample preparation. The energy of the fluorescent photons is the difference in energy between the vacancy that is the result of the ionization process and the electronic state of the electron filling this vacancy. (Beckhoff et al. 2006; Janssens et al. 2000) In this manner, the characteristic radiation emitted by the ionized atoms contains information on the nature and the abundance of the elemental constituents present. The technique is particularly efficient for studying high atomic number (high-Z) elements in low-Z matrices. Analysis of the XRF spectra involves identification of the elements present from the fluorescence lines observed and estimation of their net intensity; the latter are in principle proportional to the abundance of the corresponding chemical elements. (Semi-) quantitative analysis usually involves more complex calculations as initial absorption of the X-ray beam and absorption of the fluorescent photons in the material has to be modeled by taking the (expected) matrix composition into account in an iterative fashion. (Vincze et al. 1995, 1999, 2002) Since XRF meets a number of the requirements of the 'ideal method' for non-destructive analysis of cultural heritage materials, (Lahanier et al. 1986) such as being non-invasive, virtually non-destructive and providing multi-element and (semi-)quantitative information, analysis of objects of artistic and/or archaeological value with conventional XRF is fairly common. It is in fact one of the most often applied methods for obtaining qualitative and semi-quantitative information on such objects. Several textbooks cover the fundamental and methodological aspects of the method and its many variants. (Van Grieken and Markowicz 2002).

Several of these variants are relevant for the analysis of painted works of art or of micro-samples taken from such artifacts such as (a) portable XRF (PXRF), (b) the X-ray microprobe (XMP), involving the combined use of μ-XRF/μ-XAS and/or of μ-XRF/μ-XRD, usually based on synchrotron radiation and (c) to an increasing extent MA-XRF imaging.

11.2.1.1 XRF Mapping: Regular and Confocal Mapping

Microscopic XRF (μ-XRF) is a branch of XRF that has been developed since 1990, (Janssens et al. 1996) mainly thanks to the use and increasing availability of (i) synchrotron radiation (SR) and (ii) various devices for efficient focusing of

X-rays. (Janssens et al. 2000; Vincze et al. 1998) It can obtain information on the *local* elemental composition of inhomogeneous samples. At synchrotron facilities, a variety of micro- or nanofocus optics, based on refraction, (Lengeler et al. 2002; Schroer et al. 2010) diffraction (Gorelick et al. 2011; Sarkar et al. 2008) or total reflection (Alianelli et al. 2011; Barrett et al. 2011) of X-rays, is currently in use to create small beams with energies in the 1–100 keV range and with diameters of typically 0.1–1 μm. In laboratory μ-XRF instruments, mostly polycapillary lenses are employed for focusing, (Bichlmeier et al. 2001; Buzanich et al. 2010; Trentelman et al. 2010) providing focused X-ray beams that usually are 10–30 μm in diameter (Vittiglio et al. 2004). Among the commercial apparatus currently available, there are some specifically developed for point-based investigations of works of art. (Bronk et al. 2001) Incorporation of additional degrees of freedom of the measuring head allows for the analysis of Antique manuscripts (Christiansen et al. 2020; Rabin and Hahn 2013; Wolff et al. 2012) and bronzes, (Figueiredo et al. 2011; Valerio et al. 2012) Medieval paintings, (Herm 2008) Chinese porcelain (Cheng et al. 2011) and Baroque-era drawings. (Dietz et al. 2012)

Macroscopic X-Ray Fluorescence (MA-XRF) Imaging is a large-scale variant of μ-XRF that has come in use since 2008 when it transpired that hidden/overpainted layers in paintings can be (re)visualized in this manner; significantly more (pictorial and chemical) information can be obtained than by means of XRR. (Dik et al. 2008a, b) It involves the (moderately fast) scanning of a work of art relative to an X-ray source and XRF detector assembly. The principle is shown in Fig. 11.1.

Either the source/detector assembly is moved in front of the stationary artwork (mobile MA-XRF scanners) or vice versa.

With typical dwell times of 50–200 ms per point, a (very) large number of XRF spectra (of the order of one to several million spectra/artwork) are recorded, yielding (after appropriate spectrum evaluation) (Alfeld and Janssens 2015) large-scale elemental maps (see Figs. 11.2, 11.5, 11.8, 11.9, 11.10, 11.11, and 11.12). While its development started at a synchrotron facility, (Dik et al. 2008c) at which also the first MA-XRF studies were performed, (Alfeld et al. 2011a, b, 2013c; Dik et al. 2008a, b; Howard et al. 2012; Struick van der Loeff et al. 2012) relatively soon mobile MA-XRF instruments were developed that allowed to perform scanning experiments inside the museum or picture gallery where the works of art are normally on display or are conserved. (Alfeld et al.2011a, b, 2013a, b) With these MA-XRF scanners, it became possible to examine a great variety of artworks by well-known artists such as Rubens, (Janssens et al. 2010) Rembrandt, (Janssens et al. 2016a, b; Noble et al. 2012; Trentelman et al. 2015) Vermeer, (Verslype 2012) Goya (Bull et al. 2011), Manet, (Amato et al. 2019) Van Gogh, (Dooley et al. 2020; Monico et al. 2015a, b; Struick van der Loeff et al. 2012) Magritte, (da Silva et al. 2017; Van der Snickt et al. 2016) Mondriaan, (Martins et al. 2016a) and Pollock, (Martins et al. 2016b) and to discover new information on their artistic history and on their current state of conservation. (Cotte et al. 2017b; Miliani et al. 2018; Monico et al. 2020; Simoen et al. 2019) Next to oil paintings on panel or canvas,

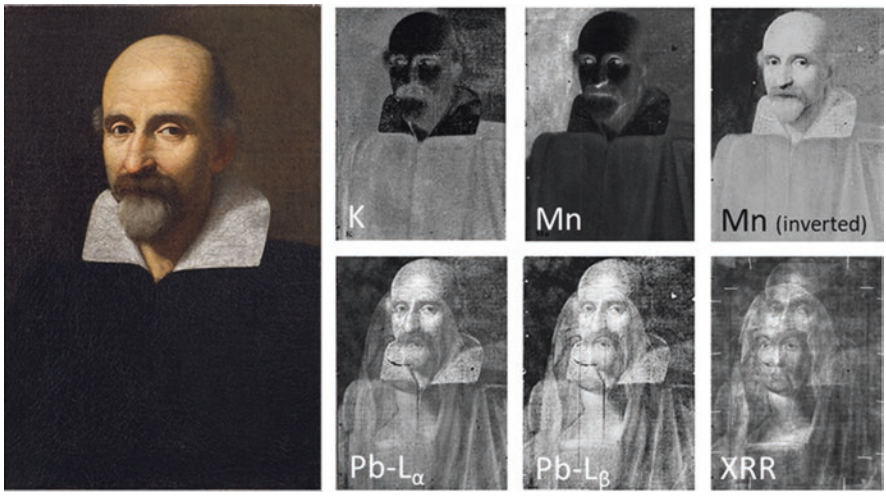

Fig. 11.2 Portrait of Prospero Farinacci (c. 1600–1618, M.M. de Caravaggio) (left panel) and various MA-XRF maps showing averaged distribution information corresponding to different sampling depths as a function of energy. For comparison, also the (transmission) X-ray radiograph of this painting is shown. Adapted from Cardinali et al. (2016)

also illuminated manuscripts (Legrand et al. 2018; Ricciardi et al. 2016) and stained-glass windows (Cagno et al.; Legrand et al. 2019) can be examined. Several X-ray instrumentation manufacturers and research institutions have described MA-XRF scanners of their own making. (Alberti et al. 2017; Dooley et al. 2014; Ravaud et al. 2016; Romano et al. 2017)

As can be seen in Fig. 11.2, the depth range below the surface from which MA-XRF collects pictorial information is energy dependent. When a distribution of an element such as K is considered, of which the XRF signal is fairly low in energy (K-K_α: 3.3 keV), the resulting map will show the lateral distribution of this element averaged over only few 10s of micrometers below the surface. However, as the XRF energy increases (such as for Mn-K_α at 5.9 keV, Pb-L_α at 10.5 keV or Pb-L_β at 12.6 keV), also the sampling range increases and thus the possibility exists that multiple overpainted representations (e.g., those present at the surface and e.g. at 100 μm below it) become visible in the same map.

11.2.1.2 Depth-Selective XRF

A specific subcategory of XRF investigations that is much more depth-selective than MA-XRF are those employing a confocal excitation-detection geometry. (Sun and Ding 2015) In such a geometry, the recorded XRF signals stem from a well-defined cube-like 'sampling' volume that is situated at the intersection of the X-ray optical devices positioned between X-ray source and sample (defining the primary beam) and between sample and X-ray detector (defining the direction from which

XRF signals can enter the detector). (Janssens et al. 2004) This type of measurement is limited to μ-XRF investigations. Often, polycapillary optics are employed for the latter purpose. (Bjeoumikhov et al. 2008; Woll et al. 2014) By moving the sample through this sampling volume, local information on the elemental composition of the material being investigated can be obtained. Sequential series of confocal XRF measurements along lines and planes allows to visualize the distribution of chemical elements of interest in one or two dimensions, creating for example virtual depth profiles, and two- or three-dimensional distributions inside the materials of interest. (Alfeld and Broekaert 2013; Luhl et al. 2013; Woll et al. 2012) After its original introduction at synchrotron radiation facilities (Beckhoff et al. 2003; Janssens et al. 2004; Smit et al. 2004; Woll et al., 2005, 2006, 2012), the feasibility of performing confocal XRF measurements using tube sources was demonstrated by several groups around the world, (Mantouvalou et al. 2010, Nakazawa and Tsuji 2013; Polese et al. 2015; Smolek et al. 2014; Tsuji et al. 2015a) along with appropriate deconvolution, quantification and simulation models. (Czyzycki et al. 2014; Huber et al. 2014; Mantouvalou et al. 2012; Mantouvalou et al. 2014; Schoonjans et al. 2012; Tsuji et al. 2015b; Wrobel and Czyzycki 2013; Wrobel et al. 2014) Several papers have been published where confocal XRF measurements are exploited for sub-surface examination of painted works of art, (Kanngiesser et al. 2012; Laclavetine et al. 2016; Reiche et al. 2012, 2015; Sun et al. 2014; Woll et al. 2008) next to pottery, (Yi et al. 2016) coins, (Buzanich et al. 2010) stained glass, (Choudhury et al. 2015; Kanngiesser et al. 2008) painted metal sheet, (Yagi and Tsuji 2015) and natural rock samples. (Li et al. 2015) Up to now, however, be it at synchrotron facilities (Mass et al. 2008) or via laboratory sources, (Lachmann et al. 2016; Nakano et al. 2016) a combination of the depth selectivity offered by confocal μ-XRF with those associated with the advantages of MA-XRF has yet to be exploited in a systematic fashion.

11.2.2 Principles of XRD

X-ray diffraction is a coherent, elastic scattering phenomenon that originates from the constructive interference of elastically scattered X-rays (of wavelength λ) by the atoms composing a crystalline structure. The basic requirement to observe a diffraction pattern is that when an X-ray interacts with an ensemble of crystallites (a priori non-oriented), a sufficient number of those crystallites should be present with suitable orientation for the diffraction phenomenon to take place along the reflection angle 2θ. If the beam size is much larger than the crystallite size and if the crystallites are randomly oriented, the diffraction pattern observed consists of so-called Debye-Scherrer rings (Fig. 11.3a). Under these conditions, the technique is labelled X-ray powder diffraction (XRPD). In the opposite case, in which only a small number of crystallites is irradiated, the pattern is limited to several bright spots (Fig. 11.3b). In the context of this review, most of the measured XRD patterns correspond to the first case. For the second case, typically a large number of diffraction

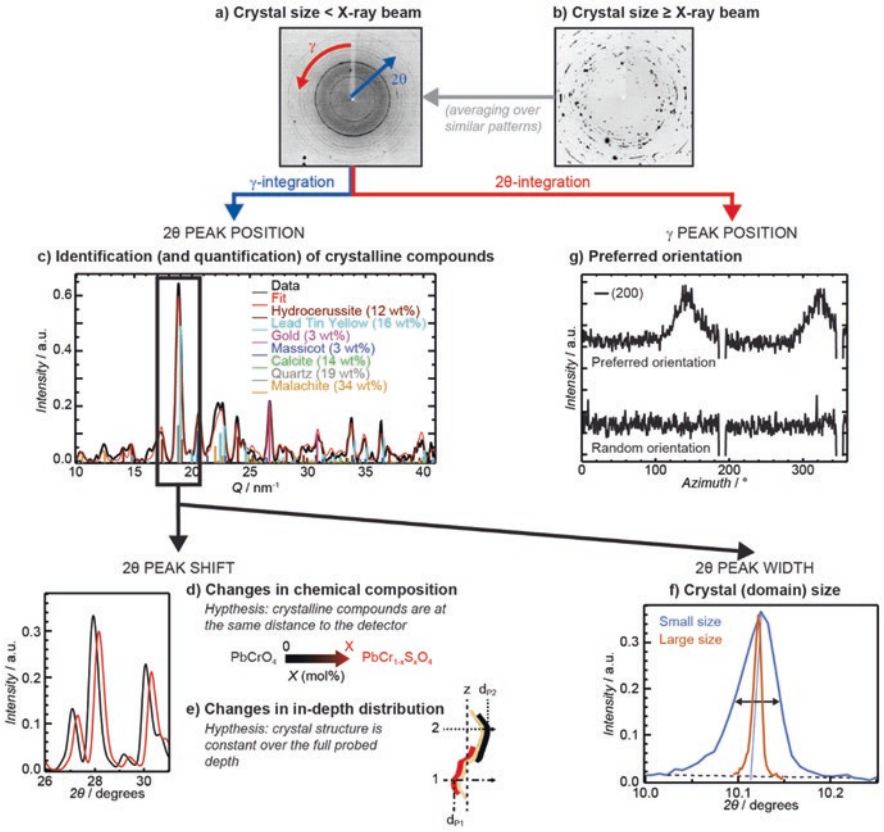

Fig. 11.3 Schematic illustration of the different types of information available from an XRD mapping experiment. Adapted from Gonzalez et al. (2020)

images from a similar area or with similar composition are averaged to obtain a 'powder-like' pattern. Different information can be derived from a diffraction pattern by looking at the variation in intensity, either along the scattering (2θ) or the azimuthal (γ) angles.

Through integration of the 2D diffraction image over the azimuth, the obtained 1D diffraction pattern shows an intensity variation of the diffracted radiation as a function of 2θ, where each peak corresponds to a specific interplanar distance (*d*). The position of these peaks follows Bragg's law: $n\lambda = 2d \sin(\theta)$, where n is a positive integer indicating the diffraction order.

Using Bragg's law, the characteristic interplanar distances can be calculated from collected peak positions. Those distances are directly connected to the lattice parameters of the crystal. Measuring a set of angular positions thus theoretically permits to determine the crystalline structure of a sample. In practice, this information will be used to identify the crystalline phases (either original compounds or degradation products) present in a material (Fig. 11.3c).

Slight variations in the position of these peaks can be caused by (i) a slight modification of the lattice parameters of a crystalline phase, e.g. through substitution of CrO_4^{2-} ions with SO_4^{2-} ions in the chrome yellow pigment (Fig. 11.3d and the example below about the different grades of chrome yellows) or (ii) can be the results of a slight variation in distance between the diffracting material and the XRD detector. When the structures of the crystalline species are known, the latter information can be used to obtain stratigraphic information of the crystalline phases without the need for invasive sampling (Fig. 11.3e).

The width of the diffraction signals also contains information about the material under investigation. Diffraction peaks can be broadened by several physical effects, such as crystallite size and strain. The amount of broadening can be quantified using the Full-Width-at-Half-Maximum (FWHM) of the diffraction peaks. In short, the FWHM of a diffraction peak increases as the dimensions of the crystallites decreases (Scherrer broadening). This information can be used to estimate the size of crystalline domains and can sometimes provide clues about the crystal formation (e.g., natural minerals versus synthetic compounds, crystals formed through precipitation, etc.) (Fig. 11.3f).

11.2.2.1 XRD Mapping in Two and Three Dimensions

As sketched in Fig. 11.1, XRD mapping consists in acquiring XRD patterns at each pixel of a two-dimensional area being either at the macro or at the micro scale. The different types of information that have been discussed in the previous section (chemical composition, depth distribution, crystallite size and preferred orientation) can be extracted from individually collected XRD patterns and employed to compose distribution maps of these properties.

In the Cultural heritage field, XRD mapping is currently mainly applied to paintings (Janssens et al. 2010, 2013) (including easel (Cotte et al. 2017a; De Nolf et al. 2011; Gonzalez et al. 2017, 2019; Klaassen et al. 2019; Monico et al. 2018; Monico et al. 2013a, b, 2015a, b; Otero et al. 2018; Pouyet et al. 2015; Price et al. 2019; Radepont et al. 2011; Salvado et al. 2002, 2009, 2010, 2013, 2014; Smieska et al. 2019; van der Snickt et al. 2009, 2012; Vanmeert et al. 2015, 2018c, 2019; Vermeulen et al. 2017; Welcomme et al. 2007) and mural (Chalmin and Reiche 2013; Cotte et al. 2008; Da Pieve et al. 2013; Dooryhee et al. 2005; Radepont et al. 2011; Salvadó et al. 2008) paintings or polychromies (Liu et al. 2007; Lynch et al. 2007)), manuscripts (such as parchments (Smieska et al. 2017; Van der Snickt et al. 2008; Vanmeert et al. 2018a, b) and papyrus (Brun et al. 2016)), ceramics, (Dejoie et al. 2015; Leon et al. 2010, 2015; Sciau et al. 2006; Wang et al. 2016) metals and metallic alloys, (Dejoie et al. 2015; Grousset et al. 2015; Kergourlay et al. 2018) as well as some more uncommon materials such as lithic materials, (Dejoie et al. 2015; Lombardo et al. 2016) concrete, (Meral et al. 2012) modern modelling clay, (Cotte et al. 2017c) or fossilized bones (Mürer et al. 2018) as well. While the technique is generally applied at SR facilities with a micrometric beam (< 50 μm, μ-XRD), in recent years also macroscopic XRD (beam >100 μm, MA-XRPD) with laboratory

instruments has been employed for the analysis of entire objects. So far, the latter form of XRD mapping has been limited to the investigation of quasi flat artefacts, such as paintings and manuscripts.

Accessing the Third Dimension Cultural heritage artefacts are very often multi-layered systems; either because the artist used a specific sequence of layers to obtain a desired visual effect, or because the original materials have evolved over time, leading to the formation of non-original layers. The location of different materials in 3D is therefore important. While XRD mapping is mostly carried out over 2D regions, the extension to 3D is sometimes possible, by exploiting one of two quite different experimental strategies. The first strategy is mainly based on a software approach (information obtained by analyzing the XRD peak shifts), while the second is a hardware (tomographic) approach (involving rotation of the sample).

The complex build-up of artistic materials (in which layers are most of the time of micrometric thickness) results in small shifts in diffraction peak position, as only a single layer of the stratigraphic system is positioned at the calibrated distance of the instrument. In the case of a painting, if all the inorganic compounds are identified and their structures known, stratigraphic information can be derived from the shift between the measured and reference peak position. This approach has been used to simultaneously identify and map pigments present on both sides of a fifteenth/sixteenth century illuminated sheet of parchment (Vanmeert et al. 2018a, b) (Fig. 11.4). The same approach has been recently exploited, together with MA-XRF, to obtain stratigraphic information, without sampling, of *Exit from the Theater*, a painting attributed to Honoré Daumier, and produced over an earlier landscape (Smieska et al. 2019) while on the iconic painting by Vermeer, *Girl with a Pearl Earring*, a cerussite-rich lead white paint was found on top of a hydrocerussite-rich underlayer (De Meyer et al. submitted).

The above approach works well for macro-scale imaging of entire paintings or parchment folios where an in-depth resolution of several 10s of micrometers is sufficient. Conversely, in μ-XRF or μ-XRD mode, the third dimension can be explored via a computed tomography (CT) approach. By rotating the paint micro-sample around an axis perpendicular to the beam and by recording 2D XRF and/or XRPD maps (or single 1D lines if acquisition time is limited) at every rotation angle, sinograms of the different elements/crystal phases can be obtained. (Bleuet et al. 2008) This approach is particularly useful for the precise location of various compounds in not-flat structures, and has been used to identify and locate degradation products in painting fragments: to identify crystalline phases constitutive of protrusions forming at the surface of *Wheat Stack Under a Cloudy Sky* by Vincent van Gogh (1889) (Vanmeert et al. 2015) and determine the nature of the lead-rich whitish surface deposits found in Rembrandt's *Homer* (1663). (Price et al. 2019) In the former case, the virtual XRPD maps revealed a complex onion-like structure around the protrusion, made up of different lead-based phases.

Added Value of XRD Mapping for Phase Identification The acquisition of elemental distributions by XRF mapping instead of a single data point not only allows to ascertain the location of different elements but may also contribute indirectly to

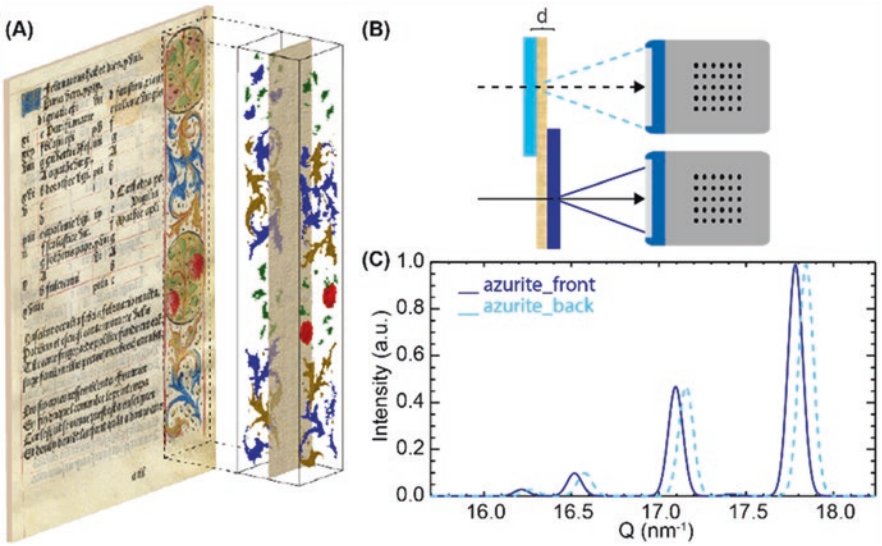

Fig. 11.4 (**a**) Fifteenth century illuminated manuscript, painted on two sides with a decorative vegetal pattern in which different pigments were employed, one of them being azurite. The (slightly) different distance of the azurite layers on the recto and verso side of the manuscript relative to the XRD detector (**b**) results in a (slight) shift of the XRD pattern (**c**), and this can be exploited to separate both contributions and reconstruct the azurite pigment distributions on both sides of the folio. Adapted from Gonzalez et al. (2020)

the identification of the compound in which the element in question is present. A simple example involved red painted areas of paintings that correspond to the Hg-rich areas of a map: since HgS (vermillion red) is the only commonly used Hg-containing red pigment, its unambiguous identification is straightforward. However, in many other cases (such as for Ca, Fe, Cu, Pb, …), specific pigment identification is not possible; additional information offered by XRD is then required. MA- or μ-XRD can detect a minor component that would be below the detection limit of bulk XRD, but which becomes a major compound when the size of the X-ray beam is restricted to a region in which this compound is concentrated.

11.3 Applications of MA-XRF and/or MA-XRD Mapping

11.3.1 Virtual Reconstructions and Retracing the Composition of the Original Artists' Materials

Main Components XRF mapping experiments may be performed for the following purposes: the motivation may be mostly art-historical in nature, requiring maps of chemical elements in visible or hidden paint layers, or may be inspired by ques-

tions related to art authentication, conservation and restoration where making the difference between original, non-original and degraded paint is more of interest. The first experiment with MA-XRF mapping was performed on a small painting by Van Gogh called 'Patch of Grass' below which a portrait of a Dutch rural lady was hidden; the original colour of her face could be reasonably approximated by combining the XRF maps of Sb (Naples yellow), Pb (lead white) and Hg (vermillion red) (Anitha et al. 2013). Other early examples in this category involved the visualization of an overpainted fountain and related garden architecture in the seventeenth c. *Portrait of Helena Fourment* by P.P. Rubens (Van der Snickt et al. 2018) and of a general's uniform below the *Portrait of Don Ramon Satué*, an eighteenth c. painting by Goya. (Bull et al. 2011) In Fig. 11.5, the results of the physical and virtual reconstruction of a small painting by Pieter Brueghel the Elder, entitled 'The Suicide of Saul' is shown. An area of the background where flame-like shapes appeared to be present in the sky, was scanned by MA-XRF. These maps revealed that originally, behind the dark green walls of the city visible in the middle of the painting, another part of the city was painted using the blue pigment smalt. This part of the city is now no longer visible because, as a result of chemical alteration, the color of smalt has faded away. However, by superimposing the Co MA-XRF map on the photograph of the physically restored painting (Fig. 11.5b), a virtual reconstruction of the original outlook of this painting (Fig. 11.5c) could be realized. This type of images is useful both for the general public, art historians and art conservators as they help to imagine what the original intention of the creating artist was. (Kirchner et al. 2018)

Many XRD mapping experiments (in particular those performed on paintings and manuscripts) aim at specifically identifying the composition of the various pigments used by the artists. (Brun et al. 2016; Cotte et al. 2008; De Nolf et al. 2011; Dooryhee et al. 2005; Gonzalez et al. 2019; Liu et al. 2007; Lynch et al. 2007; Monico et al. 2015a, b; Salvado et al. 2002, 2008, 2009, 2013, 2014; Smieska et al. 2019; Van der Snickt et al. 2008; Vanmeert et al. 2018a, b) The pioneering application of XRD mapping was on a fragment of a Roman wall painting, displaying a portrait. This experiment revealed the presence of different pigments such as hematite (Fe_2O_3), goethite (FeOOH), lead carbonate ($PbMg(CO_3)_2$) and Egyptian blue (cuprorivaïte, $CaCu(Si_4O_{10})$). Besides, calcite ($CaCO_3$) was identified not only as a pigment in the flesh tones, but also in the underlying ground layer. (Dooryhee et al. 2005) While this kind of identification can be obtained by means of a combination of other techniques (e.g. XRF, Vis/ IR imaging spectroscopy), it can be more efficiently done by exploiting the unique structural contrast and specificity offered by XRD.

Impurities in Natural Compounds Complementarily to the determination of the main crystalline compounds of an artistic artefact, the nature and precise quantification of impurities (typically crystalline phases in low amounts, i.e. < 5 w%) can be useful to elucidate the provenance of the natural (mineralogical) compounds that were employed by an artist. This was recently exemplified in a study focusing on the impurities present in azurite, an inorganic compound extensively employed as a blue pigment, both in paintings as well as in illuminated manuscripts. (Smieska et al. 2017).

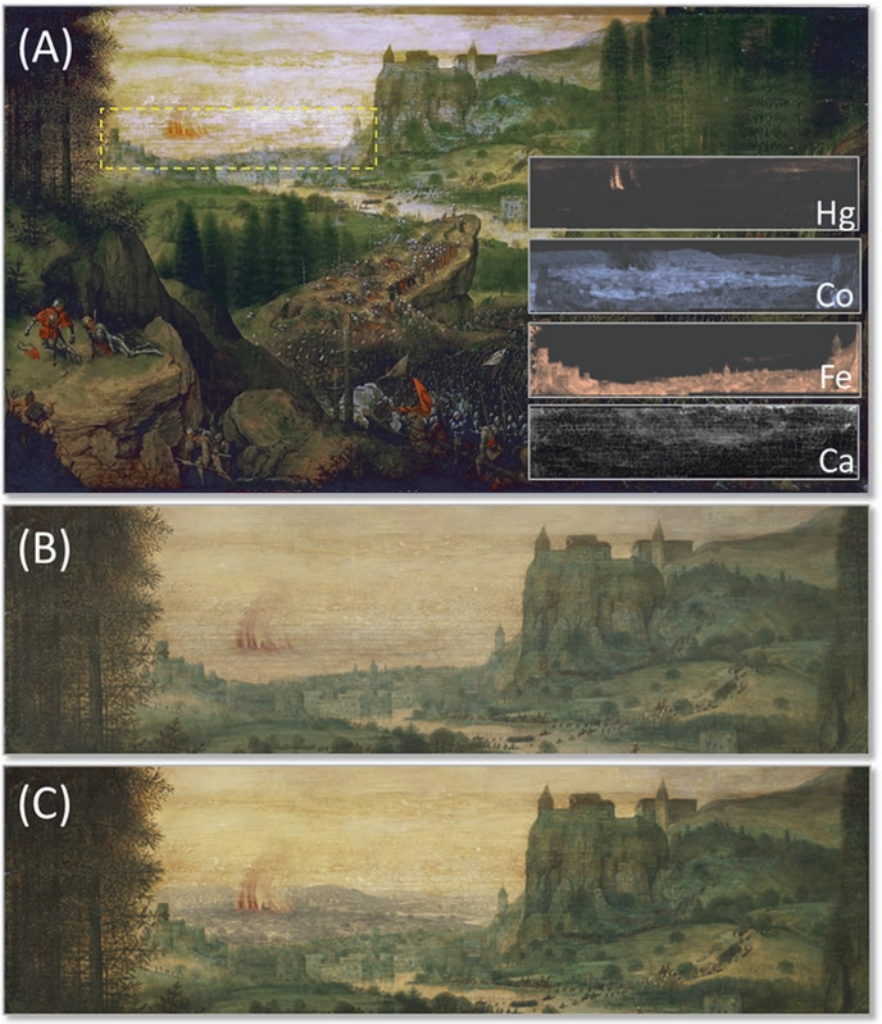

Fig. 11.5 *The Suicide of Saul* (1562, Pieter Bruegel the Elder, © Kunsthistorisches Museum Vienna): (**a**) before and (**b**) after restoration. (**c**) Virtual reconstruction of the city originally painted in the background by means of the pigment smalt. Since the smalt lost its blue color due to degradation processes, in reality the cityscape is no longer visible. In the insets of (**a**), a number of relevant MA-XRF maps of different elements are shown

Different Subtypes of Synthetic Compounds Beyond the identification of the main and minor (paint) components, XRD can be also used to highlight slight differences in the quantitative composition of specific components. Indeed, one synthetic pigment with the same generic name can exist under different grades, and different (shades of) colors. The different grades/qualities could be sold at different prices to the artists. The choice between those subtypes would depend on their budget and the

pictorial result they were aiming at. The difference between various grades is a result of the complexity of their synthesis or the possible admixture of adulterants by the merchant. Accessing today the composition of ancient materials can help to reveal those differences in grades and quality. As an example, lead white, a pigment omnipresent in painted artworks from Antiquity to the twentieth century is usually a mixture of lead carbonates: cerussite and hydrocerussite. Historical sources reveal that different grades of lead white were sold to artists through pigment markets at very different prices. The traditional way to synthesize lead white is based on acidic corrosion of lead metal foils, and mainly yields hydrocerussite and cerussite. After this step, numerous post-synthesis processes could be used by the manufacturers, such as an acidic treatment (grinding of the pigment powder in vinegar) or heating in water. The best products were praised for their exceptional optical and handling properties. While all the recipes were carefully recorded in ancient painting treatises, master painters never explicitly revealed what type of lead white they used in their artworks. Laboratory reconstructions of ancient synthesis processes and of post-synthesis treatments permitted an investigation of their effects on the composition and microstructure of the pigment. (Gonzalez et al. 2016) For example, heating the pigment in water induces the transformation of cerussite into hydrocerussite, with the newly formed hydrocerussite crystallites exhibiting large sizes (dimensions up to 5 μm instead of <1 μm without this process). Conversely, the treatment with an acidic solution (such as vinegar) leads to the formation of small (< 100 nm) cerussite crystallites, following a recrystallization process. μ-XRD and MA-XRD both allow to estimate the hydrocerussite to cerussite ratios and the dimensions of crystallites in micro-samples or paintings, thus revealing the various grades of lead white used by well-known artists such as Rembrandt and Vermeer. (De Meyer et al. submitted; Gonzalez et al. 2017)

The pigment chrome yellow is another good example of an artists' material available/used in multiple grades, shades or qualities. In a letter dated on the 5th of April 1888, van Gogh asked his brother to buy different grades of chrome yellows: "*Jaune de Chrôme citron*" (lemon), "*Jaune de Chrôme (N° deux)*" (#2), "*Jaune de Chrôme N° trois*" (#3, the latter called "orange").

These different grades and names correspond to chrome yellows with different color and composition, resulting from different synthesis protocols. The reconstruction of Winsor and Newton nineteenth century recipes revealed notably that this company produced mainly three pigment types: a lemon/pale type ($PbCr_{1-x}S_xO_4$, with $0 < x < 0.5$), a middle type ($PbCrO_4$) and orange/red type ($PbCrO_4.PbO$); these different types are obtained in acid, neutral and basic conditions, respectively. (Otero et al. 2017) In parallel to FTIR and Raman spectroscopy, these different grades can be differentiated by means of XRD. (Monico et al. 2013a, b) The $PbCrO_4$ form is crystallized under monoclinic form while the $PbCr_{1-x}S_xO_4$ can exist under both monoclinic and orthorhombic forms. Here again, both μ-XRD and MA-XRPD can be exploited to identify these different compositions in both paint fragments and paintings, respectively (Fig. 11.6c). This information is important not only to know which pigments were used by the artists, but also since these different grades exhibit

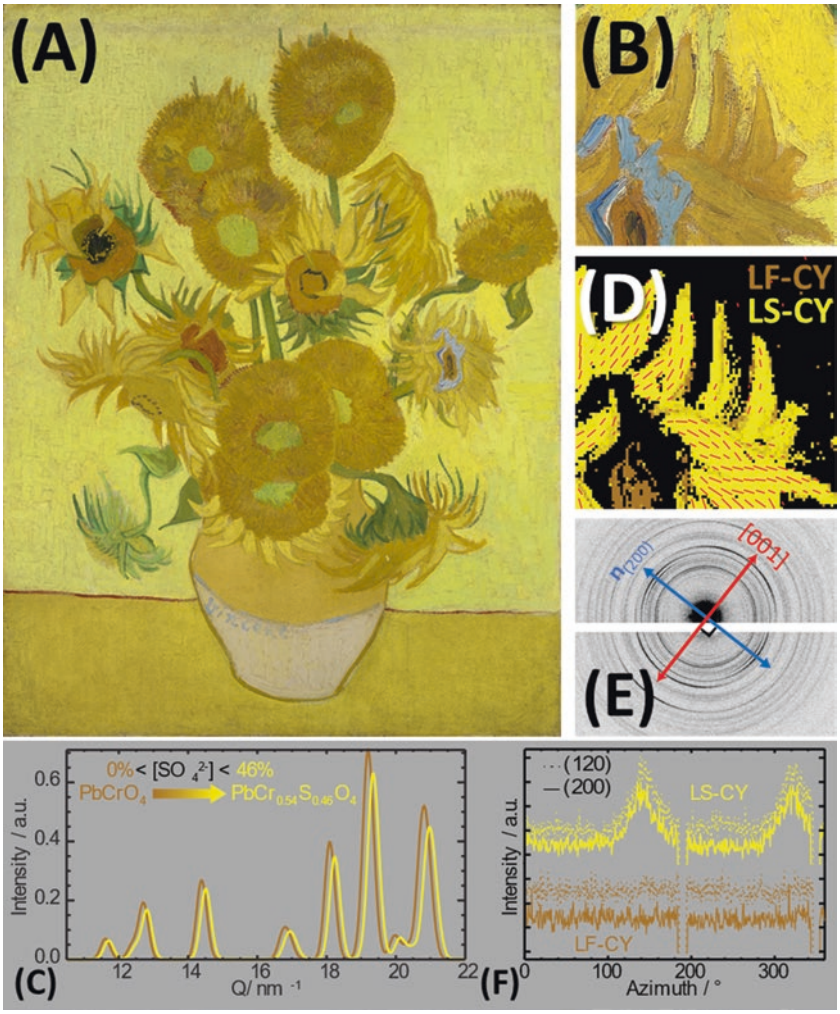

Fig. 11.6 (**a**) MA-XRD investigation in transmission mode on *Sunflowers* by Van Gogh (© Van Gogh Museum, Amsterdam) on (**b**) a detail of one of the sunflowers. (**c**) Using the small shift in diffraction peak position between LF-CY and LS-CY it is possible to visualize their distribution. (**d**) False color image showing LF-CY (brown) and LS-CY (yellow). The red lines visualize the projected [001] direction of the LS-CY crystallites on the paint surface. (**e**) 2D diffraction pattern illustrating the preferred orientation effect of the (200) reflection of LS-CY. (**f**) 2θ-integrated diffraction intensity versus azimuthal (γ) angle. The intensity maxima for reflections (120), dashed lines, and (200), full lines, for LS-CY are clearly visible, while the intensity remains constant for LF-CY. Adapted from Vanmeert et al. (2018c)

different photo stability; notably, orthorhombic $PbCr_{1-x}S_xO_4$, rich in SO_4^{2-} ($x \geq 0.4$) is prone to darken (light-sensitive chrome yellow, noted LS-CY in Fig. 11.6) while the monoclinic $PbCrO_4$ (LF-CY, for light-fast chrome yellow, Fig. 11.6) is stable. (Monico et al. 2013a, b) Laboratory MA-XRPD was used in the Van Gogh museum (Amsterdam, NL), together with many other portable imaging (MA-XRF) and micro-analytical (Raman and reflectance mid-FTIR spectroscopy) techniques (Fig. 11.6a). The full painting was scanned with MA-XRF, but, due to substantially longer acquisition times of MA-XRD (0.2 s for XRF vs. 10 s for XRD), MA-XRD was carried out only on a set of areas (Fig. 11.6b). The maps revealed that van Gogh used different chrome yellows, in different ratio and mixed with different pigments to paint the flower heart and the petals of the sunflowers (Fig. 11.6b, d). They also highlighted the areas of the painting with a higher risk for degradation (see distribution of LS-CY in Fig. 11.6d). (Vanmeert et al. 2018a, b) Besides, a combination of SR-μ-XRF, μ-XRD and micro X-ray absorption near edge spectroscopy (μ-XANES) at the Cr K-edge was used to analyze micro-fragments taken from this major work of art. (Monico et al. 2015a, b) μ-XRD was very efficient for the identification and localization of the different chrome yellow grades while μ-XANES was required to identify amorphous Cr(III) degradation compounds, invisible in μ-XRD maps. (Monico et al. 2019) This multi-modal study revealed evidence of degradation of some chrome yellows in the Van Gogh museum's version of the *Sunflowers*.

In addition to the determination of the XRD peak positions, their FWHM can also provide information about the origin of the materials used by the artists. Notably, estimating the size of the crystallites composing an inorganic compound can provide precious insights on its origin/synthesis method. For example, different calcite materials present in the flesh tones and in the ground layer of a Roman wall painting portrait were differentiated by the degree of broadening of their XRD peaks: the more finely ground pigment material in the flesh tones area showed broader peaks than the materials in the underlying ground. (Dooryhee et al. 2005) However, achieving a precise estimation of crystallite size is difficult in the case of historical materials, as they are often complex and heterogeneous mixtures. With synchrotron-based high-angular resolution XRD (SR-HR-XRD), a technique that allows achieving excellent angular resolution and avoids preferential orientation, it is possible to precisely estimate the crystallite size. This technique was recently employed to characterize different lead white pigment samples. (Gonzalez et al. 2016) It usually relies on millimetric X-ray beams and a continuous rotation of the sample, which makes it incompatible with X-ray microscopy. Using XRD microscopes, the angular resolution of the diffraction signals is usually much poorer (for experimental reasons) and the beam size can be comparable to the crystallite size leading to discrete diffraction spots (Fig. 11.3b). In this case, Scherrer broadening may still be qualitatively estimated by averaging 2D diffraction patterns from a large number of pixels over areas of similar composition. By fitting selected peaks of the crystalline phase of interest, it is then possible to measure the diffraction peak FWHM, and derive a mean crystallite size; this was done for hydrocerussite crystallites in French paintings dated to the fourteenth century. (Gonzalez et al. 2017)

However, the error intervals associated with the estimation of the FWHM by μ-XRD are much larger than those of HR-XRD, which result in a significant uncertainty on the obtained crystallite sizes (± 100 nm).

Ancient Artistic Production Techniques The phase composition of CH materials can reveal not only information on the choice of materials used by the artist (matter) but also on the way they were used to produce the final artwork (manner) and it can be specific to certain manufacturing conditions of historical artifacts. Mapping crystalline compounds at the micro-scale can also help to retrieve the lost techniques of the master painters of past periods. This was recently shown in a study on Rembrandt's *impasto*, a key pictorial technique of the Dutch Golden Age Master that allowed him to achieve striking visual effects by adding a third dimension to his paintings. (Gonzalez et al. 2019) Rembrandt's *impastos* were based on lead white paint, but the exact recipe used to obtain a paint formulation with such specific rheological properties remained unknown. By structural mapping at the micro-scale of paint samples collected in *impasto* areas and in adjacent paint layers, it was possible to identify nano-crystallites of a rare lead carbonate compound, plumbonacrite ($Pb_5O(OH)_2(CO_3)_3$), previously encountered in the degradation layers of paint from a Van Gogh painting.[127] Here, this compound was systematically found to be homogeneously distributed in the lead white matrix, within the *impasto* layers (Fig. 11.7c)

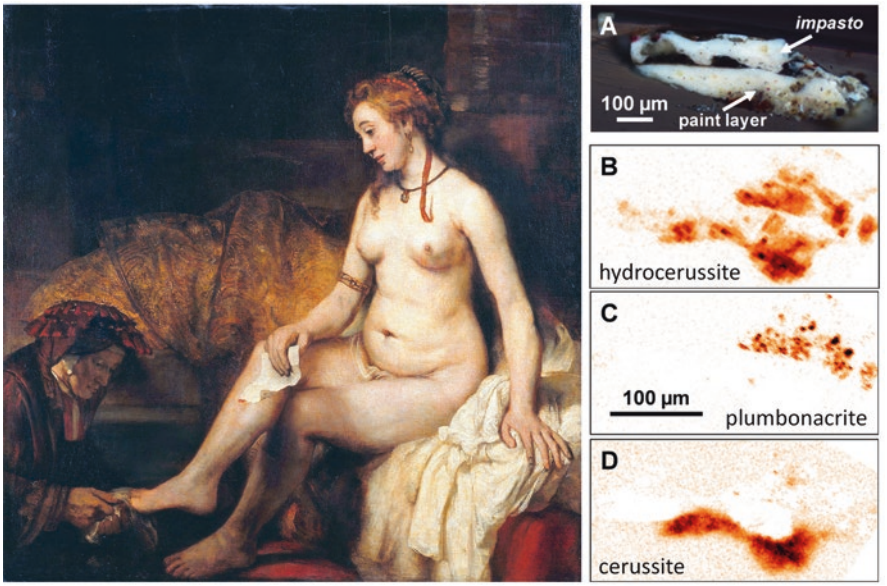

Fig. 11.7 μ-XRD analysis of a paint thin-section from Rembrandt's Bathsheba (© Musée du Louvre, left panel), sampled in an impasto area. Right panels: (**a**) Visible light photograph of the stratigraphy prepared as a cross-section. (**b–d**) μ-XRD ROI images calculated by integrating XRD intensity over several XRD peaks: (**b**) hydrocerussite, (**c**) plumbonacrite and (**d**) cerussite. In μ-XRD maps, a black/dark orange color corresponds to higher intensity. Adapted from Gonzalez et al. (2019)

and is not detected in the paint layers where only hydrocerussite and cerussite, the expected constitutive phases of lead white are present (Fig. 11.7b–d). As in the Van Gogh case, the microstructure and distribution of plumbonacrite indicates an *in-situ* formation of the compound over time. As hypothesis for its formation, the use of specific binder recipes by Rembrandt for his *impasto* (notably characterized by an addition of lead oxide (PbO)) was put forward. When associated with cerussite and/or hydrocerussite (as in the present case), plumbonacrite cannot be identified by elemental analyses alone (since the presence of Pb, C, O and H is not sufficiently specific). μ-FTIR and Raman spectroscopy are inefficient as well since these different lead hydroxyl/oxy/carbonates exhibit overlapping absorption peaks (weaker intensity for plumbonacrite), and plumbonacrite can only be reliably identified in the absence of the other carbonates. (Brooker et al. 1983) In such an example, the combined sensitivity and specificity offered by XRD was essential. Increased application of MA-XRPD and μ-XRD mapping to historical paintings is also revealing a more prevalent presence of the rare plumbonacrite than thought until now.

11.3.1.1 Crystallite Orientation Within Paint Layers

During the macroscopic investigation of *Sunflowers* by Van Gogh (Van Gogh museum, Amsterdam), next to the identification of different grades of chrome yellow, as discussed above, information about the way in which the paint was applied could be inferred. It was observed that the LS-CY showed a strong degree of preferred orientation, while for the LF-CY, a smooth intensity distribution along the Debye rings was found (Fig. 11.6e–f). By tracking the preferred orientation for two different reflections, (120) and (200), over the entire imaged area, it could be seen that the prism-like light-sensitive chrome yellow crystallites all oriented themselves along the brushstrokes made by Van Gogh (Fig. 11.6d). (Vanmeert et al. 2018a, b) It is hypothesized that this difference in microscopic behavior between both chrome yellow types could be related to different degrees of viscosity for the two paints, or to the size of the pigment particles. It remains to be seen if this information is specific for this type of chrome yellow or if it is a unique marker suggestive for the hand of Van Gogh.

11.3.2 Mapping of Degradation Products

μ-XRD mapping also has been extensively used to identify alteration products in artistic materials, and most often in paintings. As mentioned earlier, this is the case for the chemical degradation of chrome yellow, (Monico et al. 2013a, b, 2015a, b; Otero et al. 2018) cadmium yellow, (Monico et al. 2018; van der Snickt et al. 2009, 2012) cinnabar and vermilion, (Da Pieve et al. 2013; Radepont et al. 2011) copper-based pigments, (Salvado et al. 2002, 2009, 2013, 2014; Vermeulen et al. 2017) arsenate-based pigments, (Vanmeert et al. 2019; Vermeulen et al. 2017) but also for

silver foils (Salvado et al. 2010) and lead-based driers. (Cotte et al. 2017a) In the case of HgS degradation, μ-XRD could also be used to differentiate between two forms of the same degradation product: corderoite (α-$Hg_3S_2Cl_2$) and its metastable polymorph, kenhsuite (γ-$Hg_3S_2Cl_2$). Their distribution within the paint stratigraphy, as revealed by μ-XRD, showed that the former was formed as the degradation of the latter, eventually ending in the formation of calomel (Hg_2Cl_2). (Radepont et al. 2011) In many of the above studies, SR-μ-XRD is combined with other SR-based micro-analytical techniques, such as μ-XRF, μ-FTIR and μ-XAS, which can provide additional information about non-crystalline materials. Among others, oxalates are frequently identified as degradation compounds. (Cotte et al. 2008; Otero et al. 2018; Salvado et al. 2002, 2008, 2009, 2010, 2013, 2014; Van der Snickt et al. 2012) The identification and localization of such species, which can form opaque and highly disfiguring crusts, is fundamental for a state-of-the-art and well controlled conservation treatment, as recently performed on Memling's *Christ with Singing and Music-making Angels*. (Klaassen et al. 2019).

While μ-XRD mapping can provide detailed information on the sequence of degradation products, these studies are limited to a select number of small samples taken from regions that possibly show visible discoloration. Recently it has been illustrated that MA-XRD mapping is able to detect alteration products within and on the surface of paintings, often present as thin layers (Fig. 11.8) and therefor can help to select appropriate sampling locations. For the case of the photo-induced degradation of the arsenic sulfide pigments, the yellow orpiment (As_2S_3) and the red-orange realgar (α-As_4S_4), two lead arsenate species were found within and on the surface of three seventeenth century paintings, two by J.D. de Heem and one from a copy artist after de Heem (see Fig. 11.8c). (Vanmeert et al. 2019) These arsenate species, schultenite ($PbHAsO_4$) and mimetite ($Pb_5(AsO_4)_3Cl$), are believed to be the end products of the multi-step degradation pathway for these As-containing pigments. However, arsenolite (As_2O_3), which is often associated with this degradation phenomenon, was not found using MA-XRD. (Vermeulen et al. 2017) On the surface of these same paintings, various secondary formed sulfates, palmierite ($K_2Pb(SO_4)_2$), syngenite ($K_2Ca(SO_4)_2{\cdot}H_2O$) and gypsum ($CaSO_4{\cdot}2H_2O$), were also found by the same group, (Fig. 11.8b). On the surface of Vermeer's *Girl with a Pearl Earring*, next to palmierite and gypsum, a calcium oxalate (weddellite, $CaC_2O_4{\cdot}2H_2O$) was found in the dark background and shadowed areas on the Girl's face and blue headscarf. (De Meyer et al. 2019). In such degradation studies, elemental maps offered by MA-XRF are usually insufficient since original compounds and degradation products often share the same main elements and usually differ by the presence/absence of rather ubiquitous low-Z elements (such as H, C, O, P, S and Cl).

When degradation phenomena are encountered, one of the main objectives of a restoration treatment is to either counteract or inhibit as best as possible those reactions. Multiple treatments exist ranging from consolidation with new materials to the complete replacement of damaged parts of the object. While nowadays, restoration treatments are carefully monitored and documented, earlier restorations might have been performed without written records. While observation under UV light is very efficient to highlight overpaints, XRD can help to design, monitor and

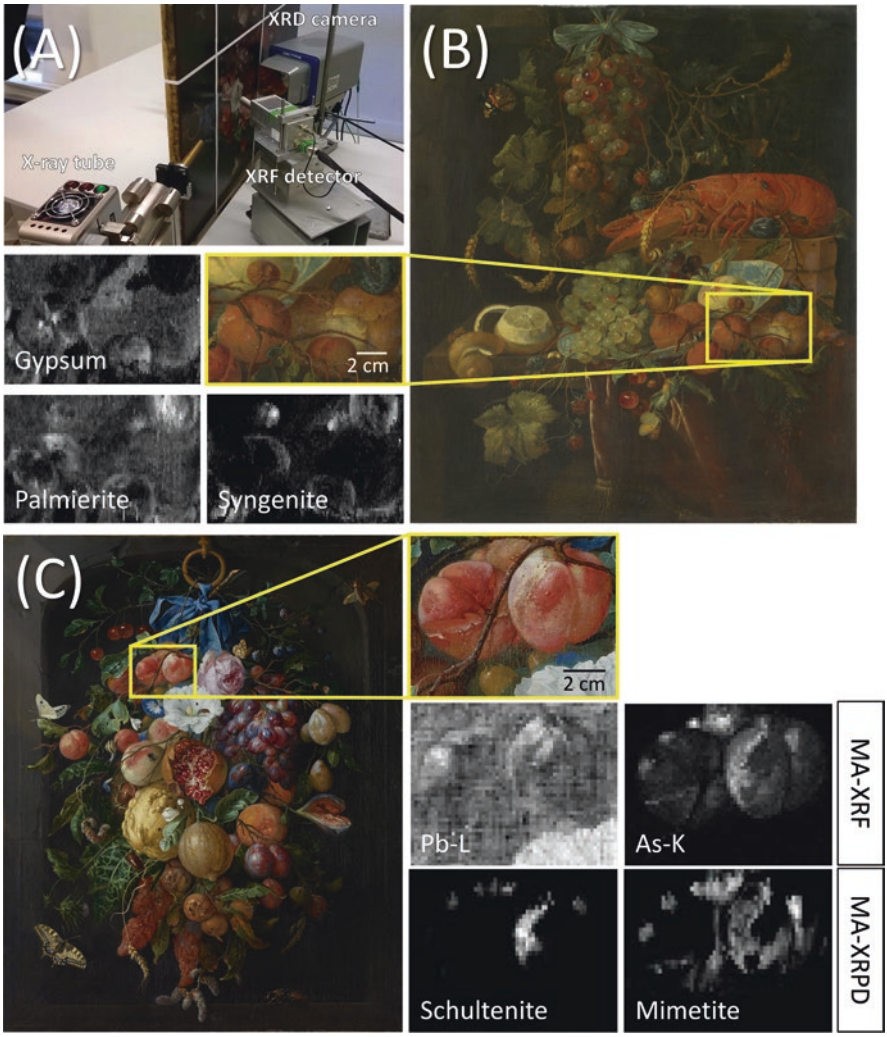

Fig. 11.8 (**a**) MA-XRF/MA-XRD investigation in reflection mode on seventeenth century still life paintings (© Rijksmuseum, Amsterdam): (**b**) *Still Life with Fruit and a Lobster*, copy after Jan Davidsz de Heem and (**c**) *Festoon of Fruit and Flowers*, Jan Davidsz de Heem. The different grey-scale images illustrate the presence of various degradation/alteration products that have formed in-situ over time. White indicates a stronger intensity of the compound. Adapted from Vanmeert et al. (2019)

optimize restoration treatments, by accurately identifying more recent inorganic materials. By mapping their distribution on the surface of an artwork, the nature of previous restorations can be retrieved and their relevance in the current context of conservation evaluated. Recently, large area MA-XRF mapping has been exploited to visualize original paint layers, to locate hidden paint losses and later overpaint on

the Ghent Altarpiece. (Van der Snickt et al. 2017) XRF mapping was fundamental to guide the restoration of this major work. In future conservation treatments, MA-XRD mapping could also be exploited in a similar manner.

11.4 Distinguishing Original from Add-On Paint and Detection of Counterfeit Artefacts

In this section several case-studies are discussed where the combination of MA-XRF and MA-XRD mapping of pigments is used to ascertain which parts/areas of a painting are consistent with the period of attribution/painting style and which are not.

11.4.1 Example 1. Identification and localization of Different Smalt Types in 'Saul and David', Rembrandt

The painting 'Saul and David', shown in Fig. 11.9, is considered to date from c. 1652 and previously was attributed to Rembrandt van Rijn and/or his studio. It is a complex work of art, recently subjected to an intensive conservation treatment and associated investigations. (Noble et al. 2012).

This painting was thought to have been started in a colorful style characterized by great detailing and smooth handling of the paint. In contrast, the adjustments of the second phase, possibly not by Rembrandt himself, are painted very loosely. This suggests that in this second phase, the painter was experimenting with the use of smalt since this pigment was found over much of the painting, and not only in the blue areas of the turban that belong to the first phase. The extensive use of smalt, especially in mixtures with bone black, lakes and earth pigments is considered typical of Rembrandt's late painting technique. (Janssens et al. 2016; van Loon et al. 2020) This pigment combination was not only useful to create coloristic effects, but also for its drying properties and to give bulk and texture to the paint. MA-XRF was used to map the presence of Cobalt-containing materials, among which is smalt.

From the Fe and Co distribution maps (Fig. 11.9), it is immediately clear that the upper right canvas piece (part γ), painted in a monochrome dark tone, does not show the same origin as the other canvas sections of *Saul and David* (parts α and β, respectively). Throughout the γ area, both Co and Fe appear to be present at high abundance; the joins between the various sub-parts as well as the entire γ-section were uniformly covered with an Fe and Co-containing paint in order to dissimulate the differences with sections α and β. The Co map of the α-section demonstrates that smalt was extensively used in the areas of the turban, the curtain, Saul's garments and his chair. K is associated with smalt but also with red lake (likely from alum or KOH added during its production). The Fe-distribution in the α-section is quite

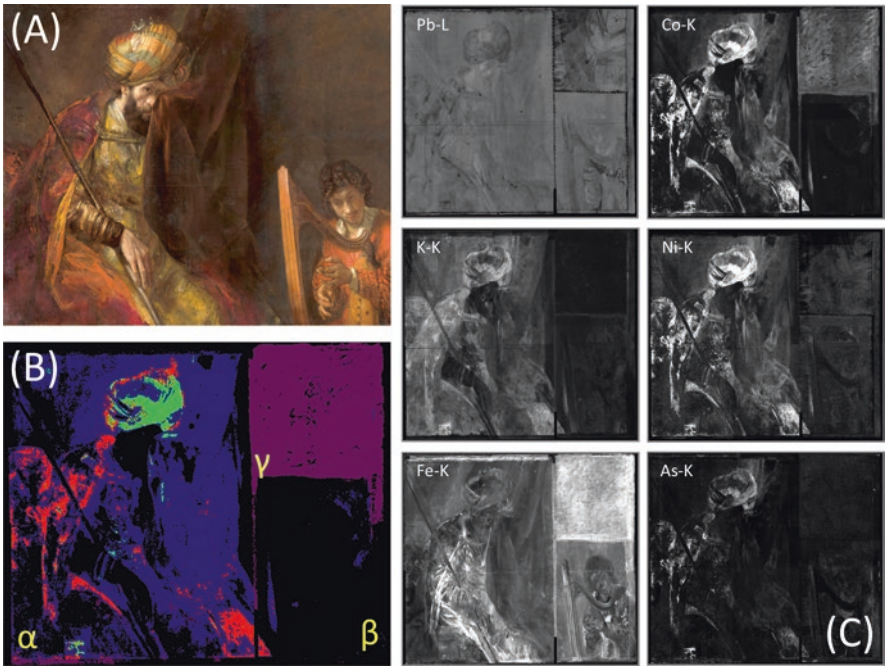

Fig. 11.9 (**a**) *Saul and David* by Rembrandt, (c. 1652, 126 x 158 cm, Royal Museum Mauritshuis, Den Haag, The Netherlands, inv. no. MH621, oil on canvas); (**b**) pixel cluster map showing locations of different Co/Ni ratio values (color codes: green: "high Ni", red: "medium Ni", magenta: "low Co/Ni", blue: "rest (Co/Ni ratio undetermined due to low Co and Ni abundance)"; black: "No smalt present"); (**c**) MA-XRF maps (1656 x 1311 pixels) of various elements present in the painting. Adapted from Janssens et al. 2016a

different from the other elements since it is dominated by the earth pigment-containing areas, where the Fe concentration is much higher than in smalt (where it is of the order of a few wt%). The Co map has a patchy appearance at the left and bottom of the picture, areas corresponding to Saul's cloak, which initially appears to have extended over the chair. The lighter (higher intensity) areas in the Co map correspond to the thicker/more intact smalt-rich paint. Paint cross-sections from the dark patchy areas in the scans of Saul show the presence of an incomplete smalt-rich top paint layer applied on top of red lake glazes. The partial removal of the smalt paint from Saul's garment and chair is most likely due to a misinterpretation during a past restoration, where a restorer tried to recover the bright red color of Saul's cloak, obscured by a discolored and darkened smalt layer. By considering the Ni-K:Co-K XRF intensity ratios throughout the painting, four groups of pixels can be distinguished (Fig. 11.9b). Next to the 'medium Ni' group of pixels (labeled red in Fig. 11.9b), a smaller group of pixels (labelled green) is present characterized by a Ni:Co ratio that is ca. 25% higher than in the 'medium Ni' group. This 'high Ni' group of pixels is situated in Saul's turban and some small parts of his clothing. The 'medium Ni' group of smalt pixels corresponds to patchy areas of paint of uneven

thickness that are present in Saul's garment in sections α and β. The pixels belonging to the curtain area in the background between the figures of Saul and David, generally showing both a low Co and Ni intensity, were labelled blue. In magenta, a fourth group of pixels, characterized by a very low Ni to Co XRF intensity ratio is also visible in Fig. 11.9b, corresponding to the paint used to cover the canvas insert γ. (Noble et al. 2012) Microscopic examination of paint samples from this section showed that Co is not present in the form of smalt pigment particles but in a more finely divided state, dispersed through the layer. The Co material was likely added to the nineteenth-century overpaint as drying agent. In sections α and β however, the Co and Ni are definitely present inside coarsely ground smalt particles. This observation is consistent with the MA-XRF data, where in the turban area, a Ni:Co intensity ratio that is ca. 25% higher than that in the garment area is observed. The difference between the 'medium Ni' and 'high Ni' areas could also be found back in the quantitative SEM-EDX data of paint samples from both areas. In this manner the combination of quantitative SEM-EDX analysis and MA-XRF scanning was used to reveal that three types of Co-containing materials are present in the original parts of the *Saul and David* painting, while a fourth Co-material was used in the non-original canvas insert.

11.4.2 Example 2: Pigment Use and Layer Buildup of a Counterfeit 'seventeenth century' Flowerpiece

In Fig. 11.10, a photograph of a colorful flower piece painting is shown that at first sight looks very similar to the seventeenth c. flower arrangements shown in Fig. 11.6; accordingly, it was described by an auction house to date from this period.

Next to a delicately painted red-and-white tulip, several white/pink roses but also red/orange/yellow marigolds, a single intensely yellow/orange eglantier rose and blue/white forget-me-nots and morning glories, together with dark green leaves are shown against a very dark blue background. Macro photographs of the surface of the tulip and the white roses show a delicate paint craquelure that is suggestive of *but not specific* for a seventeenth c. origin. The painting was examined in a non-invasive manner to verify its putative seventeenth c. origin. No definite information could be gained from the frame or lining, since the canvas was assumed to have been recently relined. In Fig. 11.10a, 14 MA-XRF maps and 10 MA-XRD maps derived from this canvas are shown. These images allow for a fairly comprehensive understanding of the (inorganic) pigment types employed to create this painting, and to (indirectly) date it. Consistent with the co-presence of the elements Cd and Se (and in part S) in the red parts of the tulip, of the roses, the red accents in various flowers and in the strawberries, a set of XRD peaks corresponding to cadmium red/orange (in this case with nominal composition $CdS_{1-x}Se_x$ and $x \approx 0.5$) was encountered while in the entire painting, no indication of the presence of the element Hg (in the MA-XRF data) nor the crystal phase HgS (vermillion red) is encountered. Considering that cadmium red has only been available to artists (from around the

1930s) while in all historic periods, the use of either cinnabar (the mineral form of α-HgS) or the synthetic pigment vermillion red is ubiquitous, the combined present and absence of these two pigments suffices to label this painting as non-authentic. Unlike seventeenth c. artists such as J.D. De Heem, A. Mignon and others who developed a complex technique of paint layer build up, allowing to capture in paint the delicate semi-transparent red-and-white petals of tulips, here a simpler juxtaposition of chalk/Ti-white rich and cadmium-red paint strokes, painted on a base layer consisting mainly of Ti-white, has been used (see detail in Fig. 11.10b). All flowers appear to have been painted on top of a uniform Prussian blue/cobalt blue or green/cerulean blue (?) background, i.e., without leaving reserves.

While the MA-XRF maps of Si and S are so noisy that the shape of a (lighter blue) *morning glory* flower is very hard to recognize, in the MA-XRD data, the unmistakable signature of natural or synthetic ultramarine (mineral: lazurite) is present in this area. The other blue flowers, however, painted in a slightly darker blue hue can be associated with high Fe-K XRF signals and the latter can be traced back to the presence of Prussian blue, a synthetic pigment that was introduced during the eighteenth century. This pigment is also present at lower abundance levels in the dark blue background, together with the mineral goethite. The presence of an earth color in the background paint can also be suspected from the correlated Mn and Fe MA-XRF maps. Co shows a similar distribution; perhaps this element is present here in the form of a drier – no additional information is available from XRD in this case.

After this second observation inconsistent with a seventeenth century origin, the co-presence of both titanium white (TiO_2, mostly present in its most stable form rutile, but also with traces of the metastable form anatase present, introduced as an artists' pigment around 1921) and zinc white (ZnO, introduced around 1834), is not surprising. In all of the brighter areas, also an abundant signal of chalk ($CaCO_3$, the mineral calcite) is encountered while in only a few areas gypsum ($CaSO_4.2H_2O$) signals can be discerned. While in a genuine seventeenth c. painting, lead white (a mixture of cerussite and hydrocerussite) would be present in all color tones and shades, here the only location rich in Pb is the eglantine rose; in which Pb is present in the form of chrome yellow ($PbCrO_4$, mineral: crocoite), a pigment introduced at the end of the 19th c, as evidenced by the co-presence of Cr and Pb in the yellow flower. Somewhat more puzzling is the presence of Zn in the same flower but also in the pale-yellow rose and in some of the green leaves. No indication of zinc-containing compounds could be found in XRD maps, such as zinc yellow ($K_2O.ZnCrO_4.3H_2O$). Finally, it is worth noting that no meaningful MA-XRF map of the element copper could be recorded, another strong inconsistency with genuine seventeenth c. flower pieces where Cu is abundantly present in all green or blue areas. (De Keyser et al. 2017; Simoen et al. 2019) Similarly, no As was encountered whereas in seventeenth c. flower still-lives this element is commonly present, either as yellowish orpiment (As_2S_3) or reddish realgar (As_4S_4) or (amorphous) compounds derived from these minerals. (Janssens et al. 2017; Vermeulen et al. 2016, 2017, 2018) All the above considerations show that the skillfully painted flower piece of Fig. 11.10 was created after 1930, with the craquelure pattern likely created by means of an accelerated aging treatment.

Fig. 11.10 (**a**) Flower piece canvas, painted in a seventeenth c. Netherlandish style and associated MA-XRF and MA-XRD maps; (**b**) detail of the tulip showing its craquelure pattern and four associated MA-XRD maps

11.4.3 Example 3: Mary Magdalene, a Counterfeit 'fifteenth century' Panel by Renowned Restorer Jef Van der Veken

The portrait of Mary Magdalene (Fig. 11.11b) was acquired by Belgian banker and art collector Emile Renders around 1920 in a very bad state of conservation, but it resurfaced in much better condition at an exhibition in Bern (CH) in 1926 and London (UK) in 1927 where it was attributed to the circle of Hans Memling. In March 1941, Alois Miedl, a Nazi art dealer who worked for Hermann Göring, made an agreement with Renders to buy his art collection for a very substantial sum. Part of this collection was shipped to Carinhall, one of Göring's residences, while other

paintings remained in the possession of Miedl. Many years after the end of WWII, Miedl sold the painting shown in Fig. 11.11b to a Scandinavian collector as a genuine fifteenth c. panel painting and copy (albeit using a different color palette) of the left panel of the *Braque Triptych* by Rogier Van der Weyden in the Louvre (Fig. 11.11a). After the death of the collector, his heirs entrusted the work to the Royal Institute for Cultural Heritage (KIK-IRPA) in Brussels for an expert appraisal of its authenticity in 2004. Very quickly, the realization was made that this work was part of the Renders collection. Consequently, the panel was seized by the Belgian state and a series of investigations were carried out to determine its authenticity. Unmistakable indications were found that this panel was in fact an authentic fifteenth c. work of poor quality that underwent an extensive and invasive intervention carried out by master- restorer/painter Jef Van der Veken (1872–1964). (Vanwijnsberghe 2008) Examination of paint cross sections and of the tree ring patterns in the wood revealed that he used as paint substrate, a genuine, late fourteenth c. oak panel from which the original paint was removed to a great extent, leaving only the ground layer, the blue of the mantle and some original paint near the edges. Part of the craquelure of this painting was original and related to the original ground layer while a second craquelure pattern was artificially induced and even some were painted on the surface.

What Van der Veken apparently did not do, however, was to consistently use fifteenth century-compatible pigments for painting Mary Magdalene's portrait. From the MA-XRF maps of Fig. 11.11, it can be assumed that in the light blue sky and grey white of the alabaster vase, the mid nineteenth c.-twentieth c. white pigment ZnO is used. Judging from the Pb MA-XRF maps, in other parts of the painting, next to ZnO also lead white was abundantly used. Other observations inconsistent with a fifteenth century origin is the presence of Co and Fe in the blue mantle as well as in some of the foliage and the green-blue landscape elements behind the figure. However, such an elemental pattern may already show up in sixteenth c. paintings. More problematic is the presence of Cr in the embroidered green sleeve and most of the yellow-green background. Another inconsistency, perhaps attributable to a later restoration is the co-presence of Sr, Ba and Br (typically associated with the red lake eosin) in the dark red line below the figure's left arm, as well as the complete absence of Hg (vermillion red) in the orange-yellow gown and in the flesh tones of the face and hand.

The counterfeit nature of the painting further shows itself when the specific composition of the lead white is considered. As shown in Fig. 11.12, in the entire face and head dress of Mary Magdalene, the lead white consists of pure (100%) hydrocerussite, suggestive of twentieth century industrial lead white production. (Gonzalez et al. 2016, 2017) The lead white in genuine fifteenth century artworks (e.g. by Jan Van Eyck or Justus van Ghent) usually shows at least 5–10% of cerussite to be present in the mixture. A second peculiarity regarding lead white is that the semi-transparent *voile* of the figure's headdress was painted with a much more cerussite-rich lead white type, containing up to 60% cerussite. Next to lead white, several other white components can be discerned in the MA-XRD data and maps: chalk, gypsum, zinc white and barite (likely filler materials, the latter two typical for

Fig. 11.11 Mary Magdalene, (**a**) Left panel of the *Braque Triptych* (1452, R. Van der Weyden, Louvre, Paris); (**b**) copy by J. Van der Veken and (**c**) MA-XRF maps of the panel in (**b**) [© KIK-IRPA]

19-twentieth c. paint). (Feller 1985; Kuhn 1985) In the blue landscape, cobalt blue and cerulean blue (a pigment introduced in 1860) appear to be present, while in the blue mantle, azurite, ultramarine, Prussian blue and cobalt blue are found (the latter two are in use only since the eighteenth and nineteenth c. respectively). Faint signals for ultramarine are also found in the sky. Finally, in one small retouched spot, a mixture of titanium white (TiO_2, rutile), crystalline wax and cadmium yellow (CdS, greenockite) is present (not shown in Fig. 11.12).

Taken together, all these indications point to a twentieth century rather than a fifteenth century date of 'genesis' of the painted representation that was applied on this late fourteenth century panel.

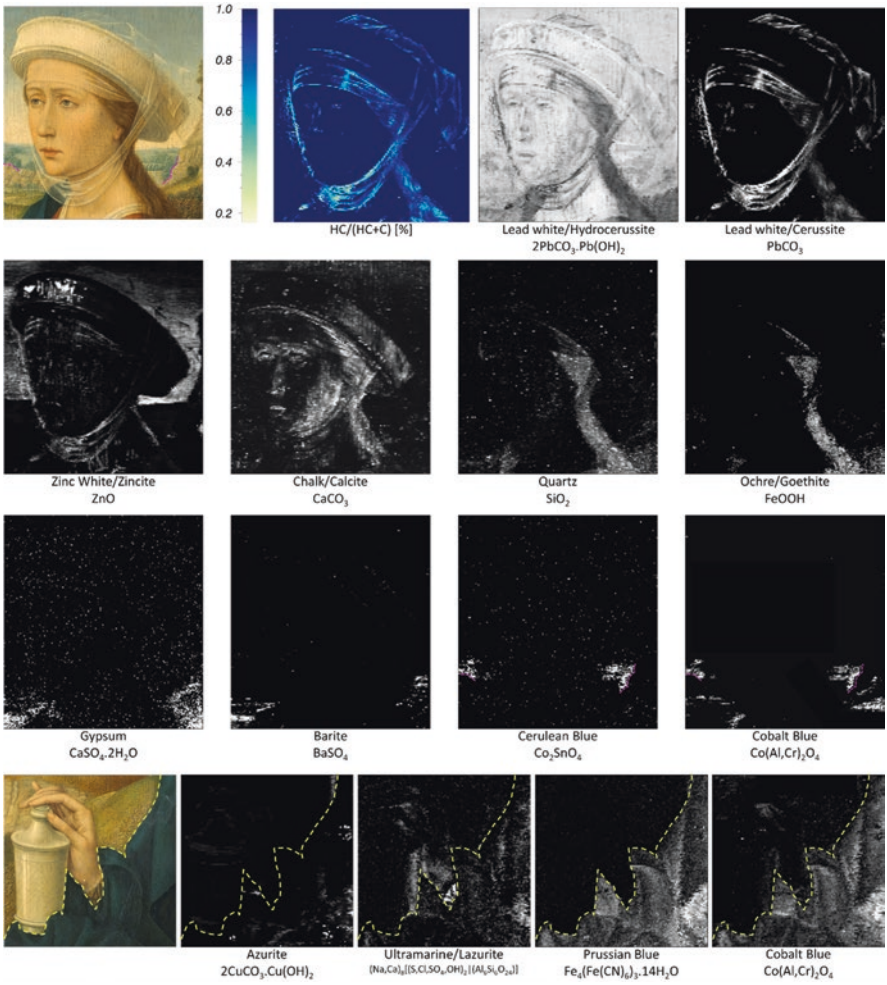

Fig. 11.12 Photographic details of the Van der Veken copy of the Mary Magdalene panel [© KIK-IRPA] with the lead white composition and associated MA-XRPD maps

11.5 Conclusions

In this chapter, an overview was presented of recent developments regarding the characterization of pigmented materials used by painters from the fifteenth to twentieth century based on various forms of X-ray based spectroscopic and imaging analysis. Both XRF and XRD cover a wide range of instrumentation that can be profitably employed for this type of investigations, ranging from fairly compact, mobile devices to sophisticated synchrotron beam lines. Microscopic XRF and XRD are well suited to visualize the elemental distribution of key elements, mostly

metals, present in paint multilayers on the length scale from 1 μm to 100 μm inside paint micro samples taken from paintings.

MA-XRF and MA-XRPD imaging are useful methods for studying degradation processes as well as for identifying pigment subtypes. Even though roughly a factor 100 slower than MA-XRF, the combination of MA-XRF and MA-XRD allows highly specific mapping of the distribution of artists pigments on the dm^2-m^2 scale. This yields information that is useful for various stakeholders in the CH community. In a number of cases, the information these methods provide is relevant for either art historians or art conservators or both. In addition, the possibility to objectively detect counterfeit paintings and to facilitate distinguishing between the original paint of the master painter and add-on paint is very useful for artworks dating from different historical periods.

References

Alberti, R., Frizzi, T., Bombelli, L., Gironda, M., Aresi, N., Rosi, F., et al.: CRONO: a fast and reconfigurable macro X-ray fluorescence scanner for in-situ investigations of polychrome surfaces. X-Ray Spectrom. **46**(5), 297–302 (2017)

Alfeld, M., Broekaert, J.A.C.: Mobile depth profiling and sub-surface imaging techniques for historical paintings – a review. Spectrochim. Acta B At. Spectrosc. **88**, 211 (2013)

Alfeld, M., de Viguerie, L.: Recent developments in spectroscopic imaging techniques for historical paintings – a review. Spectrochim. Acta B At. Spectrosc. **136**, 81–105 (2017)

Alfeld, M., Janssens, K.: Strategies for processing mega-pixel X-ray fluorescence hyperspectral data: a case study on a version of Caravaggio's painting Supper at Emmaus. J. Anal. At. Spectrom. **30**(3), 777–789 (2015)

Alfeld, M., Janssens, K., Appel, K., Thijsse, B., Blaas, J., Dik, J.: A portrait by Philipp Otto Runge – visualizing modifications to the painting using synchrotron-based X-ray fluorescence elemental scanning. Zeitschrift für Kunsttechnologie und Konservierung. **25**(1), 157–163 (2011a)

Alfeld, M., Janssens, K., Dik, J., de Nolf, W., van der Snickt, G.: Optimization of mobile scanning macro-XRF systems for the in situ investigation of historical paintings. J. Anal. At. Spectrom. **26**(5), 899–909 (2011b)

Alfeld, M., De Nolf, W., Cagno, S., Appel, K., Siddons, D.P., Kuczewski, A., et al.: Revealing hidden paint layers in oil paintings by means of scanning macro-XRF: a mock-up study based on Rembrandt's "An old man in military costume". J. Anal. At. Spectrom. **28**(1), 40–51 (2013a)

Alfeld, M., Pedroso, J.V., MvE, H., Van der Snickt, G., Tauber, G., Blaas, J., et al.: A mobile instrument for in situ scanning macro-XRF investigation of historical paintings. J. Anal. At. Spectrom. **28**(5), 760–767 (2013b)

Alfeld, M., Siddons, D.P., Janssens, K., Dik, J., Woll, A., Kirkham, R., et al.: Visualizing the 17th century underpainting in Portrait of an Old Man by Rembrandt van Rijn using synchrotron-based scanning macro-XRF. Appl. Phys. A: Mater. Sci. Process. **111**(1), 157–164 (2013c)

Alianelli, L., Sawhney, K.J.S., Barrett, R., Pape, I., Malik, A., Wilson, M.C.: High efficiency nano-focusing kinoform optics for synchrotron radiation. Opt. Express. **19**(12), 11120–11127 (2011)

Amato, S.R., Burnstock, A., Cross, M., Janssens, K., Rosi, F., Cartechini, L., et al.: Interpreting technical evidence from spectral imaging of paintings by edouard Manet in the Courtauld Gallery. X-Ray Spectrom. **48**(4), 282–292 (2019)

Anitha, A., Brasoveanu, A., Duarte, M., Hughes, S., Daubechies, I., Dik, J., et al.: Restoration of X-ray fluorescence images of hidden paintings. Signal Process. **93**(3), 592–604 (2013)

Barrett, R., Baker, R., Cloetens, P., Dabin, Y., Morawe, C., Suhonen, H., et al. (eds.): Dynamically-figured mirror system for high-energy nanofocusing at the ESRF. In: Conference on Advances in X-Ray/EUV Optics and Components VI; 2011 Aug 22–24; San Diego, CA

Beckhoff, B., Fliegauf, R., Ulm, G., Weser, J., Pepponi, G., Streli, C., et al.: Ultra-trace analysis of light elements and speciation of minute organic contaminants on silicon wafer surfaces by means of TXRF in combination with NEXAFS. In: Kolbesen, B.O., Claeys, C., Stallhofer, P., Tardif, F., Schroder, D.K., Shaffner, T.J., et al. (eds.), 2003. 120-8 p

Beckhoff, B., Kanngiesser, B., Langhoff, N., Rainer, W., Helmut, W.: Handbook of Practical X-Ray Fluorescence Analysis Berlin. Springer, Heidelberg (2006)

Bichlmeier, S., Janssens, K., Heckel, J., Gibson, D., Hoffmann, P., Ortner, H.M.: Component selection for a compact micro-XRF spectrometer. X-Ray Spectrom. **30**(1), 8–14 (2001)

Bjeoumikhov, A., Erko, M., Bjeoumikhova, S., Erko, A., Snigireva, I., Snigirev, A., et al.: Capillary mu Focus X-ray lenses with parabolic and elliptic profile. Nucl. Instrum. Methods Phys. Res. A: Accel. Spectrom. Detect. Assoc. Equip. **587**(2–3), 458–463 (2008)

Bleuet, P., Welcomme, E., Dooryhee, E., Susini, J., Hodeau, J.L., Walter, P.: Probing the structure of heterogeneous diluted materials by diffraction tomography. Nat. Mater. **7**(6), 468–472 (2008)

Bridgman, C.F.: The amazing patent on the radiography of paintings. Stud. Conserv. **9**(4), 135–139 (1964)

Bronk, H., Rohrs, S., Bjeoumikhov, A., Langhoff, N., Schmalz, J., Wedell, R., et al.: ArtTAX – a new mobile spectrometer for energy-dispersive micro X-ray fluorescence spectrometry on art and archaeological objects. Fresenius J. Anal. Chem. **371**(3), 307–316 (2001)

Brooker, M.H., Sunder, S., Taylor, P., Lopata, V.J.: Infrared and Raman spectra and X-ray diffraction studies of solid lead (II) carbonates. Can. J. Chem. **61**(3), 494–502 (1983)

Brun, E., Cotte, M., Wright, J., Ruat, M., Tack, P., Vincze, L., et al.: Revealing metallic ink in Herculaneum papyri. Proc. Natl. Acad. Sci. **113**(14), 3751–3754 (2016)

Bull, D., Krekeler, A., Alfeld, M., Dik, J., Janssens, K.: An intrusive portrait by Goya. Burlingt. Mag. **153**(1303), 668–673 (2011)

Buzanich, G., Wobrauschek, P., Streli, C., Markowicz, A., Wegrzynek, D., Chinea-Cano, E., et al.: PART II (Portable ART analyzer) – development of a XRF spectrometer adapted for the study of artworks in the Kunsthistorisches Museum, Vienna. X-Ray Spectrom. **39**(2), 98–102 (2010)

Cagno, S., van der Snickt, G., Legrand, S., Caen, J., Patin, M., Meulebroeck, W., et al.: Comparison of four mobile, non-invasive diagnostic techniques for differentiating glass types in historical leaded windows: MA-XRF, UV-Vis-NIR, Raman spectroscopy and IRT. X-Ray Spectrom. **50**(4), 293–309 (2020)

Cardinali, M., De Ruggieri, M.B., Leone, G., Prohaska, W., Alfeld, M., Janssens, K.: The Rediscovered Portrait of Prospero Farinacci by Caravaggio. Artibus Hist. **73**, 249–+ (2016)

Chalmin, E., Reiche, I.: Synchrotron X-ray microanalysis and imaging of synthetic biological calcium carbonate in comparison with archaeological samples originating from the large cave of Arcy-sur-Cure (28000-24500 BP, Yonne, France). Microsc. Microanal. **19**(6), 1523–1534 (2013)

Cheng, L., Li, M.T., Youshi, K., Fan, C.S., Wang, S.H., Pan, Q.L., et al.: The study of chemical composition and elemental mappings of colored over-glaze porcelain fired in Qing Dynasty by micro-X-ray fluorescence. Nucl. Instrum. Methods Phys. Res. B. **269**(3), 239–243 (2011)

Choudhury, S., Hormes, J., Agyeman-Budu, D.N., Woll, A.R., George, G.N., Coulthard, I., et al.: Application of a spoked channel array to confocal X-ray fluorescence imaging and X-ray absorption spectroscopy of medieval stained glass. J. Anal. At. Spectrom. **30**(3), 759–766 (2015)

Christiansen, T., Cotte, M., de Nolf, W., Mouro, E., Reyes-Herrera, J., de Meyer, S., et al.: Insights into the composition of ancient Egyptian red and black inks on papyri achieved by synchrotron-based microanalyses. Proc. Natl. Acad. Sci. U. S. A. **117**(45), 27825–27835 (2020)

Cotte, M., Susini, J., Solé, V.A., Taniguchi, Y., Chillida, J., Checroun, E., et al.: Applications of synchrotron-based micro-imaging techniques to the chemical analysis of ancient paintings. J. Anal. At. Spectrom. **23**, 820–828 (2008)

Cotte, M., Checroun, E., De Nolf, W., Taniguchi, Y., De Viguerie, L., Burghammer, M., et al.: Lead soaps in paintings: friends or foes? Stud. Conserv. **62**(1), 2–23 (2017a)

Cotte, M., Monico, L., Janssens, K., De Nolf, W., Salome, M., Langlois, J.: Synchrotron-based micro-analyses of artistic materials at ID21, ESRF. Acta Crystallogr. A. **73**, C1344-C (2017b)

Cotte, M., Pouyet, E., Salome, M., Rivard, C., De Nolf, W., Castillo-Michel, H., et al.: The ID21 X-ray and infrared microscopy beamline at the ESRF: status and recent applications to artistic materials. J. Anal. At. Spectrom. **32**, 477–493 (2017c)

Czyzycki, M., Wrobel, P., Lankosz, M.: Confocal X-ray fluorescence micro-spectroscopy experiment in tilted geometry. Spectrochim. Acta Part B At. Spectrosc. **97**, 99–104 (2014)

da Silva, A.T., Legrand, S., Van der Snickt, G., Featherstone, R., Janssens, K., Bottinelli, G.: MA-XRF imaging on Rene Magritte's La condition humaine: insights into the artist's palette and technique and the discovery of a third quarter of La pose enchantee. Herit Sci. **5**, 9 (2017)

Da Pieve, F., Hogan, C., Lamoen, D., Verbeeck, J., Vanmeert, F., Radepont, M., et al.: Casting light on the darkening of colors in historical paintings. Phys. Rev. Lett. **111**(20), 208302 (2013)

De Keyser, N., Van der Snickt, G., Van Loon, A., Legrand, S., Wallert, A., Janssens, K.: Jan Davidsz. de Heem (1606-1684): a technical examination of fruit and flower still lifes combining MA-XRF scanning, cross-section analysis and technical historical sources. Herit Sci. **5**, 13 (2017)

De Meyer, S., Vanmeert, F., Vertongen, R., van Loon, A., Gonzalez, V., van der Snickt, G., et al.: Imaging secondary reaction products at the surface of Vermeer's Girl with the Pearl Earring by means of macroscopic X-ray powder diffraction scanning. Herit Sci. **7**(1), 11 (2019)

De Meyer, S., Vanmeert, F., Vertongen, R., van Loon, A., Gonzalez, V., Delaney, J., et al.: Vermeer's discriminating use of lead white pigments in Girl with a Pearl Earring revealed by macroscopic X-ray powder diffraction imaging. Sci. Adv. 5(8), eaax1975 (2019)

De Nolf, W., Dik, J., Van der Snickt, G., Wallert, A., Janssens, K.: High energy X-ray powder diffraction for the imaging of (hidden) paintings. J. Anal. At. Spectrom. **26**(5), 910–916 (2011)

Dejoie, C., Tamura, N., Kunz, M., Goudeau, P., Sciau, P.: Complementary use of monochromatic and white-beam X-ray micro-diffraction for the investigation of ancient materials. J. Appl. Crystallogr. **48**(5), 1522–1533 (2015)

Delaney, J.K., Zeibel, J.G., Thoury, M., Littleton, R., Palmer, M., Morales, K.M., et al.: Visible and Infrared imaging spectroscopy of Picasso's Harlequin musician: mapping and identification of artist materials in Situ. Appl. Spectrosc. **64** (2010)

Delaney, J.K., Dooley, K.A., Radpour, R., Kakoulli, I.: Macroscale multimodal imaging reveals ancient painting production technology and the vogue in Greco-Roman Egypt. Sci. Rep. **7**(1), 15509 (2017)

Dietz, G., Ketelsen, T., Hoss, M., Simon, O., Wintermann, C., Wolff, T., et al.: The Egmont Master phenomenon: X-ray fluorescence spectrometric and paper studies for art history research. Anal. Bioanal. Chem. **402**(4), 1505–1515 (2012)

Dik, J., Janssens, K., Van der Snickt, G., van der Loeff, L., Rickers, K., Cotte, M.: Visualization of a lost painting by Vincent van Gogh using synchrotron radiation based X-ray fluorescence elemental mapping. Anal. Chem. **80**(16), 6436–6442 (2008a)

Dik, J., Janssens, K., van der Snickt, G., van der Loeff, L., Rickers, K., Cotte, M.: Visualization of a lost painting by Vincent van Gogh visualized by synchrotron radiation based X-ray fluorescence elemental mapping. Anal. Chem. **80**, 6436–6442 (2008b)

Dik, J., Wallert, A., Van der Snickt, G., Janssens, K.: Silverpoint underdrawing? A note on its visualization with synchrotron radiation based x-ray fluorescence analysis. Zeitschrift für Kunsttechnologie und Konservierung. **22**, 381–384 (2008c)

Dooley, K.A., Conover, D.M., Glinsman, L.D., Delaney, J.K.: Complementary standoff chemical imaging to map and identify artist materials in an early Italian Renaissance panel painting. Angew. Chem. Int. Ed. **53**(50), 13775–13779 (2014)

Dooley, K.A., Chieli, A., Romani, A., Legrand, S., Miliani, C., Janssens, K., et al.: Molecular fluorescence imaging spectroscopy for mapping low concentrations of red lake pigments: Van Gogh's painting The Olive Orchard. Angew. Chem. Int. Ed. **59**(15), 6046–6053 (2020)

Dooryhee, E., Anne, M., Bardies, I., Hodeau, J.L., Martinetto, P., Rondot, S., et al.: Non-destructive synchrotron X-ray diffraction mapping of a Roman painting. Appl. Phys. A Mater. Sci. Process. **81** (2005)

Feller, R.L.: Barium sulphate - natural and synthetic. In: Feller, R.L. (ed.) Artists' Pigments – A Handbook of Their History and Characterics, 1st edn, pp. 47–65, London, Archetype Publications (1985)

Figueiredo, E., Araujo, M.F., Silva, R.J.C., Senna-Martinez, J.C., Vaz, J.L.I.: Characterisation of Late Bronze Age large size shield nails by EDXRF, micro-EDXRF and X-ray digital radiography. Appl. Radiat. Isot. **69**(9), 1205–1211 (2011)

Gonzalez, V., Calligaro, T., Wallez, G., Eveno, M., Toussaint, K., Menu, M.: Composition and microstructure of the lead white pigment in Masters paintings using HR Synchrotron XRD. Microchem. J. **125**, 43–49 (2016)

Gonzalez, V., Wallez, G., Calligaro, T., Cotte, M., De Nolf, W., Eveno, M., et al.: Synchrotron-based high angle resolution and high lateral resolution X-ray diffraction: revealing lead white pigment qualities in old masters paintings. Anal. Chem. **89**(24), 13203–13211 (2017)

Gonzalez, V., Cotte, M., Wallez, G., van Loon, A., de Nolf, W., Eveno, M., et al.: Identification of unusual Plumbonacrite in Rembrandt's Impasto by using multimodal synchrotron X-ray diffraction spectroscopy. Angew. Chem. Int. Ed. **58**(17), 5697 (2019)

Gonzalez, V., Cotte, M., Vanmeert, F., de Nolf, W., Janssens, K.: X-ray diffraction mapping for cultural heritage science: a review of experimental configurations and applications. Chem. Eur. J. **26**(8), 1703–1719 (2020)

Gorelick, S., Vila-Comamala, J., Guzenko, V.A., Barrett, R., Salome, M., David, C.: High-efficiency Gold Fresnel Zone plates for multi-keV X-rays. In: McNulty, I., Eyberger, C., Lai, B. (eds.) 10th International Conference on X-Ray Microscopy. AIP Conference Proceedings. 13652011. 2011; pp. 88–91

Grousset, S., Kergourlay, F., Neff, D., Foy, E., Gallias, J.-L., Reguer, S., et al.: In situ monitoring of corrosion processes by coupled micro-XRF/micro-XRD mapping to understand the degradation mechanisms of reinforcing bars in hydraulic binders from historic monuments. J. Anal. At. Spectrom. **30**(3), 721–729 (2015)

Herm, C.: Mobile Micro-X-ray fluorescence analysis (XRF) on medieval paintings. Chimia. **62**(11), 887–898 (2008)

Howard, D.L., de Jonge, M.D., Lau, D., Hay, D., Varcoe-Cocks, M., Ryan, C.G., et al.: High-definition X-ray fluorescence elemental mapping of paintings. Anal. Chem. **84**(7), 3278–3286 (2012)

Huber, C., Smolek, S., Streli, C.: Simulation of layer measurement with confocal micro-XRF. X-Ray Spectrom. **43**(3), 175–179 (2014)

Janssens, K., Vekemans, B., Vincze, L., Adams, F., Rindby, A.: A micro-XRF spectrometer based on a rotating anode generator and capillary optics. Spectrochim. Acta Part B At. Spectrosc. **51**(13), 1661–1678 (1996)

Janssens, K., Adams, F., Rindby, A.: Microscopic X-ray fluorescence analysis. Wiley, Chichester (2000)

Janssens, K., Proost, K., Falkenberg, G.: Confocal microscopic X-ray fluorescence at the HASYLAB microfocus beamline: characteristics and possibilities. Spectrochim. Acta Part B At. Spectrosc. **59**(10-11), 1637–1645 (2004)

Janssens, K., Dik, J., Cotte, M., Susini, J.: Photon-based techniques for nondestructive subsurface analysis of painted cultural heritage artifacts. Acc. Chem. Res. **43**(6), 814–825 (2010)

Janssens, K., Alfeld, M., Van der Snickt, G., De Nolf, W., Vanmeert, F., Radepont, M., et al.: The use of synchrotron radiation for the characterization of artists' pigments and paintings. Annu. Rev. Anal. Chem. **6**(1), 399–425 (2013)

Janssens, K., Van der Snickt, G., Alfeld, M., Noble, P., van Loon, A., Delaney, J., et al.: Rembrandt's 'Saul and David' (c. 1652): use of multiple types of smalt evidenced by means of non-destructive imaging. Microchem. J. **126**, 515–523 (2016a)

Janssens, K., Van der Snickt, G., Vanmeert, F., Legrand, S., Nuyts, G., Alfeld, M., et al.: Non-invasive and non-destructive examination of artistic pigments, paints, and paintings by means of X-ray methods. Top. Curr. Chem. **374**(6), 52 (2016b)

Janssens, K.H., Vanmeert, F., De Meyer, S., Vermeulen, M.: Multimodal investigation of Pb- and As-based pigment degradation. Acta Crystallogr. Sect. A. **73**, C1399-C (2017)

Kanngiesser, B., Mantouvalou, I., Malzer, W., Wolff, T., Hahn, O.: Non-destructive, depth resolved investigation of corrosion layers of historical glass objects by 3D Micro X-ray fluorescence analysis. J. Anal. At. Spectrom. **23**(6), 814–819 (2008)

Kanngiesser, B., Malzer, W., Mantouvalou, I., Sokaras, D., Karydas, A.G.: A deep view in cultural heritage-confocal micro X-ray spectroscopy for depth resolved elemental analysis. Appl. Phys. A Mater. Sci. Process. **106**(2), 325–338 (2012)

Kergourlay, F., Réguer, S., Neff, D., Foy, E., Picca, F.-E., Saheb, M., et al.: Stabilization treatment of cultural heritage artefacts: in situ monitoring of marine iron objects dechlorinated in alkali solution. Corros. Sci. **132**, 21–34 (2018)

Kirchner, E., van der Lans, I., Ligterink, F., Geldof, M., Gaibor, A.N.P., Hendriks, E., et al.: Digitally reconstructing Van Gogh's Field with Irises near Arles. Part 2: pigment concentration maps. Color. Res. Appl. **43**(2), 158–176 (2018)

Klaassen, L., van der Snickt, G., Legrand, S., Higgitt, C., Spring, M., Vanmeert, F., et al.: Characterization and removal of a disfiguring oxalate crust on a large altarpiece by Hans Memling. In: Metal Soaps in Art, pp. 263–282. Springer, Cham (2019)

Kuhn, H.: Zinc white. In: Feller, R.L. (ed.) Artists' Pigments - A Handbook of Their History and Characteristics, vol. 1. Archetype Publications, London (1985)

Lachmann, T., van der Snickt, G., Haschke, M., Mantouvalou, I.: Combined 1D, 2D and 3D micro-XRF techniques for the analysis of illuminated manuscripts. J. Anal. At. Spectrom. **31**(10), 1989–1997 (2016)

Laclavetine, K., Ager, F.J., Arquillo, J., Respaldiza, M.A., Scrivano, S.: Characterization of the new mobile confocal micro X-ray fluorescence (CXRF) system for in situ non-destructive cultural heritage analysis at the CNA: mu XRF-CONCHA. Microchem. J. **125**, 62–68 (2016)

Lahanier, C., Amsel, G., Heitz, C., Menu, M., Andersen, H.H.: Proceedings of the international workshop on ion-beam analysis in the arts and archaeology - Pont-A-Mousson, Abbaye Des Premontres, France, February 18–20, 1985 - editorial. Nucl. Instrum. Methods Phys. Res. B. **14**(1), R7–R8 (1986)

Legrand, S., Ricciardi, P., Nodari, L., Janssens, K.: Non-invasive analysis of a 15th century illuminated manuscript fragment: point-based vs imaging spectroscopy. Microchem. J. **138**, 162–172 (2018)

Legrand, S., Van der Snickt, G., Cagno, S., Caen, J., Janssens, K.: MA-XRF imaging as a tool to characterize the 16th century heraldic stained-glass panels in Ghent Saint Bavo Cathedral. J. Cult. Herit. **40**, 163–168 (2019)

Lengeler, B., Schroer, C.G., Benner, B., Gerhardus, A., Gunzler, T.F., Kuhlmann, M., et al.: Parabolic refractive X-ray lenses. J. Synchrotron Radiat. **9**, 119–124 (2002)

Leon, Y., Sciau, P., Goudeau, P., Tamura, N., Webb, S., Mehta, A.: The nature of marbled Terra Sigillata slips: a combined μXRF and μXRD investigation. Appl. Phys. A Mater. Sci. Process. **99**(2), 419–425 (2010)

Leon, Y., Sciau, P., Passelac, M., Sanchez, C., Sablayrolles, R., Goudeau, P., et al.: Evolution of terra sigillata technology from Italy to Gaul through a multi-technique approach. J. Anal. At. Spectrom. **30**(3), 658–665 (2015)

Li, F.Z., Liu, Z.G., Sun, T.X., Yi, L.T., Zhao, W.G., He, J.L., et al.: Application of three dimensional confocal micro X-Ray fluorescence technology based on polycapillary X-ray lens in analysis of rock and mineral samples. Spectrosc. Spectr. Anal. **35**(9), 2487–2491 (2015)

Liu, Z., Mehta, A., Tamura, N., Pickard, D., Rong, B., Zhou, T., et al.: Influence of Taoism on the invention of the purple pigment used on the Qin terracotta warriors. J. Archaeol. Sci. **34**(11), 1878–1883 (2007)

Lombardo, T., Grolimund, D., Kienholz, A., Hubert, V., Wörle, M.: The use of flint-stone fragments as “fire-strikers” during the Neolithic period: complementary micro-analytical evidences. Microchem. J. **125**, 254–259 (2016)

Luhl, L., Mantouvalou, I., Schaumann, I., Vogt, C., Kanngiesser, B.: Three-dimensional chemical mapping with a confocal XRF setup. Anal. Chem. **85**(7), 3682–3689 (2013)

Lynch, P.A., Tamura, N., Lau, D., Madsen, I., Liang, D., Strohschnieder, M., et al.: Application of white-beam X-ray microdiffraction for the study of mineralogical phase identification in ancient Egyptian pigments. J. Appl. Crystallogr. **40**(6), 1089–1096 (2007)

Mantouvalou, I., Lange, K., Wolff, T., Grotzsch, D., Luhl, L., Haschke, M., et al.: A compact 3D micro X-ray fluorescence spectrometer with X-ray tube excitation for archaeometric applications. J. Anal. At. Spectrom. **25**(4), 554–561 (2010)

Mantouvalou, I., Malzer, W., Kanngiesser, B.: Quantification for 3D micro X-ray fluorescence. Spectrochim. Acta Part B At. Spectrosc. **77**, 9–18 (2012)

Mantouvalou, I., Wolff, T., Seim, C., Stoytschew, V., Malzer, W., Kanngiesser, B.: Reconstruction of confocal micro-X-ray fluorescence spectroscopy depth scans obtained with a laboratory setup. Anal. Chem. **86**(19), 9774–9780 (2014)

Martins, A., Albertson, C., McGlinchey, C., Dik, J.: Piet Mondrian's Broadway Boogie Woogie: non invasive analysis using macro X-ray fluorescence mapping (MA-XRF) and multivariate curve resolution-alternating least square (MCR-ALS). Herit Sci. **4**, 16 (2016a)

Martins, A.M.T., Coddington, J., Snickt, G.V.D., Driel, B.v., McGlinchey, C., Dahlberg, D., et al.: Jackson Pollock’s number 1A, 1948: a non-invasive study using macro-X-ray fluorescence mapping (MA-XRF) and multivariate curve resolution – alternating least squares (MCR-ALS) analysis. Herit Sci. **4** (2016b) in press

Mass, J.L., Woll, A.R., Ocon, N., Bisulca, C., Wazny, T., Griggs, C.B., et al.: Collaboration or appropriation? Examining a 17th c. panel by David Teniers the Younger and Jan Brueghel the Younger using confocal X-ray fluorescence microscopy. In: Vandiver, P.B., McCarthy, B., Tykot, R.H., RuvalcabaSil, J.L., Casadio, F. (eds.) Materials Issues in Art and Archaeology Viii. Materials Research Society Symposium Proceedings. 2008; 10472008

Meral, C., Jackson, M., Monteiro, P., Wenk, H. (eds.): Characterization of mineral assemblages in ancient Roman maritime concrete with synchrotron X-ray techniques. AGU Fall Meeting Abstracts; 2012

Miliani, C., Monico, L., Melo, M.J., Fantacci, S., Angelin, E.M., Romani, A., et al.: Photochemistry of artists’ dyes and pigments: towards better understanding and prevention of colour change in works of art. Angew. Chem. Int. Ed. **57**(25), 7324–7334 (2018)

Monico, L., Janssens, K.H., Miliani, C., Brunetti, B.G., Vagnini, M., Vanmeert, F., et al.: The degradation process of lead chromate in paintings by Vincent van Gogh studied by means of spectromicroscopic methods. Part III: Synthesis, characterization and detection of different crystal forms of the chrome yellow pigment. Anal. Chem. **85**(2), 851–859 (2013a)

Monico, L., Janssens, K.H., Miliani, C., Van der Snickt, G., Brunetti, B.G., Cestelli Guidi, M., et al.: The degradation process of lead chromate in paintings by Vincent van Gogh studied by means of spectromicroscopic methods. Part IV: Artificial ageing of model samples of co-precipitates of lead chromate and lead sulfate. Anal. Chem. **85**(2), 860–867 (2013b)

Monico, L., Janssens, K., Hendriks, E., Vanmeert, F., Van der Snickt, G., Cotte, M., et al.: Evidence for degradation of the chrome yellows in Van Gogh's sunflowers: a study using noninvasive in situ methods and synchrotron-radiation-based X-ray techniques. Angew. Chem., Int. Ed. **54**(47), 13923–13927 (2015a)

Monico, L., Janssens, K., Hendriks, E., Vanmeert, F., Van der Snickt, G., Cotte, M., et al.: Evidence for degradation of the chrome yellows in Van Gogh’s sunflowers: a study using noninvasive in situ methods and synchrotron-radiation-based X-ray techniques. Angew. Chem. **127**(47), 14129–14133 (2015b)

Monico, L., Chieli, A., De Meyer, S., Cotte, M., de Nolf, W., Falkenberg, G., et al.: Role of the relative humidity and the Cd/Zn stoichiometry in the photooxidation process of cadmium yellows (CdS/Cd1−xZnxS) in oil paintings. Chem. Eur. J. **24**(45), 11584–11593 (2018)

Monico, L., Sorace, L., Cotte, M., de Nolf, W., Janssens, K., Romani, A., et al.: Disclosing the binding medium effects and the pigment solubility in the (photo)reduction process of chrome yellows (PbCrO4/PbCr1-xSxO4). ACS Omega. **4**(4), 6607–6619 (2019)

Monico, L., Cartechini, L., Rosi, F., Chieli, A., Grazia, C., De Meyer, S., et al.: Probing the chemistry of CdS paints in The Scream by in situ noninvasive spectroscopies and synchrotron radiation x-ray techniques. Sci. Adv. **6**(20), 11 (2020)

Mürer, F.K., Sanchez, S., Álvarez-Murga, M., Di Michiel, M., Pfeiffer, F., Bech, M., et al.: 3D maps of mineral composition and hydroxyapatite orientation in fossil bone samples obtained by X-ray diffraction computed tomography. Sci. Rep. **8**(1), 10052 (2018)

Nakano, K., Tabe, A., Shimoyama, S., Tsuji, K.: Visualizing a black cat drawing hidden inside the painting by confocal micro-XRF analysis. Microchem. J. **126**, 496–500 (2016)

Nakazawa, T., Tsuji, K.: Development of a high-resolution confocal micro-XRF instrument equipped with a vacuum chamber. X-Ray Spectrom. **42**(5), 374–379 (2013)

Noble, P., van Loon, A., Alfeld, M., Janssens, K., Dik, J.: Rembrandt and/or Studio, Saul and David, c. 1655: visualising the curtain using cross-section analyses and X-ray fluorescence imaging. Technè. **36**, 35–45 (2012)

Otero, V., Vas Pinto, J., Carlyle, L., Vilarigues, M., Cotte, M., Melo, M.J.: 19th century chrome yellow and chrome deep from Winsor & Newton. M. A. Stud. Conserv. **62**(3), 123–149 (2017)

Otero, V., Vilarigues, M., Carlyle, L., Cotte, M., De Nolf, W., Melo, M.J.: A little key to oxalate formation in oil paints: protective patina or chemical reactor? Photochem. Photobiol. Sci. **17**(3), 266–270 (2018)

Polese, C., Cappuccio, G., Dabagov, S.B., Hampai, D., Liedl, A., Pace, E.: 2D and 3D micro-XRF based on polycapillary optics at XLab Frascati. In: Goto, S., Morawe, C., Khounsary, A.M. (eds.) Advances in X-Ray/Euv Optics and Components X. Proceedings of SPIE. 2015; 95882015

Porcier, S.M., Berruyer, C., Pasquali, S., Ikram, S., Berthet, D., Tafforeau, P.: Wild crocodile hunted to make mummies in Roman Egypt: evidence from synchrotron imaging. J. Archaeol. Sci. **110**, 105009 (2019)

Pouyet, E., Cotte, M., Fayard, B., Salomé, M., Meirer, F., Mehta, A., et al.: 2D X-ray and FTIR micro-analysis of the degradation of cadmium yellow pigment in paintings of Henri Matisse. Appl. Phys. A Mater. Sci. Process. **121**(3), 967 (2015)

Price, S.W., Van Loon, A., Keune, K., Parsons, A.D., Murray, C., Beale, A.M., et al.: Unravelling the spatial dependency of the complex solid-state chemistry of Pb in a paint micro-sample from Rembrandt's Homer using XRD-CT. Chem. Commun. (2019)

Rabin, I., Hahn, O.: Characterization of the Dead Sea Scrolls by advanced analytical techniques. Anal. Methods. **5**(18), 4648–4654 (2013)

Radepont, M., de Nolf, W., Janssens, K., Van der Snickt, G., Coquinot, Y., Klaassen, L., et al.: The use of microscopic X-ray diffraction for the study of HgS and its degradation products corderoite ([small alpha]-Hg3S2Cl2), kenhsuite ([gamma]-Hg3S2Cl2) and calomel (Hg2Cl2) in historical paintings. J. Anal. At. Spectrom. **26**(5), 959–968 (2011)

Ravaud, E., Pichon, L., Laval, E., Gonzalez, V., Eveno, M., Calligaro, T.: Development of a versatile XRF scanner for the elemental imaging of paintworks. Appl. Phys. A Mater. Sci. Process. **122**(1), 1 (2016)

Reiche, I., Mueller, K., Eveno, M., Itie, E., Menu, M.: Depth profiling reveals multiple paint layers of Louvre Renaissance paintingsusing non-invasive compact confocal micro-X-ray fluorescence. J. Anal. At. Spectrom. **27**, 1715–1724 (2012)

Reiche, I., Muller, K., Mysak, E., Eveno, M., Mottin, B.: Toward a three-dimensional vision of the different compositions and the stratigraphy of the painting L'Homme bless, by G. Courbet: coupling SEM-EDX and confocal micro-XRF. Appl. Phys. A Mater. Sci. Process. **121**(3), 903–913 (2015)

Ricciardi, P., Legrand, S., Bertolotti, G., Janssens, K.: Macro X-ray fluorescence (MA-XRF) scanning of illuminated manuscript fragments: potentialities and challenges. Microchem. J. **124**, 785–791 (2016)

Romano, F.P., Caliri, C., Nicotra, P., Di Martino, S., Pappalardo, L., Rizzo, F., et al.: Real-time elemental imaging of large dimension paintings with a novel mobile macro X-ray fluorescence (MA-XRF) scanning technique. J. Anal. At. Spectrom. **32**(4), 773–781 (2017)

Salvado, N., Pradell, T., Pantos, E., Papiz, M.Z., Molera, J., Seco, M., et al.: Identification of copper-based green pigments in Jaume Huguet's Gothic altarpieces by Fourier transform infrared microspectroscopy and synchrotron radiation X-ray diffraction. J. Synchrotron Radiat. **9**, 215–222 (2002)

Salvadó, N., Butí, S., Pantos, E., Bahrami, F., Labrador, A., Pradell, T.: The use of combined synchrotron radiation micro FT-IR and XRD for the characterization of Romanesque wall paintings. Appl. Phys. A Mater. Sci. Process. **90**(1), 67–73 (2008)

Salvadó, N., Butí, S., Nicholson, J., Emerich, H., Labrador, A., Pradell, T.: Identification of reaction compounds in micrometric layers from gothic paintings using combined SR-XRD and SR-FTIR. Talanta. **79**(2), 419–428 (2009)

Salvado, N., Buti, S., Labrador, A., Cinque, G., Emerich, H., Pradell, T.: SR-XRD and SR-FTIR study of the alteration of silver foils in medieval paintings. Anal. Bioanal. Chem. (2010)

Salvadó N, Butí S, Cotte M, Cinque G, Pradell T.: Shades of green in 15th century paintings: combined microanalysis of the materials using synchrotron radiation XRD, FTIR and XRF, Appl. Phys. A. 2013;111(1):47-57.

Salvadó, N., Butí, S., Aranda, M.A., Pradell, T.: New insights on blue pigments used in 15 th century paintings by synchrotron radiation-based micro-FTIR and XRD. Anal. Methods. **6**(11), 3610–3621 (2014)

Sarkar, S.S., Sahoo, P.K., Solak, H.H., David, C., Van der Veen, J.F.: Fabrication of Fresnel zone plates by holography in the extreme ultraviolet region. J. Vac. Sci. Technol. B. **26**(6), 2160–2163 (2008)

Schoonjans, T., Silversmit, G., Vekemans, B., Schmitz, S., Burghammer, M., Riekel, C., et al.: Fundamental parameter based quantification algorithm for confocal nano-X-ray fluorescence analysis. Spectrochim. Acta B At. Spectrosc. **67**, 32–42 (2012)

Schroer, C.G., Boye, P., Feldkamp, J.M., Patommel, J., Samberg, D., Schropp, A., et al.: Hard X-ray nanoprobe at beamline P06 at PETRA III. Nucl. Instrum. Methods. Phys. Res. A. **616**(2–3), 93–97 (2010)

Sciau, P., Goudeau, P., Tamura, N., Dooryhee, E.: Micro scanning X-ray diffraction study of Gallo-Roman Terra Sigillata ceramics. Appl. Phys. A Mater. Sci. Process. **83**(2), 219–224 (2006)

Simoen, J., De Meyer, S., Vanmeert, F., de Keyser, N., Avranovich, E., Van der Snickt, G., et al.: Combined micro- and macro scale X-ray powder diffraction mapping of degraded Orpiment paint in a 17th century still life painting by Martinus Nellius. Herit Sci. **7**(1), 12 (2019)

Smieska, L.M., Mullett, R., Ferri, L., Woll, A.R.: Trace elements in natural azurite pigments found in illuminated manuscript leaves investigated by synchrotron x-ray fluorescence and diffraction mapping. Appl. Phys. A Mater. Sci. Process. **123**(7), 484 (2017)

Smieska, L.M., Twilley, J., Woll, A.R., Schafer, M., DeGalan, A.M.: Energy-optimized synchrotron XRF mapping of an obscured painting beneath Exit from the Theater, attributed to Honoré Daumier. Microchem. J. **146**, 679–691 (2019)

Smit, Z., Janssens, K., Proost, K., Langus, I.: Confocal mu-XRF depth analysis of paint layers. Nucl. Instrum. Methods. Phys. Res. B. **219**, 35–40 (2004)

Smolek, S., Nakazawa, T., Tabe, A., Nakano, K., Tsuji, K., Streli, C., et al.: Comparison of two confocal micro-XRF spectrometers with different design aspects. X-Ray Spectrom. **43**(2), 93–101 (2014)

Struick van der Loeff, L., Alfeld, M., Meedendorp, T., Dik, J., Hendriks, E., van der Snickt, G., et al.: Rehabilitation of a flower still life in the Kröller-Müller Museum and a lost Antwerp painting by Van Gogh. In: van Tilborgh, L. (ed.) Van Gogh: New Findings Van Gogh Studies, vol. 4. Van Gogh Museum, Amsterdam, Amsterdam, Netherlands (2012)

Sun, T.X., Ding, X.L.: Confocal X-ray technology based on capillary X-ray optics. Rev. Anal. Chem. **34**(1–2), 45–59 (2015)

Sun, T.X., Liu, Z.G., Wang, G.F., Ma, Y.Z., Peng, S., Sun, W.Y., et al.: Application of confocal X-ray fluorescence micro-spectroscopy to the investigation of paint layers. Appl. Radiat. Isot. **94**, 109–112 (2014)

Thurrowgood, D., Paterson, D., De Jonge, M.D., Kirkham, R., Thurrowgood, S., Howard, D.L.: A hidden portrait by Edgar Degas. Sci. Rep. **6**, 29594 (2016)

Trentelman, K.: Analyzing the heterogeneous hierarchy of cultural heritage materials: analytical imaging. Annu. Rev. Anal. Chem. **10**(1), 247 (2017)

Trentelman, K., Bouchard, M., Ganio, M., Namowicz, C., Patterson, C.S., Walton, M.: The examination of works of art using in situ XRF line and area scans. X-Ray Spectrom. **39**(3), 159–166 (2010)

Trentelman, K., Janssens, K., van der Snickt, G., Szafran, Y., Woollett, A.T., Dik, J.: Rembrandt's An Old Man in Military Costume: the underlying image re-examined. Appl. Phys. A. **121**(3), 801–811 (2015)

Tsuji, K., Matsuno, T., Takimoto, Y., Yamanashi, M., Kometani, N., Sasaki, Y.C., et al.: New developments of X-ray fluorescence imaging techniques in laboratory. Spectrochim. Acta B Atomic Spectrosc. **113**, 43–53 (2015a)

Tsuji, K., Tabe, A., Wobrauscheck, P., Streli, C.: Secondary excitation process for quantitative confocal 3D-XRF analysis. Powder Diffract. **30**(2), 109–112 (2015b)

Valerio, P., Silva, R.J.C., Araujo, M.F., Soares, A.M.M., Barros, L.: A multianalytical approach to study the Phoenician bronze technology in the Iberian Peninsula – a view from Quinta do Almaraz. Mater. Charact. **67**, 74–82 (2012)

Van der Snickt, G., De Nolf, W., Vekemans, B., Janssens, K.: μ-XRF/μ-RS vs. SR μ-XRD for pigment identification in illuminated manuscripts. Appl. Phys. A Mater. Sci. Process. **92**(1), 59 (2008)

van der Snickt, G., Dik, J., Cotte, M., Janssens, K., Jaroszewicz, J., De Nolf, W., et al.: Characterization of a degraded cadmium yellow (CdS) pigment in an oil painting by means of synchrotron radiation based X-ray techniques. Anal. Chem. **81**, 2600–2610 (2009)

Van der Snickt, G., Janssens, K., Dik, J., De Nolf, W., Vanmeert, F., Jaroszewicz, J., et al.: Combined use of synchrotron radiation based micro-X-ray fluorescence, micro-X-ray diffraction, micro-X-ray absorption near-edge, and micro-fourier transform infrared spectroscopies for revealing an alternative degradation pathway of the pigment cadmium yellow in a painting by Van Gogh. Anal. Chem. **84**(23), 10221–10228 (2012)

Van der Snickt, G., Martins, A., Delaney, J., Janssens, K., Zeibel, J., Duffy, M., et al.: Exploring a hidden painting below the surface of Rene Magritte's Le Portrait. Appl. Spectrosc. **70**(1), 57–67 (2016)

Van der Snickt, G., Dubois, H., Sanyova, J., Legrand, S., Coudray, A., Glaude, C., et al.: Large-area elemental imaging reveals Van Eyck's original paint layers on the Ghent Altarpiece (1432), rescoping its conservation treatment. Angew. Chem. Int. Ed. **56**(17), 4797–4801 (2017)

Van der Snickt, G., Legrand, S., Slama, I., Van Zuien, E., Gruber, G., Van der Stighelen, K., et al.: In situ macro X-ray fluorescence (MA-XRF) scanning as a non-invasive tool to probe for subsurface modifications in paintings by PP Rubens. Microchem. J. **138**, 238–245 (2018)

Van Grieken, R., Markowicz, A.: Handbook of X-ray Spectrometry. Marcel Dekker, New York (2002)

van Loon, A., Noble, P., de Man, D., Alfeld, M., Callewaert, T., Van der Snickt, G., et al.: The role of smalt in complex pigment mixtures in Rembrandt'sHomer1663: combining MA-XRF imaging, microanalysis, paint reconstructions and OCT. Herit Sci. **8**(1), 19 (2020)

Vanmeert, F., Van der Snickt, G., Janssens, K.: Plumbonacrite identified by X-ray powder diffraction tomography as a missing link during degradation of red lead in a Van Gogh painting. Angew. Chem. **54**(12), 3678–3681 (2015)

Vanmeert, F., De Nolf, W., De Meyer, S., Dik, J., Janssens, K.: Macroscopic X-ray powder diffraction scanning, a new method for highly selective chemical imaging of works of art: instrument optimization. Anal. Chem. **90**(11), 6436–6444 (2018a)

Vanmeert, F., De Nolf, W., De Meyer, S., Dik, J., Janssens, K.: Macroscopic X-ray powder diffraction scanning: possibilities for quantitative and depth-selective parchment analysis. Anal. Chem. **90**(11), 6445–6452 (2018b)

Vanmeert, F., Hendriks, E., Van der Snickt, G., Monico, L., Dik, J., Janssens, K.: Highly-specific chemical mapping by macroscopic X-ray powder diffraction (MA-XRPD) of Van Gogh's sunflowers allows to identify areas with higher degradation risk. Angew. Chem. Int. Ed. **25**, 7418–7422 (2018c)

Vanmeert, F., de Keyser, N., Van Loon, A., Klaassen, L., Noble, P., Janssens, K.: Transmission and reflection mode macroscopic X-ray powder diffraction imaging for the noninvasive visualization of paint degradation in still life paintings by Jan Davidsz. de Heem. Anal. Chem. **91**(11), 7153–7161 (2019)

Vanwijnsberghe, D.: Around the Madeleine Renders. An Aspect of the History of Collections, Restoration and Counterfeiting in Belgium in the First Half of the Twentieth Century. Brussels, Royal Institute for Cultural Heritage, Brussels, Belgium (2008)

Vermeulen, M., Nuyts, G., Sanyova, J., Vila, A., Buti, D., Jussi-Peteri, S., et al.: Visualization of As(3+) and As(5+) distributions in degraded paint micro samples from a Baroque-era painting. J. Anal. At. Spectrom. (2016)

Vermeulen, M., Sanyova, J., Janssens, K., Nuyts, G., De Meyer, S., De Wael, K.: The darkening of copper- or lead-based pigments explained by a structural modification of natural orpiment: a spectroscopic and electrochemical study. J. Anal. At. Spectrom. **32**(7), 1331–1341 (2017)

Vermeulen, M., Janssens, K., Sanyova, J., Rahemi, V., McGlinchey, C., De Wael, K.: Assessing the stability of arsenic sulfide pigments and influence of the binding media on their degradation by means of spectroscopic and electrochemical techniques. Microchem. J. **138**, 82–91 (2018)

Verslype, I.: The restoration of *Woman in Blue Reading a Letter* by Johannes Vermeer. Rijksmus. Bull. **60**(1), 2–19 (2012)

Vincze, L., Janssens, K., Adams, F., Jones, K.W.: A general monte carlo simulation of energy-dispersive X-ray fluorescence spectrometers .3. Polarized polychromatic radiation, homogeneous samples. Spectrochim. Acta B Atom. Spectrosc. **50**(12), 1481–1500 (1995)

Vincze, L., Janssens, K., Adams, F., Rindby, A., Engstrom, P.: Interpretation of capillary generated spatial and angular distributions of x rays: theoretical modeling and experimental verification using the European Synchrotron Radiation Facility Optical beam line. Rev. Sci. Instrum. **69**(10), 3494–3503 (1998)

Vincze, L., Janssens, K., Vekemans, B., Adams, F.: Monte Carlo simulation of X-ray fluorescence spectra: Part 4. Photon scattering at high X-ray energies. Spectrochim. Acta B At. Spectrosc. **54**(12), 1711–1722 (1999)

Vincze, L., Somogyi, A., Osan, J., Vekemans, B., Torok, S., Janssens, K., et al.: Quantitative trace element analysis of individual fly ash particles by means of X-ray microfluorescence. Anal. Chem. **74**(5), 1128–+ (2002)

Vittiglio, G., Bichhneier, S., Klinger, P., Heckel, J., Fuzhong, W., Vincze, L., et al.: A compact mu-XRF spectrometer for (in situ) analyses of cultural heritage and forensic materials. Nucl. Instrum. Methods. Phys. Res. B. **213**, 693–698 (2004)

Wang, T., Zhu, T.Q., Feng, Z.Y., Fayard, B., Pouyet, E., Cotte, M., et al.: Synchrotron radiation-based multi-analytical approach for studying underglaze color: the microstructure of Chinese Qinghua blue decors (Ming dynasty). Anal. Chim. Acta. **928**, 20–31 (2016)

Welcomme, E., Walter, P., Bleuet, P., Hodeau, J.L., Dooryhee, E., Martinetto, P., et al.: Classification of lead white pigments using synchrotron radiation micro X-ray diffraction. Appl. Phys. A Mater. Sci. Process. **89**(4), 825–832 (2007)

Wolff, T., Rabin, I., Mantouvalou, I., Kanngiesser, B., Malzer, W., Kindzorra, E., et al.: Provenance studies on Dead Sea scrolls parchment by means of quantitative micro-XRF. Anal. Bioanal. Chem. **402**(4), 1493–1503 (2012)

Woll, A.R., Mass, J., Bisulca, C., Huang, R., Bilderback, D.H., Gruner, S., et al.: Development of confocal X-ray fluorescence (XRF) microscopy at the Cornell high energy synchrotron source. Appl. Phys. A. Mater. Sci. Process. **83**(2) (2006)

Woll, A.R., Mass, J., Bisulca, C., Cushi-Nan, M., Griggs, C., Wanzy, T., et al.: The unique history of the Armorer's Shop an application of confocal x-ray fluorescence microscopy. Stud. Conserv. **53**(2), 93–109 (2008)

Woll, A.R., Agyeman-Budu, D., Bilderback, D.H., Dale, D., Kazimirov, A.Y., Pfeifer, M., et al.: 3D x-ray fluorescence microscopy with 1.7 mu m resolution using lithographically fabricated micro-channel arrays. In: Goto, S., Morawe, C., Khounsary, A.M. (eds.) Advances in X-Ray/Euv Optics and Components Vii. Proceedings of SPIE. 2012; 85022012

Woll, A.R., Agyeman-Budu, D., Choudhury, S., Coulthard, I., Finnefrock, A.C., Gordon, R., et al.: Lithographically-fabricated channel arrays for confocal x-ray fluorescence microscopy and XAFS. In: Arp, U., Reversz, P., Williams, G.P. (eds.) 17th Pan-American Synchrotron Radiation Instrumentation Conference Sri2013. J. Phys. Conf. Ser. 2014; 4932014

Woll, A.R., Bilderback, D.H., Gruner, S., Gao, N., Huang, R., Bisulca, C., et al.: Confocal x-ray fluorescence (XRF) microscopy: a new technique for the nondestructive compositional depth profiling of paintings. In: Vandiver, P.B., Mass, J.L., Murray, A. (eds.) Materials Issues in Art and Archaeology VII. Materials Research Society Symposium Proceedings. 2005; 8522005

Wrobel, P., Czyzycki, M.: Direct deconvolution approach for depth profiling of element concentrations in multi-layered materials by confocal micro-beam X-ray fluorescence spectrometry. Talanta. **113**, 62–67 (2013)

Wrobel, P., Wegrzynek, D., Czyzycki, M., Lankosz, M.: Depth profiling of element concentrations in stratified materials by confocal microbeam X-ray fluorescence spectrometry with polychromatic excitation. Anal. Chem. **86**(22), 11275–11280 (2014)

Yagi, R., Tsuji, K.: Confocal micro-XRF analysis of light elements with Rh X-ray tube and its application for painted steel sheet. X-Ray Spectrom. **44**(3), 186–189 (2015)

Yi, L.T., Liu, Z.G., Wang, K., Lin, X., Chen, M., Peng, S.Q., et al.: Combining depth analysis with surface morphology analysis to analyse the prehistoric painted pottery from Majiayao Culture by confocal 3D-XRF. Appl. Phys. A Mater. Sci. Process. 2016;122(4)

Chapter 12
Microchemical Imaging of Oil Paint Composition and Degradation: State-of-the-Art and Future Prospects

Selwin Hageraats, Mathieu Thoury, Marine Cotte, Loïc Bertrand, Koen Janssens, and Katrien Keune

Abstract Oil paint is a dynamic system that undergoes chemical alteration on several time and length scales. At the short term, curing reactions are necessary for oil

S. Hageraats
Rijksmuseum Amsterdam, Conservation and Science, Amsterdam, The Netherlands

Université Paris-Saclay, CNRS, Ministère de la culture, UVSQ, MNHN, IPANEMA, Saint-Aubin, France

Van't Hoff Institute for Molecular Science, University of Amsterdam, Amsterdam, The Netherlands
e-mail: selwin.hageraats@wur.nl

M. Thoury
Université Paris-Saclay, CNRS, Ministère de la culture, UVSQ, MNHN, IPANEMA, Saint-Aubin, France
e-mail: mathieu.thoury@synchrotron-soleil.fr

M. Cotte
European Synchrotron Radiation Facility (ESRF), Experimental Division, Grenoble, France

Laboratoire d'Archéologie Moléculaire et Structurale, Sorbonne Université, CNRS, Paris, France
e-mail: marine.cotte@esrf.fr

L. Bertrand (✉)
Université Paris-Saclay, ENS Paris-Saclay, CNRS, PPSM, Gif-sur-Yvette, France
e-mail: loic.bertrand@ens-paris-saclay.fr

K. Janssens
AXES, Faculty of Science, University of Antwerp, Antwerp, Belgium
e-mail: koen.janssens@uantwerpen.be

K. Keune (✉)
Rijksmuseum Amsterdam, Conservation and Science, Amsterdam, The Netherlands

Van't Hoff Institute for Molecular Science, University of Amsterdam, Amsterdam, The Netherlands
e-mail: K.Keune@rijksmuseum.nl

M. P. Colombini et al. (eds.), *Analytical Chemistry for the Study of Paintings and the Detection of Forgeries*, Cultural Heritage Science,
https://doi.org/10.1007/978-3-030-86865-9_12

to dry properly. At longer time scales, a wide variety of other chemical processes can negatively affect the visual appearance or mechanical properties of historical artistic paint systems. The development of chemical imaging methods capable of covering length scales continuously from the millimetric to micro- or even nanoscale is key in understanding the chemical composition of a painting and the historical changes thereof. Such imaging methods can help in assessing to which extent the original painting's composition may have been modified by chemical degradation processes. Processes that occur in the highly heterogeneous mixtures of binders, pigments, additives, alteration products and possibly later repainting and restoration treatments. Establishing the precise biography of the painting contributes to evaluate its authenticity. New modalities and novel methods of microchemical imaging provide access to previously unexplored length scales, are capable of better differentiation between the various oil paint components (original composition or later addition), and allow performing faster analysis to produce higher definition images. In this review, we report on recent methodological developments and future prospects to determine oil paints composition using microchemical imaging at the micro- and nanoscale.

Keywords Imaging · Spectroscopy · Microscopy · Paint · Pigments

12.1 Introduction

For centuries, oil paint has been one of the most important artistic media. It was used as the medium of choice for some of the world's most recognized artworks, such as Leonardo da Vinci's *Mona Lisa*, Rembrandt's *The Night Watch*, and Vincent van Gogh's *Starry Night*. Despite their static appearance, oil paintings are in fact dynamic systems that undergo a wide variety of chemical changes. A fresh oil paint undergoes various chemical reactions, resulting in a dry and mechanically stable paint system. However, at longer time scales a multitude of chemical reactions take place that may (severely) deteriorate the painting's visual appearance or mechanical stability. Since these degradative processes are chemically complex and hard to predict, they pose a monumental challenge to art curators and conservators worldwide. By modifying the painting chemical composition, they may also impact the authentication evaluation which usually aims at identifying which materials were used, in which parts of the paintings, when applied and above all by whom (main artist, copyist, conservators, or even forgers!)

Past studies have shown that forgers have tried various strategies to speed up the drying of the oil paint, such as accelerated ageing conditions or the use of additives to create a hard paint film (Blumenroth et al. 2019; Breek and Froentjes 1975). Access to suitable analytical techniques and an understanding of the drying processes of oil paint are important factors in unravelling these frauds. The use of pigments that have come onto the market after the dating of the painting is a good marker for authenticity issues, but often the pallet of the painting is not

characteristic enough and needs further investigation into the material and its context (Craddock 2009; Sloggett 2019). Focusing on past conservation treatments, conservators are confronted with paint retouches which can be very difficult to distinguish from the original paint (Noble et al. 2018). Paint morphologies, trace elements, layer build-ups, degradation components and their distribution can help identify these later additions to the painting. In all cases, knowledge of various chemical alteration and degradation processes is needed to address authenticate specific sections of oil paintings, or oil paintings as a whole (Doménech-Carbó et al. 2012; Tanasa et al. 2020).

The most basic description of oil paint is that of a mixture of a drying oil binder (triacylglycerol with a high degree of polyunsaturated fatty acid chains) and one or more organic or inorganic pigments, mixed in a ratio such that it is *workable* by the artist. Upon application of the paint, the drying oil binder is exposed to oxygen and the double bonds of the unsaturated fatty acids start to undergo autoxidation and form cross-links (van den Berg et al. 1999). This process is called the *curing* of the oil paint and eventually leads to a 3D-polymerized network that holds the pigment particles in place. As the curing process tends to take multiple days or even weeks, driers or other additives may be added to speed up the solidification of the oil paint.

On a longer timescale, the ongoing autoxidation and hydrolysis start to break down the polymerized oil binder network to form carboxylic acids—either still covalently bonded to the oil network or present as free or metal-bound dicarboxylic or monocarboxylic fatty acids. Previous studies have shown that—for a mature oil paint—the degree of carboxylic acid formation due to autoxidation is in the order of one acid group per triacylglycerol, while hydrolysis increases the free fraction of saturated fatty acids from less than 1% for fresh oils to over 90% for some historical oil paints (Baij et al. 2019; van den Berg et al. 1999). Like the binding medium, many pigments also undergo certain alteration and degradation processes. Some pigments react with saturated free fatty acids to form metal soaps (Heeren et al. 1999; Van der Weerd et al. 2004). Although this process is not necessarily disadvantageous for an oil paint (Cotte et al. 2017a), in some cases, the metal soaps agglomerate, forming brittle domains that may occupy a larger volume than the separate starting materials. In such cases, metal soap formation has been shown to lead to conservation issues such as paint layer delamination and the formation of protrusions (Ebert et al. 2011; Heeren et al. 1999; Keune and Boon 2007; Van Loon et al. 2019; Noble et al. 2002; Osmond et al. 2013; Van der Weerd et al. 2004). Another phenomenon that affects many oil paintings is the light-induced transformation of pigments into polymorphs or oxidation products (Van Der Snickt et al. 2009; Trentelman et al. 1996). As these polymorphs and oxidation products may have a different color than the original pigment material, these processes can lead to discoloration of the painting over time and therefore loss of the original artistic intention.

Aged oil paint leads to the formation of systems that are chemically complex and spatially highly heterogeneous. This heterogeneity shows up on multiple length scales: both in the plane of the painting as well as in-depth, due to the multi-layered build-up of oil paintings. A paint stratigraphy typically consists of several

chemically distinct paint layers, each 10–100 μm thick, containing pigment particles with dimensions of about 0.05–10 μm that are embedded in a medium of organic binder and various micrometric and submicrometric domains of organic and inorganic alteration and degradation products. The existence of these various distinct scales of chemical heterogeneity means that information on composition and degradation processes can also be found on various length scales, ranging from tens of micrometers to nanometers. Given these length scales, there is a strong interest in analyses using high-resolution microchemical imaging (techniques hereafter denoted with the prefix μ, e.g., μ-XRF). Due to the multiscale nature of oil paints, the scale of analysis needs to be chosen such that relevant details can be spatially resolved while the total sampled area (or volume) provides a representative chemical overview.

For the purpose of performing microchemical analysis on oil paints, microsamples can sometimes be obtained from historical works of art. Microsamples typically have dimensions in the order of a few hundred micrometers and are mostly taken by conservators from small pre-existing cracks, other surface damages, or from the edge, so as not to leave any marks that can be distinguished by the naked eye. An alternative and complementary approach is to mimic oil paint composition and degradation phenomena by ageing (naturally or artificially) paint mock-ups. This approach allows to control the type and extent of ageing, paint composition, and has less strict limitations when it comes to sampling, but may not always accurately represent the chemistry that occurs in actual historical works of art.

What measurement modality will be applied for the study of either a historical microsample or a sample obtained from a paint mock-up strongly depends on the specific chemical question. For instance, an investigation of oxidative discoloration of an inorganic pigment may require that a measurement can provide reliable chemical contrast between the different oxidation states of the affected element, while a study of delamination in saponified zinc white (ZnO) paints requires a measurement that can provide chemical contrast between metal carboxylates and one or more of the organic and inorganic reactants. If the migration of a reactant or a degradation product is of interest, it may be insightful to resolve chemical distributions throughout one or multiple paint layers, directly around the pigment, or in the vicinity of a possible catalytically active compound. Depending on what distribution is being studied, a spatial resolution may be required in the order of tens of micrometers (multilayer gradients), a few micrometers (gradients within layers), or tens to hundreds of nanometers (distributions around pigment particles or particles of possibly catalytically active compounds). The study of all the various aspects of oil paint degradation requires an extensive methodological toolbox with a wide variety of contrasting mechanisms and the ability to perform analysis at multiple length scales. Due to the complexity of oil paints and their degradation phenomena, answering chemical questions typically requires the use of multiple methods from this toolbox.

Over the past few decades, rapid advances have been made in the development of spectroscopic, spectrometric, and diffraction tools that are capable of characterizing and identifying organic and inorganic compounds in terms of molecular

fragments, functional groups, elemental composition, coordination chemistry, defect chemistry, crystalline structure, and physical texture. Developments in focusing optics and sources for mid-IR to hard X-ray photons and charged particles have led to the availability of microanalytical tools that can perform these chemical characterizations and identifications on the micro- or even nanoscale. As the various developments progress, the time necessary to perform chemical microanalysis at single points decreases further and further. Reduced measurement times have made it possible to implement almost all spectroscopic, spectrometric and diffraction modalities as microchemical imaging tools; allowing to resolve—in two or even three dimensions—the spatial distributions of specific chemical species at micrometric or nanometric spatial resolution. Microchemical imaging is therefore particularly useful for detecting trends and patterns in chemical distributions, which can inform on the underlying chemistry of migration and degradation processes. Especially for the study of systems that are as chemically complex and spatially heterogeneous as oil paints, such trends and patterns may only be detected through the analysis of many spatial points and the use of some form of microchemical imaging is essential to collect the required information.

The first part of this chapter will review the state-of-the-art applications of microchemical imaging methodologies to the study of oil paint composition and degradation. As there may be some ambiguity with regards to the term *microchemical imaging*, in this review it is defined as any technique that can probe compound-specific spectroscopic transitions, diffraction patterns, or mass fragments, and resolve their distributions at a sub-10 μm lateral resolution over a certain area or volume of interest. The following four sections will discuss recent advances in microchemical imaging instrumentation, covering optics, detectors, and light sources, and go over what types of chemical information can be obtained and at what length scales analysis can currently be performed. This review is structured along the working principles of the discussed analytical tools; separating infrared-, UV-Vis-, X-ray-, and charged particle-based methods. The second part of this chapter will critically discuss the capabilities and limitations of the current methodological toolbox and formulate perspectives on future research endeavors in oil paint studies. Such perspectives are illustrated by identifying four general research objectives that address the technological limitations of the microchemical imaging techniques reviewed previously: improved retrieval of spatial information, improved retrieval of chemical information, addressing the limited statistical relevance of analysis on paint microsamples, and integration of computational methods in the processing of microchemical data.

12.2 Infrared-based Methods

Starting at the lower-end of the energy range, infrared-based analysis is primarily used for the characterization of the organic phase of paint systems. Especially in the mid-infrared (mid-IR) range (2.5–25 μm, 400–4000 cm^{-1}), most functional groups

exhibit fundamental vibrational modes. Since each fundamental mode has a narrow corresponding absorption feature, mid-IR absorption spectroscopy has a very high chemical specificity. This property has made mid-IR spectroscopy one of the most widely applied methods for the study of oil paint degradation. In the wider context of paint analysis, mid-IR spectroscopy has been used extensively to identify and analyze pigments, additives, binding medium (Meilunas et al. 1990; Shearer et al. 1983), metal carboxylates (Cotte et al. 2007; Gabrieli et al. 2017; Henderson et al. 2019; Keune and Boon 2007; Mass et al. 2013a; Mazzeo et al. 2008; Noble et al. 2002; Osmond 2014; Osmond et al. 2012; Pouyet et al. 2015; Romano et al. 2020; Van der Weerd et al. 2004), as well as environmentally-induced inorganic pigment degradation products (Mass et al. 2013a; Pouyet et al. 2015). Here, we will cover the state-of-the-art of two approaches to microscale mid-IR analysis of oil paints: μ-FTIR and AFM-IR.

12.2.1 μ-FTIR

A detailed description of the μ-FTIR technique and its various measuring modalities can be found in ref. (Salzer and Siesler 2009).

Fourier-transform infrared microscopy (μ-FTIR) is a technique in which an FTIR spectrometer is coupled to a microscope so as to obtain full mid-IR absorption spectra either on single points (using a single-element detector) or on many points at once (using array detectors). Although the high chemical specificity and sensitivity to the organic phase makes μ-FTIR a suitable technique for studies of oil paint degradation, its use of mid-IR radiation inherently comes with restrictions in terms of spatial resolution. Even in the most ideal optical set-up, the spatial resolution of conventional far-field μ-FTIR is limited by the diffraction limit according to:

$$d = \frac{0.61\lambda}{NA} \tag{12.1}$$

Where d is the minimum distance between adjacent features where both features can still be resolved, λ is the wavelength of the used electromagnetic radiation, and NA is the numerical aperture of the optical system. In transmission μ-FTIR experiment, lenses with numerical apertures of 0.3–0.8 are most common, meaning features smaller than 10 μm can typically not be resolved. Obviously, for oil paint samples with a characteristically high degree of heterogeneity, this puts significant limits on the types of phenomena that can be studied.

As a means to improve the applicability of μ-FTIR for studies of oil paint composition and degradation, one instrumental development has gained particular popularity. Attenuated total reflectance (ATR) is a measurement geometry that is somewhat comparable to specular reflectance (see Fig. 12.1), but makes use of a high refractive index crystal that is pressed onto the sample. Rather than reflecting

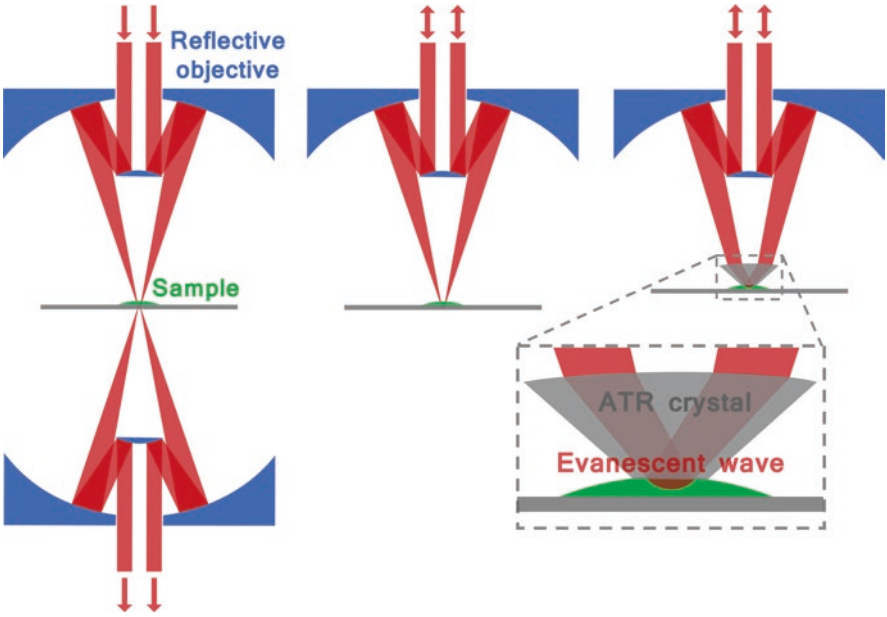

Fig. 12.1 The three common measurement geometries in μ-FTIR using a conventional (reflection) Schwarzschild objective. From left to right: transmission, specular reflectance and ATR. The red arrows indicate the direction of the mid-IR beam

directly on the sample surface, the mid-IR beam reflects internally on the crystal surface pressed onto the sample. In the process of reflecting internally on the crystal-sample interface, parts of the electromagnetic wave penetrate several micrometers into the sample (known as an evanescent wave). The reflected light will therefore be partially absorbed by the sample, as would be the case in a specular reflectance geometry. As an ATR crystal, germanium is typically used. Besides being IR-transparent, germanium possesses a refractive index of around 4.0 in the mid-IR spectral range. Due to the proportionality between numerical aperture and refractive index, substantial improvements can be made in terms of spatial resolution. Although this value depends on the wavelength, detector, and other optics used in the set-up, the spatial resolution of μ-ATR-FTIR with a germanium ATR crystal is thought to be in the order of several μm.

Two of the earliest applications of μ-ATR-FTIR for microchemical studies of oil paint were reported by Spring et al. (2008) and Mazzeo et al. (2007). Both on historical cross-sections and model samples they show the ability to identify and map various metal carboxylate species. More recently, Gabrieli et al. (2017) showed how μ-ATR-FTIR allows to resolve the morphology of zinc soap agglomerates and their formation relative to particles of the jellifying agent aluminum stearate. Maps of ionomeric zinc carboxylates, zinc soaps, aluminum stearate, and corresponding FTIR spectra are shown in Fig. 12.2.

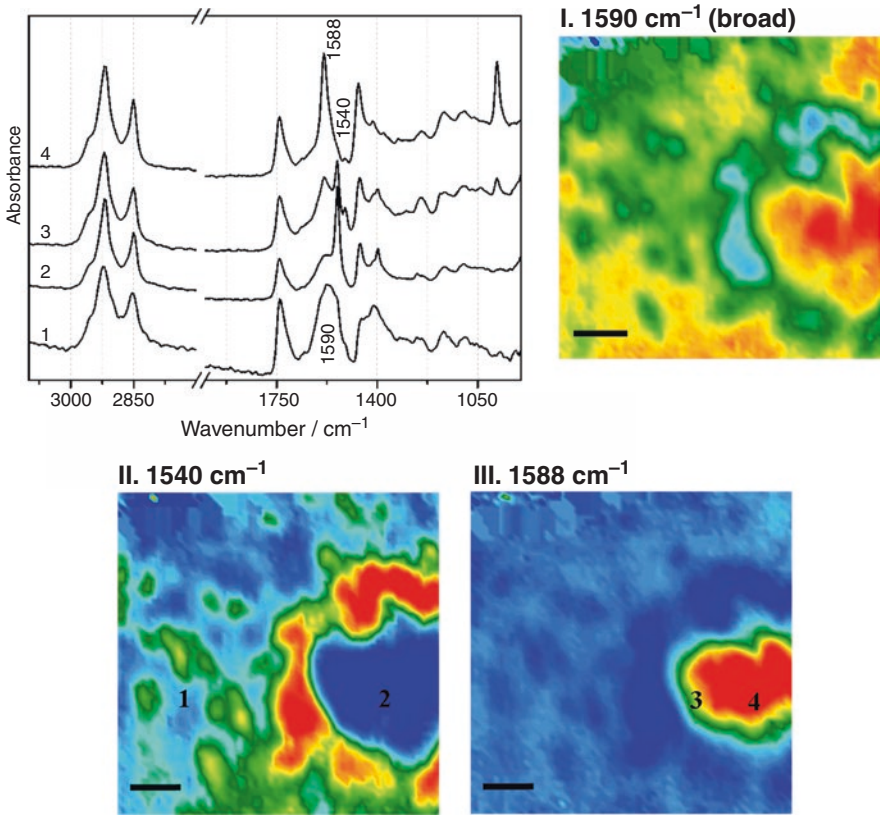

Fig. 12.2 μ-FTIR data recorded in ATR geometry on a sample obtained from Jackson Pollock's *Alchemy*. The four FTIR spectra were recorded on locations indicated by numbers 1–4 in the heat-maps, representing the distributions of ionomeric zinc carboxylates (1590 cm^{-1} broad), crystalline zinc carboxylates (1540 cm^{-1}), and aluminum stearate (1588 cm^{-1}). The black scale bars correspond to 10 μm. Reprinted with permission from ref. (Gabrieli et al. 2017)

For studies in which a high signal-to-noise ratio (SNR) is of primary concern, the use of synchrotron-generated IR beams is a development that has gained particular attention the last 10–15 years. Although mid-IR synchrotron beams are not necessarily brighter than the regular Globar IR sources, their low divergence make that the actual photon flux delivered to the focal volume is substantially higher (Cotte et al. 2007). While the most significant benefits are obtained when working in a confocal configuration with diffraction-limit-sized apertures and single-element mercury cadmium telluride (MCT) detectors (Cotte et al. 2007; Levenson et al. 2006; Osmond 2014; Osmond et al. 2012; Pouyet et al. 2015; Schiering et al. 2000), synchrotron radiation has also been used as an IR source for studies of oil paint degradation in external reflection and transmission geometries (see Fig. 12.1) using 2D focal plane array (FPA) detectors (Henderson et al. 2019; Kidder et al. 1997; Mass et al. 2013a).

Another development in the use of μ-FTIR applied to studies of oil paint is the use of chemical derivatization of the sample surface to separate otherwise overlapping absorption features. This approach was first reported in the context of degraded oil paint by Zumbühl et al. (Zumbühl et al. 2014), who demonstrate how exposure of polished cross-sections to gaseous sulfur tetrafluoride (SF_4) can for instance help in distinguishing absorption features coming from non-hydrolyzed triglyceride esters with those coming from free fatty acids and metal carboxylates. In addition, it has been shown that differences in the sensitivity of different metal carboxylates to SF_4 exposure allows to readily differentiate metal oxalates from other metal carboxylate species.

12.2.2 AFM-IR

A detailed description of the AFM-IR technique can be found in ref. (Dazzi et al. 2005), *while a schematic illustration of the technique is shown in Fig. 12.3.*

A lot of methodological research has been conducted over the years to combine the powerful capabilities of mid-IR microspectroscopy with the ability to perform analysis on length scales smaller than the diffraction limit. A near-field approach that couples atomic force microscopy with mid-IR absorption spectroscopy (AFM-IR) has been demonstrated to be especially powerful (Dazzi et al. 2005; Dazzi and Prater 2017). AFM-IR makes use of an AFM cantilever to probe local thermal expansion induced by a pulsed mid-infrared laser (see Fig. 12.3). Due to the

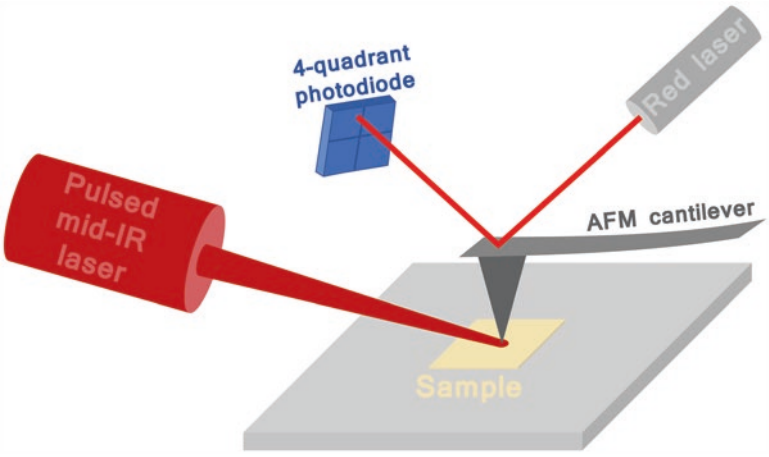

Fig. 12.3 Schematic representation of the AFM-IR technique. A pulsed mid-IR laser is focused onto the sample and directed to coincide with the apex of the AFM cantilever. Absorption of mid-IR pulses by the sample induces transient or resonant oscillations of the AFM cantilever that are monitored by the deflection of a red laser

nanometric radius of the apex of the AFM cantilever, field exaltation induced by the tip, and the fast dissipation of thermal energy induced by the laser pulses, lateral resolutions in the order of several tens of nanometers can readily be obtained.

Two studies have been published so far that involve the use of AFM-IR for the study of oil paints. Morsch et al. (2017) demonstrate how AFM-IR can inform on the photocatalytic activity of titanium white (TiO_2), showing that radical oxygenation of the oil binder is induced in the direct vicinity of nanometric TiO_2 pigment crystallites. Ma et al. (2019) studied the effects of aluminum stearate on the formation of zinc soaps in naturally aged paint-outs. Resolving the distributions of zinc carboxylates around a micrometric aluminum stearate agglomerate informs on how it acts as a local source of free fatty acids, hereby fostering the growth of zinc stearate crystallites.

As Ma et al. studied the same systems as Gabrieli et al. (2017), but used AFM-IR instead of μ-FTIR, it is interesting to note the different types of information that can be obtained at different length scales. A false-color image showing the distribution of crystalline zinc soaps and glycerol esters around an aluminum stearate agglomerate is shown in Fig. 12.4. It is clear from resolving the zinc soap distributions at the nanoscale that the formation of zinc soap crystallites at the rim of the aluminum stearate mass only constitutes a small fraction of all saponification. Moreover, it can be seen that the distribution of the zinc soap crystallites does not exhibit a clear (anti-) correlation with the distribution of non-hydrolyzed triglyceride esters. Both observations imply an important role for the diffusion of free fatty acids in the saponification of oil paints; something that could not be concluded from the distributions resolved at micrometric resolution (Fig. 12.2). On the other hand, the very small field of view of the AFM-IR maps means that certain trends and patterns cannot be observed. Whereas it is clear from Fig. 12.2 that in the *Alchemy* sample zinc soap formation is fostered as much as 20 μm away from the aluminum stearate

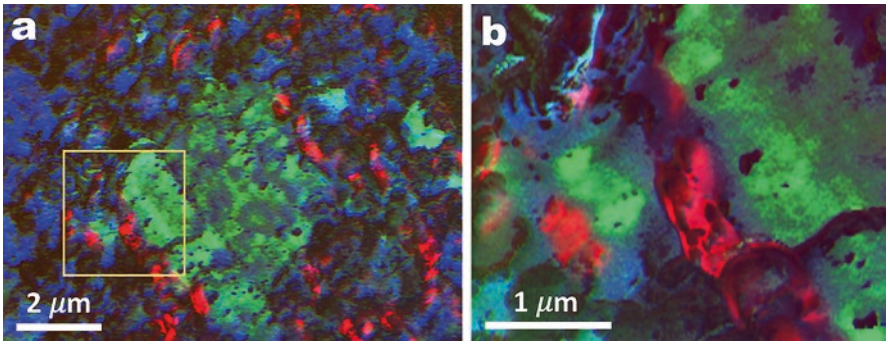

Fig. 12.4 False-color AFM-IR images obtained on a thin section of a naturally aged titanium white/zinc white paint-out. Colors were assigned as follows: crystalline zinc carboxylates (1540 cm^{-1}, red), ionomeric zinc carboxylates plus aluminum stearate (1590 cm^{-1}, green), glycerol esters (1742 cm^{-1}, blue). The yellow rectangle on the left indicates where the high-resolution map on the right was recorded. Reprinted from (Ma et al. 2019)

mass, but not beyond, the occurrence of this phenomenon in the naturally aged paint-outs could not be confirmed due to the much smaller scale of analysis.

It is important to note that AFM-IR is still heavily under development, with different instrumental approaches rapidly succeeding one another. Comparing the two examples mentioned in the previous paragraph, the approach taken by Morsch et al. involves an optical parametric oscillator (OPO) light source pulsed at 1 kHz, which induces a transient resonance in the AFM cantilever, while Ma et al. operate the AFM-IR with a high-frequency heterodyne detection scheme and a quantum cascade laser (QCL) light source (Dazzi et al. 2015). Moreover, Morsch et al. report the operation of the AFM in contact mode, working on paint films cut straight from the substrate, while Ma et al. operate in tapping mode, working on samples cut with an ultramicrotome to a thickness of around 200 nm. Although high-frequency heterodyne detection and samples prepared as thin sections are thought to provide significant benefit in terms of measurement speed and spatial resolution, a lot remains as of yet unknown about the exact effects of these parameters on the analysis of degraded paint samples.

12.3 Methods Based on UV and Visible Light

Moving up in energy from the infrared, one reaches the visible and UV regions of the electromagnetic spectrum. In this particular spectral region, two spectroscopic principles have been most widely applied in studies of oil paint: Raman scattering and photoluminescence (PL).

12.3.1 PL Microimaging

More detailed descriptions of the various aspects of PL microspectroscopy and microimaging specifically applied to cultural heritage samples can be found in refs. (Thoury et al. 2011, Nevin et al. 2014)

PL is a process in which a compound absorbs a photon of a given energy (excitation) and then emits a photon of a lower energy (emission). Although the macroscopic use of PL for the study of heritage objects has been reported as far back as the late 1920s and early 1930s (Rorimer 1929, 1931), it has only been over the last 10 years that a wide range of PL-based methods have started to become widely used as microanalytical tools for studies of oil paint degradation. In most common modern PL microimaging set-ups, a sample area of interest is illuminated with a defocused UV beam, the emitted PL is magnified by an optical objective, and full-field images are captured through one or more emission bandpass filters. This multispectral approach has become commonplace, because PL emission spectra of most materials of interest exhibit relatively broad bands that can often be selectively

imaged even with relatively broad emission bandpass filters (see Fig. 12.5). Due to the use of visible and UV photons, PL microimaging has the ability to routinely achieve submicrometric spatial resolutions. Chemical specificity can be achieved along no less than three dimensions (absorption wavelength, emission wavelength, and emission lifetime).

Two research themes have particularly benefited from the contribution of microchemical imaging by PL: the study of semiconductor pigments and that of metal soap formation. Semiconductor pigments are often brightly luminescing under suitable excitation and exhibit emission properties informative both about their characteristic band gap and intrinsic crystal defects. The hypothesized relation between crystal defects and the (photo-) catalytic activity of semiconductor pigments such as zinc white and cadmium yellow (CdS) make the identification of these defects of especially high interest in the context of oil paint degradation (Comelli et al. 2019; Drouilly et al. 2013; French et al. 2001; Hageraats et al. 2019b; Kurtz et al. 2005). As was discussed in Sect. 12.2.2, metal soap formation is usually studied using techniques based on absorption in the mid-IR, where metal carboxylates have

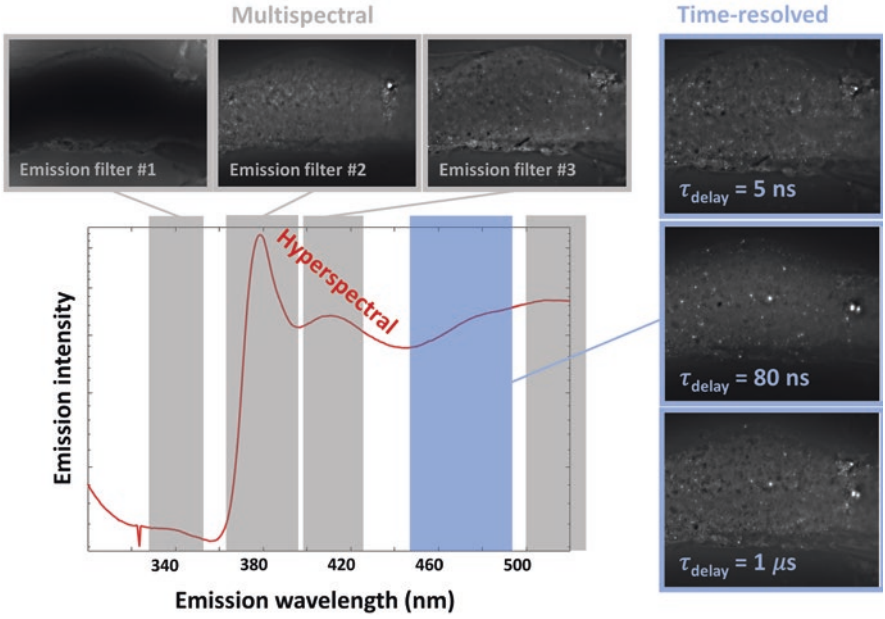

Fig. 12.5 Schematic representation of the three main approaches to PL microanalysis. The bottom left shows a high-resolution emission spectrum retrieved from a hyperspectral map recorded on a zinc white oil paint microsample that was excited at 280 nm. The figures shown in grey frames represent full-field images recorded through emission band pass filters of which the spectral ranges are indicated in the full emission spectrum with grey rectangles. The figures shown in blue frames represent full-field images taken through one emission bandpass filter at different time delays. NB: PL images are for illustration purposes only and have not necessarily been obtained using the indicated parameters

multiple distinct and characteristic absorption features. However, due to the intrinsically limited spatial resolution of conventional μ-FTIR, there is significant interest to complement μ-FTIR observations of metal soaps with PL microimaging, which works with ultraviolet and visible light and can therefore produce images at submicrometric spatial resolution.

Notable recent additions to the PL microimaging toolbox include methods based on excitation in the deep-UV regime (deep-UV PL) and methods based on resolving the emission dynamics over time (time-resolved PL, see Fig. 12.5). Deep-UV excited PL microspectroscopy and microimaging have been shown particularly useful for studies of the brightly luminescing semiconductor pigment zinc white and its zinc carboxylate alteration products. With its characteristic band gap emission centered around 380 nm and the various defect-related emissions at longer wavelengths (Bertrand et al. 2013a; Zhang et al. 2019), the PL-based study of degraded zinc white oil paints has been shown to benefit from excitation around 280 nm. As zinc white does not luminescence at energies higher than its bandgap, excitation at 280 nm opens up a significant spectral region (280–380 nm) without spectral interference from the brightly luminescing zinc white pigment. To illustrate this principle, Fig. 12.5 shows the average PL emission spectrum of a degraded zinc white oil paint microsample, recorded with an excitation energy of 280 nm. Whereas the spectral region above 380 nm is dominated by zinc white emission, the spectrum shows a clear low-intensity emission band around 340 nm which is thought to be emitted by crystalline zinc soaps (Hageraats et al. 2019a; Van Loon et al. 2019; Thoury et al. 2019). According to a previous evaluation of the optical system used in these studies, this method provides chemically specific analysis of zinc white degradation products close to the diffraction limit of about 150 nm (Bertrand et al. 2013a).

Particularly interesting results have been reported using time-resolved PL microspectroscopy and microimaging (also known as fluorescence lifetime imaging or FLIM) to study of the semiconductor pigments cadmium yellow and zinc white. Besides differing in emission wavelength, band gap and defect-related emissions can also be distinguished based on their emission lifetime, with band gap emission typically occurring in the ps or ns regime, and defect-related emission typically occurring in the μs regime. This principle has been exploited by Comelli et al. (2017) and Artesani et al. (2019) in studies combining multispectral PL microimaging with time-gated detection to aid the identification of pigments in chemically complex historical samples. It has been shown that the measurement of PL lifetimes can inform on the chemical interaction of the reactive pigment with the organic binding medium (Artesani et al. 2017, 2018). However, the retrieval of such information in the context of a microchemical imaging study has not yet been reported.

12.3.2 Raman Microspectroscopy

A more detailed account of Raman (micro-)spectroscopy applied to studies of oil paint degradation and authentication can be found in Chap. 13. This section therefore presents only a concise summary of the technique and its applications in microscopic studies of oil paint degradation.

Raman scattering is an inelastic scattering phenomenon in which a scattered visible or near-IR photon loses an amount of energy corresponding to a vibrational transition in the scattering molecule. Following this principle, Raman scattering (like mid-IR absorption) can therefore be used to probe vibrational transitions. Raman spectroscopy experiments are performed by focusing a laser (with a wavelength of typically 500–800 nm) onto the sample and recording a high-resolution spectrum of the scattered light (Opilik et al. 2013). Besides an elastic scattering peak and possible broad luminescence bands, Raman spectra contain a series of narrow peaks with a small energy offset relative to the laser energy. The offset of each peak then corresponds to the energies of certain vibrational transitions that are expressed in terms of a Raman shift.

Within studies of oil paint, Raman scattering has mostly been applied in microspectroscopy experiments where only one or several spatial points are analyzed (Chen-Wiegart et al. 2017; Higuchi et al. 1997; Keune et al. 2013; Mahon et al. 2020; Monico et al. 2011, 2013, 2014; Otero et al. 2014; Spring and Grout 2002; Trentelman et al. 1996). In some studies, where resolving spatial distributions is of crucial importance, raster scans are performed (Cato et al. 2017; Lau et al. 2008; Monico et al. 2015b, 2020a; Ropret et al. 2010). This yields hyperspectral Raman spectroscopy maps with micrometric spatial resolution, from which specific features can be integrated to obtain chemically specific distribution images on the microscale. Monico et al. (2015b, 2020a) show how this approach can be used to map out different types of chrome yellows and to detect poorly crystalline, hexagonal CdS and some of its degradation products. Cato et al. (2017) show how mapping a specific vibration of the blue $S^{\bullet}_{3}{}^{-}$ radical anion chromophore over an ultramarine oil paint surface reveals a local decrease in the chromophore concentration in optically altered regions: implying that the oxidation of sulfur chromophores may have caused ultramarine discoloration.

12.4 Methods Based on X-Rays

The X-ray regime is very broad in terms of energy range and provides a variety of analytical methods to study oil paint degradation. Photons on the lower end of this energy range—spanning roughly from 100 eV to 1 keV—are collectively referred to as soft X-rays, while photons on the upper end of the energy range (>5 keV) are typically referred to as hard X-rays. The intermediate range (1–5 keV) is sometimes colloquially called the tender X-ray regime. Applications in each energy range

largely depend on the penetration depth in the sample of interest. Generally speaking, the higher the X-ray photon energy, the greater the attenuation depth, and the heavier the element, the shorter the attenuation depth.

All the X-ray based studies reviewed in this following section were conducted at synchrotron facilities. Synchrotron-based light sources offer low-divergence beams of an extremely high brightness that can be over 10 orders of magnitude greater than that of conventional X-ray tube sources. These properties make them particularly suitable for use with tunable monochromators and focusing optics. Although the high energy (and therefore short wavelength) of X-rays makes that the diffraction limit at most energies is subnanometric, their focusing is generally technically challenging due to the small difference in refractive index between air (or vacuum) and condensed matter and the very small critical angle for total external reflection (Ice et al. 2011). Still, a number of techniques were developed over the years that address these physical limitations in different ways. The four most commonly applied focusing optics for microscopic X-ray experiments are Kirkpatrick-Baez (KB) mirrors (Kirkpatrick and Baez 1948), Fresnel zone plates (FZP) (Rösner et al. 2018), compound refractive lenses (CRL), and X-ray capillary optics (illustrated in Fig. 12.6). Depending on the type of optics, design, X-ray energy, and beam divergence of the beamline, beam diameters can be obtained in the order of tens of micrometers (capillary optics) down to several nanometers (FZP).

A detailed review of X-ray focusing optics can be found in ref. (Ice et al. 2011), *while an overview of applications of synchrotron techniques for the study of ancient materials can be found in ref.* (Bertrand et al. 2012).

For microchemical imaging applications, X-rays are primarily used to probe core-level transitions and to perform crystal diffraction. Probing core-level transitions, chemically-specific information can be obtained by making use of either of two dependencies: the element-dependency of core-level transition energies, or the dependency of the density-of-states (DOS) of core-level transitions to the oxidation state and to the coordination environment of the target atom. X-ray fluorescence

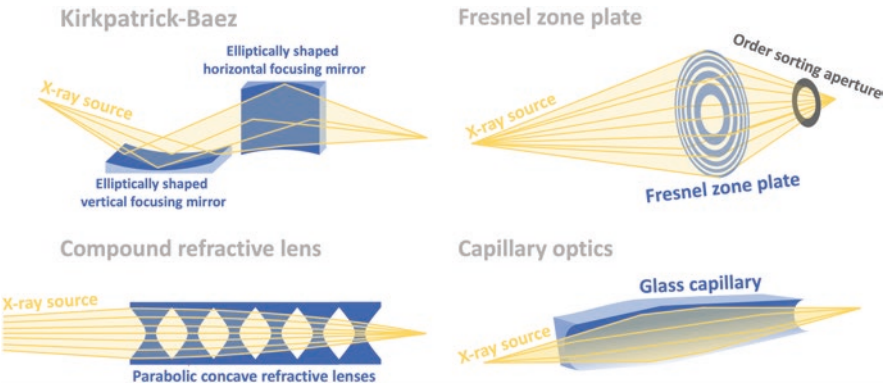

Fig. 12.6 Schematic representations of the four main X-ray focusing optics

spectrometry (XRF) uses this element-dependency of core-level transition energies, whereas the dependency of the DOS of core-level transitions to the oxidation state and coordination environment is exploited in X-ray absorption spectroscopies (XAS). While XRF is especially useful for elemental mapping, XAS has its main applications in determining oxidation states, coordination numbers, and the bond lengths for the first few coordination shells. Microfocused X-ray beams can also be used for crystal diffraction experiments (X-ray diffraction, XRD) to determine the crystalline phases present in a sample of interest.

The principles and state-of-the-art of μ-XRF, μ-XAS, and μ-XRD as applied to oil paint research are discussed in the following three sub-sections. In addition, to demonstrate the capabilities and complementarity of these three techniques, Figs. 12.8, 12.9, and 12.11 show the X-ray based chemical microimaging of an extraordinarily thick (~3 mm) stratigraphy of historical white oil paints, taken from the window frame of a historical home (*De Witte Roos*) in Delft, The Netherlands (see Fig. 12.7). These wooden frames have been repainted regularly over the past three centuries, as can be seen from the ~50 yellowish/whitish paint layers composing the stratigraphy (Fig. 12.7b. c). This sample therefore presents the recording of most of the commonly used white pigments over the past ~300 years. Besides, it can provide relevant information about their long-term stability and degradation. Therefore, its analysis established a record biography of a painting fragment. After embedding the paint fragment in resin, it was prepared as a cross-section (Fig. 12.7b) and as a microtomed 15 μm thin section (Fig. 12.7c).

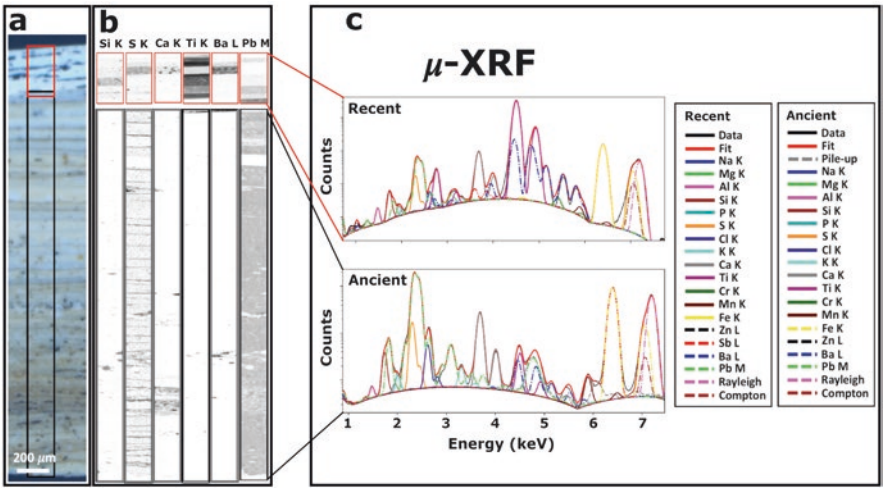

Fig. 12.8 μ-XRF data obtained on a cross-section of the Delft sample. (**a**) Optical microscopy image, with the red and black rectangles indicating the recent and ancient paint layers respectively. (**b**) μ-XRF maps of Si, S, Ca, Ti, Ba, and Pb. (**c**) Fits to the raw data using known energies of K, L, and M emission lines. Data was obtained at ID21, ESRF (Cotte et al. 2017b), using an X-ray beam tuned to 7.2 keV and focused down to 0.5 × 1.0 μm using a Kirkpatrick-Baez mirror system (see Fig. 12.6).

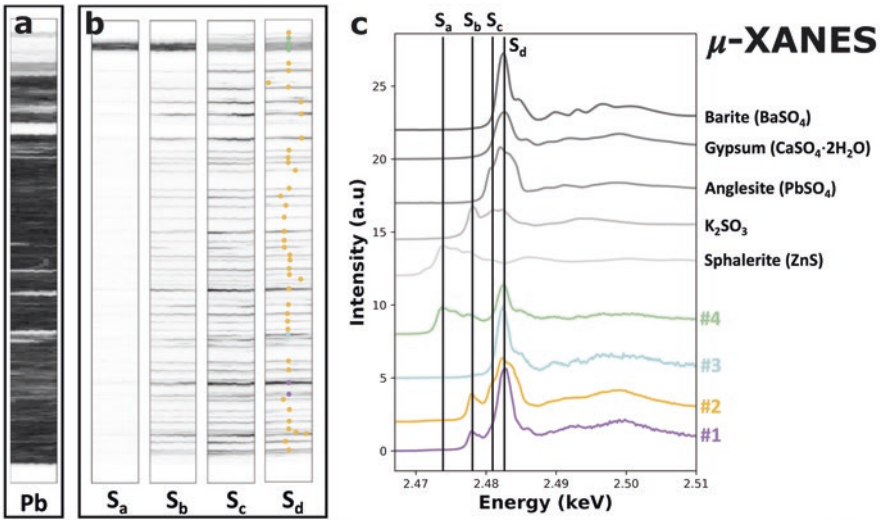

Fig. 12.9 μ-XANES data obtained on the Delft sample. (**a**) Elemental map of Pb as a reference for the distribution of lead pigments (acquired at 2.55 keV, above Pb M_5-edge). (**b**) XRF S-K maps recorded at the four absorption features identified in (**c**). (**c**) The bottom four spectra show averages of S K-edge XANES acquired at 51 points, represented as colored dots in (**b**) (#1–4), while the top five spectra shown S K-edge XANES from five reference compounds (grey). Data was obtained at ID21, ESRF, using an X-ray beam focused down to 0.5 μm × 1.0 μm using a Kirkpatrick-Baez mirror system (see Fig. 12.6).

12.4.1 μ-XRF

A description of the principle of XRF can be found in ref. (Mantler and Schreiner 2000)*, while a more detailed account of the instrumental aspects of modern μ-XRF instrumentation can be found in ref.* (Cotte et al. 2017b).

The ability of μ-XRF to map elemental distributions makes the technique particularly suitable to map pigment distributions in oil paint cross-sections. μ-XRF usually requires microfocused synchrotron-generated X-ray beams, making this technique less accessible than its electron-based counterpart (SEM-EDX) which is routinely used for mapping pigments. μ-XRF is mostly applied to studies of oil paint systems when sensitivity to certain (low concentration) elements is of concern or when other forms of synchrotron-based X-ray microanalysis are involved and μ-XRF can be performed for parallel characterization of the sample at the same location using the same instrumentation and set-up (Chen-Wiegart et al. 2017; Cotte et al. 2008; Cotte and Susini 2009; Van Der Snickt et al. 2009, 2012). Some research findings that were obtained through μ-XRF include the role played by chlorine contamination in the blackening of cinnabar (HgS) (Cotte et al. 2008; Cotte and Susini 2009; Radepont et al. 2011), the formation of a cadmium-sulfur degradation compound on the surface of cadmium yellow paints (Van Der Snickt et al. 2009, 2012),

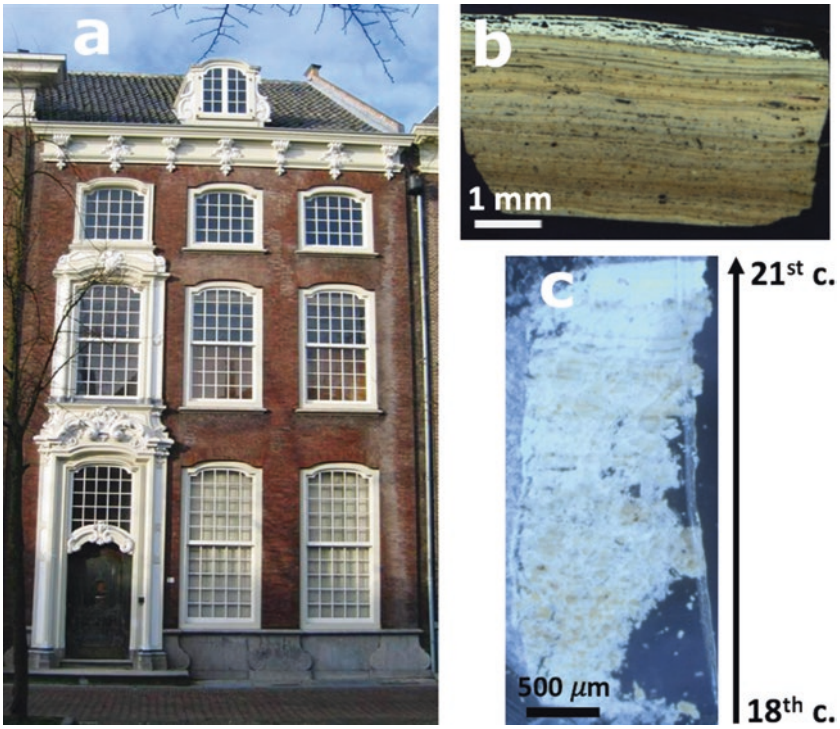

Fig. 12.7 (**a**) *De Witte Roos* in Delft. (**b** and **c**) Optical microscopy image of a paint fragment prepared as a polished cross-section and as a thin section, respectively. The most ancient (yellowish) paint layers are at the bottom while the most recent (whiter) layers are at the top of the section

and the disintegration of lead tin yellow to form lead soap aggregates (Chen-Wiegart et al. 2017). Combined with macro- X-ray imaging techniques on the entire painting itself (see Chap. 11), μXRF can be used to distinguish originally paint layers from repainted layers in micro-samples, and help in reorienting and optimizing the conservation strategy, as recently done during the restoration of van Eyck's renowned Ghent Altarpiece (Van der Snickt et al. 2017).

State-of-the-art applications of μ-XRF to studies of oil paint include the simultaneous recording of μ-XRF and μ-XRD by making use of fluorescence and transmission geometry respectively (Cotte et al. 2008; Van Der Snickt et al. 2012), and the ability to perform hard X-ray μ-XRF at spatial resolutions as high as 200 nm (Casadio and Rose 2013; Cotte et al. 2008). More routinely, beam sizes in the order of one to a few μm are being used, with μ-XRF experiments typically being combined with μ-XAS—enabled by the tunability of synchrotron-generated X-ray beams and the shared ability to record data in fluorescence geometry.

The application of the μ-XRF technique to the Delft sample is shown in Fig. 12.8. Two maps were acquired at 7.2 keV (above the Fe K-edge), one covering the older, yellowish paint layers and one covering the more recent, whiter, upper paint layers.

The elemental maps show that in the older paint layers, lead is the main element, with some layers containing calcium, barium, and sulfur. The finding of lead in the older paint layers is in line with the common use of lead white in that time period, and based on similar knowledge of pigment use in modern times, the finding of titanium in the upper paint layers can for instance be hypothesized to be due to the pigment titanium white. However, in these cases, μ-XRF data cannot provide a definitive identification, for which one relies on techniques with a higher chemical specificity. This is also the case for a number of other μ-XRF observations—such as the finding of barium and titanium in some of the oldest paint layers and the presence of many thin layers of sulfur—for which more precise identification is necessary in order to determine their origin.

12.4.2 μ-XAS

Detailed information about the methodological and theoretical principles behind XAS can be found in refs. (Penner-Hahn 1999) *and* (Rehr and Albers 2000).

μ-XAS refers to a set of techniques that aim to extract chemical information from the spectral structure around and above elemental absorption edges. Since the collection of X-ray absorption spectra requires extensive tunability and high monochromaticity of the X-ray beam, it is still today essentially a synchrotron-based technique, particularly for heterogenous complex systems as encountered in paint composition and alteration studies. XAS is performed in two distinct energy ranges: X-ray absorption near-edge structure (XANES) and extended X-ray absorption fine structure (EXAFS). XANES focuses on the energy range close to the absorption edge—containing the discrete orbital-to-orbital transition features—and is particularly useful for probing oxidation states and identifying compounds. EXAFS focuses on the higher energy range that corresponds to core-shell-to-continuum transitions. It can be used to extract precise quantitative measurements of the average coordination numbers and bond lengths. As EXAFS has as of yet not been shown in a microchemical imaging application in the context of oil paint degradation studies, this section will be focused on μ-XANES, while the prospects of the capabilities of μ-EXAFS imaging are discussed in Sect. 12.6.

The capability of XANES to probe oxidation states of elements makes μ-XANES a particularly powerful technique to study (mostly) environmentally induced degradation processes of inorganic pigments on the microscale. Some notable examples of results obtained through μ-XANES on degradation oil paint systems include the identification of cinnabar degradation products (Cotte and Susini, 2009), the identification of oxidative cadmium yellow degradation products (Van Der Snickt et al. 2009, 2012), the elucidation of the various factors that affect the reduction of lead chromate (Monico et al. 2011, 2015a, 2016), and the characterization of the degradation-migration pathways of realgar (As_4S_4), orpiment (As_2S_3), and emerald green ($3Cu(AsO_2)_2{\cdot}Cu(CH_3COO)_2$) (Keune et al. 2015, 2016). Besides degradation

studies, μ-XANES can also be used to distinguish different qualities. It was used for example to identify a marker for the preparation method (in particular heat treatment) of ultramarine pigment from lapis lazuli in historical paints (Gambardella et al. 2020).

One of the primary goals of μ-XANES analysis on oil paints is to resolve spatial distributions of the different components, in particular degradation products relative to the original pigment and possible other reactants. Two main approaches are currently taken, depending on the chemical species under study and the available instrumentation. The first approach is sometimes called chemical state (or speciation) mapping and works particularly well when absorption edges exhibit markedly different spectral features. Chemical state mapping involves the recording of a small number (2–4) of XRF maps at different excitation energies (see also examples below). When the excitation energies are chosen so as to correspond to XANES absorption features that are specific for certain compounds or oxidation states, chemical maps can be reconstructed that specifically show the distribution of one compound or the other (Monico et al. 2015a, 2016; Pouyet et al. 2015; Radepont et al. 2011; Van Der Snickt et al. 2009, 2012).

The second approach is based on recent developments in detector technology and involves the recording of hyperspectral μ-XANES maps and subsequent fitting with reference spectra. This approach is particularly useful when the X-ray absorption behavior of the species of interest is more subtly different, or when complex mixtures of compounds are present. Using single-element X-ray detectors, hyperspectral maps can only be recorded by raster scanning the same area many times for different excitation energies. With conventional detector technology, this approach is only feasible for low-definition images. One demonstrated solution involves the use of the recently developed new-generation Maia detector: an annular X-ray detector with a much larger solid angle that enables faster raster scanning of samples and has been used to record hyperspectral XANES maps to study chrome yellow degradation (Monico et al. 2015a). The second solution is to employ a full-field imaging approach using scintillators and very sensitive CCD or CMOS cameras. Megapixel hyperspectral images can be recorded at once, circumventing time-costly raster scanning and the need for tightly focused X-ray beams. This principle has been demonstrated for the study of the degradation of cadmium yellow and for the characterization of sulfur chemistry in ultramarine pigments as a function of their post-synthesis treatments, mentioned above (Gambardella et al. 2020; Pouyet et al. 2015).

The application of the μ-XANES technique to the Delft sample is shown in Fig. 12.9. The goal of these experiments was to determine more precisely the identity of the sulfur species, in particular in the many thin layers observed using μ-XRF (see Fig. 12.8). First, a μ-XRF map was acquired at 2.55 keV (i.e., above the S K-edge and Pb M_5-edge) to localize lead and the thin sulfur layers. 51 XANES spectra were then acquired at the maximum XRF emission intensity of each of these S layers. These spectra could be grouped into four main classes and averaged (Fig. 12.9c). They reveal different sulfur species, ranging from reduced sulfur

(sulfide, S^{2-}, here preliminary attributed to ZnS), to more oxidized forms (sulfite and sulfate, S^{4+} and S^{6+}). The reference spectra of three sulfates ($PbSO_4$, $CaSO_4.2H_2O$ and $BaSO_4$) show that they all have a maximum absorption at a similar energy position (around 2.482 keV), but differ by their fine structure. Comparing the four experimental XANES with these five reference spectra, experimental spectrum 1 can be hypothesized to have been recorded on a mixture of $CaSO_4{\cdot}2H_2O$ and a sulfite, spectrum 2 on a mixture of $PbSO_4$ and a sulfite, spectrum 3 on $BaSO_4$, and spectrum 4 on a mixture of ZnS and $BaSO_4$. Based on these spectra, four energies were chosen to map these different species: S_a = 2.4736 keV (maximum absorption for ZnS), S_b = 2.477 keV (maximum absorption for sulfite), S_c = 2.481 keV (shoulder in the $PbSO_4$ spectrum) and S_d = 2.4822 keV (maximum absorption for all sulfates). From these maps and the experimental S K-edge XANES spectra, it could be concluded that the top paint layers contain sulfur in the forms of ZnS and $BaSO_4$, suggesting the use of the white pigment lithopone. Furthermore, μ-XANES analyses of the thin sulfur-rich layers reveal a mixture of sulfites and sulfates. The sulfates in the layers found among lead-pigmented layers were found to most closely resemble anglesite ($PbSO_4$), whereas those found on top of the calcium-rich layer more closely resemble gypsum ($CaSO_4{\cdot}2H_2O$). Although these compounds have been used as paint components in the past (anglesite as Flemish white and gypsum as an extender), here, their mixture with sulfites and their systematic distribution as thin layers alternated with lead white layers suggests a degradative origin; likely due to prolonged exposure to atmospheric pollutants, such as SO_2.

12.4.3 μ-XRD

A comprehensive review of both the instrumental and theoretical aspects of XRD and μ-XRD can be found in refs. (Giacovazzo et al. 2009; Gonzalez et al. 2020). *The application of μ-XRD to cultural heritage in general has been reviewed previously* (Gonzalez et al. 2020).

When scattered elastically off a material with crystalline properties, X-rays form diffraction patterns that are highly characteristic of the chemical make-up of the material and its various crystalline phases. X-ray diffractograms are recorded by irradiating a crystalline sample with a monochromatic X-ray beam and recording the intensity of reflected X-rays as a function of the outgoing angle. According to Bragg's law, positive interference occurs for specific angles θ, under the condition that the following relation holds:

$$2d \sin\theta = n\lambda \tag{12.2}$$

Here, d is the spacing between certain crystallographic planes, λ is the wavelength of the X-ray beam, and n is an integer that corresponds to the order of the interference maximum. X-ray diffractograms typically consist of many (>10) narrow peaks,

making the technique highly chemically specific for the analysis of crystalline compounds.

Common applications of μ-XRD in studies of oil paint include the identification and mapping of crystalline metal carboxylates and inorganic degradation products (Cotte et al. 2008; Radepont et al. 2011; Salvadó et al. 2009; Simoen et al. 2019; Van Der Snickt et al. 2009, 2012), and the characterization of certain pigments (Cotte et al. 2008; Gonzalez et al. 2017b; Monico et al. 2013; Welcomme et al. 2007). In currently reported μ-XRD analyses of oil paint, both mapping and characterization experiments are performed in transmission geometry. For mapping, the use of a transmission geometry (as compared to reflection geometry) reduces the on-sample lateral spot size of microfocused X-ray beams and prevents shadowing of Debye-Scherrer rings, especially at small diffraction angles (Welcomme et al. 2007).

One approach to recording transmission geometry μ-XRD maps is currently shown to be particularly useful for applications in oil paint analysis. In this approach, the sample is raster scanned under an X-ray microbeam and diffraction patterns are imaged in full-field using a scintillator in combination with a 2D CCD (Cotte and Susini 2009; Gonzalez et al. 2017b; Radepont et al. 2011; Van Der Snickt et al. 2009, 2012). Compared to the more conventional way of recording powder X-ray diffractograms, in which an angular range is scanned using a single-element X-ray detector, the full-field approach is substantially faster, allowing many points to be analyzed in a relatively short period of time. Some of the previously referenced papers show how it allows the imaging of oxidation products of cadmium yellow (Cotte and Susini 2009; Van Der Snickt et al. 2009), lead sulfates, copper oxalates, and copper hydroxyl chlorides (Mantler and Schreiner 2000), different grades of lead white (Welcomme et al. 2007), and degradation products of vermillion (Cotte and Susini 2009).

A second approach that is particularly noteworthy in discussing the state-of-the-art of μ-XRD analysis of oil paints is X-ray diffraction tomography. Reported first in this context by Vanmeert et al. (2015), the technique is used to preserve the depth information that is normally lost when recording diffraction data in transmission. As reported by Vanmeert et al. and later by Price et al. (2019), it works by repeatedly scanning a line of the microsample with a microfocused X-ray beam and recording diffractograms in transmission with a 2D scintillator-CMOS or hybrid photon counting (HPC) detector system. After each repetition the sample is rotated by a few degrees, such that a rotation of 180° or 360° is reached after about 100 successive rotational steps. After reconstruction with a filtered back-projection (FBP) or maximum-likelihood expectation-maximization (MLEM) algorithm, a virtual 2D cross-section is obtained with a full X-ray diffractogram for each pixel. The spatial resolution of this technique is determined by the diameter of the X-ray beam and the number of rotational steps and is in the order of one to a few μm (Vanmeert et al. 2015; Price et al. 2019). A comparison of 2D XRD tomograms and a regular μ-XRD map recorded on a pustular mass from a painting by Vincent van Gogh is shown in Fig. 12.10. Here, it can be seen that voids in the distribution of crystalline material have formed in the pustular mass—something that cannot be observed in the regular 2D μ-XRD map.

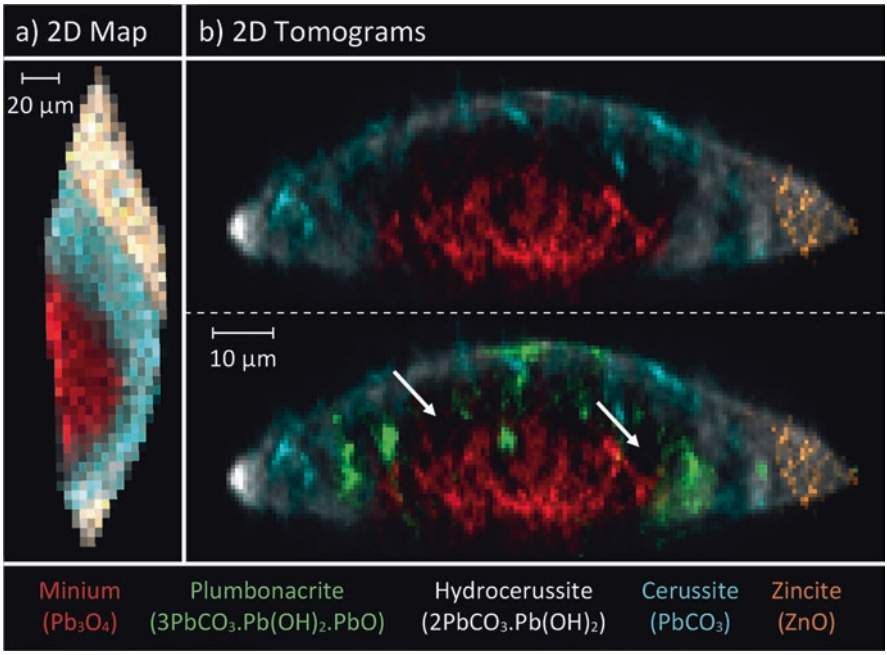

Fig. 12.10 2D µ-XRD mapping (**a**) versus 2D XRD tomography (**b**) of a pustular mass sampled from Vincent van Gogh's *Wheat Stack Under a Cloudy Sky* (Kröller-Müller Museum). The two 2D tomograms show identical virtual cross-sections with the green color in the bottom tomogram representing a plumbonacrite phase. The white arrows indicate the voids in the distribution of crystalline material. Reprinted from ref. (Vanmeert et al. 2015)

The application of the µ-XRD technique to the Delft sample is shown in Fig. 12.11. The diffraction data was recorded on a microtomed 15 µm thin section in a transmission geometry (Fig. 12.7c) in order to have good control of the probed volume and optimize the absorption and diffraction intensity. Having access to full X-ray diffractograms for each pixel, it is now possible to unambiguously identify all crystalline compounds present throughout the 50+ different paint layers. Hydrocerussite and cerussite are both detected in the lead-pigmented layers in various ratios, indicating the presence of lead white produced using different manufacturing processes or having undergone different post-synthesis treatments (Gonzalez et al. 2017b). In the more recently applied paint layers towards the top of the sample, zincite (ZnO) is detected, indicating the use of the pigment zinc white, introduced in the first half of the nineteenth century. Here, alternating zinc white and lead white layers show the gradual progression in the use of different white pigments. TiO_2 (rutile) is the main component of five recent layers, separated by one $ZnS/BaSO_4$ layer, indicating the use of the modern pigment titanium white and lithopone respectively. In addition, a lead titanate ($PbTiO_3$) phase was observed in some of the upper titanium white paint layers. The use of lead titanate as a highly durable pigment for use in protective paint has been proposed in the 1930s, but has

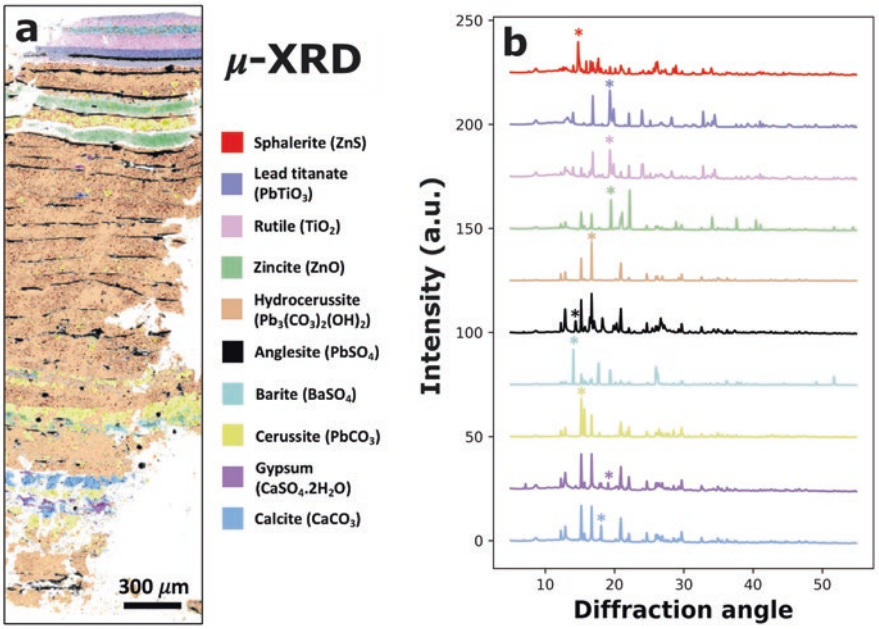

Fig. 12.11 μ-XRD data obtained on the thin section of the Delft sample. (**a**) False color image showing the distribution of different crystalline phases, calculated by integrating the XRD intensity at specific diffraction peaks, indicated by colored asterisks in (**b**). (**b**) Diffractograms obtained by averaging XRD patterns over pixels exhibiting corresponding colors in the phase maps. Data was obtained at ID13, ESRF, using an X-ray beam tuned to 13 keV and focused down to 1.5 μm × 2.2 μm using a compound refractive lens (see Fig. 12.6).

never found widespread use, reportedly due to its high cost of production (Robertson 1936). In terms of (possible) degradation products, anglesite could now be identified with a high degree of certainty, and its distribution mapped with respect to the many lead white paint layers. Gypsum is also confirmed at the surface of the early calcite layers.

Comparing the information obtained from μ-XRD with the information obtained using μ-XRF and μ-XANES, it is clear that μ-XRD is particularly powerful for unambiguously identifying pigments and crystalline degradation products. On the other hand, only μ-XANES appears to be able to show the presence of sulfite species in the bottom lead white layers, most likely because this phase is (mostly) amorphous. Overall, for studies of oil paint, the choice of (X-ray) based imaging method strongly depends on the research question, the sample composition, as well as on constraints with regards to sample preparation.

12.5 Methods Based on Charged Particle Beams

The two main principles involving charged particles beams that are applied to the study of paint are electron scattering and secondary ion generation. Electron scattering forms the basis for electron microscopy and the commonly integrated energy dispersive X-ray spectrometry, while secondary ion generation forms the basis for secondary ion mass spectrometry (SIMS). In the following sections three different techniques will be discussed: scanning electron microscopy energy-dispersive X-ray spectrometry (SEM-EDX), transmission electron microscopy (TEM), and imaging SIMS.

12.5.1 SEM-EDX

A comprehensive overview of the instrumental aspects of SEM-EDX can be found in ref. (Goldstein et al. 2003).

SEM-EDX works with a tightly focused electron beam that is scattered off the analyzed sample and subsequently detected using an electron-sensitive detector. For imaging purposes, the most common approach is to detect the elastically backscattered electrons—analogous to the use of reflection geometry in optical microscopy. As compared to photon-based imaging methods, SEM has a clear advantage in terms of spatial resolution. While the diffraction limit of IR, visible, and UV photons and the physically limited focusability of X-rays pose substantial challenges for photon-based imaging at the nanoscale, electron beams can readily be focused down to only a few nanometers to obtain images of comparable spatial resolution.

Besides scattering elastically on the sample surface and inelastically generating secondary electrons, the focused electron beam also induces the ejection of core electrons from the measurement volume. This process is similar to the X-ray-induced core electron ejection that forms the basis for XRF and likewise results in the emission of characteristic X-rays. In this respect, the elemental mapping capabilities of SEM-EDX are comparable to the capabilities of μ-XRF, with the clear advantage that SEM-EDX does not require synchrotron-generated X-rays. A conscious choice may be made for either one, depending on whether there is an interest in low-concentration elements and whether the study of a sample is already planned to involve the use of synchrotron-generated microfocused X-ray beams (see Sects. 12.4.2 and 12.4.3).

Due to the unique combination of high-resolution imaging and elemental mapping capabilities and the fact that mature lab-based instrumentation has been around for several decades (Goldstein et al. 2003), SEM-EDX has evolved to become one of the primary methods of oil paint microanalysis. Common ways by which SEM-EDX analysis can inform on oil paint composition and degradation is through identifying the elements in degradation-related surface crusts (Van Loon et al. 2011; Mass et al. 2013b; Spring and Grout 2002), visualizing and identifying aggregates

and protrusions of degradation products (Gabrieli et al. 2017; Helwig et al. 2014; Keune et al. 2011; Osmond et al. 2013; Romano et al. 2020; Van der Weerd et al. 2004), studying early signs of paint delamination (Helwig et al. 2014; Van Loon et al. 2019; Rogala et al. 2010), and resolving surface texture for studies of water sensitivity, blanching, and ultramarine disease (Burnstock et al. 2006; de la Rie et al. 2017; Mills et al. 2008). Two examples that show the value of the high-resolution imaging capabilities of SEM and the elemental mapping capabilities of EDX are shown in Fig. 12.12. a and b show SEM backscatter images of lead soap aggregates in two distinct stages of development, demonstrating how contrast in electron density can inform on migration and remineralization phenomena in degraded oil paints. Figure 12.12c, d show an example of a 2D EDX raster scan and corresponding SEM backscatter image, recorded on a whole cross-section taken from an oil painting suffering from cracking. Lead white and zinc white can be identified in the top and middle layer respectively, which—due to some discontinuity—are both in contact with a carbon black layer that is painted on top, but cannot be observed clearly using SEM-EDX.

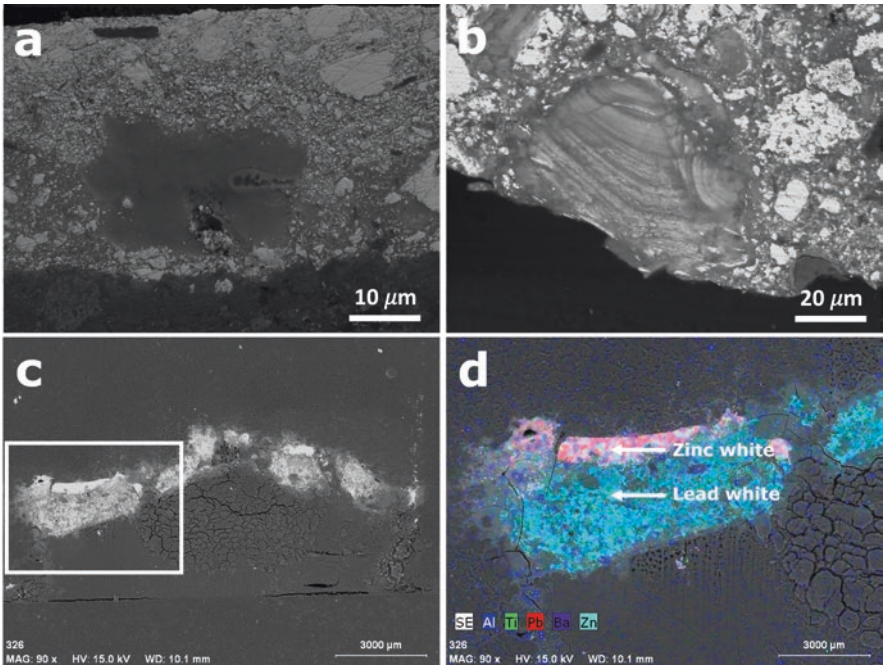

Fig. 12.12 SEM backscatter images of lead soap aggregates in early (**a**) and later (**b**) stages of development. (**c**) SEM backscatter image of a cross-section a painting whose upper layers have suffered from cracking. The white rectangle indicates the region that was scanned using EDX. (**d**) Overlay of SEM backscatter image and false color EDX map. (**a**) and (**b**) reproduced with permission from ref. (Keune et al. 2011). (**c**) and (**d**) Reprinted from ref. (Rogala et al. 2010) with the permission of Taylor and Francis Ltd.

One alternative approach to EDX for elemental mapping using the SEM platform is wavelength-dispersive X-ray spectrometry (WDS). This approach is based on the wavelength-dependent diffraction angle of X-rays on a single crystal and actually predates the EDX approach. Although WDS is much slower than EDX due to the mechanical scanning of diffraction angles, its spectral resolution and quantitative capabilities are superior. One example of how SEM-WDS can be used for studies of oil paint degradation was reported by Geldof et al. (2019). Here, WDS is chosen over EDX for the characterization of chrome yellows ($PbCr_{1-x}S_xO_4$) in terms of the stoichiometric factor x, due to the strong spectral overlap of the sulfur Kα and lead Mα emission lines.

12.5.2 TEM

A detailed account of the instrumental aspects of TEM and the associated sample preparation can be found in ref. (Williams and Carter 2009).

TEM is based on the imaging of transmitted electrons either by scanning a focused electron beam (scanning transmission electron microscopy, STEM) or by employing a full-field configuration with a 2D electron detector array. Due to complex interplay between higher accelerating voltages (shorter electron wavelength), lower electron densities, and different scattering and absorption processes of the detected electrons, TEM has a spatial resolution that is about an order of magnitude better than conventional SEM. Despite this interesting capability, TEM is much less widely applied than SEM-EDX for the study of oil paint. This can mostly be traced back to one primary reason; since TEM is based on the transmission of electrons,

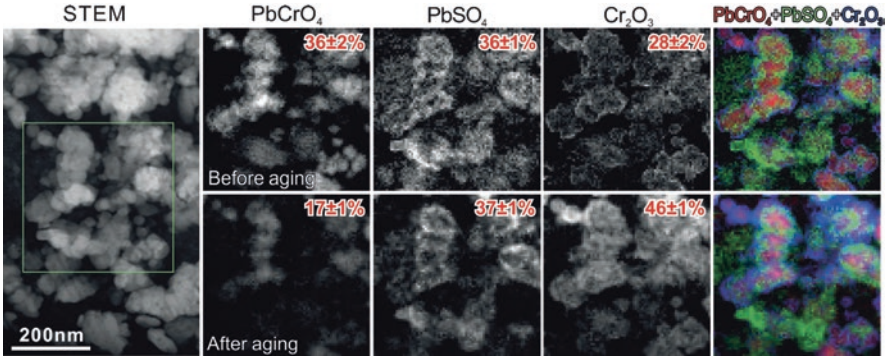

Fig. 12.13 TEM-EELS images of chrome yellow before (top row) and after aging (bottom row) under UV-Vis light. The numbers in the top right of each map show the estimated fraction of each compound in the analyzed sample. Reprinted from ref. (Tan et al. 2013) with the permission of Wiley-VCH

samples need to be extremely thin. Depending on the material, a sample thickness of no more than a few hundred nanometers is required.

In the paint studies, TEM was initially used as an alternative to SEM-EDX for pigment identification (Barba et al. 1995; Papillon et al. 1987; San Andres et al. 1997). In these cases, the reason to choose TEM over SEM-EDX is the ability to perform electron diffraction; providing direct structural information that allows unambiguous identification of paint components. A TEM modality that is of particular interest for studies of oil paint degradation is electron energy loss spectroscopy (EELS). EELS measures the loss in energy of transmitted electrons using an electron spectrometer. These energy losses tend to correspond to core-level electronic transitions in a way that is conceptually similar to XANES. Similar transitions are probed; providing information about the oxidation state and coordination environment of certain elements. Combining STEM and EELS, Casadio et al. (2011) were able to elucidate the chemical process leading to the darkening of zinc yellow ($K_2O{\cdot}4ZnCrO_4{\cdot}3H_2O$) oil paints. Here, EELS works by recording electron losses in resonance with Cr L-edge transitions, providing highly localized information about the oxidation state of chromium. Monico et al. (2011) and Tan et al. (2013) show how the extraordinarily high lateral resolution of TEM-EELS allows to visualize the core-shell structure of degraded chrome yellow particles—identifying up to three different phases based on O K-edge and Cr $L_{2,3}$-edge speciation. Taken from Tan et al. distribution maps of these three phases obtained through fitting reference spectra to the hyperspectral maps are shown in Fig. 12.12. Comparing the pigment before and after light-induced aging reveals that the $PbCrO_4$ core is reduced to a Cr_2O_3 shell. Given the nanometric thickness of the reduced shell structure, it is evident that the ability to perform chemically specific analysis at the nanoscale is an important asset in the microchemical imaging toolbox.

The combination of STEM and EDX was demonstrated by Vandivere et al. (2019a, b) to obtain very detailed information on pigmentation in Vermeer's *The Girl with a Pearl Earring*. Here, preparation of samples as 200 nm thin sections by means of a focused ion beam (FIB) was shown to drastically improve the spatial resolution of the obtained elemental maps. STEM-EDX was also shown by Van Driel et al. (2018) to be able to perform mapping and identification of different types of inorganic surface coatings and non-stoichiometric surfaces on titanium whites. The ability to resolve coatings and the stoichiometry of titanium white surfaces has previously been hypothesized to be related to the pigment's photocatalytic properties (Cushing et al. 2017; van Driel et al. 2016; Pan et al. 2013; Zhao et al. 2017), again showing the utility of chemical imaging at the nanoscale for the study of oil paint composition.

Another particularly noteworthy application of TEM to the study of oil paint was recently published by Hermans et al. (2018). They report on the use of TEM to produce 3D reconstructions of nanometric zinc soap agglomerates in degraded zinc white oil paint model systems. Similar to most other tomography methods, transmission images are recorded under a series of tilt angles. From the obtained set of projections, a 3D reconstruction can algorithmically be retrieved. Reconstructions of a single agglomerate show a lamellar structure with a high degree of disorder.

The crystalline domains are in the order of several tens of nanometers, with many domains measuring no more than a few unit cells.

12.5.3 Imaging SIMS

A detailed account of the various aspects of imaging SIMS and some other imaging mass spectrometry techniques can be found in ref. 136. (Massonnet and Heeren 2019).

Moving from electrons to ions, imaging SIMS is the last technique to be discussed in this review. It is unique in the context of all other discussed methods, as it derives its chemical specificity from the mass of atoms and molecules. SIMS uses a primary ion beam to generate secondary ions on the surface of a sample. These primary ions are metallic ions or ionic clusters of gallium, indium, gold, or bismuth, while the secondary positive or negative ions consist of sample material (or fragments thereof) and are separated based on their weight-to-charge ratio m/z. Analysis of m/z in SIMS is typically done using either a time-of-flight (TOF) or quadrupole mass analyzer (Dawson 1975; Massonnet and Heeren 2019; Niehuis et al. 1987). Due to the limited ability of these primary ions or ionic clusters to penetrate into the sample and the limited ability of secondary ions to escape from the sample, SIMS is very much a surface technique, probing only the first 1–2 nm. Spatially resolved SIMS analysis is enabled by the use of a microfocused ion beam which is raster scanned over the sample surface. For imaging applications, the ion beam is slightly defocused, yielding beam diameters ranging from several hundreds of nanometers to several micrometers.

In the context of oil paint studies, SIMS has a broad chemical sensitivity that can perform chemically specific analysis of low- and high-Z elements (Baij et al. 2019; Boon et al. 2001; Keune et al. 2009; Keune and Boon 2004, 2007; Voras et al. 2015), common moieties such as sulfates or carbonates (Boon et al. 2001), lead chloride alteration products (Keune et al. 2009), as well as fatty acids and their salts such as lead and zinc soaps (Baij et al. 2019; Boon et al. 2001; Keune et al. 2009; Keune and Boon 2004, 2005, 2007; Noun et al. 2016; Richardin et al. 2011; Sanyova et al. 2011). One recent study that shows some of the wider capabilities of imaging SIMS enabled by using Bi_3^+ clusters was reported by Voras et al. (Voras et al. 2015). Here, as a follow-up to two previous studies of Matisse's *Le Bonheur de Vivre* (Mass et al. 2013a, b), the authors demonstrate how imaging SIMS can perform chemically specific analysis of the intact cadmium yellow pigment, its various oxidation products, and amino acid fragments, while also resolving elemental distributions. The demonstration of such analyses at an estimated spatial resolution of 7.5 μm shows that modern imaging SIMS instrumentation can retrieve a wide range of information that may otherwise have required XRD, EDX, XANES, and FTIR analyses.

12.6 Future Prospects

Sections 12.2, 12.3, 12.4 and 12.5 reviewed the state-of-the-art of microchemical imaging currently applied to the study of oil paint composition and degradation. The aim of this final section is to critically discuss the capabilities and limitations of the current methodological toolbox and formulate perspectives on future research endeavors in oil paint studies. Such perspectives are illustrated by identifying four general research objectives that address the technological limitations of the microchemical imaging techniques reviewed previously: improved retrieval of spatial information, improved retrieval of chemical information, addressing the limited statistical relevance of analysis on paint microsamples, and integration of computational methods in the processing of microchemical data.

12.6.1 Improved Retrieval of Spatial Information

The spatial information captured in a chemical image is hard to define formally and has aspects far beyond the scope of this chapter (Yu and Winkler 2013), but here the discussion will be limited to the two aspects of spatial information that are considered most relevant for the study of highly heterogeneous degraded oil paint samples: spatial resolution and definition (Bertrand et al. 2013b). Here, spatial resolution is defined as the dimensions of the smallest detail that can still be resolved, while definition is defined as the total number of spatial points that can be analyzed in a reasonable timeframe. An improvement in spatial resolution reduces the smallest scale at which chemical information can be gathered, whereas an increase in the total number of analyzed spatial points allows access to different length scales at once and can increase the statistical relevance of the obtained information (Bertrand et al. 2013b). Here, a perspective is formulated on how certain technological developments and statistical approaches could lead to improvements in the retrieval of spatial information of degraded oil paint samples at various length scales through microchemical imaging.

12.6.1.1 Improvements in Spatial Resolution

In studies of oil paint, different chemical questions need to be addressed at different length scales. For instance, while the origin of metal soap-related delamination issues can typically be identified through chemical imaging on a length scale in the order of 10 μm (Van Loon et al. 2019), some fundamental, chemically relevant properties of oil paints only show up on length scales in the order of tens to hundreds of nanometers (Bertrand et al. 2013a; Casadio and Rose 2013). Especially in studies that aim to specifically address the earliest signs of degradation (e.g., microfissure formation) or the chemical interactions between submicrometric pigment

particles and the binding medium, crucial information is expected to be found in the nanometric reaction volume at the pigment-medium interface. The following section discusses some technologies that are capable of significant improvements in spatial resolution, but has so far only been applied sparsely (or not at all) in studies of oil paint.

As was discussed in Chap. 2, Sect. 2.1, μ-FTIR is a technique that has proven very powerful for the study of oil paint composition, but also suffers from intrinsic limitations in terms of spatial resolution. AFM-IR circumvents these intrinsic limitations by employing an ultrafine mechanical probe, reaching a spatial resolution in the order of tens of nanometers (see Chap. 2, Sect. 2.2). Despite its demonstrated potential for oil paint studies (Ma et al. 2019; Morsch et al. 2017), preliminary experiments by the authors have revealed that the mechanical heterogeneity of cured oil paint samples severely hampers the routine application of the technique. Furthermore, AFM-IR is a relatively young technique which is still under rapid development. For these reasons, further studies are required to fully elucidate the compatibility of this technique with mechanically heterogeneous samples and to explore the positive and negative effects of the various measurement modalities that already have been developed or are currently under development. A recent demonstration of how specific preparations of mechanically heterogeneous cultural heritage samples can facilitate compatibility with AFM-IR was reported by Reynaud et al. (2020).

In Sect. 12.3.2, some previously reported applications of Raman microspectroscopy were discussed. The Raman scattering modality was shown to be very useful in complementing other means of analysis, providing chemical specificity for compounds that are challenging to discriminate otherwise. The spatial resolution of the technique is determined by the focal volume of the excitation laser and is in the order of 1–2 μm. Significant improvements to this resolution can be realized by making use of wide-field Raman imaging or tip-enhanced Raman scattering (TERS). Wide-field Raman imaging is a technique that is operationally similar to PL microimaging (see Chap. 2, Sect. 2.3), but instead of broadband emission filters, employs tunable narrow-band emission filters (Schaeberle et al. 1999). As the technique works according to a full-field configuration and records images in the visible or near-IR range, a submicrometric spatial resolution can readily be achieved (Schaeberle et al. 1999). Moreover, this full-field approach means that millions—instead of hundreds—of spatial points can be analyzed in a reasonable timeframe. Wide-field Raman imaging therefore also addresses the focus of Sect. 12.6.1.2: increasing the number of analyzed spatial points.

TERS is based on the phenomenon of surface-enhanced Raman scattering (SERS) (Campion and Kambhampati 1998). SERS is induced when the probed molecule is in contact with a nanostructured metallic surface and can locally enhance the Raman signal by several orders of magnitude. The SERS phenomenon is particularly useful as the unenhanced Raman process has an extremely low cross-section, which prohibits analysis of low-concentration compounds and necessitates the use of intense laser irradiation—posing a substantial risk in terms of radiation damage. Using a gold-coated AFM tip to induce the SERS effect, it is possible to

record Raman spectra well below the diffraction limit, improving further upon the diffraction-limited spatial resolution of wide-field Raman microimaging (Anderson 2000). This technique does not employ the mechanical detection scheme used for AFM-IR, so the compatibility issues with mechanically heterogeneous cured oil paint samples are not expected to show up as strongly.

As described in Sect. 12.4, methods in the X-ray range are widely applied in oil paint studies. Microscopic X-ray based methodologies provide access to information on redox chemistry, coordination chemistry, while allowing discrimination between compounds of high chemical similarity. Besides beam divergence, measurement volume, and sample thickness, the spatial resolution of X-ray based techniques is for a large part limited by the X-ray focusing optics. Recent developments in synchrotron technology and X-ray focusing optics have led to more routine application of both soft and hard X-ray nanoprobes with sizes in the order of tens of nanometers (Sakdinawat and Attwood 2010). Moreover, similar focusing optics can be applied as imaging optics in full-field X-ray transmission experiments. The two main techniques associated with X-ray nanoprobes and full-field X-ray nanoimaging are called scanning transmission X-ray microscopy (STXM) and transmission X-ray microscopy (TXM) respectively. Due to the tunability of synchrotron-generated X-ray beams, STXM and TXM can be operated in XANES contrasting mode and are therefore for instance foreseen to have the ability to provide crucial information on the early stages of the formation and migration of oxidation and reduction products.

12.6.1.2 Increasing the Number of Analyzed Spatial Points

The second point of focus in this section is the projected increase in the total number of spatial points that can be analyzed in a reasonable timeframe. The retrieval of chemically specific information at a single spatial point may take anywhere between a few milliseconds (e.g., multispectral PL microimaging) to several minutes (e.g., Raman microspectroscopy), meaning that the total amount of spatial information obtained in a reasonable experimental timeframe may be anywhere between several tens and several millions of spatial points. Especially when studying highly heterogeneous samples, the information obtained from the analysis of several tens of points may hold very little statistical relevance. Moreover, when analyzing certain radiation sensitive compounds, long exposure times may cause radiation damage, which often changes the outcome of the measurement and can prevent subsequent chemical analysis on the same sample. As oil paint samples exhibit a high degree of heterogeneity and can contain materials prone to photo-induced reactions, technological developments aimed at speeding up microchemical analysis are considered crucial. Here, a perspective is proposed on the implementation of both instrumental and statistical methods to increase the total number of analyzed spatial points in the same timeframe.

The first approach is an instrumental one and has been developed specifically to speed up X-ray absorption spectroscopy analysis. All of the currently reviewed studies that involve the use of μ-XAS record spectra by scanning the energy of the excitation beam with a monochromator and recording either a raster-scanned or full-field image. Energy-dispersive XAS uses an elliptically bent polychromator to select a broad energy range that covers an entire absorption edge at once, while simultaneously focusing the beam to micrometric dimensions (Couves et al. 1990). As the transmitted divergent beam is energy-dispersed, a linear detector array placed some distance behind the sample allows to record a full absorption spectrum at once. Due to the extremely high brightness of third-generation synchrotron beamlines, it has recently been shown that full X-ray absorption spectra can be recorded using only a single 100-ps electron bunch (Pascarelli et al. 2016). Besides its applications for time-resolved XAS studies (Gervais et al. 2013b), the technique has specific potential for dramatically reducing the exposure time needed to record full hyperspectral X-ray absorption maps on thin sections of oil paint samples.

The second approach is based on the XANES/XRF speciation mapping method described in Sect. 12.4.2 (Pouyet et al. 2015; Radepont et al. 2011; Van Der Snickt et al. 2009, 2012) and the previously discussed multispectral PL microimaging method (Bertrand et al. 2013a; Comelli et al. 2017; Hageraats et al. 2019a; Van Loon et al. 2019; Thoury et al. 2011, 2019), but is foreseen to be similarly applicable to any other technique that relies on scanning an excitation or emission energy. Both XANES/XRF speciation mapping and multispectral PL microimaging essentially compromise the spectral resolution from hundreds of spectral points to just a few, in order to drastically reduce the measurement time per point. The rationale behind reducing the number of spectral points is (1) the notion that the intrinsic width of absorption and emission features tends to exceed the spectral resolution of most spectrometers and (2) the notion that, within a typically probed spectral range, many spectral features provide redundant information about the same compound. In the previously referenced examples on XANES/XRF speciation mapping and multispectral PL microimaging, energies were chosen either based on visual inspection of XANES spectra or simply based on the availability of spectral bandpass filters. It is postulated here that studies of oil paint could greatly benefit from the development of statistical models (for instance based on discriminant analysis) that determine from high-resolution spectra the number and energy of spectral points required to obtain certain threshold fractions of information. In this way, maps recorded in a multispectral manner could approach the chemical specificity of hyperspectral maps while significantly lowering the analysis time and radiation dose.

A detailed account of the theoretical background of this approach applied to as well as an example on cerium speciation in a paleontological sample was recently reported by Cohen et al. (2020).

Just like a full spectrum contains many redundant spectral points, the signal in any data set can be said to manifest a certain level of redundancy with respect to the noise level. That is, the information content in a data set with a high signal-to-noise ratio may be approximately equal to a similar data set with a low signal-to-noise

ratio, even though the latter took less time to record. Therefore, the third method for increasing the number of analyzed spatial points is based on a critical evaluation of the signal-to-noise ratio (SNR) that is required to discriminate between different compounds. It is here proposed to make use of the principle of zeta-scores, which measure the distance between two data points $\boldsymbol{x}_i$ and $\boldsymbol{x}_j$ normalized to the expected standard deviation σ in this distance if the two data points were recorded on exactly the same sample (Analytical Methods Committee 2016):

$$\zeta_{\boldsymbol{x}_i,\boldsymbol{x}_j} = \frac{\left\|\boldsymbol{x}_i - \boldsymbol{x}_j\right\|}{\sqrt{\sigma_{\boldsymbol{x}_i}^2 + \sigma_{\boldsymbol{x}_j}^2}} \tag{12.3}$$

Recognizing that the SNR of a spectrum $\boldsymbol{R}$ can be calculated by taking the ratio between its mean value μ and its standard deviation, the zeta-score equation for spectra can be rewritten as:

$$\zeta_{\boldsymbol{R}_i,\boldsymbol{R}_j} = \frac{\left\|\boldsymbol{R}_i - \boldsymbol{R}_j\right\|}{\sqrt{\left(\frac{\mu_{\boldsymbol{R}_i}}{SNR_{\boldsymbol{R}_i}}\right)^2 + \left(\frac{\mu_{\boldsymbol{R}_j}}{SNR_{\boldsymbol{R}_j}}\right)^2}} \tag{12.4}$$

A rough estimate of the SNR required to determine the chemical identity of a sample based on some spectrum $\boldsymbol{X}$ and two reference spectra $\boldsymbol{R_1}$ and $\boldsymbol{R_2}$ could then be made as follows:

$$SNR_X = \frac{\mu_{\mathbf{X}}}{\sqrt{\left(\frac{\left\|\boldsymbol{R}_1 - \boldsymbol{R}_2\right\|}{\zeta}\right)^2 - \left(\frac{\mu_{\boldsymbol{R}_{\min}}}{SNR_{\boldsymbol{R}_{\min}}}\right)^2}} \tag{12.5}$$

Where $\|\boldsymbol{R}_1 - \boldsymbol{R}_2\|$ is the Cartesian distance between the two reference spectra, $\boldsymbol{R}_{min}$ is the reference spectrum with the lowest SNR, and ζ is the zeta-score, which sets the required level of confidence for the identification based on spectrum $\boldsymbol{X}$ and reference spectra $\boldsymbol{R}_1$ and $\boldsymbol{R}_2$. For instance, for a 95% confidence level, ζ needs to be set to 1.96. This expression for SNR_X can be generalized to n reference spectra simply by finding the set of two reference spectra for which the zeta score is minimal (according to Eq. 12.4) and plugging the values for $\boldsymbol{R}_i$ and $\boldsymbol{R}_j$ into Eq. 12.5.

12.6.2 Improved Retrieval of Chemical Information

Besides the instrumental and statistical methods to improve the retrieval of spatial information for a given analytical approach, there is a continuous interest to improve upon the ability of microchemical imaging techniques to discriminate between different chemical species. Here, seven methodologies are briefly discussed that are meant to improve upon the chemical specificity of PL microimaging, μ-XANES, and SIMS, and extend the analytical capabilities of SEM.

12.6.2.1 Semi-hyperspectral Total Synchronous PL Microimaging

In Sect. 12.3.1 a number of PL-based microimaging and microspectroscopy methods were described that have so far been shown to be powerful analytical tools for the study of semiconductor pigments and zinc carboxylate degradation products. Still, the authors identify a recurring issue with PL-based methodologies in terms of chemical specificity, which limits the number of possible applications in oil paint studies. This issue is thought to be related primarily to the width of PL emission bands at room temperature and the large dynamic range of photoluminescence quantum yields of different paint components. This makes that emission bands of interest are often obscured either by emission bands with a similar energy, or even by emission bands with a very different energy, but a much higher quantum yield. In order to improve upon the chemical specificity of PL-based microimaging, there may be a strong interest in exploiting both the absorption and emission behavior of compounds by implementing total synchronous PL approaches in PL microanalysis methodologies. Total synchronous PL spectroscopy works by recording 2D absorption-emission spectra and has demonstrated potential in the classification of organic paint media and the characterization of differently produced lead whites (Gonzalez et al. 2017a; Nevin et al. 2009), but has so far not been demonstrated for microanalytical purposes.

It is proposed here to extend the multispectral PL microimaging methodology with a tunable narrow-band excitation source to obtain high-resolution spectral information without compromising on spatial resolution. Such a semi-hyperspectral total synchronous PL microimaging set-up could be realized by performing the excitation using a monochromatized tunable xenon arc lamp and recording full-field images for a large series of excitation wavelengths. Repeating the series through a number of emission band pass filters then yields a total synchronous PL dataset with the ability to reach diffraction-limited lateral resolutions. Of course, in order for total synchronous PL microimages to be translated into chemically specific maps of organic compounds, comprehensive (standardized) studies into the PL properties of binders, pigments, additives, and degradation products are first required. Moreover, spectral unfolding (see Sect. 12.6.4) will foster the ability to map compounds with strongly overlapping absorption and/or emission features.

12.6.2.2 Site-Selective and High-Energy Resolution μ-XANES

Within the current state-of-the-art, μ-XANES on oil paint microsamples is often recorded in a fluorescence geometry. Detection of the X-ray fluorescence signal typically occurs using energy-dispersive silicon drift or high purity germanium (HPGe) detectors, providing for each excitation energy an X-ray fluorescence spectrum with low energy resolution (< 130 eV). By either recording all signal, irrespective of energy (total fluorescence mode), or binning the emission signal falling only in a detector channel region over the element emission lines of interest, a measurement is obtained of the local X-ray absorption at that specific excitation energy. It must be stressed that the low spectral resolution of energy-dispersive detectors has an effect on the spectral resolution of X-ray absorption spectra and consequently also has an effect on the chemical specificity of the technique.

This effect is best described by considering a resonant X-ray emission spectroscopy (RXES) plane, such as the one shown in Fig. 12.14. An RXES plane shows a high-resolution X-ray emission spectrum for each X-ray excitation energy—exhibiting multiple narrow resonant emission bands whose energies and intensities depend strongly on the excitation energy. In case of negligible molecular motion, the resonant emission bands follow diagonal lines each characterized by a definite energy transfer corresponding to $\omega - \omega'$: the difference between the excitation and emission energies. When recording XANES with a low-energy-resolution detector,

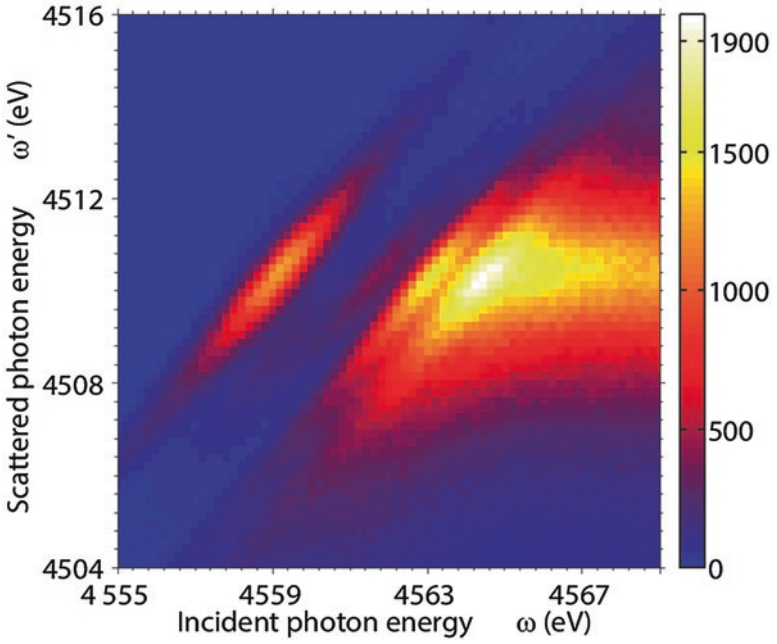

Fig. 12.14 RXES plane of CH_3I recorded close to the I L_3-edge. Reprinted from ref. (Marchenko et al. 2011) with the permission of AIP Publishing

the whole RXES plane is effectively projected onto a single energy channel, significantly broadening absorption features and often losing important spectral and therefore chemical information. Looking for instance at the RXES plane shown in Fig. 12.14, there are clearly two (or even three) separate peaks in the region of incident photon energies between 4560 and 4567 eV, which would all be observed as one using a low-resolution energy-dispersive detector (Marchenko et al. 2011).

Methods have therefore been proposed to improve the spectral resolution of fluorescence detection systems, in order to record X-ray absorption spectra for specific X-ray emission energies (Glatzel and Bergmann 2005). Glatzel et al. (2002) reported on a setup in which—using a Rowland geometry wavelength-dispersed spectrometer—the X-ray emission energy of different Kβ lines could be selectively probed. It was shown that with this site-selective approach it is possible to selectively probe different iron species in mixed-valence Prussian blue. A demonstration of how this approach can be made to work with X-ray nanoprobes was reported by Cotte et al. (2011), showing significant improvements on the spectral resolution of Sb L_3-edge XANES using a compact double-crystal wavelength-dispersive detection system operated in a confocal configuration. Due to the high chemical heterogeneity of oil paint samples, site-selective and high-resolution μ-XANES are anticipated to provide increased chemical specificity in studies of pigment degradation that involve complex redox chemistry. For imaging purposes, it must be noted that the wavelength-dispersed detection scheme requires a higher radiation dose to be deposited onto the sample as compared to regular μ-XAS. Therefore, there is an elevated risk of radiation damage in the analyzed sample (Bertrand et al. 2015; Monico et al. 2020b).

12.6.2.3 Energy-Dispersive μ-EXAFS

EXAFS is conceptually similar to XANES (see Sect. 12.4.2), but rather than focusing on discrete near-edge transitions, information is retrieved from the oscillations that appear at higher energies corresponding to core-shell-to-continuum transition. These oscillations are interference patterns of ejected electrons that are scattered off atoms in the first few coordination shells; corresponding spectra can be transformed and fitted to retrieve information about a compound's coordination number and bond lengths. μ-EXAFS has been applied previously to studies of oil paint degradation, providing unique insights into the discoloration of smalt and the blackening of copper resinate (Cartechini et al. 2008; Cianchetta et al. 2012; Robinet et al. 2011). These μ-EXAFS studies all make use of point analysis, due to the fact that experiments were performed in fluorescence geometry with stepwise scanning of the excitation energy, leading to measurement times per spectrum in the order of tens of minutes.

As was discussed in Sect. 12.6.1.2, the measurement time of μ-XAS measurements can be reduced by several orders of magnitude by making use of a transmission geometry in combination with an energy-dispersive detection scheme. The fact that the elliptically bent polychromator crystals can disperse a range of X-ray

energies that is much wider than a typical XANES make this approach also highly suitable—and in fact primarily designed—for EXAFS analysis (Couves et al. 1990; Pascarelli et al. 2016). Given the previously reported relationship between changes in coordination chemistry and pigment discoloration (Cianchetta et al. 2012; Couves et al. 1990; Robinet et al. 2011), the implementation of an energy-dispersive detection scheme in the EXAFS regime is anticipated to provide unique information on the precise chemical processes that underlie the discoloration of certain pigments.

12.6.2.4 X-Ray Raman Scattering

A limitation of XAS techniques for light elements (such as carbon, oxygen or nitrogen) is the high attenuation of X-rays which requires working on TEM-class (∼100 nm) thin samples. Yet, the preparation necessary to obtain samples that thin may not be compatible with mechanically heterogeneous cured oil pains. An alternative is the excitation of the same transitions (such as C, O or N K edges) using the energy loss in the sample resulting from inelastic scattering processes in the hard X-ray domain; a modality called X-ray Raman scattering (XRS). Using such an approach on historical materials, Gueriau et al. (2017) could for instance differentiate chemical compositions among carbon black pigments. Apart from the study of carbonaceous pigments, XRS is thought to be particularly promising to gain a deeper understanding of the transformation of the organic binder in oil paints.

On chemically heterogenous samples, a micrometric beam (typically 50 μm) can be raster-scanned across the sample, with XRS spectral information being recorded for each position. With this approach, chemical speciation maps can be collected on heterogeneous samples without the hassle and limitations of preparing thin sections. Due to the low attenuation of hard X-rays in most materials, XRS also lends itself as a contrasting method in 3D imaging techniques. To demonstrate this ability, Sahle et al. (2017a, b) have shown that the detected (scattered) X-ray beams can be resolved on a pixelated detector. The point-to-point correlation between voxels illuminated along the beam path in the depth of the sample allows to attain 3D reconstructed volumes of chemical speciation of carbon, oxygen and other elements in organic materials following the *direct tomography* method (Georgiou et al. 2019).

Currently, the limited spatial resolution of XRS-based methodologies prohibits them from providing spatially resolved chemical information on oil paints at resolutions better than a few tens of micrometers. Still, currently reported values are not due to fundamental physical limitations, but rather to the very low cross-section of the XRS process, which makes it challenging to obtain a sufficient signal-to-noise ratio from small measurement volumes while keeping radiation damage below acceptable thresholds. It is anticipated that improved detection systems with higher solid angles of detection can eventually bring the spatial resolution to ∼10 μm or below. Here, it must be noted that, due to the low cross-section of the XRS process, a high photon flux is often required to obtain sufficient signal. Exposure of organic materials to such high photon fluxes has been shown to induce radiation damage that is observable with the human eye (Gueriau et al. 2017).

12.6.2.5 SEM-Raman & Electron Backscatter Diffraction

One of the primary limitations of SEM—even when equipped with an EDX system—is its limited chemical specificity. For this reason, many research efforts have been focused on combining scanning electron microscopes with various other measurement modalities. Here, based on their prospective applications in studies of oil paint, two of such *hyphenated techniques* are discussed: SEM-Raman and electron backscatter diffraction (EBSD). SEM-Raman has been developed very recently to introduce the analytical capabilities of Raman microspectroscopy into a SEM—hereby circumventing the need to transfer the sample between microscopes and allowing easy correlation between high-resolution electron backscatter images and Raman scattering data. It works by leading the beam of an excitation laser into the chamber, focusing it onto the sample, and directing the scattered light to a spectrometer using collection optics and an optical fiber (Wille et al. 2014). The technique has already been shown to work well for the identification and characterization of pigments obtained from an ancient cave painting from *Grottes de la Garenne*. In the context of oil paint, the technique can be expected to provide quick identification of pigments and degradation products in and around the degradation features observed using SEM.

EBSD is a more established technique that combines SEM electron backscatter imaging with the exceptional chemical specificity of crystal diffraction (Schwartz et al. 2009). Instead of using X-rays, EBSD makes use of the wave properties of electrons. By firing the electron beam at a crystalline sample at a large angle and imaging the scattered electrons using a scintillator-CCD/CMOS detection system, complex (Kikuchi) patterns are observed that are representative of the local crystal structure. For highly heterogeneous samples, EBSD can be used to identify crystalline phases with dimensions in the order of tens of nanometers. Its application for the study of historical artworks has already been demonstrated by Berrie et al. (2016), who used EBSD to identify various pigments in a microscopic cross-section. Just like SEM-Raman, the technique can be envisioned to provide direct and accurate chemical identification of compounds found in features resolved using SEM backscatter imaging.

12.6.2.6 Imaging MALDI Mass Spectrometry

In Sect. 12.5.3 the imaging applications of secondary ion mass spectrometry (SIMS) were discussed. Using a focused beam of ions or small ionic clusters, secondary ions can be generated locally on the sample surface. Chemical maps are then obtained by scanning the beam over an area of interest, and integrating the signal coming from certain chemical species. Imaging MALDI mass spectrometry is a technique that is conceptually similar, but uses matrix-assisted laser desorption (MALDI) as an ionization mechanism (Sabatini et al. 2016). By using a focused laser beam, a spatial resolution in the order of 25 μm can be obtained. Despite this compromise on spatial resolution as compared to imaging SIMS, the MALDI

ionization method is extremely soft and is therefore useful for analysis of large molecules, such as proteins. For this reason, MALDI mass spectrometry has for instance been used in identification and characterization studies of proteinaceous binders and organic dyes (Kuckova et al. 2007; Sabatini et al. 2016). In the future, imaging MALDI mass spectrometry may for instance be applied to map distributions of more complex organic original and degradation products. In this regard, the method would be unique within the conservation scientist's microchemical imaging toolbox.

12.6.3 Addressing the Limited Statistical Relevance of Analysis on Paint Microsamples

One fundamental problem that is inherent to the analysis of oil paint microsamples is the limited statistical relevance of the sample in the context of the object as a whole. Moreover, microchemical imaging of paint microsamples conducted in a reflection or fluorescence geometry is often only sensitive to the uppermost micrometers (e.g., μ-ATR-FTIR, μ-XANES) or uppermost nanometers (e.g., AFM-IR, imaging SIMS) of the sample. The authors identify two main perspectives for improving the statistical relevance of the analysis of oil paint microsamples: three-dimensional microchemical imaging techniques to resolve chemical distributions throughout entire microsamples and object-based sub-surface microchemical imaging to perform cross-sectional microanalysis without the need for invasive sampling.

12.6.3.1 Three-Dimensional Microchemical Imaging

Within the current state-of-the-art of microchemical imaging of oil paints, the focus lies primarily on two-dimensional imaging of paint cross-sections, fragments, or pigment powders. Still, extending microchemical analysis into the third dimension is foreseen to strongly increase the amount of information that can be obtained from a single microsample, thereby decreasing the risk of false positives that are inherent to interpretations of data sets with limited spatial representation. Depending on the purpose of the study, there are two general groups of 3D imaging techniques that may see applications for the microchemical study of oil paints: those relying solely on material density and those relying on compound-specific X-ray absorption or emission transitions.

The principle of material density-based 3D imaging applied to oil paints was first demonstrated in a series of three studies by Ferreira et al. (2009, 2011) and Gervais et al. (2013a), who show how X-ray absorption tomography can help in determining the porosity of oil paints. Here, the use of tomography—instead of a 2D imaging method—allows to obtain much better statistics on overall porosity, but also permits to calculate accurate porosity metrics as a function of depth. Instead of imaging the

absorption of X-rays to detect differences in density, the coherence of synchrotron-generated X-rays also allows to detect density differences based on differences in the phase shift. This principle is used by ptychographic X-ray computed tomography and is particularly useful for imaging small differences in density (Dierolf et al. 2010).

An alternative to X-ray tomography for 3D imaging has also been developed that eliminates the need for synchrotron radiation and is based on a SEM instead. Serial block-face scanning electron microscopy (SBFSEM) is a method in which an ultramicrotome is introduced into the SEM experimental chamber to cut many consecutive thin (∼30 nm) slices off the surface of the sample (Denk and Horstmann 2004). After each cut, the surface is imaged to obtain a stack of images that can be reconstructed to a 3D volume with voxel sizes in the order of 20 × 20 × 30 nm. Although no applications have yet been demonstrated on oil paint, multiple reports have been published of SBFSEM applied to distinguish the various phases in coatings (Chen et al. 2013, 2014; Hughes et al. 2014).

In all these studies, no direct chemical information could be obtained. In an effort to retrieve chemical information from SBFSEM or single-energy X-ray tomography data, processing algorithms have recently been developed that can quantitatively assess local attenuation lengths and electron densities (Andres et al. 2008; Li et al. 2019; Maldanis et al. 2020; Reynaud et al. 2020). In studies of oil paint, this could allow coupling microscopic observation of morphological features with phase identification at micrometric to nanometric resolutions. The collection of billions of voxels means that statistical processing can be performed, which can produce a more complete description of samples and can help to identify previously unidentified phases in complex heterogenous degraded oil paint samples (Li et al. 2019).

The second way to obtain microchemical information in 3D is by making use of the chemical information embedded in elemental absorption edges or by collecting the XRF signal. The principle of using XAS contrast in X-ray absorption tomography has for instance been demonstrated on composite electrodes (Meirer et al. 2011), where rotational tomography series were repeated for 154 X-ray energies, covering the full Ni K-edge. The principle of using XRF contrast in X-ray absorption tomography has recently been demonstrated on catalyst particles (Bossers et al. 2020). Here, consecutive XRF images are recorded by raster scanning a nanofocused X-ray beam and recording the full XRF spectrum per sample position using a fast annular X-ray detector.

In the context of oil paint, three-dimensional reconstructions of elemental distributions or their oxidation states are foreseen to provide invaluable, statistically sound information on the presence and migration of original and degradative species. Moreover, with spatial resolutions being reported in the order of tens of nanometers (Meirer et al. 2011), these techniques can provide a unique view to a variety of interface effects and early stages of degradation.

12.6.3.2 Object-Based Sub-surface Microchemical Imaging

Technologies that possess the ability to analyze paintings as a whole are commonly referred to as macroscopic techniques and include for instance visible-NIR hyperspectral reflectance imaging, macroscopic XRF (MA-XRF) and macroscopic X-ray powder diffraction (MA-XRPD) (Cucci et al. 2016; Dik et al. 2008; Vanmeert et al. 2018). Although such techniques have proven exceptionally powerful for studying artistic composition, underpaintings, and pigmentation, the ability to resolve chemical distributions in-depth and/or on the microscale is still underdeveloped. One particularly promising research objective is therefore to bridge the current gap between macroscopic and microscopic methodologies, by developing object-based sub-surface microchemical imaging methodologies.

One of the primary advantages of performing analysis on microsamples is the ability to analyze paint layers in cross-section. In order to bring chemical microanalysis to whole objects, the ability to probe underneath the paint surface is therefore a crucial point of focus. Here, we will discuss four techniques that have a proven ability to probe samples in-depth and rely on contrasting methods that could be exploited for the study of oil paint sub-surface composition: confocal XRF/XAS, pump-probe microscopy, and Compton scattering tomography.

Confocal XRF makes use of a set of two perpendicularly placed X-ray focusing optics so as to only detect X-ray fluorescence from the intersection between the two foci (Kanngießer et al. 2003). Most commonly, polycapillary optics are used, providing lateral and axial resolutions in the order of tens of micrometers. With the ability to discriminate between elements, this technique is capable of distinguishing different paint layers and identifying with some degree of certainty the pigmentation in each layer. Although these capabilities can for instance provide virtual cross-sectional elemental distributions (Alfeld and Broekaert 2013; Kanngießer et al. 2012), the limited chemical specificity of XRF and the low spatial resolution provided by polycapillary optics make conventional confocal XRF largely unsuitable for studies of oil paint degradation. Instead, it is proposed to make use of the tunability of synchrotron radiation and use the confocal X-ray excitation-detection scheme in conjunction with XAS. Confocal XAS follows the same principle as confocal XRF, but measures the total fluorescence yield as a function of the excitation energy at certain absorption edges (Denecke et al. 2009). In order to combine the higher chemical specificity of XAS with a spatial resolution suitable for microanalytical studies of oil paint sub-surface layers, a KB mirror can be used to focus the excitation beam, while collimating channel array (CCA) optics can be used to define the measurement volume. This combination has been shown to provide a lateral resolution of 2.0 μm and a depth resolution of 2.5 μm (Sun et al. 2008), thereby making the confocal XAS technique a potentially powerful tool for noninvasive subsurface microchemical imaging of oil paintings.

Pump-probe microscopy is a technique that originates from biology and exploits de-excitation dynamics as a means to achieve chemical contrast in the overlapping excitation volume of two pulsed light sources (Helmchen and Denk 2005). Due to the use of a confocal configuration, pump-probe microscopy is a suitable technique

to obtain virtual cross-sections. This principle has been demonstrated by Villafana et al. (2014), where the different absorption spectra and de-excitation dynamics of ultramarine and quinacridone red are used to compose cross-sectional distributions maps of both pigments in mock-ups and a fourteenth century painting. As was shown by Yu et al. (2019) in a pump-probe microscopy study on vermillion powders and a historical cross-section, the technique can also be used to study pigment degradation. It is foreseen that such principles could be similarly applied in object-based studies.

Compton scattering tomography is a technique that is highly promising for applications in subsurface imaging of oil paintings, but has not been demonstrated in practice yet (Norton 1994). Recently, Guerrero Prado et al. (2017) provided the numerical support for the feasibility of this technique for the three-dimensional electron density imaging of flat objects. The proposed approach to Compton scattering tomography does not require relative rotations of the object with respect to the imaging set-up and can be performed even when the object is supported by an electronically dense material. In combination with the processing algorithms discussed briefly in Sect. 12.6.3.1, it ought to be possible to use this technique to obtain subsurface microchemical information on oil paintings.

12.6.4 Integrating Computational Methodologies in the Processing of Microchemical Data

In the current state-of-the-art of microchemical analysis of oil paint degradation, the overwhelming majority of all chemical information is still retrieved through manual data analysis by means of the expert eye. However, with the current and prospective technological developments discussed in all foregoing sections, there is a strong tendency for microchemical images to consist of more and more spectral and/or spatial points. With all this extra information, relying solely on the expert eye will often mean missing patterns or compounds that computer algorithms can identify. Following the rapid increase in readily available computational power, more and more methods are becoming available for the retrieval of chemical information through algorithmic processing (Gendrin et al. 2008). Due to the complex nature of degraded oil paints and the increasing volume of data sets, the authors identify a significant opportunity for the integration of computational methodologies for the improved retrieval of chemical information from microanalytical data.

For the study of samples that are chemically as complex and heterogeneous as mature oil paint samples, particularly useful computational methodologies are those involved in dimensionality reduction. Given a large microspectroscopic dataset, dimensionality reduction algorithms aim to find so-called latent variables: variables that reflect certain chemical parameters, but are hidden in the dataset. In this way, a series or map of spectra with several hundreds of spectral variables (e.g., excitation or emission energies) can be reduced to less than 10 variables—each of which can

be interpreted chemically. Common examples of such algorithms include principal component analysis (PCA), partial least squares (PLS), non-negative matrix factorization (NMF), and singular value decomposition (SVD). As a follow-up, each spectrum in the dataset can be expressed (i.e., modeled) as a linear combination of the calculated latent variables, returning chemically relevant weight matrices. A more detailed review of methods to perform dimensionality reduction to obtain chemical maps can be found in (Guerrero Prado et al. 2017).

As has been expressed previously, the application of such approaches to microspectroscopic datasets obtained in oil paint degradation studies has been rather rare. The most noteworthy applications have been reported very recently and include the work by Romano et al. (2020) and Gambardella et al. (2020). Although the microspectroscopic data sets were recorded using μ-FTIR and full-field μ-XANES respectively, in both cases NMF is used to retrieve the latent variables. Romano et al. use the weight matrices retrieved through modeling of the μ-FTIR data cube using NMF factors to reconstruct chemical phase maps of cadmium red paint, zinc white paint, and a gel-like zinc carboxylate protrusion. Similarly, Gambardella et al. visualize the distributions of two distinct chemical phases in ultramarine pigments by color-coding the difference between the NMF weight matrices of the first and third factor.

These examples illustrate two instances in which the different chemical phases cannot directly be identified by mapping single spectral points or single integrated absorption features, but are rather hidden in the complex sets of data. For instance, looking at the result reported by Romano et al. the pigments zinc white and cadmium red have no significant absorption in the mid-IR range themselves, but the two paints could still be distinguished computationally; likely due to different chemical interactions with the infrared-active oil binder. Considering the chemical contrast within ultramarines reported by Gambardella et al. and its origin in subtle spectral differences in S K-edge XANES, it is hard to imagine a manual approach to yield the same chemical information as the reported computational procedure.

Even without the previously described dimensionality reduction algorithms, there are still significant improvements that can be made in the retrieval of information from microchemical imaging datasets by making use of spectral unfolding. Spectral unfolding is based on the notion that most spectra are essentially made up of sums of probability distributions, such as Gaussians, Lorentzians, or Voigt profiles. These probability distributions reflect instrumental peak broadening, statistical variance in molecular structure, and—especially for rapid transitions—natural broadening. In chemically complex samples, there tends to be a high degree of overlap between adjacent probability distributions, often obscuring the precise peak locations of spectral bands. As the adjacency of spectral bands may for instance reflect the occurrence of relevant chemical transitions or the presence of one compound in two or more structural configurations, it is often favorable to be able to analyze the separate spectral contributions. Spectral unfolding is an exclusively computational endeavor that fits a model consisting of sums of probability distributions to raw spectral data.

This procedure is currently routinely applied to XRF data obtained with energy-dispersive X-ray detectors, where emission energies are known and peak widths can be approximated by knowing the spectral resolution of the detector. For this particular purpose, the PyMCA software has been developed at the European Synchrotron Radiation Facility (ESRF) (Solé et al. 2007), and has been used extensively among the μ-XRF studies discussed in part I of this chapter (see for instance Fig. 12.8). Still, in oil paint studies involving μ-FTIR or PL microspectroscopy—where spectral overlap similarly obscures chemically relevant information—spectral unfolding is not yet commonly applied. Explanations as to why spectral unfolding has so far been limited to XRF studies include lack of prior knowledge about the location and width of spectral features and complex and unpredictable baselines.

12.7 Conclusion

In part I of this chapter, we reviewed the current state-of-the-art of microchemical imaging studies on oil pain tcomposition. Based on the specific characteristics of oil paint samples, techniques have been applied that are based on the absorption of mid-IR radiation, the emission of photoluminescence, the absorption, reflection, and emission of X-rays, the scattering and absorption of electrons, and the mass-specific detection of secondary ions. By either employing tightly focused beams of electromagnetic radiation or charged particles, or full-field detection in combination with dedicated microscopy objectives, spatially resolved analysis can be performed at the micro- or even nanoscale. The current toolbox that makes up the state-of-the-art has for instance been applied to the identification and localization of (different grades of) original and degraded pigments and later added paint layers. By combining multiple microchemical imaging modalities, it is often possible to obtain the information necessary to elucidate the entire painting life history.

From the review of over a hundred reports on the microchemical imaging of oil paints, one can conclude that the conservation science community has shown an eagerness to adapt new developments, such as synchrotron-generated micro- and nanobeams, full-field X-ray imaging detectors, XRD tomography, and AFM-based infrared nanospectroscopy. Still, due to the complexity of oil paints and the current challenges associated both with object-based and sample-based microanalysis, even current state-of-the-art technology comes with substantial limitations in terms of the chemical information that can be obtained and the statistical relevance thereof. Ways in which these limitations can be addressed were discussed in Sect. 12.6.

In this sectioncond part, it was proposed that by making use of certain recent instrumental developments, smart statistical evaluations of data requirements, and subsequent computational data analysis, some of these limitations could potentially be tackled. The authors foresee particularly promising prospects for nanoscale chemical imaging methodologies (see Sect. 12.6.1.1), object-based sub-surface microchemical imaging techniques (see Sect. 12.6.3.2), and data dimensionality reduction approaches for mapping chemical contrast in complex, heterogeneous

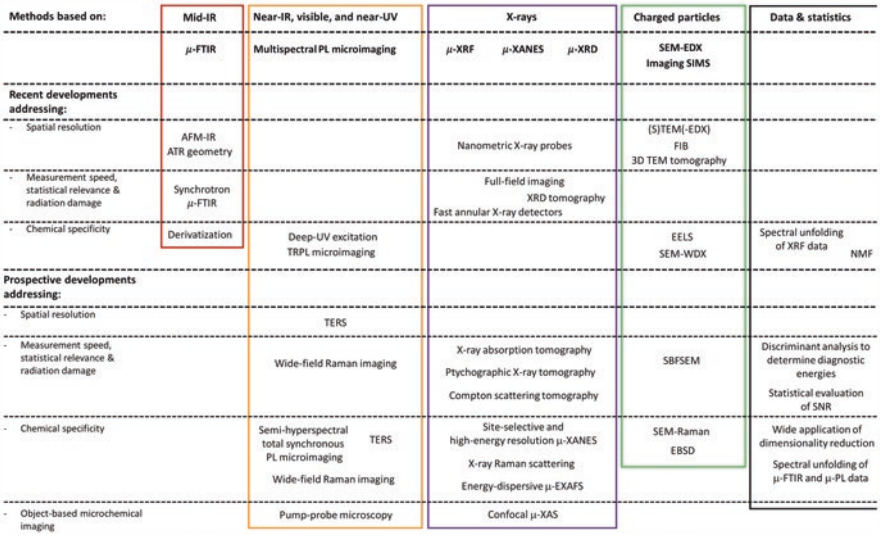

Fig. 12.15 Graphical summary of the microchemical imaging methods currently employed for the study of oil paint and their recent and prospective developments

samples (see Sect. 12.6.4). A summary of all methodologies discussed in the first and second part of this chapter is presented in Fig. 12.15. In this respect, the specific properties of ancient painting materials (which are inherently heterogeneous, aged, and unique) not only constitute a set of constraints on analytical studies concerning the identification of their composition and the understanding of degradation pathways, they also constitute an important source of inspiration, encouraging the optimization and development of analytical techniques sensitive to small chemical contrasts at high spectral and spatial resolution, and their coupling to advanced statistical processing of data, for the heritage science field and far beyond.

Acknowledgements The authors would like to express their gratitude to The Bennink Foundation for funding this research, to Edwin Verweij for providing the sample from the window frame of *De Witte Roos* in Delft, and to Dawn Rogala, Frederik Vanmeert, and Xiao Ma for providing figures for and/or proofreading the examples of SEM-EDX, XRD tomography and AFM-IR. They also warmly thank ESRF for granting in-house beamtime and Manfred Burghammer and Wout de Nolf for their support in data acquisition and data processing. SH, MT, LB and KK acknowledge support from the France–Netherlands Van Gogh program (Partenariat Hubert Curien MEAE/MESRI and NUFFIC).

Glossary

Concept/ abbreviation	Description
Absorption edge	Distinct step in the absorption spectrum of a compound, corresponding to element-specific electronic transitions from a core-level orbital to other core-level orbitals, valence-level orbitals, and continuum states.
AFM	Atomic force microscopy
Annular detector	A ring-shaped detector primarily used to collect signal from a large solid angle, while permitting transmission of an excitation beam through the center.
ATR	Attenuated total reflectance
Band gap	Property of a semiconductor: the gap between the highest occupied and lowest unoccupied energy levels. The bandgap strongly influences the ability of the semiconductor to absorb (or emit) ultraviolet, visible, and /or infrared light.
CCD detector	Charge-coupled device: a 2D photodetector array used primarily for the detection of ultraviolet and visible light. See also: CMOS detector.
Chemical contrast	*Ambiguous term*, here defined as: differences in the signal recorded by a measurement modality from different chemical compounds.
Chemical specificity	*Ambiguous term*, here defined as: the ability of a measurement modality to distinguish different chemical compounds. A modality with a high chemical specificity is capable of recording signal from specific compounds without interference from any others.
CMOS detector	Complementary metal oxide semiconductor: a 2D photodetector array used primarily for the detection of ultraviolet and visible light. Similar to, but operated differently than CCD detectors.
Compton scattering	An inelastic scattering effect in which energy is transferred from an X-ray photon to an electron.
Core-level transition	An electronic transition in which the lower energy level corresponds to a tightly bound core-orbital. Core-level transition energies are diagnostic of certain elements.
Cross-section (of a process)	The probability that a certain process will take place. Primarily used in the context of scattering, absorption, and emission processes.
Energy-dispersive detection	*Ambiguous term.* In the context of SEM-EDX: a means of detecting photon energy directly by probing the amount of ionization the photon produces in a detector material. In the context of energy-dispersive XAS: a detection method in which the energies in a polychromatic X-ray beam are spatially dispersed and detected separately on a detector array. See also: wavelength-dispersive detection.
EXAFS	Extended X-ray absorption fine structure
Far-field	An approach in optics in which the distance between the sample and the collection or focusing elements is far greater than the wavelength of the photons being used.
FTIR	Fourier-transform infrared
Full-field imaging	An approach to imaging in which a whole region-of-interest is projected onto a 2D detector array at once.

Hyperspectral	An approach to spectral imaging in which full spectra are collected for each pixel.
Length scale	*Ambiguous term.* Imaging at a certain length scale is here defined to be done with a spatial resolution and field of view that allows to resolve physical features whose dimensions lie in a certain range.
Measurement modality	*Ambiguous term*, here defined as: the physical principle according to which an analytical measurement is performed.
Metal soap	A salt consisting of metal ions and fatty acids. Often found in oil paints as a result of pigment degradation.
Method	*Ambiguous term*, defined in the context of microchemical imaging as: a physical or computational tool that can be used to prepare or analyze a sample or dataset.
Methodology	*Ambiguous term*, defined in the context of microchemical imaging as: the overarching approach by which analysis is performed; includes sample preparation, instrumental analysis, and data treatment.
Multispectral	An approach to spectral imaging in which absorption, emission, or scattering is probed at a small number of energies (typically 5-15) for each pixel.
Near-field	An approach in optics in which the distance between the sample and the collection or focusing elements is smaller than the wavelength of the photons being used.
Numerical aperture	A metric of optical elements that measures the angular range over which light is accepted or emitted. See also: solid angle
PL	Photoluminescence
Polymorph	A compound that exists in a particular crystal structure, but can exist in one or more others.
Pump-probe	An approach to spectroscopy in which one light source (the pump) promotes electrons from one energy level to another and a second light source (the probe) is used to measure the population or depopulation of certain energy levels.
RXES	Resonant X-ray emission spectroscopy, sometimes referred to as resonant inelastic X-ray scattering (RIXS)
Saponification	The process of fatty acids being converted into (metal) soaps.
SEM-EDX	Scanning electron microscopy-energy-dispersive X-ray spectrometry. See also: energy-dispersive detection.
Semiconductor pigment	An inorganic pigment that consists of crystallites that possess semiconducting properties, such as a bandgap and the ability to luminesce. Due to its bandgap structure, small changes in the composition of the pigment can strongly affect its color or luminescing properties.
SIMS	Secondary ion mass spectrometry
SNR	Signal-to-noise ratio
Solid angle	The angular range over which an optical element or detector accepts incoming photons.
STEM	Scanning transmission electron microscopy
Synchrotron	A large cyclic particle accelerator that can be used as a source of high-intensity and tunable X-rays, infrared, visible, and ultraviolet radiation.
TEM	Transmission electron microscopy
Tomography	A collection of techniques that are aimed at reconstructing sections through a sample.

Voxel	The three-dimensional equivalent of a pixel.
Wavelength-dispersive detection	A means to detect a spectrum in which different wavelengths are separated based on some form of diffraction and directed towards a 2D detector array.
XANES	X-ray absorption near-edge structure
XAS	X-ray absorption spectroscopy
XRD	X-ray diffraction
XRF	X-ray fluorescence

References

Alfeld, M., Broekaert, J.A.C.: Mobile depth profiling and sub-surface imaging techniques for historical paintings—a review. Spectrochim. Acta Part B Atom. Spectrosc. **88**, 211–230 (2013). https://doi.org/10.1016/j.sab.2013.07.009

Analytical Methods Committee. (2016). z-Scores and other scores in chemical proficiency testing-their meanings, and some common misconceptions. Anal. Methods. **8**, 5553–5555. https://doi.org/10.1039/C6AY90078J

Anderson, M.S.: Locally enhanced Raman spectroscopy with an atomic force microscope. Appl. Phys. Lett. **76**, 3130–3132 (2000). https://doi.org/10.1063/1.126546

Andres, B., Köthe, U., Helmstaedter, M., Denk, W., Hamprecht, F.A.: Segmentation of SBFSEM Volume Data of Neural Tissue by Hierarchical Classification. Pattern Recognit, pp. 142–152. Springer Berlin Heidelberg, Berlin/Heidelberg (2008). https://doi.org/10.1007/978-3-540-69321-5_15

Artesani, A., Gherardi, F., Nevin, A., Valentini, G., Comelli, D.: A photoluminescence study of the changes induced in the zinc white pigment by formation of zinc complexes. Materials (Basel). **10**, 340 (2017). https://doi.org/10.3390/ma10040340

Artesani, A., Gherardi, F., Mosca, S., Alberti, R., Nevin, A., Toniolo, L., et al.: On the photoluminescence changes induced by ageing processes on zinc white paints. Microchem. J. **139**, 467–474 (2018). https://doi.org/10.1016/j.microc.2018.03.032

Artesani, A., Ghirardello, M., Mosca, S., Nevin, A., Valentini, G., Comelli, D.: Combined photoluminescence and Raman microscopy for the identification of modern pigments: explanatory examples on cross-sections from Russian avant-Garde paintings. Herit. Sci. **7**, 17 (2019). https://doi.org/10.1186/s40494-019-0258-x

Baij, L., Chassouant, L., Hermans, J.J., Keune, K., Iedema, P.D.: The concentration and origins of carboxylic acid groups in oil paint. RSC Adv. **9**, 35559–35564 (2019). https://doi.org/10.1039/C9RA06776K

Barba, C., Andrés, M.S., Peinado, J., Báez, M.I., Baldonedo, J.L.: A note on the characterization of paint layers by transmission electron microscopy. Stud. Conserv. **40**, 194–200 (1995). https://doi.org/10.1179/sic.1995.40.3.194

Berrie, B.H., Leona, M., McLaughlin, R.: Unusual pigments found in a painting by Giotto (c. 1266-1337) reveal diversity of materials used by medieval artists. Herit. Sci. **4**, 1 (2016). https://doi.org/10.1186/s40494-016-0070-9

Bertrand, L., Cotte, M., Stampanoni, M., Thoury, M., Marone, F., Schöder, S.: Development and trends in synchrotron studies of ancient and historical materials. Phys. Rep. **519**, 51–96 (2012). https://doi.org/10.1016/j.physrep.2012.03.003

Bertrand, L., Réfrégiers, M., Berrie, B., Échard, J.-P., Thoury, M.: A multiscalar photoluminescence approach to discriminate among semiconducting historical zinc white pigments. Analyst. **138**, 4463 (2013a). https://doi.org/10.1039/c3an36874b

Bertrand, L., Thoury, M., Anheim, E.: Ancient materials specificities for their synchrotron examination and insights into their epistemological implications. J. Cult. Herit. **14**, 277–289 (2013b). https://doi.org/10.1016/j.culher.2012.09.003

Bertrand, L., Schöeder, S., Anglos, D., Breese, M.B.H., Janssens, K., Moini, M., et al.: Mitigation strategies for radiation damage in the analysis of ancient materials. TrAC Trends Anal. Chem. **66**, 128–145 (2015). https://doi.org/10.1016/j.trac.2014.10.005

Blumenroth, D., Dietz, S., Müller, W., Zumbühl, S., Caseri, W., Heydenreich, G.: Inside the Forger's oven: identification of drying products in oil paints during and after accelerated drying with increased temperatures. In: Conservation of Modern Oil Paintings, pp. 437–450. Springer International Publishing, Cham (2019). https://doi.org/10.1007/978-3-030-19254-9_34

Boon, J.J., Keune, K., Van der Weerd, J., Geldof, M., Van Asperen de Boer, J.: Imaging microspectroscopic, secondary ion Mass spectrometric and electron microscopic studies on Discoloured and partially Discoloured smalt in cross-sections of 16th century paintings. Chimia (Aarau). **55**, 952–960 (2001)

Bossers, K.W., Valadian, R., Zanoni, S., Smeets, R., Friederichs, N., Garrevoet, J., et al.: Correlated X-ray Ptychography and fluorescence Nano-tomography on the fragmentation behavior of an individual catalyst particle during the early stages of olefin polymerization. J. Am. Chem. Soc. **142**, 3691–3695 (2020). https://doi.org/10.1021/jacs.9b13485

Breek, R., Froentjes, W.: Application of pyrolysis gas chromatography on some of Van Meegeren's faked Vermeers and Pieter de Hooghs. Stud. Conserv. **20**, 183 (1975). https://doi.org/10.2307/1505738

Burnstock, A., van den Berg, K.J., de Groot, S., Wijnberg, L.: An investigation of water-sensitive oil paints in twentieth-century paintings. In: Modern Paints Uncovered, pp. 177–188. Getty Conservation Institute, Los Angeles (2006)

Campion, A., Kambhampati, P.: Surface-enhanced Raman scattering. Chem. Soc. Rev. **27**, 241 (1998). https://doi.org/10.1039/a827241z

Cartechini, L., Miliani, C., Brunetti, B.G., Sgamellotti, A., Altavilla, C., Ciliberto, E., et al.: X-ray absorption investigations of copper resinate blackening in a XV century Italian painting. Appl. Phys. A Mater. Sci. Process. **92**, 243–250 (2008). https://doi.org/10.1007/s00339-008-4498-y

Casadio, F., Rose, V.: High-resolution fluorescence mapping of impurities in historical zinc oxide pigments: hard X-ray nanoprobe applications to the paints of Pablo Picasso. Appl. Phys. A Mater. Sci. Process. **111**, 1–8 (2013). https://doi.org/10.1007/s00339-012-7534-x

Casadio, F., Xie, S., Rukes, S.C., Myers, B., Gray, K.A., Warta, R., et al.: Electron energy loss spectroscopy elucidates the elusive darkening of zinc potassium chromate in Georges Seurat's A Sunday on La Grande Jatte—1884. Anal. Bioanal. Chem. **399**, 2909–2920 (2011). https://doi.org/10.1007/s00216-010-4264-9

Cato, E., Scherrer, N., Ferreira, E.S.B.: Raman mapping of the S 3 − chromophore in degraded ultramarine blue paints. J. Raman Spectrosc. **48**, 1789–1798 (2017). https://doi.org/10.1002/jrs.5256

Chen, B., Guizar-Sicairos, M., Xiong, G., Shemilt, L., Diaz, A., Nutter, J., et al.: Three-dimensional structure analysis and percolation properties of a barrier marine coating. Sci. Rep. **3**, 1177 (2013). https://doi.org/10.1038/srep01177

Chen, B., Hashimoto, T., Vergeer, F., Burgess, A., Thompson, G., Robinson, I.: Three-dimensional analysis of the spatial distribution of iron oxide particles in a decorative coating by electron microscopic imaging. Prog. Org. Coat. **77**, 1069–1072 (2014). https://doi.org/10.1016/j.porgcoat.2014.03.005

Chen-Wiegart, Y.K., Catalano, J., Williams, G.J., Murphy, A., Yao, Y., Zumbulyadis, N., et al.: Elemental and molecular segregation in oil paintings due to Lead soap degradation. Sci. Rep. **7**, 11656 (2017). https://doi.org/10.1038/s41598-017-11525-1

Cianchetta, I., Colantoni, I., Talarico, F., D'Acapito, F., Trapananti, A., Maurizio, C., et al.: Discoloration of the smalt pigment: experimental studies and ab initio calculations. J. Anal. At. Spectrom. **27**, 1941–1948 (2012). https://doi.org/10.1039/c2ja30132f

Cohen, S.X., Webb, S.M., Gueriau, P., Curis, E., Bertrand, L.: Robust framework and software implementation for fast speciation mapping. J. Synchrotron Radiat. **27**, 1049–1058 (2020). https://doi.org/10.1107/S1600577520005822

Comelli, D., Artesani, A., Nevin, A., Mosca, S., Gonzalez, V., Eveno, M., et al.: Time-resolved photoluminescence microscopy for the analysis of semiconductor-based paint layers. Materials (Basel). **10**, 1335 (2017). https://doi.org/10.3390/ma10111335

Comelli, D., MacLennan, D., Ghirardello, M., Phenix, A., Schmidt Patterson, C., Khanjian, H., et al.: Degradation of cadmium yellow paint: new evidence from photoluminescence studies of trap states in Picasso's femme (Époque des "demoiselles d'Avignon"). Anal. Chem. **91**, 3421–3428 (2019). https://doi.org/10.1021/acs.analchem.8b04914

Cotte, M., Susini, J.: Watching ancient paintings through synchrotron-based X-ray microscopes. MRS Bull. **34**, 403–405 (2009). https://doi.org/10.1557/mrs2009.115

Cotte, M., Checroun, E., Susini, J., Walter, P.: Micro-analytical study of interactions between oil and lead compounds in paintings. Appl. Phys. A Mater. Sci. Process. **89**, 841–848 (2007). https://doi.org/10.1007/s00339-007-4213-4

Cotte, M., Susini, J., Solé, V.A., Taniguchi, Y., Chillida, J., Checroun, E., et al.: Applications of synchrotron-based micro-imaging techniques to the chemical analysis of ancient paintings. J. Anal. At. Spectrom. **23**, 820–828 (2008). https://doi.org/10.1039/b801358f

Cotte, M., Szlachetko, J., Lahlil, S., Salomé, M., Solé, V.A., Biron, I., et al.: Coupling a wavelength dispersive spectrometer with a synchrotron-based X-ray microscope: a winning combination for micro-X-ray fluorescence and micro-XANES analyses of complex artistic materials. J. Anal. At. Spectrom. **26**, 1051–1059 (2011). https://doi.org/10.1039/c0ja00217h

Cotte, M., Checroun, E., De Nolf, W., Taniguchi, Y., De Viguerie, L., Burghammer, M., et al.: Lead soaps in paintings: friends or foes? Stud. Conserv. **62**, 2–23 (2017a). https://doi.org/10.1080/00393630.2016.1232529

Cotte, M., Pouyet, E., Salomé, M., Rivard, C., De Nolf, W., Castillo-Michel, H., et al.: The ID21 X-ray and infrared microscopy beamline at the ESRF: status and recent applications to artistic materials. J. Anal. At. Spectrom. **32**, 477–493 (2017b). https://doi.org/10.1039/C6JA00356G

Couves, J.W., Thomas, J.M., Catlow, C.R.A., Greaves, G.N., Baker, G., Dent, A.J.: In situ studies of the dehydration of zeolitic catalysts by time-resolved energy-dispersive x-ray absorption spectroscopy. J. Phys. Chem. **94**, 6517–6519 (1990). https://doi.org/10.1021/j100380a001

Craddock, P. (ed.): Scientific Investigation of Copies, Fakes and Forgeries. Butterworth-Heinemann, Oxford (2009)

Cucci, C., Delaney, J.K., Picollo, M.: Reflectance hyperspectral imaging for investigation of works of art: old master paintings and illuminated manuscripts. Acc. Chem. Res. **49**, 2070–2079 (2016). https://doi.org/10.1021/acs.accounts.6b00048

Cushing, S.K., Meng, F., Zhang, J., Ding, B., Chen, C.K., Chen, C.-J., et al.: Effects of defects on photocatalytic activity of hydrogen-treated titanium oxide Nanobelts. ACS Catal. **7**, 1742–1748 (2017). https://doi.org/10.1021/acscatal.6b02177

Dawson, P.H.: Quadrupoles for secondary ion mass spectrometry. Int. J. Mass Spectrom. **17**, 447–467 (1975). https://doi.org/10.1016/0020-7381(75)80018-0

Dazzi, A., Prater, C.B.: AFM-IR: technology and applications in nanoscale infrared spectroscopy and chemical imaging. Chem. Rev. **117**, 5146–5173 (2017). https://doi.org/10.1021/acs.chemrev.6b00448

Dazzi, A., Prazeres, R., Glotin, F., Ortega, J.M.: Local infrared microspectroscopy with subwavelength spatial resolution with an atomic force microscope tip used as a photothermal sensor. Opt. Lett. **30**, 2388 (2005). https://doi.org/10.1364/OL.30.002388

Dazzi, A., Saunier, J., Kjoller, K., Yagoubi, N.: Resonance enhanced AFM-IR: a new powerful way to characterize blooming on polymers used in medical devices. Int. J. Pharm. **484**, 109–114 (2015). https://doi.org/10.1016/j.ijpharm.2015.02.046

de la Rie, E.R., Michelin, A., Ngako, M., Del Federico, E., Del Grosso, C.: Photo-catalytic degradation of binding media of ultramarine blue containing paint layers: a new perspective on the phenomenon of "ultramarine disease" in paintings. Polym. Degrad. Stab. **144**, 43–52 (2017). https://doi.org/10.1016/j.polymdegradstab.2017.08.002

Denecke, M.A., Brendebach, B., De Nolf, W., Falkenberg, G., Janssens, K., Simon, R.: Spatially resolved micro-X-ray fluorescence and micro-X-ray absorption fine structure study of a fractured granite bore core following a radiotracer experiment. Spectrochim. Acta Part B Atom. Spectrosc. **64**, 791–795 (2009). https://doi.org/10.1016/j.sab.2009.05.025

Denk, W., Horstmann, H.: Serial block-face scanning electron microscopy to reconstruct three-dimensional tissue nanostructure. PLoS Biol. **2**, 1900–1909 (2004). https://doi.org/10.1371/journal.pbio.0020329

Dierolf, M., Menzel, A., Thibault, P., Schneider, P., Kewish, C.M., Wepf, R., et al.: Ptychographic X-ray computed tomography at the nanoscale. Nature. **467**, 436–439 (2010). https://doi.org/10.1038/nature09419

Dik, J., Janssens, K., Van Der Snickt, G., van der Loeff, L., Rickers, K., Cotte, M.: Visualization of a lost painting by Vincent van Gogh using synchrotron radiation based X-ray fluorescence elemental mapping. Anal. Chem. **80**, 6436–6442 (2008). https://doi.org/10.1021/ac800965g

Doménech-Carbó, M.T., Edwards, H.G.M., Doménech-Carbó, A., del Hoyo-Meléndez, J.M., de la Cruz-Cañizares, J.: An authentication case study: Antonio Palomino versus Vicente Guillo paintings in the vaulted ceiling of the Sant Joan del Mercat church (Valencia, Spain). J. Raman Spectrosc. **43**, 1250–1259 (2012). https://doi.org/10.1002/jrs.3168

Drouilly, C., Krafft, J.-M., Averseng, F., Lauron-Pernot, H., Bazer-Bachi, D., Chizallet, C., et al.: Origins of the deactivation process in the conversion of methylbutynol on zinc oxide monitored by operando DRIFTS. Catal. Today. **205**, 67–75 (2013). https://doi.org/10.1016/j.cattod.2012.08.011

Ebert, B., Macmillan, A.S., Singer, B.W., Grimaldi, N.: Analysis and conservation treatment of vietnamese paintings. In: ICOM-CC 16th Triennial Conference Lisbon 19–23 September 2011 Preprints (2011)

Ferreira, E.S.B., Boon, J.J., van der Horst, J., Scherrer, N.C., Marone, F., Stampanoni, M.: 3D synchrotron x-ray microtomography of paint samples. In: Pezzati, L., Salimbeni, R. (eds.) SPIE 7391, O3A Optics for Arts, Architecture, and Archaeology II, p. 73910L (2009). https://doi.org/10.1117/12.837366

Ferreira, E.S.B., Boon, J.J., Stampanoni, M., Marone, F.: Study of the mechanism of formation of calcium soaps in early 20th century easel paintings with correlative 2D and 3D microscopy. In: ICOM Lisbon 2011 Preprints 16th Triennial Conference Lisbon, 19–23 September 2011. ICOM (2011)

French, S.A., Sokol, A.A., Bromley, S.T., Catlow, C.R.A., Rogers, S.C., King, F., et al.: From CO2 to methanol by hybrid QM/MM embedding this work was supported by EU Esprit IV project 25047. S.A.F. is grateful to ICI and Synetix for funding. K. Waugh, L. Whitmore, S. Cristol, and P. Sushko are thanked for their helpful insights. QM/MM=quantum. Angew. Chem. Int. Ed. **40**, 4437–4440 (2001). https://doi.org/10.1002/1521-3773(20011203)40:23<4437::AID-ANIE4437>3.0.CO;2-L

Gabrieli, F., Rosi, F., Vichi, A., Cartechini, L., Pensabene Buemi, L., Kazarian, S.G., et al.: Revealing the nature and distribution of metal carboxylates in Jackson Pollock's Alchemy (1947) by micro-attenuated Total reflection FT-IR spectroscopic imaging. Anal. Chem. **89**, 1283–1289 (2017). https://doi.org/10.1021/acs.analchem.6b04065

Gambardella, A.A., Cotte, M., de Nolf, W., Schnetz, K., Erdmann, R., van Elsas, R., et al.: Sulfur K-edge micro- and full-field XANES identify marker for preparation method of ultramarine pigment from lapis lazuli in historical paints. Sci. Adv. **6**, eaay8782 (2020). https://doi.org/10.1126/sciadv.aay8782

Geldof, M., van der Werf, I.D., Haswell, R.: The examination of Van Gogh's chrome yellow pigments in 'Field with irises near Arles' using quantitative SEM–WDX. Herit. Sci. **7**, 100 (2019). https://doi.org/10.1186/s40494-019-0341-3

Gendrin, C., Roggo, Y., Collet, C.: Pharmaceutical applications of vibrational chemical imaging and chemometrics: a review. J. Pharm. Biomed. Anal. **48**, 533–553 (2008). https://doi.org/10.1016/j.jpba.2008.08.014

Georgiou, R., Gueriau, P., Sahle, C.J., Bernard, S., Mirone, A., Garrouste, R., et al.: Carbon speciation in organic fossils using 2D to 3D x-ray Raman multispectral imaging. Sci. Adv. **5**, eaaw5019 (2019). https://doi.org/10.1126/sciadv.aaw5019

Gervais, C., Boon, J.J., Marone, F., Ferreira, E.S.B.: Characterization of porosity in a 19th century painting ground by synchrotron radiation X-ray tomography. Appl. Phys. A Mater. Sci. Process. **111**, 31–38 (2013a). https://doi.org/10.1007/s00339-012-7533-y

Gervais, C., Languille, M.-A., Reguer, S., Gillet, M., Vicenzi, E.P., Chagnot, S., et al.: "Live" Prussian blue fading by time-resolved X-ray absorption spectroscopy. Appl. Phys. A Mater. Sci. Process. **111**, 15–22 (2013b). https://doi.org/10.1007/s00339-013-7581-y

Giacovazzo, C., et al.: Fundamentals of crystallography. Oxford University Press, Oxford/New York (2009). https://doi.org/10.1093/acprof:oso/9780199573653.001.0001

Glatzel, P., Bergmann, U.: High resolution 1s core hole X-ray spectroscopy in 3d transition metal complexes—electronic and structural information. Coord. Chem. Rev. **249**, 65–95 (2005). https://doi.org/10.1016/j.ccr.2004.04.011

Glatzel, P., Jacquamet, L., Bergmann, U., de Groot, F.M.F., Cramer, S.P.: Site-selective EXAFS in mixed-valence compounds using high-resolution fluorescence detection: a study of iron in Prussian blue. Inorg. Chem. **41**, 3121–3127 (2002). https://doi.org/10.1021/ic010709m

Goldstein, J.I., Newbury, D.E., Echlin, P., Joy, D.C., Lyman, C.E., Lifshin, E., et al.: Scanning Electron Microscopy and X-Ray Microanalysis. Springer US, Boston (2003). https://doi.org/10.1007/978-1-4615-0215-9

Gonzalez, V., Gourier, D., Calligaro, T., Toussaint, K., Wallez, G., Menu, M.: Revealing the origin and history of Lead-white pigments by their photoluminescence properties. Anal. Chem. **89**, 2909–2918 (2017a). https://doi.org/10.1021/acs.analchem.6b04195

Gonzalez, V., Wallez, G., Calligaro, T., Cotte, M., De Nolf, W., Eveno, M., et al.: Synchrotron-based high angle resolution and high lateral resolution X-ray diffraction: revealing Lead white pigment qualities in old masters paintings. Anal. Chem. **89**, 13203–13211 (2017b). https://doi.org/10.1021/acs.analchem.7b02949

Gonzalez, V., Cotte, M., Vanmeert, F., Nolf, W., Janssens, K.: X-ray diffraction mapping for cultural heritage science: a review of experimental configurations and applications. Chem. Eur. J. **26**, 1703–1719 (2020). https://doi.org/10.1002/chem.201903284

Gueriau, P., Rueff, J.-P., Bernard, S., Kaddissy, J.A., Goler, S., Sahle, C.J., et al.: Noninvasive synchrotron-based X-ray Raman scattering discriminates carbonaceous compounds in ancient and historical materials. Anal. Chem. **89**, 10819–10826 (2017). https://doi.org/10.1021/acs.analchem.7b02202

Guerrero Prado, P., Nguyen, M.K., Dumas, L., Cohen, S.X.: Three-dimensional imaging of flat natural and cultural heritage objects by a Compton scattering modality. J. Electron. Imaging. **26**, 011026 (2017). https://doi.org/10.1117/1.JEI.26.1.011026

Hageraats, S., Keune, K., Réfrégiers, M., van Loon, A., Berrie, B., Thoury, M.: Synchrotron deep-UV photoluminescence imaging for the submicrometer analysis of chemically altered zinc white oil paints. Anal. Chem. **91**, 14887–14895 (2019a). https://doi.org/10.1021/acs.analchem.9b02443

Hageraats, S., Keune, K., Thoury, M., Hoppe, R.: A synchrotron photoluminescence microscopy study into the use and degradation of zinc white in 'the woodcutters' by Bart van der. In: Conservation of Modern Oil Paintings, pp. 275–288. Springer International Publishing, Cham (2019b). https://doi.org/10.1007/978-3-030-19254-9_21

Heeren, R.M.A., Boon, J.J., Noble, P., Wadum, J.: Integrating imaging FTIR and secondary ion mass spectrometry for the analysis of embedded paint cross-sections. In: ICOM-CC Triennial Meeting, (12th), Lyon, 29 August-3 September 1999 Preprint, pp. 228–233 (1999)

Helmchen, F., Denk, W.: Deep tissue two-photon microscopy. Nat. Methods. **2**, 932–940 (2005). https://doi.org/10.1038/nmeth818

Helwig K, Poulin J, Corbeil M-C, Moffatt E, Duguay D. Conservation issues in several twentieth-century Canadian oil paintings: the role of zinc carboxylate reaction products. In: van den Berg KJ, Burnstock A, de Keijzer M, Krueger J, Learner T, de Tagle A, et al.. Issues in Contemporary Oil Paint, Cham: Springer International Publishing; 2014, p. 167–184. doi: https://doi.org/10.1007/978-3-319-10100-2_11

Henderson, E.J., Helwig, K., Read, S., Rosendahl, S.M.: Infrared chemical mapping of degradation products in cross-sections from paintings and painted objects. Herit. Sci. **7**, 71 (2019). https://doi.org/10.1186/s40494-019-0313-7

Hermans, J., Osmond, G., van Loon, A., Iedema, P., Chapman, R., Drennan, J., et al.: Electron microscopy imaging of zinc soaps nucleation in oil paint. Microsc. Microanal. **24**, 318–322 (2018). https://doi.org/10.1017/S1431927618000387

Higuchi, S., Hamada, T., Gohshi, Y.: Examination of the photochemical curing and degradation of oil paints by laser Raman spectroscopy. Appl. Spectrosc. **51**, 1218–1223 (1997). https://doi.org/10.1366/0003702971941782

Hughes, A.E., Trinchi, A., Chen, F.F., Yang, Y.S., Cole, I.S., Sellaiyan, S., et al.: The application of multiscale quasi 4D CT to the study of SrCrO4 distributions and the development of porous networks in epoxy-based primer coatings. Prog. Org. Coat. **77**, 1946–1956 (2014). https://doi.org/10.1016/j.porgcoat.2014.07.001

Ice, G.E., Budai, J.D., Pang, J.W.L.: The race to X-ray microbeam and Nanobeam science. Science (80-). **334**, 1234–1239 (2011). https://doi.org/10.1126/science.1202366

Kanngießer, B., Malzer, W., Reiche, I.: A new 3D micro X-ray fluorescence analysis set-up – first archaeometric applications. Nucl. Instrum. Methods Phys. Res. Sect. B Beam Interact Mater. Atoms. **211**, 259–264 (2003). https://doi.org/10.1016/S0168-583X(03)01321-1

Kanngießer, B., Malzer, W., Mantouvalou, I., Sokaras, D., Karydas, A.G.: A deep view in cultural heritage—confocal micro X-ray spectroscopy for depth resolved elemental analysis. Appl. Phys. A Mater. Sci. Process. **106**, 325–338 (2012). https://doi.org/10.1007/s00339-011-6698-0

Keune, K., Boon, J.J.: Imaging secondary ion Mass spectrometry of a paint cross section taken from an early Netherlandish painting by Rogier van der Weyden. Anal. Chem. **76**, 1374–1385 (2004). https://doi.org/10.1021/ac035201a

Keune, K., Boon, J.J.: Analytical imaging studies clarifying the process of the darkening of vermilion in paintings. Anal. Chem. **77**, 4742–4750 (2005). https://doi.org/10.1021/ac048158f

Keune, K., Boon, J.J.: Analytical imaging studies of cross-sections of paintings affected by Lead soap aggregate formation. Stud. Conserv. **52**, 161–176 (2007). https://doi.org/10.1179/sic.2007.52.3.161

Keune, K., Hoogland, F., Boon, J.J., Peggie, D., Higgitt, C.: Evaluation of the "added value" of SIMS: a mass spectrometric and spectroscopic study of an unusual Naples yellow oil paint reconstruction. Int. J. Mass Spectrom. **284**, 22–34 (2009). https://doi.org/10.1016/j.ijms.2008.10.016

Keune, K., van Loon, A., Boon, J.J.: SEM backscattered-electron images of paint cross sections as information source for the presence of the Lead white pigment and Lead-related degradation and migration phenomena in oil paintings. Microsc. Microanal. **17**, 696–701 (2011). https://doi.org/10.1017/S1431927610094444

Keune, K., Boon, J.J., Boitelle, R., Shimadzu, Y.: Degradation of Emerald green in oil paint and its contribution to the rapid change in colour of the Descente des vaches (1834–1835) painted by Théodore Rousseau. Stud. Conserv. **58**, 199–210 (2013). https://doi.org/10.1179/2047058412Y.0000000063

Keune, K., Mass, J., Meirer, F., Pottasch, C., van Loon, A., Hull, A., et al.: Tracking the transformation and transport of arsenic sulfide pigments in paints: synchrotron-based X-ray microanalyses. J. Anal. At. Spectrom. **30**, 813–827 (2015). https://doi.org/10.1039/C4JA00424H

Keune, K., Mass, J., Mehta, A., Church, J., Meirer, F.: Analytical imaging studies of the migration of degraded orpiment, realgar, and emerald green pigments in historic paintings and related conservation issues. Herit. Sci. **4**, 10 (2016). https://doi.org/10.1186/s40494-016-0078-1

Kidder, L.H., Levin, I.W., Lewis, E.N., Kleiman, V.D., Heilweil, E.J.: Mercury cadmium telluride focal-plane array detection for mid-infrared Fourier-transform spectroscopic imaging. Opt. Lett. **22**, 742–744 (1997). https://doi.org/10.1364/OL.22.000742

Kirkpatrick, P., Baez, A.V.: Formation of optical images by X-rays. J. Opt. Soc. Am. **38**, 766–774 (1948). https://doi.org/10.1364/JOSA.38.000766

Kuckova, S., Hynek, R., Kodicek, M.: Identification of proteinaceous binders used in artworks by MALDI-TOF mass spectrometry. Anal. Bioanal. Chem. **388**, 201–206 (2007). https://doi.org/10.1007/s00216-007-1206-2

Kurtz, M., Strunk, J., Hinrichsen, O., Muhler, M., Fink, K., Meyer, B., et al.: Active sites on oxide surfaces: ZnO-catalyzed synthesis of methanol from CO and H 2. Angew. Chem. Int. Ed. **44**, 2790–2794 (2005). https://doi.org/10.1002/anie.200462374

Lau, D., Villis, C., Furman, S., Livett, M.: Multispectral and hyperspectral image analysis of elemental and micro-Raman maps of cross-sections from a 16th century painting. Anal. Chim. Acta. **610**, 15–24 (2008). https://doi.org/10.1016/j.aca.2007.12.043

Levenson, E., Lerch, P., Martin, M.C.: Infrared imaging: synchrotrons vs. arrays, resolution vs. speed. Infrared Phys. Technol. **49**, 45–52 (2006). https://doi.org/10.1016/j.infrared.2006.01.026

Li, J., Guériau, P., Bellato, M., King, A., Robbiola, L., Thoury, M., et al.: Synchrotron-based phase mapping in corroded metals: insights from early Copper-Base artifacts. Anal. Chem. **91**, 1815–1825 (2019). https://doi.org/10.1021/acs.analchem.8b02744

Ma, X., Beltran, V., Ramer, G., Pavlidis, G., Parkinson, D.Y., Thoury, M., et al.: Revealing the distribution of metal carboxylates in oil paint from the micro- to nanoscale. Angew. Chem. Int. Ed. **58**, 11652–11656 (2019). https://doi.org/10.1002/anie.201903553

Mahon, D., Centeno, S.A., Iacono, M., Caró, F., Stege, H., Obermeier, A.: Johannes Vermeer's mistress and maid: new discoveries cast light on changes to the composition and the discoloration of some paint passages. Herit. Sci. **8**, 30 (2020). https://doi.org/10.1186/s40494-020-00375-2

Maldanis, L., Hickman-Lewis, K., Verezhak, M., Gueriau, P., Guizar-Sicairos, M., Jaqueto, P., et al.: Nanoscale 3D quantitative imaging of 1.88 Ga Gunflint microfossils reveals novel insights into taphonomic and biogenic characters. Sci. Rep. **10**, 8163 (2020). https://doi.org/10.1038/s41598-020-65176-w

Mantler, M., Schreiner, M.: X-ray fluorescence spectrometry in art and archaeology. X-Ray Spectrom. **29**, 3–17 (2000). https://doi.org/10.1002/(SICI)1097-4539(200001/02)29:1<3::AID-XRS398>3.0.CO;2-O

Marchenko, T., Journel, L., Marin, T., Guillemin, R., Carniato, S., Žitnik, M., et al.: Resonant inelastic x-ray scattering at the limit of subfemtosecond natural lifetime. J. Chem. Phys. **134**, 144308 (2011). https://doi.org/10.1063/1.3575514

Mass, J., Sedlmair, J., Patterson, C.S., Carson, D., Buckley, B., Hirschmugl, C.: SR-FTIR imaging of the altered cadmium sulfide yellow paints in Henri Matisse's Le Bonheur de vivre (1905–6) – examination of visually distinct degradation regions. Analyst. **138**, 6032 (2013a). https://doi.org/10.1039/c3an00892d

Mass, J.L., Opila, R., Buckley, B., Cotte, M., Church, J., Mehta, A.: The photodegradation of cadmium yellow paints in Henri Matisse's le Bonheur de vivre (1905–1906). Appl. Phys. A Mater. Sci. Process. (2013b). https://doi.org/10.1007/s00339-012-7418-0

Massonnet, P., Heeren, R.M.A.: A concise tutorial review of TOF-SIMS based molecular and cellular imaging. J. Anal. At. Spectrom. **34**, 2217–2228 (2019). https://doi.org/10.1039/C9JA00164F

Mazzeo, R., Joseph, E., Prati, S., Millemaggi, A.: Attenuated Total reflection–Fourier transform infrared microspectroscopic mapping for the characterisation of paint cross-sections. Anal. Chim. Acta. **599**, 107–117 (2007). https://doi.org/10.1016/j.aca.2007.07.076

Mazzeo, R., Prati, S., Quaranta, M., Joseph, E., Kendix, E., Galeotti, M.: Attenuated total reflection micro FTIR characterisation of pigment–binder interaction in reconstructed paint films. Anal. Bioanal. Chem. **392**, 65–76 (2008). https://doi.org/10.1007/s00216-008-2126-5

Meilunas, R.J., Bentsen, J.G., Steinberg, A.: Analysis of aged paint binders by FTIR spectroscopy. Stud. Conserv. **35**, 33–51 (1990). https://doi.org/10.1179/sic.1990.35.1.33

Meirer, F., Cabana, J., Liu, Y., Mehta, A., Andrews, J.C., Pianetta, P.: Three-dimensional imaging of chemical phase transformations at the nanoscale with full-field transmission X-ray microscopy. J. Synchrotron Radiat. **18**, 773–781 (2011). https://doi.org/10.1107/S0909049511019364

Mills, L., Burnstock, A., Duarte, F., De Groot, S., Margens, L., Bisschoff, M., et al.: Water sensitivity of modern artists' oil paints. In: ICOM Preprint International Council Museums-Committee for Conservation 15th Triennial Conference New Delhi, pp. 651–659. Allied Publishers PVT, New Delhi (2008)

Monico, L., Van der Snickt, G., Janssens, K., De Nolf, W., Miliani, C., Verbeeck, J., et al.: Degradation process of Lead chromate in paintings by Vincent van Gogh studied by means of synchrotron X-ray Spectromicroscopy and related methods. 1. Artificially aged model samples. Anal. Chem. **83**, 1214–1223 (2011). https://doi.org/10.1021/ac102424h

Monico, L., Janssens, K., Miliani, C., Brunetti, B.G., Vagnini, M., Vanmeert, F., et al.: Degradation process of Lead chromate in paintings by Vincent van Gogh studied by means of Spectromicroscopic methods. 3. Synthesis, characterization, and detection of different crystal forms of the chrome yellow pigment. Anal. Chem. **85**, 851–859 (2013). https://doi.org/10.1021/ac302158b

Monico, L., Janssens, K., Hendriks, E., Brunetti, B.G., Miliani, C.: Raman study of different crystalline forms of PbCrO 4 and PbCr 1−x S x O 4 solid solutions for the noninvasive identification of chrome yellows in paintings: a focus on works by Vincent van Gogh. J. Raman Spectrosc. **45**, 1034–1045 (2014). https://doi.org/10.1002/jrs.4548

Monico, L., Janssens, K., Alfeld, M., Cotte, M., Vanmeert, F., Ryan, C.G., et al.: Full spectral XANES imaging using the Maia detector array as a new tool for the study of the alteration process of chrome yellow pigments in paintings by Vincent van Gogh. J. Anal. At. Spectrom. **30**, 613–626 (2015a). https://doi.org/10.1039/C4JA00419A

Monico, L., Janssens, K., Hendriks, E., Vanmeert, F., der Snickt, G., Cotte, M., et al.: Evidence for degradation of the chrome yellows in van Gogh's sunflowers : a study using noninvasive in situ methods and synchrotron-radiation-based X-ray techniques. Angew. Chem. Int. Ed. **54**, 13923–13927 (2015b). https://doi.org/10.1002/anie.201505840

Monico, L., Janssens, K., Cotte, M., Sorace, L., Vanmeert, F., Brunetti, B.G., et al.: Chromium speciation methods and infrared spectroscopy for studying the chemical reactivity of lead chromate-based pigments in oil medium. Microchem. J. **124**, 272–282 (2016). https://doi.org/10.1016/j.microc.2015.08.028

Monico, L., Cartechini, L., Rosi, F., Chieli, A., Grazia, C., De Meyer, S., et al.: Probing the chemistry of CdS paints in the scream by in situ noninvasive spectroscopies and synchrotron radiation x-ray techniques. Sci. Adv. **6**, eaay3514 (2020a). https://doi.org/10.1126/sciadv.aay3514

Monico, L., Cotte, M., Vanmeert, F., Amidani, L., Janssens, K., Nuyts, G., et al.: Damages induced by synchrotron radiation-based X-ray microanalysis in chrome yellow paints and related Cr-compounds: assessment, quantification, and mitigation strategies. Anal. Chem. **92**, 14164–14173 (2020b). https://doi.org/10.1021/acs.analchem.0c03251

Morsch, S., van Driel, B.A., van den Berg, K.J., Dik, J.: Investigating the photocatalytic degradation of oil paint using ATR-IR and AFM-IR. ACS Appl. Mater. Interfaces. **9**, 10169–10179 (2017). https://doi.org/10.1021/acsami.7b00638

Nevin, A., Cesaratto, A., Bellei, S., D'Andrea, C., Toniolo, L., Valentini, G., Comelli, D.: Time-resolved photoluminescence spectroscopy and imaging: New approaches to the analysis of cultural heritage and its degradation. Sensors. **14**(4), 6338–6355 (2014). https://doi.org/10.3390/s140406338

Nevin, A., Comelli, D., Valentini, G., Cubeddu, R.: Total synchronous fluorescence spectroscopy combined with multivariate analysis: method for the classification of selected resins, oils, and protein-based media used in paintings. Anal. Chem. **81**, 1784–1791 (2009). https://doi.org/10.1021/ac8019152

Niehuis, E., Heller, T., Feld, H., Benninghoven, A.: Design and performance of a reflectron based time-of-flight secondary ion mass spectrometer with electrodynamic primary ion mass separation. J. Vac. Sci. Technol. A Vac. Surf. Film. **5**, 1243–1246 (1987). https://doi.org/10.1116/1.574781

Noble, P., Boon, J.J., Wadum, J.: Dissolution, aggregation, and protrusion: Lead soap formation in 17th century grounds and paint layers. Art Matters. **1**, 46–61 (2002)

Noble, P., Van Duijn, E., Hermens, E., Keune, K., Van Loon, A., Smelt, S., et al.: An exceptional commission. Rijksmus Bull. **66**, 308–345 (2018). https://doi.org/10.52476/trb.9762

Norton, S.J.: Compton scattering tomography. J. Appl. Phys. **76**, 2007–2015 (1994). https://doi.org/10.1063/1.357668

Noun, M., Van Elslande, E., Touboul, D., Glanville, H., Bucklow, S., Walter, P., et al.: High mass and spatial resolution mass spectrometry imaging of Nicolas Poussin painting cross section by cluster TOF-SIMS. J. Mass Spectrom. **51**, 1196–1210 (2016). https://doi.org/10.1002/jms.3885

Opilik, L., Schmid, T., Zenobi, R.: Modern Raman imaging: vibrational spectroscopy on the micrometer and nanometer scales. Annu. Rev. Anal. Chem. **6**, 379–398 (2013). https://doi.org/10.1146/annurev-anchem-062012-092646

Osmond, G.: Zinc white and the influence of paint composition for stability in oil based media. In: Issues in Contemporary Oil Paint, pp. 263–281. Springer International Publishing, Cham (2014). https://doi.org/10.1007/978-3-319-10100-2_18

Osmond, G., Boon, J.J., Puskar, L., Drennan, J.: Metal stearate distributions in modern artists' oil paints: surface and cross-sectional investigation of reference paint films using conventional and synchrotron infrared microspectroscopy. Appl. Spectrosc. **66**, 1136–1144 (2012). https://doi.org/10.1366/12-06659

Osmond, G., Ebert, B., Drennan, J.: Zinc oxide-centred deterioration in 20th century Vietnamese paintings by Nguyễn Trọng Kiệm (1933–1991). AICCM Bull. **34**, 4–14 (2013). https://doi.org/10.1179/bac.2013.34.1.002

Otero, V., Sanches, D., Montagner, C., Vilarigues, M., Carlyle, L., Lopes, J.A., et al.: Characterisation of metal carboxylates by Raman and infrared spectroscopy in works of art. J. Raman Spectrosc. **45**, 1197–1206 (2014). https://doi.org/10.1002/jrs.4520

Pan, X., Yang, M.-Q., Fu, X., Zhang, N., Xu, Y.-J.: Defective TiO2 with oxygen vacancies: synthesis, properties and photocatalytic applications. Nanoscale. **5**, 3601–3614 (2013). https://doi.org/10.1039/c3nr00476g

Papillon, M., Lefevre, R., Lahanier, C., Duval, A., Rioux, J.: Analyses de pigments blancs appliquées à l'étude chronologique des peintures de chevalet—blanc de titane. In: Grimstad, K. (ed.) Committee for Conservation; 8th Triennial Meeting. Getty Conservation Institute, Los Angeles (1987)

Pascarelli, S., Mathon, O., Mairs, T., Kantor, I., Agostini, G., Strohm, C., et al.: The time-resolved and extreme-conditions XAS (TEXAS) facility at the European Synchrotron Radiation Facility: the energy-dispersive X-ray absorption spectroscopy beamline ID24. J. Synchrotron Radiat. **23**, 353–368 (2016). https://doi.org/10.1107/S160057751501783X

Penner-Hahn, J.E.: X-ray absorption spectroscopy in coordination chemistry. Coord. Chem. Rev. **190–192**, 1101–1123 (1999). https://doi.org/10.1016/S0010-8545(99)00160-5

Pouyet, E., Cotte, M., Fayard, B., Salomé, M., Meirer, F., Mehta, A., et al.: 2D X-ray and FTIR micro-analysis of the degradation of cadmium yellow pigment in paintings of Henri Matisse. Appl. Phys. A Mater. Sci. Process. **121**, 967–980 (2015). https://doi.org/10.1007/s00339-015-9239-4

Price, S.W.T., Van Loon, A., Keune, K., Parsons, A.D., Murray, C., Beale, A.M., et al.: Unravelling the spatial dependency of the complex solid-state chemistry of Pb in a paint micro-sample from Rembrandt's Homer using XRD-CT. Chem. Commun. **55**, 1931–1934 (2019). https://doi.org/10.1039/C8CC09705D

Radepont, M., de Nolf, W., Janssens, K., Van der Snickt, G., Coquinot, Y., Klaassen, L., et al.: The use of microscopic X-ray diffraction for the study of HgS and its degradation products corderoite (α-Hg3S2Cl2), kenhsuite (γ-Hg3S2Cl2) and calomel (Hg2Cl2) in historical paintings. J. Anal. At. Spectrom. **26**, 959–968 (2011). https://doi.org/10.1039/c0ja00260g

Rehr, J.J., Albers, R.C.: Theoretical approaches to x-ray absorption fine structure. Rev. Mod. Phys. **72**, 621–654 (2000). https://doi.org/10.1103/RevModPhys.72.621

Reynaud, C., Thoury, M., Dazzi, A., Latour, G., Scheel, M., Li, J., et al.: In-place molecular preservation of cellulose in 5,000-year-old archaeological textiles. Proc. Natl. Acad. Sci. **117**, 19670–19676 (2020). https://doi.org/10.1073/pnas.2004139117

Richardin, P., Mazel, V., Walter, P., Laprévote, O., Brunelle, A.: Identification of different copper green pigments in renaissance paintings by cluster-TOF-SIMS imaging analysis. J. Am. Soc. Mass Spectrom. **22**, 1729–1736 (2011). https://doi.org/10.1007/s13361-011-0171-3

Robertson, D.W.: Lead Titanate. Ind. Eng. Chem. **28**, 216–218 (1936). https://doi.org/10.1021/ie50314a017

Robinet, L., Spring, M., Pagès-Camagna, S., Vantelon, D., Trcera, N.: Investigation of the discoloration of smalt pigment in historic paintings by micro-X-ray absorption spectroscopy at the Co K-Edge. Anal. Chem. **83**, 5145–5152 (2011). https://doi.org/10.1021/ac200184f

Rogala, D., Lake, S., Maines, C., Mecklenburg, M.: Condition problems related to zinc oxide Underlayers: examination of selected abstract expressionist paintings from the collection of the Hirshhorn Museum and Sculpture Garden, Smithsonian Institution. J. Am. Inst. Conserv. **49**, 96–113 (2010). https://doi.org/10.1179/019713610804489937

Romano, C., Lam, T., Newsome, G.A., Taillon, J.A., Little, N., Tsang, J.: Characterization of zinc carboxylates in an oil paint test panel. Stud. Conserv. **65**, 14–27 (2020). https://doi.org/10.1080/00393630.2019.1666467

Ropret, P., Miliani, C., Centeno, S.A., Tavzes, Č., Rosi, F.: Advances in Raman mapping of works of art. J. Raman Spectrosc. **41**, 1462–1467 (2010). https://doi.org/10.1002/jrs.2733

Rorimer, J.: Marble sculpture and the ultra-violet ray. Metrop. Mus. Art Bull. **24**, 185–186 (1929)

Rorimer, J.J.: Ultra-Violet Rays and Their Use in the Examination of Works of Art. Metropolitan Museum of Art, New York (1931)

Rösner, B., Koch, F., Döring, F., Bosgra, J., Guzenko, V.A., Kirk, E., et al.: Exploiting atomic layer deposition for fabricating sub-10 nm X-ray lenses. Microelectron. Eng. **191**, 91–96 (2018). https://doi.org/10.1016/j.mee.2018.01.033

Sabatini, F., Lluveras-Tenorio, A., Degano, I., Kuckova, S., Krizova, I., Colombini, M.P.: A matrix-assisted laser desorption/ionization time-of-flight Mass spectrometry method for the identification of Anthraquinones: the case of Historical Lakes. J. Am. Soc. Mass Spectrom. **27** (2016). https://doi.org/10.1007/s13361-016-1471-4

Sahle, C.J., Mirone, A., Vincent, T., Kallonen, A., Huotari, S.: Improving the spatial and statistical accuracy in X-ray Raman scattering based direct tomography. J. Synchrotron Radiat. **24**, 476–481 (2017a). https://doi.org/10.1107/S1600577517000169

Sahle, C.J., Rosa, A.D., Rossi, M., Cerantola, V., Spiekermann, G., Petitgirard, S., et al.: Direct tomography imaging for inelastic X-ray scattering experiments at high pressure. J. Synchrotron Radiat. **24**, 269–275 (2017b). https://doi.org/10.1107/S1600577516017100

Sakdinawat, A., Attwood, D.: Nanoscale X-ray imaging. Nat. Photonics. **4**, 840–848 (2010). https://doi.org/10.1038/nphoton.2010.267

Salvadó, N., Butí, S., Nicholson, J., Emerich, H., Labrador, A., Pradell, T.: Identification of reaction compounds in micrometric layers from gothic paintings using combined SR-XRD and SR-FTIR. Talanta. **79**, 419–428 (2009). https://doi.org/10.1016/j.talanta.2009.04.005

Salzer, R.W., Siesler, H. (eds.): Infrared and Raman Spectroscopic Imaging. John Wiley & Sons, Ltd, Weinheim (2009)

San Andres, M., Baez, M.I., Baldonedo, J.L., Barba, C.: Transmission electron microscopy applied to the study of works of art: sample preparation methodology and possible techniques. J. Microsc. **188**, 42–50 (1997). https://doi.org/10.1046/j.1365-2818.1997.2460804.x

Sanyova, J., Cersoy, S., Richardin, P., Laprévote, O., Walter, P., Brunelle, A.: Unexpected materials in a Rembrandt painting characterized by high spatial resolution cluster-TOF-SIMS imaging. Anal. Chem. **83**, 753–760 (2011). https://doi.org/10.1021/ac1017748

Schaeberle, M.D., Morris, H.R., Ii, J.F.T., Treado, P.J.: Peer reviewed: Raman chemical imaging spectroscopy. Anal. Chem. **71**, 175A–181A (1999). https://doi.org/10.1021/ac990251u

Schiering, D.W., Tague, T.J., Reffner, J.A., Vogel, S.H.: A dual confocal aperturing microscope for IR microspectrometry. Analusis. **28**, 46–52 (2000). https://doi.org/10.1051/analusis:2000280046

Schwartz, A.J., Kumar, M., Adams, B.L., Field, D.P. (eds.): Electron Backscatter Diffraction in Materials Science. Springer US, Boston (2009). https://doi.org/10.1007/978-0-387-88136-2

Shearer, J.C., Peters, D.C., Hoepfner, G., Newton, T.: FTIR in the service of art conservation. Anal. Chem. **55**, 874A–880A (1983). https://doi.org/10.1021/ac00259a002

Simoen, J., De Meyer, S., Vanmeert, F., de Keyser, N., Avranovich, E., Van der Snickt, G., et al.: Combined micro- and macro scale X-ray powder diffraction mapping of degraded orpiment paint in a 17th century still life painting by Martinus Nellius. Herit. Sci. **7**, 83 (2019). https://doi.org/10.1186/s40494-019-0324-4

Sloggett, R.: Unmasking art forgery: scientific approaches. In: The Palgrave Handbook on Art Crime, pp. 381–406. Palgrave Macmillan UK, London (2019). https://doi.org/10.1057/978-1-137-54405-6_19

Solé, V.A., Papillon, E., Cotte, M., Walter, P., Susini, J.: A multiplatform code for the analysis of energy-dispersive X-ray fluorescence spectra. Spectrochim. Acta Part B Atom. Spectrosc. **62**, 63–68 (2007). https://doi.org/10.1016/j.sab.2006.12.002

Spring, M., Grout, R.: The blackening of Vermillion: an analytical study of the process in paintings. Natl. Gall Tech. Bull. **23**, 50–61 (2002)

Spring, M., Ricci, C., Peggie, D.A., Kazarian, S.G.: ATR-FTIR imaging for the analysis of organic materials in paint cross sections: case studies on paint samples from the National Gallery, London. Anal. Bioanal. Chem. **392**, 37–45 (2008). https://doi.org/10.1007/s00216-008-2092-y

Sun, T., Ding, X., Liu, Z., Zhu, G., Li, Y., Wei, X., et al.: Characterization of a confocal three-dimensional micro X-ray fluorescence facility based on polycapillary X-ray optics and Kirkpatrick–Baez mirrors. Spectrochim. Acta Part B Atom. Spectrosc. **63**, 76–80 (2008). https://doi.org/10.1016/j.sab.2007.11.003

Tan, H., Tian, H., Verbeeck, J., Monico, L., Janssens, K., Van Tendeloo, G.: Nanoscale investigation of the degradation mechanism of a historical chrome yellow paint by quantitative electron energy loss spectroscopy mapping of chromium species. Angew. Chem. Int. Ed. **52**, 11360–11363 (2013). https://doi.org/10.1002/anie.201305753

Tanasa, P.O., Sandu, I., Vasilache, V., Sandu, I.G., Negru, I.C., Sandu, A.V.: Authentication of a painting by Nicolae Grigorescu using modern multi-analytical methods. Appl. Sci. **10**, 3558 (2020). https://doi.org/10.3390/app10103558

Thoury, M., Echard, J.-P., Réfrégiers, M., Berrie, B., Nevin, A., Jamme, F., et al.: Synchrotron UV−visible multispectral luminescence microimaging of historical samples. Anal. Chem. **83**, 1737–1745 (2011). https://doi.org/10.1021/ac102986h

Thoury, M., Van Loon, A., Keune, K., Hermans, J.J., Réfrégiers, M., Berrie, B.H.: Photoluminescence micro-imaging sheds new light on the development of metal soaps in oil paintings. In: Casadio, F., Keune, K., Noble, P., Van Loon, A., Hendriks, E., Centeno, S., et al. (eds.) Metal Soaps in Art, pp. 211–225 (2019). https://doi.org/10.1007/978-3-319-90617-1_12

Trentelman, K., Stodulski, L., Pavlosky, M.: Characterization of Pararealgar and other light-induced transformation products from Realgar by Raman microspectroscopy. Anal. Chem. **68**, 1755–1761 (1996). https://doi.org/10.1021/ac951097o

van den Berg, J.D.J., van den Berg, K.J., Boon, J.J.: Chemical changes in curing and ageing oil paints. In: ICOM Committee for Conservation, 12th Triennial Meeting. Lyon 29 August – 3 September 1999. James & James (Science Publishers) Ltd, Lyon (1999)

Van Der Snickt, G., Dik, J., Cotte, M., Janssens, K., Jaroszewicz, J., De Nolf, W., et al.: Characterization of a degraded cadmium yellow (CdS) pigment in an oil painting by means of synchrotron radiation based X-ray techniques. Anal. Chem. **81**, 2600–2610 (2009). https://doi.org/10.1021/ac802518z

Van Der Snickt, G., Janssens, K., Dik, J., De Nolf, W., Vanmeert, F., Jaroszewicz, J., et al.: Combined use of synchrotron radiation based micro-X-ray fluorescence, micro-X-ray diffraction, micro-X-ray absorption near-edge, and micro-Fourier transform infrared spectroscopies for revealing an alternative degradation pathway of the pigment cadmium ye. Anal. Chem. **84**, 10221–10228 (2012). https://doi.org/10.1021/ac3015627

Van der Snickt, G., Dubois, H., Sanyova, J., Legrand, S., Coudray, A., Glaude, C., et al.: Large-area elemental imaging reveals Van Eyck's original paint layers on the Ghent altarpiece (1432), Rescoping its conservation treatment. Angew. Chem. Int. Ed. **56**, 4797–4801 (2017). https://doi.org/10.1002/anie.201700707

Van der Weerd, J., Geldof, M., Van der Loeff, L., Heeren, R., Boon, J.J.: Zinc soap aggregate formation in 'falling leaves' (Les Alyscamps)' by Vincent van Gogh. Zeitschrift Für Kunsttechnologie Und Konserv. **17**, 407–416 (2004)

van Driel, B.A., Kooyman, P.J., van den Berg, K.J., Schmidt-Ott, A., Dik, J.: A quick assessment of the photocatalytic activity of TiO2 pigments — from lab to conservation studio! Microchem. J. **126**, 162–171 (2016). https://doi.org/10.1016/j.microc.2015.11.048

van Driel, B., Artesani, A., van den Berg, K.J., Dik, J., Mosca, S., Rossenaar, B., et al.: New insights into the complex photoluminescence behaviour of titanium white pigments. Dyes Pigments. **155**, 14–22 (2018). https://doi.org/10.1016/j.dyepig.2018.03.012

Van Loon, A., Noble, P., Boon, J.J.: White hazes and surface crusts in Rembrandt's homer and related paintings. In: ICOM-CC 16th Triennial Conference Lisbon 19–23 September 2011 Preprint. ICOM (2011)

Van Loon, A., Hoppe, R., Keune, K., Hermans, J.J., Diependaal, H., Bisschoff, M., et al.: Paint delamination as a result of zinc soap formation in an early Mondrian painting. In: Casadio, F., Keune, K., Noble, P., Van Loon, A., Hendriks, E., Centeno, S., et al. (eds.) Metal Soaps in Art, pp. 359–373. Springer, Houten (2019). https://doi.org/10.1007/978-3-319-90617-1_21

Vandivere, A., van Loon, A., Callewaert, T., Haswell, R., Proaño Gaibor, A.N., van Keulen, H., et al.: Fading into the background: the dark space surrounding Vermeer's girl with a pearl earring. Herit. Sci. **7**, 69 (2019a). https://doi.org/10.1186/s40494-019-0311-9

Vandivere, A., van Loon, A., Dooley, K.A., Haswell, R., Erdmann, R.G., Leonhardt, E., et al.: Revealing the painterly technique beneath the surface of Vermeer's girl with a pearl earring using macro- and microscale imaging. Herit. Sci. **7**, 64 (2019b). https://doi.org/10.1186/s40494-019-0308-4

Vanmeert, F., Van der Snickt, G., Janssens, K.: Plumbonacrite identified by X-ray powder diffraction tomography as a missing link during degradation of red Lead in a van Gogh painting. Angew. Chem. Int. Ed. **54**, 3607–3610 (2015). https://doi.org/10.1002/anie.201411691

Vanmeert, F., De Nolf, W., De Meyer, S., Dik, J., Janssens, K.: Macroscopic X-ray powder diffraction scanning, a new method for highly selective chemical imaging of works of art: instrument optimization. Anal. Chem. **90**, 6436–6444 (2018). https://doi.org/10.1021/acs.analchem.8b00240

Villafana, T.E., Brown, W.P., Delaney, J.K., Palmer, M., Warren, W.S., Fischer, M.C.: Femtosecond pump-probe microscopy generates virtual cross-sections in historic artwork. Proc. Natl. Acad. Sci. **111**, 1708–1713 (2014). https://doi.org/10.1073/pnas.1317230111

Voras, Z.E., DeGhetaldi, K., Wiggins, M.B., Buckley, B., Baade, B., Mass, J.L., et al.: ToF–SIMS imaging of molecular-level alteration mechanisms in Le Bonheur de vivre by Henri Matisse. Appl. Phys. A Mater. Sci. Process. **121**, 1015–1030 (2015). https://doi.org/10.1007/s00339-015-9508-2

Welcomme, E., Walter, P., Bleuet, P., Hodeau, J.-L., Dooryhee, E., Martinetto, P., et al.: Classification of lead white pigments using synchrotron radiation micro X-ray diffraction. Appl. Phys. A Mater. Sci. Process. **89**, 825–832 (2007). https://doi.org/10.1007/s00339-007-4217-0

Wille, G., Bourrat, X., Maubec, N., Lahfid, A.: Raman-in-SEM, a multimodal and multiscale analytical tool: performance for materials and expertise. Micron. **67**, 50–64 (2014). https://doi.org/10.1016/j.micron.2014.06.008

Williams, D.B., Carter, C.B.: Transmission Electron Microscopy. Springer US, Boston (2009). https://doi.org/10.1007/978-0-387-76501-3

Yu, H., Winkler, S.: Image complexity and spatial information. In: 2013 Fifth International Workshop on Quality of Multimedia Experience, pp. 12–17. IEEE (2013)

Yu, J., Warren, W.S., Fischer, M.C.: Visualization of vermilion degradation using pump-probe microscopy. Sci. Adv. **5**, eaaw3136 (2019). https://doi.org/10.1126/sciadv.aaw3136

Zhang, M., Averseng, F., Haque, F., Borghetti, P., Krafft, J.-M., Baptiste, B., et al.: Defect-related multicolour emissions in ZnO smoke: from violet, over green to yellow. Nanoscale. **11**, 5102–5115 (2019). https://doi.org/10.1039/C8NR09998G

Zhao, H., Pan, F., Li, Y.: A review on the effects of TiO2 surface point defects on CO2 photoreduction with H2O. J. Mater. **3**, 17–32 (2017). https://doi.org/10.1016/j.jmat.2016.12.001

Zumbühl, S., Scherrer, N.C., Eggenberger, U.: Derivatization technique to increase the spectral selectivity of two-dimensional Fourier transform infrared focal plane Array imaging: analysis of binder composition in aged oil and tempera paint. Appl. Spectrosc. **68**, 458–465 (2014). https://doi.org/10.1366/13-07280

Part IV
Isotopic Analysis for Authentication

Chapter 13
Dating of Artwork by Radiocarbon

Johannes van der Plicht and Irena Hajdas

Abstract The Radiocarbon method, which allows analysis of carbon bearing material and its potential for dating artwork is reviewed. The development of the ^{14}C measurement techniques (conventional and AMS) and its significance for dating art is discussed. This includes the present state-of-the-art of the Radiocarbon dating method on timescale calibration, sample quality aspects, and sample pretreatment. Dating of paintings and textiles are discussed as case studies.

Keywords Radiocarbon · Dating · Paintings · Textiles

13.1 Radiocarbon Dating

13.1.1 Introduction

The Radiocarbon (^{14}C) dating method was developed during the years around 1950 (Libby 1952; Taylor and Aitken 1997). The method enables direct dating of organic remains back to about 50,000 years ago. Since that time, several "revolutions" have improved the method considerably. Among the most significant ones are the introduction of AMS in the 1980s, and calibration of the ^{14}C timescale to obtain absolute dates.

AMS (Accelerator Mass Spectrometry) enables small (milligram size) sample analysis (Tuniz et al. 1998; Jull 2013). This is a factor of 1000 less than the original, so-called conventional method based on radiometry (e.g. Cook and van der Plicht 2013). AMS therefore enables ^{14}C dating of intrinsically small samples such as

J. van der Plicht (✉)
Center for Isotope Research, University of Groningen, Groningen, the Netherlands
e-mail: j.vander.plicht@rug.nl

I. Hajdas
Laboratory of Ion Beam Physics, ETH Zürich, Zürich, Switzerland

M. P. Colombini et al. (eds.), *Analytical Chemistry for the Study of Paintings and the Detection of Forgeries*, Cultural Heritage Science,
https://doi.org/10.1007/978-3-030-86865-9_13

botanical remains (pollen and seeds) and of precious samples, such as archaic human bones and artefacts and valuable works of art (Caforio et al. 2014; Fedi et al. 2013).

Calibration now enables absolute dating back to 50,000 years ago (Reimer et al. 2020), i.e. the complete dating range. In turn, this spawned "revolutions" in many applications among which archaeology, palaeontology and quaternary geology. Radiocarbon provides a "yardstick of time", enabling the measurement of past time by scientific means, independent of associations and assumptions (e.g. van der Plicht and Bruins 2001).

While the principle of the method is basically simple, it is complex in detail and errors in matters concerning both sampling and technical laboratory aspects. Stringent quality control is necessary, which involves regular laboratory intercomparisons, duplicate measurements, sample selection, association, and others (van Strydonck et al. 1999; Scott 2003). In addition to ^{14}C dating, the contents of the stable carbon isotope ^{13}C of the sample is also measured (Mook 2006). This provides insight in chemical processes applied to the sample, like conservation material.

In this paragraph, a short review of the principles of the ^{14}C method and conventions is given. The application discussed here is dating of artwork, in particular paintings. Selected case studies will be discussed.

13.1.2 The ^{14}C Dating Method

The element carbon consists of 3 naturally occurring isotopes: ^{12}C, ^{13}C and ^{14}C with abundances of ca. 98.9%, 1.1% and 10^{-10}%, respectively. The isotope ^{14}C (Radiocarbon) is continuously produced in the earth's atmosphere by cosmic radiation. Radiocarbon is radioactive and decays with a currently accepted half-life of 5700 years (Kutschera 2019). A stationary state of production, distribution between the main carbon reservoirs (atmosphere, ocean and biosphere) and decay results in a more or less constant ^{14}C concentration in atmospheric CO_2 and the terrestrial biosphere (e.g. Libby 1952). Upon death of an organism, the radioactive ^{14}C decays, and by measuring the amount of remaining ^{14}C in the sample its time of death can be derived. For accurate Radiocarbon dating, only the ^{14}C that was part of the organism when it died should be measured. This requires so-called pretreatment of the sample (described below).

It is known for some time that the ^{14}C concentration of atmospheric CO_2 has not always been the same in the past. In tree rings, natural variations of the atmospheric $^{14}CO_2$ abundance were discovered on a time scale of one decade to a few centuries (de Vries 1958). Later it was discovered that these variations can be attributed to variations in solar activity (Stuiver 1965), which in turn influence the production of ^{14}C in the atmosphere. Also changes of the geomagnetic field strength influence the production of ^{14}C in the atmosphere (Bucha 1970). This is understood because both solar activity and geomagnetic field strength determine the amount of cosmic radiation impinging on the earth (van der Plicht 2013 and references therein). In addition,

the atmospheric $^{14}CO_2$ concentration also depends on exchange between the atmosphere and ocean.

Because of these variations in the natural ^{14}C concentration, the ^{14}C clock runs at a varying pace, different from real clocks: ^{14}C time is not equivalent to calender time. Therefore, the ^{14}C timescale has been defined and needs to be calibrated to establish the relationship between ^{14}C time and historical time. This definition is known as the "Radiocarbon convention".

The ^{14}C Convention

The convention consists of the following four parts (i–iv), and is subsequently explained in more detail below.

(i) The ^{14}C radioactivity is measured relative to that of a modern reference material, which is Oxalic Acid with a radioactivity of 0.226 Bq/gC.[1]
(ii) From this measured radioactivity the "Radiocarbon date" is calculated using a half-life of 5568 years.
(iii) The Radiocarbon dates are expressed in the unit BP.
(iv) The Radiocarbon dates are corrected for isotope effects (called fractionation) using the stable isotope ^{13}C by standardizing to $\delta^{13}C = -25‰$.

The convention is largely "historic" and was established among laboratories to standardize methods and reporting, and avoiding confusion in interpretations. See Flint and Deevey 1962. The conventions (i)–(iv) need some clarification.

(i) Various standard materials from modern samples appeared to have different activities, caused by natural and anthropogenic effects. The chosen standard oxalic acid relates to AD 1950. However, a batch of wood from AD 1950 has a specific activity of 95% of the oxalic acid standard.
(ii) The original half-life value used in the first decade of Radiocarbon dating, the so-called Libby value is 5568 years. However, the proper value was later established as 5700 ± 30 years (Kutschera 2019 and references therein) which is significantly larger than the Libby value. Nevertheless, the Libby value is chosen as convention; any change would cause confusion with the many dates already published at the time. The convention ensures that all ^{14}C dates keep the same meaning. The deviation between the defined ^{14}C timescale and the calendar introduced this way is taken care of by calibration as explained below.
(iii) Radiocarbon dates were originally reported in "BP" which means Before Present, present being 1950. This later appeared not to be correct calendar years because of the half-life ambiguity and the varying ^{14}C contents in nature.

One has chosen to keep using the unit BP, to avoid introducing confusion with earlier published dates. But it means now Before Present on the ^{14}C timescale, and not on the calendar timescale. There is one confusion left unfortunately, "Present" is not to be taken in the literal sense. It does not mean today, nor AD 1950.

[1] Becquerel (Bq) per gram Carbon; 1 Bq equals 1 decay per second.

(iv) Fractionation arises from the differences in natural and laboratory processes for the different isotopes, caused by their different masses. For example, in biological pathways lighter isotopes are taken up preferentially, reducing the proportion of ^{14}C in a sample making it seem older. The proportion of ^{13}C is also changed. This isotope is stable, i.e. its concentration is constant throughout time. Therefore, the ratio of the stable isotopes ^{13}C and ^{12}C in a sample can be used to estimate the fractionation effect for ^{14}C. The Radiocarbon convention implies that the fractionation correction must be to a standardized value for the $^{13}C/^{12}C$ ratio to $\delta^{13}C = -25‰$. The δ values are defined as the relative difference of the $^{13}C/^{12}C$ ratio of a sample to that of a reference material:

$$\delta^{13}C = \left[{}^{13}R_{\text{sample}} - {}^{13}R_{\text{reference}} \right] / {}^{13}R_{\text{reference}}$$

where we introduced the so-called isotope ratio

$${}^{13}R = \left[{}^{13}C / {}^{12}C \right].$$

The δ values are usually expressed in permil (‰). The reference material is Vienna PeeDee Belemnite (VPDB) (see Mook 2006 and references therein).

Since $\delta^{14}C \approx 2\,\delta^{13}C$, fractionation effects can be normalized out as is done by the convention. For more technical details, we refer to the literature (e.g. Mook 2006).

In the following we will use both the ^{14}C age (in BP) and the "activity ratio" ^{14}a, defined as the measured ^{14}C radioactivity A(t) (A at time t in Bq) relative to that of the standard: $^{14}a = A(t)/A(t = 0)$. Thus, for the Oxalic Acid standard $^{14}a = 1$ or 100%; for a sample with a (conventional) half-life of 5568 years $^{14}a = 0.5$ or 50%. See Mook and van der Plicht 1999 for details, other definitions and references.

The exponential decay law for the activity ratio is

$${}^{14}a = A(t) / A(t = 0) = \exp(-\lambda t) \text{ with } \lambda = \ln(2) / T_{1/2}$$

Use of the half-life value $T_{1/2} = 5568$ years then leads to the conventional age t:

$$t = -8033 \ln\left({}^{14}a \right) BP.$$

13.2 Measuring Techniques

13.2.1 Sample Pretreatment

The ^{14}C content in natural (organic) materials is small: $^{14}C/^{12}C \approx 10^{-12}$ for recent material, decreasing to $^{14}C/^{12}C \approx 10^{-15}$ for samples of about 50,000 years old. The latter is the detection limit for the method. This is the attomole sensitivity regime

(Vogel et al. 1995) and also means that the method is rather sensitive to contamination of other Carbon containing materials, which are present abound.

In archaeology, contamination most often results in younger dates because of penetration with younger materials from above in the stratigraphy. In art, contamination can go in different directions. For example, in historical times glue could have been applied which is made from bone contemporaneous with the sample. Today, conservation and restauration materials are usually "fossil" (originating from the oil industry) and thus do not contain ^{14}C. When not removed, that would make the date too old.

Quantitively, the effect of contaminants can be calculated by the mixing equation:

$$^{14}a(m) = (1-f)^{14}a(s) + f^{14}a(c)$$

where f is the mass fraction of the contamination, $^{14}a(m)$ is the measured activity, $^{14}a(s)$ is the true activity of the sample and $^{14}a(c)$ is the activity of the contaminant. For modern contamination, $^{14}a(c) = 1$, and for fossil contamination, $^{14}a(c) = 0$. Worked examples can be found in Mook and Streurman (1983).

Therefore, so-called pretreatment of sample materials is needed, consisting of isolating the datable fraction, and removing foreign contaminants. This is done by a mixture of physical and chemical methods.

In general, the sample is subject to subsequent Acid/Base/Acid baths, the so-called ABA method. The first acid bath removes carbonates and fulvic acids, the base bath removes humates, and the final acid bath removes any CO_2 absorbed during the base step. Standard procedures include 4% HCl for the A steps at 80 °C during 24 h, and 1% NaOH at 80 °C during 24 h for the B step (Mook and Streurman 1983; Bayliss et al. 2004; Hajdas 2008, Brock et al. 2010, Brock et al. 2018). For more fragile samples, acid/base strength, temperature and duration can be softened, and/or only the first A step can be applied. In combination with such a cleaning procedure, a datable fraction can be prepared. Relevant for the subject of this article, cellulose can be prepared for wood (for example Nemec et al. 2010; Dee et al. 2020). Treatment with solvents is applied whenever an addition of exogenous carbon in a process of conservation is suspected or detected (Hajdas et al. 2004). Such treatment is often performed in a Soxhlet apparatus shown in the application to art objects.

There are two different techniques available for measuring the ^{14}C content in a sample: radiometry and mass spectrometry (AMS). These will be discussed below. They differ mainly in the sample quantity needed for analysis. For radiometry this is typically 1 gram of Carbon; for AMS, this is 1 mg of C. The pretreatment for both methods is the same (except for the quantity of materials involved). AMS is usually required for dating works of art, but radiometry is still in use in limited cases; mostly wooden artefacts when it is not a problem to sample 1 gram of material.

13.2.2 Radiometry

The original technique for measuring ^{14}C is radiometry, developed in the late 1940s by Libby who received the Nobel prize for chemistry for his work in 1960 (Olsson 1970). We will only briefly summarize this method here, because recently it has been to a large part replaced by AMS.

Radiometry for ^{14}C is not straightforward for two reasons. First, ^{14}C is a β^-emitter; the energy of the β rays is very low. Second, the activity is very low and is hampered by environmental radioactivity.

The first is solved by combusting the pre-treated sample material into CO_2. This CO_2 is led into a proportional gas counter. The CO_2 acts as both counting gas and internal radioactive source ($^{14}CO_2$).

The second problem is solved by shielding the equipment and locating it in a low background environment. The shielding is both passive (low activity lead bricks) and active (measuring the background radiation in anti-coincidence with the radiation from the $^{14}CO_2$ gas).

The above describes radiometry by proportional gas counting (PGC). There is another radiometric method, liquid scintillation counting (LSC). Here the CO_2 gas is transferred into benzene (C_6H_6). An amount of scintillant is added, which emits light when a β particle is emitted by ^{14}C. This light is subsequently detected by a photomultiplier.

Both radiometric methods (PGC and LSC) have been developed into very reliable dating methods, reaching precision of 2‰ in age. However, a major disadvantage is that they require large samples, typically 1 gram of Carbon.

For more details on both radiometric methods, we refer to the literature, e.g., Cook and van der Plicht (2013).

13.2.3 Accelerator Mass Spectrometry

Mass spectrometry as a technique for measuring isotope concentrations require small sample amounts, 1 mg of Carbon. For the stable isotopes of major relevance for natural processes like ^{13}C, ^{18}O and also ^{2}H and ^{15}N, IRMS (Isotope Ratio Mass Spectrometry) has been developed since the 1950s (e.g., Craig 1953; Mook and Grootes 1973). For ^{14}C with abundances many orders of magnitude less than the stable isotopes, this method does not work because of the "isobar problem" in molecular mass spectrometry: $^{14}CO_2$ has the same molecular mass as (mainly) $^{12}C^{16}O^{18}O$ and several other isotopic combinations of C and O.

This problem is solved by using mass spectrometry of nucleons instead of molecules. The molecular method is based on the acceleration of beams of CO_2^+ ions by voltages of a few kV. These beams are steered through a magnet which separates this beam according to mass, i.e., isotope. The CO_2^+ beam is split into separate beams of $^{12}CO_2$, $^{13}CO_2$ and $^{12}C^{16}O^{18}O$ with masses 44, 45 and 46, respectively. The

isobar $^{14}CO_2$ is hidden in the mass 46 signal and cannot be separated this way. However, separation is possible when we use mass spectrometry at the nuclear level: ^{12}C, ^{13}C and ^{14}C. That means one has to accelerate beams of C ions with much higher voltages, in the MV range. One has to use a particle accelerator as a mass spectrometer: AMS, or Accelerator Mass Spectrometry.

AMS started as a spinoff of nuclear science, using relatively large tandem accelerators operating with voltages of typically 5 MV. Detecting the minute abundances of natural ^{14}C needs to be made possible in a practical way, together with control issues such as machine stability and isotopic fractionation processes.

Also here the main issue is dealing with the isobars, in this case with mass 13. The main isobars are ^{14}N and molecular fragments like $^{12}CH_2$ and ^{13}CH. The "Nitrogen problem" is solved by starting with negative ions; $^{14}C^-$ is stable, whereas $^{14}N^-$ is not stable. Negative ions can be produced from a solid surface by a so-called sputtering ion source. When we consider a source accepting solid state samples to be sputtered, carbon has to be in the form of graphite. Thus the ion source produces a C^- beam, which is injected in the accelerator. The accelerator is a tandem-type: a positive high voltage is applied in the middle of the accelerator tube. The negative ion beam is accelerated towards the high voltage, which is applied to a so-called "stripper" part of the tube. This is usually a gas that strips the electrons from the negative ions, which then become positively charged. These are then accelerated away from the high voltage (hence the name tandem). During the stripping process, the molecular fragments are broken up. A beam of C^+ ions then emerges from the accelerator, are steered through a magnet (in combination with other analysers) which then separates the beam into ^{12}C, ^{13}C and ^{14}C.

The first generation of AMS systems were large nuclear science machines with voltages of 5 MV or even higher. The first detection of natural ^{14}C took place in 1977 (Nelson and Korteling 1977; Bennett et al. 1977). Such large machines are still used, in particular for detection of natural isotopes of the heavier elements (Elmore and Phillips 1987). For ^{14}C, lower voltages are sufficient. The second generation of AMS machines uses 2.5 MV which is has the optimum efficiency for $^{14}C^{3+}$ ions (Purser et al. 1990; Purser 1992). The most recent machines of this type are characterized by using simultaneous injection of the 3 C isotopes, enabling the measurement of $\delta^{13}C$ for fractionation correction by the AMS itself. These machines were mostly dedicated to Radiocarbon analysis. Most recently a third generation the ^{14}C dedicated AMS system using 200 kV became available. This is the so-called Micadas (MIni CArbon Dating System). For a technical description, see Synal et al. (2007) and Synal (2013).

The MICADAS systems indeed revolutionized AMS, as they have also driven other companies to develop machines operating at lower voltages.

For more details on AMS systems and research we refer to the book by Tuniz et al. (1998) and review articles by Jull (2013), Kutschera (2013), Litherland et al. (2010), Synal and Wacker (2010), and Synal (2013).

AMS allows the measurement of intrinsically small samples, as compared with the radiometric method (Mook 1984). The sample pretreatment is for both methods (radiometry and AMS) the same, except for sample size. The sample size is in the

same regime as for the stable isotopes like ^{13}C. This enables combustion of pre-treated sample material by an Elemental Analyzer (EA). For radiometry that would be impossible because typically 1 liter of CO_2 is required (Mook and Streurman 1983). In practice, EA-IRMS combinations are used yielding CO_2 gas and stable isotope ratios of the sample.

AMS does require an extra preparation step: the preparation of graphite (Vogel et al. 1984). Organic material can be combusted to CO_2 in closed quartz tubes or an Elemental Analyzer (EA). The CO_2 is then trapped by liquid nitrogen, and at a later stage reduced into graphite powder by the reaction $CO_2 + 2H_2 \rightarrow 2H_2O + C$, using Fe as a catalyst and a temperature of around 600 °C. The modified method has been applied in AGE systems where the step of trapping is in liquid nitrogen is replaced by trapping in zeolite mineral as described by Wacker et al. (2010a, b).

AMS is more sensitive to contaminants than radiometry which is applied to large samples. See Lanting and van der Plicht (1994) for examples.

AMS much more efficient than radiometry; 1 mg C easily gives more than 100 ^{14}C counts per second for a modern sample, where for radiometry the registrations are 0.226 Bq for 1 g C for the standard. That amounts to 5–6 orders of magnitude more in the case of AMS.

A relatively new development for AMS is a workable CO_2 gas source. Indeed, over the past years, interest in going below the milligram level in sample size requirements has pushed research to overcome poor graphitization yields and increased contamination issues, the two main drawbacks when dealing with smaller samples sizes (Brown and Southon 1997). While the graphitization step could be improved (Santos et al. 2007; Walter et al. 2015), the development of gas ion sources allowing the direct measurement of carbon dioxide offered a very interesting alternatives (Middleton 1984; Bronk Ramsey and Hedges 1987). This reduced sample size requirements to tens of micrograms of carbon.

In 2007 at ETH Zurich the hybrid ion source of the MICADAS instrument, which enabled the measurement of both CO_2 and solid graphite targets, was equipped with a gas handling system and enabled the measurement of micrograms of material (Ruff et al. 2010), thereby setting a new milestone. The conversion of the sample to carbon dioxide through thermal oxidation in a quartz tube (Ruff et al. 2010) allowed to prepare the CO_2 in glass ampoules, which could then be collected in a gas-tight syringe, where it is mixed with helium. Using a stepping motor to move the syringe plunger forward, the carbon dioxide is dosed at a constant rate into the ion source via a glass capillary, hereby allowing stable measurement conditions on 3–30 micrograms Carbon.

Growing demand for the measurement of small samples in various fields has led to the coupling of various gas handling introduction systems to the AMS (see review in Wacker et al. 2013), the coupling of an elemental analyzer (EA) to the AMS being one of them (Bronk Ramsey et al. 2004; Uhl et al. 2004).

This skips the graphite step, and enables dating sub-milligram size samples, even down to 10 μg C (Ruff et al. 2010).

In conjunction to technical developments, the extent of contamination when dealing with such small samples, and procedures have been determined to reduce

and control contamination (Bour et al. 2016; Shah and Pearson 2007), as well as to correct the data for the constant contamination, enabling the analysis of extremely small samples (>5 μg C) with an acceptable accuracy (Haghipour et al. 2019; Welte et al. 2018).

Another important direction of study regarding minute amounts of material was the development of Compound Specific Radiocarbon Analysis (CSRA), enabling the isolation of selected biomarkers using preparative capillary gas chromatography (Eglinton et al. 1996). The combination of sample size downscaling, contamination correction as well as the possibility of targeting precise compounds has opened the field of radiocarbon dating to new directions of research for environmental studies (see review by Mollenhauer and Rethemeyer 2009). Applications in dating art and items of cultural heritage are still rare but dating pottery (Casanova et al. 2020) might be the first step in applying the CSRA in this research area.

13.3 Timescale Calibration

The Radiocarbon convention applies to both radiometry and AMS. Both measure $^{14}C/^{12}C$ and $^{13}C/^{12}C$ ratios, using the same reference and fractionation correction. Therefore, BP has the same meaning for both methods.

By convention the ^{14}C timescale is defined, and is different from the calendar timescale. Calibration is needed to establish the relationship between these 2 timescales.

Calibration curves give this relation. They are constructed by measuring samples by both the ^{14}C method and another method. Ideally this other method has to be independent from ^{14}C, yielding absolute dates (in AD/BC or the equivalent CE/BCE), and the samples have to be from the terrestrial (or atmospheric) reservoir. The paired dates (in the units BP and AD/BC, respectively) then are used to construct a calibration curve. For the dates calibrated using this curve, the chosen convention for half-life and fractionation correction are taken into account. It is important to note that the variations in the natural ^{14}C content cause the relation between both timescales to be not linear.

We also note here that the unit calBP is used as well; this is defined as calendar years relative to AD 1950 (calBP = 1950-AD).

The most ideal samples for calibration are tree rings, because they can be dated absolutely by means of dendrochronology. Following the early work of Suess (1980), the ^{14}C community has issued special issues of the journal *Radiocarbon* with calibration curves based on a variety of records available. These issues are updated regularly. The main data are tree rings dated by both ^{14}C and dendrochronology. Beyond the available absolutely dated dendrochronological dataset, records from varves (laminated sediments containing botanical remains), plus corals/foraminifera and speleothems which are also dated by isotopes in the Uranium decay chain are used. The main varved record is from terrestrial sediment of Lake Suigetsu in Japan (Bronk Ramsey et al. 2012).

Using these datasets, the calibration curve named IntCal20 has been constructed. It is the presently recommended calibration curve, and is shown in Fig. 13.1 (Reimer et al. 2020). The dendro-chronological part and the part derived from other records are indicated, separated at 13.910 calBP (Reimer et al. 2020). For examples using the curve in various fields of application see van der Plicht et al. (2020).

In practice for artwork and forgeries, the most relevant period is the last two millennia. This part of IntCal20 is shown in Fig. 13.2. Since the recent upgrade of the calibration curve to IntCal20, this part of the curve has an annual resolution for the calender timescale.

Unfortunately, the most recent period (since ca. 1700) is characterised by strong variations in the natural ^{14}C content, caused by the solar fluctuations. This obviously strongly hampers the application of the ^{14}C method for a lot of artwork.

In modern times, the ^{14}C content in nature is strongly influenced by anthropogenic effects. First, in the atmosphere and terrestrial samples, the greenhouse gas emissions (which are of geological age and thus do not contain ^{14}C) dilute the natural atmospheric $^{14}CO_2$ content since around 1900 AD. This is known as the Suess effect which is apparent in terrestrial samples like tree rings (Stuiver and Quay 1981). Further, after the second world war test explosions of nuclear bombs in the

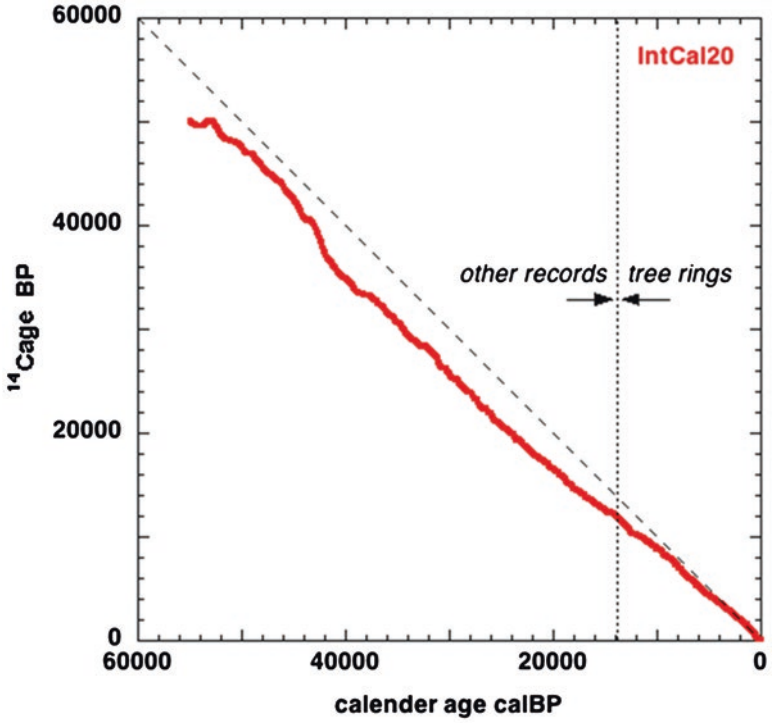

Fig. 13.1 Radiocarbon calibration curve IntCal20 (Reimer et al. 2020) for the complete dating range. (Calender years are shown in calBP, calender years relative to AD 1950)

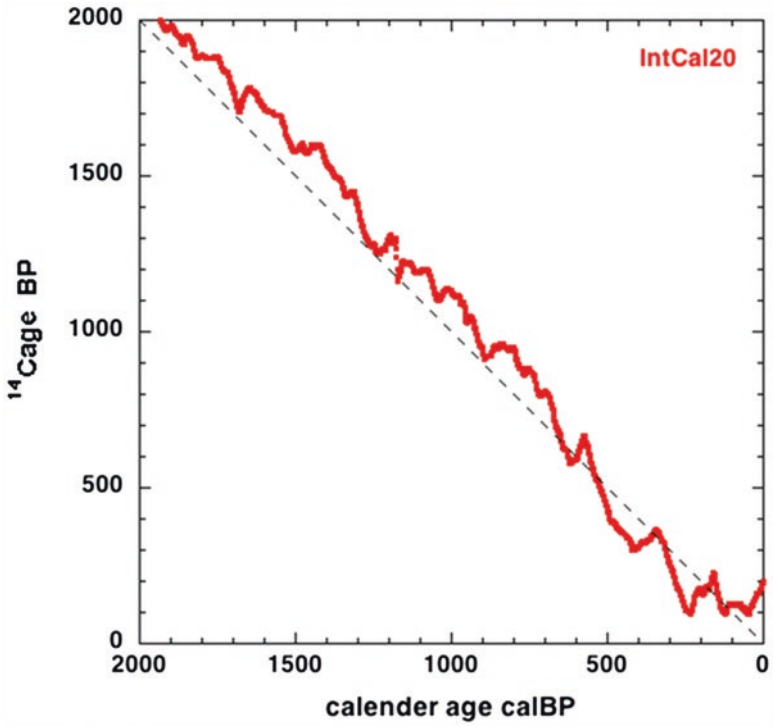

Fig. 13.2 Radiocarbon calibration curve IntCal20 (Reimer et al. 2020) for the last two millennia. (Calender years are shown in calBP, calender years relative to AD 1950)

atmosphere produced extra ^{14}C. In the northern hemisphere this (almost) doubled the ^{14}C concentration ($^{14}a \approx 2 = 200\%$) in 1963.

Since 1963, the year of the partial treaty on nuclear tests, atmospheric explosions took no longer place (except for a few small bomb tests). Since then, the ^{14}C content decreased in the atmosphere and increased in the oceans by exchange of $^{14}CO_2$ (e.g. Levin and Hesshaimer 2000). Figure 13.3 shows what is generally known as the "bomb peak" and is valid for the Northern Hemisphere (Hua et al. 2013). At present, the interplay of ^{14}C in the global carbon cycle (bomb peak, fossil fuels, and the reservoirs atmosphere, biosphere and the oceans) causes the natural ^{14}C content in the atmosphere close to the "normal" value $^{14}a = 100\%$ (Graven 2015).

Calibrated ^{14}C dates are given in calAD, calBC or calBP (Mook 1986). Recently, the Common Era (CE) has been applied as well as a unit, and consequently the calibrated age are defined as calCE or calBCE.

We also note that we discuss here only the northern atmosphere. The southern atmosphere, which has slightly lower ^{14}C signature of the atmosphere, has a different calibration curve: Shcal20 (Hogg et al. 2020) and for the bomb period we refer to Hua et al. (2013).

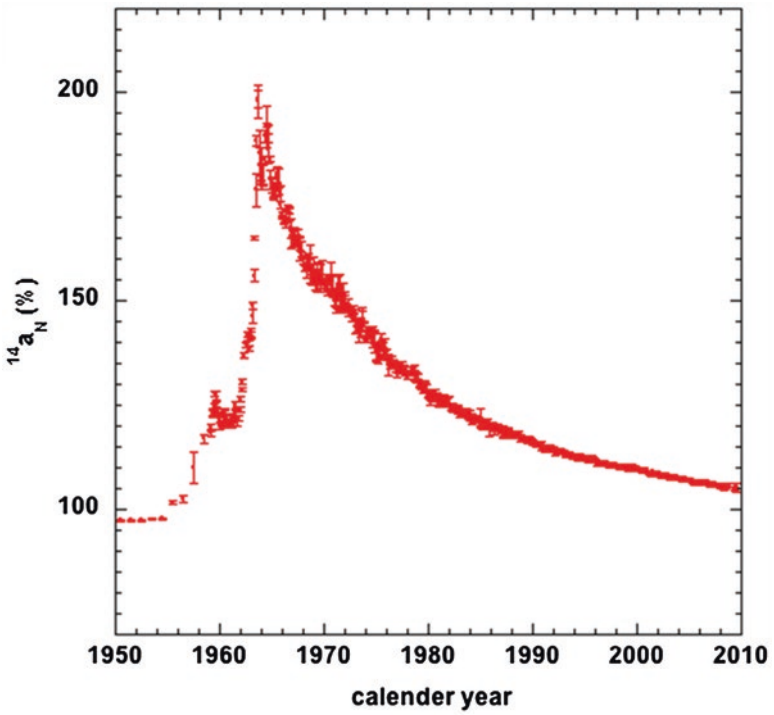

Fig. 13.3 Radiocarbon calibration curve for modern (post-1950) samples, clearly showing the so-called "bomb peak" with a maximum at 1963. (Hua et al. 2013)

For how to go about calibration we refer to e.g. van der Plicht and Mook (1987), Bronk Ramsey et al. (2006), Hajdas (2014) and van der Plicht et al. (2020). Calibration can be performed online by software available on the internet, we refer here to OxCal: https://c14.arch.ox.ac.uk/oxcal.html.

13.4 Dating Artwork

13.4.1 General

Since the early days of radiocarbon dating, the community has sought ways to date works of art by the method. However the original method, radiometry, requires large samples (grams of carbon) which is prohibitive for this category of samples.

This changed since the introduction of AMS. Among the first samples dated by AMS is the Shroud of Turin, arguably a piece of art but a classic example. Small samples of the textile were dated by 3 indepentent laboratories, resulting in an

average ^{14}C date of 691 ± 31 BP (Damon et al. 1989). Calibrated this is AD 1260–1390 AD (2-sigma, rounded to 10).

A prime question for dating of art (and also for other fields like archaeology) is given by the title of the article by van Strydonck et al. (1999): "what's in a date". The phrase refers to what fraction is dated and what does it represent. Radiocarbon is a measure of time, but not necessarily the moment of creation of the artwork. We mention here as an illustrative example the "old wood problem", an association problem also known from archaeology. Artefacts can be made from wood which is already old at the time of manufacturing. A clear example is a wooden statue of Christ from a medieval church in the Netherlands, which yields a miraculous ^{14}C date of 4000 ± 60 BP. Obviously, the artist used a piece of wood which was already many centuries old at the time of sculpturing.

Quality control of the measurements is established by laboratory protocols, standardization (such as the Radiocarbon convention mentioned above) and calibration by recommended calibration curves. In addition there are organised mutual intercomparisons between the laboratories. See for example Scott (2003) and information on the website of the journal Radiocarbon: www.radiocarbon.org.

Considering absolute dating, the measuring precision today can be 15 BP (1sigma). This number can be significantly detoriated by the calibration process. This makes art dating in particular often problematic, because the calibration curve is very erratic for the last 300 years. It shows strong natural variations in the ^{14}C signal, known as "wiggles" (Fig. 13.2). As a result, a sample dated as 300 ± 15 BP calibrates into multiple solutions between the year 1525 and today.

This does not mean that ^{14}C dating artwork for the last three centuries is meaningless; it depends on the research question. For example, the result of 300 BP does mean that the sample can not date to the fourteenth century. So it can be used for falsification purposes.

The wiggles can be applied to our advantage by a technique called "wiggle matching" (Bronk Ramsey et al. 2001). For a piece of wood, this is based on a series of (typically 10) ^{14}C dates of tree rings which can be counted (dendrochronology). The series of dates can be matched to the calibration curve. This increases precision, and can even exclude a certain wiggle as calibrated solution. The method has been applied to relatively large wood statues from South Korea (Park et al. 2010).

13.4.2 Dating of Wood

Arguably the primary example of artwork that can be dated by ^{14}C is that made of wood: wood statues, other wood sculpture work, paintings on wood panels (including icons), wood from musical instruments and of course frames of paintings. The method is destructive, a sample of about 1 mg of C is needed for high precision AMS dating by standard methods, which requires at least 3 mg of clean material (wood, but also textile). Obviously ethical reasons guide what can be sampled, but

the same is true for ^{14}C dating concerning the quality of the material. Important quality aspects are preservatives which are contaminants, and degraded material.

Among the most precious samples of wood art dating we discuss here are medieval icons from the National Art Gallery in Kiev, Ukraine. Icon painters in Kiev were famous and highly skilled since the twelfth century AD. The fourteenth to fifteenth centuries AD are considered the "golden age" of icon painting in the Ukraine (Chlenova 1999).

Historic dating is not always certain, even for some well known icons. Seven icons from the museum were selected for ^{14}C dating. They were all painted on wooden boards, specially made for the purpose of icon painting. Chips of wood were taken from the edges of the boards, which correspond to the youngest tree rings; this is the best material representing the time of painting. The series of icons was dated by three laboratories, for reason mutual intercomparison.

We discuss here the results of one icon: "the intercession" (Fig. 13.4). For a full report we refer to Kovalyukh et al. (2001).

The wood was pretreated chemically using the standard ABA method (see above). The combined ^{14}C date (average of 4 dates, rounded to 5) is 1055 ± 20 BP. The calibrated result is shown in Fig. 13.5. The calibrated ^{14}C dates (now done using the updated calibration curve IntCal20) are AD 960–925 (1-sigma probability) and 1050–1030 plus 980–920 (2-sigma), al numbers rounded to 5.

Wood has the advantage that it is generally not difficult to date by Radiocarbon. In addition, icons have a clear association: the artwork is directly made on wood panels. For paintings, but the wooden frames can be dated. Here association can become an issue, because a ^{14}C date of the frame does not necessarily give the date of the painting.

An interesting example in this respect is a medieval painting from the museum Huis Bergh in the Netherlands; see Fig. 13.6. The wood frame of the painting dates to 180 ± 30 BP. Calibration yields 3 possible time ranges (see Fig. 13.2) of AD 1665–1685, 1735–1805 and 1930–1950 (all numbers rounded to 5, 1sigma uncertainty). Clearly this is not an example of accurate historical dating of the artwork. Nevertheless, the result is meaningful. The research question was wether the wooden frame is original (i.e. medieval), or replaced in later times. The ^{14}C date clearly shows that the latter is the case.

13.4.3 Contamination

For more than a century, conservation and restoration, securing archeological objects and excavation sites rely on organic consolidants, adhesives and coatings (Horie 2010). Most of these substances are of high molecular weight with ample Carbon atoms. Many of these conservation materials are produced from fossil carbon, which is free of ^{14}C and introduces significant old contamination.

Fig. 13.4 Icon (painting on wood) "the Intercession" (Kovalyukh et al. 2001). (National Art Gallery, Kiev, Ukraine)

The effect has been recognized in various studies (for example Bruhn et al. 2001) and methods of potential treatment were investigated by Dee et al. (2011) and more recently by Brock et al. (2018) who employed Chromosorb®, a non-carbon-containing absorbent, silica-based polymer with a high surface to volume ratio which was artificially aged before simulation of contamination with various conservation materials. The tests performed by Brock et al. (2018) were done for 11 substances, and a combination of 17 treatment steps involving solvents was applied. FTIR spectroscopy and Mass Spectrometry can be used to control the efficiency of specific treatment with solvents.

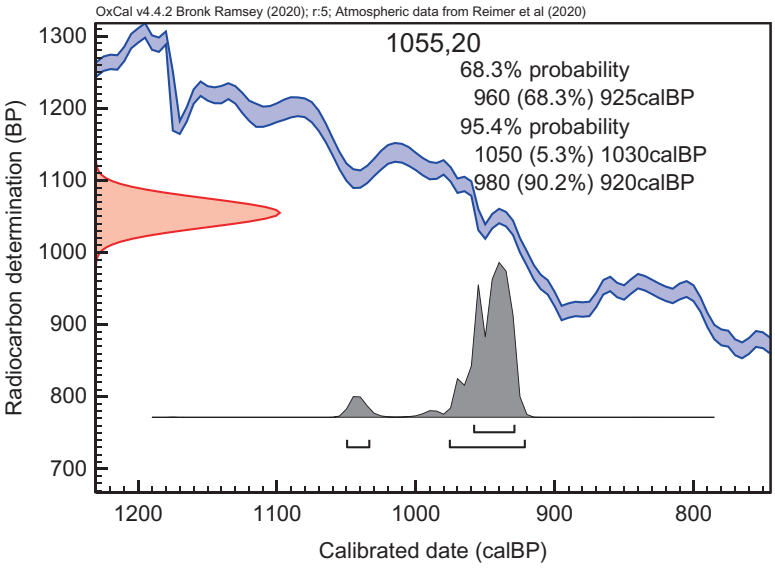

Fig. 13.5 Calibrated result for the icon "the Intercession". (Fig. 13.4)

Fig. 13.6 Painting from the museum "Huis Bergh". (Huis Bergh, the Netherlands)

13.4.4 New Materials

Upon the introduction of AMS and the gas ion source, radiocarbon dating has become less invasive. This allowed the consideration of more differentiated strategies for dating art (Fedi et al. 2013). When considering materials used by the artist, not only the support material can be carbon based but the binding media, pigments

or additives may also contain carbon atoms and are therefore potentially datable by ^{14}C.

Keisch and Miller (1972) discussed dating linseed oil or other drying oils used as painting media to detect post-1950 forgeries, i.e. from times including the "bomb peak" (Fig. 13.3). But using radiometry to measure the ^{14}C content would require as much as 100 mg of sample material.

This changed significantly with the advent of AMS which enabled dating samples of sizes as little as 1 mg. For rock art, charcoal or the vehicle used to bind the pigments has been dated (Baker and Armitage 2013; Li et al. 2012; Bonneau et al. 2011, 2016).

The introduction of the gas ion source and scaling down samples to micrograms of carbon allowed wider application to modern and contemporary art. It allows dating natural binder (oil) as shown by Hendriks et al. (2016): 0.5 mg paint from artist palette was dated. The method is however complex and requires complementary spectroscopic analysis to ensure suitable sample selection. Ideal are inorganic pigment zones, free of varnish or restoration (Hendriks et al. 2018). Nevertheless, micro samples have been successfully applied in case study for the detection of forged painting (Hendriks et al. 2019).

For Radiocarbon dating of lead white, the lead white corresponds to the ^{14}C level of the atmosphere at the time of its production.

In addition, ^{14}C dating was combined with lead isotopes studies, maximizing the gain from sampling artworks (Hendriks et al. 2020a).

Different approaches were proposed for the extraction of ^{14}C from lead white, either by acid hydrolysis or by thermal extraction. The latter was found to enhance the process selectivity and thus overcome the presence of calcium carbonate contaminations, allowing more realistic applications (Messager et al. 2020; Quarta et al. 2020). The challenges of dating lead white in artwork, effect of binder matrix and its consequence for isolating a specific ^{14}C signature of lead white are presented and discussed by Hendriks et al. (2020b).

13.4.5 Forgeries

The 1950 the "bomb-peak" (see Fig. 13.3) provides a unique opportunity for authentication studies, i.e. detection of modern forgeries created after 1950. It is a sharp signal: the peak is narrow in time and high in ^{14}C activity, is well monitored since 1950, and results of the atmospheric ^{14}C content measured in the clean environment are available for comparison (Hua et al. 2013).

The bomb peak provides unique possibilities for to detect forgeries for a very simple reason: when a sample has a ^{14}C activity $^{14}a>100\%$, it must originate post 1950. In this paragraph we discuss possibilities and show examples of analysed works of art.

Forgery issues are generally one of the main reasons why one might want to accurately date materials in artworks. Other reasons include technological and

provenience research, as measured ^{14}C ages can establish whether the dated material in an artwork is consistent with the period when the attributed artist was active. Detection of forgeries is seldom published, but part of the daily work of radiocarbon laboratories are ^{14}C dates, which provide a chronological context to undated objects as well as help replace wrongly attributed authentic artworks (Jull and Burr 2014; Richardin and Gandolfo 2013). For example, in the study of two canvas paintings, van Strydonck and co-workers (1998) brought new evidence regarding the attribution of a piece under debate, namely it was most likely realized by Pieter Bruegel the elder but rather one of his followers as the canvas date to the 2nd half of seventeenth century, after the purported artist's death.

In a different case the potential of unmasking forgeries where ^{14}C analyses provided decisive evidence, was put forward by a group of Italian physicists. In their work an alleged painting by Fernard Léger (1881–1955) belonging to the prestigious Peggy Guggenheim Collection in Venice, was proven to be a fake by dating of the canvas. In fact, Caforio and her team (2014) were able to establish that the canvas was made in 1959, 4 years after the artist's death, thus providing a decisive argument in establishing the forgery. The particular feature of the bomb peak enables accurate dating of contemporary art and may be exploited as a marker for twentieth century objects.

Another example is illustrated in the work of Hajdas et al. (2019a, b), where 14 suspected counterfeit works of the Chinese artist T'ang Haywen (1927–1991) could be identified as such. A comparison between the measured ^{14}C age for 7 legitimate works of the artists and the dubious ones revealed that the support material of the latter (Arches® cotton paper) was produced more than a decade after the death of the artist (Fig. 13.7); this time correlates with an increase in the reputation of the artist.

A similar case is shown by Fiorillo et al. (2021) researching a wooden panel attributed to the seventeenth century Dutch artist Jan Ruyscher (1625–1675). While many anachronistic features were discovered in the pictorial layer, the investigation of the support material revealed the first signs of inconsistency with the attribution. Radiocarbon analysis conducted on the wooden panel dated the object between the sixteenth and beginning of the twentieth centuries. The broad time range is caused by the wiggles of the calibration curve (see Fig. 13.2), and was narrowed later by wiggle matching (see above). As a result, it was shown that the tree was still growing at the time of the Ruyscher's death; the tree lived until the mid-eighteenth century. Moreover, spectroscopic analyses pinpointed the twentieth century as a timeframe for the application of the pictorial layers. The study highlights furthermore that this forgery was most likely created as a consequence of the "rediscovery" of Ruyscher.

Figure 13.8 shows an overview of the amount required for standard high precision analysis performed on targets of 1 mg of carbon. When sampling the fact that material will be lost in the chemical pretreatment must be taken into the account. Figure 13.8 shows examples of paper, wood and fiber materials which all lost ca. 10–50% of the original mass. It is a good illustration of what can be done. Detection of (post-1950) forgeries can be addressed by Radiocarbon dating of minute samples because the clear high concentration of ^{14}C in the bomb peak period. However, one

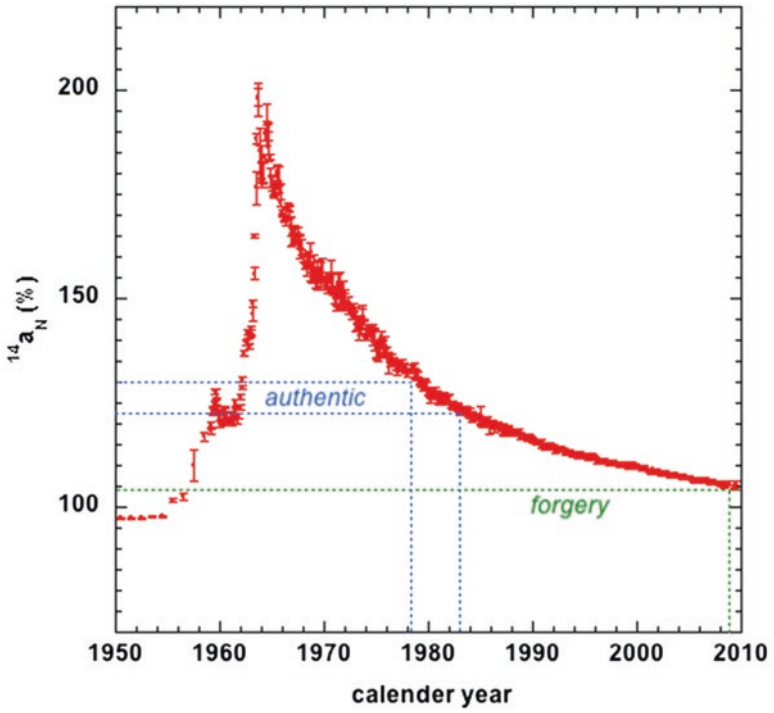

Fig. 13.7 Detection of forgeries using the ^{14}C analysis of Arches® cotton paper. Authentic paintings by T'ang Haywen (1927–1991) (light blue) yield a ^{14}C signal close to the creation time of the paper (the last decades of his life). The green line shows the ^{14}C signal of 14 suspected paintings that postdate 1991, the year of his death. (Hajdas et al. 2019a, b)

must note that nowadays the signal has been almost obscured by CO_2 from fossil fuel combustion (Graven 2015).

Nevertheless, finding proofs of falsification may become challenging, as forgers gain in sophistication, hereby manipulating scientific expertise to their advantage. For instance, a broadly known trick is the recycling of older support materials by forgers. Sample selection is therefore crucial for reliable interpretation of the results and identifying counterfeit artworks by relying solely on the dating of the support material is insufficient to ensure authenticity. This problem was raised recently by Hendriks et al. (2019), who demonstrated that radiocarbon dating of the paint layer is a powerful strategy for detecting modern (post-1950) forgeries. Two microsamples taken from the canvas as well as the pictorial weighing no more than 250 micrograms showed discordant ages. Where the dating of the canvas did not contradict an nineteenth century attribution, it is the dating of the organic binder which revealed the fraud. The study revealed the forger's scheme in recycling an appropriately aged canvas to convey the illusion of authenticity. In comparison to pigment anachronism, ^{14}C analysis of the pictorial layer binder offers decisive evidence,

Fig. 13.8 (**a**) Sample of canvas. Original weight 9 mg, reduced to 5.2 mg after solvent washes in Soxhlet and ABA treatment (on the picture). Sufficient amount for 1 target with 1 mg of carbon and one with 0.5 mg C. (**b**) Sample of paper fiber. Original weight 19 mg, reduced to 17 mg after solvent washes in Soxhlet (on the picture) and subsequently to 13 mg after ABA treatment. Sufficient amount for 3–4 targets with 1 mg of carbon. (**c**) Sample of wood. Original weight (here on the picture) 15 mg, reduced to 12.6 mg after solvent washes in Soxhlet and to 8.1 mg after ABA treatment. Sufficient amount for 2 targets with 1 mg of carbon

regardless of the level of sophistication of the forger, as it targets the only material which accurately reflects the image being assessed.

Radiocarbon dating of material used in paintings can provide a series of possible radiocarbon ages which in combination with material analysis, stylistic and provenance evaluation, can be an important piece in the puzzle of artwork authentication.

13.4.6 The Radiocarbon "Artwork Convention"

Since its conception, ^{14}C dating provides an excellent opportunity for dating ancient objects. The basis of the method is the so called 'curve of known' and includes dating of wood and textiles from an archeological context (Arnold and Libby 1949; Jull et al. 2018). The advance of AMS allowed for less invasive dating of art and antique items (Damon et al. 1989; Krzemnicki and Hajdas 2013; Hajdas et al. 2014). Moreover, the bomb peak signal is useful for the detection of forgeries (Zoppi et al. 2004; Caforio et al. 2014; Hajdas et al. 2019a, b; Hendriks et al. 2019). Such development has been swiftly recognized by the antiquities trade and employed in detection of forgeries (Huysecom et al. 2017). However, the radiocarbon community recently established standard procedures and guidelines for ethical handling items of cultural heritage (Hajdas et al. 2019a, b). Numerous radiocarbon laboratories joined the initiative (http://radiocarbon.webhost.uits.arizona.edu/node/11).

13.5 Conclusions

In this chapter we have shown that radiocarbon dating can be a useful chronometer in art research and for detection of forgeries. The ^{14}C signature measured in sample material of the studied object can only indicate the time period in which the material is being used; therefore, it does not provide authentication of the artist. However, detection of anachronic material indicates forgeries. Moreover, the new field of measuring the ^{14}C signal in different components (such as support, pigment and binder) provides a new potential yielding information for art researchers. The potential of ^{14}C analysis in the field of cultural heritage is growing and requires awareness and care in applying this most useful dating method.

Acknowledgments Many thanks to Laura Hendriks for her input to this article. The teams of LIP ETH (Zürich) and CIO (Groningen) are thanked for their continuous support with ^{14}C sample preparation and measurement.

References

Arnold, J.R., Libby, W.F.: Age determinations by radiocarbon content: checks with samples of known age. Science. **110**, 678–680 (1949)

Baker, S.M., Armitage, R.A.: Cueva La Conga: first Karst Cave Archaeology in Nicaragua. Lat. Am. Antiq. **24**, 309–329 (2013)

Bayliss, A., McCormac, G., van der Plicht, J.: An illustrated guide to measuring radiocarbon from archaeological samples. Phys. Educ. **39**, 137–144 (2004)

Bennett, C.L., Beukens, R.P., Clover, M.R., Gove, H.E., Liebert, R.B., Litherland, A.E., et al.: Radiocarbon dating using electrostatic accelerators: negative ions provide the key. Science. **198**, 508–510 (1977)

Bonneau, A., Brock, F., Higham, T., Pearce, D.G., Pollard, A.M.: An improved pretreatment protocol for radiocarbon dating black pigments in San Rock Art. Radiocarbon. **53**, 419–428 (2011)

Bonneau, A., Staff, R.A., Higham, T., Brock, F., Pearce, D.G., Mitchell, P.J.: Successfully dating rock art in Southern Africa using improved sampling methods and new characterization and pretreatment protocols. Radiocarbon. **59**, 1–19 (2016)

Bour, A.L., Walker, B.D., Broek, T.A.B., McCarthy, M.D.: Radiocarbon analysis of individual amino acids: carbon blank quantification for a small-sample high-pressure liquid chromography purification method. Anal. Chem. **88**, 3521–3528 (2016)

Brock, F., Higham, T., Ditchfield, P., Bronk Ramsey, C.: Current pretreatment methods for Ams radiocarbon dating at the oxford radiocarbon accelerator Unit (Orau). Radiocarbon. **52**, 103–112 (2010)

Brock, F., Dee, M., Hughes, A., Snoeck, C., Staff, R., Bronk Ramsey, C.: Testing the effectiveness of protocols for removal of common conservation treatments for radiocarbon dating. Radiocarbon. **60**, 35–50 (2018)

Bronk Ramsey, C., Hedges, R.E.M.: A gas ion source for radiocarbon dating. Nucl. Inst. Methods Phys. Res. B. **1-2**, 45–49 (1987)

Bronk Ramsey, C., van der Plicht, J., Weninger, B.: 'Wiggle matching' radiocarbon dates. Radiocarbon. **43**, 381–389 (2001)

Bronk Ramsey, C., Ditchfield, P., Humm, M.: Using a gas ion source for radiocarbon AMS and GC-AMS. Radiocarbon. **46**, 25–32 (2004)

Bronk Ramsey, C., Buck, C.E., Manning, S.W., Reimer, P., van der Plicht, J.: Developments in radiocarbon calibration for archaeology. Antiquity. **80**, 783798 (2006)
Bronk Ramsey, C., Staff, R.A., Bryant, C.L., Brock, F., Kitagawa, H., van der Plicht, J., et al.: A complete terrestrial radiocarbon record for 11.2 to 52.8 kyr BP. Science. **338**, 370–374 (2012)
Brown, T.A., Southon, J.R.: Corrections for contamination background in AMS C-14 measurements. Nucl. Inst. Methods Phys. Res. B. **123**, 208–213 (1997)
Bruhn, F., Duhr, A., Grootes, P.M., Mintrop, A., Nadeau, M.J.: Chemical removal of conservation substances by 'soxhlet'-type extraction. Radiocarbon. **43**, 229–237 (2001)
Bucha V. Influence of the earth's magnetic field on radiocarbon dating. In: Olsson IU, editor. Radiocarbon Variations and Absolute Chronology, Proceedings of the 12th Nobel Symposium. Stockholm: Almquist and Wiksells; 1970. P. 501-512.
Caforio, L., Fedi, M., Mando, P., Minarelli, F., Peccenini, E., Pellicori, V., Petrucci, F., Schwartzbaum, P., Taccetti, F.: Discovering forgeries of modern art by the C-14 Bomb Peak. Eur. Phys. J. Plus. **129**, 1 (2014)
Casanova, E., Knowles, T.D.J., Bayliss, A., Dunne, J., Baranski, M.Z., Denaire, A., Lefranc, P., di Lernia, S., Roffet-Salque, M., Smyth, J., Barclay, A., Gillard, T., Classen, E., Coles, B., Ilett, M., Jeunesse, C., Krueger, M., Marciniak, A., Minnitt, S., Rotunno, R., van de Velde, P., van Wijk, I., Cotton, J., Daykin, A., Evershed, R.P.: Accurate compound-specific C-14 dating of archaeological pottery vessels. Nature. **580**, 506–510 (2020)
Chlenova, L.G.: Masterpieces of Ukrainian Iconpainting of the 12th–19th Centuries. Kiev (1999) ISBN 966-577-035-7
Cook GT, van der Plicht J. Radiocarbon dating. In: Elias S, Mock CJ, editors. Encyclopedia of Quaternary Science. 2nd ed. Elsevier Amsterdam; 2013. p.305-315.
Craig, H.: The geochemistry of the stable carbon isotopes. Geochim. Cosmochim. Acta. **3**, 53–92 (1953)
Damon, P.E., Donahue, D.J., Gore, B.H., Hatheway, A.L., Jull, A.J.T., Linick, T.W., Sercel, P.J., Toolin, L.J., Bronk Ramsey, C., Hall, E.T.: Radiocarbon dating of the Shroud of Turin. Nature. **337**, 611–615 (1989)
de Vries, H.: Variation in concentration of Radiocarbon with time and location on earth. KNAW Proc. Ser. B. **61**, 1–9 (1958)
Dee, M., Brock, F., Bowles, A., Bronk Ramsey, C.: Using a silica substrate to monitor the effectiveness of radiocarbon pretreatment. Radiocarbon. **53**, 705–711 (2011)
Dee, M.W., Palstra, S.W.L., Aerts-Bijma, A.T., Bleeker, M.O., de Bruijn, S., Ghebru, F., et al.: Radiocarbon dating at Groningen: new and updated chemical pretreatment procedures. Radiocarbon. **62**, 63–74 (2020)
Eglinton, T.I., Pearson, A., McNichol, A.P., Currie, L.A., Benner, B.A., Wise, S.A.: Compound specific radiocarbon analysis as a tool to quantitatively apportion modern and fossil sources of polycyclic aromatic hydrocarbons in environmental matrices. In: Abstracts of Papers of the American Chemical Society, vol. 212, p. 65, ENVR (1996)
Elmore, D., Phillips, F.M.: Accelerator mass spectrometry for measurement of long-lived radioisotopes. Science. **236**, 543–550 (1987)
Fedi, M., Caforio, L., Mando, P., Petrucci, F., Taccetti, F.: May ^{14}C be used to date contemporary art? Nucl. Instr. Meth. Phys. Res. Sect. Phys. Res. B. **294**, 662–665 (2013)
Fiorillo, F., Hendriks, L., Hajdas, I., Vandini, M., Huysecom, E.: The rediscovery of Jan Ruyscher and its consequence. J. Am. Inst. Conserv. (2021). https://doi.org/10.1080/01971360.2020.1822702
Flint, R.S., Deevey, E.S.: Editorial statement. Radiocarbon. **1962**, 4 (1962)
Graven, H.D.: Impact of fossil fuel emissions on atmospheric radiocarbon and various applications of radiocarbon over this century. Proc. Natl. Acad. Sci. **112**, 9542–9545 (2015)
Haghipour, N., Ausin, B., Usman, M.O., Ishikawa, L., Wacker, L., Welte, K., et al.: Compound specific radiocarbon: analysis by elemental analysis accelerator mass spectrometry: precision and limitations. Anal. Chem. **91**, 2042–2049 (2019)

Hajdas, I.: The radiocarbon dating method and its applications in quaternary studies. Eiszeit. Gegenw. **57**, 2–24 (2008)
Hajdas, I.: Radiocarbon: calibration to absolute time scale. In: Turekian, H.D.H.K. (ed.) Treatise on Geochemistry, 2nd edn, pp. 37–43. Elsevier, Oxford (2014)
Hajdas, I., Bonani, G., Thut, H., Leone, G., Pfenninger, R., Maden, C.: A report on sample preparation at the ETH/PSI AMS facility in Zurich. Nucl. Inst. Methods Phys. Res. B. **223**, 267–271 (2004)
Hajdas, I., Cristi, C., Bonani, G., Maurer, M.: Textiles and radiocarbon dating. Radiocarbon. **56**, 637–643 (2014)
Hajdas, I., Jull, A.J.T., Huysecom, E., Mayor, A., Renold, M.A., Synal, H.A., et al.: Radiocarbon dating and the protection of cultural heritage. Radiocarbon. **61**, 1133–1134 (2019a)
Hajdas, I., Koutouzis, P., Tai, K., Hendriks, L., Maurer, M., Rottig, M.B.: Bomb C-14 on paper and detection of the forged paintings of T'ang Haywen. Radiocarbon. **61**, 1905–1912 (2019b)
Hendriks, L., Hajdas, I., McIntyre, C., Küffner, M., Scherrer, N.C., Ferreira, E.S.B.: Microscale radiocarbon dating of paintings. Appl. Phys. A. **122**, 167 (2016)
Hendriks, L., Hajdas, I., Ferreira, E.S.B., Scherrer, N.C., Zumbühl, S., Küffner, M., et al.: Selective dating of paint components: radiocarbon dating of lead white pigment. Radiocarbon. **61**, 473–493 (2018)
Hendriks, L., Hajdas, I., Ferreira, E.S.B., Scherrer, N.C., Zumbuhl, S., Smith, G.D., et al.: Uncovering modern paint forgeres by radiocarbon dating. Proc. Natl. Acad. Sci. **116**, 13210–13214 (2019)
Hendriks, L., Kradolfer, S., Lombardo, T., Hubert, V., Küffner, M., Khandekar, N., et al.: Dual isotope system analysis of lead white in artworks. Analyst. **145**, 1310–1318 (2020a)
Hendriks, L., Caseri, W., Ferreira, E.S., Scherrer, N.C., Zumbühl, S., Küffner, M., et al.: The ins and outs of ^{14}C dating lead white paint for artworks application. Anal. Chem. **92**, 7674–7682 (2020b)
Hogg, A., Heaton, T.J., Hua, Q., Palmer, J.G., Turney, C., Southon, J.S., et al.: SHCal20 Southern Hemisphere calibration, 0-55,000 years cal BP. Radiocarbon. **62**, 759–778 (2020)
Horie, C.V.: Materials for Conservation: Organic Consolidants, Adhesives and Coatings. Routledge (2010) ISBN 0750669055
Hua, Q., Barbetti, M., Rakowski, A.Z.: Atmospheric radiocarbon for the period 1950-2010. Radicoarbon. **55**, 2059–2072 (2013)
Huysecom, E., Hajdas, I., Renold, M.A., Synal, H.A., Mayor, A.: The "enhancement" of cultural heritage by AMS dating: ethical questions and practical proposals. Radiocarbon. **59**, 559–563 (2017)
Jull AJT. AMS radiocarbon dating. In: Elias SA, Mock CJ, editors. Encyclopedia of Quaternary Science (2nd ed.). Elsevier: Amsterdam; 2013. ISBN 9780444536433. p.316-323.
Jull, A.J.T., Burr, G.: Some interesting applications of radiocarbon dating to art and archaeology. Archeometriai Muhely. **11**, 139–148 (2014)
Jull, A.J.T., Pearson, C.L., Taylor, R.E., Southon, J.R., Santos, G.M., Kohl, C.P., et al.: Radiocarbon dating and intercomparison of some early historical radiocarbon samples. Radiocarbon. **60**, 535–548 (2018)
Keisch, B., Miller, H.H.: Recent art forgeries – detection by C-14 measurements. Nature. **240**, 491–492 (1972)
Kovalyukh, N., van der Plicht, J., Possnert, G., Skripkin, V., Chlenova, L.: Dating of ancient icons from Kiev art collections. Radiocarbon. **43**, 1065–1075 (2001)
Krzemnicki, M.S., Hajdas, I.: Age determination of pearls: a new approach for pearl testing and identification. Radiocarbon. **55**, 1801–1809 (2013)
Kutschera, W.: Applications of accelerator mass spectrometry. Int. J. Mass Spectrom. **349/350**, 203–218 (2013)
Kutschera, W.: The half-life of ^{14}C – why is it so long? Radiocarbon. **61**, 1135–1142 (2019)
Lanting, J.N., van der Plicht, J.: ^{14}C-AMS: Pros and cons for archaeology. Palaeohistoria **35/36**, 1–12 (1994)

Levin, I., Hesshaimer, V.: Radiocarbon, a unique tracer of global carbon cycle dynamics. Radiocarbon. **42**, 69–80 (2000)

Li, R., Baker, S., DeRoo, C.S., Armitage, R.A.: Characterization of the binders and pigments in the rock paintings of Cueva la Conga, Nicaragua. Coll. Endeavors Chem. Anal. Art Cult. Herit. Mater. **1103**, 75–89 (2012)

Libby, W.F.: Radiocarbon Dating. University of Chicago press (1952)

Litherland, A.E., Zhao, X.L., Kieser, W.E.: Mass spectrometry with accelerators. Mass Spectrom. Rev. **30**, 1037–1072 (2010)

Messager, C., Beck, L., De Viguerie, L., Jaber, M.: Thermal analysis of carbonate pigments and linseed oil to optimize CO2 extraction for radiocarbon dating of lead white paintings. Microchem. J. **154**, 104637 (2020)

Middleton, R.: A review of ion sources for accelerator mass spectrometry. Nucl. Inst. Methods Phys. Res. B. **5**, 193–199 (1984)

Mollenhauer, G., Rethemeyer, J.: Compound-specific radiocarbon analysis – analytical challenges and applications. IOP Conf. Ser. Earth Environ. Sci. **5**, 012006 (2009)

Mook, W.G.: Archaeological and geological interest in applying ^{14}C AMS to small samples. Nucl. Inst. Methods Phys. Res. B. **5**, 297–302 (1984)

Mook, W.G.: Business meeting, 12th international radiocarbon conference. Radiocarbon. **28**, 799 (1986)

Mook, W.G.: Introduction to Isotope Hydrology. Taylor and Francis, London (2006) ISBN 0415381975

Mook, W.G., Grootes, P.M.: The measuring procedure and corrections for the high-precision mass spectrometric analysis of isotopic abundance ratios, especially referring to carbon, oxygen and nirrogen. Int. J. Mass Spectrom. **12**, 273–298 (1973)

Mook, W.G., Streurman, H.J.: Physical and chemical aspects of radiocarbon dating. PACT Publ. **8**, 31–55 (1983)

Mook, W.G., van der Plicht, J.: Reporting ^{14}C activities and concentrations. Radiocarbon. **41**, 227–239 (1999)

Nelson, D.E., Korteling, R.G.: Carbon-14: direct detection at natural concentrations. Science. **198**, 507–508 (1977)

Nemec, M., Wacker, L., Hajdas, I., Gaggeler, H.: Alternative methods for cellulose preparation for AMS measurement. Radiocarbon. **52**, 1358–1370 (2010)

Olsson, I.U.: Radiocarbon variations and absolute chronology. In: Proceedings of the 12th Nobel Symposium, Uppsala University. Almquist and Wiksells, Stockholm (1970)

Park, W.K., Kim, Y., Jeong, A.R., Kim, S.K., Oh, J.A., Park, S.Y., et al.: Tree-ring dating and AMS wiggle matching of wooden statues at Neunggasa Temple in South Korea. Radiocarbon. **52**, 924–932 (2010)

Purser, K.H.: A high throughput ^{14}C accelerator mass spectrometer. Radiocarbon. **34**, 459–467 (1992)

Purser, K.H., Smick, T.H., Purser, R.K.: A precision ^{14}C accelerator mass spectrometer. Nucl. Instr. Meth. Phys. Res. Sect. Phys. Res. B. **52**, 263–268 (1990)

Quarta, G., D'Elia, M., Paparella, S., Serra, A., Calcagnile, L.: Characterisation of lead carbonate white pigments submitted to AMS radiocarbon dating. J. Cult. Herit. **46**, 102–107 (2020)

Reimer, P.J., Austin, W.E.N., Bard, E., Bayliss, A., Blackwell, P.G., Bronk Ramsey, C., et al.: The IntCal20 Northern Hemisphere radiocarbon age calibration curve (0-55 kcal BP). Radiocarbon. **62**, 725–757 (2020)

Richardin, P., Gandolfo, N.: Radiocarbon dating and authentication of ethnographic objects. Radiocarbon. **55**, 1810–1818 (2013)

Ruff, M., Fahrni, S., Gaggeler, H.W., Hajdas, I., Suter, M., Synal, H.A., et al.: On-line radiocarbon measurements of small samples using elemental analyzer and micadas gas ion source. Radiocarbon. **52**, 1645–1656 (2010)

Santos, G.M., Southon, J.R., Griffin, S., Beaupre, S.R., Druffel, E.R.M.: Ultra small-mass AMS C-14 sample preparation and analyses at KCCAMS/UCI facility. Nucl. Inst. Methods Phys. Res. B. **259**, 293–302 (2007)

Scott, E.M.: The Third International Radiocarbon Intercomparison (TIRI). Radiocarbon. **45**, 293–328 (2003)

Shah, S.R., Pearson, A.: Ultra-scale analysis of individuallipids by ^{14}C AMS: assessment and correction for sample processing blanks. Radiocarbon. **49**, 69–82 (2007)

Stuiver, M.: Carbon-14 content of 18th and 19th century wood: variations correlated with sunspot activity. Science. **149**, 533–535 (1965)

Stuiver, M., Quay, P.: Atmospheric ^{14}C changes resulting from fossil fuel CO_2 release and cosmic ray flux variability. Earth Planet. Sci. Lett. **53**, 349–362 (1981)

Suess, H.E.: The radiocarbon record in tree rings of the last 8000 years. Radiocarbon. **22**, 200–209 (1980)

Synal, H.A.: Developments in accelerator mass spectrometry. Int. J. Mass Spectrom. **349–350**, 192–202 (2013)

Synal, H.A., Wacker, L.: AMS measurement technique after 30 years: possibilities and limitations of low energy systems. Nucl. Inst. Methods Phys. Res. B. **268**, 701–707 (2010)

Synal, H.A., Stocker, M., Suter, M.: MICADAS: a new compact rediocarbon AMS system. Nucl. Inst. Methods Phys. Res. B. **B259**, 7–13 (2007)

Taylor, R.E., Aitken, M.J.: Chronometric Dating in Archaeology, New York, Springer (1997) ISBN 9781475796964

Tuniz, C., Bird, J.R., Fink, D., Herzog, G.F.: Accelerator Mass Spectrometry: Ultrasensitive Analysis for Global Science. CRC Press, Boca Raton (1998) ISBN 9780849345388

Uhl, T., Kretschmer, W., Luppold, W., Scharf, A.: Direct coupling of an elemental analyzer and a hybrid ion source for AMS measurements. Radiocarbon. **46**, 65–75 (2004)

van der Plicht J. 2013. Variations in atmospheric ^{14}C. In: Elias SA, Mock CJ, Encyclopedia of Quaternary Science (2nd ed.). Elsevier: Amsterdam; ISBN 9780444536433. p.329-335.

van der Plicht, J., Bruins, H.J.: Radiocarbon dating in Near-Eastern Mediterranean contexts: confusion and quality control. Radiocarbon. **43**, 1155–1166 (2001)

van der Plicht, J., Mook, W.G.: 1987. Automatic Radiocarbon calibration: illustrative examples. Palaeohistoria. **29**, 173–182 (1987)

van der Plicht, J., Bronk Ramsey, C., Heaton, T.J., Scott, E.M., Talamo, S.: Recent developments in calibration for archaeological and environmental samples. Radiocarbon. **62**, 1095–1117 (2020)

Van Strydonck, M., Masschelein-Kleiner, L., Alderliesten, C., de Jong, A.F.M.: Radiocarbon dating of canvas paintings: 2 case studies. Stud. Conserv. **43**, 209–214 (1998)

van Strydonck, M., Nelson, D.E., Combre, P., Bronk Ramsey, C., Scott, E.M., van der Plicht, J., et al.: What's in a ^{14}C date. In: Proceedings of the third conference on ^{14}C and Archaeology (1998). Lyon, pp. 433–440 (1999)

Vogel, J.S., Southon, J.R., Nelson, D.E., Brown, T.A.: Performance of catalytically condensed carbon for use in accelerator mass spectrometry. Nucl. Inst. Methods Phys. Res. B. **233**, 289–293 (1984)

Vogel, J.S., Turteltaub, K.W., Finkel, R., Nelson, D.E.: Accelerator mass spectrometry: isotope quantification at attomole sensitivity. Anal. Chem. **67**, 353A–359A (1995)

Wacker, L., Christl, M., Synal, H.A.: Bats: a new tool for AMS data reduction. Nucl. Inst. Methods Phys. Res. B. **268**(7–8), 976–979 (2010a)

Wacker, L., Nemec, M., Bourquin, J.: A revolutionary graphitisation system: fully automated, compact and simple. Nucl. Inst. Methods Phys. Res. B. **268**, 7–8 (2010b)., 931–4

Wacker, L., Fahrni, S., Hajdas, I., Molnar, M., Synal, H., Szidat, S., Zhang, Y.: A versatile gas interface for routine radiocarbon analysis with a gas ion source. Nucl. Inst. Methods Phys. Res. B. **294**, 315–319 (2013)

Walter, S.R.S., Gagnon, A.R., Roberts, M.L., McNichol, A.P., Lardie Gaylord, M.C., Klein, E.: Ultra-small graphitization reactors for ultra-microscale 14C analysis at the National Ocean Sciences Accelerator Mass Spectrometry (NOSAMS) facility. Radiocarbon. **57**, 109–122 (2015)

Welte, C., Hendriks, L., Wacker, L., Haghipour, N., Eglinton, T.I., Gunther, D., et al.: Towards the limits: analysis of microscale 14C samples using EA-AMS. Nucl. Inst. Methods Phys. Res. B. **437**, 66–74 (2018)

Zoppi, U., Skopec, Z., Skopec, J., Jones, G., Fink, D., Hua, Q., Jacobsen, G., Tuniz, C., Williams, A.: Forensic applications of C-14 bomb-pulse dating. Nucl. Inst. Methods Phys. Res. B. **223**, 770–775 (2004)

Chapter 14
Lead Isotope Ratios of Lead White: From Provenance to Authentication

Paolo D'Imporzano and Gareth R. Davies

Abstract The chapter reports the latest developments on the use of lead isotope analysis in the field of painting study, highlighting the contribution that this technique can bring to authentication of paintings and forgery detection. The chapter discusses the state of the art and the novel applications of lead isotope analysis to characterise paintings, using a detailed study of seventeenth century Dutch paintings as an example. Topics covered include: pigment/paintings provenance, regional isotopic variation, time-dependant lead isotope ratio variation and the travel of artists. Determining lead isotope ratio variation contributes to an increased understanding of paint-making, adding new and necessary knowledge useful for painting authentication. The work presented will help the reader understand the great potential contribution of lead isotope analysis to cultural heritage.

Keywords Lead isotope ratios · Analytical methods · Lead white · Provenance

14.1 Introduction

Is it possible to identify a forged painting by using the lead isotope ratios of lead white? As usual, the answer to such a relatively simple question is not definitive: yes, but it depends. Lead isotope analysis of lead white is a technique that has been used since the 1970s in order to identify the isotopic composition of the pigment (Keisch and Callahan 1976). In initial studies, the focus was on tracking the provenance of the lead used to produce lead white. In subsequent decades, associated with the development of more sensitive mass spectrometry, this technique also contributed to studies focusing on characterisation of artistic periods based on their lead white isotopic signature (Fabian and Fortunato 2010; Fortunato et al. 2005; Hendriks

P. D'Imporzano · G. R. Davies (✉)
Faculty of Science, Vrije Universiteit Amsterdam, Amsterdam, the Netherlands
e-mail: g.r.davies@vu.nl

M. P. Colombini et al. (eds.), *Analytical Chemistry for the Study of Paintings and the Detection of Forgeries*, Cultural Heritage Science,
https://doi.org/10.1007/978-3-030-86865-9_14

et al. 2020). In these latter studies, however, the bulk of the isotopic data were obtained from sixteenth to seventeenth century Italian or Netherlandish painters, meaning that many important artistic periods and regions have yet to be characterised.

The use of lead isotope ratios for identification of a painting's source or age is not straight forward and requires knowledge on several factors that influence the production of the painting and the production of the pigment. The latter needs knowledge of the source and nature of the smelting process used to extract the raw materials and how metallic lead is traded and processed prior to the paint production process. It is perhaps correct to conclude that the several days preparation to perform isotopic analyses of lead white is, arguably, the easiest part for the characterisation of the pigment. Information about which mines were active, which trade routes were used, in which region or time the painting was produced are fundamental in order to be able to use lead isotope data for authentication or attribution. Once these conditions are met then undoubtedly it is possible to use lead isotope ratios to distinguish certain groups of paintings, and use this information for attribution, authentication or even to detect later modification and potentially forgeries. This chapter will outline how lead isotope analyses of lead white are undertaken and how the data can be interpreted. Initially background information is provided on how lead white was produced, traded and used and a brief review of the analytical technique is also given. How the technique can be applied and the limitations will focus on the seventeenth century, with special attention to Dutch painters, as this period has been the most extensively studied and provides the best database to consider the potential of lead isotope analysis for authentication or attribution.

14.2 Lead White Production

Lead white almost invariably consists predominantly of a mixture of two lead carbonates: (C) cerussite ($PbCO_3$) and (HC) hydrocerussite ($2PbCO_3 \bullet Pb(OH)_2$) (Olby 1966). Other lead salts such as plumbonacrite ($Pb_5O(OH)_2(CO_3)_3$) are rare but have been reported in a number of synchrotron studies and appear to be a function of the ambient pH during paint production (Gonzalez et al. 2019; Stols-Witlox et al. 2012; Welcomme et al. 2007). The high content of lead (~ 77–80% by weight depending upon the C/HC ratio in the pigment) makes lead white the perfect candidate for lead isotope analysis. Coupled with the quasi-ubiquitous presence of this pigment in every painting until the twentieth century, it is possible to examine how paintings clusters based on painter, geography or time.

Lead white has been used as a pigment since before ancient Egyptian (Walter et al. 1999) and the synthesis of the pigment has not changed significantly over time. Detailed written description of its use were given during Roman times by

Theophrastus (fourth century B.C.), Vitruvius (first century B.C.) and Pliny the elder (first century A.D.)[1] (Eastaugh et al. 2004; Welcomme, 2007).

Lead white production consists of the transformation of metallic lead to a carbonate by exposure to acetic acid vapours (vinegar) in a fermentation medium (typically horse manure). Venice was the main production centre for this pigment from the twelfth until the sixteenth century (Berrie and Matthew 2011). The pigment was produced directly in the city, and enormous quantities of metallic lead were transported and processed in Venice. Documents report that in Venice, at least one lead foundry and one lead white factory ('luogo dale sbiacche'), as well as a shop specially dedicated to the sale of lead white ('la botega dalle sbiacche et altro posta sopra el ponte di Rialto') were active in the sixteenth to seventeenth century (Berrie and Matthew 2011). At the end of the sixteenth century, lead white production was implemented by Dutch craftsmen on a commercial scale and the production of the pigment increased in order to meet a constantly increasing demand. In this period the main production centre for lead white became the Netherlands, which would maintain this position until the 1800s. The rise of the Dutch industry was initiated at the end of the sixteenth century when the fall of Antwerp to the Spanish in 1585 forced many craftsmen to move north toward the Netherlands where they created the basis of the lead white industry in the country (Homburg and de Vlieger 1996). Producers in the Netherlands managed to improve the efficiency and increase the scale of the production process. This was achieved by using thin coils of metallic lead that were placed into pots with vinegar and staked in successive layers. The innovation was that the metallic lead coil increased the active surface area. In addition, the reaction time was increased to maximise acid attack of the lead sheets. The synthesis process reached quasi-industrialised productivity yielding large quantities (tons) of lead white. This improved process led to a production boom in Holland, and it became common to refer to the process as the Dutch stack process (Homburg and de Vlieger 1996). From the end of the sixteenth century, the Dutch started to produce and trade lead white on a large scale, becoming the main production centre in the seventeenth and eighteenth century (Stols-Witlox 2014). The details of the Dutch stack process are well explained by Homburgh (Homburg and de Vlieger 1996), and references within, and this work can be taken as a reference of lead white production until the nineteenth century. Records suggest that at the peak of the activity, a single lead white producer was able to process four tons of lead in a single production batch. The process started by melting together the metallic lead, which included mixing new and unreacted metallic lead recycled from previous lead white production. The lead was then cast into metallic sheets (or in thin lead coil in the Dutch stack process) and exposed to vinegar under a CO_2-rich atmosphere. The process to convert metallic lead into lead white required 6 to 8 weeks, depending on the ambient temperature and humidity. After conversion of the metallic lead, the pigment was washed and ground several times according to various recipes in order

[1] Theophrastus, De lapidibus, 56; Vitruvius, De Architectura, 8, 6, 1; Pliny the old, Histoire Naturelle, 34, 175.

to obtain the desired final grain size and purity (Stols-Witlox et al. 2012). After a final drying step, the product was ready to be sold. Documentary evidence indicates that lead white produced in the north of Europe could be mixed with chalk ($CaCO_3$) in order to cut the production cost, whereas the lead white from Venice was known to be pure and considered of a higher quality (Berrie and Matthew 2011; Homburg and de Vlieger 1996; Stols-Witlox et al. 2012). This fact allowed Venetian lead white to maintain a position as a high quality product on the international lead white market, which was dominated by the Dutch in the seventeenth century. It is estimated that in 1790, 1350 tons of lead white were shipped out the harbours of Amsterdam and Rotterdam (Stols-Witlox 2014; Vlieger and Homburg 1992) and that at the end of the eighteenth century more than 35 factories were active in the Netherlands with a production of 4000 tons per year.

Lead white is not the only lead based pigment produced, but it is the only one that has been well-characterised with lead isotope analysis. The other notable lead based pigments used in history are: minium (Pb_3O_4), lead thin yellow (Pb_2SnO_4), Naples yellow ($Pb_2Sb_2O_7$) used between eighteenth and nineteenth century and chrome yellow ($PbCrO_4$ used from the nineteenth century) (Feller 1986; Roy 1993). These pigments, however, have not been studied as much as lead white and, therefore, their isotopic compositions remain unknown.

Knowing the production process and the trading of the lead white is fundamental for lead isotope data interpretation. The implication of the commercial production is that large quantities of lead white were produced at one time from lead that was melted and hence homogenised before being re-casted into the required shape. The lead used was either new or recycled from previous production batches, meaning that potentially different sources of lead were mixed together. This suggests that the final lead white product should be isotopically homogenous due to rapid diffusion of the element within a melt and due to physical mixing during the processes of grinding and washings after the lead was transformed in lead white. Depending on variations in the amount of recycled lead used, each lead white batch could potentially have a different isotopic composition. This conclusion is due, not only to the recycling of lead but also to changes in lead isotope composition of individual lead ore deposits during their progressive exploitation or changes in the supply chain of lead ore. Although Dutch lead white, was adulterated with chalk, the difference in lead content (~77–80 wt. % Pb in lead white compared to less than 10 ppm in chalk) means that adulteration is expected to have minimal effect on the final lead isotope composition.

14.3 Lead Ore Deposits

Large quantities of lead commonly occur in ore deposits in association with zinc and less commonly with copper and iron. In all cases these elements occur in sulphide minerals that were formed by precipitation from ore fluids due to processes such as cooling, mixing with other fluids, and pH change. The most common

sulphide minerals are galena (PbS, 87 wt.% Pb), sphalerite (ZnS), chalcopyrite ($CuFeS_2$), pyrite(FeS_2), and pyrrhotite (FeS). The largest mineralised regions can contain up to 10×10^6 tons (t) of Pb, in addition to the other metals.

Significant lead accumulations occur in oceanic and continental crust in seven main types of ore deposits that are conventionally grouped based on geological occurrence (Eckstrand et al. 1995). Skarn and manto deposits are hosted in carbonate rocks and associated with igneous intrusive bodies such as granite. Fluids expelled during cooling of the igneous bodies reacted with, and replaced, the carbonate rocks precipitating sulphides. Skarn deposits were formed at high temperatures (>350 °C) associated with formation of calcium silicate minerals. Manto deposits form further from the igneous bodies and lack the distinctive calcium silicate assemblage. Both deposit-types form large, "massive" (i.e., typically >60% sulphide) deposits containing mainly Pb and Zn sulphides, although silver is commonly an important by-product. Mississippi Valley-type (MVT) deposits are also hosted in sedimentary carbonate rocks and named after three mineralised regions in the Mississippi Valley, USA, although other large MVT sphalerite and galena deposits with low pyrite content occur world-wide. They formed due to the tectonically driven expulsion of metal sulphide-rich hydrothermal fluids from shale into surrounding carbonate rocks. Igneous intrusions were not involved and depositional temperatures were lower than manto and skarn type deposits (100–150 °C). Deposits are normally Zn-rich and the silver content is low. MVT deposits generally occur as clusters ranging from a few to more than 300 separate deposits.

Volcanogenic massive sulphide (VMS) deposits are found in volcanic rocks as old as 3.5 billion years and are still forming at mid ocean ridges today. The deposits commonly contain Cu, Pb, Zn, Ag and Au. Although VMS deposits form in variable geological environments, all form by metals being leached from the surrounding sub-seafloor volcanic rocks by seawater circulating in a hydrothermal system. Sulphides precipitate on or near the seafloor due to changes in temperature, pressure, and pH when the rising hydrothermal fluids interact with seawater. Sedimentary-exhalative (SEDEX) deposits represent the largest known Pb and Zn deposits with several containing in excess of 10×10^6 t of metal. SEDEX deposits were formed close to the seafloor by seawater circulating through underlying sediments. The deposits are bi-mineralic, sphalerite and galena with highly variable Ag contents, 0 to ~300 g/t. Sandstone-lead deposits do not represent major sources of Pb on a world scale but were the major source of Pb in Sweden and Germany. Galena, usually accompanied by lesser amounts of pyrite or sphalerite, is disseminated within sandstone at relatively low ore grades. The sedimentary sandstone host rock usually overlies older rocks of granitic composition, which are the source of the Pb. The final lead occurrence is vein deposits. Veins formed in a series of narrow fractures, cutting through the host rock and filled with ore minerals that precipitated from hydrothermal fluids. Lead-bearing veins are associated with a variety of sulphides, Ag-bearing minerals, quartz, and calcite. Although generally small compared with the other deposits, vein deposits have been exploited from prehistoric up to the nineteenth century.

14.4 The Isotopes of Lead

Lead has four stable isotopes, ^{204}Pb, ^{206}Pb, ^{207}Pb and ^{208}Pb. ^{204}Pb is non radiogenic while ^{206}Pb, ^{207}Pb and ^{208}Pb are the product of radioactive decay of respectively ^{238}U, ^{235}U and ^{232}Th. The decay rates of the parent isotopes differ by more than a factor of 10. ^{232}Th has the slowest decay with a half-life of 1.4×10^{10} y. The half-life of ^{238}U, 4.47×10^{9} y, is comparable to the age of the Earth whereas the half-life of ^{235}U is almost seven times shorter (7.07×10^{8} y) such that the vast majority (> 95%) of ^{235}U has now decayed away. This means that the rate of change in the ingrowth of the daughter Pb isotopes has changed significantly over time with notably more ^{207}Pb formed during early Earth evolution. Rocks formed in the Achaean period therefore had notably higher ^{207}Pb/^{206}Pb ratios. Galena contains such large amounts of Pb that it has U/Pb and Th/Pb ratios close to zero so that once formed, there is no change in the Pb isotope ratios in galena. This means that the Pb isotope ratios are "frozen" at the time of formation and represent a record of the Pb isotope ratio at that time. Lead ore deposits formed in different geological periods therefore generally have distinct Pb isotope ratios.

Lead ore deposits are formed from lead derived from two major sources: (i) the continental crust that is enriched in U and Th such that the crust is characterised by elevated (radiogenic) Pb isotope ratios or (ii) Earth's upper mantle, either directly or from recently formed lower continental crust. Earth's mantle has a predictable Pb isotope compositions with time that approximately follows a two stage evolution model (Galer and Goldstein 1996; Stacey and Kramers 1975). In this model, Pb develops from primordial Pb, defined by troilite recovered from meteorites with ^{238}U/^{204}Pb and ^{232}Th/^{204}Pb of 7.19 and 32.21 respectively. Following a major differentiation event at 3.7 Ga, ^{238}U/^{204}Pb and ^{232}Th/^{204}Pb increased to 9.74 and 37.19. Many ore bodies have compositions that approximate the mantle evolution model and have been variously described as ordinary or common (Pollard and Heron 2008). In these cases, there is little contribution of radiogenic lead from the upper continental crust. A second group of lead deposits, described as anomalous, indicate the involvement of lead sources derived from continental crust of different age (Gulson 1986; Sangster et al. 2000).

All the factors described above contribute to the understanding of the nature and timing of the processes that form lead deposit, and make it possible to use the Pb isotope system to determine Pb provenance in cultural heritage studies. Common lead deposits formed in the same period, will have the same Pb isotope composition, even if the geographical regions of the two deposits are distant. In contrast, anomalous deposits may have distinct isotopic compositions even if they are formed in close proximity. This characteristic of lead deposits is what makes the Pb isotope system so powerful for provenance studies as potentially most ore deposits have a distinct signature.

Within Europe, however, ore deposits often formed in regions with similar geological backgrounds and histories (Germany, Poland and U.K). Nevertheless, even in these areas it is possible to distinguish ore bodies formed in local regions. Hence,

if the exploitation history of individual ore deposits is known, Pb isotope compositions can be used to determine the provenance of lead in cultural heritage objects.

14.5 Lead Production

Lead, due to its low melting point and association with silver was one of the first metals to be smelted by humans. Since antiquity lead extraction from galena (PbS) was almost ubiquitously connected with silver recovery, and many silver-rich lead deposits were used in order to obtain the precious metal. For many centuries lead was considered a by-product of silver production and the usefulness of metallic lead was not widely recognised (Henderson 2013). The first documented trade in lead was recorded in an inscription found in a temple from the 18th Egyptian dynasty (~3400 BP). The use of lead from that time onwards is documented in ice cores from Greenland, where lead pollution is recorded at concentrations four times higher than previously (Hong et al. 1994). Peaks in lead pollution are dated at 2500 and 1700 years ago, which coincides with mining and smelting activity at the height of Greek and Roman societies. The peak of pollution due to the processing of lead during the Roman period was not reached again until the industrial revolution (Cooke and Bindler 2015; Hong et al. 1994). During Greco-Roman times, lead mining and processing were most active in Spain, which represented around 40% of production of the Roman Empire with significant production in Central Europe, Britain, Greece and Asia minor (Cooke and Bindler 2015; Fortunato et al. 2005; Hong et al. 1994; Pollard and Heron 2008; Stos-Gale and Gale 2009).

Detailed lead pollution records obtained from European lakes have been used to indicate that the use of lead after the decline of the Roman Empire decreased considerably and only started to rise again around 1000 years ago (Cooke and Bindler 2015). From this time on, the lead contents of lake sediments closely correlate with lead production in Europe. By the eleventh and twelfth century, many old Roman lead production centres had re-opened in Germany, Britain and Spain. By the sixteenth century the main lead production centres were Germany, Poland and U.K., with the latter becoming the world leading lead producer in the seventeenth century.

During the industrial revolution lead production exceeded that of the Roman Empire. Britain was no longer the leading lead production centre by the mid-nineteenth century, in association with the depletion of its mines and the re-development of lead mining in Germany, Spain, and major expansion in the United States. In the same period major lead deposits were discovered in Australia. The United States became the leading global lead producer at the end of the nineteenth century, and associated with increasing production from other non-European nations such as Canada, Mexico, and Australia, non-European lead production surpassed European mines (Rich 1994). Today, Australia is the world's leading producer and exporter of lead, with large mines at Broken Hill, Mt Isa and Hilton in Queensland and McArthur River in the Northern Territory. In deposits mined today, lead is usually found in ores which also contain zinc, silver and commonly copper and is

extracted as a co-product of these metals. Much of this lead production is from regions characterised by ancient geology (1.0–3.0 Billion years old) and has characteristic lead isotope ratios. Lead sulphide, the major ore mineral, contains insignificant amounts of U and Th and hence undergoes essentially no radioactive decay after formation. As such the Pb isotope ratios of exported Australian lead ores are generally low, typically with $^{206}Pb/^{204}Pb$ ratios < 16.5 (Sangster et al. 2000), making this lead easily distinguishable from European lead, for example that used in seventeenth century Dutch paintings (Fabian and Fortunato 2010; Fortunato et al. 2005; Keisch and Callahan 1976; Sangster et al. 2000; van Loon et al. 2019). These major changes in long-term lead trade mean that lead whites produced and used as pigment in different centuries are liable to have significantly different Pb isotope ratios enabling recent renovation-retouching to be recognised.

14.5.1 European Lead Production (Fifteenth to Seventeenth Century)

In order to understand the lead isotope compositions of European paintings it is important to know the history of European lead mining. As most studies of lead white have focused on the sixteenth to seventeenth century, we will summarise which regions were active lead producers in this period, and how lead was used and traded. The two most important regions for lead production were Derbyshire in central England and the Harz region of Germany (Fabian and Fortunato 2010; Fortunato et al. 2005; Keisch and Callahan 1976). The lead mining history of these two regions is well known in the period between 1400 and 1600 because lead was key to silver production (Blanchard 1995). During this period, European silver was obtained using the Saigerprozess, which allows silver extraction from argentiferous copper by using large quantities of lead. Between 1450 and 1560, European lead production increased from 250 tons per year to 2250 tons, with a peak around 1530 with an annual production of 4200 tons (Blanchard 1995). At the peak of the silver production in the 1530s it was estimated that around two-thirds of lead in Europe was used to treat argentiferous copper with between 0.4 and 0.55 tons of lead used to process each ton of copper (Blanchard 1995).

The use of the Saigerprozess, together with fluctuation of the silver price during the sixteenth century, caused the lead mining industry to adapt multiple times and Derbyshire, Harz and Poland alternated as the main lead production centres (Blanchard 1995; Burt 1995). Lead production was affected by a series of technical and socio-political developments that had a major influence on trade in the middle of the sixteenth century. First, as a result of the earlier dissolution of the monasteries, priories, convents and friaries in the UK, there was an over-supply of cheap lead recycled from buildings that flooded the market and caused a drop in the lead price (from 1545 until 1549 (Burt 1995)). Second, a new silver extraction technique was developed around 1560. Mercury rather than Pb was used for silver extraction in a

process known as amalgamation. This change in the silver recovery process resulted in a drop in the demand for lead in a market that was already over supplied. In addition, the development of a new furnace smelting technique in the Mendip Hills in the UK allowed the waste (slag) of previous lead production to be reprocessed, again resulting in an increase in lead supply. This process was exported to the main lead production region of Derbyshire in the middle of the 1500s (Burt 1995).

These factors allowed England to become the main lead production centre from the end of the sixteenth century onwards, with the Derbyshire the focal point. The rise in the British mining industry contrasted with the fortunes of the generally deep mines in Germany and Poland. British lead deposits were relatively shallow while German and Polish mine were deep and required expensive technologies and a specialised workforce. Moreover, British lead mines were almost exempt from taxation in contrast to the high government taxes applied in Germany and Poland. The dramatic decrease of the lead price in the mid 1500s made the continental lead mine industry uncompetitive (Blanchard 1995, Burt 1995). This series of events resulted in an increase in British lead export from 450 tons in 1540 to 12300 tons in 1630 making the U.K. the major producer of Pb and its dominance continued for most of the seventeenth century.

14.6 Lead Isotope Analysis

One of the main issues in lead isotope analyses of lead white is obtaining samples as sampling paintings, especially when they are considered a masterpiece, is a delicate task, both physically and politically. Generally, the samples are kept to a minimum in both number and size, and restricted to areas of the paintings such as the border or areas of existing damage (Fortunato et al. 2005). Painting samples generally are taken manually by trained conservators using a scalpel under a magnification lens or with the help of stereo microscope. The small samples taken in this way can vary between hundreds of ng to μg in weight. This way of sampling, however, has some intrinsic problems:

- Unknown and variable amounts of contamination are included due to the sampling in different institutions/museums.
- Different operators perform the sampling leading to substantial differences in the way the samples are taken.
- Manual sampling causes variable amounts of sample to be taken such that sample size can differ by many orders of magnitude in weight, and it is not always possible to know how much painting matrix is contained in the samples.

These problems are not usually critical for the final analytical results, as lead white samples contain enough lead that contamination is irrelevant. Moreover the samples are treated and chemically purified before analysis to remove surface varnish layers that contain most of any environmental pollution. In some cases, however, the amount of lead white in the samples is low and possible contaminations,

either coming from the painting matrix that is not lead white or the surface, can produce unrepresentative data. This scenario is a problem because, in most of the cases, the samples are unique and no replicates are available. Importantly, however, quality control can be checked by monitoring the amount of lead in the samples so that, despite their unique nature, samples with little lead white can be discarded. These problems have the effect of reducing the available lead isotope data.

The issue of precise sampling was addressed by D'Imporzano et al. (2020a). The authors develop a micro-scalpel method to precisely sample lead white directly from cross sections of paintings. This method was designed to standardise the sampling procedure, reduce blank contamination, and minimise the amount of material obtained from a painting, and to store the sample material unused for isotopic analyses for further study. The possibility to store the painting material in cross-sections that can be re-utilised after lead isotope analysis, makes curators more willing to allow multiple sampling from a single painting and hence replicate analyses. Importantly, sampling from an existing cross-section negates the need to remove new material from a painting. If new samples are required, these can be taken as scrapings, embedded, sampled and then stored for future study. The developed tool can easily be transported. Moreover cross-sections can be shipped temporally to the laboratory and the sampling performed in a clean laboratory reducing any effect of blank contamination.

The improvement in the sampling method to expand available samples is crucial for lead isotope analyses, because data interpretation is heavily dependent on the database of lead isotope ratios of lead white of paintings. Increasing the number of analysed well-characterised paintings is necessary for the correct interpretation of lead isotope ratios of lead white from new and unknown paintings. Portable laser ablation techniques that use pulsed lasers may offer a potential solution for the future sampling of lead white to reduce the damage to painting/cross section and improve the precision of sampling (Knaf et al. 2017). The hope is that developing new, less invasive sampling methods will encourage institutions to allow more extensive sampling of paintings for lead isotope analysis.

There are two main techniques used for the analyses of lead isotope ratios: Thermal Ionisation Mass Spectrometry (TIMS) and Multi Collector Inductively Coupled Plasma Mass Spectrometry (MC-ICPMS). In the last decades, MC-ICPMS instruments have been used regularly to characterise lead isotope ratios of lead white. The reason of the preference of this technique over the TIMS is due to:

- MC-ICPMS can analyse samples directly in solution, reducing greatly the time of sample preparation.
- The data acquisition is faster and more automated compared to TIMS, meaning that sample throughput is more efficient.
- Instrumental fractionation between the different Pb isotopes (mass fractionation) cannot be directly monitored using TIMS and the long term accuracy is assessed by measuring a series of standards (see below). This issue can be overcome using an artificially enriched double Pb isotope "spike" but that requires multiple analysis and the use of expensive spikes.

– For samples containing between 50 and 100 ng of lead the MC-ICPMS provides the same accuracy and precision as the double spiked TIMS technique (D'imporzano et al. 2020a).

Typical samples of lead white contain several hundreds of ng of lead such that sample dilution is required. Hence, the MC-ICPMS is the best option for lead isotope analyses of lead white. The use of TIMS, that have a higher precision and accuracy for smaller ion beam, is required when the samples contain smaller amounts of lead (< 10 ng). The recent development of 10^{13} Ohm resistor amplifiers, however, allows MC-ICPMS measurement of 5 ng of lead while maintaining similar accuracy and precision compared to 75 ng Pb sample using normal amplifier (Klaver et al. 2015; Koornneef et al. 2014, 2019). If such small samples are analysed, however, it becomes important to precisely monitor the blank contamination.

The general procedure to prepare the sample is based on the dissolution of the lead white in nitric acid. Subsequent sample preparation can vary slightly from laboratory to laboratory. After dissolution, the sample is treated with chromatography in order to obtain a pure lead fraction (D'imporzano et al. 2020a). Other works argued that for samples containing only pure lead white, chromatographic purification with chromatography can be avoided provided that Ca content is not below 200 ppm (Fortunato et al. 2005).

Avoiding any matrix interference is, however, important because isotope analyses on an MC-ICPMS are subject to large instrumental mass fractionation that can be influenced by even small (ppm) levels of other elements, and chromatographic separation to ensure the highest quality data is highly recommended. Details of how corrections are applied to account for mass fractionation and more information on isotope analysis, MC-ICPMS theory and mass-bias can be found in (Albarède and Beard 2004) and only briefly summarised below.

Lead has only one stable isotope, ^{204}Pb, and therefore internal sample correction for mass bias fractionation produced in the mass spectrometer is impossible, as at least two stable isotopes are required. Correction for instrumental fractionation is typically performed by analyses of reference materials (usually pure Pb solution in 1% HNO_3) with known isotopic composition in between analyses of unknown samples (so-called standard sample bracketing—SSB). The advantage over the TIMS method is that switching between sample and standard can be performed within a few minutes. The known isotopic composition of the reference material is used to calculate, following an exponential law, the instrumental mass fractionation factor that is then used to correct the samples data. This approach, however, cannot correct for differences in instrumental mass fractionation between the sample and reference material caused by variations in the sample matrix, therefore requiring a chromatographic purification step to assure the best accuracy possible of the analysis.

An alternative method is to use the Double Spike (DS) technique. DS allows for internal correction of the instrumental mass fractionation, and the use of a standard solution between samples is unnecessary. The accuracy of the DS is independent of the matrix composition of the sample, and the purification of the lead of the sample is less important in this case. The intense use of the DS, however, can cause memory

effects in the instrument making this technique unsuitable for routine analysis (D'imporzano et al. 2020b) and it is expensive and more time consuming.

14.7 Current State-of-the-Art

14.7.1 Lead Isotope Ratios in Paintings: Provenance and Identification

Lead isotope analyses of lead white in paintings have provided information about: (i) pigment provenance; (ii) artistic periods which can lead to; (iii) distinction between modern and historical lead white; iv) valuable information for attribution of paintings.

Place of origin, provenance, of lead in the lead white of a painting can only be determined by direct comparison to data obtained from lead ore deposits. Ideally isotopic analysis of ore minerals should be confined to lead deposits that were active at the time of creation of the artwork. In that case, the isotopic data can be used to provide useful insights into the trading history of past societies. This has been successfully applied for archaeological artefacts (Pollard and Heron 2008; Stos-Gale and Gale 2009). The vast majority of the archaeological studies using lead isotope ratios, however, are focused to reveal the trade in metals in the Mediterranean in the bronze age (Pollard and Heron 2008) and it is these data that currently form the majority of the Pb isotope database used for provenance studies.

When all the isotopic data from individual regions are combined, the result is a graph with overlapping Pb isotope ratios. As an example, lead isotope data from European ore deposits are summarised in Fig. 14.1. A key aspect to the data interpretation is knowledge of which mines were active at the relevant time.

Figure 14.1 demonstrates that the Pb isotope ratios from lead white present in seventeenth century Dutch/Flemish paintings fall in an area characteristic of three different countries. These represent mines in Poland, England and Germany, specifically Harz Mountains, Germany, Nidderdale, Derbyshire in the UK. Fortunato et al. 2005, concluded it is impossible to identify provenance based on lead isotope ratios alone. If the information about the mining industry in Europe during the seventeenth century are taken in account, however, it is most likely that the lead has a British origin, probably Derbyshire, as this region was the most active for the production of lead in the seventeenth century (Blanchard 1995; Burt 1995). This discussion emphasises the need to know the lead production history in order to interpret the isotopic data. Importantly, however, there are also some clear regional variations in the Pb isotope compositions of mining districts. Fabian and Fortunato 2010 pointed out the distinction between seventeenth century Dutch paintings and sixteenth to seventeenth century Italian paintings (Fig. 14.2). The Pb isotope data show two well resolved clusters, consistent with the different geological environments of the lead mines in the Alps and northern Europe.

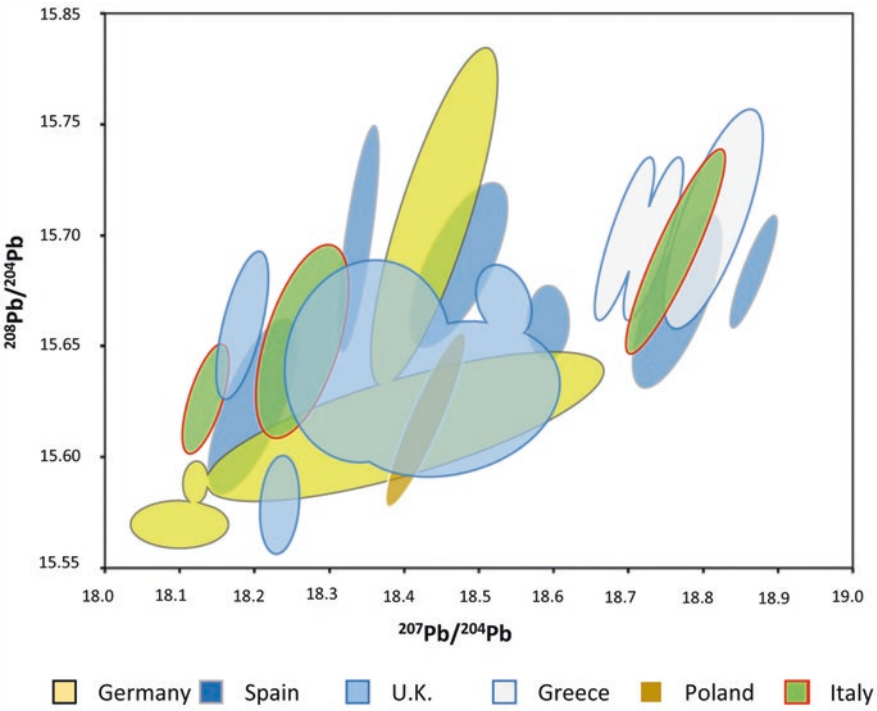

Fig. 14.1 Lead isotope ratio figure showing the $^{206}Pb/^{204}Pb$ and $^{207}Pb/^{204}Pb$ ratios for lead deposit in Europe. The data are taken from the literature (e.g. (Fortunato et al. 2005) and Oxford lead isotope database OXALID). The red circle indicates the range of seventeenth century Dutch/Flemish paintings. (Fortunato et al. 2005)

The marked isotopic difference between Italian and Dutch lead white is particularly useful due to the many study-visits made by Dutch painters to Italy. The Pb isotope differences make it possible to recognise if a painting was made by a painter while studying abroad because it is unlikely that painters would have transported bulky and dense pigments with them, especially when lead white was readily available in Italy. The painting by Willem Drost, presented in the study of D'Imporzano et al. (D'Imporzano et al. 2020a) provides an interesting case study. The artist was active in Amsterdam (1652–1654) before he travelled and died in Venice in 1659. The painting entitled, *Roman Charity* (SK-C-1802) was thought to derive from his Italian period (1655–1659) due to strong Italian stylistic influences. The lead isotope ratios of the painting are, however, consistent with seventeenth Century Dutch lead white, in particular in the years around 1650 (star in Fig. 14.2). In this period the artist was known to be active in Amsterdam either in Rembrandt's studio or in his own. The isotopic data are within analytical error of samples from Rembrandt's workshop painting "Holy Family" (SK-A-4119), which was painted in the period 1642–1648. Italian influences in the painting can be explained by the numerous Italian works that were in Amsterdam at the time. Further support for a Dutch

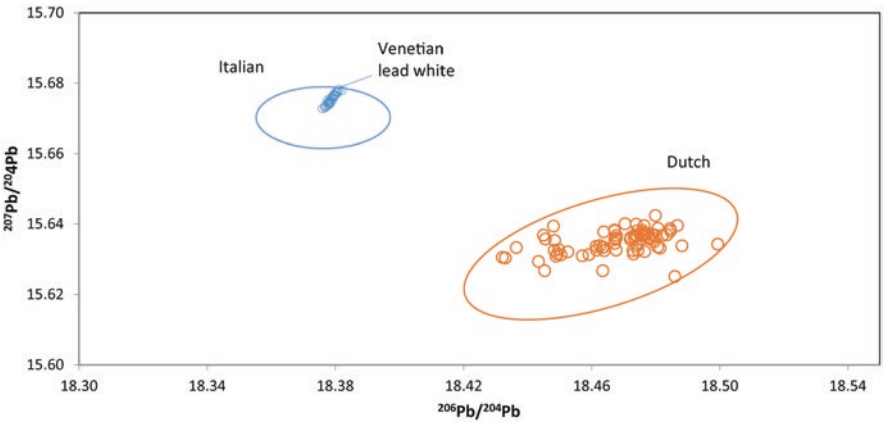

Fig. 14.2 Lead isotope ratio figure showing a comparison between seventeenth century Dutch paintings and sixteenth to seventeenth century Italian paintings (Fabian and Fortunato 2010; Fortunato et al. 2005; D'Imporzano et al. 2020a). The Italian group is characterised by samples analysed by (Fabian and Fortunato 2010), light blue ellipse, while the blue dots are from lead white cones representing pure Venetian lead white found in a shipwreck (D'Imporzano et al. 2020). The star represents an analysis of a painting from Drost, see text for details

provenance comes from the fact that Drost made a preparatory drawing for the painting that dates from his Amsterdam period. Integrating this information with the lead isotope data, it is considered highly probable that the painting was produced by the artist in Amsterdam before his departure to Rome in 1655 (D'Imporzano et al. 2021).

Currently available Pb isotope data from well characterised paintings from other regions and periods are limited, primarily due to the difficulty in obtaining samples for destructive analysis. Unfortunately this means that Spanish, German, British and French paintings cannot be easily characterised. The database for lead isotope ratios of lead white will be expanded further in the future in order to have more information on these paintings.

14.7.2 Post Production Retouching and Modification

Lead isotope ratios of lead white can help identify retouching made to paintings significantly post production. Equally if a painting has been restored several decades or centuries after its initial production, it is almost inevitable that lead isotope analysis will resolve the different generations of lead white. In their pioneering work, Keisch and Callahan 1976 analysed 429 paintings produced between the thirteenth to the twentieth century and demonstrated that lead isotope compositions of lead white changed over time. In particular, the data show that lead isotope ratios of lead white are markedly more variable after the eighteenth century (>x 10).

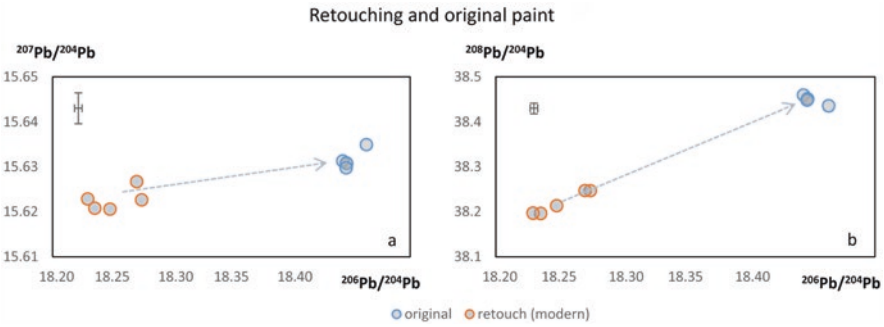

Fig. 14.3 Pb isotope ratio diagram contrasting original and retouched paint sampled for a painting from De Gelder (D'Imporzano et al. 2020a). The cross indicates the long term reproducibility of the instrument (analytical error) after D'Imporzano et al. 2020b

The increase in variability of lead isotope ratios of lead white was also reported in two other papers Fortunato et al. 2005 and D'Imporzano et al. 2020a. Fortunato et al. 2005, compare data from Flemish and Dutch paintings with samples of "modern lead white". Figure 14.3 demonstrates that the Flemish/Dutch paintings form a distinct cluster compared to modern lead white (D'Imporzano et al. 2020a). The study from Fortunato et al. 2005 reports that a specific sample taken from a Rembrandt painting (sample G26-G, painting Minerva in her study, Mauritshuis, NL) falls among the region of modern lead white. The sample is from an area of the painting that was restored most probably at the end of the eighteenth century. Similarly, D'Imporzano et al. 2020a, found that 5 samples, taken from retouched part of a painting from De Gelder, have isotopic compositions that are consistent with modern lead white (Fig. 14.3).

In all these cases, lead isotope ratios were able to distinguish different generations of lead white used on an individual painting. In this context, it is notable that the variability in lead isotope ratios of lead white increased markedly after the eighteenth century. This change happened in a period when the world was going through unprecedented socio-economical change, with the advent of the industrial revolution and the establishment extensive extra-European lead production. These observed long-term temporal changes can be used in order to identify retouching and paintings made before or after a certain period, and could be a powerful tool to identify forgeries.

14.7.3 From Macro to Micro: Lead Isotope Ratios Within a Painting

As outlined above, lead isotope data can distinguish different artistic periods/geographical regions. One important parameter that has not been fully assessed is how well lead isotope analyses can distinguish two paintings produced in the same

period/region. This information will be crucial in studies of authentication or when an unknown painting requires attribution. In order to answer this question it is crucial to know the range of lead isotope heterogeneity present within a certain artistic cluster and the heterogeneity of lead isotope ratios of the lead white within an individual painting. This question arises because authentication studies are generally made based on the analyses of a limited number of samples and compared against a small database or just one or two other samples from a comparison painting. The case of the *Saint Praxedis* (1655, Private Collection) provides a good example as the attribution of the painting is highly debated with some arguing that it represents an early Vermeer while others suggest it to be an Italian copy after Felice Ficherelli's Saint Praxedis (Wheelock 1986). Prior to auction in 2014, the *Saint Praxedis* was subjected to Pb isotope analysis. Lead isotope data were determined from two samples of the Saint Praxedis and then directly compared with a sample from Vermeer's *Diana and her Nymphs* (1653–4, Mauritshuis, The Hague, inv. n. 406). The Pb isotope data of the two paintings were analytically identical and this evidence was used to support an attribution to Vermeer (Christie's London Auction Cat. July 2014, The Barbara Piasecka Johnson Collection, Lot 39). The interpretation was based on the assumption that samples from works by the same artist have the same Pb isotope ratios. Based on the current state of knowledge, however, this assumption was not proven. Lead isotope data available at that time establish that paintings produced in the same region and time have limited lead isotope variation. A conclusion that the *Saint Praxedis* was not produced in Italy but in the Netherlands is therefore supported. There was, however, insufficient information about the Pb isotope variation within individual paintings or within the oeuvre of individual artists from the Netherlands to make a direct attribution. Equally it was unknown if or how Pb isotope ratios of lead white change during the seventeenth century and across the continent.

As the heterogeneity of lead isotope ratios within an individual painting is unknown, this makes the direct comparison of individual samples from a limited number of different paintings by the same artist difficult to interpret. To address these questions a study on the heterogeneity within individual paintings was conducted by analysing five paintings from the Rijksmuseum Amsterdam (D'Imporzano et al. 2020a). The study focused on paintings created during the seventeenth century in the Netherlands. The paintings were sampled multiple times, with a minimum of five samples taken from different locations from each painting. The study also investigated the potential isotopic differences in lead between different paint layers, including the ground.

The study found that while all the samples have isotopic values in line with those previously reported for seventeenth century Dutch/Flemish paintings, four out of five paintings have lead isotope ratios that vary more than analytical error (Fig. 14.4). The isotopic heterogeneity found in the paintings corresponds to several time the long term reproducibility of the analytical method on each of the reported lead isotope ratios. In particular, the highest variation was found for the case of the painting of de Gheyn II where data show that the heterogeneity was 7.6 times the long term reproducibility for $^{206}Pb/^{204}Pb$, 2.6 for $^{207}Pb/^{204}Pb$ and 3.4 for $^{208}Pb/^{204}Pb$. The

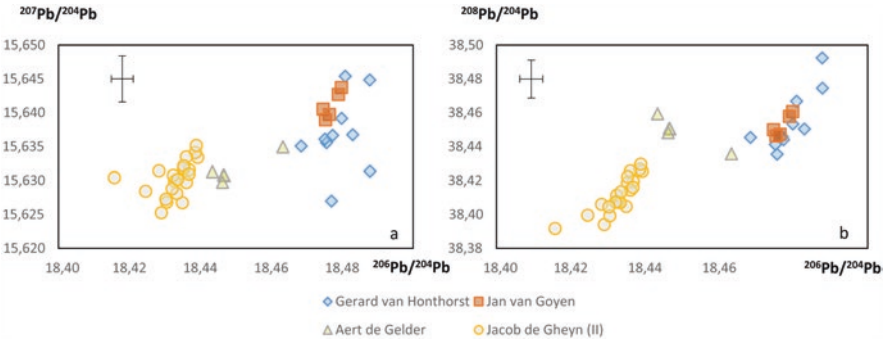

Fig. 14.4 Lead isotope distribution from four Dutch artists. The data show the lead isotope ratios distribution obtained by analyses of several samples coming from 5 different paintings (two paintings for van Honthorst made in the same period were analysed and are reported using the same symbol). The cross indicates the long term reproducibility of the instrument (analytical error) after reference (D'Imporzano et al. 2020a)

variation of lead isotope ratios of lead white in this painting, especially on the ratio $^{206}Pb/^{204}Pb$ was controlled by two samples taken from the ground layer. If these samples were ignored, the Pb isotope heterogeneity still remains outside analytical error, up to 4 times (D'Imporzano et al. 2020a).

The study investigated the reason for the isotopic heterogeneity in individual paintings and included analyses of a large number of samples of contemporary (sixteenth century) commercially produced pure lead white. Lead white was sampled from cones of pure pigment recovered from a ship wreck that was trading goods from Venice to Constantinople (Batur 2019) and sunk in the Mediterranean sea. The lead white was studied because it was produced around 1580, as the ship sunk in 1583 and can give insight on lead white produced at that time. In this way, it was possible to analyse historical lead white that was untouched for centuries and that retains the original lead isotope composition of its production. Although the lead white was under water for hundreds of years, it was unaffected by alteration due to the high content of lead in lead white and the low concentration of lead in seawater and the pristine preservation of all but the outside of the lead white cone. The Pb isotope data of multiple lead white cones are within analytical error and demonstrate that the product was homogeneous when shipped. This conclusion should not come as a surprise because the lead white production method involves steps of melting metallic lead, washing and grinding of huge quantities of lead white that will produce homogenisation (Stols-Witlox 2014). The study used Venetian lead white but the similarity of the general production methods across Europe (Stols-Witlox 2014) implies all commercially produced batches of lead white would be homogeneous. The heterogeneity recorded by the individual paintings analysed in D'Imporzano et al. 2020b imply either mixing of different batches of lead white or the mixing of lead white with other lead bearing material in the matrix of the painting that had different lead isotope compositions. This heterogeneity can have two explanations:

The first hypothesis would imply that the lead white used for paintings come from different batches having different isotopic values. It is possible that different lead white batches contain different lead isotope ratios if different starting lead was used. Based on trading records, however, the sources of lead appear to be stable for extended periods (several years), which would argue against significant short term isotopic variations, a point explored in more detail in Sect. 14.7.3.

The second hypothesis to consider is that the production of a painting involves the combination of many different lead bearing materials. In particular, many recipes advise to use of oils that have been processed by a variety of methods. Recipes for preparatory layers mention boiled oil, fat oil and drying oil (Stols-Witlox 2014). These preparations aim to improve the drying rate (polymerisation) of the oil. Usually lead based compounds were used as a siccative agents, as written in a recipe for fat oil treatment with siccatives. Stols-Witlox et al. 2014 list multiple recipes for oil preparation using lead as siccative agent: De Mayerne's recipe for siccative oil written between 1620 and 1646 suggests to treat the oil with water and PbO (PbO/oil/water ratio of 1/4/4 (w%)) (Mayerne 1620–1646). King (1653–7) provides a recipe for a fat oil that is prepared by placing linseed oil in the sun for three weeks after the oil had been mixed with lead white, minium, sawdust and crumbs of brown bread (Stols-Witlox 2014). Stalker and Parker (1688) advised to place linseed oil in the sun in a lead glazed vessel. Dutens (1779) describes how fat oil is made by slowly heating litharge (lead II oxide) and lead white with linseed oil. In a later edition, Dutens (1803) gives a recipe for a 'fat or drying oil' that is prepared by exposing linseed oil with lead white and litharge to the sun for eight days, stirring it once or twice per day (Stols-Witlox 2014). The use of siccatives, metal salts such as those containing lead, manganese or zinc, which act as a catalyst for the polymerisation of the oil binder, not only appear in recipes for the preparation of oil binders advised for use in preparatory layers, but also appear as additions during the ground preparation itself, e.g. for earth or clay-bound layers, addition of small amounts of lead white or minium are suggested (Stols-Witlox 2014).

The combination and mixing of these lead-based compounds in different layers of the painting could cause a variation of lead isotope ratios within and between paintings according to the amount of lead sources mixed in the process. In order to cause a significant isotopic change, however, the lead composing the PbO should come from a different source, which as explained below would imply lead sources produced at different times.

14.7.4 Temporal Change in Lead Isotope Ratios of Lead White: A Case of Study for Seventeenth Century Dutch Paintings

The first documented variation in lead isotope ratios of lead white with time was documented by Keisch and Callahan (Keisch and Callahan 1976). The study found that after the nineteenth century lead isotope ratios of lead white are more variable.

The Pb isotope composition of lead white undergoes significant change and becomes more variable after the industrial revolution in the mid-eighteenth century (Fig. 14.5), and remains highly variable during the nineteenth and twentieth century. This change in isotopic composition of the pigment is due to a combination of the opening of many extra-European lead mines, changes in the lead trading and the opening of new centres of lead white production.

The variation of lead isotope ratios of lead white in paintings made after the eighteenth century have not been studied systematically, however, a detailed investigation has been made for seventeenth century Dutch paintings (D'Imporzano et al. 2021). Analyses of this artistic group (Fabian and Fortunato 2010; Fortunato et al. 2005; Wheelock 1986) indicate that the lead isotope compositions of lead white from seventeenth century Dutch paintings forms a cluster but also record significant Pb isotope variation equivalent, to 44.5 times the analytical error for $^{206}Pb/^{204}Pb$. D'Imporzano et al. 2021 evaluate the processes that control the observed variation in seventeenth century Dutch paintings. Based on the analysis of 77 painting from 27 Netherlandish painters, the study examined if the isotopic variation reflected artistic groups or the time of production. Lead white samples were taken from authenticated paintings from the collections of the Rijksmuseum and Mauritshuis. In all cases, the date of production was known with an uncertainty of a maximum ± 2.5 years. These data, reproduced in Fig. 14.6, demonstrated that by using lead isotope ratios alone, it was impossible to achieve a clear distinction between paintings produced within the oeuvre or workshop of an individual artist (D'Imporzano et al. 2021).

The lead isotope ratios of most terrestrial sources define general co-linearity because the isotopic ratios are controlled by geological age and U/Pb and Th/Pb ratios. This is because U and Th generally have similar geochemical behaviour. The $^{206}Pb/^{204}Pb$ ratio records the largest variation and is the best ratio to identify patterns

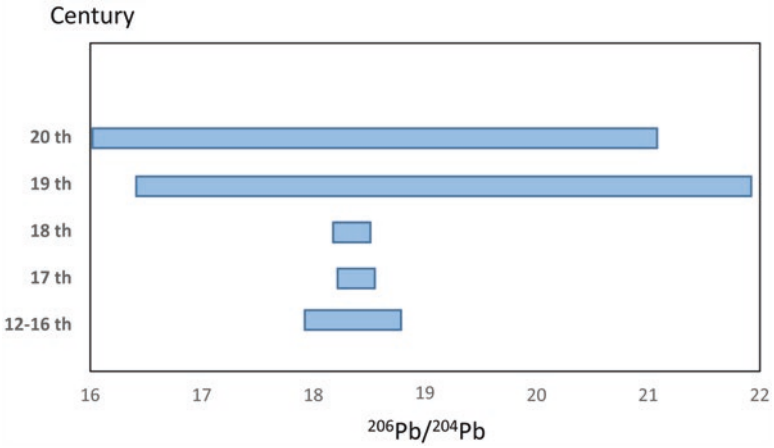

Fig. 14.5 Temporal variation in lead isotope ratios in lead white reported by Keisch & Callahan (1976)

of lead isotope variation in lead white. Using a single Pb isotope ratio, however, fails to fully utilise all the Pb isotope variation, $^{206}Pb/^{204}Pb$, $^{207}Pb/^{204}Pb$, $^{208}Pb/^{204}Pb$, $^{206}Pb/^{207}Pb$, $^{208}Pb/^{206}Pb$, $^{208}Pb/^{207}Pb$. In order to better visualise all aspects of the Pb isotope data, Keisch and Callahan 1976 [1] developed the Lead Isotope Ratio Index (LIRI). The method applies a correction to the $^{206}Pb/^{204}Pb$ ratio based on $^{207}Pb/^{204}Pb$ and $^{208}Pb/^{206}Pb$ values following the empirical equation:

$$\begin{aligned} \mathrm{LIRI} = {} & 35.385 + 0.4729 * \left({}^{206}\mathrm{Pb} / {}^{204}\mathrm{Pb} \right) \\ & - 0.5519 * \left({}^{206}\mathrm{Pb} / {}^{204}\mathrm{Pb} \right) * \left({}^{207}\mathrm{Pb} / {}^{206}\mathrm{Pb} \right) \\ & - 8.2561 * \left({}^{208}\mathrm{Pb} / {}^{206}\mathrm{Pb} \right) \end{aligned}$$

The LIRI index gives an indication of whether a sample lies within a specific cluster of isotopic ratios and allows the integrated isotopic data to be easily plotted against time, Fig. 14.6. Using the LIRI to visualise the isotopic data, using information from all the relevant Pb isotope ratios. However, if direct comparison of two samples is required, it is important to analyse the data using the original lead isotope ratios because identical LIRI values can be obtained from different raw data and therefore using only the LIRI could lead to false interpretation (Keisch and Callahan 1976). This method of data analysis is, however, useful when lead white samples come from an artistic group.

The data reported in Fig. 14.6 establish that the paintings produced in the Netherlands between 1588 and 1642 have LIRI values between 18.271 and 18.304 (D'Imporzano et al. 2021). The 5 years following 1642 show a transition to higher LIRI values that reach an "equilibrium" in the period 1647–1680. In these three

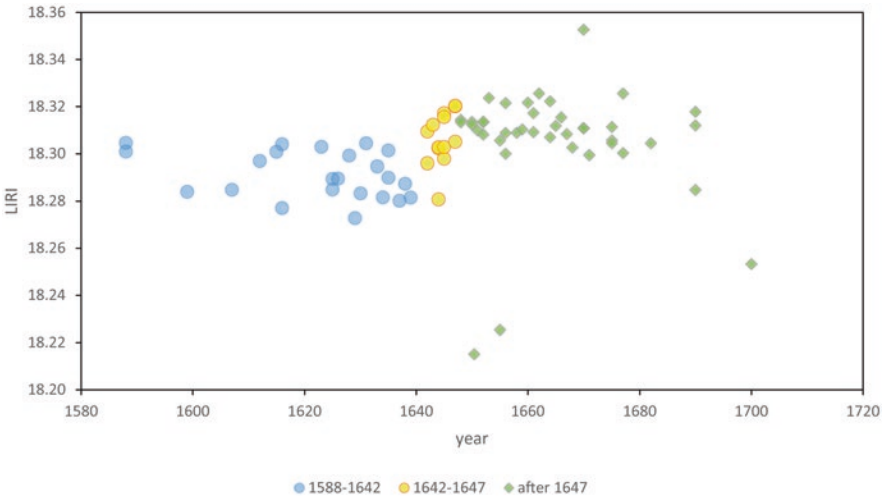

Fig. 14.6 Lead Isotope Ratio Index (LIRI) against time. The graph shows the data for lead white samples from 77 different Dutch paintings plotted against time (D'Imporzano et al. 2021)

decades LIRI values are between of 18.297 and 18.326. Samples from paintings made after 1680 appear to be more variable but the dataset from this period is limited, as is the coverage of paintings from the start of the seventeenth century. Despite these limitations, the study appears able to distinguish paintings from the seventeenth century Dutch period, based on their time of production. The explanation for variation in the lead isotope ratios of lead white appears related to changes in the socio-political and economic factors that controlled the lead trade in the seventeenth century. The major change in Pb isotope compositions between 1642 and 1647 is coincident with the English civil war. England was the main producer of lead before that period, and most lead white in north Europe was probably made using English lead. Changes in the supply chain during the English civil war led to changes in lead supply. The limited data available for the end of the seventeenth century show that the LIRI is more variable, and it appears that the LIRI values start to lower to values comparable to the beginning of the century. The end of the seventeenth Century was a period of major tension between the Dutch Republic, England and France, with a series of wars starting in the 1670s until the end of the century. This period of social turbulence would undoubtedly have altered the Pb supply chain and therefore explains the variance of the lead isotope ratios found in lead white. More data are needed in order to clarify this hypothesis and determine the exact changes in the source of Pb to the Netherlands. At the actual state of the art, the time-dependant variation of the lead isotope ratios of lead white is able to distinguish lead white used between 1588 and 1642 and between 1647 and 1680. This can be used in order to distinguish the work of artist active in different decades, in particular if they were active before and after the transition recorded in the period 1642–1647. In this optic lead isotope analysis could also help to distinguish the early and late work of an artist active in the middle decades of the century. The study of D'Imporzano et al. 2021 represents a first step to obtaining a better understanding a detailed record of the temporal changes in Pb isotope ratios in lead white over time but additional studies are required from other European countries to examine the extent that Pb trade was local or regional.

14.8 Lead Isotope Tool Box for Identification

The previous sections discussed how lead isotope ratios of lead white have been used in order to study paintings, and how information about provenance, affiliation to artistic groups and variance of lead isotope ratios within painting or artistic group can be used in cultural heritage studies. The majority of the information obtained to date, however, is relevant for the seventeenth century Dutch paintings. This section will provide guidelines of how to use lead isotope analyses on paintings that derive from artistic groups that have not yet been studied. The methodology is designed to help attribute the artist or discover forgeries.

In a case that a painting is analysed for lead isotope ratios, and the artist is unclear the following approach can be used. The first step is to gather as much background

information as possible. Information about date of production, artist name or artistic affiliation and region of provenance all can contribute greatly to interpretation of lead isotope data. As explained previously, the sampling strategy is fundamental for the correct characterisation of lead isotope ratios. Consequently, the study of a painting should be based on the analysis of multiple samples and these samples should be taken from areas of the painting containing lead white as pure as possible, in order to limit any unwanted external contamination. Ideally, 3–5 samples would be sufficient in order to assess correctly the variability of lead isotope ratios within the painting.

If the painting does not belong to a period of which the lead isotope composition is known (sixteenth to seventeenth century Dutch or Italian), then lead isotopes data interpretation requires the analyses of samples from paintings produced at the same time and in the same region. Based on the current state-of-the-art, however, it is not essential (but recommended when possible) to have paintings from the same artist, especially if not painted in the same period. These requirements may prove difficult, as obtaining sample material from well-characterised paintings (painter and time) is usually difficult and time consuming. Comparison of lead white samples of known provenance, i.e. which artistic period and region, is fundamental for correct attribution. If these steps are followed then lead isotope analyses can be used to help identify the artist.

As an example, we use the uncertain origin of a Spanish paintings purported to be from the seventeenth century. Currently there are extremely limited data from Spanish paintings and a lead isotope database for these painting, dated between the 1600 and 1750, does not exist. The information obtained from the analysis of a single sample would be therefore limited. In the absence of a comparison database, only three data interpretation outcomes are possible: (i) the lead white is consistent with one of the artistic groups characterised so far (Dutch, Italian); (ii) the lead white has isotopic ratios that fall in an area where modern lead white is found; (iii) the lead white has values inconsistent with previously analysed paintings. Option one would imply that the artist, if Spanish, used a foreign lead white or that the painting is not Spanish. The second option would suggest that the painting is a modern copy, or that seventeenth century Spanish lead white has a similar isotopic distribution to modern lead white. The third option does not allow attribution of the artist. In all these scenarios, the lead isotope analyses provide little concrete information. If, however, samples from other Spanish paintings of the same period were analysed, then it would be possible to have a control group to compare the data with, and lead isotope analysis would provide a clear indication for attribution. Without following the proposed approach the identification of many paintings using lead isotope analysis would be impossible, or worse, could give incorrect information. Currently, it is only possible to use lead isotope analysis to identify or discover forgeries of Dutch and Italian paintings in respectively the sixteenth and seventeenth centuries.

14.9 Conclusion

The study of lead isotope ratios of lead white demonstrates that is possible to identify the provenance of the Pb used in the pigment and the difference in lead provenance can identify pigment originating from different regions. In this way, it is possible use lead isotope ratios to identify Italian and Flemish/Dutch paintings produced in the sixteenth to seventeenth century. Lead isotope variation in lead white increases in modern time, and it is possible to identify an increase in lead isotope variation starting after the mid-eighteenth century, when extra-European lead deposits started to dominate the lead trade.

The lead isotope analysis of paintings in recent years focused on the identification of isotopic variance at different levels in order to provide a more quantitative interpretation of the data. Variance has been identified at three different levels: within a painting, within an artistic group and relative to time, most notably in seventeenth century Dutch paintings. The variation of lead isotope ratios found within a single painting and in seventeenth century Dutch paintings suggests that future studies employ a multi-sampling method for lead isotope analyses of lead white, especially when an analysis is applied for authentication. The heterogeneity found within individual paintings implies that the comparison of single samples of lead white between two paintings may provide insufficient information to make attribution to a region or an artist.

Available data suggest that it is possible to identify different artistic groups within a specific time and region using lead isotope analysis. Within these groups, however, it is impossible to distinguish different artists, especially if active at the same time, using lead isotope data alone. The detailed study of the seventeenth century Dutch period, however, establishes that lead isotope ratios of lead white follow a time-dependant trend. This variation is best illustrated using LIRI and indicates that it is possible to assign a Dutch painting to a certain part of the century, and potentially distinguish artists active in different decades, or can help to distinguish between the young or old work of the artists. This information represents a powerful tool to help in authentication of seventeenth century Dutch paintings.

For the study of paintings coming from other periods and regions, lead isotope analysis can still be a powerful tool if guidelines listed in Sect. 14.9 are followed. This review suggests that lead isotope analysis of lead white will become a powerful tool in the field of cultural heritage. The information obtained via this method cannot be obtained with other techniques and the isotopic composition can give insight on the material used that can allow distinction of original and modern paintings and as the database is expanded, a far greater understanding of lead trading will be established and how this was influenced by socio-political events in Europe and beyond.

Bibliography

Albarède, F., Beard, B.: Analytical methods for non-traditional isotopes. Rev. Mineral. Geochem. **55**(1), 113–152 (2004)

Batur, K.R.R.: I Archaeological evidence of Venetian trade in colouring materials: the case of the Gnalić shipwreck'. In: Trading Paintings and Painters' Materials 1550–1800, Proceeding from IV CATS Conference, Copenhagen 2018, pp. 111–120. Archetype Publications, Copenhagen (2019)

Berrie, B., Matthew, L.: Lead white from Venice: a whiter shade of pale. In: Studying Old Master Paintings: Technology and Practice, pp. 295–301 (2011)

Blanchard, I.: International Lead Production and Trade in the "Age of the Saigerprozess": 1460–1560, pp. 167–193. Franz Steiner Verlag Wiesbaden GmbH (1995)

Burt, R.: The transformation of the non-ferrous metals industries in the seventeenth and eighteenth centuries. Econ. Hist. Rev. **48**(1), 23–45 (1995)

Cooke, C.A., Bindler, R.: Lake sediment records of preindustrial metal pollution. In: Environmental Contaminants, pp. 101–119. Springer (2015)

D'Imporzano, P., Batur, K., Keune, K., Koornneef, J.M., Hermens, E., Noble, P., et al.: Lead isotope heterogeneity in lead white: from lead white raw pigment to canvas. Microchem. J. **105897** (2020a)

D'Imporzano, P., Keune, K., Koornneef, J., Hermens, E., Noble, P., Van Zuilen, K., et al.: Micro-invasive method for studying lead isotopes in paintings. Archaeometry. **62**(4), 796–809 (2020b)

D'Imporzano, P., Keune, K., Koornneef, J.M., Hermens, E., Noble, P., Vandivere, A. L. S., Davies, G.R.: Time-dependent variation of lead isotopes of lead white in 17th century Dutch paintings. Science Advances. In press (2021)

Eastaugh, N., Walsh, V., Chaplin, T., Siddall, R.: In: Heinemann, E.-B. (ed.) The Pigment Compendium: A Dictionary of Historical Pigments, pp. 233–235. Routledge, Amsterdam/ London (2004)

Eckstrand, O.R., Sinclair, W., Thorpe, R.: Geology of Canadian Mineral Deposit Types. Geological Survey of Canada (1995)

Fabian, D., Fortunato, G.: Tracing white: a study of lead white pigments found in seventeenth-century paintings using high precision lead isotope abundance ratios. In: Trade in Artists' Materials: Markets and Commerce in Europe to 1700, pp. 426–443 (2010)

Feller, R.L.: Artist's Pigments: A Handbook of Their History and Characteristics, pp. 187–219. National Gallery of Art, Washington, DC (1986)

Fortunato, G., Ritter, A., Fabian, D.: Old Masters' lead white pigments: investigations of paintings from the 16th to the 17th century using high precision lead isotope abundance ratios. Analyst. **130**(6), 898–906 (2005)

Galer, S.J., Goldstein, S.L.: Influence of accretion on lead in the Earth. Geophys. Monogr. Am. Geophys. Union. **95**, 75–98 (1996)

Gonzalez, V., Cotte, M., Wallez, G., van Loon, A., De Nolf, W., Eveno, M., et al.: Unraveling the Composition of Rembrandt's Impasto through the Identification of Unusual Plumbonacrite by Multimodal X-ray Diffraction Analysis. Angewandte Chemie International Edition (2019)

Gulson, B.L.: Lead Isotope in Mineral Exploration. Elsevier, Amsterdam (1986)

Henderson, J.: The Science and Archaeology of Materials: An Investigation of Inorganic Materials. Routledge, New York (2013)

Hendriks, L., Kradolfer, S., Lombardo, T., Hubert, V., Küffner, M., Khandekar, N., et al.: Dual isotope system analysis of lead white in artworks. Analyst. **145**(4), 1310–1318 (2020)

Homburg, E., de Vlieger, J.H.: A victory of practice over science: the unsuccessful modernisation of the Dutch white lead industry. Hist. Technol. **13**, 33–52 (1996)

Hong, S., Candelone, J.-P., Patterson, C.C., Boutron, C.F.: Greenland ice evidence of hemispheric lead pollution two millennia ago by Greek and Roman civilizations. Science. **265**(5180), 1841–1843 (1994)

Keisch, B., Callahan, R.C.: Lead isotope ratios in artists' lead white: a progress report. Archaeometry. **18**(2), 181–193 (1976)
Klaver, M., Smeets, R., Koornneef, J., Davies, G., Vroon, P.Z.: Pb isotope analysis of ng size samples by TIMS equipped with a 1013 Ω resistor using a 207Pb-204Pb double spike. J. Anal. At. Spectrom. **31** (2015)
Knaf, A.C.S., Koornneef, J.M., Davies, G.R.: "Non-invasive" portable laser ablation sampling of art and archaeological materials with subsequent Sr–Nd isotope analysis by TIMS using 1013 Ω amplifiers. J. Anal. At. Spectrom. **32**(11), 2210–2216 (2017)
Koornneef, J., Bouman, C., Schwieters, J., Davies, G.: Measurement of small ion beams by thermal ionisation mass spectrometry using new 10(13) Ohm resistors. Anal. Chim. Acta. **819**, 49–55 (2014)
Koornneef, J.M., Nikogosian, I., van Bergen, M.J., Vroon, P.Z., Davies, G.R.: Ancient recycled lower crust in the mantle source of recent Italian magmatism. Nat. Commun. **10**(1), 3237 (2019)
Mayerne, T.: Pictoria, Sculptoria, Tinctoria, et quae subalternarum artium (manuscript). Brit. Mus. Lond. Ms Sloane. **2052** (1620–1646)
Olby, J.: The basic lead carbonates. J. Inorg. Nucl. Chem. **28**(11), 2507–2512 (1966)
Pollard, M., Heron, C.: Chapter 9 – lead isotope geochemistry and the trade in metals. Archaeol. Chem. R. Soc. Chem. **2**, 302–345 (2008)
Rich, V.: Chapter 1 – origins and history. In: Rich, V. (ed.) The International Lead Trade, pp. 3–13. Woodhead, Cambridge (1994)
Roy, A.: Artists' Pigments. A Handbook of Their History and Characteristics, 2. National Gallery of Art, Washington, DC (1993)
Sangster, D.F., et al.: Stable lead isotope characteristics of lead ore deposits of environmental significance. Environ. Rev. **8**(2), 115–147 (2000)
Stacey, J.S., Kramers, J.D.: Approximation of terrestrial lead isotope evolution by a two-stage model. Earth Planet. Sci. Lett. **26**(2), 207–221 (1975)
Stols-Witlox, M.: Historical Recipes for Preparatory Layers for Oil Paintings in Manuals, Manuscripts and Handbooks in North West Europe, 1550–1900: Analysis and Reconstructions. Amsterdam School of Historical Studies, Amsterdam (2014)
Stols-Witlox, M., Megens, L., Carlyle, L.: To prepare white excellent...: reconstructions investigating the influence of washing, grinding and decanting of stack-process lead white on pigment composition and particle size. Artist's Proc. Technol. Interpret., 112–129 (2012)
Stos-Gale, Z.A., Gale, N.H.: Metal provenancing using isotopes and the Oxford archaeological lead isotope database (OXALID). Archaeol. Anthropol. Sci. **1**(3), 195–213 (2009)
van Loon, A., Vandivere, A., Delaney, J.K., Dooley, K.A., De Meyer, S., Vanmeert, F., et al.: Beauty is skin deep: the skin tones of Vermeer's Girl with a Pearl Earring. Herit. Sci. **7**(1), 102 (2019)
Vlieger, J., Homburg, E.: Technische vernieuwing in een oude trafiek, De Nederlandse loodwitindustrie 1600–1870. Jaarboek voor de Geschiedenis van bedrijf en techniek. **9**, 10–19 (1992)
Walter, P., Martinetto, P., Tsoucaris, G., Brniaux, R., Lefebvre, M., Richard, G., et al.: Making make-up in ancient Egypt. Nature. **397**(6719), 483–484 (1999)
Welcomme, E.: Développement de techniques combinées de microanalyse par rayonnement synchrotron pour l'étude des pigments à base de carbonates de plomb, pp. 21–72. These de Doctorat en Chimie, Paris (2007)
Welcomme, E., Walter, P., Bleuet, P., Hodeau, J.L., Dooryhee, E., Martinetto, P., et al.: Classification of lead white pigments using synchrotron radiation micro X-ray diffraction. Appl. Phys. A. **89**, 825–832 (2007)
Wheelock, A.K.: "St. Praxedis": new light on the early career of Vermeer. Artibus et Historiae. **7**(14), 71–89 (1986)

Part V
Case Studies

Chapter 15
The Role of Technical Study and Chemical Analysis on Questions of Attribution and Dating of Paintings and on Easel Painting Conservation Practice: Selected Case Studies

Aviva Burnstock

Abstract This chapter uses case studies to illustrate the challenges and ambiguities in interpreting technical and historical evidence to determine whether a painting may be categorised as an original or first version, as sketch or preliminary work, contemporary or later copy, pastiche or a forgery, made with the intention to deceive. The introduction of selected novel methods of analysis in the last decades and their impact on the assignment of paintings to these categories is discussed, with an emphasis on collaborative investigations between experts in science, art history and conservation in defining the questions and interpreting the evidence in the case studies. These new methods of technical study have been used to examine the physical history of paintings together with a significant and increasing body of knowledge of artists' studio practice, painting materials, their use and deterioration provide context for identification of forgeries and makes the task of the forger more difficult.

Keywords Attribution · Chemical analysis · Case studies

15.1 Introduction

The application of methods of technical study and chemical analysis of painting materials has for over a century provided evidence to inform a range of historical questions related to the origin authorship and condition of paintings. Technical imaging using microscopy, incident ultraviolet light and X-ray radiography were

A. Burnstock (✉)
Department of Conservation, Courtauld Institute of Art, London, UK
e-mail: aviva.burnstock@courtauld.ac.uk

M. P. Colombini et al. (eds.), *Analytical Chemistry for the Study of Paintings and the Detection of Forgeries*, Cultural Heritage Science,
https://doi.org/10.1007/978-3-030-86865-9_15

applied for technical examination of paintings from early in the twentieth century; from the later part of the century imaging in the infrared range, together with the opportunity for molecular characterisation of pigment and organic media in micro samples, provided evidence for materials and techniques used for paintings and studies of deterioration using a range of methods. The body of knowledge of artists materials and techniques, and new methods applied to examine the condition and physical history of paintings have provided a foundation for broad assignment of works of art to a century of creation, and indication of geographical origin. Although there have been significant technical developments since the IIC Nordic group conference on Art Forgeries in Reykjavik in 2003 (Amsgaard Ebsen et al. 2003), it is still true that technical evidence alone cannot provide conclusive argument for attribution of a painting to a particular artist, without context given by the provenance and history of the work, and the intention to deceive. However, there are a range of historical questions where technical evidence can provide critical evidence. These include questions about the physical history of the painting, its original presentation and additions and changes made to the work by or after the artist and the effects of previous conservation campaigns. The same evidence can be used together with historical documentary evidence to assign a painting as an original, contemporary or later copy, pastiche or forgery.

While in some instances the purpose of technical study is to address historical questions, more often as a prelude to conservation treatment analysis is carried out as part of an assessment of the materials, technique and condition of the work. This may include examination of the original materials and methods used to create the painting and characterisation of subsequent additions, by those other than the artist. This involves the application and interpretation of appropriate methods for technical and materials analysis, together with historical and contextual considerations to formulate a holistic technical and historical profile of the painting to be treated. This work then forms the basis for conservation treatment proposal.

In the last 20 years or so a range of novel methods have been applied to study paintings, including non- sampling techniques that provide imaging an analytical information. Notable is the application of non-invasive multispectral imaging and analysis and hand-held X ray fluorescence spectrometers (XRF) and MA-XRF for elemental analysis and mapping, and improved microscopy for characterisation of surface phenomena. Molecular characterisation of microsamples using Fourier Transform Infrared (FTIR) and Raman microscopy have provided advanced layer and particle specific analysis of paintings. These techniques have been fairly widely adopted in museums, research organizations and in some education institutions. Other advances in molecular characterisation using combinations of methods have spurred research that provides a framework of reference for new studies. The application of new technologies has led to new technical discoveries and evidence for re-interpretation of historical questions. Some of the techniques are sufficiently accessible to conservators, and offer the opportunity for diagnostic tools for material analysis in the studio that can inform conservation practice. While other methods including mass spectrometric methods for analysis of organic materials, radiocarbon dating, and dendrochronology require specialist expertise, the

engagement of scientists with the questions posed by conservators and historians has produced collaborative research and application and development of novel methods of analysis.

This essay discusses case studies, both published and new, that provide examples of the advantages and limitations of current methods used for technical study of paintings to address different questions related to the dating and attribution of paintings, their creation and physical history. The framework for evaluation of analytical and technical evidence that is critical for interpretation of the results is also outlined.

15.2 Case Studies

15.2.1 Dating, Assigning Geographical Origin

Material analysis has for decades been used to estimate the age and in some cases to assign a geographical origin to a painting for which there is no provenance or other information. The assessment may be made based on the condition and composition of support and its preparatory layers, its attachment to an original or non-original stretcher or strainer, and evidence of former treatments such a relining, damages and restoration paints. Analysis of the original inorganic materials used for paint and ground, and organic binding media may provide broad criteria for estimating the age and perhaps origin of the work. The context for interpretation was informed by evidence of the original painting and technique, and the identification of later additions and restoration campaigns. The identification of pigments not available at the time of making the original work may either be part of a mimetic restoration or if it is cogent with the original scheme of the artist, suggest a date of creation that postdates the introduction of the pigments. This can be quite broad as the benchmarks for the introduction of new pigments are largely limited to new materials introduced for use after 1700, in the nineteenth century, and apart from Titanium white that was introduced in the mid- 1920s, a range of modern synthetic organic pigments that may be characterised using Raman spectroscopy and HPLC (see Chaps. 10 and 11 in this volume).

Paintings made using materials that were available to artists for many centuries, such as iron oxides, chalk, gypsum, in oil media provide more limited criteria. An example is provided by a painting on canvas of a *Cumaean Sibyl*, similar to that at depicted by Bolognese artist Domenico Zampieri, known as Domenichino 1581–1641 (Fig. 15.1). The painting came with no date or provenance; preliminary superficial examination of the subject and style would suggest a date from the end of the seventeenth century to the nineteenth or even early part of the twentieth century. Damage to the support – an unlined and embrittled canvas – might suggest a date before the twentieth century. The painting was examined using a combination of microscopy, X radiography, infrared reflectography and X ray fluorescence spectroscopy to characterise the materials and techniques and condition of the painting,

Fig. 15.1 *Cumaean Sibyl*, private collection

and samples were taken of the canvas fibres and paint and ground layers prepared as cross section for assessment of the ground and layer structure. Results suggest that the painting was executed on linen canvas, primed with a layer of chalk, gypsum and lead white. The pigments used for the original paint included iron containing brown, red and ochres, umber mixed with lead white, all available from early times, with the exception of lead white that became less commonly used in the later part of the twentieth century. The infrared image showed no clear evidence of underdrawing, that may have been executed in a medium such as chalk or iron containing pigment that is transparent in the IR range used for reflectography. The X-radiograph showed limited areas of paint loss that had been inpainted in a previous restoration campaign.

While characterisation of the original materials here provided little indication of the date of the work, the layer structure and observations of the edge of the canvas and its method of attachment to the wooden stretcher provided key evidence. The canvas was attached to the strainer with a single set of tacks and no additional tack holes, suggesting that the support and strainer were original (Fig. 15.2). The canvas was primed to the edges and been cut from a larger piece of primed canvas. The surface deformations that included cupping of paint suggested that the canvas was

Fig. 15.2 Tacking margin of the commercially primed canvas for *Cumaean Sibyl*

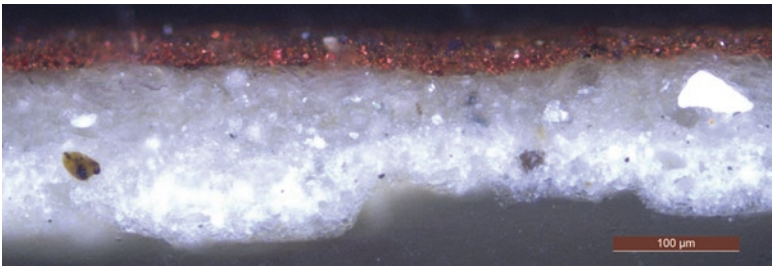

Fig. 15.3 Section from the brown background paint of the *Cumaean Sibyl* showing size layer and commercial priming layer with iron oxide pigment in the paint layer

primed with a layer of cold size before applying the ground layers, that rendered the canvas more responsive to moisture that could have led to cupping and flaking paint. This was confirmed by examination of the paint cross section (Fig. 15.3) that showed the application of a size layer followed by the white priming and red-brown paint. The composition and evenness of the priming and the application of a cold size layer pointed to the use of a commercially primed canvas typical of those produced from the early nineteenth century onwards.

The infrared image suggested that the artist made minor alterations, including slight widening of the width of the Sibyl's arms. No significant changes in composition were visible in the radiograph. An hypothesis could be constructed that the work may be a copy of an earlier motif, from the nineteenth century or later, based on the absence of changes made during painting, that are more usually present in the first version of a painting, where the artist is making adjustments to the composition. The lack of evidence for methods of transfer of the composition, that may have been done using a cartoon, grid or freely copied and the absence of another version of the composition made by Domenichino might suggest that the image is a pastiche, or image in the style of the seventeenth century master. Alternatively, the original version may have been lost since the copy was made.

Evidence for the production of the work in a geographical region presents more challenging inferences. While the materials used for the primed canvas are typical for those produced by leading manufacturers such as Roberson and Winsor & Newton in England in the nineteenth and early twentieth century, the same materials were used for commercial priming in France, the Netherlands and Germany (Carlyle 2001).

This case illustrates both the limitations of inferring date and origin of a paintings based on material analysis alone, and the importance of contextual evidence in forming hypotheses. There are some basic assumptions that have been made in this discussion: that the conservator, perhaps in collaboration with scientists, interpreted the technical evidence, to determine what was original and which materials were associated with earlier restoration campaigns. In this case, consideration of different pieces of evidence from each analytical method are integrated into an holistic understanding of the technique and condition of the painting. However, in relation to the attribution of the work, critical was the context provided by historical research into the history of depiction of the Cumaean Sibyl, workshop production by Domenichino and his assistants, and the enduring the popularity of the image in the centuries that followed. Technical studies of another painted image of the Cumaean Sibyl using a combination of analytical methods identified a version postulated to postdate 1750 based on the identification and use of Prussian blue and Naples Yellow (Daniilia et al. 2008). The authors also suggest that the painting was by the hand of Angelica Kaufmann based on stylistic evidence, and the use of similar pigments. A number of copies of this painting can be found on a google search that may have been made at any time after the original, and in this case further comparative technical evidence of works by Kaufmann together with provenance of the work would be needed to make a confident attribution.

An internet search yields more than one hundred painted versions of the Cumaen Sibyl in a similar style to that of Domenichino's original and was clearly a popular subject from the early seventeenth century onwards; these versions may have been produced in the artists studio by assistants, or may be copies or pastiches made at any time afterwards. The production of these versions and copies may have been for sale but not necessarily as the original version, or made as part of art school practice with no intention to deceive.

Further evidence for dating has been attempted using radiocarbon dating of micro-samples of paint and canvas (Hendriks et al. 2019). The authors reported a broad date range in the nineteenth century for the repurposed canvas support used for a known twentieth century forgery, confirmed by analysis of a sample of the oil medium used for the painting based on the C14 profile of the linseeds produced in the mid twentieth century. The problems with interpretation of analysis of complex mixtures of materials in paint samples is discussed by the authors. They acknowledge that interpretation of carbon dating of oil from paint samples would be further complicated by the addition of materials as part of the physical history of the works. For example, the application of oleoresinous varnishes as part of one or more restoration campaign will penetrate every crack and loss in the paint surface and may react with original inorganic materials to form soaps, making it difficult to distinguish the added oil from the oil binding medium used for the original paint. This further supports the necessity of holistic technical and historical study in dating a painting. For works on oak panels, dendrochronology is a reliable method for dating the felling of oak trees from which boards have been prepared for painting (Tyers 2010). While this method alone cannot date paintings that are made on re-purposed

oak supports, the boards can be characterised to Baltic or English origin, and thus provides evidence of the trade in artists' materials.

15.2.2 Physical History

15.2.2.1 Characterising and Imitating the Aging of Materials

Developments in technical analysis in the last decades have included research into the aging and deterioration of artists' pigments and painting materials, and identification of a range of deterioration phenomena in paintings. Molecular level analytical studies have led to hypotheses about the chemical processes underlying deterioration that link with optical and physical changes in paint, including colour change, formation of metal soaps in oil media, fatty acid efflorescence and blanching, and the material characteristics of paint that exhibit water sensitivity on cleaning. Methods for characterising organic materials that identify the molecular characteristics of the range of organic materials found in paintings, including original materials and modern synthetic materials have been useful in studies of the physical and conservation history of paintings (see Chaps. 7 and 8 in this volume).

Another outcome of the improvements in material characterisation is a deeper understanding of aging properties of paint and paintings, both in terms of what can be expected in aged works using both visual and chemical indicators. This makes it more challenging to replicate the effect of age convincingly in complex composite of materials from which paintings are made. This has long been a concern of forgers of works intended to be linked with traditional pre-nineteenth century varnished paintings where cracking and patination of varnish might convincingly disguise elements of the painting technique beneath. An example is a letter of enquiry as to how to create an antique effect in a picture varnish (Fig. 15.4). Imitating a painting with an understanding of an artist's technique and materials from published studies, it is still important to mimic convincingly the manifestation of the physical history of the whole object and not only the surface. A small panel painting *Portrait of a child with a bird* (Fig. 15.5) in the style of Peter Paul Rubens, with no documented provenance, provides an example of a work with a fabricated material physical history. The reverse of the unbevelled single piece of oak support measuring 25.5 × 19.6 cm (Fig. 15.6) showed evidence of rough marks made by a hand tool similar to that seen on panel paintings dated before the introduction of the mechanical saw in the early nineteenth century (Tyers 2015). Visual examination showed that the edges of the panel had been cut or sawn, and the back of the panel was stained brown after being cut as the satin has settled into fractures in the wood. An X radiograph of the panel (Fig. 15.7) showed an underlying composition comprising architecture with a series of arches and a balcony beneath the surface composition of the boy with a bird. The fractured edges of paint of the underlying composition suggested that the panel was cut after the paint had dried, before the final composition was painted. Dense areas on the radiograph suggested that the wood had been filled and repaired before

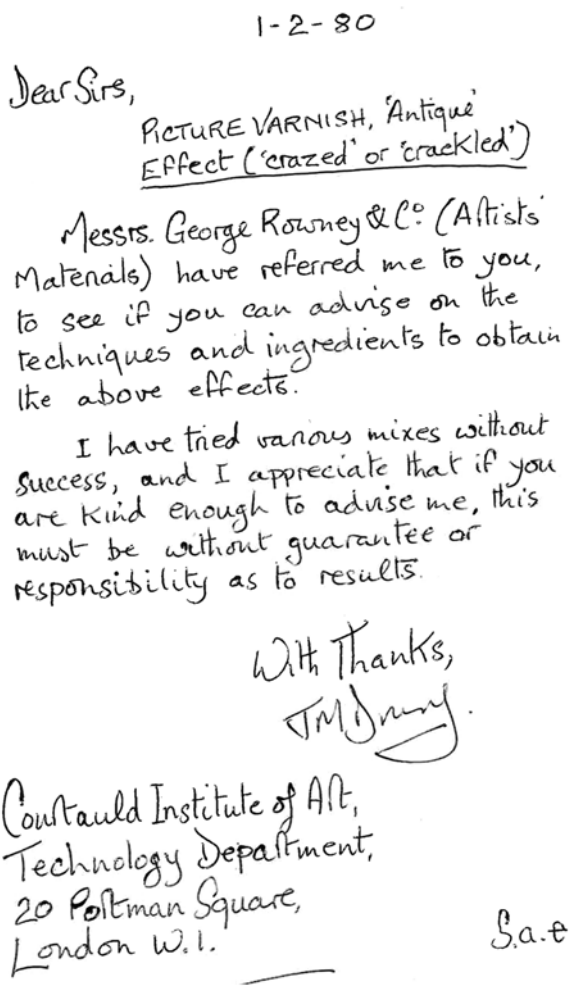

1-2-80

Dear Sirs,

PICTURE VARNISH, 'Antique' Effect ('crazed' or 'crackled')

Messrs. George Rowney & Co. (Artists' Materials) have referred me to you, to see if you can advise on the techniques and ingredients to obtain the above effects.

I have tried various mixes without success, and I appreciate that if you are kind enough to advise me, this must be without guarantee or responsibility as to results.

With Thanks,

T M Jenny.

Courtauld Institute of Art,
Technology Department,
20 Portman Square,
London W.1.

S.a.e

Fig. 15.4 Letter of enquiry as to how to make a picture varnish look antique

painting the upper image. Also visible in the radiograph are nail heads on the left and lower edges that could suggest that the oak wood board was repurposed, perhaps originally having been part of a piece of furniture, wainscot or a floorboard. Although not carried out as part of the present study, the owner reported that the wood had been dated to the fourteenth century by a respected expert in dendrochronology. Elemental analysis suggested that the upper composition was painted using a range of pigments available in the seventeenth century, however the presence of zinc in the white for the boy's costume and lead chromate yellow for his collar led to the conclusion that the portrait was painted in or after the mid nineteenth century.

More revealing was evidence of an attempt at fabricated ageing that was visible using the light microscope. The surface of the painting appeared to have been smeared with soot and abraded using sand before varnishing. Details show black

Fig. 15.5 *Portrait of a child with a bird, private collection*

particles of soot and granules of silica on the surface that have sunk into the paint, suggesting that the abrasion and application was done while the paint was wet (Figs. 15.8 and 15.9). Areas of more extreme abrasion in the boy's jacket had removed the brown paint entirely in a series of horizontal marks (Fig. 15.10). The combination of soot and abrasion rendered the surface with a muted, aged appearance that might be typical of a work on panel from the seventeenth century.

In this case, the painting was clearly executed on an old piece of oak that had been repurposed more than once for painting. The pigments used to paint the *Boy with a bird* included materials available only from the nineteenth century, when the fashion spread for viewing paintings as if affected by the smoke from the pipe of old father time, depicted in a print by William Hogarth (Fig. 15.11). This raises the question of whether the evidence of abrasion, the application of soot and the tinted varnish coating was part of the intention of the nineteenth century creator of the panting rather than the efforts of a forger to give the appearance of a work from Rubens's time.

The status of the painting might be clarified further, as a copy of the original version by Rubens now in the Gemaldegalerie der Staatlichen Museen in Berlin (Fig. 15.12). The work is also on an oak panel measuring 50.9 × 41 cm, approximately double the height and width of the support for the copy. The original dated

Fig. 15.6 Reverse of the oak panel support for *Portrait of a child with a bird*, showing tool marks and brown staining

around 1616 is very famous, and even inspired a stamp in use in 1953 (Fig. 15.13) and may have been copied many times once it was in the public domain. In the nineteenth century the image may have been known in print form and accessible to art students and copyists. The copy examined in this case study shows none of the hallmarks of Rubens's painting technique on panel, such as the use of a beige imprimatura for the mid tones and shadows and swift economical application of highlights in the flesh and drapery, and touches of red that give translucency and three-dimensionality to the forms. For the copy the paint is more thickly applied and worked with no visible underlayers.

A search for versions of this work also leads to websites that promise to reproduce the image using "real oil, real brushes, real artists, real art" and for a small extra cost to be aged and cracked (https://www.1st-art-gallery.com/cracked-aged-craquelure-paintings.html n.d.). The case study *Portrait of a boy with a bird* discussed here is clearly not a modern aged copy on canvas made to order, nor a copy of the whole object made by another process such as laser scanning and 3-D reproduction available today that can reproduce surfaces very accurately using a polymeric material (https://www.factum-arte.com/ n.d.). The status of the work as a nineteenth century copy made to the taste of the era or a forgery relies on the intention to deceive.

Fig. 15.7 X radiograph of *Portrait of a child with a bird*

15.2.3 Attribution

There are now many published studies and popular media productions that have used technical evidence to review attribution to a specific artist. Examples presented here are selected either because they present challenges for interpretation or where new evidence has proved decisive.

15.2.3.1 Signatures, Studio Practice and Collaborative Production

It has long been recognized that signatures are not a reliable means for attributing paintings to an artist; many if not most artists do not sign their works, and those that have been signed are often reinforced or altered in past treatments. For those artists who are known to have regularly signed their paintings the use of methods of handwriting analysis may be useful, but beyond the scope of this essay. The question of who signed the works might also be investigated, for example, Degas signed his works before sale by hand or using a name or atelier degas stamp; the same stamp may have been used to mark unfinished or unsigned works after the death of the

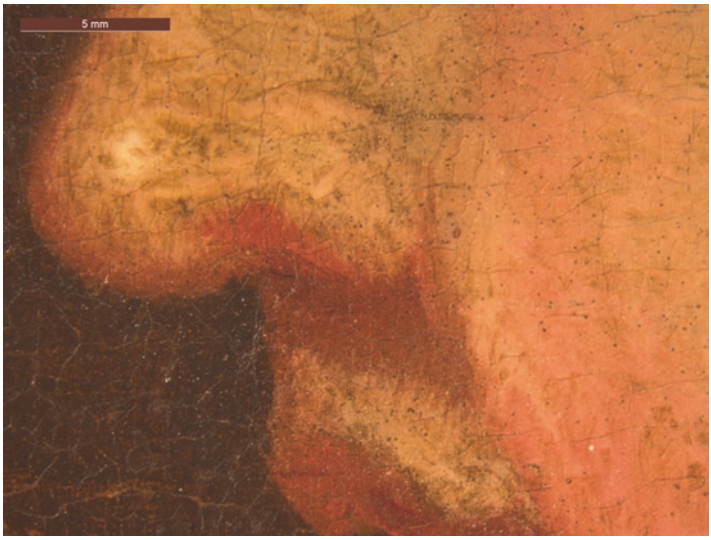

Fig. 15.8 Micrograph of a detail of the child's face with soot smeared on the surface of *Portrait of a child with a bird*

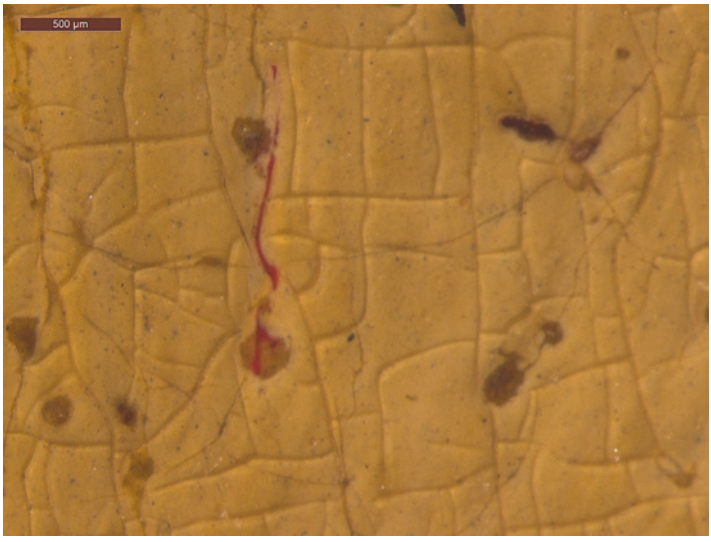

Fig. 15.9 Micrograph showing granular sandy material smeared on the surface in pits, *Portrait of a child with a bird*

artist (http://www.degas-catalogue.com/methodologie.html n.d.). Other paintings may simply have been signed by dealers, at the point of sale. Unfinished works left in the studio of deceased artists may have been "finished" and signed by a dealer before sale.

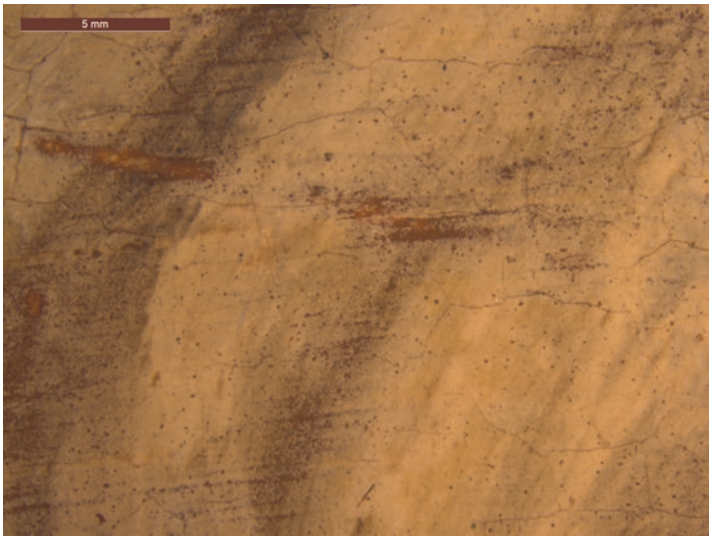

Fig. 15.10 Micrograph showing abraded paint of child's jacket**,** *Portrait of a child with a bird*

Further debate on signatures in relation to Rembrandt's paintings was addressed as part of the Rembrandt Research project (1968–2011) in which technical imaging and close object based study was used as part of an historical investigation that aimed to redefine the artist's oeuvre, resulting in the publication of six volumes *A corpus of Rembrandt Paintings*. Relevant to signatures it was proposed that Rembrandt signed works by some of his most talented pupils (Bruyn et al. 1989). This hypothesis could explain the variation in painting techniques of paintings that carried Rembrandt's signature. The challenge faced by technical research in this project was to characterise the painting techniques of the artist as distinct from his pupils and contemporaries who used many of the same materials and techniques. The possibility of collaborative production was also considered, that was common practice in the production of art long before and after Rembrandt's era. Although close object based study highlighted repaint and strengthening of signatures, the proposal devalued the artist's signature and relied on judgment of the particular method of handing of paint for arguments about attribution.

15.2.3.2 Review of Attribution Using New Analytical Evidence

In 2003 Johannes Rød presented a case for attribution of a *Portrait/Self Portrait? Of Vincent Van Gogh* acquired by the Nasjonalgalleriet Oslo in 1910 from Paris dealer E. Blot (Rød 2002). Although the provenance of the painting could be traced back to the dealer Vollard in the first years of the twentieth century, questions of authorship of the painting were raised based on the painting technique that differs from the artist's other self-portraits made in Paris from 1886 or later. Following its

Fig. 15.11 Print of *Father time smoking a painting* by William Hogarth 1761

recovery by police after it was stolen from the museum in 1984, conservators/scientists Unn and Leif Plahter examined the painting and provided interpretation of the materials and techniques. They noted small changes in the composition and the use of pigments lead and zinc white both used by van Gogh and contemporary artists of the time. Rød made a case for the presence of another portrait beneath the uppermost image, based on interpretation of the radiograph and proposed that the paint of the underlying head was partly scraped before developing the final image. Rod concluded that the painting technique is different from other self portraits by the artist, but nonetheless was in his view a work left unfinished or rejected by Van Gogh.

In the decade following Rød's publication there was intensive research into the materials and techniques used by Van Gogh, resulting in many publications including *Van Gogh's Studio Practice*, that included chapters that describe the application of weave pattern analysis in canvas supports used by van Gogh (Hendriks et al.

Fig. 15.12 *Child with a Bird* probably his son Albert by Peter Paul Rubens c.1616 Gemaldegalerie der Staatlichen Museen Berlin

2013; Johnson et al. 2013). The results showed matching weave patterns for paintings that were cut from the same bolt of canvas, providing new evidence for both attribution and the chronology of the paintings. This relies on the notion that the artist had exclusive use of bolts of canvas (letters to his brother Theo record Vincent's request for artists materials) from which sections were cut for individual paintings when required. Thread counting is based on scanned X radiographs of the paintings, and thus new evidence for the attribution of the Oslo portrait was gleaned from the application of this method. Johnson found that he portrait has a warp-direction match with F557, Flowering Almond Tree in the Van Gogh Museum Amsterdam dated 1888.[1] This provides significant evidence for the attribution of the self-portrait and an indication of the date it was painted, given that the support was cut from the same roll of primed canvas. With this strong evidence for the association between works by Van Gogh himself, an interpretation of the anachronistic painting technique noted by Rød would be considered in the attribution to the artist. Rød noted that the Oslo portrait has a mutilated ear on the right rather than the left side depicted in other self-portraits of the artist painted in 1889. One plausible explanation is that

[1] Don Johnson, personal communication August 26th 2020.

Fig. 15.13 Stamp from 1953 after Rubens's original version of *Child with a bird*

the painting was reworked later by the artist, or by another hand that would explain the mistaken depiction of the ear, and the difference in paint handling. Another possibility is that an artist has a broader spectrum of production and wide variation in technique. This argument has also been applied to works by Rembrandt, who was capable of painting using a range of styles from closely blended to broad freely applied brushwork.

Considering specific elements of artistic practice together with the history and the function of a work of art in relation to other versions of the subject may be critical in determining attribution of a painting. An example is the question of the relationship between two versions of Edouard Manet's *Le Dejeuner sur l'herb*, the larger scale painting now in the Musée D'Orsay, Paris dated 1863 and a smaller version of the same subject in the Courtauld Gallery, London (Fig. 15.14), for which the date is uncertain and the attribution to Manet has been questioned by some scholars. Recent cleaning of the Courtauld painting, together with technical imaging using MA-XRF and material analysis using hyperspectral imaging and other methods contributed to a review of the status of the smaller work (Amato et al. 2020). Ambiguities interpreting the provenance of the Courtauld painting, with regard to its production as a preparatory sketch, or alternatively as a copy of the larger painting was re-evaluated in the context of new technical evidence. The Courtauld panting is smaller and the paint more sketchy applied than the Orsay painting that has a more finished blended brushwork. The figures in the smaller work are laid in using diluted brownish paint composed of a mixture of pigments, a technique that is characteristic of Manet and his contemporaries mid-nineteenth century painting practice. The pigments used for the Courtauld painting were

Fig. 15.14 Le Dejeuner sur L'herb, Edouard Manet, Courtauld Gallery

similar to those reported in published studies of paintings by the artist, and were used throughout his painting career. While an X ray of the larger composition shows many changes to the composition, only minor changes were noted in the Courtauld painting. Critical new evidence provided by MA-XRF mapping of elemental calcium showed a grind beneath the composition probably applied using chalk, that was not detectable using Infrared reflectography (Fig. 15.15). Evidence of a second grid was observed at the edges of the painting at intervals marked in red paint, that may indicate that a copy was made after the work was completed, perhaps using a grid of strings. The presence of the chalk grind beneath the paint suggests that the composition was copied from another version, while the second grid may have been used to make a copy of the Courtauld picture. In this case, it is clear that close similarities between the materials used for the painting place it in Manet's oeuvre, but a wider survey of Manet's use of sketches and the production of copies and versions is needed to contextualise the findings; in particular, close examination of the Orsay version may provide more evidence about the links between the paintings.

Fig. 15.15 MA-XRF scan for Ca showing grid beneath the Courtauld painting, image from (Amato et al. 2020)

15.3 Conclusion

The question of whether a work is the original, a copy, a version or a deliberate forgery requires consideration of a combination of technical and historical evidence, and consideration of the history of studio practice and the history of production of art. Collaboration between masters and assistants and the sharing of images between workshops using copies and cartoons was common practice before the nineteenth century when artists such as Vincent van Gogh worked alone. Context provided by evidence both technical and historical is needed to determine whether a copy or version of a painting was made as with the intention to deceive and be sold as an original, that would define it as a forgery. Thus the individual proposing to sell a work that was originally made as an innocent copy may redefine the painting as a forgery.

The development of new methods that characterise the date of painting materials makes the creation of a forgery more difficult. However technical evidence must be carefully interpreted to consider the function and condition of the work and the changes it has undergone since its creation. This requires collaboration between scientists, historians, curators and conservators for effective interpretation of the status of the work based on technical and historical evidence.

As the body of knowledge about artists materials, techniques and studio practice grows together with instrumental methods for characterising modern materials, new

criteria for dating and attribution may be possible. This contextual knowledge in published studies may appear to favour forgers by making available detailed information on key elements of an artist's work, however increasing confidence in material characterisation and dating using novel techniques will present challenges for future forgers of paintings.

References

Amato, S., Cross, M., Burnstock, A., Janssens, K., Dik, J., Cartechini, L., et al.: Examining Édouard Manet's Le Déjeuner sur l'herbe from the Courtauld Gallery using spectral imaging techniques. In: Kempski, M., Kirby, J., Leanse, V., Mandy, K. (eds.) 'Tales of the Unexpected' in Paintings Conservation, pp. 98–110. Archetype Publications Ltd, London (2020)

Amsgaard Ebsen, J., Jacqueminet, N., Ásgeirsdóttir, H.: Preprints of the IIC Nordic Group 16th Congress "Art Forgeries", 4–7th June 2003. The University Press, Reykjavik (2003)

Bruyn J. A selection of signatures, 1635–1642. In: Bruyn J, Haak B, Levie SH, van Thiel PJJ, van de Wetering E, editors. A Corpus Rembrandt Paint. vol. III 1635–1642, Springer; 1989, p. 51–56

Carlyle, L.: The Artist's Assistant: Oil Painting Instruction Manuals and Handbooks in Britain 1800–1900 with Reference to Selected Eighteenth-Century Sources. Archetype Publications Ltd, London (2001)

Daniilia, S., Minopoulou, E., Andrikopoulos, K.S., Karapanagiotis, I., Kourouklis, G.A.: Evaluating a Cumaean Sibyl: Domenichino or later? A multi analytical approach. Anal. Chim. Acta. **611**, 239–249 (2008). https://doi.org/10.1016/j.aca.2008.01.079

Hendriks, E., Johnson, J.C., Johnson, D.H., Geldof, M.: Automated thread counting and the studio practice project. In: Vellekoop, M., Geldof, M., Hendriks, E., Jansen, L., de Tagle, A. (eds.) Van Gogh's Studio Practice, pp. 156–181. Mercatorfonds, Brussels (2013)

Hendriks, L., Hajdas, I., Ferreira, E.S.B., Scherrer, N.C., Zumbühl, S., Smith, G.D., et al.: Uncovering modern paint forgeries by radiocarbon dating. Proc. Natl. Acad. Sci. **116**, 13210–13214 (2019). https://doi.org/10.1073/pnas.1901540116

http://www.degas-catalogue.com/methodologie.html. n.d.

https://www.1st-art-gallery.com/cracked-aged-craquelure-paintings.html. n.d.

https://www.factum-arte.com/. n.d.

Johnson, D., Johnson, J.C., Hendrinks, E.: Automated thread counting. In: Vellekoop, M., Geldof, M., Hendriks, E., Jansen, L., de Tagle, A. (eds.) Van Gogh's Studio Practice, pp. 142–155. Mercatorfonds, Brussels (2013)

Rød, J.: Vincent van Gogh's self portrait in Nasjonalgalleriet Oslo, genuine of fake? In: Art Forgeris. Prints of the Contribution to the Nordic Group 16th Congress, 4–7th June 2003, pp. 22–30 (2002)

Tyers, I.: Aspects of the European Trade in Oak Boards to England 1200-1700. In: Kirby, J., Nash, S., Cannon, J. (eds.) Aspects of the European Trade in Oak Boards to England 1200–1700, pp. 42–49. Archetype Publications Ltd, London (2010)

Tyers, I.: Panel making, sources of wood, construction "trademarks" and conclusions on the making and trade in the UK. In: Cooper, T., Burnstock, A., Howard, M., Town, E. (eds.) Painting in Britain 1500–1630: Production, Influences and Patronage, pp. 107–115. Oxford University Press/British Academy (2015)

Chapter 16
Approaches to Current Issues with Art Forgery, Restoration and Conservation: Legal and Scientific Perspectives

Jana S. Farmer and Jennifer Mass

Abstract With the soaring values of artworks over the past few decades, it is increasingly important for art buyers to be mindful of the risks associated with art forgeries and potential mistakes in conservation of artworks, both of which may affect the value of their investment (the rising art prices are in part attributable to the inflation considerations). The authors of this chapter offer art law and scientific perspectives on these issues as well as make recommendations as to what an art purchaser should look out for and how art collectors and conservators may most safely approach their dealings with the market. The first part of this chapter will discuss the contractual protections, scientific tools, and legal remedies that may be available to a buyer of a fake or forged artwork. The second part of this chapter is dedicated to the potential impacts of conservation on artworks, as well as the risks and remedies in connection with the process of conservation and restoration of artworks. Most of the discussion of legal issues is based on the United States law perspective.

Keywords Art forgery · Restoration · Conservation · Legal issues

J. S. Farmer (✉)
Partner and Chair of Art Law Practice, Wilson Elser Moskowitz Edelman and Dicker LLP, New York, NY, USA
e-mail: Jana.Farmer@wilsonelser.com

J. Mass
President and Founder of Scientific Analysis of Fine Art, LLC and Mellon Professor of Cultural Heritage Science, Bard Graduate Center, New York, NY, USA

M. P. Colombini et al. (eds.), *Analytical Chemistry for the Study of Paintings and the Detection of Forgeries*, Cultural Heritage Science,
https://doi.org/10.1007/978-3-030-86865-9_16

16.1 Case Studies Involving Art Forgery

"Follow the money" is a catchphrase made popular by the film *All the President's Men* (1976). Art crime does exactly that: with the soaring art prices in the past few decades, the limited supply of coveted artworks, and the risk that a buyer may "fall in love" with the piece, clouding their judgment, the art market is unfortunately attractive to bad actors of all manner. In April of 2018, more than 60% of the works on display at the Musée Terrus in Elne, France, were revealed to be fakes after the signature on one of the paintings easily wiped away when a visiting art historian passed over it with a white glove (Neuendorf 2018). Earlier that same year, top art curators and dealers issued an open letter criticizing the Meseum voor Schone Kunsten in Ghent, Belgium for displaying questionable artworks of Russian avant-garde artists (Fake Kandinskys, Malevichs, Jawlenskys? Top curators and dealers accuse Ghent museum of showing dud Russian avant-garde works (January 15, 2018), following which the museum removed the show (Cascone 2018).

The curators of this show relied predominately on art historical analysis for their due diligence prior to the loan of the privately held works. However, two of the works were also accompanied by materials analysis certificates that seemed to demonstrate the use of period- and artist-appropriate materials (Cascone 2018). This is an excellent example of how a multidisciplinary approach must be taken with respect to due diligence, whether it is prior to a loan of a private collection for an exhibition or prior to a sale.

In 2017, an exhibit of the works of Amadeo Modigliani in Genoa, Italy, closed following the allegations by the Italian prosecutors that 21 of the 60 artworks shown were possible fakes (Povoledo 2017). In fact, in 2014, Switzerland's Fine Art Expert Institute (FAEI) issued a sobering report estimating that at least 50% of the art circulating in the art market is forged or misattributed, and that is a conservative estimate (Over 50 Percent of Art is Fake (October 13, 2014) 2014).

Any suspicions before a sale should ideally be followed by a scientific examination of the works for anachronistic media or for materials that may be period-appropriate but were not used by the artist. Innovations in portable and non-destructive spectroscopy and spectroscopic imaging have meant that cultural heritage scientists increasingly have reference data on the artist in question when this situation arises. However, we still find ourselves in a technological "arms race" with art forgers, famously including Wolfgang Beltracchi who tried to "science-proof" his forgeries by using period-appropriate pigments (Finn 2014). Beltracchi's forgery methods were closely studied by paintings conservator Gunnar Heydenreich and his colleagues (see generally (Blumenroth et al. 2019; Nadolny and Eastaugh 2014)). Heydenreich revealed that Beltracchi would obtain period-appropriate canvases for his forgeries, and then sand down the original painting to obtain a priming layer, canvas, and stretcher of the appropriate age. He would sometimes leave some paint media from the original painting so that if x-rayed the forgery would even be revealed to have pentimenti. He would then purchase what he thought were period-appropriate and artist-appropriate pigments for the early twentieth-century artists

whose work he forged, including Max Ernst, Heinrich Campendonk, and Fernand Léger. However, Beltracchi understood some features of the history of artists' materials exceedingly well but overlooked others. For example, he used vermilion red (a mercury sulfide, HgS) in paintings that were supposed to date from the early decades of the twentieth century. This would be a perfectly appropriate red pigment to observe for this time period, however by the twentieth century all of the vermilion red pigment available to artists was laboratory-synthesized HgS, not the mineral analog of this bright red material – cinnabar. Cinnabar has the same chemical formula as vermilion, but it has the clastic morphology and impurities that are to be expected of a pigment made from a ground mineral source. Vermilion red has been synthesized since the ninth century AD, and so the identification of cinnabar was a "red flag" for Beltracchi's work.

Beltracchi also endeavored to make the physical characteristics of his forgeries correct by drilling fake worm holes into paintings on panel, as well as sprinkling dust and debris between canvases and their stretchers to give the impression of appropriate age (Schmidt 2019). He would even apply a layer of surface soil to his paintings that stopped at the edge of the frame to give the impression of appropriate patterns of dirt collection for his framed paintings. One of his most important contributions to using physical methods to obtain a faux patina of age was his oven-drying of his paintings. He built a specially programed furnace to create a craquelure consistent with the age of a given work. However, again we see that his physical aging methods were not perfect. The worm holes in the wooden panel supports were made with a power drill and so they do not meander in the manner of real worm tunnels. Likewise, he sometimes sanded too much of the original priming/ground layer of the painting revealing the canvas weave in an atypical manner, or would create paintings with tacking margins that were readily distinguishable from the original artist's works.

Wolfgang Beltracchi's rigorous attempts at deception also included creating a deceptive provenance, in one case taking photographs of his wife Helene dressed up as her grandmother with the paintings in the background to create false documentation/history of ownership. This type of deception was combined with a keen understanding of the art market. He never tried to forge artists whose work was so valuable that it would inevitably come under intense scrutiny. By sticking to the mid-range of the market, he was able to capitalize on the fact that only works selling at the very top of the market are subject to the type of rigorous inspection that might reveal his carefully constructed forgeries. The level of planning and sophistication that Beltracchi put into his forgeries, in terms of their false provenances, stylistic attributes, carefully considered artists' materials, and position in the art market meant that the exceedingly diligent inspection of the works required to identify them was unlikely to occur. However, Beltracchi was caught when a titanium white pigment (not available until 1916) was identified in one of his "Campendonk" preparation layers that was purported to date to 1914. While Beltracchi understood pigment chronologies and the history of artists' materials to a large extent, he was unaware additives and fillers that can be present even in a tube of a historic paint such as zinc oxide white. He was sentenced to six years in prison following his conviction of

forgery and corruption in 2011, and he maintains that many of his paintings still hang in major European collections.

Given the remarkable care with which Beltracchi constructed a work designed to fool conservators, scientists, art historians, and provenance researchers, what due diligence lessons can our fields learn from studying his crimes? One of the first is that the type of rigorous study required to identify a forgery of this quality is unlikely to take place before a sale, no matter how ideal this would be. Such due diligence would certainly require a full complement of research techniques. These would include elemental analysis, molecular analysis, microscopic analysis, stratigraphic analysis, multispectral imaging, provenance research, examination of the work's support and its construction, and even a study of the work's conservation history and paint degradation products. Given the intensive nature of this type of research, the construction of an agreement that allows for due diligence to take place for some period of time after the sale makes sense. We have seen that it can take years for a forgery circulating in the market to be questioned, and some sort of transactional protection for this commonly occurring circumstance is needed. An understanding of Beltracchi's methods also speaks to the need for deeper and more substantive collaborations between experts in allied fields studying artworks. All too often a painting receives a thorough scientific study but not the connoisseurship or provenance research that should accompany such research. Similarly the art market has traditionally heavily relied on connoisseurship expertise in the absence of the other allied disciplines. It is this type of oversight that allowed the Knoedler scandal to occur, and there are both legal and best practices lessons to be learned from this Abstract Expressionist fiasco that can prevent this type of large-scale fraud in the future.

In the art market, the principle of *caveat emptor* (Latin for "let the buyer beware") controls, with the buyer running the risk that their often considerable investment may be for naught and that they will not be able to simply return the purchase and get their money back. With art being a passion asset as one of its attributes, purchasing art is an emotionally charged decision and the experience of discovering that one's artwork is a forgery is also intensely personal. Art advisors highlight the importance of knowing your dealer, doing one's due diligence, carefully examining the ownership history, as well as consulting provenance researchers, connoisseurship and scientific experts (Goukassian 2020). The problem, however, is that the bad actors are often talented artists and knowledgeable researchers themselves (Goukassian 2020), and documentation can be forged just as the artwork itself, as the Art Newspaper's investigation into the Ghent Russian avant garde exhibition suggested (Hewitt 2018). A strong contract is important to give the buyer additional protections and the ability to recoup at least part of their investment should the artwork be determined to be a forgery. After a forgery is revealed, a buyer may also be able to pursue claims sounding in tort (typically, fraud and misrepresentation) or breach of contract against the seller of forged art or the forger itself, and possibly against other participants in the transaction. It is important to know, however, that an element of fraud that the buyer needs to prove (at least as far as the U.S. litigation is concerned) is that his or her reliance on the misrepresentation was justified. We

will discuss the meaning of what justifiable reliance means in the following case studies.

16.2 Defining the Terminology: Fake v. Forgery

Initially, while in common parlance the terms "fake" and "forgery" are interchangeable, it is important to remember that specialists apply these terms in restricted ways (Casement 2020). As the meaning of the term "forgery" is not uniformly established, legal terminology typically avoids the term altogether in regard to artworks (Casement 2020). Typically, a forgery is a work that intends to deceive (Biggest Art Fakes and Forgeries Revealed in 2018). In contrast, a "fake" often refers to a work that is a copy or a replica, or a work that is misattributed (Biggest Art Fakes and Forgeries Revealed in 2018).

Throughout this chapter, we will use the term "forgery" to refer to artworks that are intentionally meant to deceive the buyer as to the artwork's authorship.[1]

16.2.1 Contractual Protections for Buyers of Art

For a buyer who is finally able to purchase that coveted artwork that they have been hunting, it is often tempting to throw caution to the wind and secure the piece at any cost. And yet, this is the time to pause and think, is this deal too good to be true? In the art market, the disparity of knowledge of material facts about the artwork between the buyer and the seller may be remedied by the use of contractual representations and warranties[2] in the art purchase agreement. Among the representations that should be included are that the seller owns the artwork and has full authority to sell it, as well as that the artwork is not encumbered by any third-party claims, such as liens, or possible or pending restitution claims by alleged prior owners. With many art transactions being international or art crossing international borders at some point in its history, it is also important to confirm that the artwork was not imported in violation of the relevant jurisdictions' export/import, customs and cultural patrimony laws (see e.g., McKinley Jr. 2018; Prada 1998). In the United

[1] It should be noted that art scholars and authenticators may reasonably disagree about the provenance or authenticity of a piece of art. *See* Christine E. Weller, Lessons from Two Recent Art Forgery Cases, 3 Stetson J. Advoc. & L. 1 (2016), p. 3. While such disagreements indubitably affect value, they are outside the scope of such chapter as we focus solely on the artworks created or modified with an express intent to deceive.

[2] Representations have been defined as statements of fact that generally relate to past or existing facts and warranties have been defined as promises that existing or future facts are or will be true. *See* Stephen Glover, Representations and Warranties in Acquisition Agreement, Practice Note, available via plus.lexis.com.

States, the guiding principle is that a thief cannot pass good title, which means that if art was purchased and sold in violation of property, import/export, customs or other laws at any point in its history, there is a risk that even a good-faith purchaser for value cannot obtain good title for such art.[3] This means that even if the buyer bought an artwork at a reputable gallery or an auction house, and the artwork is later shown to be stolen or illegally exported, the art may need to be restituted, (see e.g., Cohan 2019; Duron 2021). By contrast, in most civil law countries (e.g., most of Europe), good title may be obtained so long as the art was not bought directly from a thief and/or was held by the collector for decades (Prowda 2013, p. 222).

Additionally, given that in the art market, scholarship and scientific methods are rapidly evolving and provenance research resources are increasingly digitized and accessible, facts may emerge as to an artworks condition, ownership and authorship in the future that were possibly not available or not completely available at the time of purchase, (see, e.g., Moynihan 2018). It is critically important for the buyer to have the same information as the seller before entering into a transaction. As such, a buyer should require a representation from the seller that they are not aware of any information pertinent to the issues of authorship, authenticity, provenance and prior ownership that was not disclosed to the buyer. In the *Knoedler* cases discussed below, there was evidence that the gallery received a very negative report from the International Foundation for Art Research (IFAR), of which the buyers should have been made aware of (Bono 2013; Goukassian 2020).

Provided that there is an art purchase contract in place (which, sadly, is not always the case even when millions are at stake (Haigney 2017, pt. "[t]he two sides had no written contract regarding the commission")), the buyer will have an option to rely on the contractual provisions to seek repayment of the purchase price in exchange for the return of the artwork if one or more of the representations discussed above turn out to be false.[4] Alternatively, the doctrine of mutual mistake of

[3] *See, e.g., Reif v. Nagy*, 2018 NY Slip Op 28253, ¶ 2, 61 Misc. 3d 319, 323, 80 N.Y.S.3d 629, 632 (Sup. Ct., New York Cty., 2018); *Farm Bureau Mut. Auto. Ins. Co. v. Moseley*, 47 Del. 256, 8 Terry 256, 90 A.2d 485, 488 (1952) ("The general rule is well established that no one can transfer a better title to personal property or chattels than he himself has. … Even a bona fide purchaser acquires no title to property which has been stolen") (citing Heckle and other cases); *Motors Ins. Corp. v. State of South Carolina*, 313 S.C. 279, 282, 437 S.E.2d 555, 557 (1993) ("Because a person can pass to his successor no greater title than he acquired, a thief or one in the subsequent chain of title cannot grant good title to stolen property, even to a bona fide purchaser."); *In re "Paysage Bords De Seine," 1879 Unsigned Oil Painting on Linen by Pierre-Auguste Renoir*, 991 F. Supp. 2d 740, 744–745 (E.D. Va. 2014) ("even a good-faith purchaser for value cannot acquire title to stolen goods"); *Brown Univ. v. Tharpe*, No. 4:10CV167, 2013 U.S. Dist. LEXIS 79164, 2013 WL 2446527, at *11 (E.D. Va. June 5, 2013) ("a thief cannot pass title to stolen goods even to an innocent purchaser who pays for the stolen goods.")

[4] When art is purchased online, for example at an online action, the platform's Terms of Sale and Terms of Use will operate as the contract between the buyer and the seller. The buyer should review these terms and conditions before purchase, including specifically the (No) Representations and Warranties section, the Limitation of Liability and the Governing Law/Dispute resolution clauses. These provisions will affect the buyer's rights in trying to unwind the transaction in the event the art they purchased turns out to be forged.

fact may also allow a party to a contract to rescind the contract and restore the matters to the position before the contract was entered into, provided that both parties to the contact were unaware of a material fact or circumstance.[5] Art buyers in many jurisdictions may also be able to rely on statutory provisions (such as the Uniform Commercial Code Article 2 or §13.01(1)(b) of the New York State Arts and Cultural Affairs Law) to assert a claim of breach of express or implied warranties by the counterparty in an art transaction and to seek a recover their damages. As discussed in further detail below, however, a written contract may provide a buyer with more favorable remedies that are available under statutory or common law.

16.2.2 Tort Claims

In addition to contract claims, common law in the United States recognizes causes of action sounding in tort (a wrongful act or infringement outside of a breach of contract that may lead to liability) that may be asserted by an art purchaser in the event of a forgery against other parties in an art transaction. A false representation of the author of an artwork can constitute an unfair trade practice, civil fraud or conspiracy to defraud, unjust enrichment, unfair and deceptive business practices, a private right of action arising from a RICO violation,[6] and a number of additional causes of action as may be permitted by the jurisdiction where the civil case is brought. *Intentional* misrepresentation that a forged artwork is authentic may also serve as a basis of criminal charges, such as criminal fraud, tax evasion and money laundering. The discussion of criminal prosecution of art forgeries is outside the scope of this chapter. That said, civil and criminal cases arising out of the same transaction typically go hand in hand, sometimes with the civil case following the conclusion of the criminal case after the available information about the criminal case in unsealed, other times proceeding concurrently.[7]

The matter of *Hall v. Gascardi*[8] is an example of a successful lawsuit by the defrauded collector against the defendants accused of selling forged artworks. There, plaintiff Andrew Hall, a collector of post-war and contemporary art, purchased twenty-four artworks from Lorettann and Nikolas Gascard over the course of two years.[9] Some of the artworks were purchased directly and some through auction houses where the Gascards had consigned the works.[9]

---

[5] Mutual mistakes are false assumptions of fact made by both parties to an agreement. In the event of a mutual mistake, the court may reform or invalidate the agreement. Restatement 2d of Contracts, § 155.

[6] The Racketeer Influenced and Corrupt Organizations Act, 18 U.S.C. §§ 1961–1968 ("RICO") provides a private right of action for treble damages by a person "injured in his business or property by reason of" a RICO violation. 18 U.S.C. § 1964(c).

[7] *See Weller*, s*upra* note 1, at p. 7.

[8] *Hall v. Gascard*, Case No. 16-cv-418-SM (U.S.D.C. D.N.H. 2018).

[9] *Hall v. Gascard*, 2018 DNH 152.

According to Mr. Hall, the Gascards claimed that each of the twenty-four works that Mr. Hall purchased from them were original artworks by artist Leon Golub (1922–2004). The Gascards made affirmative representations to Mr. Hall about the source of these artworks, such as "acquired directly from the artist" or "acquired directly from the artist by descent to the present owner."[9] Mr. Hall first discovered that the works were not authentic when he and the Hall Art Foundation began planning an exhibition of the works of Leon Golub and asked the Golub Foundation to verify the names and dates of the subject artworks; the Foundation responded that it had no record of the artworks purchased from the Gascards.[9] During his deposition (pretrial testimony under oath), Nicholas Gascard admitted that he fabricated the names of each artwork he sold to Mr. Hall as well as the supposed dates of creation for each artwork.[9]Additional evidence adduced during the course of the litigation discovery process established that Nicholas Gascard misled various auction houses and potential purchasers about how he and his mother came into possession of various works.[10]

Mr. Hall advanced six common law and statutory claims against the Gascards – fraud, conspiracy to defraud, breach of warranty, breach of contract, unjust enrichment, and unfair and deceptive trade practices – in violation of New Hampshire's Consumer Protection Act. On a motion for summary judgment filed by the Gascards (a dispositive motion that seeks to resolve some or all of the claims or defenses advanced by the parties as a matter of law and before trial), the breach of warranty claim was dismissed because it was untimely under the applicable statute of limitations.

The fraud claim in *Hall* survived the motion for summary judgment, with the court noting that "to prevail on his fraud claim at trial, Hall must demonstrate that the Gascards made a representation with knowledge of its falsity or with conscious indifference to its truth, with the intention to cause Hall to rely upon it. Additionally, Hall must show that his reliance upon that false representation was reasonable." In the context of this case, the Gascards argued that it was not reasonable for Mr. Hall to rely on their representations as to the artwork's authenticity because he was a "sophisticated purchaser" who collected Leon Golub's artworks and had demonstrated access to multiple experts. However, the evidence in the case was that the forgeries were in fact very good and were not detected by many experts earlier. For example, Mr. Hall noted that he "hosted an event at his home in late 2010, at which he displayed some of the fake works he had acquired from the Gascards. Attending that event were a number of Golub "aficionados," including Golub's son Stephen, and Golub's former studio manager, Samm Kunce. Neither man raised any question about the potential authenticity of those works." Mr. Hall also knew that the Gascards sold works to reputable auction houses, which as the court noted "make reasonable efforts to avoid dealing in forged works of art." Under the circumstances, the court reasoned, Mr. "Hall was not, as the Gascards suggest, obligated to secure the

[10]It should be noted that Mr. Hall also brought claims against the auction houses from which he bought some of the artworks, which were settled.

services of an independent expert to determine the authenticity of each of the works – particularly since the information bearing on the works' authenticity (e.g., how they were acquired and from whom) was peculiarly within the Gascards' own knowledge." This reasoning is interesting because it leaves open the possibility that under a different set of facts, a collector may potentially be held to not have justifiably relied on representations of authenticity made to him or her. This is a reminder for collectors that they cannot justifiably rely on someone's representation merely because it comes from what they think is a reputable source.

Following a trial of the *Hall* matter, a jury in New Hampshire found for Mr. Hall on the fraud/conspiracy to commit fraud claim and required Lorettann and Nikolas Gascard to repay $465,000 to Mr. Hall[11] (Bowley 2018). Many art buyers in his place will not be so lucky, however. Frequently, the forger or the bad actor selling forged art are never caught or have no assets from which a compensation may be recovered.

The recent litigations involving the Knoedler Gallery and forged American Abstract Expressionist works illustrate the considerations in lawsuits against an art gallery, where there are allegations that the gallery withheld material information from buyers. Many will be familiar with the circumstances of the matter from a recent Netflix documentary, *Made You Look* (Netflix 2020). Briefly, the facts of this controversy were as follows: Knoedler & Company was one of Manhattan's oldest art galleries with a 165 year history (Cohen 2011). Ann Freedman, the gallery's long-time director, was approached by a relatively obscure art dealer Glafira Rosales, who offered to sell a number of newly discovered mid-century Modernist masterpieces with no documented provenance from an anonymous collector (Cohen 2012). Between 1996 and 2008, Knoedler purchased or accepted on consignment approximately forty artworks, generating approximately $40 million in profits (Cohen 2012).

In 2010, Pierre Lagrange attempted to sell one of the paintings, believed to be by Jackson Pollock, which he purchased from Knoedler in 2007. [12] He encountered difficulties due to the doubts as to the work's provenance.[12] Because of concerns about the authenticity of the painting, Mr. Lagrange subjected the work to forensic testing and discovered that two of the paints used to create the painting did not exist at the time of Pollock's death in 1956.[12] This scientific work included the identification of synthetic organic pigments using microRaman spectroscopy, a tool of increasing importance for cultural heritage scientists. The international collaborations of scientists for the creation of web-searchable databases of these materials, such as the KIK-IRPA SOPRANO database and the IRUG spectral database, have

[11] *Hall v. Gascard*, 2019 DNH 069 ("Plaintiff's counsel methodically challenged every aspect of defendants' narrative, exposed many misrepresentations made about the works' provenance, and offered uncontradicted expert opinion evidence that the works were crude fakes. The jury had little difficulty in expeditiously rejecting the defense and returning a verdict in Hall's favor against Nikolas for fraud and against both Nikolas and Lorettann for conspiracy to commit fraud. Hall was awarded $465,000.00 in damages, the full amount paid for the works.")

[12] *Lagrange v. Knoedler Gallery*, 2011 U.S. Dist. LEXIS 163035, at *2 (S.D.N.Y. Dec. 23, 2011).

been key to the advancement of this aspect of research on twentieth-century artist's materials. Armed with evidence of the materials, connoisseurship, and provenance shortcomings of his painting, Mr. Lagrange commenced a lawsuit against Knoedler and Ann Freedman. This suit alleged that they made a number of false representations to him about the painting before it was purchased, including that it would be listed in an upcoming Pollock catalogue raisonné and that twelve scholars of Pollock's work opined that it was in fact a Pollock, and that the painting was being sold by a collector who had inherited it, when in fact it was co-owned by the Gallery and an investor.[12] The lawsuit was resolved by settlement (Hurtado and Pettersson 2012).

During the ensuing eight years, nine more similar lawsuits were asserted against Knoedler by art purchasers and settled (Kinsella 2019). Of these, the most significant from the art law perspective is *De Sole v. Knoedler Gallery, LLC*, which, albeit also ultimately settled, is the only one of the Knoedler litigations to reach the trial stage. Collectors Eleanor and Domenico De Sole purchased a purported Mark Rothko painting in 2004 from Ms. Freedman (Neuendorf 2016), which upon evaluation was concluded to be fake (Kinsella 2016a). In 2016, the De Soles sued both Ann Freedman and Knoedler Gallery, among others, seeking $25 million in damages (Neuendorf 2016). Their complaint alleged causes of action sounding in (1) fraud and fraudulent concealment claims against Knoedler and Ms. Freedman; (2) substantive RICO and RICO conspiracy claims against all defendants; (3) an aiding and abetting fraud claim against Jaime Andrade (gallery employee), Glafira Rosales, Bergantinos Diaz (a "longtime companion" of Ms. Rosales), and Michael Hammer (Knoedler's managing member and owner of the gallery's holding company); and (4) a fraud conspiracy claim against all defendants.[13] The $25 million in damages was triple the De Soles's actual damages and was only available had the De Soles proved at trial that the defendants violated RICO (Gilbert 2016). On February 7, 2016, only two weeks after plaintiffs began presenting their case, a settlement was reached between the De Soles and Ms. Freedman (Kinsella 2016a); shortly thereafter Knoedler and its affiliate holding company settled with plaintiffs (Kinsella 2016a).

The Knoedler scandal highlights the importance of the buyer consulting with their own experts and doing their due diligence in connection with purchases of artworks, even if the seller is a well-established gallery. For example, collector Jack Levy set a condition on his purchase of a Jackson Pollock work from Knoedler that the artwork must be authenticated as a Pollock by the International Foundation for Art Research; when it was not, Mr. Levy received a refund (Cohen 2013).[14] As discussed above, it is also critically important that the buyer demands that the art purchase contract should set forth a representation by the gallery that they are not aware of any information pertinent to the issues of authorship, authenticity, provenance and prior ownership that was not disclosed to the buyer. Such a provision may

[13] *De Sole v. Knoedler Gallery, LLC*, 974 F. Supp. 2d 274, 286 (S.D.N.Y. 2013).

[14] *De Sole*, *supra*, 974 F. Supp. 2d at 286 (S.D.N.Y. 2013).

protect a buyer who did not condition their purchase on an independent authentication as had Mr. Levy.

A troubling result of some art collectors' ill-advised and misplaced effort to recoup losses from purchase of forged artworks (or due to contested attributions) from authenticators, artists' foundations and authentication boards became the silencing of the very experts that the art market needs to rely upon in guarding against forgeries (Bresler 2018). Although the law is usually on the side of the experts that render opinions on authenticity, litigation costs and difficulties in obtaining insurance coverage have led many experts, authentication boards and artists' foundations to stop issuing opinions as to authenticity (Bresler 2018). As James Martin, the expert who performed forensic analysis on many of the Knoedler paintings noted, "Due diligence in evaluating the authenticity of works of art is not merely showing works to others, then acting only on favorable comments (or the absence of negative comments) – especially after questions have been raised about more than one work that share the same provenance." (Kinsella and Cascone 2016) A buyer should take the responsibility to conduct due diligence and heed the red flags that may come up as a result, and as stated, require that all the pertinent information be disclosed to them by the seller or their representatives.

16.3 Case Studies Involving Art Conservation

Our society has a collective sense of ownership in our art and cultural artifacts and concerns itself with their preservation for artistic, cultural, historical, educational and heritage purposes. This desire to preserve and protect our art sometimes resulted in a schism between two camps of experts in the twentieth-century art world. Is it preferable to let the evidence of damage and destruction remain when an artwork had suffered at the hand of a vandal or negligent restoration practices? Do such changes become part of the "object biography"? Should we strip the old varnish of the canvasses darkened with age to reveal the bright colors that we think existed when the Old Masters first created them, or is there a possibility that original translucent glazes could be harmed in the process? The application of scientific monitoring of such conservation treatments starting in the fourth quarter of the twentieth century has largely reduced, but not fully eliminated, such controversies. On the one hand, there are those who seek to preserve and restore art to the appearance it had during it creator's lifetime. On the other hand, groups comprising art historians and critics of some of the more interventionist restoration and conservation approaches seek to preserve the integrity of the artwork and protect it from overzealous treatments that may remove and replace the layers created by the hand of the original artist. The battle between John Richardson (1983) and Carolyn Keck (Keck et al. 1983), starting with his "Crimes Against the Cubists" article in *The New York Times Book Review* is one example where varnishes added to early modernist paintings in the name of preservation ran counter to the intended play of matt, gloss, and textural effects intended by the artists. The Sistine Chapel cleaning controversy (Kimmelman

1990) that played out in the international news and the National Gallery Old Master cleaning controversies that played out on the pages of *Burlington Magazine* (Burlington Index 2015) are two more examples of misunderstandings between art historians and art conservators about where the line between "clean" versus "stripped" lies. Many of these controversies can be (and in the case of the Sistine Chapel were) settled by a careful study of the painting's stratigraphy or layer structure prior to conservation treatment. The notion of a painting having a patina goes all the way back to the writings of Pliny the Elder, however, and misunderstandings of an artist's working practice have without a doubt led to the overcleaning of masterworks such as, for example, Thomas Eakins' *The Gross Clinic* (1875) (see Philadelphia Museum of Art - Research: Conservation 2001).

When the Louvre Museum in Paris, France recently announced plans to restore Leonardo da Vinci's *St. John the Baptist*, many critics in the art world protested, fearing that the restoration may permanently damage the painting (Lewis 2016; Muñoz-Alonso 2016). In fact, the Louvre's prior attempt at restoring another da Vinci painting, *The Virgin and Child With Saint Anne*, was criticized by many art historians for having excessively lightened the piece; two art conservation experts on the panel advising on the restoration of this artwork resigned in protest over the restoration methods employed (Lewis 2016; Muñoz-Alonso 2016). That these types of disputes can still occur within the past decade (regarding whether materials removed were solely prior restorations or included glazes applied by Leonardo) points to the need for intensive collaboration between conservators, art historians, and scientists at all stages of such an endeavor. Holistic imaging methods such as MA-XRF scanning and hyperspectral imaging can increasingly contribute to these questions in a totally nondestructive manner. In addition, as highly publicized botched art restorations carried out by untrained hands have in recent years occurred alarmingly often, there is always a fear that the damage that an unskilled restorer or a well-intended layperson may inflict will be irreversible (Jones 2020; Phillips 2013). The recent proliferation of satisfying-to-watch but profoundly careless and unethical painting cleaning videos on social media platforms such as YouTube or Instagram ironically generate great interest in the field of art conservation while simultaneously portraying it as the opposite of the carefully considered and painstakingly executed field of endeavor that it truly is. And yet, with the practice of art conservation becoming commonplace since the 1800s, "[the] more famous the painting, the more often it's been redone because people simply cannot keep their hands off it." ((Chalkley 2010) citing Ian McClure, chief conservator for the Yale University Art Gallery). This section will focus on the review of the existing legal frameworks that give some options to owners of artworks and to living artists to object to improper art restoration techniques and perhaps to seek a measure of recourse for the damages caused by restoration errors. Conversely, this section will also discuss considerations for the art conservators in ways to limit their exposure to expensive lawsuits and the reasons why a well-written conservation contract is advisable.

16.4 Defining Terminology: Distinctions Between Conservation, Restoration and Preservation

For the avoidance of confusion, it is necessary to begin with discussing briefly what we mean by art preservation, conservation and restoration. In the professional art world, these terms have been defined in various ways and are occasionally used interchangeably (see generally (Ramsay and Jacobs 2015)). The term art conservation may refer both to the profession dedicated to preserving art and to the practice comprising "activities of preservation (preventive care) *and* restoration." ((Ramsay and Jacobs 2015) emphasis in the original). Conservation encompasses the treatment of artworks that are informed by scientific study and that are rigorously documented by technical imaging methods before, during, and after treatment. In addition, conservation is carried out by practitioners that hold a terminal degree in the field of art conservation, which in the United States and Canada is an M.A. or an M.S. degree in one of the recognized graduate programs. The professionalization of the field of art conservation in the United States transitioned from an apprentice-based system to an academic system between 1960 and 1970 with the opening of four graduate programs for obtaining a master's degree in the field (at Oberlin, NYU, State University of New York at Cooperstown, and University of Delaware). The term restoration refers to "repair or replacement of damaged or missing elements in a work of art, with the goal of returning the object to its original appearance." (Ramsay and Jacobs 2015). In the United States, the people who work as restorers are commonly apprentice-trained and may carry out sensitive, skilled treatments but lack the rigorous scientific and documentation training of their conservation peers. Various laws also contain operative definitions of these terms.[15] For the purposes of this chapter, we will use the terms "conservation" and "conservator" generally to refer to all of these practices and practitioners, given that damage may result from errors in handling any of the stages of care for an artwork.

16.4.1 Artwork Owner's Claims Against Conservators

Owners of any damaged property traditionally have two main approaches to seek recourse from a professional who has performed below the standard of care in the profession and caused damage: tort claims and claims sounding in breach of contract. Tort claims exist to address the wrongs that arise in the course of a business

[15] Pennsylvania's Fine Art Preservation Act defines the term "conserve" as "[t]o preserve a work of fine art by retarding or preventing deterioration or damage through appropriate treatment in accordance with prevailing standards in order to maintain the physical integrity of a work of fine art;" and the term "restore" as "[t]o return, as nearly as feasible, a deteriorated or damaged work of fine art to its original state or condition in accordance with prevailing standards." 73 P.S. § 2102; *see also*, California Art Preservation Act (Cal Civ Code § 987) for similar definitions.

relationship between the parties, whereas contract claims are based on violations of an agreement between the parties. As many property owners chose to enter into a written agreement as a matter of course when engaging a professional, tort and contract claims can often overlap. In fact, a complaint filed in a court of law may assert causes of action dealing with breach of contract and with torts arising out of the same set of facts.

16.4.2 Tort Claims

In the context of art conservation, some of the claims that an owner of the artwork may assert against a conservator may include fraud/misrepresentation, negligence and/or professional malpractice. Additional causes of action may be appropriate depending on the facts of each specific case (see Adelman 1994), p.527, discussing torts such as defamation, invasion of privacy and conversion (violation of ownership interests, when an artwork is "so radically damage[d] or alter[ed] […] that its character is substantially changed") in the context of art conservation. (Internal citations omitted)). Fraud or fraudulent misrepresentation occurs when one party (here, a conservator) misstates or omits important facts pertaining to the transaction, and the other party (the owner of the artwork) relies on the statements or omissions to their detriment, which causes them to suffer damages. To state a claim of negligence, the owner of the artwork will need to allege that the conservator owed certain duties to the owner, and breached such duties, which caused damages. A professional malpractice claim is essentially a negligence claim against a member of a profession who allegedly failed to exercise ordinary skill and knowledge in the performance of their duties, resulting in damages.

The difficulty in asserting a negligence or a malpractice claim in the context of art conservation is that the conservator may not have breached any of the accepted practices in the conservation community and yet changed the character of the artwork ((Adelman 1994), p. 525 and note 29) as was alleged to be the case with the restoration of *The Virgin and Child With Saint Anne,* discussed above. Judges and juries, not being experts in the art world, must rely on the opinion testimony of expert witnesses that the parties introduce during a trial. When there is an ongoing disagreement as to various conservation practices within the conservation community itself, for example with respect to overall restorations versus localized treatments, it is very likely that such disagreement will translate into what is called a "battle of experts" at the time of trial. When presented with conflicting testimony, a judge or a jury will need to make a judgment call as to which expert they find more persuasive, which makes the prospects of a successful recovery by an art owner against a conservator less than certain. A party may have no choice but to bring a tort action, however, when no contract was signed before the art restoration or when a contract is poorly drafted and does not adequately protect the owner of the artwork.

From the perspective of an art conservator defending against claims of negligence and malpractice, it is important to be able to show that their conservation

practices met the accepted standards of care, and follow the American Institute for Conservation's Code of Ethics and Guidelines for Practice.[16] This may be accomplished by securing the testimony of a well-established and respected expert in the area, who would support that the art conservators' actions met the standards of care. With respect to fraud/misrepresentation claims asserted in litigation in the United States, the conservator and their legal counsel should confirm that the false statements and omissions attributable to the conservator are plead with reasonable particularity, a heightened pleading standard required in the United States federal courts[17] and in some state jurisdictions.[18] If the fraud claim is not properly plead, the conservator would typically have an option to bring a pre-answer motion to dismiss, which is a litigation procedural device that may allow the conservator to end litigation against him or her quickly, saving on their legal costs. Truth is a defense in misrepresentation claims; however, the conservator will likely not be able to assert this defense on the merits until after the process of document discovery (exchange of records by litigants), depositions (on the record interviews of parties and non-party witnesses by litigation counsel for the parties), and expert discovery (exchange of expert reports and expert depositions, where allowed by law) is completed. These discovery procedures are typically costly and take many months to complete. This should be one of the incentives to an art conservator to enter into a contract with the owner of the artwork, at least in an effort to limit the conservator's liability or try and contain the costs of the possible litigation.

16.4.3 Contract Claims

To assert a breach of contract claim, a plaintiff will need to show that a valid contract was formed between the parties, that the plaintiff performed his or her obligations under the contract and that the defendant failed to perform such obligations, resulting in damages. A possible related claim to that of a breach of contract is a cause of action of a breach of the implied covenant of good faith and fair dealing. In the context of the existence of a contractual relationship between a plaintiff and a defendant, the plaintiff can also claim that he or she was unfairly prevented by the defendant from receiving the benefits they were entitled to under the contact, even

[16] American Institute for Conservation, Code of Ethics, https://www.culturalheritage.org/about-conservation/code-of-ethics.

[17] Federal Rules of Civil Procedure, Rule 9(b).

[18] To state a claim for fraud, a plaintiff must allege a material misrepresentation of fact, knowledge of its falsity, an intent to induce reliance, justifiable reliance by the plaintiff and damages. *Eurycleia Partners, LP v. Seward & Kissel, LLP*, 12 N.Y.3d 553, 558 (2009). The plaintiff must provide sufficient facts to support a "reasonable inference" that the allegations of fraud are true. *Id*. at 559–60. Conclusory allegations will not suffice. *Id*. Neither will allegations based on information and belief. *See Facebook, Inc. v. DLA Piper LLP (US)*, 134 A.D.3d 610, 615 (1st Dept. 2015) ("Statements made in pleadings upon information and belief are not sufficient to establish the necessary quantum of proof to sustain allegations of fraud.").

when a specific contractual provision may not technically be breached. As with the breach of contract claim, a plaintiff asserting a breach of implied covenant claim must also show that plaintiff has performed (or is excused from performance of) its obligations under the contract and that plaintiff suffered an injury as a result of defendant's conduct.

Provided that the art owner invested the effort into negotiating the express terms of their contract with the art conservator, it will likely be more attractive for them to assert breach of contract claims. The art owner may, for example, be able to negotiate a contract term that an alteration of an artwork's character is considered a breach or agree on the set of criteria by which an acceptable restoration is to be judged.

An art conservator entering into a contract with the art owner should take care to limit his or her liability against the risks and uncertainties of the conservation process, where the chosen restoration methods may expose the artwork to dangers even in the hands of a trained conservator. Each artwork is a unique chemical and physical composite of the artists' materials, the alteration products that have formed over time through exposure to agents of degradation, and the results of any prior interventions. For an Old Master painting, it is not unusual for the work to have gone through five or more previous treatments and/or interventions. It is helpful for the art conservator to specify upfront which techniques and approaches, tools and materials will be used, and to try and secure the art owner's agreement (and acceptance of the risks) at every stage of the process. An art conservator should negotiate a strong limitation of liability clause to the full extent permitted by law and be discerning in their choice of which law will govern the parties' obligations under the contract (so long as their jurisdiction permits such choice of law provisions). It may also be possible to shorten the statutory period during which claims against the conservator may be brought, i.e., if a malpractice claim must be brought within three years of the occurrence by law, a contract may specify that all claims resulting from the transaction must be commenced within one year of the completion of the restoration.

The art conservator may also demand that any disputes arising out of the restoration be resolved by mandatory arbitration, for example, by the International Court of Arbitration for Art (Den Haag) or WIPO Art and Cultural Heritage Dispute Resolution, which is often preferable in art disputes for a number of reasons. First, the proceedings are non-public and may be made confidential, unlike traditional litigation, which is often open to the public. Second, the costs of arbitration are usually considered to be less than the costs of litigation, as the discovery process is usually abbreviated and less formal. Third and perhaps most significantly, in arbitration the parties have an opportunity to appoint arbitrators with technical experience in the art world including the most up-to-date conservation methodologies and ethics, and a scientific knowledge of the materials and techniques being practiced. Less time and effort will thus be required to educate such arbitrators on the accepted conservation practices, as would not be the case with judges and juries, for many of whom this would be a matter of first impression. It is also often commented that the outcomes of art arbitrations are thus more predictable.

16.4.4 Remedies

Remedies available for tort claims can differ from those available for breach of contract claims. Absent contractual provisions that may exclude or limit certain categories of damages, the law seeks to protect the expectations of the parties to the contract. A successful plaintiff in a tort claim may be able to recover compensatory damages to reimburse the plaintiff for all the harm caused by the defendant, which may be broader than damages contemplated in a contract, and punitive damages, which are meant to deter similar conduct by others or to punish truly reprehensible conduct. The available tort remedies may also be affected by federal or state statutes and case law, which will differ from jurisdiction to jurisdiction.

Damages available for breach of contract are usually compensatory and their purpose is to put a plaintiff in the position they would have been in if the contract had been fully performed. If such damages may be contemplated when a contract is executed, consequential damages may be recoverable (for example, cost of future attempts to correct defective restoration, loss of reputation, loss of anticipated profits, etc.). Punitive damages are typically not awarded in breach of contract claims. A contract may also specify what damages may be awarded in the event of the breach, known as liquidated damages.

As the recoverable damages may differ between tort and contract claims, it may be advisable for an art owner seeking redress for the damages suffered to add tort claims to breach of contract claims in order to claim different damages. One caveat to keep in mind is that some jurisdictions do not allow parties to assert tort claims to recover purely economic losses (financial losses as opposed to a physical injury or destruction of property) arising out of a contract. As such, the precedent followed in the local jurisdiction must be reviewed, and at the very least, the art owner and their legal counsel should make certain that the tort damages sought do not simply mirror the damages that may be recoverable under a contract.

Contracts also may be used to limit the damages recoverable as a result of a transaction, both in contract and in tort, which is again one of the incentives for the art conservator to require a written contract for each of their conservation projects (the contract may be a standard form that the conservator uses for each project, as appropriate). One such limitation, for example, may be a liability cap clause limiting the conservator's liability, for example, to the total fee that the conservator receives for their work.

16.4.5 City of Amsterdam v. Daniel Goldreyer (1995)

The matter of *City of Amsterdam v. Daniel Goldreyer*[19] is instructive as to the types of claims that may be asserted by an owner of the artwork that is claimed to be damaged because of a restoration. This matter arose out of the restoration of Barnett Newman's painting *Who's Afraid of Red, Yellow and Blue III*, which was slashed with a knife by a vandal on March 21, 1986 (Kimmelman 1991). The director of the Stedelijk Museum, Wilhelmus A.L. Beeren, decided on a full restoration concealing the slashes. This decision was criticized by proponents of less extensive restoration (James 1991). Mr. Beeren, however, explained that to have left such extensive damage visible would have destroyed the integrity of the painting (James 1991).

To conduct the restoration, the Museum selected Daniel Goldreyer, who specialized in the restoration of artwork and whose company, Daniel Goldreyer, Ltd. (Goldreyer, Ltd.), served as the official conservator for the work of Barnett Newman (1905–1970). The City of Amsterdam entered into a written restoration agreement with Mr. Goldreyer and Goldreyer, Ltd. (the Restoration Agreement), which called for Mr. Goldreyer to restore the painting to the best possible condition. The Restoration Agreement also obligated Mr. Goldreyer to make a specification in writing of the work to be carried out and to keep the City informed of all action taken on the Artwork via bi-monthly progress reports. A committee was formed to advise the City on the conservation proceedings, but the final methodology was in at Mr. Goldreyer's discretion.

The restoration was completed on August 5, 1991, and the artwork was returned to the Stedelijk Museum on August 12, 1991.[20] The Museum's representatives signed two letter agreements or releases on each of these respective dates, both of which stated that the painting was in a "good and satisfactory condition" after the restoration and the transportation.[20]

Once the artwork was returned to the Museum and once again placed on public display, the art community in Amsterdam and internationally and several publications claimed that the artwork had been "overpainted".[21] See (Adelman 1994, p. 523) and (Stroh 2006) discussing overpainting. In light of the public criticism of the restoration, the City proceeded to submit the artwork to the Forensic Laboratory of the Netherlands Ministry of Justice for testing, which revealed that the damaged area of the oil painting had been painted over using acrylic paint applied with a paint roller and that an alkyd varnish had been applied as a sealer.[22] The *New York Times*

[19] *City of Amsterdam v. Daniel Goldreyer, Ltd*., 882 F. Supp. 1273 (USDC EDNY 1995). Full text of the court's decision on the motion to dismiss is available at https://law.justia.com/cases/federal/district-courts/FSupp/882/1273/1603601/

[20] *City of Amsterdam v. Daniel Goldreyer, Ltd*., *supra*.

[21] *Id*. Overpainting is a controversial treatment due to it being irreversible and masking the artist's original surface.

[22] *See supra* note 19, *City of Amsterdam v. Goldreyer,* 882 F. Supp. at 1278.

article "Roller Controversy in Amsterdam: The Restoration of Modern Art" raised ethical issues in restoration of this painting (James 1991):

> One Dutch expert, Ijsbrand Hummelen, a member of a commission that examined the painting after the attack, said that Goldreyer, without consulting the museum, had overlaid acrylic paint onto Newman's original oils. He said the restoration had destroyed a shimmering, silky effect that the artist had achieved by the subtle juxtaposition of magenta and sienna, turning the painting into a mere monochrome.

Mr. Hummelen also expressed an opinion, as reported by the *New York Times*, that the repair had violated one of the fundamental tenets of art conservation in that it is not reversible and that the repair was not confined only to the damaged parts. In art conservation, this is known as overpainting versus inpainting. Overpainting was widely practiced in the nineteenth century and into the first half of the twentieth century, but it is now considered unacceptable to cover over the original unaltered paint of the artist, even in some cases when there is discoloration or fading. For instance, the chrome yellows of several works by Vincent van Gogh have discolored to brown and his eosin reds have faded nearly to white, but conservators have made the decision not to overpaint these large regions of color. A similar minimally interventionist approach has been taken for the faded and discolored cadmium yellows in paintings by Henri Matisse.

The conservation of color field paintings from the Abstract Expressionist period (and beyond) represents a tremendous challenge for the field of paintings conservation, and the quote above reveals how the seemingly two-dimensional nature of these fields painted not only by Barnett Newman but also by contemporaries Ad Reinhardt (1913–1967) and Mark Rothko (1903–1970) are actually three-dimensional compositions that are rich in complexity and depth. Cross-section microanalysis and binding media identification of works by Mr. Newman and Mr. Rothko confirm their use of precise pigment mixtures and unconventional combinations of media to obtain variations in sheen and depth in their paintings (see for example (Glanzer et al. 2006; Hensick and Whitmore 1988; Langley and Burnstock 1999; Wijnberg et al. 2011)). To create a discrete and invisible repair of such a large and subtly variegated surface is next to impossible because any break in the broad field of color immediately draws the viewer's eye. The situation is complicated in the case of Mr. Goldreyer because he was the trusted restorer of artworks not only by Newman but also Rothko, and one can assume that he held this position because he was considered to be sensitive to their techniques. However, there can be little question in this case that he did not comply with the accepted standards of practice of his profession.

On November 5, 1993, the City of Amsterdam filed a suit against Mr. Goldreyer and Goldreyer, Ltd., alleging six causes of action, including that Mr. Goldreyer and his company committed fraud, made misrepresentations, were negligent and failed to honor the terms of a written agreement with the City.[23] At the heart of the City's claims was the allegation that Mr. Goldreyer represented that he was utilizing the

[23] *City of Amsterdam v. Daniel Goldreyer, Ltd*., *supra*.

"pinpointing" method of restoring the damaged section of the painting, a restoration technique that involves layering many dots over the cracks in the red paint formed by the slash. These representations were allegedly made several times during the course of the restoration as well as in the Complete Conservation Report, which Mr. Goldreyer submitted upon the completion of the restoration on August 5, 1991.[23] The City also later claimed that during a five-month period from September 1990 through February 1991, Mr. Goldreyer failed to submit bi-monthly progress reports on the restoration.[23] According to the City, it had the right to withdraw from the Restoration Agreement if it was not satisfied with the restoration progress. The City also alleged that the overpainting and the application of the sealer were inconsistent with industry restoration standards because the new paint and sealer were not removable without damage to the original artwork. According to the City, these actions allegedly destroyed the translucency of Newman's original work. The City claimed damages in the amount of US$3.5 million, representing the reduction in the value of the artwork. The City also claimed that the general public was deprived of the opportunity to view a valuable work of art by Barnett Newman.

Mr. Goldreyer and Goldreyer, Ltd. disputed the City of Amsterdam's assertions as to the breach of the Restoration Agreement. They filed a motion to dismiss[24] the **breach of contract** and other claims, relying on the two written releases signed by the City's representatives, acknowledging that the painting was in a "good and satisfactory condition," as a bar to the City's right to claim a breach of the Restoration Agreement. In reviewing the legal merits of the breach of contract claim, the court held that this claim was properly plead: Mr. Goldreyer and Goldreyer, Ltd. did not argue that any of the City's allegations were not suitable for recovery of damages. Rather, they sought to show that there was evidence of them having properly discharged their obligations, which is not something that a court may consider on a motion to dismiss stage. As such, the court upheld the breach of contract claim. With respect to the two releases signed by the City's representatives, the court noted that a finding of fraud (if proven) will invalidate any signed release under the law of the State of New York, which governed the dispute. Furthermore, a release or waiver may be attached or set aside due to other defects, including flaws in its execution, illegality, duress and mutual mistakes. Because the City alleged misrepresentations by Mr. Goldreyer, the court held that the issue of the validity of the two releases was a question of fact that must be resolved at the trial stage and not on a motion to dismiss stage.

The City also asserted a claim of "**conversion**" against Mr. Goldreyer and Goldreyer, Ltd. The State of New York interprets this tort to consist of either unauthorized exercise of dominion over the property of another to the exclusion of the

[24] A motion to dismiss is a procedural tool in the U.S. litigation, which allows a party, usually a defendant, to claim that the complaint is legally invalid and should be dismissed by the court. This motion is typically filed early in the life of a case and before any substantial discovery takes place. The role of the court on such a motion is not to weigh in on the available evidence, but only to determine whether the plaintiff asserted cognizable legal claims based on the allegations set forth in the Complaint, which are presumed to be true for the purposes of the motion only.

owner's right, or the unauthorized use of that property. The court upheld this claim also, stating that even when a defendant had a right to limited possession (as Mr. Goldreyer had), when such defendant takes actions with respect to the property that are not contemplated by the agreement with an owner, conversion is properly plead. The City also asserted a related claim of "**trespass to chattel**," which occurs when a party intentionally damages or interferes with the use of property belonging to another. For the similar reasons as in the discussion of the conversion claim, the court held that the trespass to chattel claim was sufficiently plead.

With respect to the City's **fraud claim**, Mr. Goldreyer and Goldreyer, Ltd. claimed that the City could not have relied on Mr. Goldreyer's alleged misrepresentations because the City was on actual notice of the falsity of the statements attributed to Mr. Goldreyer. Specifically, it was claimed that one of the Museum's representatives had suspicions that the artwork was in fact overpainted. The court held that the issue of whether reliance on defendants' statements was justified was also an issue of fact that must be litigated at trial, and furthermore, that suspicions do not amount to an actual notice of a fact.

Finally, the City also asserted claims sounding in **negligence** and **negligent misrepresentation**. Mr. Goldreyer and Goldreyer, Ltd. also sought to dismiss these claims, again on the grounds that releases were signed by the City's representatives and on their "actual notice" theory, same as with the claims above. The court again determined that the claims themselves were sufficiently alleged, declining to dismiss them at the motion to dismiss stage.

Mr. Goldreyer and Goldreyer, Ltd. also claimed that the City's claims should be barred because the City did not procure insurance for the artwork, which would have indemnified them for any damage allegedly caused to the artwork during the conservation. The court was not persuaded by this argument, noting that the law of "all-risk" insurance policies specifically exempts from coverage the losses resulting from misconduct or fraud. Because fraud, international wrongdoing and negligence were alleged in this litigation (but not yet proven at the motion to dismiss stage), if the City's claims are taken as true as the court must do on a motion to dismiss, the existence of insurance coverage would not have indemnified Mr. Goldreyer and Goldreyer, Ltd. for their actions. Moreover, the court noted, the defendants had recourse to their own insurance policies for indemnification.

Based on this reasoning, the court declined to dismiss any of the claims against Mr. Goldreyer as legally insufficient. Following this motion, this litigation and Mr. Goldreyer's defamation countersuit lingered for several years because of differences between the American and Dutch legal system. In January 1997, both lawsuits were settled through the payment of $100,000 by the City of Amsterdam to Mr. Goldreyer, with both sides agreeing not to further discuss the restoration or the legal case (Greensboro 1997).

16.4.6 Practical Considerations for Drafting Conservation Contracts

Besides illustrating the possible claims and defenses that may be asserted in disputes over art conservation, the *Goldreyer* matter offers insights to drafters of conservation contracts in outlining the parties' obligations as well as provisions that may be included in an effort to protect an artwork against damage. The key issues in the *Goldreyer* matter appear to have been the breakdowns in contemporaneous communication as to what restoration method was being used. Although the plaintiffs had a committee advising them on the process of restoration, if periodic reports from Mr. Goldreyer that were called by the contract were not available and the final choice of the restoration techniques was up to the conservator, the City of Amsterdam had no practical ability to prevent the use of the techniques with which they did not agree. As such, in drafting a conservation contract, the owner of an artwork may want to become familiar in advance with the professional industry standards and acceptable restoration techniques and obtain written proposals from conservators outlining the treatments to be performed in detail. The owner may consider requiring not only periodic reports on the restoration progress but also approvals to begin each subsequent stage of the restoration. It is important to achieve the right balance between transparency and communication on the one hand, and micromanagement of the conservation project on the other, which is not desirable to either side. In the alternative, a conservation contract may provide that the treatment may not be substantially modified without the owner's written authorization but that treatments may be modified to a reasonable degree at the discretion of the conservator.

Regardless of the treatment methods used, the conservation contract should contain a prohibition on modification of the character of the work and possibly a liquidated damages clause in the event such modification does in fact occur. It is furthermore important to remember that what constitutes "damage" to the artwork may be disputed, with experts disagreeing as to whether any damage occurred. As such, parties should also agree in advance to a set of criteria by which any modification to the character of the artwork is to be judged, as it is expected that conservation will involve some degree of modification to the original work.

Finally, the drafters of conservation contracts should pay special attention to the limitation of liability clauses, representations and warranties, and insurance provisions to make sure that if damage occurs, the owner has appropriate recourse. On the other hand, the conservator should make sure to secure appropriate disclaimers of liability as to the losses that are part of the risk of the conservation process and should not be born solely by the conservator. Finally, as discussed, choice of law and dispute resolution clauses may have a significant impact on the parties' costs and prospect of recovery and the implications of these clauses should be carefully considered at the drafting stage.

16.4.7 Moral Rights of Artists and Art Conservation

In addition to the rights of the owners with respect to art conservation, the laws of a number of countries recognize moral rights of living artists to exercise a degree of influence over the fate of the artworks they created. These rights afford the artists an opportunity to have a say in conservation of their artworks.[25]

Moral rights have been recognized since 1928 under the Berne Convention for the Protection of Literary and Artistic Works (Article 6bis).[26] These are "rights of a spiritual, non-economic and personal nature" that exist "independently of an artist's copyright in his or her work" and "spring from a belief that an artist in the process of creation injects his spirit into the work and that the artist's personality, as well as the integrity of the work, should therefore be protected and preserved."[27] Because they are personal to the artist, moral rights exist independently of an artist's copyright in his or her work or ownership rights in the physical object of an artwork.[28] These general principles result in recognition of the artist's right of paternity or attribution, and the right of integrity.[29] The right of attribution gives the artist the right to be recognized as an author of an artwork and to not be associated with an artwork that the artist did not create and with which they do not wish to be associated. The right of integrity protects an artwork from subsequent modification, distortion or mutilation by others.

The scope of implementation of these rights into national laws of the country members of the Berne Convention differs from jurisdiction to jurisdiction. Moral rights have been accepted and adopted within every civil law system within the European Union (Schere 2018), where their application is much broader than in the United States. In the United States, where moral rights is a relatively recent addition to our jurisprudence, initially several states recognized moral rights of artists: California was the first to take up the task of protecting artists with the passage in

[25] In addition, artists have an option to set up contractual or quasi-contractual arrangements that may also allow them to control conservation of their artworks. *See* (Donati 2018) discussing contractual systems organized by artists Carl Andre, Daniel Buren, Sol LeWitt and Lawrence Weiner, which allow these artists and their estates to track circulation, guarantee authenticity and exert authorial control through the use of contracts, certificates of authenticity and artists' archives. Where each change of ownership of the work must be registered with the artist or their estate, each subsequent collector may also be contractually required to submit to the guidance as to conservation or risk not being able to sell the artwork in the future in the event of a breach of the procedures set up by the artist.

[26] The Berne Convention for the Protection of Literary and Artistic Works art. 6bis, Jul. 24, 1971, 828 U.N.T.S. 221. As of September 2020, there are 179 states that are parties to the Berne Convention.

[27] *Mass. Museum of Contemporary Art Found., Inc. v. Buchel*, 593 F.3d 38, 49 (1st Cir. 2010) (discussing moral rights in the context of the Visual Artists Rights Act).

[28] *See,* 2 Nimmer on Copyright 8D-4 & n.2 (1994) (Nimmer).

[29] Arathi Ashok, Moral Rights – TRIPS and Beyond: The Indian Slant, 59 J. COPYRIGHT SOC'Y U.S.A. 697, 700 (2013).

1979 of the California Art Preservation Act,[30] followed in 1983 by New York's enactment of the Artist's Authorship Rights Act.[31] In 1990, the U.S. Congress first recognized moral rights on a national level when it enacted the Visual Artists Rights Act (VARA) as an amendment to the Copyright Act, [32] and which largely superseded the moral rights laws of the various states.

VARA's principal provisions afford protection only to authors of works of visual art, a very limited subset of artworks that includes only paintings, drawings, prints, sculptures, or photographs produced for exhibition purposes, existing in a single copy or limited edition of 200 copies or fewer.[33] The moral rights recognized under VARA are the right of integrity and the right of attribution. Specifically, under VARA[34] an artist author of a work of visual art may:

1. claim authorship of that work;
2. prevent the use of his or her name as the author of any work of visual art that he or she did not create;
3. prevent the use of his or her name as the author of the work of visual art in the event of a distortion, mutilation, or other modification of the work that would be prejudicial to his or her honor or reputation;
4. prevent any intentional distortion, mutilation, or other modification of that work that would be prejudicial to his or her honor or reputation, and any intentional distortion, mutilation, or modification of that work is a violation of that right; and
5. prevent any destruction of a work of recognized stature, and any intentional or grossly negligent destruction of that work is a violation of that right.

The artists' rights to protect their artworks from destruction under VARA have several important limitations. As seen in point 4 above, the "distortion, mutilation, or other modification" must be intentional for there to be a breach of an artist's right. When a conservator negligently modifies the artwork during restoration, the intentional component will not be met. Similarly, the right to prevent destruction (point 5 above) is limited to "works of recognized stature," meaning that no every artwork may be protected by this right under VARA. What works are of "recognized stature" is determined by the courts on a case-by-case basis, using a two-prong test: (1) determining that the visual art in question has "stature," i.e., is viewed as meritorious, and (2) that this stature is 'recognized' by art experts, other members of the artistic community, or by some cross-section of society.[35]

Another important exception under VARA is that the modification of a work of visual art that is the result of conservation of the work is not a destruction,

[30] Cal. Civ. Code § 987 *et seq*.

[31] N.Y. Arts & Cult. Aff. Law § 14.03.

[32] 17 USCS § 106A.

[33] *Id*., 17 U.S.C. § 101.

[34] *Id.*, 17 USCS § 106A.

[35] *Cohen v. G&M Realty L.P.*, 988 F. Supp. 2d 212, 217 (E.D.N.Y. 2013), citing *Carter v. Helmsley-Spear, Inc*., 861 F.Supp. 303, 325 (S.D.N.Y. 1994), *rev'd and vacated in part and aff'd in part, by* 71 F.3d. 77 (2d Cir. 1995).

distortion, mutilation, or other modification within the meaning of this statute unless the modification is caused by gross negligence.[36] There is no settled meaning for gross negligence among the courts, but it generally contemplates a conduct that falls somewhere between ordinary negligence and willful misconduct. Courts in California, for example, have found gross negligence to be either a "want of even scant care" or "an extreme departure from the ordinary standard of conduct." In contrast, courts in New York have opined that in order for conduct to be grossly negligent, it must "smack of intentional wrongdoing" and reflect a "reckless indifference to the rights of others." In any event, these are not easy thresholds for an artist to overcome in order to protect their work from modification or destruction under VARA.

The right of attribution or paternity, however, gives an artist more choices. The conservation exception applies only to VARA's right of integrity, and not to the right of attribution.[37] The art market recognizes the name of an artist as a form of branding (Buskirk 2018), which carries value by virtue of the name of the artist being attached to the artwork and because the artist is supporting the artwork's authenticity. Street artist Banksy illustrated this phenomenon during his 2013 New York residency, when he set up a stall in Central Park for one day and sold his works anonymously for $60 (Simpson 2013), with most people walking by and missing the opportunity to get their hands on the original Banksy works.

The degree of importance that the art world attaches to the name of the artist gives artists an opportunity to threaten the disavowal or actually disavow authorship of artworks that are conserved or restored without consulting the artist. Cady Noland disavowed the artwork *Log Cabin Blank With Screw Eyes and Cafe Door* (1990), which was restored without her knowledge and approval, thus presumably stripping the artwork of its economic value (Kinsella 2015). This artwork consisted of a wooden façade with a U.S. flag placed above the entrance and it was reportedly made with the intention that it be displayed outdoors (Kinsella 2015). It is unclear, however, if Ms. Noland intended for the artwork to deteriorate and not be conserved. The owner of this artwork, Wilhelm Schürmann, loaned it to a museum in Aachen, Germany, which did display the work outdoors. After approximately ten years of exposure to the elements, the wood began to rot (Kaplan 2017). Mr. Schürmann consulted with conservators, who recommended that all of the logs should be replaced (Kaplan 2017). He did not consult with Ms. Noland. In light of the conservators' advice, Mr. Schürmann authorized remaking the artwork and conservators replaced the original logs with new ones from the same Montana fabricator that Ms. Noland used for the original artwork (Kinsella 2020). Mr. Schürmann subsequently sold the artwork to an Ohio art collector, Scott Mueller (Kinsella 2020). Subsequent to the sale, Ms. Noland learned that the artwork has undergone extensive restoration. She faxed a handwritten note to the purchaser, Mr. Mueller, stating "This is not an artwork," and that it was "repaired by a consevator [sic] BUT

[36] 17 USCS § 106A.

[37] *Id*., 17 USC. § 106A(a)(1–3).

THE ARTIST WASN'T CONSULTED."[38] This disavowal resulted in a lawsuit by Mr. Mueller against the gallery and art advisor, from whom he purchased the artwork, which was ultimately dismissed on procedural grounds (Kinsella 2016b). This lawsuit left open the question whether Ms. Noland rightfully disavowed her work under VARA,[39]which was partially addressed in another lawsuit resulting from these transactions, which was filed by Ms. Noland herself.

Ms. Noland subsequently filed her own lawsuit against Mr. Schürmann and the gallery that sold the artwork after the restoration, claiming that the unauthorized conservation and later attempt to sell the refurbished work infringed her copyright in the artwork and violated her moral rights under VARA. [40] This lawsuit, however, failed because each of the alleged copyright violations occurred in Germany and the artist failed to allege a basis for the extraterritorial application of the U.S. copyright laws (which includes VARA) to defendants' conduct in Germany. Even though Ms. Noland alleged that defendants' purchase of the replacement wood logs in the United States and attempted to sell the work to an American collector pursuant to a contract calling for delivery of the work to the United States, these acts in and of themselves did not constitute copyright infringement.[41] Ms. Noland also argued that defendants distributed and displayed photographs and plans of the refurbished artwork, which was an independent violation of the copyright laws. The court, however, concluded that such distribution in connection with an attempted sale constituted "fair use,"[42] a construct of U.S. law, which allows limited use of copyrighted material for "transformative" purposes, including criticism, commentary and parody. The court also rejected Ms. Noland's claims under VARA because the subject artwork was created before the statute's effective date.[43] Despite the dismissal of Ms. Noland's claim, however, an artist's claim involving conduct in the United States and a work of visual art that was created after June 1, 1991 may merit a different outcome.

In any event, it is important for owners of artworks to remember that artists may object to the conservation or other modification of their artworks (or even due to a simple failure to properly care for the artwork) and should be consulted before such modifications or conservation are attempted. Ms. Noland is certainly not unique in

[38] *See supra* note 9*4.

[39] In fact, VARA did not apply to this artwork, created in 1990, where VARA's effective is June 1, 1991. In her lawsuit discussed below, Ms. Noland argued, however, that when she permitted Mr. Schürmann to stain the sculpture sometime after the effective date of the statute, and that derivative work is entitled to VARA protection. The court was unpersuaded by her argument, holding that she is not able to grandfather in her preexisting sculpture to VARA's coverage simply by virtue of the later derivative work, of which she is not the author.

[40] *Noland v. Janssen*, No. 17-CV-5452 (JPO), 2019 U.S. Dist. LEXIS 37781 (S.D.N.Y. Mar. 8, 2019) and subsequent decisions in the same matter.

[41] *Noland v. Janssen*, No. 17-CV-5452 (JPO), 2020 U.S. Dist. LEXIS 95454, at *5 (S.D.N.Y. June 1, 2020).

[42] *Noland v. Janssen*, 2020 U.S. Dist. LEXIS 95454, at *10.

[43] *Id.,* at *19.

her approach. In mid-1980s, sculptor Elyn Zimmerman disavowed her fountain artwork created for the plaza outside of an office building in Bethesda, Maryland, when a contractor could not figure out where the water would drain out and drilled a big hole in the bottom (Grant 2016). Sculptor Athena Tacha had her name removed from an installation in Smithtown, New York, after the artwork's owners failed to properly conserve it.[44] In fact, as the contemporary art practice involves a number of non-traditional mediums, such as chocolate, soap and even bologna, it is prudent for buyers of artworks to establish a dialogue with the artist on the artwork's conservation early on to gain an understanding of the artist's intentions about the work. For example, degradation of an artwork may be the artist's intention in the first place, in which case it is unlikely that such artist will authorize conservation attempts. It would be important for the buyer to learn this information prior to investing in order to avoid disputes later on (and to consider incorporating the agreed-upon conservation practices into the purchase agreement with the artist, at least where artworks in non-traditional media are concerned). Conservation decision making with respect to artists such as Matthew Barney and Joseph Beuys who work with materials such as waxes and fats that, while not necessarily ephemeral, are certainly highly reactive, requires carefully documented discussions with the artists about their wishes while they are alive (such as the artist interview program carried out by INCCA (International Network for the Conservation of Contemporary Art, Artist Interview Project INCCA-NA 2011)). In the absence of such detailed wishes and instructions after the artist's death (in the case of Mr. Beuys) conservators and the artist's estate face challenging and often uncomfortable decisions about which artworks should follow the artist to the grave (Barker and Bracker 2021). In the case of artists such as Naum Gabo and Antoine Pevsner, who used cellulose nitrate and cellulose acetate in their sculptures, the construction of multiple copies and replicas of their works both during their lifetimes and posthumously can create confusion in the understanding and documentation of their oeuvres (Lodder 2008; Rankin 1988).

Potential legal concerns that come to mind with respect to VARA, moral rights, and the current art market include the individual reselling of dots from one of Damien Hirst's spot paintings by the MSCHF art collective (Dafoe 2020), the burning of Banksy's print *Morons (White)* to create a non-fungible token (NFT) (Criddle 2021), and Gerhard Richter's disavowal of early works from his West German period (Neuendorf 2015). What, if any, are the rights of the collectors who now own these zombie Richter works that have been struck from the catalogue raisonné?

[44] The owners reportedly failed to take care of the waterfall and the pool and planted a tree in the middle of the installation (Grant 2016).

16.5 Conclusion

As the case studies discussed in this chapter illustrate, it is important for the owners of artworks to be familiar with the legal landscape pertaining to buyer due diligence, art purchase contracts, conservation of art and artists' moral rights in their jurisdiction in order to protect their investments. As we have seen through the case studies discussed in this chapter, a buyer has the responsibility to investigate the documentation accompanying the artworks that they are purchasing and would do well to consult with experts and have an appropriate art purchase agreement drawn up to increase the chances of having a recourse if the purchase is later found out to be a forgery. With respect to art conservation, certainly, it cannot be expected that art objects will look pristine indefinitely and conservation generally is associated with a certain degree of risk. An artwork may also degrade through no fault of the owner or conservator due to the nature of the materials used by the artist (inherent vice). Even within the last decade, we have gained a greater understanding of the mechanisms through which oil paintings degrade (through metal soap aggregation, for example), which demonstrates how much we have yet to learn about the chemical instabilities of most artists' media. These instabilities can be minimized using proper storage and display conditions but not eliminated. With all of this in mind, well-drafted contractual provisions may be utilized to protect art owners' investments both at the point of purchase and in advance of any conservation attempts. Conservators also should be aware of the applicable moral rights laws (given the artist's ability to disavow the artworks under certain circumstances) in order to protect themselves against disputes with artists and the owners whose property may be seriously impacted by a conservator's work.

Acknowledgments The authors gratefully acknowledge Taylor Bialek, Law Clerk at Wilson Elser Moskowitz Edelman and Dicker LLP (USA) for her contribution to the research and citation checks.

References

Adelman, P.: Conservator overreaching and the art owner: contractual protections against the overzealous restoration of fine art. Cardozo AELJ - Arts Entertain Law J. **12**, 521–544 (1994)

Barker, R., Bracker, A.: Beuys is Dead: Long Live Beuys! Characterising Volition, Longevity, and Decision-Making in the Work of Joseph Beuys. Tate Pap (2021)

Biggest Art Fakes and Forgeries Revealed in 2018. Artwork Arch (2018). https://www.artworkarchive.com/blog/biggest-art-fakes-and-forgeries-revealed-in-2018

Blumenroth, D., Dietz, S., Müller, W., Zumbühl, S., Caseri, W., Heydenreich, G.: Inside the Forger's Oven: Identification of Drying Products in Oil Paints During and After Accelerated Drying with Increased Temperatures. Conserv. Mod. Oil Paint., pp. 437–450. Springer, Cham (2019). https://doi.org/10.1007/978-3-030-19254-9_34

Bono, M.A.: Fraud Cases Against the Knoedler Gallery Move Forward (NY), October 17, 2013. WCM Law Blog (2013)

Bowley, G.: Wall Street Titan to Get a Refund Over Fake Art (November 30, 2018). New York Times (2018)
Bresler, J.: Brave New Art Market: Unsilencing the Authenticators. In: McClean, D. (ed.) Artist. Authorsh. Leg. a Read., p. 203–215. Ridinghouse, London (2018)
Burlington Index.: The Burlington Magazine and the National Gallery Cleaning Controversy (1947–1963). Burlingt Mag (2015)
Buskirk, M.: Retraction. In: McClean, D. (ed.) Artist. Authorsh. Leg., p. 55. Ridinghouse, London (2018)
Cascone, S.: Belgian Museum Removes Show of Disputed Russian Avant-Garde Works After Damning Exposé (January 30, 2018). Artnet News (2018). https://news.artnet.com/art-world/russian-avant-garde-exhibition-closes-expose-1210742
Casement, W.: Is it a forgery? Ask a semanticist. J. Aesthetic Educ. **54**, 51–68 (2020). https://doi.org/10.5406/jaesteduc.54.1.0051
Chalkley, M.: Art Restoration: The Fine Line Between Art and Science (December 1, 2010). Yale Sci Mag (2010)
Cohan, W.D.: Court Says Heirs of Holocaust Victim Can Keep Nazi-Looted Works (July 10, 2019). New York Times (2019)
Cohen, P.: A Gallery that Helped Create the American Art World Closes Shop After 165 Years (November 30, 2011). New York Times (2011)
Cohen, P.: Lawsuits Claim Knoedler Made Huge Profits on Fakes (October 21, 2012). New York Times (2012)
Cohen, P.: From One Garage in Queens, a World of Fakes (December 26, 2013). New York Times (2013)
Criddle, C.: Banksy Art Burned, Destroyed and Sold as Token in "Money-Making Stunt" (March 9, 2021). BBC News (2021)
Dafoe, T.: An Art Collective Bought a $30,000 Damien Hirst Spot Print and Cut It Up. Now, They're Selling the Spots for $480 a Pop (April 27, 2020). Artnet News (2020). https://news.artnet.com/art-world/artist-collective-cut-up-damien-hirst-print-1844958
Donati, A.: From the Object to the Archive: Guaranteeing Authorship and Ownership in Contemporary Art. In: McClean, D. (ed.) Artist. Authorsh. Leg., pp. 143–146 Ridinghouse, London (2018)
Duron, M.: Turkey Seeks to Recover $14.4 M. Stargazer Sculpture in U.S. Federal Court (April 12, 2021). ARTnews (2021)
Fake Kandinskys, Malevichs, Jawlenskys? Top Curators and Dealers Accuse Ghent Museum of Showing Dud Russian Avant-Garde Works (January 15, 2018). Art Newsp (2018)
Finn, C.: The devil in the detail. Apollo. **179**, 50–55 (2014)
Gilbert, L.: Why would the De Soles Settle Their Claim Against Knoedler and Freedman (February 11, 2016). Art Newsp (2016)
Glanzer, I., Bracht, E., Wijnberg, L.: Cathedra, Barnett Newman. Zeitschrift Für Kunsttechnologie Und Konserv ZKK. **20**, 63–86 (2006)
Goukassian, E.: How to Make Sure You're Not Buying a Forgery (April 30, 2020). Artsy (2020). https://www.artsy.net/article/artsy-editorial-buying-forgery
Grant, D.: Artistic Paternity: When and How Artists Can Disavow Their Work (July 28, 2016). Obs (2016)
Greensboro.: Amsterdam Agrees to Pay Art Restorer $100,000, News & Record (January 11, 1997) (1997)
Haigney, S.: Lawsuit Reveals Gauguin Painting Was Not World's Most Expensive (July 3, 2017). New York Times (2017)
Hensick, T., Whitmore, P.: Mark Rothko's Harvard Murals. Center for Conservation and Technical Studies, Harvard University Art Museums, Massachusetts (1988)
Hewitt, S.: The Art Newspaper's exposé helps close dubious Russian avant-garde art display in Ghent museum (January 29, 2018). Art Newsp (2018)

Hurtado, P., Pettersson, E.: Closed New York Gallery Settles Suit Over 'Forged' Pollock (October 5, 2012). Bloom News (2012). https://www.bloomberg.com/news/articles/2012-10-05/defunct-new-york-gallery-settles-suit-over-fake-pollock-1-

International Network for the Conservation of Contemporary Art, Artist Interview Project INCCA-NA (2011). https://www.incca.org/articles/artist-interview-project-incca-na-2011

James, B.: Roller Controversy in Amsterdam: The Restoration of Modern Art (November 2, 1991). New York Times (1991)

Jones, S.: Experts call for regulation after latest botched art restoration in Spain (June 22, 2020). Guard (2020)

Kaplan, I.: Cady Noland Sues Seeking Destruction of Artwork "Copy" She Disavowed (July 21, 2017). Artsy (2017)

Keck, C.K., Lank, H., Miller, S., Golding, J., Zander, G., Rudenstine, A., et al. 'Crimes Against the Cubists': An Exchange (October 13, 1983). New York Rev (1983)

Kimmelman, M.: After a Much-Debated Cleaning, A Richly Hued Sistine Emerges (May 14, 1990). New York Times (1990)

Kimmelman, M.: Restoration of a Painting Worries Dutch Art Experts (Dec. 17, 1991). New York Times (1991): Section C page 15

Kinsella, E.: Cady Noland Disowns $1.4 Million 'Log Cabin' Artwork Sparking Collector Lawsuit (June 25, 2015). Artnet News (2015)

Kinsella, E.: Domenico De Sole Speaks About the Knoedler Fraud Trial (February 17, 2016). Artnet News (2016a)

Kinsella, E.: Judge Throws Out Lawsuit Over $1.4 Million Cady Noland Artwork After Artist Disavows It (December 13, 2016). Artnet News (2016b)

Kinsella, E.: The Final Knoedler Forgery Lawsuit, Over a $5.5 Million Fake Rothko, Has Been Settled, Closing the Book on a Sordid Drama (August 28, 2019). Artnet News (2019)

Kinsella, E.: Cady Noland Said a Collector Restored Her Log Cabin Sculpture Beyond Recognition. A Judge Has Thrown Out Her Lawsuit—for the Third Time (June 3, 2020). Artnet News (2020)

Kinsella, E., Cascone, S.: Top 9 Takeaways From Knoedler Forgery Trial (February 12, 2016). Artnet News (2016)

Langley, A., Burnstock, A.: The Analysis of Layered Paint Samples from Modern Paintings Using FTIR Microscopy. ICOM Comm. Conserv. 12th Trienn. Meet. Lyon 29 August–3 Sept. 1999, pp. 234–241, James & James (Science Publishers) Ltd (1999)

Lewis, D.: The Louvre has Restored St. John the Baptist (Nov. 9, 2016). Smithson Mag (2016)

Lodder, C.: Naum Gabo and the Quandries of the Replica. Tate Pap (2008)

McKinley Jr, J.C.: Looted Antiques Seized From Billionaire's Home, Prosecutors Say (January 5, 2018). New York Times (2018). https://www.nytimes.com/2018/01/05/nyregion/antiques-seized-from-billionaire-michael-steinhardt-cyrus-vance.html

Moynihan, C.: Did Christie's Do Its Homework? Buyer of Nazi-Tainted Work Says No (June 3, 2018). New York Times (2018)

Muñoz-Alonso, L.: Louvre Unveils Controversial Restoration of Leonardo Da Vinci Masterpiece (November 7, 2016). Artnet News (2016). https://news.artnet.com/art-world/louvre-unveils-controversial-leonardo-da-vinci-restoration-masterpiece-736250

Nadolny, J., Eastaugh, N.: The analytical results of a group of beltracchi forgeries and some historical context to their reception, Der Fall Beltracchi Und Die Folgen. In: Keazor, H., Öcal, T. (eds.) Interdiszip. Fälschungenforsch. heute, pp. 59–78. De Gruyter, Berlin (2014)

Netflix: Made You Look: A True Story About Fake Art (2020)

Neuendorf, H.: Collectors Alarmed as Gerhard Richter Disowns Early Works From West German Period (July 21, 2015). Artnet News (2015)

Neuendorf, H.: Former Knoedler Gallery Director Ann Freedman Settles Out of Court in Fraud Trial (February 8, 2016). Artnet News (2016). https://news.artnet.com/market/knoedler-ann-freedman-de-sole-settlement-421727

Neuendorf, H.: A French Museum Just Discovered That Half of Its Collection Is Fake (April 30, 2018). Artnet News (2018). https://news.artnet.com/art-world/france-terrus-museum-fake-art-1275536

Over 50 Percent of Art is Fake (October 13, 2014). Artnet News (2014). https://news.artnet.com/market/over-50-percent-of-art-is-fake-130821

Philadelphia Museum of Art - Research: Conservation (2001). https://philamuseum.org/conservation/14.html?page=5

Phillips, T.: Restorers Paint over Qing Dynasty fresco in Chinese Temple (October 22, 2013). Telegr (2013)

Povoledo, E.: Modigliani Exhibit Closes Early Amid Allegations of Fakes, The New York Times (July 19, 2017). New York Times (2017). https://doi.org/https://www.nytimes.com/2017/07/19/arts/design/modigliani-fakes-palazzo-ducale-genoa.html

Prada, P. Museums, Collectors Watch Case of Italy vs. Steinhardt (October 9, 1998). Wall Str J (1998)

Prowda, J.B.: Visual Arts and the Law: A Handbook for Professionals. Lund Humphries in association with Sotheby's Institute of Art (2013)

Ramsay, B.A., Jacobs, J.K.: Art Conservation and Restoration. Fine Art High Financ, pp. 263–286. Wiley, Hoboken (2015). https://doi.org/10.1002/9781119204688.ch11

Rankin, E.: A betrayal of material: problems of conservation in the constructivist sculpture of Naum Gabo and Antoine Pevsner. Leonardo. **21**, 285 (1988). https://doi.org/10.2307/1578657

Richardson, J.: Crimes Against the Cubists (June 16, 1983). New York Rev (1983)

Schere, E.: Where is the morality? Moral rights in international intellectual property and trade law. Fordham Int. Law J. **41**, 773–784 (2018)

Schmidt, N.: Hope in Science. Restauro (2019). https://www.restauro.de/hoffnung-in-die-wissenschaft/

Simpson, D.: Big-ticket graffiti artist Banksy says he offered paintings for $60 in Central Park (October 15, 2013). CNN (2013). https://www.cnn.com/2013/10/14/living/banksy-street-art-sale

Stroh, H.: Comment: preserving fine art from the ravages of art restoration. Alb. LJ Sci. Tech. **16**, 256–257 (2006)

Wijnberg, L., Bracht, E., van den Berg, K.J., de Keijzer, M., van Keulen, H.: Study of the grounds used by three post-war American Artists (1954–1974): Barnett Newman, Ellsworth Kelly and Brice Marden. In: Bridgland, J. (ed.) ICOM Lisbon 2011 Prepr. 16th Trienn. Conf. Lisbon, 19–23 Sept. 2011, Almada, Portugal: Criterio Producao Grafica, pp. 1–10 (2011)